TARGETING HUMAN INFLAMMATORY SKIN DISEASES WITH NATURAL PRODUCTS: EXPLORING POTENTIAL MECHANISMS AND REGULATORY PATHWAYS

EDITED BY: Bey Hing Goh, Andrei Mocan, Jianbo Xiao, Wei Hsum Yap and Siau Hui Mah
PUBLISHED IN: Frontiers in Pharmacology

frontiers Research Topics

About Frontiers

Frontiers is more than just an open-access publisher of scholarly articles: it is a pioneering approach to the world of academia, radically improving the way scholarly research is managed. The grand vision of Frontiers is a world where all people have an equal opportunity to seek, share and generate knowledge. Frontiers provides immediate and permanent online open access to all its publications, but this alone is not enough to realize our grand goals.

Frontiers Journal Series

The Frontiers Journal Series is a multi-tier and interdisciplinary set of open-access, online journals, promising a paradigm shift from the current review, selection and dissemination processes in academic publishing. All Frontiers journals are driven by researchers for researchers; therefore, they constitute a service to the scholarly community. At the same time, the Frontiers Journal Series operates on a revolutionary invention, the tiered publishing system, initially addressing specific communities of scholars, and gradually climbing up to broader public understanding, thus serving the interests of the lay society, too.

Dedication to Quality

Each Frontiers article is a landmark of the highest quality, thanks to genuinely collaborative interactions between authors and review editors, who include some of the world's best academicians. Research must be certified by peers before entering a stream of knowledge that may eventually reach the public - and shape society; therefore, Frontiers only applies the most rigorous and unbiased reviews.
Frontiers revolutionizes research publishing by freely delivering the most outstanding research, evaluated with no bias from both the academic and social point of view. By applying the most advanced information technologies, Frontiers is catapulting scholarly publishing into a new generation.

What are Frontiers Research Topics?

Frontiers Research Topics are very popular trademarks of the Frontiers Journals Series: they are collections of at least ten articles, all centered on a particular subject. With their unique mix of varied contributions from Original Research to Review Articles, Frontiers Research Topics unify the most influential researchers, the latest key findings and historical advances in a hot research area! Find out more on how to host your own Frontiers Research Topic or contribute to one as an author by contacting the Frontiers Editorial Office: frontiersin.org/about/contact

TARGETING HUMAN INFLAMMATORY SKIN DISEASES WITH NATURAL PRODUCTS: EXPLORING POTENTIAL MECHANISMS AND REGULATORY PATHWAYS

Topic Editors:
Bey Hing Goh, Monash University Malaysia, Malaysia
Andrei Mocan, Iuliu Hațieganu University of Medicine and Pharmacy, Romania
Jianbo Xiao, University of Vigo, Spain
Wei Hsum Yap, Taylor's University, Malaysia
Siau Hui Mah, Taylor's University, Malaysia

Table of Contents

Editorial: Targeting Human Inflammatory Skin Diseases With Natural Products: Exploring Potential Mechanisms and Regulatory Pathways

Bey Hing Goh[1,2]*, Andrei Mocan[3,4], Jianbo Xiao[5], Siau Hui Mah[6,7]* and Wei Hsum Yap[6,7]*

[1]Biofunctional Molecule Exploratory Research Group (BMEX), School of Pharmacy, Monash University Malaysia, Bandar Sunway, Malaysia, [2]College of Pharmaceutical Sciences, Zhejiang University, Hangzhou, China, [3]Department of Pharmaceutical Botany, "Iuliu Haţieganu" University of Medicine and Pharmacy, Cluj-Napoca, Romania, [4]Laboratory of Chromatography, ICHAT, University of Agricultural Sciences and Veterinary Medicine Cluj-Napoca, Cluj-Napoca, Romania, [5]Nutrition and Bromatology Group, Department of Analytical Chemistry and Food Science, Faculty of Food Science and Technology, University of Vigo, Ourense, Spain, [6]School of Biosciences, Taylor's University, Subang Jaya, Malaysia, [7]Centre for Drug Discovery and Molecular Pharmacology (CDDMP), Faculty of Health and Medical Sciences (FHMS), Taylor's University, Subang Jaya, Malaysia

Editorial on the Research Topic

Targeting Human Inflammatory Skin Diseases With Natural Products: Exploring Potential Mechanisms and Regulatory Pathways

INTRODUCTION

For decades, researchers have explored the potential of natural products with immunomodulatory and antioxidant effects for targeting human skin diseases. Skin diseases can be caused by multiple factors including exposure to allergens, genetic inheritance, as well as autoimmune responses, and they cause major health concerns. The use of natural products is gaining popularity due to their long history of use and as a potential source of biologically active agents with anti-inflammatory, immunomodulatory, antioxidant, and chemo-preventive effects. Thus, natural products are continuously being explored for targeting multiple signaling pathways and acting as potential bioactive agents for targeting skin diseases. In this Research Topic, a total of eleven articles were published, illustrating the immunomodulatory mechanisms and regulatory pathways of diverse natural products and their formulations in targeting human skin diseases.

NATURAL PRODUCTS–HERBAL FORMULATIONS AND BIOACTIVE AGENTS

There is growing interest in the search for novel, effective and safe herbal formulations derived from combinations of medicinal plants which contain active ingredients with multiple effects. The potential of herbal formulations in dermatological applications for the treatment of psoriasis, atopic dermatitis, contact dermatitis, oral ulcers and many other inflammatory skin diseases were highlighted. Herbal medicines are formulated in various forms, including topical agents such as ointment, creams, and emulsions, as well as in oral forms like capsule, tablet, and soup. Lee et al.

reported that Chijabyukpi-tang (CBT), an oriental herbal formula traditionally shown to treat eczema, has shown to improve atopic dermatitis-associated symptoms in 2,4-dinitrochlorobenzene (DNCB) treated mice. Lee et al. demonstrated that Socheongryong-tang (SCRT), a traditional formulation originating from East Asia that has been used for treating respiratory and allergic diseases, reduced dependence on steroidal ointment in patients with mild-moderate atopic dermatitis without any significant toxicity effects. On the other hand, LiangXueJieDu (LXJD), an herbal formula that has been commonly used in China to treat psoriasis vulgaris, was also shown to suppress IMQ-induced psoriasis-like lesions in mice (Zhao et al.). Besides, Jo et al. identified the potential of Derma-H which has been used as traditional herb for treating swelling, dryness, and itchiness, to inhibit skin hyperplasia and mast cell infiltration in DNCB-induced allergic contact dermatitis in mice.

Herein, Chen et al. reported that Kouyanqing Granule (KYQG) reduces sleep-deprivation-induced symptoms in oral ulcers by regulating neuro-immunoendocrine system, oxidative stress levels, and tryptophan metabolism. Kuai et al. revealed the mechanisms of Taodan granules (TDGs) in inhibiting keratinocyte cell growth and inflammatory responses to suppress psoriasis symptoms in IMQ-induced mice. Apart from the improvement of inflammatory reactions in skin lesions, another research reported by Gan et al. has shown that burn ointment (BO), a traditional Chinese medical formulation, can be used to promote cutaneous wound healing due to its antimicrobial and anti-inflammatory qualities. Meanwhile, phenolic phytochemicals such as xanthones and flavonoids which comprise oxygenated heterocycles structures are well-known antioxidants with multi-targeting mechanisms. Many studies reported that prenylated α- and γ-mangostin, glucosylated mangiferin and xanthone gambogic acid can be used for treating skin diseases (Gunter et al.). Zhang et al. identified the role of isovitexin, a flavonoid found in the leaf of Celtis sinensis, in ameliorating contact dermatitis. Other key metabolites from microalgae including carotenoids, astaxanthine and lutein known to possess anti-inflammation and anti-oxidative properties are also used in the remedy of various skin diseases (Choo et al.). Despite the promising therapeutic effects, natural products were limited in terms of their stability, solubility, and bioavailability. The development of novel delivery approaches, such as micro- and nano-emulsions, nanocarriers, microneedles, and cryogels could help to alleviate these limitations (How et al.; Xie et al.). These strategies could help to achieve the therapeutic effect through its delivery to the skin lesions and interact with underlying immune cells and inflammatory mediators.

REGULATING IMMUNO-PATHOGENESIS OF SKIN DISEASES–PATHWAYS AND MECHANISMS

Inflammatory skin diseases are mostly characterized by skin lesions with systemic manifestations. The immune system plays a crucial pathogenetic role. Mechanistically, immune mediators that trigger molecular changes in the local tissue cells are driving inflammatory responses (Richmond and Harris, 2014; Schön, 2019). Translational immunology has contributed significantly to the understanding and controlling of inflammatory skin diseases. Therapeutics targeting IL-23 and IL-17 are approved for clinical use and they showed high efficacy (Gaffen et al., 2014; Ghoreschi et al., 2021). The detailed mechanism of natural products in targeting immuno-pathogenesis of skin diseases have been reported.

Herein, the LXJD formula was shown to inhibit keratinocyte proliferation and suppressed CD3$^+$ T cells infiltration in IMQ-induced mice. LXJD formula treatment suppressed IL-1β, IL-6, TNF-α, COX2 by regulating several signaling pathways including MAPK, PI3K/AKT, and NF-κB (Zhao et al.). Meanwhile, CBT suppressed serum immunoglobulin E (IgE) levels and pro-inflammatory cytokines (IL-4 and IL-6) and chemokines (IL-8 and CXCL10) expression in DNCB-treated mice with AD-like lesions (Lee et al.; Lee et al.). Mechanistically, CBT activates Nrf2 and HO-1 signaling in HaCaT cells stimulated with TNF-α/IFN-γ. Derma-H, a mixture that contains Astragalus membranaceus Fisch. ex Bunge and Nepeta tenuifolia Benth, inhibit Th2-mediated cytokines expression and suppress NGF-TrkA signaling, all which improved the skin lesions in DNCB-treated mice (Jo et al.).

It has been reported that KYQG inhibit systemic inflammation by reducing the expression of TNF-α, IL-1β, IL-6, IL-18, and MCP-1 (Chen et al.). BO on the other hand have shown to suppress TNF-α and inhibit VEGF and TGF-β1 levels in the serum. As a wound healing agent, BO also resulted in the increase of collagen-I expression, possibly through regulating the PI3K, AKT, and mTOR signaling pathways (Gan et al.). Interestingly, TDGs attenuate IMQ-induced lesions in a psoriatic mouse model and were shown to reduce IL-17a, TNF-α, and NF-κB expression, and upregulation of the Gly- Ser-Thr metabolism axis (Kuai et al.). Isovitexin decrease proinflammatory cytokines (TNF-α, IFN-γ, IL-2 and IL-17A) expression, and modulated the MAPK and STAT signaling pathways as well as SHP2 phosphorylation (Zhang et al.).

SYSTEMATIC EXPERIMENTAL PHARMACOLOGICAL EVALUATION APPROACHES OF NATURAL PRODUCTS

To elucidate the mechanistic pathways targeted by phytochemicals and herbal mixtures, a systematic experimental pharmacological evaluation approach is needed. Natural products which comprise herbal formulation mixtures are most often based on their theory of medicine with multiple ingredients interactions. The complex herbal mixtures along with their pharmacological activity could complicate the understanding of their mechanisms of action. Chemical profiling based on UPLC-MS analysis is the most often used approach in identifying chemical ingredients of natural products extracts and formulations, followed by experimental evaluation of their pharmacological activities in cellular and animal models. Systems pharmacology can be used as an approach to integrate data on oral bioavailability, drug targets prediction and validation, as well as disease network pharmacology. Recent studies have reported the use of in silico ADME (absorption,

distribution, metabolism, and excretion) model to select active agents with favorable pharmacokinetic properties (Ru et al., 2014; Yuan et al.). In addition, in-depth metabolomic profiling serves to provide insights into the biological targets regulated by natural products. Gan et al. combined the use of pharmacological and metabolomics approaches in identifying the biomarkers of KYQG. It was highlighted that identification and quantification of absorbed chemicals and its metabolites should be performed to correlate biomarkers targeted in response to their corresponding active constituents.

CONCLUSION

In summary, this Research Topic enhances our knowledge on recent exciting progress in the field of molecular pharmacology of natural products in skin diseases. Herbal formulations and their active constituents can improve inflammatory skin lesions in animal models and human disease patients, and they regulate pro-inflammatory cytokines expression and its corresponding

signaling pathways. Furthermore, the combination of technologies between chemical profiling, metabolomics and pharmacodynamics will continue to uncover the mechanisms and regulatory pathways of natural products in targeting human skin diseases.

AUTHOR CONTRIBUTIONS

All authors listed have made a substantial, direct, and intellectual contribution to the work and approved it for publication.

FUNDING

REFERENCES

Gaffen, S. L., Jain, R., Garg, A. V., and Cua, D. J. (2014). The IL-23-IL-17 Immune axis: from Mechanisms to Therapeutic Testing. *Nat. Rev. Immunol.* 14 (9), 585–600. doi:10.1038/nri3707

Ghoreschi, K., Balato, A., Enerbäck, C., and Sabat, R. (2021). Therapeutics Targeting the IL-23 and IL-17 Pathway in Psoriasis. *The Lancet* 20397 (10275), 754–766. doi:10.1016/S0140-6736(21)00184-7

Richmond, J. M., and Harris, J. E. (2014). Immunology and Skin in Health and Disease. *Cold Spring Harb Perspect. Med.* 4 (12), a015339. doi:10.1101/cshperspect.a015339

Ru, J., Li, P., Wang, J., Zhou, W., Li, B., Huang, C., et al. (2014). TCMSP: a Database of Systems Pharmacology for Drug Discovery from Herbal Medicines. *J. Cheminform* 6, 13. doi:10.1186/1758-2946-6-13

Schön, M. P. (2019). Adaptive and Innate Immunity in Psoriasis and Other Inflammatory Disorders. *Front. Immunol.* 10, 1764. doi:10.3389/fimmu.2019.01764

Pharmacodynamic and Metabolomics Studies on the Effect of Kouyanqing Granule in the Treatment of Phenol-Induced Oral Ulcer Worsened by Sleep Deprivation

Pan Chen[1], Hongliang Yao[2], Weiwei Su[1], Yuying Zheng[1], Weiyang Fan[1], Liping Zhang[1], Tingting Chen[1], Shuling Wu[1], Weijian Zhang[1], Yan He[1], Zenghao Yan[1], Yonggang Wang[1] and Peibo Li[1]*

[1] Guangdong Engineering and Technology Research Center for Quality and Efficacy Re-evaluation of Post-marketed TCM, Guangdong Key Laboratory of Plant Resources, School of Life Sciences, Sun Yat-sen University, Guangzhou, China, [2] Guangdong Key Laboratory of Animal Conservation and Resource Utilization, Guangdong Public Laboratory of Wild Animal Conservation and Utilization, Drug Synthesis and Evaluation Center, Guangdong Institute of Applied Biological Resources, Guangzhou, China

Oral ulcers are the most prevalent oral mucosal diseases globally, and no specific treatment schemes are currently available due to the complexity of oral ulcer diseases. Sleep deprivation increases the risk of a deterioration in oral health. Kouyanqing Granule (KYQG) has been used for decades in China to treat inflammatory diseases of the mouth and throat associated with the hyperactivity of fire due to yin deficiency syndrome. However, the mechanisms underlying the effects of KYQG in the treatment of oral ulcers are still unclear. The aims of this study were to investigate whether KYQG treatment could attenuate the symptoms of oral ulcers worsened by sleep deprivation and identify the involved metabolic pathways. First, we conducted chemical profiling of KYQG via UPLC–MS analysis. We then combined pharmacological and metabolomics approaches in a phenol-induced rat model of oral ulcers worsened by sleep deprivation. A total of 79 compounds were initially identified. Our observations showed that KYQG treatment induced a significantly higher healing rate in oral ulcers worsened by sleep deprivation. KYQG significantly reduced the levels of 5-HT and GABA in serum, and only decreased the 5-HT level in brain tissue after phenol injury followed by sleep deprivation. Moreover, KYQG administration significantly suppressed systemic inflammation by inhibiting TNF-α, IL-1β, IL-6, IL-18, and MCP-1. Immunohistochemical analysis further revealed that KYQG inhibited IL-6 expression in buccal mucosa tissues. KYQG treatment also significantly decreased the serum levels of ACTH, CORT, IgM, and 8-OHdG. Serum metabolomics analysis showed that a total of 30 metabolites showed significant differential abundances under KYQG intervention, while metabolic pathway analysis suggested that the altered metabolites were associated with the dysregulation of eight metabolic pathways. Taken together, our results indicated that KYQG attenuates the symptoms of oral ulcers

worsened by sleep deprivation probably through the regulation of the neuroimmunoendocrine system, oxidative stress levels, and tryptophan metabolism. This study also provides a novel approach for addressing the increased health risks resulting from sleep deficiency using an herbal medicine formula.

INTRODUCTION

Oral ulcers are among the most painful and common mucosal diseases. These conditions have uncertain and complex etiology, including mechanical injuries, immunologic dysregulation, genetic predisposition, hormonal level fluctuations, systemic diseases, microelement deficiencies, nutritional imbalances, microbial infections, allergic factors, adverse drug reactions, and psychological stress (Scully and Shotts, 2000; Guimaraes et al., 2007; Akintoye and Greenberg, 2014). The breakdown of immune regulation at mucosal sites plays a crucial role in the development of oral ulcers. Recurrent aphthous stomatitis (RAS) is one of the most common oral ulcer diseases, and it has a prevalence in the general population that ranges between 5% and 60% (Taylor et al., 2014). Oral ulcers usually expose nerve endings in the underlying lamina propria and can severely affect patients' quality of life. Due to their complexity, no specific or ideal treatment approach is currently available for the treatment of these diseases.

Traditional Chinese medicine (TCM) formulas are used for oral ulcer therapy, acting through the synergistic effects of multiple constituents. Kouyanqing Granule (KYQG), a TCM formula, comprises parts of five species of herbs, namely, the flower bud of Lonicera macrantha (D.Don) Spreng. (syn. *Lonicera macranthoides* Hand.-Mazz., 1936) (FL), tuberous root of *Ophiopogon japonicus* (Thunb.) Ker Gawl., 1807 (TO), root of *Scrophularia ningpoensis* Hemsl. (RS), tuberous fibrous root of *Asparagus cochinchinensis* (Lour.) Merr. (TA), and root of *Glycyrrhiza uralensis* Fisch. ex DC. (RG). In China, KYQG has been used for decades to treat inflammatory diseases of the mouth and throat, such as RAS, traumatic ulcers, oral leukoplakia, and oral lichen planus. KYQG is also recorded in the Chinese Pharmacopoeia of 2015 as a treatment for oral diseases associated with the hyperactivity of fire due to Yin deficiency (HFYD) syndrome (China, 2015). The symptoms of HFYD, a type of TCM syndrome, have characteristics of sleeplessness, thirst, dry mouth, and dysphoria with a feverish sensation (Poon et al., 2012; Jiang et al., 2015). Sleep loss usually leads to HFYD (Yan et al., 2009; Poon et al., 2012). Inadequate sleep is a prevalent issue in today's society and can increase the risk of numerous disorders, such as cardiovascular disease (Tobaldini et al., 2017), obesity (Fatima et al., 2015), diabetes (Lee et al., 2017), inflammatory bowel disease (Ananthakrishnan et al., 2013), pregnancy complications (Romero and Badr, 2014), hypertension (Pepin et al., 2014), and neurobehavioral and cognitive impairment (Kreutzmann et al., 2015).

Epidemiological evidence indicates that a link exists between sleep loss and oral health, such as the increased risk of periodontitis (Lee et al., 2014) and gingivitis (Carra et al., 2017) that results from sleep deprivation. We have previously shown that sleep deprivation exacerbates the symptoms of oral ulcers and delays the healing process in the rat, and that oxidative stress and the neuro-immuno-endocrine system may have roles in worsening oral ulcer symptoms (Chen et al., 2019). However, the mechanisms underlying the therapeutic effects of KYQG against oral ulcers associated with the HFYD syndrome remain poorly understood. To address this, we performed chemical profiling of KYQG *via* UPLC–MS and investigated the treatment effects and potential mechanisms by combining pharmacological and metabolomics approaches in a phenol-induced rat model of oral ulcers worsened by sleep deprivation.

MATERIALS AND METHODS

Chemical Profiling Based on UPLC–MS Analysis

The reference standards of lysine, arginine, aspartic acid, and citrulline were purchased from Jianglai Biotechnology co., LTD (Shanghai, China). Chelidonic acid and diosmetin were purchased from Sigma-Aldrich (St Louis, MO, USA). Phenylalanine, chlorogenic acid, caffeic acid, liquiritin, isoquercitrin, angoroside C, isoliquiritoside, harpagoside, macranthoidin B, luteolin, quercetin, and formononetin were purchased from the National Institute for the Control of Pharmaceutical and Biological Products (Beijing, China). KYQG extracts (Batch number: A19M025) were provided by Hutchison Whampoa Guangzhou Baiyunshan Chinese Medicine Co., Ltd (Guangzhou, China), and KYQG was prepared by extracting the five herbs in the following proportion: flower bud of Lonicera macrantha (D.Don) Spreng. (syn. *Lonicera macranthoides* Hand.-Mazz., 1936) (FL), 26%; tuberous root of *Ophiopogon japonicus* (Thunb.) Ker Gawl., 1807 (TO), 21%; root of *Scrophularia ningpoensis* Hemsl. (RS), 21%; tuberous fibrous root of *Asparagus cochinchinensis* (Lour.) Merr. (TA), 21%; root of *Glycyrrhiza uralensis* Fisch. ex DC. (RG), 11%, as described in our previous study (Liu et al., 2015). One gram of KYQG extract was ultrasonically extracted with 80% methanol for 30 min. The mixture was precipitated overnight and filtered (pore size 0.22 μm; Jinteng, China) before chemical profiling analyses. The UPLC system was equipped with a Shimadzu CBM-20Alite controller. Chromatographic separation of the sample was

conducted on a Dionex Bonded Silica C18 column (4.6 mm × 150 mm, 3 μm; Sunnyvale, California, USA) maintained at 40 °C. The mobile phase consisted of acetonitrile containing 0.1% formic acid (mobile phase A) and water containing 0.1% formic acid (mobile phase B) and the gradient elution program was as follows: 0–7 min, 2 to 10% A; 7–95 min, 10% to 41% A; 95–105 min, 41% to 100% A; 105–115 min, 100% A. The flow rate was 0.3 mL/min, and the sample injection volume was 3 μL. The mass spectral analyses were performed using a hybrid triple quadrupole time-of-flight mass spectrometer (Triple TOF™ 5600+, AB Sciex, Forster City, CA, USA). The electrospray ionization (ESI) source was operated in both positive and negative ion mode with the following settings: ion spray voltage was 5500 V in positive ion mode and 4500 V in negative mode, ion source gas 1 = 55 psi, ion source gas 2 = 55 psi, curtain gas = 35 psi, and collision gas pressure = 10 psi. The components of the KYQG sample were identified *via* the mass spectrum data, chromatographic retention time (RT), MS/MS fragmentation pathway, and comparisons with available standards, references, and a mass spectral library (Natural Products HRMS/MS Spectral Library, Version 1.0; AB Sciex).

Quantification Analysis

To perform a quantification analysis, 1 mg of KYQG extract was ultrasonically extracted with 9 ml of 50% methanol in volumetric flask (10 ml) for 30 min and then diluted to volume. The mixture was diluted to appropriate concentration filtered through a 0.22 μm filter for quantification analysis. The stock solutions of arginine, liquiritin, chlorogenic acid, harpagoside, luteolin-7-O-glucoside, and glycyrrhizic acid were prepared in methanol and then mixed and diluted to serial concentrations in 50% methanol. Linearity of the method was examined by using the serial mixed standards and the calibration curves were calculated by the least squares linear regression method. The separation of the sample was conducted on a Phenomenex Kinetex C18 100A (2.10mm × 100 mm, 2.6 μm, Torrance, USA). The mobile phase consisted of acetonitrile containing 0.1% formic acid (mobile phase A) and water containing 0.1% formic acid (mobile phase B), and the gradient elution program was as follows: 0–30 min, 5 to 62% A; 30–33 min, 62% to 100% A. The flow rate was 0.3 mL/min, and the sample injection volume was 5 μL. MS conditions were set as described above (Part 2.1).

Animals and Treatment

Eight-week-old male Sprague–Dawley rats were purchased from the Laboratory Animal Center of Sun Yat-sen University. The animals were randomly divided into six groups (*n* = 7 per group): a Control group, Model group, KYQG-Low group, KYQG-Mid group, KYQG-High group, and Levamisole group. The KYQG-Low, KYQG-Mid, and KYQG-High groups were treated with KYQG extract at the doses of 0.522, 1.57, and 4.70 g/kg/d, respectively, by oral administration from day 1 to day 9. The Levamisole group was treated with levamisole (20 mg/kg/d, levamisole solution was prepared at a concentration of 2 mg/ml in water and then intragastrically administered to rats at a dose of 10 ml/kg/d), and the other groups were treated with distilled water. On day 4, oral ulcers were induced on the cheek

mucosa of rats in the Model group, KYQG groups, and Levamisole group by phenol-induced chemical injury, as described in our previous study (Chen et al., 2019). Ulcers that were almost uniformly round formed in the oral mucosal region on day 6. The rats in the Model group, KYQG groups, and Levamisole group were then subjected to sleep deprivation for 72 h using a modified multiple platform technique as described in our previous study (Chen et al., 2019). At the end of the sleep deprivation period, all the animals were anesthetized, and blood was collected from the abdominal aorta. The blood was centrifuged at 5,000 rpm for 20 min at 4°C to obtain serum, which was stored at −80°C. Whole brains and buccal mucosa tissues were collected and immediately frozen at −80°C. The animal experimental protocol is depicted in **Figure 1**. All animal experiments were approved by the Institutional Animal Care and Use Committee of Sun Yat-sen University (Approval No. SYSU-IACUC-2019-000181). All efforts were made to minimize the suffering of the experimental animals.

Measurement of Ulcer Area

Measurement of the ulcer area was started on day 6 after induction of ulceration using Image-Pro Plus 6.0 (Media Cybernetics Inc., Rockville, MD, USA) as described in our previous study (Chen et al., 2019). The degree of healing was expressed as ulcer healing rate = $(A_6 − A_t)/A_6 × 100\%$, where A_6 and A_t represent the initial ulcer area and the ulcer area at the time of observation, respectively.

Enzyme-Linked Immunosorbent Assay (ELISA)

The serum concentrations of tumor necrosis factor-alpha (TNF-α), interleukin (IL)-1β, IL-6, monocyte chemoattractant protein 1 (MCP-1), adrenocorticotropin hormone (ACTH), corticosterone (CORT), immunoglobulin M (IgM), and 8-hydroxy-deoxyguanosine (8-OHdG) were measured using commercial ELISA kits (Nanjing Jiancheng Bioengineering Institute, Nanjing, Jiangsu, China) according to the manufacturer's instructions.

Measurement of Neurotransmitter Levels

The levels of γ-aminobutyric acid (GABA) and 5-hydroxytryptamine (5-HT) in serum and whole-brain tissues were determined using ultra-high performance liquid chromatography–tandem mass spectrometry as described in our previous study (Chen et al., 2019).

Immunohistochemistry

Immunohistochemistry was performed to determine the expression of IL-6 in healthy buccal mucosa tissues. All specimens were fixed in 4% paraformaldehyde (BioSharp, Hefei, China), embedded in paraffin (Guangdong Dachuan special wax Co. Ltd, Maoming, China), and sliced into 5-μm sections. Subsequently, the sections were dewaxed with xylene and dehydrated with ethanol. The processed sections were preincubated with 3% H_2O_2 in PBS for 10 min to block endogenous peroxidases. The sections were rinsed three times with PBS (5 min each wash) and then blocked with 5% (*w/v*)
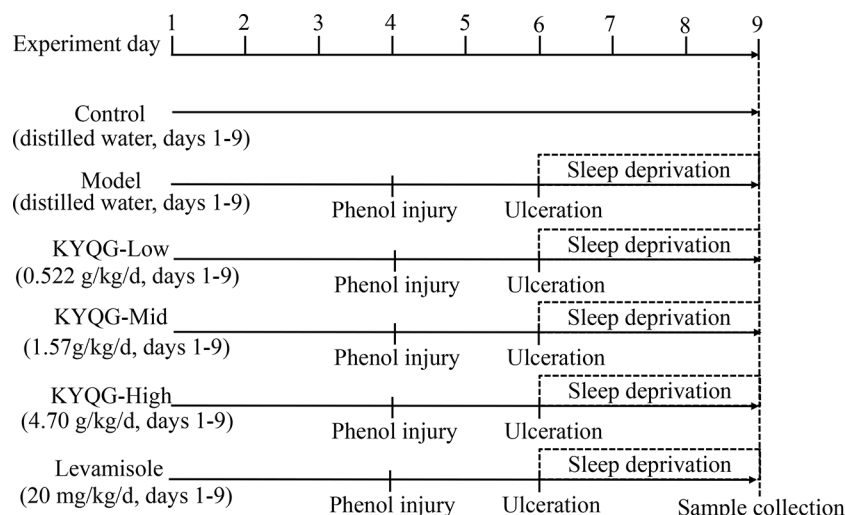
FIGURE 1 | Schematic representation of the experimental protocol showing the sequence of events throughout the experiment.

bovine serum albumin for 30 min at 37°C. Then, the sections were incubated with an anti-IL-6 primary antibody (1:5000, ab9324, Abcam, Cambridge, UK) at 37°C for 2 h, followed by incubation with the secondary antibody at 37°C for 30 min. Subsequently, the samples treated with diaminobenzidine tetrahydrochloride. To stop the reaction and clear unbound antibody, the incubated sections were rinsed three times with PBS before and after the corresponding treatments. Staining was developed by incubation in a diaminobenzidine solution for 10 min followed by staining with hematoxylin for 5 min. Images of these sections were obtained using an optical microscope (Olympus BX43; Olympus Co., Tokyo, Japan). The mean optical density of each field (epithelial tissue section) was represented as integrated optical density (IOD)/area using Image-Pro Plus 6.0.

Metabolomics Analysis of Serum Samples

Metabolomic profiling was performed using LC–QTOF/MS. For the untargeted metabolomics analysis, an LC system (Shimadzu CBM20Alite controller) combined with a hybrid triple quadrupole time-of-flight mass spectrometer (Triple TOF™ 5600+, AB Sciex) was used. A Kinetex® C18 100A column (2.6 μm, 150 mm × 3.0 mm, Phenomenex Corp, Torrance, CA, USA) was used for sample separation. Water containing 0.1% formic acid (*v/v*) (mobile phase A) and acetonitrile (mobile phase B) were used at a flow rate of 0.3 mL/min. The gradient elution program was as follows: 0–20 min, 5% to 80% B; 20–30 min, 80% to 90% B; 30–40 min, and 90% to 95% B. The serum samples of the Control, Model, and KYQG-High groups were used for metabolomics analysis. Each serum sample (100 μL) was added to 200 μL of a cold acetonitrile/methanol solution (1:1, *v/v*) to precipitate the proteins. After vortexing for 5 min, the solution

was centrifuged at 13,000 rpm for 20 min at 4°C. Afterwards, 10 μL of the supernatant was injected into the LC–QTOF/MS system for analysis. The mass spectrometry data were acquired in negative ion mode, and the electrospray source settings were as follows: gas 1 = 55 psi, gas 2 = 55 psi, source temperature = 550°C, and ion spray voltage was −4500 V with 35 psi curtain gas. Samples were analyzed with scanning mass-to-charge (*m/z*) ratio ranging from 50 to 1500 Da (30 V collision energy, 15 eV collision energy spread, and 80 V declustering potential). Nitrogen was used as nebulizer and auxiliary gas.

The raw data were converted to the mzXML format using ProteoWizard and processed using the R package 'XCMS' for peak detection, extraction, alignment, and integration. Then, an in-house MS2 database was applied in metabolite annotation. The cutoff for annotation was set at 0.3. The metabolomics data were analyzed by orthogonal partial least squares discriminant analysis (OPLS-DA) using SIMCA (version 15.0.2, Umea, Sweden). Furthermore, the value of variable importance in the projection (VIP) of the first principal component in OPLS-DA analysis was obtained and summarizes the contribution of each variable to the model. Metabolites with VIP >1 and $P < 0.05$ (Student's *t*-test) were considered as having significantly changed abundance. In addition, the KEGG (http://www.genome.jp/kegg/) and MetaboAnalyst (http://www.metaboanalyst.ca/) databases were used for pathway enrichment analysis.

Statistical Analysis

Data analyses were performed using GraphPad Prism 8.0.2 (GraphPad Prism Software, La Jolla, CA, USA). The results are presented as means ± SD for each group. To assess the differences between the groups, one-way ANOVA was carried out followed by Tukey test. Results were considered significant at $P < 0.05$.

RESULTS

Chemical Profiling and Quantification Analysis of KYQG

The retention time, exact molecular mass, and MS/MS data for each compound were obtained and applied in the KYQG chemical profiling analysis performed using Peakview software. The total ion chromatograms of KYQG in the positive and negative modes are shown in **Supplementary Figure S1**. A total of 79 compounds were initially identified, including phenolics, flavonoids, triterpenoid saponins, and amino acids. The identified compounds are shown in **Table 1**, and the mass spectrum data of standards are shown in **Supplementary Figure S2** and **Supplementary Table S1**. The results of quantification analysis of six components in KYQG are shown in **Tables 2** and **3**. The linear correlations of the calibration curves over the test range were acceptable. Chlorogenic acid was the most abundant component among the six components detected.

Effects of KYQG on Oral Ulcer Area

Representative images of buccal mucosa regions are shown in **Figure 2A**. On day 6, baseline ulcer areas of the Model, KYQF-Low, KYQF-Mid, KYQF-High, and Levamisole groups were 12.15 ± 0.68, 12.20 ± 0.66, 11.99 ± 0.74, 12.16 ± 1.05, and $12.18 \pm 0.50 \text{ mm}^2$, respectively, and the differences were not significant. The ulcer healing rate was calculated to assess the treatment effects of KYQG (**Figure 2B**). The oral ulcer area was decreased in all groups on days 7–9, with the highest ulcer healing rate being found in the KYQG-High group; the KYQG-Mid group, KYQG-high group, and Levamisole group showed significantly higher ulcer healing rates than the Model group on days 7–9. However, the difference between the Model group and the KYQG-Low group on days 7–9 was not significant.

Effects of KYQG on Serum and Brain Neurotransmitter Levels

As shown in **Figures 2C–F**, KYQG treatment decreased the 5-HT level in serum and brain tissue and the GABA level in serum. However, compared with the Model group, KYQG treatment did not lead to a reduction in the GABA level in brain tissue.

Effects of KYQG on the Serum Levels of ACTH and CORT

Figures 2G, H show the serum levels of ACTH and CORT. Levamisole and KYQG treatments resulted in a significant decrease in the serum level of ACTH. The serum level of CORT was also significantly reduced in the KYQG (4.70 g/kg/d)- and Levamisole-treated groups when compared with that in the Model group. The above results demonstrated that the protective effect of KYQG in oral ulcers may be modulated through the hypothalamic-pituitary-adrenocortical (HPA) axis.

Effects of KYQG on the Levels of Inflammatory Cytokines, 8-OHdG, and IgM

As shown in **Figures 2I–O**, at the concentration of 4.70 g/kg/d, KYQG significantly reduced the serum levels of TNF-α, IL-1β,

and IL-18, while at the concentrations of 1.57 and 4.70 g/kg/d, KYQG treatment lowered the serum levels of IL-6 and MCP-1. KYQG treatment also led to reduced serum levels of 8-OHdG and IgM, indicating that KYQG reduced oxidative stress and was involved in the regulation of immunological responses.

Effects of KYQG on IL-6 Expression in Buccal Mucosa Tissues

To investigate the protective effects of KYQG on oral ulcers, the expression of IL-6 in epithelial tissue sections was investigated by immunohistochemistry. As illustrated in **Figures 2P, Q**, the expression of IL-6 in epithelial tissue sections from the Model group was significantly increased when compared with that of the Control group; however, IL-6 level was markedly lower in the KYQG-High group than in the Model group.

Metabolic Profiling Analysis

Serum metabolic profiling in the Control group, Model group, and KYQG-High group was assessed by multivariate analysis. A clear separation was observed among the Control, Model, and KYQG-High groups in OPLS-DA score plots (**Figures 3A, B**), suggesting differential metabolic profiles between two groups. A permutation test was used to verify the model to avoid the transition fit of the OPLS-DA mode (**Figures 3C, D**). The quantification parameters for this OPLS-DA model (R2Y and Q2) were all positive, indicating that the OPLS-DA model was robust.

Identification of Metabolites and Pathway Analysis

According to the OPLS-DA analysis, the levels of the metabolites identified in the Model group were significantly different from those in the Control and KYQG-High groups. The metabolites showing significantly differential abundance were visualized through volcano plots (**Figures 3E, F**). A total of 59 differential metabolites were identified in the Model and Control groups, and 68 in the Model and KYQG groups, using a VIP >1.0 in the OPLS-DA models and a *p*-value <0.05 (two-tailed Student's *t*-test). The generated heat map clearly depicts the relationships between these differential metabolites in different samples (**Figures 3G, H**). Based on the heatmaps, the Control and Model groups, as well as the Model and KYQG groups, could be completely separated. A total of 30 metabolites showed significantly differential abundance with KYQG treatment (**Figure 4A**), and these metabolites were used for pathway analysis. The metabolic pathway analysis using Metaboanalyst based on KEGG database (www.kegg.jp) revealed that eight pathological processes were associated with KYQG treatment, including D-Glutamine and D-glutamate metabolism, tryptophan metabolism, alanine, aspartate, and glutamate metabolism, arachidonic acid metabolism, and arginine and proline metabolism (**Figure 4B**). The important differential metabolites were summarized in **Figure 4C**, and we found that tryptophan metabolism plays an important role in the protection of KYQG against phenol-induced oral ulcer worsened by sleep deprivation.

TABLE 1 | Identification of the chemical composition of Kouyanqing Granule (KYQG).

No.	RT (min)	Formula	[M+H]$^+$(Error, ppm)	[M−H]$^−$(Error, ppm)	MS/MS fragments (Positive mode)	MS/MS fragments (Negative mode)	Identification	Plant material
1	5.28	$C_6H_{14}N_2O_2$	147.1128 (−0.4)		130.0867 [M+H−NH$_3$]$^+$, 84.0826 [M+H−NH$_3$−HCOOH]$^+$, 67.0566 [M+H−2NH$_3$−HCOOH]$^+$		Lysine	TA/TO
2	5.63	$C_6H_{14}N_4O_2$	175.1190 (0.0)	173.1058 (+8.1)	158.0934 [M+H−NH$_3$]$^+$, 130.0985 [M+H−NH$_3$−CO]$^+$, 116.0716 [M+H−CN$_3$H$_5$]$^+$ 70.0681 [M+H−CN$_3$H$_5$−HCOOH]$^+$, 60.0594	156.0767 [M−H−NH$_3$]$^−$, 131.0827 [M−H−C$_3$H$_6$]$^−$	Arginine	TA/TO
3	5.74	$C_4H_8N_2O_3$	133.0606 (+0.3)		116.0336 [M+H−NH$_3$]$^+$, 87.0565 [M+H−HCOOH]$^+$, 74.0259 [M+H−C$_2$H$_5$NO]$^+$, 70.0312 [M+H−HCOOH−NH$_3$]$^+$		Asparagine	TA/TO
4	5.84	$C_4H_7NO_4$		132.0315 (+9.7)		115.0045 [M−H−NH$_3$]$^−$, 88.0413 [M−H−CO$_2$]$^−$, 71.0154 [M−H− CO$_2$−NH$_3$]$^−$	Aspartic acid	TA/TO
5	5.89	$C_5H_{13}NO$	104.1074 (+3.5)		60.0836 [M+H-C$_2$H$_4$O]$^+$, 58.0681 [M+H−H$_2$O−C$_2$H$_4$]$^+$		Choline	TA/TO
6	6.14	$C_6H_{13}N_3O_3$	176.1029 (−0.5)		159.0765 [M+H−NH$_3$]$^+$, 113.0709 [M+H−NH$_3$−HCOOH]$^+$, 70.0673 [M+H−NH$_3$−CO$_2$−CH$_3$NO]$^+$		Citrulline	TA/TO
7	6.21	$C_4H_9NO_2$	104.0709 (−0.1)		87.0457 [M+H−NH$_3$]$^+$, 69.0359 [M+H−NH$_3$−H$_2$O]$^+$, 60.0835 [M+H−CO$_2$]$^+$		γ-Aminobutyric acid	TA/TO
8	6.46	$C_{30}H_{52}O_{26}$		827.2671 (−0.3)		545.1759 [M−H−C$_{10}$H$_{18}$O$_9$]$^−$, 383.1197 [M−H−C$_{10}$H$_{18}$O$_9$−Glc]$^−$, 179.0539 [M−H−4Glc]$^−$	MDG−1	TO
9	6.51	$C_7H_7NO_2$	138.0550 (+0.7)		94.0662 [M+H−CO$_2$]$^+$, 92.0506 [M+H−HCOOH]$^+$, 78.0355 [M+H−CO$_2$−CH$_4$]$^+$, 65.0412 [M+H−CO$_2$−NCH$_3$]$^+$		Trigonelline	FL/RG
10	6.59	$C_5H_9NO_2$	116.0709 (+0.8)		70.0677 [M+H−HCOOH]$^+$, 68.0521		Proline	TA/TO
11	6.64	$C_{24}H_{42}O_{21}$		665.2142 (+0.9)		485.1530 [M−H−Glc−H$_2$O]$^−$, 383.1197 [M−H−Glc−C$_4$H$_8$O$_4$]$^−$, 341.1085 [M−H−2Glc]$^−$, 179.0558 [M−H−3Glc]$^−$,	Stachyose	TA/TO/RG
12	6.75	$C_{10}H_{17}N_3O_6$	276.1188 (−0.8)		147.0763 [M+H−C$_5$H$_7$NO$_3$]$^+$, 130.0497 [M+H−C$_5$H$_{10}$N$_2$O$_3$]$^+$		QGE dipeptide	TA/TO
13	6.82	$C_{12}H_{22}O_{11}$		341.1088 (+0.7)		179.0560 [M−H−Glc]$^−$, 161.0459 [M−H−Glc−H$_2$O]$^−$, 119.0346,89.0249	Sucrose/maltose	TA/TO
14	6.85	$C_{30}H_{52}O_{26}$		827.2671 (−0.3)		545.1759[M−H−Glc−C$_4$H$_8$O$_4$]$^−$, 383.1197 [M−H−2Glc−C$_4$H$_8$O$_4$]$^−$	Verbascose	TA/RS

(Continued)

TABLE 1 | Continued

No.	RT (min)	Formula	[M+H]+(Error, ppm)	[M–H]−(Error, ppm)	MS/MS fragments (Positive mode)	MS/MS fragments (Negative mode)	Identification	Plant material
15	6.91	$C_{18}H_{32}O_{16}$		503.1610 (+1.1)		383.1205 [M–H–$C_4H_8O_4$]−, 341.1092 [M–H–Glc]−, 221.0650 [M–H–Glc–$C_4H_8O_4$]−, 179.0558 [M–H–2Glc]−, 89.0250 [M–H–2Glc–$C_3H_6O_3$]−	Raffinose	TA/TO
16	7.13	$C_5H_5N_5$	136.0619 (+0.6)		119.0358 [M+H–NH_3]+, 92.0252 [M+H–NH_3–HCN]+, 65.0161 [M+H–CH_2N_2–CH_3N]+		Adenine	FL/RG/RS
17	10.21	$C_6H_5NO_2$	124.0396 (+0.6)		106.0289 [M+H–H_2O]+, 80.0514 [M+H–CO_2]+, 78.0357 [M+H–HCOOH]+,		Nicotinic acid	FL
18	10.61	$C_7H_4O_6$	185.0082 (+0.7)	182.9939 (+2.1)	141.0173 [M+H–CO_2]+, 97.0297 [M+H–2CO_2]+, 71.0152 [M+H–2CO_2–C_2H_2]+	139.0038 [M–H–CO_2]−, 68.9988 [M–H–$C_4H_2O_4$]−, 67.0207 [M–H–2CO_2–CO]−	Chelidonic acid	TA
19	10.86	$C_5H_{11}O_2NS$	150.0582 (−1.0)		133.0298 [M+H–NH_3]+, 104.0534 [M+H–HCOOH]+, 102.0549 [M+H–CH_4S]+, 61.0129 [M+H–$C_3H_9NO_2$]+, 56.0529 [M+H–CH_4S–HCOOH]+		Methionine	TA/TO
20	11.61	$C_5H_7NO_3$	130.0500 (+1.1)		84.0461 [M+H–HCOOH]+, 56.0531 [M+H–HCOOH–CO]+		Pyroglutamic acid	TA/FL/RG
21	12.16	$C_4H_4N_2O_2$	113.0348 (+1.8)		96.0090 [M+H–NH_3]+ 70.0309 [M+H-CHNO]+		Uracil	FL/RG
22	12.81	$C_{10}H_{13}N_5O_4$	268.1043 (+1.0)		136.0620 [M+H–Rib]+, 119.0357 [M+H– Rib–NH_3]+		Adenosine	RS
23	12.95	$C_9H_{11}NO_3$	182.0811 (−0.2)		165.0543 [M+H–NH_3]+, 147.0435 [M+H–NH_3–H_2O]+, 136.0755 [M+H–HCOOH]+, 119.0490 [M+H–HCOOH–NH_3]+, 91.0553 [M+H–HCOOH–NH_3–CO]+, 77.0403,65.04111		Tyrosine	TA/TO
24	13.37	$C_{10}H_{13}N_5O_5$	284.0992 (+0.9)		152.0569 [M+H–Rib]+, 135.0298 [M+H– Rib–NH_3]+		Guanosine	RS
25	16.27	$C_{15}H_{24}O_{10}$		363.1291 (+0.9)		201.0759 [M–H–Glc]−, 183.0656 [M–H–Glc–H_2O]−, 165.0549 [M–H–Glc–2H_2O]−, 139.0388 [M–H–Glc–2H_2O–C_2H_2]−,	Harpagide	RS
26	17.03	$C_9H_{11}NO_2$	166.0864 (+0.9)	164.0725 (+4.6)	120.0816 [M+H–HCOOH]+, 103.0554 [M+H–HCOOH–NH_3]+	147.0445 [M–H–NH_3]−, 103.0555 [M–H–NH_3–CO_2]−, 72.0096	Phenylalanine	TA/TO/RS
27	19.16	$C_8H_8O_4$		167.0361 (+1.2)		123.0445 [M–H–CO_2]−, 93.0351 [M–H–CO_2–OCH_2]−	Vanillic acid	TO/RG
28	21.83	$C_{16}H_{18}O_9$	355.1025 (+0.3)	353.0877 (−0.2)	163.0396 [M+H–$C_7H_{12}O_6$]+, 145.0288 [M+H–$C_7H_{12}O_6$–H2O]+, 117.0342 [M+H–$C_7H_{12}O_6$–H_2O–CO]+, 89.0402 [M+H–$C_7H_{12}O_6$–H_2O–2CO]+	191.0557 [M–H–$C_9H_6O_3$]−, 179.0344 [M–H–$C_7H_{10}O_5$]−, 135.0450 [M–H–$C_7H_{10}O_5$–CO_2]−	Neochlorogenic acid	FL

(Continued)

TABLE 1 | Continued

No.	RT (min)	Formula	[M+H]⁺(Error, ppm)	[M–H]⁻(Error, ppm)	MS/MS fragments (Positive mode)	MS/MS fragments (Negative mode)	Identification	Plant material
29	22.40	$C_7H_6O_4$	155.0339 (0)	153.0195 (+0.9)	137.0242 $[M+H–H_2O]^+$, 109.0279 $[M+H–H_2O–CO]^+$, 93.0352 $[M+H–H_2O–CO_2]^+$, 81.0324 $[M+H–H_2O–2CO]^+$, 65.0413 $[M+H–H_2O–CO_2–CO]^+$	109.0280 $[M–H–CO_2]^-$, 91.0178 $[M–H–CO_2–H_2O]^-$	Protocatechuic acid	FL
30	22.76	$C_{21}H_{28}O_{13}$	511.1404 (−3.5)	487.1444 (−2.8)	365.0824 $[M+Na–Rha]^+$	179.0338 $[M–H–Rha–Caffeoyl]^-$, 161.0224 $[M–H–Caffeoyl–Rha–H_2O]^-$ 135.0440 $[Caffeic acid–CO_2]^-$	Cistanoside F	RS
31	24.81	$C_7H_8O_3$	141.0547 (0.2)		126.0309 $[M+H–CH_3]^+$, 97.0304 $[M+H–CH_4–CO]^+$, 81.0682 $[M+H–CH_4O–CO]^+$, 71.0144, 55.0230		5-Methoxymethyl furfural	TA
32	28.13	$C_{16}H_{18}O_9$	355.1026 (+0.6)	353.0870 (−1.3)	163.0394 $[M+H–C_7H_{12}O_6]^+$, 145.0290 $[M+H–C_7H_{12}O_6–H_2O]^+$, 117.0344 $[M+H–C_7H_{12}O_6–H_2O–CO]^+$, 89.0405 $[M+H–C_7H_{12}O_6–H_2O–2CO]^+$	191.0549 $[M–H–C_9H_6O_3]^-$	Chlorogenic acid	FL
33	29.64	$C_{16}H_{18}O_9$	355.1027 (+0.9)	353.0869 (−0.5)	163.0390 $[M+H–C_7H_{12}O_6]^+$, 145.0284 $[M+H–C_7H_{12}O_6–H_2O]^+$, 117.0338 $[M+H–C_7H_{12}O_6–H_2O–CO]^+$	191.0548 $[M–H–C_9H_6O_3]^-$, 173.0442 $[M–H–C_9H_6O_3–H_2O]^-$, 135.0441 $[M–H–C_7H_{10}O_5–CO_2]^-$, 93.0345	Cryptochlorogenic acid	FL
34	33.42	$C_8H_8O_3$	153.0546 (−0.2)	151.0409 (3.1)	135.1159 $[M+H–H_2O]^+$, 107.0866 $[M+H–H_2O–CO]^+$, 77.0399 $[M+H–2CH_2O]^+$	136.0169 $[M–H–CH_3]^-$, 108.0210 $[M–H–CH_3–CO]^-$	Vanillin	RG/TO
35	34.92	$C_9H_8O_4$	181.0409 (−0.7)	179.0354 (+2.5)	163.0387 $[M+H–H_2O]^+$, 135.0439 $[M+H–HCOOH]^+$, 89.398 $[M+H–H_2O–CO–HCOOH]^+$	135.0446 $[M–H–CO_2]^-$	Caffeic acid	FL
36	36.14	$C_{16}H_{18}O_8$		337.0926 (−0.9)		191.0556 $[M–H–C_9H_6O_2]^-$, 173.0437 $[M–H–C_9H_6O_2–H_2O]^-$, 93.0347 $[M–H–C_{10}H_{12}O_7]^-$	5-(p-Coumaroyl) quinic acid	FL
37	39.11	$C_9H_8O_3$	165.0545 (−0.9)		121.0286 $[M+H–CO_2]^+$, 77.0405 $[M+H–H_2O–C_3H_2O_2]^+$,		p-coumaric acid	FL
38	39.15	$C_{17}H_{20}O_9$		367.1014 (−3.8)		191.0552 $[M–H–C_7H_{12}O_5]^-$, 173.0446 $[M–H–C_7H_{12}O_5–H_2O]^-$, 93.0340 $[M–H–C_{11}H_{14}O_7–H_2O]^-$	3-O-Caffeoylquinic acid methyl ester	FL
39	43.08	$C_{27}H_{32}O_{14}$	581.1847 (−1.5)	579.1703 (−1.0)	419.1332 $[M+H–Glc]^+$, 257.0802 $[M+H–2Glc]^+$, 239.0745 $[M+H–2Glc–H_2O]^+$	417.1207 $[M–H–Glc]^-$, 297.0661 $[M–H–C_{14}H_{18}O_6]^-$, 255.0647 $[M–H–2Glc]^-$, 135.0066 $[M–H–2Glc–RDA]^-$	Liquiritigenin 7,4'-diglucoside	RG
40	45.99	$C_{27}H_{30}O_{16}$	611.1601 (−1.4)	609.1447 (−1.9)	465.1076 $[M+H–Rha]^+$, 303.0502 $[M+H–Glc–Rha]^+$, 287.0603,229.0507,85.0248	300.0258 $[M–H–Glc–Rha]^-$, 271.0244 $[M–H–Glc–Rha–CH_2O]^-$	Rutin	FL
41	47.09	$C_{26}H_{30}O_{13}$	551.1742 (−1.0)	549.1610 (−0.7)	419.1273 $[M+H–Api]^+$, 257.0794 $[M+H–Api–Glc]^+$, 145.0480, 137.0230 $[M–H–C_{19}H_{26}O_{10}]^-$	255.0659 $[M–H–Api–Glc]^-$, 135.0084 $[M–H–C_{19}H_{26}O_{10}]^-$	Liquiritin apioside	RG

(Continued)

TABLE 1 | Continued

No.	RT (min)	Formula	[M+H]⁺(Error, ppm)	[M–H]⁻(Error, ppm)	MS/MS fragments (Positive mode)	MS/MS fragments (Negative mode)	Identification	Plant material
42	48.23	$C_{27}H_{30}O_{15}$	595.1643 (–0.7)	593.1491 (–3.4)	287.0541 [M+H–Rut]⁺	285.0388 [M–H–Rut]⁻	Kaempferol-3-O-rutinoside	FL
43	48.33	$C_{29}H_{36}O_{15}$		623.1976 (–0.9)		461.1678 [M–H–O–Rha]⁻, 161.0235 [M–H– Rha–$C_8H_9O_2$–$C_9H_7O_4$]⁻, 133.0289 [M–H– Rha–$C_8H_9O_2$–$C_9H_7O_4$– CO]⁻	Acteoside	RS
44	48.41	$C_{21}H_{22}O_9$	419.1334 (–0.7)	417.1189 (–0.6)	257.0803 [M+H–Glc]⁺, 137.0224 [M+H–$C_{14}H_{18}O_6$]⁺	255.0645 [M–H–Glc]⁻, 135.0073 [M–H–Glc–RAD]⁻, 119.0489	Liquiritin	RG
45	49.18	$C_{21}H_{20}O_{12}$	465.1027 (–0.1)	463.0876 (–1.2)	303.0489 [M+H–Glc]⁺	301.0351 [M–H–Glc]⁻, 271.0240 [M–Glc–CH_2O]⁻, 255.0285 [M–H–Glc–O–CH_2O]⁻, 151.0016 [M–H–Glc–RDA]⁻	Isoquercitrin	RG
46	49.25	$C_{21}H_{20}O_{11}$	449.1077 (–0.3)	447.0917 (–2.3)	287.0554 [M+H–Glc]⁺	285.0404 [M–H–Glc]⁻	Luteolin-7-O-glucoside	FL/RG
47	52.22	$C_{29}H_{36}O_{15}$		623.1975 (–1.0)		461.1675 [M–H–O–Rha]⁻, 161.0238 [M–H–$C_{20}H_{28}O_{11}$–H_2O]⁻, 135.0440 [M–H–$C_{20}H_{28}O_{11}$–H_2O–C_2H_2]⁻	Isoacteoside	RS
48	53.10	$C_{25}H_{24}O_{12}$	517.1335 (–1.0)	515.1188 (–1.3)	499.1231 [M+H–H_2O]⁺, 163.0389 [M+H–$C_6H_{18}O_9$]⁺ 145.0286 [M+H–$C_6H_{18}O_9$–H_2O]⁺	353.0861 [M–H–$C_9H_6O_3$]⁻, 191.0546 [M–H–$2C_9H_6O_3$]⁻, 173.0439 [M–H–$2C_9H_6O_3$–H_2O]⁻,	3,4-Dicaffeoylquinic acid	FL
49	55.23	$C_{21}H_{20}O_{11}$	449.1077 (–0.3)	447.0919 (–3.2)	287.0552 [M+H–Glc]⁺	285.0387[M–H–Glc]⁻, 255.0284 [M–H–Glc–CH_2O]⁻, 227.0327 [M–H–Glc–CH_2O–CO]⁻	Quercitrin	FL
50	55.74	$C_{25}H_{24}O_{12}$	517.1325 (–0.6)	515.1177 (–2.1)	499.1229 [M+H–H_2O]⁺, 163.0390 [M+H–$C_6H_{18}O_9$]⁺, 145.0280 [M+H–$C_6H_{18}O_9$–H_2O]⁺	353.0867 [M–H–$C_9H_6O_3$]⁻, 191.0547 [M–H–$2C_9H_6O_3$]⁻, 173.0336 [M–H–$2C_9H_6O_3$–H_2O]⁻,	3,5-Dicaffeoylquinic acid	FL
51	56.82	$C_{36}H_{48}O_{19}$	807.2675 (–0.9)	783.2723 (+0.7)	807.2675 [M+Na]⁺	607.2276 [M–H–$C_6H_{11}O_4$–CHO]⁻, 193.0492 [M–H–$C_{26}H_{38}O_{15}$]⁻, 175.0383 [M–H–$C_{26}H_{38}O_{15}$–H_2O]⁻	Angoroside C	RS
52	56.98	$C_{21}H_{20}O_{10}$	433.1127 (–0.5)	431.0965 (–4.4)	271.0614 [M+H–Glc]⁺	269.0446 [M–H–Glc]⁻,	Afzelin	RG/FL
53	58.88	$C_{25}H_{24}O_{12}$	517.1336 (–0.8)	515.1181 (–0.9)	499.1240 [M+H–H_2O]⁺, 163.0397 [M+H–$C_{16}H_{18}O_9$]⁺, 145.0289 [M+H–$C_{16}H_{18}O_9$–H_2O]⁺	353.0853 [M–H–$C_9H_6O_3$]⁻, 191.0541 [M–H–$2C_9H_6O_3$]⁻, 173.0435 [M–H–$2C_9H_6O_3$–H_2O]⁻,	4,5-Dicaffeoylquinic acid	FL
54	62.84	$C_{26}H_{30}O_{13}$	551.1762 (+0.5)	549.1595 (–3.3)	419.1367 [M+H–Api]⁺, 257.0813 [M+H–Api–Glc]⁺, 239.0680 [M+H– Api–Glc–H_2O]⁺, 269.0809 [M+H–Glc]⁺	255.0649 [M–H–Api–Glc]⁻, 135.0074 [M–H–Api–Glc–C_6H_4–CO]⁻	Isoliquiritin apioside	RG
55	66.06	$C_{22}H_{22}O_9$	431.1335 (–0.4)	475.1224 (–1.3)		267.0639 [M–H–Glc]⁻, 252.0403 [M–H–Glc–CH_3]⁻	Ononin	RG
56	66.21	$C_{21}H_{22}O_9$	419.1334 (–0.7)	417.1179 (–2.9)	257.0812 [M+H–Glc]⁺, 137.0224 [M+H–Glc–C_8H_6O]⁺	255.0648 [M–H–Glc]⁻, 148.0150,135.0077, 119.0489 [M–H–Glc–C_8H_6O–H_2O]⁻, 92.0260 [M–H–Glc–$C_9H_7O_3$]⁻	Isoliquiritoside	RG
57	73.66	$C_{24}H_{30}O_{11}$	517.1675 (–1.0)	493.1679 (–1.8)	369.1170,203.0533	345.1161 [M–H–$C_9H_7O_2$]⁻, 147.0434 [M–H–$C_{15}H_{22}O_9$]⁻, 165.0535,103.0544	Harpagoside	RS

(Continued)

TABLE 1 | Continued

No.	RT (min)	Formula	[M+H]$^+$(Error, ppm)	[M–H]$^-$(Error, ppm)	MS/MS fragments (Positive mode)	MS/MS fragments (Negative mode)	Identification	Plant material
58	73.68	$C_9H_8O_2$	149.0598 (–0.6)		121.0650 [M+H–CO] $^-$, 93.0713 [M+H–2CO] $^-$		Dihydrocoumarin	RG
59	73.75	$C_{25}H_{32}O_{13}$		539.1745 (+1.0)		493.1679 [M–H–HCOOH]$^-$, 345.1169 [M–H–$C_{10}H_{10}O_4$]$^-$, 147.0429	8-O-Feruloylharpagide	RS
60	74.42	$C_{15}H_{12}O_4$	257.0810 (–2.3)	255.0658 (–3.9)	239.0675 [M+H–H_2O]$^+$, 211.0752 [M+H–H_2O–CO]$^+$, 147.0440 [M+H–$C_6H_6O_2$]$^+$, 137.0232 [M+H–C_8H_8O]$^+$	135.0081 [M–H–C_8H_8O]$^-$, 119.0500 [M–H–$C_7H_4O_3$]$^-$	Liquiritigenin	RG
61	75.02	$C_{65}H_{106}O_{32}$		1397.6516 (–1.1)		1073.5549 [M–H–2Glc]$^-$, 744.3308	Macranthoidin B	FL
62	76.60	$C_{15}H_{10}O_6$	287.0552 (–0.5)	285.0393 (–2.1)	153.0169 [M+H–$C_8H_6O_2$]$^+$	175.0389 [M–H–$C_6H_6O_2$]$^-$, 133.0289 [M–H–$C_7H_4O_4$]$^-$	Luteolin	TO/FL
63	77.19	$C_{47}H_{76}O_{17}$	913.5130 (+0.8)		781.4760 [M-Ara]$^+$, 751.4601 [M+H–Glc]$^+$, 455.3512 [M+H– Ara–Rha–Glc]$^+$, 437.3398 [M+H–Ara–Rha–Glc–H_2O]$^+$,		Macranthoside A	FL
64	77.23	$C_{59}H_{96}O_{27}$		1235.5997 (–1.9)		911.5033 [M–H–2Glc]$^-$	Macranthoidin A	FL
65	77.24	$C_{47}H_{76}O_{17}$		911.4993 (–2.3)		749.4506 [M–H–Glc]$^-$, 603.3903 [M–H–Glc–Rha]$^-$	3-O-α-L-arabinopyranosyl (2→1)-O-α-L-rhamnopyranosyl-hederagenin-28-O-β-D-glucopyranosyl ester	FL
66	77.79	$C_{15}H_{10}O_7$		301.0341 (–1.9)		178.9966 [M–H–$C_7H_6O_2$]$^-$, 151.0020 [M–H–$C_8H_6O_3$]$^-$	Quercetin	RG
67	79.70	$C_{53}H_{86}O_{22}$		1073.5496 (–4.1)		749.4489 [M–H–2Glc]$^-$, 323.0972[Mal]	Dipsacoside B	FL
68	81.62	$C_{47}H_{76}O_{18}$		927.4934 (–2.0)		603.3911 [M–H–2Glc]$^-$	Akebia saponin D	FL
69	89.34	$C_{17}H_{14}O_7$	331.0811 (–0.3)	329.0648 (–3.3)	315.0507 [M+H–OH]$^+$, 316.0569 [M+H–CH_3]$^+$, 203.0333 [M+H–$C_6H_8O_3$]$^+$, 153.0168 [M+H–$C_{10}H_{10}O_3$]$^+$	299.0171 [M–H–CHO]$^-$, 271.0235 [M–H–CHO–CO]$^-$, 243.0300 [M–H–CHO–2CO]$^-$, 203.0353,161.0214	Tricin	FL
70	90.34	$C_{53}H_{86}O_{22}$		1073.5437 (-6.4)		911.4934 [M–H–Glc]$^-$	Macranthoside B	FL
71	90.99	$C_{16}H_{12}O_6$	301.0706 (+0.7)	299.0544 (–3.7)	286.0473 [M+H–CH_3]$^+$, 258.0511 [M+H–CH_3–CO]$^+$, 119.0487,153.0189	284.0292 [M–H–CH_3]$^-$, 256.0335 [M–H–CH_3–CO]$^-$, 227.0349 [M–H–CH_3–CO–CHO]$^-$	Diosmetin	FL
72	95.18	$C_{42}H_{68}O_{14}$		795.4455 (–3.3)		471.3444 [M–H–2Glc]$^-$, 323.0961	Dipsacussaponin A	FL
73	96.33	$C_{16}H_{12}O_6$	301.0707 (+0.8)	299.0536 (–0.9)	286.0467 [M+H–CH_3]$^+$, 285.0388 [M+H–OH]$^+$, 258.0529 [M+H–CH_3–CO]$^+$, 121.0276 [M+H–$C_7H_8O_2$–CO–CO]$^+$	284.0294 [M–H–CH_3]$^-$, 255.0282 [M–H–CH_3–CHO]$^-$, 227.0333 [M–H–CH_3–CHO–CO]$^-$	Chrysoeriol	FL
74	100.92	$C_{42}H_{62}O_{16}$	823.4098 (–1.1)		471.3453 [M+H–$2C_6H_8O_6$]$^+$, 453.3362 [M+H–$2C_6H_8O_6$–H_2O]$^+$,	351.0554 [M–H–$C_{28}H_{42}O_3$–CO_2]$^-$	Glycyrrhizic acid	RG

(Continued)

TABLE 1 | Continued

No.	RT (min)	Formula	[M+H]+(Error, ppm)	[M-H]-(Error, ppm)	MS/MS fragments (Positive mode)	MS/MS fragments (Negative mode)	Identification	Plant material
75	101.48	$C_{15}H_{12}O_4$	257.0806 (0.7)	255.0646 (−0.8)	239.0696 $[M+H-H_2O]^+$, 137.0232 $[M+H-C_8H_8O]^+$, 119.0500, 81.0353	135.0074 $[M-H-C_8H_8O]^-$, 119.0492 $[M-H-C_7H_4O_3]^-$, 91.0183 $[M-H-C_7H_4O_3-CO]^-$,	Isoliquiritigenin	RG
76	102.69	$C_{16}H_{12}O_4$	269.0809 (+0.3)	267.0645 (+0.7)	253.0491 $[M+H-CH_3]^+$, 197.0598 $[M-CH_3 -CO-CO]^+$, 181.0641 $[M-OCH_3 -CO-CO]^+$	252.0404 $[M-H-CH_3]^-$, 223.0373 $[M-H-CH_3-CHO]^-$, 195.0418 $[M-H-CH_3-CHO-CO]^-$, 132.0190 $[M-H-C_7H_7O- CO]^-$,	Formononetin	RG
77	104.50	$C_{21}H_{20}O_6$	369.1335 (+0.6)		313.0705 $[M+H-2CO]^+$, 271.0607 $[M+H-CO-CO-C2H2O]^+$, 211.0391, 215.0698 $[M+H-C_6H_6O_2-CO_2]^+$	91.0175 $[M-H-C_9H_8O- CO-OH]^-$	Glycycoumarin	RG
78	106.36	$C_{41}H_{66}O_{12}$		749.4381 (−0.2)		603.3814 $[M-H-Rha]^-$	Sapindoside A	FL
79	107.93	$C_{21}H_{22}O_4$		337.1413 (−3.6)		305.1168 $[M-H-CH_2O]^-$	4'-O-methylglabridin	RG

The losses are Glc, glucose moiety; Rha, rhamnose moiety; Ara, arabinose moiety; Api, apiose moiety; Rib, ribose moiety; Mal, maltose.

TABLE 2 | Regression equation of UHPLC-TOF-MS method for the quantification analysis.

Name	Regression equation	R²	Linear range (µg/ml)
Chlorogenic acid	y = 461220x + 170230	0.9985	0.44~43.76
Luteolin-7-O-glucoside	y= 1651116 x + 169046	0.9987	0.10~5.05
Arginine	y = 803438x + 245940	0.9955	0.11~11.05
Harpagoside	y = 715849x − 42021	0.9999	0.08~8.48
Liquiritin	y = 1392671 x + 590609	0.9920	0.11~11.45
Glycyrrhizic acid	y = 1459525 x + 456361	0.9912	0.20~10.09

TABLE 3 | The quantification results of six components in KYQG.

Name	Peak area	Dilution ratio	Contents (mg/g)
Chlorogenic acid	1.18E+06	10000	2.82
Luteolin-7-O-glucoside	2.30E+06	30	0.06
Arginine	4.22E+05	30	0.01
Harpagoside	4.67E+06	30	0.31
Liquiritin	4.97E+06	100	0.43
Glycyrrhizic acid	6.69E+06	100	0.64

DISCUSSION

In this study, we have combined data obtained by different experimental methods, and explored the associations between oral ulcer progression, metabolomics, inflammation, oxidative stress, neurotransmitter levels, and HPA activity in a rat model of oral ulcers.

We examined the effects of KYQG on the levels of inflammatory cytokines in our oral ulcer rat model. Our results demonstrated that KYQG could inhibit the increased levels of IL-1, IL-18, IL-6, and MCP-1 levels in serum. Notably, the expression of IL-6 in epithelial tissue sections was ameliorated by KYQG treatment. Excessive production of IL-6, IL-1β, and TNF-α is known to be associated with an increased risk of developing RAS (Bazrafshani et al., 2002; Guimaraes et al., 2007; Scully and Porter, 2008). Therefore, the inhibitory effects of KYQG on the production of inflammatory cytokines may account for its anti-oral ulcer activity.

Our data also showed that KYQG treatment inhibited the excessive release of ACTH and CORT when compared with the Model group. It has been shown that sleep deprivation can activate the HPA axis (Ganz, 2012; Opp and Krueger, 2015). However, the direct links between the HPA axis and oral ulcers are poorly understood, and further studies are required to elucidate whether the KYQG-mediated regulation of the HPA axis contributes to its anti-ulcer activity.

Our data suggested that KYQG could downregulate the levels of 5-HT and GABA in serum but could only decrease the 5-HT level in the brain. 5-HT, an important pronociceptive mediator, can induce inflammation and hyperalgesia or allodynia (Oliveira et al., 2007). Neurotransmitter levels are correlated with detrimental psychological factors, including depression and stress, and depression is one of the psychological factors with a role in the etiopathogenesis of oral ulcers (Alshahrani, 2014). This suggests that regulation of neurotransmitter levels by KYQG may contribute to its treatment effects. Furthermore,
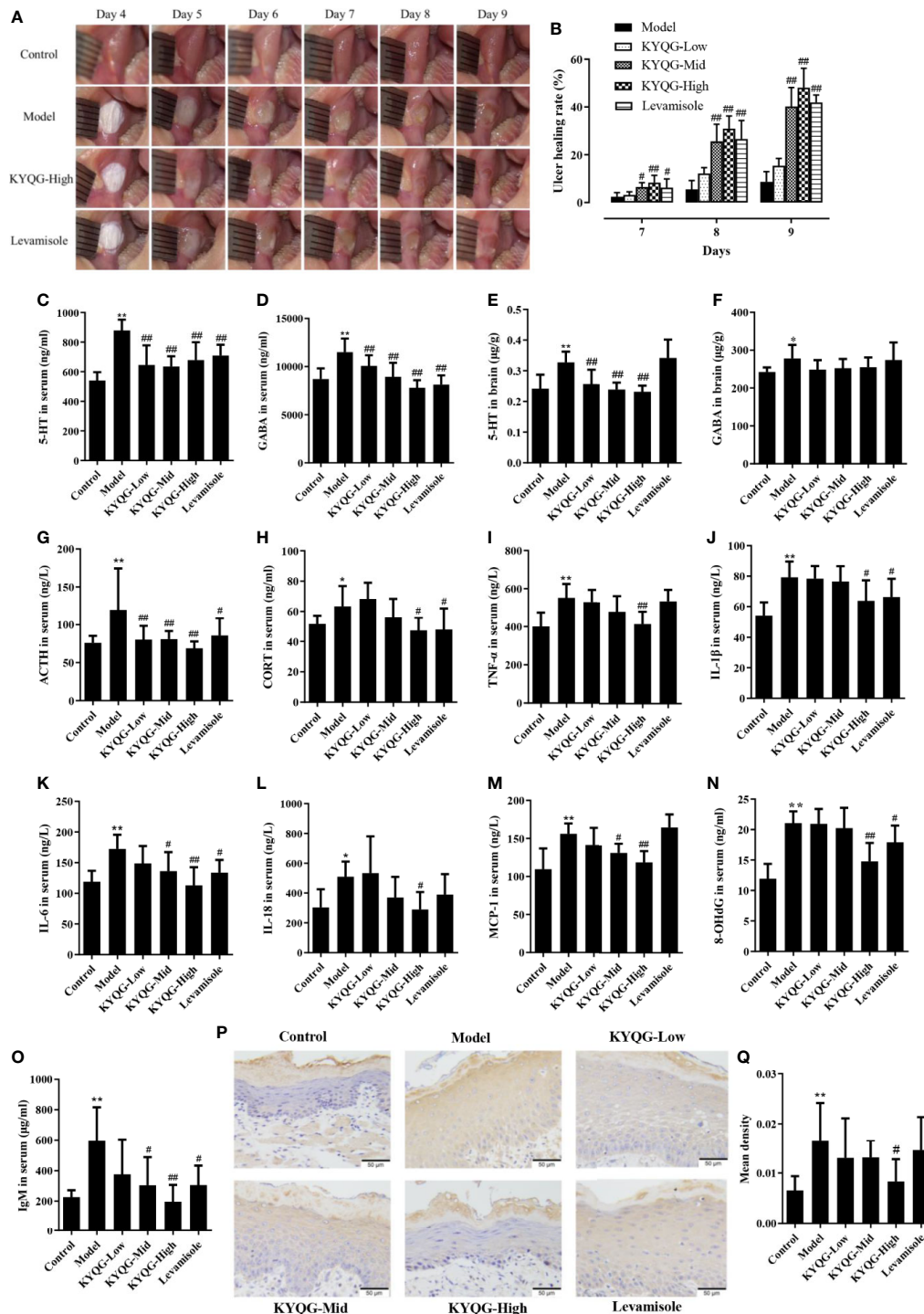
FIGURE 2 | Results of the effect of Kouyanqing Granule (KYQG) in the treatment of phenol-induced oral ulcer worsened by sleep deprivation. Representative images of oral ulcers **(A)**; Effects of KYQG on the ulcer healing rate **(B)**, ulcer healing rate = $[(A_6 - A_t)/A_6] \times 100\%$, where A_6 represents the initial ulcer area on day 6, and A_t represents the ulcer area on days 7–9. Effects of KYQG on 5-hydroxytryptamine (5-HT) and γ-aminobutyric acid (GABA) levels in serum **(C, D)** and brain tissue **(E, F)**. Effects of KYQG on the serum levels of adrenocorticotropin hormone (ACTH) **(G)** and corticosterone (CORT) **(H)**. Effects of KYQG on the levels of inflammatory cytokines **(I–M)**, 8-hydroxy-2'-deoxyguanosine (8-OHdG) **(N)**, and immunoglobulin M (IgM) **(O)**. Interleukin (IL)-6 protein expression in epithelial tissue sections of buccal mucosa by immunohistochemistry in Control group, Model group, Kouyanqing Granule (KYQG)-Low group, KYQG-Mid group, KYQG-High group, and Levamisole group **(P)**. Quantification of IL-6 expression in epithelial tissue section of buccal mucosa **(Q)**. Data are expressed as means ± SD. $*P < 0.05$, $**P < 0.01$ compared with the Control group; $^{\#}P < 0.05$, $^{\#\#}P < 0.01$ compared with the Model group.

FIGURE 3 | Continued

this result is consistent with the results of our serum metabolic analysis.

Metabolic analysis indicated that tryptophan, kynurenine, and indole lactic acid, metabolites involved in tryptophan metabolism, were highly induced in the Model group, and decreased after KYQG treatment. There are two main pathways for tryptophan metabolism, resulting in two different metabolites – 5-HT and kynurenine (Agus et al., 2018). The results of this preliminary study suggested that breakdown of tryptophan metabolism was involved in the pathogenesis of oral ulcers *via* both pathways. It is known that tryptophan metabolites, as aryl hydrocarbon receptor ligands, play important roles in the regulation of immune responses (Hubbard et al., 2015). In the present study, KYQG treatment also downregulated serum IgM levels. Neurotransmitters can also serve as immunomodulators (Pacheco et al., 2010). Numerous studies have confirmed the crucial role of immune responses in the pathogenesis of oral ulcers (Slebioda et al., 2014; Johnson et al., 2017). Tryptophan metabolism, oxidative stress, and inflammation have also been associated with various conditions, including neurological disorders and inflammatory bowel disease (Roager and Licht, 2018). Li et al. compared the salivary nontargeted metabolite profiles between healthy individuals and RAS patients and found that dysregulation of tryptophan metabolism was involved in the pathogenesis of this condition (Li Y. T. et al., 2018). A previous study reported that the tryptophan metabolism enzyme, L-kynureninase, is highly expressed in patients with chronic inflammatory skin disease (Harden et al., 2016). In summary, tryptophan metabolism plays a crucial role in the etiopathogenesis and therapeutics of oral ulcers, probably through the regulation of immune responses, inflammation, and oxidative stress; however, the exact mechanism through which tryptophan metabolism regulates the development of oral ulcers remains unknown and requires further study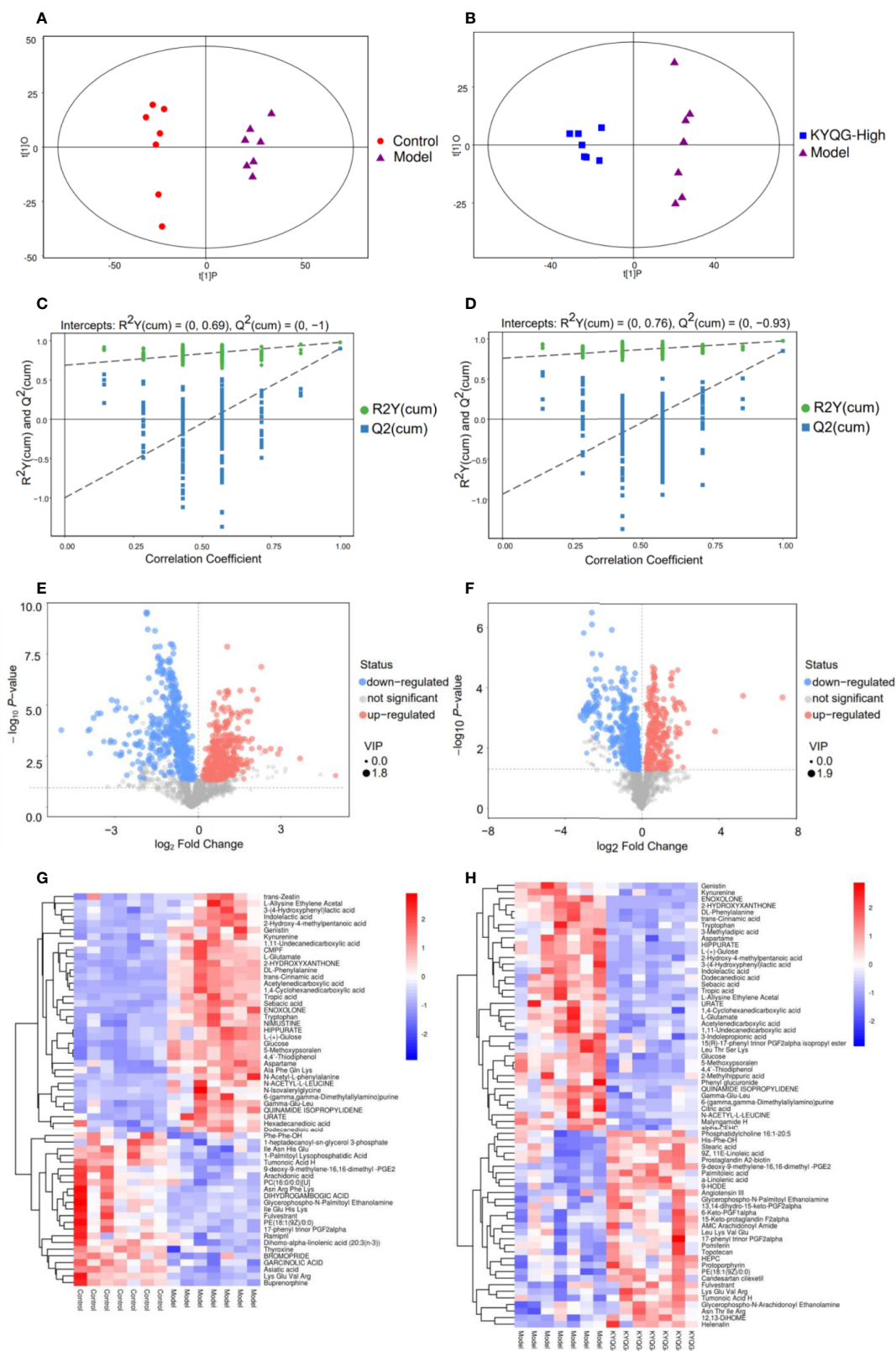. According to the results of the metabolic pathway analysis, the level of D-glucose, a metabolite of energy metabolism, was higher in the Model group than in the Control group, but the levels were restored by KYQG treatment. Sleep deprivation has been reported to affect glucose metabolism (Knutson et al., 2007). However, the relationship between energy metabolism and oral ulcers is unclear, and whether KYQG-mediated regulation of energy metabolism contributes to its anti-oral ulcer effects requires further investigation. L-Glutamic acid is involved in four metabolic pathways, namely, those of D-glutamine and D-glutamate metabolism, alanine, aspartate and glutamate metabolism, glutathione metabolism, and arginine and proline metabolism. Increases in the levels of glutamic acid have been reported to reduce GSH levels and eventually stimulate ROS release

in Riluzole-treated cells (Seol et al., 2016). In addition, the serum level of 8-OHdG was increased in rats of the Model group and decreased by KYQG treatment. Combined, these results indirectly suggest that KYQG reduces oxidative stress in the treatment of oral ulcers. A previous study reported that arginine and proline metabolism was the characteristic metabolic signature of dental plaque in patients with periodontal inflammation, which may be related to the metabolic profiles of disease-associated communities (Sakanaka et al., 2017). In addition, it has been suggested that an increase in the serum levels of uric acid represents an inflammatory response associated with obesity, metabolic syndrome, dysglycemic conditions, diabetes mellitus, hypertension, endothelial dysfunction, cardiovascular disease, and chronic kidney disease (Spiga et al., 2017). These results showed that comprehensive metabolomic profiling can provide further insights into the molecular mechanisms underlying the beneficial effects of KYQG on the symptoms of oral ulcers. Notably, the modulation of tryptophan metabolism by KYQG may be important for the treatment of oral ulcers. All the above changes suggest that KYQG may affect multiple aspects of the neuroimmunoendocrine system, which correlate with improved oral ulcer symptoms.

Our phytochemical analysis indicated that the main constituents of KYQG were phenolics, flavonoids, and triterpenoid saponins. The KYQG phenolics, such as neochlorogenic acid (Kim et al., 2015), chlorogenic acid (Naveed et al., 2018), cryptochlorogenic acid (Villalva et al., 2018), 3,4-dicaffeoylquinic acid (Wan et al., 2019), and 3,5-dicaffeoylquinic acid (Hong et al., 2015), reportedly exhibit antioxidant and anti-inflammatory activities. Isoquercitrin, a bioactive flavonoid in KYQG, possesses a variety of biological properties, including antioxidant (Li et al., 2016), anti-inflammatory (Rogerio et al., 2007), anti-ulcer, and hepatoprotective (Xie et al., 2016) effects. Luteolin-7-O-glucoside, another flavonoid constituent of KYQG, exhibits antioxidative activity through the regulation of the HO-1 signaling cascade in RAW 264.7 cells (Song and Park, 2014). Liquiritigenin has been reported to exert anti-inflammatory, antioxidant, antidiabetic, and antitumor activities (Lee et al., 2018). Liquiritin could protect against UVB–induced skin injury by inhibiting TLR4/MyD88/NF−κB mitogen−activated protein kinases and caspase pathways, which lead to alleviating the inflammatory response, oxidative stress, and apoptosis in mice and cells (Li X.-Q. et al., 2018).

Triterpenoid saponins such as glycyrrhizic acid, dipsacussaponin A, and akebia saponin D are also active constituents of KYQG. Glycyrrhizic acid reportedly inhibits inflammation by activating the glucocorticoid receptor and the PI3K/AKT/GSK3β signaling pathway (Kao et al., 2010), and it acts as a neuroprotectant in the postischemic brain by inhibiting HMGB1 phosphorylation and
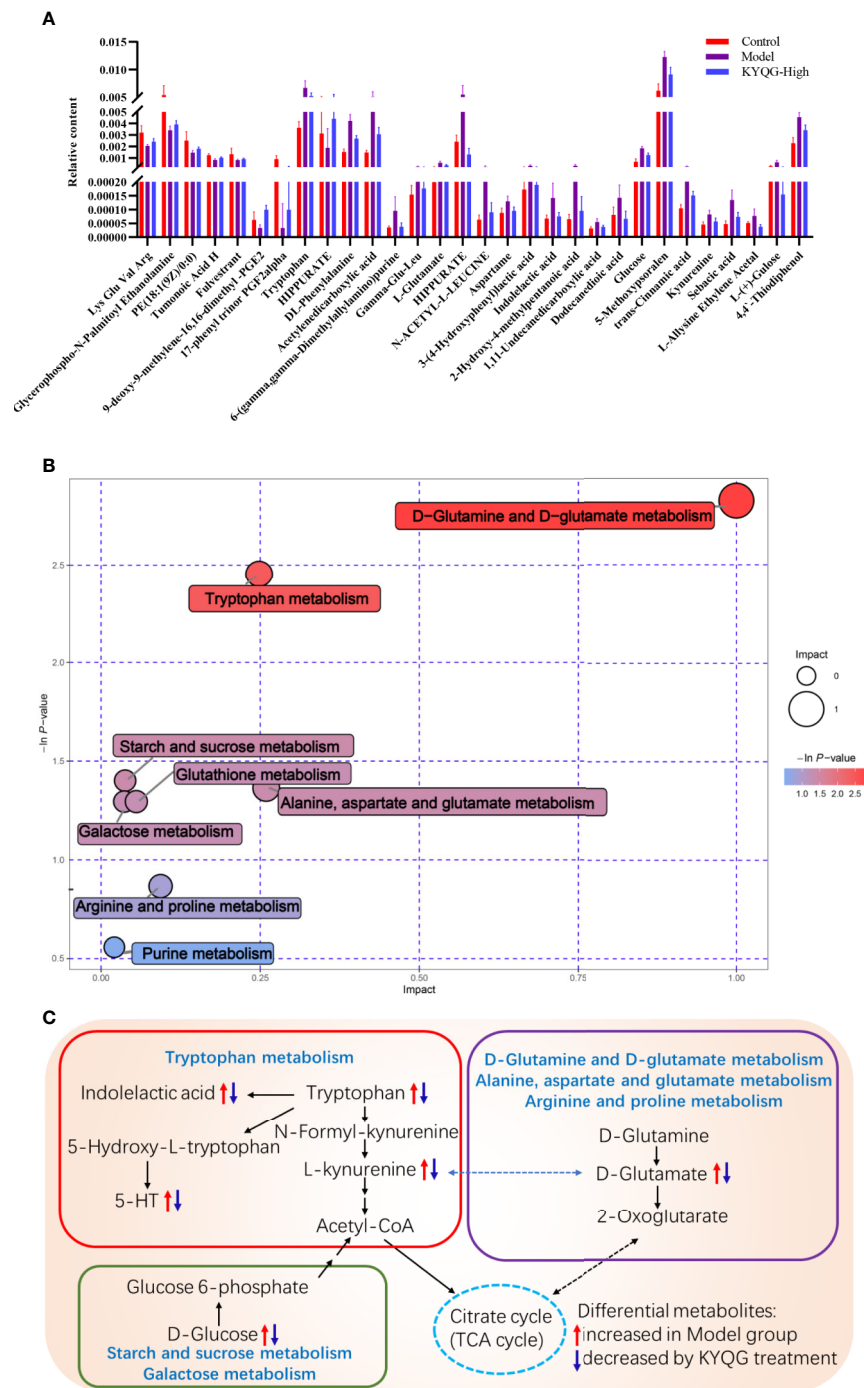
FIGURE 4 | The relative levels of 30 regulated serum metabolites in rats after Kouyanqing Granule (KYQG) treatment **(A)**. Metabolic pathway analysis results based on the 30 regulated serum metabolites after Kouyanqing Granule (KYQG) treatment **(B)**. Summaries of metabolic pathways **(C)**.

secretion (Kim et al., 2012). A different study reported that dipsacussaponin A inhibits TNF-α-induced NF-kB transcriptional activity in HepG2 cells (Quang et al., 2011). Akebia saponin D has been shown to inhibit amyloid beta-induced inflammatory responses and cognitive deficits in rats (Yu et al., 2012), and suppress corticosterone overproduction in

an Alzheimer's disease model (Wang et al., 2018). Amino acids such as lysine, tyrosine, and arginine potentially regulate immune function and promote wound healing (Li et al., 2007; Rahayu et al., 2016). Lysine has been reported to treat RAS (Singh et al., 2011), while arginine supplementation significantly improved the rate of healing of pressure ulcers (Desneves et al.,

2005). Tyrosine could reportedly inhibit gelatin-induced inflammation (Meyers et al., 1979). It has shown that harpagoside and harpagide have an inhibitory effect on IFNγ/LPS-induced secretion of TNFα in differentiated THP-1 cells (Schopohl et al., 2016). We inferred that the diverse constituents of KYQG may be holistically responsible for the amelioration of oral ulcer symptoms worsened by sleep deprivation.

Metabolomics strategy was widely applied for investigation of pharmacodynamics (Zhang et al., 2019), screening of active constituents (Caesar et al., 2019), prediction of targets (Sun et al., 2019), discovery of quality-markers (Ding et al., 2018) in herbal medicines. In this study, we performed the chemical profiling of KYQG *in vitro* and investigated the treatment effects and biomarkers by combining pharmacological and metabolomics approaches. Nonetheless, an acknowledged limitation of this study is that the absorbed chemicals and their metabolites in serum have not been identified and quantified, which could be correlated with biomarkers to further elucidate the active constituents. Identification and quantification of the absorbed chemical markers of KYQG in serum are needed in future study.

In summary, our observations suggest that KYQG therapy could attenuate phenol-induced oral ulcers worsened by sleep deprivation in a rat model. Amelioration of symptoms was primarily associated with regulation of the neuroimmunoendocrine system, levels of oxidative stress, and tryptophan metabolism. The multiple functionalities of the diverse constituents of KYQG make it an efficient therapy for hard-to-treat oral ulcers. These findings may contribute to a better understanding of the clinical application of KYQG. This study also provides a novel approach for addressing the increased health risk resulting from sleep deficiency using an herbal medicine formula. Nevertheless, further studies are needed to elucidate the precise mechanisms by which KYQG ameliorates oral ulcer symptoms as well as the interactions between components and targets.

DATA AVAILABILITY STATEMENT

The datasets generated for this study are available on request to the corresponding author.

ETHICS STATEMENT

The animal study was reviewed and approved by Institutional Animal Care and Use Committee, Sun Yat-sen University.

AUTHOR CONTRIBUTIONS

PL, HY, and WS provided the concept and designed the experiment. PC, YZ, WF, LZ, TC, WZ, ZY, YH, and SW performed the experiments. PC and YW analyzed the data. PC and PL wrote the manuscript. All authors contributed to the article and approved the submitted version.

SUPPLEMENTARY MATERIAL

The Supplementary Material for this article can be found online at: https://www.frontiersin.org/articles/10.3389/fphar.2020.00824/full#supplementary-material

REFERENCES

Agus, A., Planchais, J., and Sokol, H. (2018). Gut microbiota regulation of tryptophan metabolism in health and disease. *Cell Host Microbe* 23 (6), 716–724. doi: 10.1016/j.chom.2018.05.003

Akintoye, S. O., and Greenberg, M. S. (2014). Recurrent aphthous stomatitis. *Dent. Clin. North Am.* 58 (2), 281–297. doi: 10.1016/j.cden.2013.12.002

Alshahrani, S. (2014). Psychological screening test results for stress, depression, and anxiety are variably associated with clinical severity of recurrent aphthous stomatitis and oral lichen planus. *J. Evidence-Based Dental Pract.* 14 (4), 206–208. doi: 10.1016/j.jebdp.2014.10.004

Ananthakrishnan, A. N., Long, M. D., Martin, C. F., Sandler, R. S., and Kappelman, M. D. (2013). Sleep disturbance and risk of active disease in patients with Crohn's disease and ulcerative colitis. *Clin. Gastroenterol. Hepatol.* 11 (8), 965–971. doi: 10.1016/j.cgh.2013.01.021

Bazrafshani, M. R., Hajeer, A. H., Ollier, W. E., and Thornhill, M. H. (2002). IL-1B and IL-6 gene polymorphisms encode significant risk for the development of recurrent aphthous stomatitis (RAS). *Genes Immun.* 3 (5), 302–305. doi: 10.1038/sj.gene.6363882

Caesar, L. K., Kellogg, J. J., Kvalheim, O. M., and Cech, N. B. (2019). Opportunities and Limitations for Untargeted Mass Spectrometry Metabolomics to Identify Biologically Active Constituents in Complex Natural Product Mixtures. *J. Nat. Prod.* 82 (3), 469–484. doi: 10.1021/acs.jnatprod.9b00176

Carra, M. C., Schmitt, A., Thomas, F., Danchin, N., Pannier, B., and Bouchard, P. (2017). Sleep disorders and oral health: a cross-sectional study. *Clin. Oral. Investig.* 21 (4), 975–983. doi: 10.1007/s00784-016-1851-y

Chen, P., Yao, H., Su, W., He, Y., Cheng, K., Wang, Y., et al. (2019). Sleep deprivation worsened oral ulcers and delayed healing process in an experimental rat model. *Life Sci.* 116594. doi: 10.1016/j.lfs.2019.116594

China, C.o.P.o. (2015). *Pharmacopoeia of the People's Republic of China (Part 1)* (Beijing, China: Pharmacopoeia Commission of the Ministry of Public Health of PRC).

Desneves, K. J., Todorovic, B. E., Cassar, A., and Crowe, T. C. (2005). Treatment with supplementary arginine, vitamin C and zinc in patients with pressure ulcers: A randomised controlled trial. *Clin. Nutr.* 24 (6), 979–987. doi: 10.1016/j.clnu.2005.06.011

Ding, M., Jiang, Y., Yu, X., Zhang, D., Li, J., Wang, H., et al. (2018). Screening of Combinatorial Quality Markers for Natural Products by Metabolomics Coupled With Chemometrics. A Case Study on Pollen Typhae. *Front. Pharmacol.* 9, 691. doi: 10.3389/fphar.2018.00691

Fatima, Y., Doi, S. A., and Mamun, A. A. (2015). Longitudinal impact of sleep on overweight and obesity in children and adolescents: a systematic review and bias-adjusted meta-analysis. *Obes. Rev.* 16 (2), 137–149. doi: 10.1111/obr.12245

Ganz, F. D. (2012). Sleep and Immune Function. *Crit. Care Nurse* 32 (2), E19–E25. doi: 10.4037/ccn2012689

Guimaraes, A. L., Correia-Silva Jde, F., Sa, A. R., Victoria, J. M., Diniz, M. G., Costa Fde, O., et al. (2007). Investigation of functional gene polymorphisms IL-1beta, IL-6, IL-10 and TNF-alpha in individuals with recurrent aphthous stomatitis. Arch. Oral. Biol. 52 (3), 268–272. doi: 10.1016/j.archoralbio.2006.08.008

Harden, J. L., Lewis, S. M., Lish, S. R., Suarez-Farinas, M., Gareau, D., Lentini, T., et al. (2016). The tryptophan metabolism enzyme L-kynureninase is a novel inflammatory factor in psoriasis and other inflammatory diseases. J. Allergy Clin. Immunol. 137 (6), 1830–1840. doi: 10.1016/j.jaci.2015.09.055

Hong, S., Joo, T., and Jhoo, J. W. (2015). Antioxidant and anti-inflammatory activities of 3,5-dicaffeoylquinic acid isolated from Ligularia fischeri leaves. Food Sci. Biotechnol. 24 (1), 257–263. doi: 10.1007/s10068-015-0034-y

Hubbard, T. D., Murray, I. A., and Perdew, G. H. (2015). Indole and tryptophan metabolism: endogenous and dietary routes to Ah receptor activation. Drug Metab. Dispos. 43 (10), 1522–1535. doi: 10.1124/dmd.115.064246

Jiang, T. T., Wang, C., Wei, L. L., Yu, X. M., Shi, L. Y., Xu, D. D., et al. (2015). Serum protein gamma-glutamyl hydrolase, Ig gamma-3 chain C region, and haptoglobin are associated with the syndromes of pulmonary tuberculosis in traditional Chinese medicine. BMC Complement. Altern. Med. 15. doi: 10.1186/s12906-015-0686-4

Johnson, L., Perschbacher, K., Leong, I., and Bradley, G. (2017). Oral manifestations of immunologically mediated diseases. Atlas Oral. Maxillofac. Surg. Clin. North Am. 25 (2), 171–185. doi: 10.1016/j.cxom.2017.04.009

Kao, T. C., Shyu, M. H., and Yen, G. C. (2010). Glycyrrhizic Acid and 18 beta-Glycyrrhetinic Acid Inhibit Inflammation via PI3K/Akt/GSK3 beta Signaling and Glucocorticoid Receptor Activation. J. Agric. Food Chem. 58 (15), 8623–8629. doi: 10.1021/jf101841r

Kim, S. W., Jin, Y., Shin, J. H., Kim, I. D., Lee, H. K., Park, S., et al. (2012). Glycyrrhizic acid affords robust neuroprotection in the postischemic brain via anti-inflammatory effect by inhibiting HMGB1 phosphorylation and secretion. Neurobiol. Dis. 46 (1), 147–156. doi: 10.1016/j.nbd.2011.12.056

Kim, M., Choi, S. Y., Lee, P., and Hur, J. Y. (2015). Neochlorogenic acid Inhibits lipopolysaccharide-induced activation and pro-inflammatory responses in BV2 microglial cells. Neurochem. Res. 40 (9), 1792–1798. doi: 10.1007/s11064-015-1659-1

Knutson, K. L., Spiegel, K., Penev, P., and Van Cauter, E. (2007). The metabolic consequences of sleep deprivation. Sleep Med. Rev. 11 (3), 163–178. doi: 10.1016/j.smrv.2007.01.002

Kreutzmann, J. C., Havekes, R., Abel, T., and Meerlo, P. (2015). Sleep deprivation and hippocampal vulnerability: changes in neuronal plasticity, neurogenesis and cognitive function. Neuroscience 309, 173–190. doi: 10.1016/j.neuroscience.2015.04.053

Lee, C. F., Lin, M. C., Lin, C. L., Yen, C. M., Lin, K. Y., Chang, Y. J., et al. (2014). Non-apnea sleep disorder increases the risk of periodontal disease: a retrospective population-based cohort study. J. Periodontol. 85 (4), E65–E71. doi: 10.1902/jop.2013.130284

Lee, S. W. H., Ng, K. Y., and Chin, W. K. (2017). The impact of sleep amount and sleep quality on glycemic control in type 2 diabetes: a systematic review and meta-analysis. Sleep Med. Rev. 31, 91–101. doi: 10.1016/j.smrv.2016.02.001

Lee, E. H., Park, K. I., Kim, K. Y., Lee, J. H., Jang, E. J., Ku, S. K., et al. (2018). Liquiritigenin inhibits hepatic fibrogenesis and TGF-beta1/Smad with Hippo/YAP signal. Phytomedicine 62, 152780. doi: 10.1016/j.phymed.2018.12.003.

Li, P., Yin, Y. L., Li, D., Kim, S. W., and Wu, G. Y. (2007). Amino acids and immune function. Br. J. Nutr. 98 (2), 237–252. doi: 10.1017/S000711450769936x

Li, X. C., Jiang, Q., Wang, T. T., Liu, J. J., and Chen, D. F. (2016). Comparison of the antioxidant effects of quercitrin and isoquercitrin: Understanding the role of the 6 "-OH group. Molecules 21 (9). doi: 10.3390/molecules21091246

Li, X.-Q., Cai, L.-M., Liu, J., Ma, Y.-L., Kong, Y.-H., Li, H., et al. (2018). Liquiritin suppresses UVB−induced skin injury through prevention of inflammation, oxidative stress and apoptosis through the TLR4/MyD88/NF−κB and MAPK/caspase signaling pathways. Int. J. Mol. Med. 42 (3), 1445–1459. doi: 10.3892/ijmm.2018.3720

Li, Y. T., Wang, D. M., Zeng, C. W., Liu, Y. C., Huang, G. Y., and Mei, Z. L. (2018). Salivary metabolomics profile of patients with recurrent aphthous ulcer as revealed by liquid chromatography-tandem mass spectrometry. J. Int. Med. Res. 46 (3), 1052–1062. doi: 10.1177/0300060517745388

Liu, H., Zheng, Y. F., Li, C. Y., Zheng, Y. Y., Wang, D. Q., Wu, Z., et al. (2015). Discovery of anti-inflammatory ingredients in chinese herbal formula

kouyanqing granule based on relevance analysis between chemical characters and biological effects. Sci. Rep. 5, 18080. doi: 10.1038/srep18080

Meyers, B. E., Moonka, D. K., and Davis, R. H. (1979). The effect of selected amino acids on gelatin-induced inflammation in adult male mice. Inflammation 3 (3), 225–233. doi: 10.1007/bf00914179

Naveed, M., Hejazi, V., Abbas, M., Kamboh, A. A., Khan, G. J., Shumzaid, M., et al. (2018). Chlorogenic acid (CGA): A pharmacological review and call for further research. Biomed. Pharmacother. 97, 67–74. doi: 10.1016/j.biopha.2017.10.064

Oliveira, M. C. G., Pelegrini-Da-Silva, A., Parada, C. A., and Tambeli, C. H. (2007). 5-HT acts on nociceptive primary afferents through an indirect mechanism to induce hyperalgesia in the subcutaneous tissue. Neuroscience 145 (2), 708–714. doi: 10.1016/j.neuroscience.2006.12.021

Opp, M. R., and Krueger, J. M. (2015). Sleep and immunity: A growing field with clinical impact. Brain Behav. Immun. 47, 1–3. doi: 10.1016/j.bbi.2015.03.011

Pacheco, R., Riquelme, E., and Kalergis, A. M. (2010). Emerging evidence for the role of neurotransmitters in the modulation of T cell responses to cognate ligands. Cent. Nerv. Syst. Agents Med. Chem. 10 (1), 65–83. doi: 10.2174/187152410790780154

Pepin, J. L., Borel, A. L., Tamisier, R., Baguet, J. P., Levy, P., and Dauvilliers, Y. (2014). Hypertension and sleep: overview of a tight relationship. Sleep Med. Rev. 18 (6), 509–519. doi: 10.1016/j.smrv.2014.03.003

Poon, M. M. K., Chung, K. F., Yeung, W. F., Yau, V. H. K., and Zhang, S. P. (2012). Classification of insomnia using the traditional chinese medicine system: A systematic review. Evidence-Based Complement. Altern. Med. 2012. doi: 10.1155/2012/735078

Quang, T. H., Ngan, N. T. T., Minh, C. V., Kiem, P. V., Nhiem, N. X., Tai, B. H., et al. (2011). Anti-inflammatory Triterpenoid Saponins from the Stem Bark of Kalopanax pictus. J. Natural Prod. 74 (9), 1908–1915. doi: 10.1021/np200382s

Rahayu, P., Marcelline, F., Sulistyaningrum, E., Suhartono, M. T., and Tjandrawinata, R. R. (2016). Potential effect of striatin (DLBS0333), a bioactive protein fraction isolated from Channa striata for wound treatment. Asian Pac. J. Trop. Biomed. 6 (12), 1001–1007. doi: 10.1016/j.apjtb.2016.10.008

Roager, H. M., and Licht, T. R. (2018). Microbial tryptophan catabolites in health and disease. Nat. Commun. 9. doi: 10.1038/s41467-018-05470-4

Rogerio, A. P., Kanashiro, A., Fontanari, C., da Silva, E. V. G., Lucisano-Valim, Y. M., Soares, E. G., et al. (2007). Anti-inflammatory activity of quercetin and isoquercitrin in experimental murine allergic asthma. Inflammation Res. 56 (10), 402–408. doi: 10.1007/s00011-007-7005-6

Romero, R., and Badr, M. S. (2014). A role for sleep disorders in pregnancy complications: challenges and opportunities. Am. J. Obstetr. Gynecol. 210 (1), 3–11. doi: 10.1016/j.ajog.2013.11.020

Sakanaka, A., Kuboniwa, M., Hashino, E., Bamba, T., Fukusaki, E., and Amano, A. (2017). Distinct signatures of dental plaque metabolic byproducts dictated by periodontal inflammatory status. Sci. Rep. 7. doi: 10.1038/srep42818

Schopohl, P., Gruneberg, P., and Melzig, M. F. (2016). The influence of harpagoside and harpagide on TNFalpha-secretion and cell adhesion molecule mRNA-expression in IFNgamma/LPS-stimulated THP-1 cells. Fitoterapia 110, 157–165. doi: 10.1016/j.fitote.2016.03.005

Scully, C., and Porter, S. (2008). Oral mucosal disease: recurrent aphthous stomatitis. Br. J. Oral. Maxillofac. Surg. 46 (3), 198–206. doi: 10.1016/j.bjoms.2007.07.201

Scully, C., and Shotts, R. (2000). Mouth ulcers and other causes of orofacial soreness and pain. Br. Med. J. 321 (7254), 162–165. doi: 10.1136/bmj.321.7254.162

Seol, H. S., Lee, S. E., Song, J. S., Lee, H. Y., Park, S., Kim, I., et al. (2016). Glutamate release inhibitor, Riluzole, inhibited proliferation of human hepatocellular carcinoma cells by elevated ROS production. Cancer Lett. 382 (2), 157–165. doi: 10.1016/j.canlet.2016.08.028

Singh, M., Rao, D. M., Pande, S., Battu, S., Dutt, K. R., and Ramesh, M. (2011). Medicinal uses of L-lysine: past and future. Int. J. Res. Pharm. Sci. 2 (4), 637–642. https://pharmascope.org/ijrps/article/view/976

Slebioda, Z., Szponar, E., and Kowalska, A. (2014). Etiopathogenesis of recurrent aphthous stomatitis and the role of immunologic aspects: literature review. Arch. Immunol. Ther. Exp. (Warsz) 62 (3), 205–215. doi: 10.1007/s00005-013-0261-y

Song, Y. S., and Park, C. M. (2014). Luteolin and luteolin-7-O-glucoside strengthen antioxidative potential through the modulation of Nrf2/MAPK

mediated HO-1 signaling cascade in RAW 264.7 cells. *Food Chem. Toxicol.* 65, 70–75. doi: 10.1016/j.fct.2013.12.017

Sun, H, Zhang, A.-H., Yang, L., Li, M.-X., Fang, H., Xie, J., et al. (2019). High-throughput chinmedomics strategy for discovering the quality-markers and potential targets for Yinchenhao decoction. *Phytomedicine* 54, 328–338. doi: 10.1016/j.phymed.2018.04.015

Spiga, R., Marini, M. A., Mancuso, E., Di Fatta, C., Fuoco, A., Perticone, F., et al. (2017). Uric acid is associated with inflammatory biomarkers and induces inflammation via activating the NF-kappa B Signaling pathway in HepG2 cells. *Arterioscler. Thromb. Vasc. Biol.* 37 (6), 1241–1249. doi: 10.1161/Atvbaha.117.309128

Taylor, J., Glenny, A. M., Walsh, T., Brocklehurst, P., Riley, P., Gorodkin, R., et al. (2014). Interventions for the management of oral ulcers in Behcet's disease. *Cochrane Database Syst. Rev.* 9. doi: 10.1002/14651858.CD011018.pub2

Tobaldini, E., Costantino, G., Solbiati, M., Cogliati, C., Kara, T., Nobili, L., et al. (2017). Sleep, sleep deprivation, autonomic nervous system and cardiovascular diseases. *Neurosci. Biobehav. Rev.* 74, 321–329. doi: 10.1016/j.neubiorev.2016.07.004

Villalva, M., Jaime, L., Aguado, E., Nieto, J. A., Reglero, G., and Santoyo, S. (2018). Anti-inflammatory and antioxidant activities from the basolateral fraction of Caco-2 dcells exposed to a rosmarinic acid enriched extract. *J. Agric. Food Chem.* 66 (5), 1167–1174. doi: 10.1021/acs.jafc.7b06008

Wan, P., Xie, M. H., Chen, G. J., Dai, Z. Q., Hu, B., Zeng, X., et al. (2019). Anti-inflammatory effects of dicaffeoylquinic acids from Ilex kudingcha on lipopolysaccharide-treated RAW264.7 macrophages and potential mechanisms. *Food Chem. Toxicol.* 126, 332–342. doi: 10.1016/j.fct.2019.01.011

Wang, Y. H., Shen, J. Y., Yang, X. L., Jin, Y., Yang, Z. L., Wang, R. F., et al. (2018). Akebia saponin D reverses corticosterone hypersecretion in an Alzheimer's disease rat model. *Biomed. Pharmacother.* 107, 219–225. doi: 10.1016/j.biopha.2018.07.149

Xie, W. Y., Wang, M., Chen, C., Zhang, X. Y., and Melzig, M. F. (2016). Hepatoprotective effect of isoquercitrin against acetaminophen-induced liver injury. *Life Sci.* 152, 180–189. doi: 10.1016/j.lfs.2016.04.002

Yan, B., JiYe, A., Hao, H. P., Wang, G. J., Zhu, X. X., Zha, W. B., et al. (2009). Metabonomic phenotype and identification of "heart blood stasis obstruction pattern" and "qi and yin deficiency pattern" of myocardial ischemia rat models. *Sci. China Ser. C-Life Sci.* 52 (11), 1081–1090. doi: 10.1007/s11427-009-0136-y

Yu, X., Wang, L. N., Du, Q. M., Ma, L., Chen, L., You, R., et al. (2012). Akebia Saponin D attenuates amyloid beta-induced cognitive deficits and inflammatory response in rats: Involvement of Akt/NF-kappa B pathway. *Behav. Brain Res.* 235 (2), 200–209. doi: 10.1016/j.bbr.2012.07.045

Zhang, A. H., Ma, Z. M., Sun, H., Zhang, Y., Liu, J. H., Wu, F. F., et al. (2019). High-Throughput Metabolomics Evaluate the Efficacy of Total Lignans From Acanthophanax Senticosus Stem Against Ovariectomized Osteoporosis Rat. *Front. Pharmacol.* 10, 553. doi: 10.3389/fphar.2019.00553

Chijabyukpi-Tang Inhibits Pro-Inflammatory Cytokines and Chemokines *via* the Nrf2/HO-1 Signaling Pathway in TNF-α/IFN-γ-Stimulated HaCaT Cells and Ameliorates 2,4-Dinitrochlorobenzene-Induced Atopic Dermatitis-Like Skin Lesions in Mice

Ji-Hyun Lee[1], Ji-Ye Lim[1], Eun Hee Jo[2,3], Hyeon Min Noh[4], Sunggu Park[5], Min Cheol Park[2,5*] and Dae-Ki Kim[1*]

[1] Department of Immunology and Institute of Medical Sciences, Medical School, Chonbuk National University, Jeonju, South Korea, [2] Research Center of Traditional Korean Medicine, Wonkwang University, Iksan, South Korea, [3] Department of Acupuncture and Moxibustion, College of Korean Medicine, Wonkwang University, Iksan, South Korea, [4] Korean Traditional Medicine Institute, Wonkwang University, Iksan, South Korea, [5] Department of Korean Medical Ophthalmology & Otolaryngology & Dermatology, College of Korean Medicine, Wonkwang University, Iksan, South Korea

Chijabyukpi-tang (CBT) is an oriental herbal formula consisting of three herbs (Gardeniae Fructus (*Gardenia jasminoides* J.Ellis.), Phellodendri Cortex (*Phellodendron amurense* Rupr.), Glycyrrhizae Radix (*Glycyrrhiza uralensis* Fisch. ex DC.) at the ratio of 2: 2: 1. CBT has traditionally been used to treat eczema with inflammation in Northeast Asia. The components of CBT have been shown to have anti-inflammatory and anti-oxidant properties, but the exact role and mechanism of CBT on atopic dermatitis (AD) remain unclear. In this study, we investigated the anti-inflammatory effect and mechanism of CBT in the HaCaT human keratinocyte cell line and investigated the anti-atopic effect in mice models of atopic dermatitis-like skin lesions. In the tumor necrosis factor alpha (TNF)-α/ interferon (IFN)-γ-stimulated HaCaT cells, CBT inhibited the production of pro-inflammatory cytokines and chemokines and elevated the nuclear translocation of NF-E2 p45 related factors 2 (Nrf2) and subsequent production of heme oxygenase-1 (HO-1). CBT improved the symptoms of atopic dermatitis-like lesions in 2,4-dinitrochlorobenzene (DNCB)-treated mice by suppressing the levels of serum immunoglobulin E (IgE), and various pro-inflammatory cytokines and chemokines. The improvement effect of CBT on atopic dermatitis-like lesions can be predicted to be due to increased Nrf2 and HO-1 gene expression. These results suggest that CBT is an herbal medicine with the potential for use as a therapeutic agent for inflammatory skin diseases such as atopic dermatitis.

Keywords: *Chijabyukpi-tang*, atopic dermatitis, keratinocytes, cytokine, chemokine, inflammation

INTRODUCTION

Atopic dermatitis (AD) is a chronic relapsing inflammatory skin disease, and the incidence of AD worldwide has been increasing rapidly over the past 30 years (Kapoor et al., 2008). AD occurs most often during childhood and occurs equally in both females and males. In developed countries, about 2–4% of adults and 15–20% of children suffer from AD, and most AD patients are known to have symptoms that last approximately five years (Shaw et al., 2011). AD is characterized by severe skin lesions such as pruritus, erythema, rash, edema, dryness, and skin hypersensitivity (Guttman-Yassky et al., 2011). Because of these features, AD patients often suffer from sleep deprivation, anxiety, and stress, which can lower their quality of life (Kiebert et al., 2002). Many sufferers of AD are also prone to developing other chronic inflammatory diseases including asthma and allergic reactions.

AD is caused by a complex interaction between extrinsic and intrinsic factors. The main risk factor of AD is not yet known, but it is known that mostly immune system dysfunction and environmental factors impair the skin's barrier and exacerbate immunoglobulin E (IgE)-mediated sensitization, severe skin inflammation and immune responses (Darlenski et al., 2014).

AD skin inflammation is orchestrated by the production of pro-inflammatory cytokines and chemokines by keratinocytes that subsequently induces the invasion of immune cells. The immune cells create inflammatory skin lesions following the production of further pro-inflammatory cytokines and chemokines (Homey et al., 2006). According to previous studies, AD patients are known to have increased levels of chemokines (such as IL-8, CCL17, and CXCL10) and cytokines (such as IL-4, IL-6, and IL-13), compared to healthy individuals (Yamanaka and Mizutani, 2011). It is also known that the activation of several oxidative stress-related inflammatory signaling pathways, such as NF-E2 p45 related factors 2 (Nrf2) and heme oxygenase-1 (HO-1), is related to inflammation in AD (Choi et al., 2014; Akram et al., 2016).

Currently, topical ointments and oral medications such as corticosteroids, antihistamines, and immunosuppressive drugs are used to treat AD inflammation and reduce itching (Cury Martins et al., 2015). However, these drugs have serious side effects when repeatedly administered over a long period of time. Therefore, in order to minimize the adverse effects of the long-term use of AD drugs, there is a need for the development of new alternative drugs derived from natural resources with fewer side effects.

Abbreviations: AD, atopic dermatitis; CBT, *Chijabyukpi-tang*; Dexa, dexamethasone; DMSO, dimethyl sulfoxide; DNCB, 2,4-dinitrochlorobenzene; ECL, enhanced chemi-luminescence; ELISA, Enzyme-linked immunosorbent assay; FBS, fetal bovine serum; HO-1, heme oxygenase-1; HPLC, high performance liquid chromatography; H&E, Hematoxylin and eosin; IFN-γ, interferon-γ; IgE, immunoglobulin E; KIOM, Korea Institute of Oriental Medicine; MTT, 3-(4,5-Dimethyl-2-thiazolyl)-2,5-diphenyl-2H-tetrazolium bromide; Nrf2, NF-E2 p45 related factors 2; PDA, photodiode array; qPCR, Quantitative real-time polymerase chain reaction; SDS-PAGE, sodium dodecyl sulfate-polyacrylamide; SEM, standard error of the mean; Th2, T helper 2; TNF-α, tumor necrosis factor-α.

Chijabyukpi-tang (CBT) is an oriental herbal formula consisting of three herbs (Gardeniae Fructus, Phellodendri Cortex, Glycyrrhizae Radix), in a 2:2:1 ratio. CBT is a traditional medicine first reported thousands of years ago in the ancient Chinese medicine book "Sang han-lun". CBT has long been used as a treatment for eczema with inflammation (Mie et al., 2009). In addition, it is an oriental herbal formula that is known to eliminate heat in the body, cure humid, jaundice and epidemic diseases. It has also been used to treat severe pain in the lower abdomen, burns, and various infectious symptoms (Chen et al., 2009). The various effects of each herb that constitutes CBT are well known; previous studies have shown that Gardeniae Fructus and Phellodendri Cortex have anti-inflammatory and anti-allergic effects (Hon et al., 2011; Debnath et al., 2018). In addition, Glycyrrhizae Radix has been previously shown to relieve inflammation (Yang et al., 2013). However, there is few scientific research on the CBT in which these herbs are combined. Previous studies have reported that CBT relieves fever and dizziness, and pruritic skin disease (Higashi and Kanzaki, 2006; Choi and Lee, 2017).

Since AD is characterized by inflammation and pruritus, eczema, we first studied the effect of CBT on AD and its mechanism of action. Therefore, the aim of this study was to investigate the anti-inflammatory effect and action mechanism of CBT on TNF-α/IFN-γ-stimulated HaCaT cells (human keratinocyte cell line) and 2,4-dinitrochlorobenzene (DNCB)-induced AD-like skin lesions in mice.

MATERIALS AND METHODS

Cell Culture and Reagents

The HaCaT cell line was obtained from the laboratory of Wonkwang university (Prof. Min Cheol Park). The HaCaT cells were incubated in Dulbecco's modified Eagle's medium (DMEM) supplemented with 10% fetal bovine serum (FBS), 100 units/ml of penicillin, and streptomycin (Welgene, Seoul, Korea). The HaCaT cells were cultured at 37°C in an incubator with a humidified atmosphere of 5% CO_2 and 95% air. DMEM and FBS were purchased from GIBCO BRL (Grand Island, NY, USA). Penicillin and streptomycin were purchased from Welgene (Seoul, Korea). Recombinant human TNF-α, IFN-γ, and IgE mouse ELISA kit were obtained from BioLegend (San Diego, CA, USA). Primary antibodies for Nrf2, Lamin B, HO-1, β-actin, and secondary antibodies used in the western blot analysis were purchased from Santa Cruz Biotechnology (Santa Cruz, CA, USA). 3-(4,5-Dimethyl-2-thiazolyl)-2,5-diphenyl-2H-tetrazolium bromide (MTT), dexamethasone (#D2915), and DNCB were purchased from Sigma-Aldrich. (St. Louis, Mo., USA).

Preparation of CBT

The herb components used in CBT were obtained from the K-herb Research Center, Nong-Lim and Ja-Dam. The identity of the herbs was confirmed by Prof. Min-Chel Park from Wonkwang University of traditional korean medicine. Voucher specimens of Gardeniae Fructus (NLGF-1803) and Phellodendri

Cortex (NLPC-1801) have been deposited at Nong-Lim. Voucher specimen of Glycyrrhizae Radix (JD8KZ-1902) has been deposited at Ja-Dam. CBT was constructed by mixing the herbs in accordance with each component composition in **Table 1** (www.theplantlist.org). 18 g of CBT was boiled at 100°C in 1,000 ml water for 30 min. Then the extract was collected, and as above, the residue was twice boiled in water. The extracted CBT was filtered and freeze-dried, and the weight of the dried extract was measured, and kept at 4°C until use.

Analysis of High Performance Liquid Chromatography (HPLC)

To perform the HPLC analysis of CBT, the Waters e2695 separation module, 2998 photodiode array (PDA) detector (Waters Corporation, USA) was used. The analytical column used was Phenomenex Luna C18 (250× 4.6 mm). The column temperature was at 40°C, the samples temperature was at 25°C, and the injection volume was 10 µl. The mobile phases were composed of solvent (A) = 0.1% trifluoroacetic acid in water, and solvent (B) = Acetonitrile. The total run time was 120 min and the mobile phase process gradient flow was as follows: (A)/(B) = 80/20 (0-10 min) → (A)/(B) = 80/20 (10-90 min) → (A)/(B) = 40/60 (90-91 min) → (A)/(B) = 0/100 (91-111 min) → (A)/(B) = 80/20 (111-120 min). The mobile phase flow rate was 1.0 ml/min. Samples were detected with a UV detector at a wavelength of 260 nm.

MTT Assay

The viability of HaCaT cells was evaluated using the MTT assay. The MTT assay was carried out as previously described (Lee et al., 2018). Briefly, cells were seeded into a 96-well plate at 1×10^4 cells/well, and treated with various concentrations of CBT (0, 12.5, 25, 50, 100 µg/ml) for 24 h in a 37°C incubator. MTT reagents were added to each well, and the plate was incubated for a further 4 h. After removing the supernatant, the crystallized formazan was dissolved in dimethyl sulfoxide (DMSO), and the absorbance was read at 570 nm using an ELISA plate reader.

Preparation of the HaCaT Nuclear and Cytosol Fractions

The nuclear and cytosol fractions of the HaCaT cells were isolated using the Nuclear/Cytosol Fractionation Kit (BioVision, Inc., CA, USA), according to the manufacturer's instructions. The nuclear and cytosol fractions were stored at -80°C until use.

Quantitative Real-Time Polymerase Chain Reaction (qPCR)

qPCR was carried out to confirm the expression levels of several genes *in vitro* and *in vivo*. Total RNA was isolated from *dorsal skin tissues* and HaCaT cells using 1 ml Trizol *reagent* (Invitrogen, Carlsbad, CA, USA). After the RNA was extracted, cDNA was synthesized using the Prime Script ™ II 1st strand cDNA synthesis kit (Takara Bio, Inc. USA), according to the *manufacturer's protocols*. The cDNA was amplified with SYBR Green PCR Master Mix (Applied Biosystem, CA, USA) using an ABI Real-Time PCR system (Applied Biosystems, Inc., CA, USA). *The primer sequences are shown in* **Table 2**. The RNA gene expression levels of each sample were analyzed three times and normalized to the internal control gene, GAPDH.

Western Blot Analysis

The protein production levels of cells were evaluated using western blot analysis. HaCaT cells were pretreated with various concentrations of CBT (0, 12.5, 25, 50, and 100 µg/ml) for 2 h, and treated with TNF-α/IFN-γ (10 ng/ml each) for 3 h. The cells were harvested, and proteins were extracted using cell lysis buffer (Millipore, Bedford, MA, USA) supplemented with a protease and phosphatase inhibitor cocktail (Thermo Fisher Scientific, Waltham, MA, USA). Proteins (25 µg) were separated *via* electrophoresis in 10% sodium dodecyl sulfate-polyacrylamide (SDS-PAGE) gels, and transferred to PVDF membranes.

TABLE 2 | *Primer sequences for* quantitative real-time polymerase chain reaction (qPCR).

Gene	Forward	Reverse
hIL-6	CTCCACAAGCGCCTTCGGTC	TGTGTGGGGCGGCTACATCT
hIL-13	ACCACGGTCATTGCTCTCACT	GTCAGGTTGATGCTCCATAC
hIL-8	ACCGGAGCACTCCATAAGGCA	AGGCTGCCAAGAGAGCCACG
hCCL17	CCATTCCCCTTAGAAAGCTG	CTCTCAAGGCTTTGCAGGTA
hCXCL10	TTGCTGCCTTATCTTTCTGACTC	ATGGCCTTCGATTCTGGATT
mIL-4	ATGGGTCTCAACCCCCAGCTA	TGCATGGCGTCCCTTCTCCT
mIL-6	GACAACCACGGCCTTCCCTA	GGTACTCCAGAAGACCAGAGG
mIL-8	TTTGGGAGACCTGAGAACAAG	TGCCTGTCAAGCTGACTTCA
mCXCL10	CTGAGTGGGACTCAAGGGAT	TCGTGGCAATGATCTCAACAC
mHO-1	CAGAACCAGCCTGAACTAGC	TGGATGTGTACCTCCTTGGT
mNrf2	ACCAAGGGGCAC CATATAAAAG	CTTCGCCGAGTTGCACTCA
GAPDH	GAAGGTGAAGGTCGGAGT	GAAGATGGTGATGGGATTTC

IL-, Interleukin-; CCL17, Chemokine (C-C motif) ligand 17; CXCL10, C-X-C motif chemokine 10; HO-1, heme oxygenase-1; Nrf2, NF-E2 p45-related factor 2; GAPDH, glyceraldehyde 3-phosphate dehydrogenase.

TABLE 1 | The composition of *Chijabyukpi-tang* (CBT).

Herb medicine	Latin scientific name	Family	Source	Weight (g)/Ratio (%)
Gardeniae Fructus	*Gardenia jasminoides* J.Ellis.	Rubiaceae	Korea	6/40
Phellodendri Cortex	*Phellodendron amurense* Rupr.	Rutaceae	Korea	6/40
Glycyrrhizae Radix	*Glycyrrhiza uralensis* Fisch. ex DC.	Fabaceae	Korea	3/20
Total Amount				**15/100**

Membranes were blocked with 5% BSA in TBS-T at room temperature for 1 h, and incubated with primary antibodies (Nrf2, Lamin B, HO-1, and β-actin; 1:1,000 dilution in 5% BSA) overnight at 4°C. Then, the membranes were washed several times with TBS-T, and incubated with horseradish peroxidase (HRP)-conjugated secondary antibody (1:5,000 dilution in 5% BSA) at room temperature for 1 h. The proteins were detected with enhanced chemi-luminescence (ECL) detection kit (Millipore, Billerica, MA, USA) using the Fusion Fx gel documentation system (Davinch-Invivo™ Imaging System, USA).

Animals

Four-week-old male BALB/c mice were purchased from Samtako Bio Korea (Osan, Korea). All mice (22 ± 2 g) were randomly housed in a controlled environment with 50–60% humidity and a temperature of 21–23°C, under a 12-h dark/light cycle. Mice were allowed free access to standard laboratory chow and tap water. After a one-week period of new environment acclimation, mice were randomly divided into five groups of six mice. This research was performed in accordance with the guidelines of the Animal Experiment Ethics Committee of Chonbuk National University (CBNU-IACUC) (Confirmation No. CBNU 2016-0011).

Experimental Protocols of the Mouse Study

Thirty mice were divided into five groups (n=6) as follows: (1) control (vehicle treatment), (2) DNCB, (3) DNCB + CBT-low dose (CBT-150 mg/kg), (4) DNCB + CBT-high dose (CBT-300 mg/kg) and (5) positive control (dexamethasone (Dexa)-1 mg/kg). Except for the control group, AD-like skin lesions were induced using DNCB as described previously. Briefly, the dorsal skin hairs of all mice were removed. After 24 h, DNCB was dissolved in an acetone and olive oil mixture (4:1 v/v), and the dorsal skin was treated with 1% DNCB solution once a day for three days. Furthermore, 0.5% DNCB solution was treated to the dorsal skin once every two days for ten days to promote AD-like skin lesions. CBT samples and dexamethasone were dissolved in water and orally administered once a day for 11 days (days 4–14) (**Figure 4A**). The experimental animals were anesthetized by ether and euthanized by cervical dislocation for collecting skin tissues and blood serum.

Measurement of Dorsal Skin Moisture Content, Atopic Dermatitis Score, and Dorsal Skin Thickness

On the last day of the experiment, the dorsal skin moisture content (%) was measured using a TS-skin diagnostic system (Aram Huvis Co., Seongnam, Korea), according to the manufacturer's protocol. We assessed the severity of erythema, edema, and stretches on AD-like skin lesions on the dorsal skin five times according to Fan's criteria (Fan et al., 2018). After the dorsal skin tissues of mice were isolated, the thicknesses of the dorsal skin were gauged three times using a micrometer.

Hematoxylin and Eosin (H&E) Staining

After the mice were sacrificed, their dorsal skin tissue specimens (100 μm²) were fixed in 10% formalin solution at room temperature for 24 h, and then embedded in paraffin wax. The paraffin blocks were sectioned serially into a thickness of 6-μm (n=6), and stained with hematoxylin and eosin (H&E; hematoxylin, 1 min and eosin, 3 min) to examine skin histological changes. Histological changes were observed using a microscope (Olympus CX21, Olympus Corporation, Tokyo, Japan). All images were observed at ×100 magnification.

Enzyme-Linked Immunosorbent Assay (ELISA)

After the mice were anesthetized, blood samples were collected. Blood samples were allowed to clot by incubation at room temperature for 30 min. Then, bloods were centrifuged at 3,000 rpm for 10 min and serum samples were obtained. IgE in serum was analyzed using a total IgE mouse ELISA kit, according to the manufacturer's instructions.

Statistical Analysis

Graph Pad Prism software 5.0 was used for data statistical analysis. All data are represented as means ± standard error of the mean (SEM) of triplicate experiment, and evaluated using one-way ANOVA (analysis of variance) with Tukey's *post-hoc* test to locate differences between groups. A value of $p < 0.05$ was defined as statistically significant.

RESULTS

HPLC Analysis of CBT

The final extraction yield (%) of CBT was 37.77%. The CBT indicator ingredient compounds (crocin, berberine hydrochloride, and glycyrrhizic acid) were analyzed using HPLC. We confirmed the peak of three compounds in the CBT extract by comparison with the standard ingredients' peak. As shown in **Figure 1**, the CBT used in our experiments contains these three components. The content of crocin, berberine hydrochloride, and glycyrrhizic acid in CBT was 28.671 mg/g, 6.255 mg/g, and 6.249 mg/g, respectively.

CBT Reduces the mRNA Expression of Pro-Inflammatory Cytokines and Chemokines in TNF-α/IFN-γ-Stimulated HaCaT Cells

The cytotoxicity of HaCaT cells was examined at various concentrations (12.5, 25, 50, and 100 μg/ml) of CBT for 24 h. As shown in **Figure 2A**, CBT did not show cytotoxicity at all concentration ranges. To evaluate the anti-inflammatory effects of CBT, the production of pro-inflammatory cytokines and chemokines was measured in TNF-α/IFN-γ-treated HaCaT cells. HaCaT cells were pretreated with CBT (0, 12.5, 25, 50, and 100 μg/ml) for 2 h, and stimulated with TNF-α/IFN-γ (10 ng/ml each) for 3 h. Then, the mRNA expression levels of cytokines (IL-6 and IL-13), and chemokines (IL-8, CCL17, and CXCL10) were analyzed using qPCR. CBT was shown to significantly inhibit the
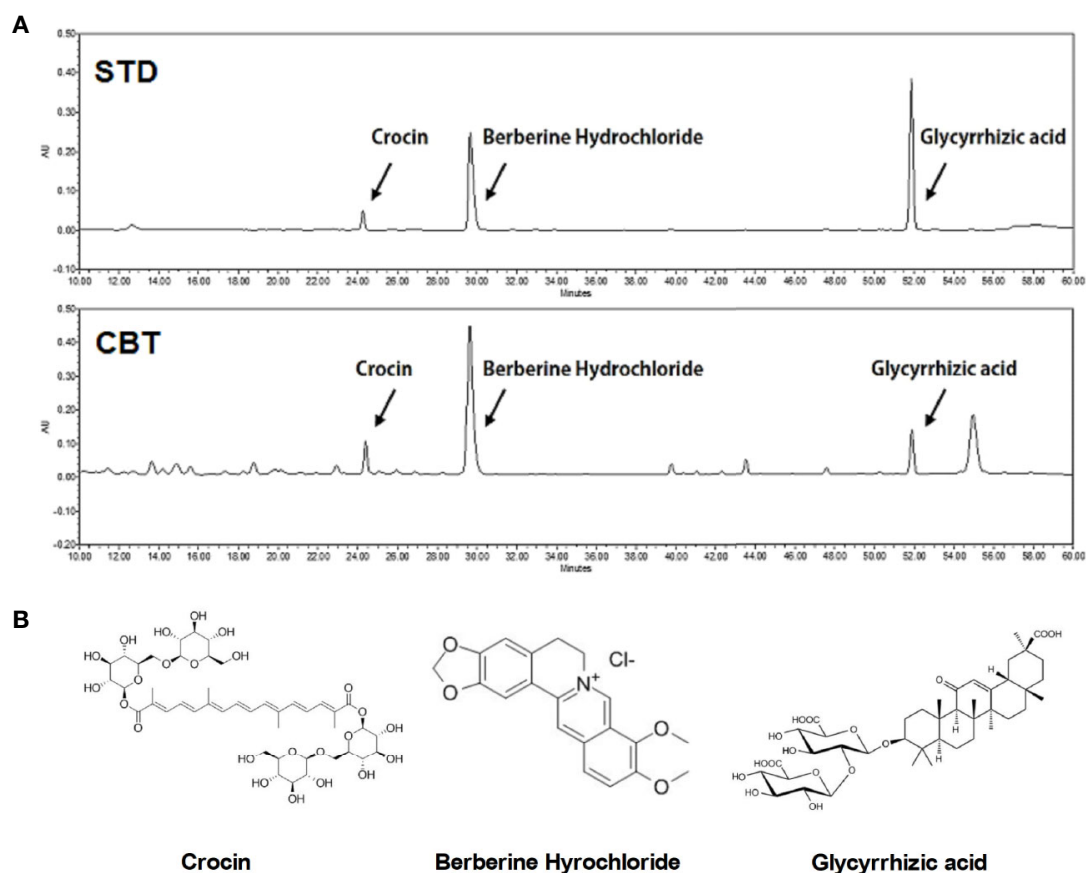
FIGURE 1 | High performance liquid chromatography (HPLC) analysis of *Chijabyukpi-tang* (CBT). HPLC chromatograms of standard compound mixtures (STD) and CBT samples **(A)**. Chemical structures of crocin, berberine hydrochloride, and glycyrrhizic acid **(B)**.
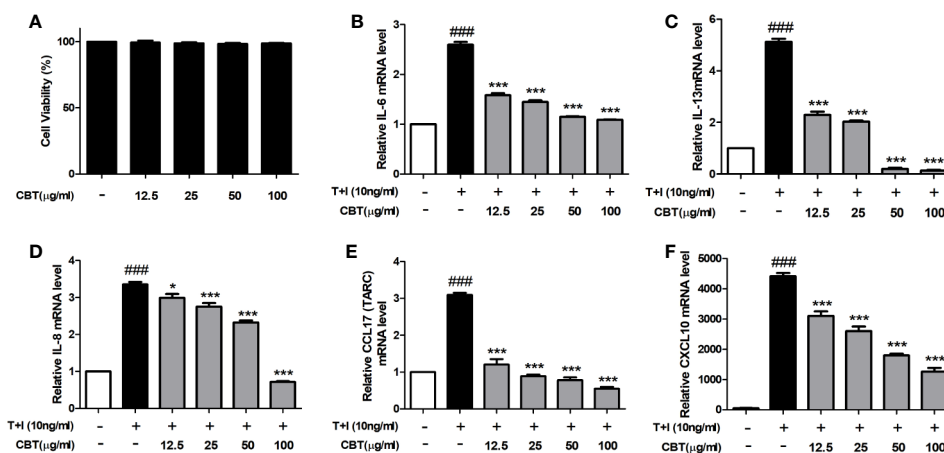
FIGURE 2 | Effects of *Chijabyukpi-tang* (CBT) on the mRNA expression levels of pro-inflammatory cytokines and chemokines in TNF-α/IFN-γ-stimulated HaCaT cells. Cell viability of CBT was measured using MTT assay. The group that did not treatment anything was set as negative control **(A)**. Cells were incubated for 24 h in the presence of CBT (12.5 to 100 µg/ml) or in the absence of CBT (media only). HaCaT cells were pretreated with several concentrations of CBT (12.5, 25, 50, and 100 µg/ml) for 2 h and then stimulated with TNF-α/IFN-γ (each 10 ng/ml) for 3 h. The mRNA expression levels of IL-6 **(B)**, IL-13 **(C)**, IL-8 **(D)**, CCL17 **(E)**, and CXCL10 **(F)** were determined using quantitative real-time polymerase chain reaction (qPCR). Data are shown as mean ± SEM of the three independent experiments. $^{###}p < 0.001$ compared with the no-treatment condition, $^{*}p < 0.05$, and $^{***}p < 0.001$ compared with the only TNF-α/IFN-γ treatment condition.

production of TNF-α/IFN-γ-induced cytokines and chemokines in a dose-dependent manner (**Figures 2B–F**).

CBT Up-Regulates Nuclear Nrf2 and HO-1 Protein Levels in TNF-α/IFN-γ-Stimulated HaCaT Cells

The Nrf2/HO-1 signaling pathway plays a crucial mediator role in cell protection from oxidative stress (Loboda et al., 2016). To evaluate whether CBT affects the Nrf2/HO-1 signaling pathway, we investigated the levels of nuclear Nrf2 and HO-1 proteins using western blot. As shown in **Figure 3**, protein levels of nuclear Nrf2 and HO-1 were decreased following cellular stimulation with TNF-α/IFN-γ, however in the groups pretreated with CBT, the nuclear Nrf2 and HO-1 activation was increased in a dose-dependent manner.

CBT Improves DNCB-Induced AD-Like Skin Lesions and Suppresses the Secretion of Serum IgE in Mice

AD-like skin lesions were induced by repeated exposure of the dorsal skin regions of BALB/c mice to DNCB. A significant improvement in dorsal skin condition was observed in mice administrated CBT orally compared to the only DNCB-induced group (n=6) (**Figure 4B**). There were no mouse deaths by CBT (150 and 300 mg/kg) oral administration. We examined H&E staining slides to study the therapeutic effects of CBT on epidermal hyperplasia and the infiltration of inflammatory cells in AD-like dorsal skin tissue. As a result, we found that the dorsal skin thickness of DNCB-induced mice was increased, and that oral administration of CBT reduced the dorsal skin thickness and relieved AD-like lesions in a dose dependent manner (**Figures 4C, D**). The severity scores of the dorsal skin lesions were evaluated with reference to known criteria. We observed that AD-severity scores were suppressed in the CBT-orally administrated mice groups in a dose-dependent manner (**Figure 4E**). We observed a significant decrease in dorsal skin moisture content (%) of approximately 60.9% in the DNCB-treated mice group compared

to the non-DNCB-treated mice group. When orally administered with CBT, the DNCB-treated mice group's skin moisture content was elevated. However, no significant difference was observed (**Figure 4F**). IgE is associated with the T helper 2 (Th2) immune response and is known to play an important role in the pathogenesis and progression of AD (Liu et al., 2011). Thus, total IgE measurements have been used to confirm the severity of AD. We analyzed the effect of CBT on serum IgE levels using ELISA. As a result, serum total IgE was increased in the DNCB-treated mice group compared with the control mice group (control mice group: 267.81 ± 84.81 ng/ml; DNCB-treated mice group: 1,932.53 ± 79.57 ng/ml), and it was reduced by oral administration of CBT (CBT 300 mg/kg administered group: 1,503.92 ± 181.21 ng/ml). In particular, the CBT 300 mg/kg and dexamethasone 1 mg/kg mice groups were significantly inhibited (dexamethasone administered group: 1,500.47 ± 236.26 ng/ml) (**Figure 4G**).

CBT Inhibits the mRNA Expression of Pro-Inflammatory Cytokines and Chemokines in DNCB-Treated Mice

Dorsal skin tissues were collected from each mouse, and the effect of CBT on pro-inflammatory cytokines and chemokines was analyzed using qPCR. In dorsal skin tissues, the expression levels of pro-inflammatory cytokines (IL-4 and IL-6), and chemokines (IL-8 and CXCL10) were remarkably increased in the DNCB-treated mice group compared with the control mice group. Expression levels of pro-inflammatory cytokines and chemokines in the CBT-orally administered mice groups were reduced compared to the DNCB-treated mice group in a dose-dependent manner (**Figure 5**).

CBT Elevates the mRNA Expression of Nrf2 and HO-1 in DNCB-Treated Mice

The mRNA expression levels of Nrf2 and HO-1 were measured using qPCR. We observed that the mRNA expression levels of Nrf2 and HO-1 decreased by treatment with DNCB were increased by oral administration of CBT in a dose-dependent manner (**Figure 6**).
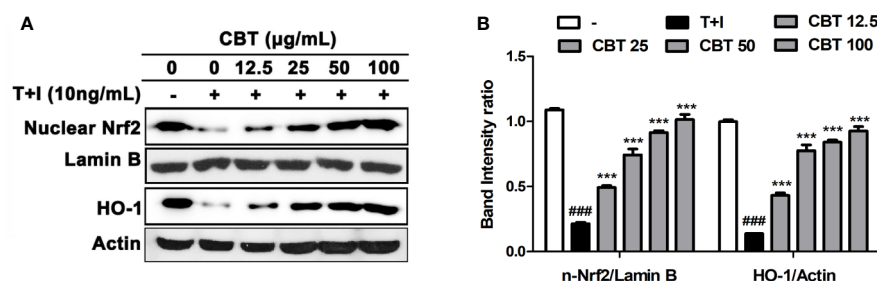
FIGURE 3 | Effects of *Chijabyukpi-tang* (CBT) on the nuclear Nrf2 and HO-1 proteins in TNF-α/IFN-γ-stimulated HaCaT cells. HaCaT cells were pretreated with several concentrations of CBT (12.5, 25, 50, and 100 μg/ml) for 2 h and then stimulated with TNF-α/IFN-γ (each 10 ng/ml) for 3 h. The proteins of nuclear Nrf2, lamin B, HO-1, and actin **(A)** were analyzed using western blotting. The bar graphs represent quantitative density of the bands; nuclear Nrf2/Lamin B, and HO-1/Actin **(B)**. Data are shown as mean ± SEM of the three independent experiments. $^{###}p < 0.001$ compared with the no-treatment condition, $^{***}p < 0.001$ compared with the only TNF-α/IFN-γ treatment condition.
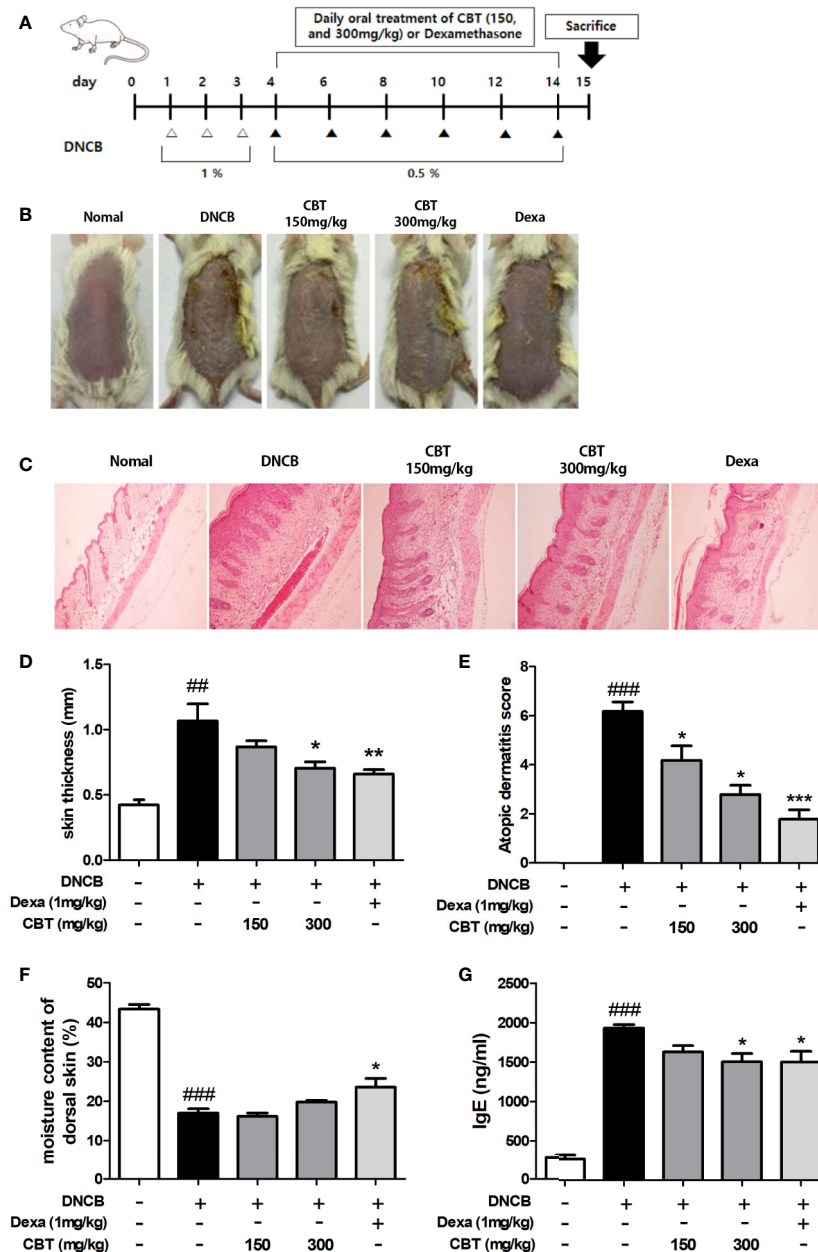
FIGURE 4 | Effects of *Chijabyukpi-tang* (CBT) on clinical signs in 2,4-dinitrochlorobenzene (DNCB)-treated mice skin tissues. The DNCB treatment and oral administration (CBT 150 and 300 mg/kg, and Dexa) schedule used in this experiment **(A)**. On the last day of the experiment, photographs were taken for comparison of skin lesions before the mice were sacrificed. Each dorsal skin picture is representative of each group **(B)**. The histological status of the dorsal skin tissues was observed using hematoxylin and eosin (H&E) staining **(C)**. Images were taken at 100x magnification. The dorsal skin tissue thickness of mice was measured using a micrometer **(D)**. The atopic dermatitis score of mouse dorsal skin lesion was evaluated using the standard evaluation criteria **(E)**. The moisture content of mouse dorsal skin was measured using a Tewameter TM 210 device **(F)**. Serum IgE level was analyzed using enzyme-linked immunosorbent assay (ELISA) **(G)**. Data are shown as mean ± SEM of the three independent experiments. $^{###}p < 0.001$ compared with the control group, $^*p < 0.05$, $^{**}p < 0.01$, and $^{***}p < 0.001$ compared with the DNCB-induced group. The Dexa group was set as positive control.

DISCUSSION

AD is a chronic inflammatory skin disease that occurs frequently in infancy and has a high rate of both recurrence and persistence. AD is characterized by severe itching, eczema, erythema, dry skin, and skin hyperplasia, and is also closely related to other inflammatory diseases (Peng and Novak, 2015). In inflammatory AD skin lesions, the levels of serum IgE, cytokines and chemokines are increased, and there is infiltration of Th cells (Leung and Bieber, 2003). Although these factors causing AD
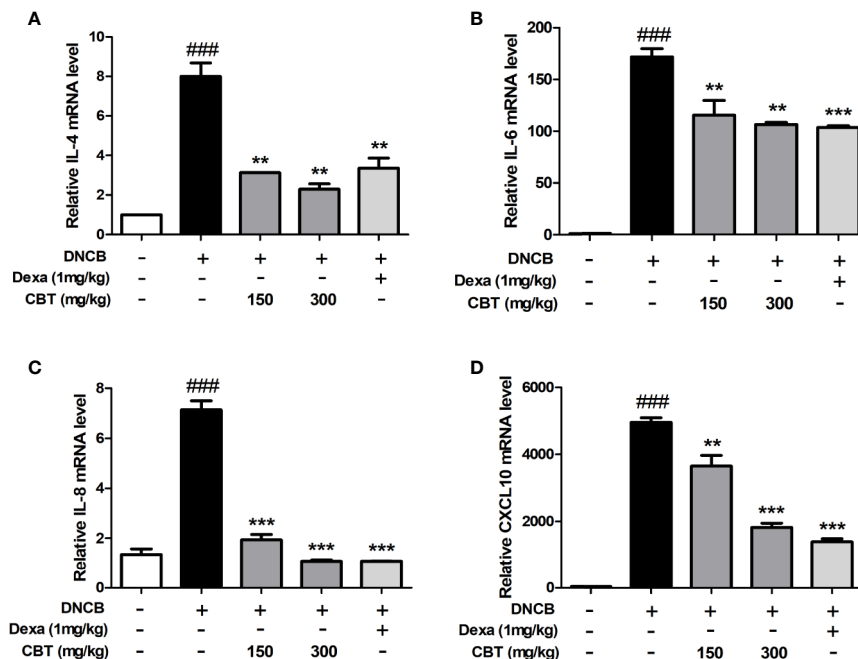
FIGURE 5 | Effects of *Chijabyukpi-tang* (CBT) on the mRNA expression levels of pro-inflammatory cytokines and chemokines in 2,4-dinitrochlorobenzene (DNCB)-treated mice skin tissues. The mRNA expression levels of IL-4 **(A)**, IL-6 **(B)**, IL-8 **(C)**, and CXCL10 **(D)** were analyzed using the quantitative real-time polymerase chain reaction (qPCR). Data are shown as mean ± SEM of the three independent experiments. $^{###}p < 0.001$ compared with the control group, $^{**}p < 0.01$, and $^{***}p < 0.001$ compared with the DNCB-induced group. The Dexa group was set as positive control.
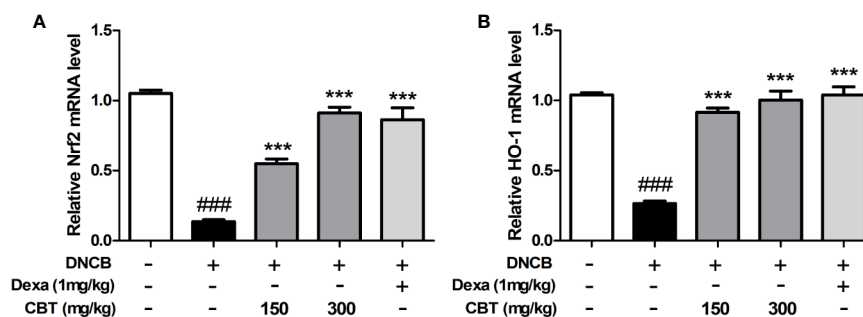
FIGURE 6 | Effects of *Chijabyukpi-tang* (CBT) on the mRNA expression level of HO-1 in DNCB-treated mice skin tissues. The mRNA expression levels of Nrf2 **(A)** and HO-1 **(B)** were analyzed using the quantitative real-time polymerase chain reaction (qPCR). Data are shown as mean ± SEM of the three independent experiments. $^{###}p < 0.001$ compared with the normal group, $^{***}p < 0.001$ compared with the DNCB-treated group. The Dexa group was set as positive control.

progression have been outlined, the exact causes of AD and treatments without side effects have yet to be clarified (Dupuy, 1994). Therefore, there is a need to develop safe and effective therapies for AD, using natural extracts and herbal medicines.

For thousands of years, Northeast Asia (Korea, China, and Japan) has used traditional medicinal herb formulas to treat many diseases. However, since there is no scientific evidence for the efficacy and safety of these medicinal herb formulas, consumers have doubts concerning their use. CBT has been used as a treatment for eczema accompanied with inflammation, but there is still no definitive evidence for the efficacy of CBT

treatment on AD. Therefore, we conducted this study to investigate the anti-inflammatory effects of CBT on AD and its mechanism of action.

Keratinocytes are the main cells that compose the stratum corneum and play a key role in AD pathogenesis. When keratinocytes are damaged by repetitive mechanical stimulations such as scratching behavior, various keratinocyte-derived cytokines and chemokines are secreted to promote inflammatory skin disease progression (Asahina and Maeda, 2017). These secreted factors also cause additional responses by recruiting immune cells such as neutrophils, monocytes, and T cells to AD inflammatory skin

lesions (Giustizieri et al., 2001). T cells recruited to AD inflammatory skin lesions secrete various cytokines such as IL-4, IL-5, IL-6, and IL-13, and chemokines such as IL-8, CCL17, and CXCL10 (Leung and Sorter, 2001). This secretion of pro-inflammatory cytokines and chemokines is known to be caused by the activation of various signaling pathways. Oxidative stress is one of the factors that drive the progression of AD. Since anti-oxidant enzymes play a major role in protecting cells from oxidative stress, increasing anti-oxidant enzymes is an important strategy for treating AD. As a defense against oxidative stress in cells, Nrf2, a transcription factor, moves from the cytosol to the nucleus and increases the expression of anti-oxidant enzyme genes including HO-1. The increased level of HO-1 protein induces cell protection (Ahmed et al., 2017). The Nrf2/HO-1 signaling pathway is involved in the recruitment of various inflammatory cells into inflammatory lesions and is known to contribute to the anti-inflammatory process (Chen et al., 2006; Ryter et al., 2006). In addition, previous studies have indicated that increased HO-1 gene expression attenuates the development of AD skin lesions (Kirino et al., 2008).

Based on these mechanisms, we investigated the anti-inflammatory effect of CBT on TNF-α/IFN-γ-stimulated keratinocytes, and on DNCB-induced AD-like skin lesions in mice.

Firstly, the major compounds of CBT were identified by HPLC, and it was confirmed that it contains crocin (28.671

mg/g), berberine hydrochloride (6.255 mg/g), and glycyrrhizic acid (6.249 mg/g). Previous studies have reported these compounds have anti-inflammatory and anti-oxidant effects (Fagot et al., 2018; Wang et al., 2018).

HaCaT cells are used in many skin disease studies as they can mimic the symptoms of AD in response to inflammatory stimuli such as TNF-α/IFN-γ. In this study, we observed that CBT induces no toxicity in HaCaT cells, and significantly inhibits the increase in mRNA levels of pro-inflammatory cytokines and chemokines in TNF-α/IFN-γ-stimulated HaCaT cells. To further understand the mechanisms of the regulation of the immune response by CBT, we investigated the effects of CBT on the Nrf2/HO-1 signaling pathway. As a result, we confirmed that CBT promoted the migration of Nrf2 into the nucleus and increased the expression levels of the HO-1 gene in a dose-dependent manner. These results suggest that CBT has anti-inflammatory and protective effects on cells by inhibiting the production of pro-inflammatory cytokines and chemokines *via* the Nrf2/HO-1 signaling pathway.

To establish the AD experimental animal model, DNCB was repeatedly applied to the hairless dorsal skin of BALB/c mice (Matsumoto et al., 2004). The mice treated with DNCB were found to exhibit general AD symptoms such as increasing skin thickness, keratinization, and skin dryness. CBT attenuated the symptoms of mice with AD-like skin lesions in a dose-dependent manner. CBT

FIGURE 7 | A graphic summary of atopic dermatitis (AD)-like symptoms and related genes regulated by *Chijabyukpi-tang* (CBT).
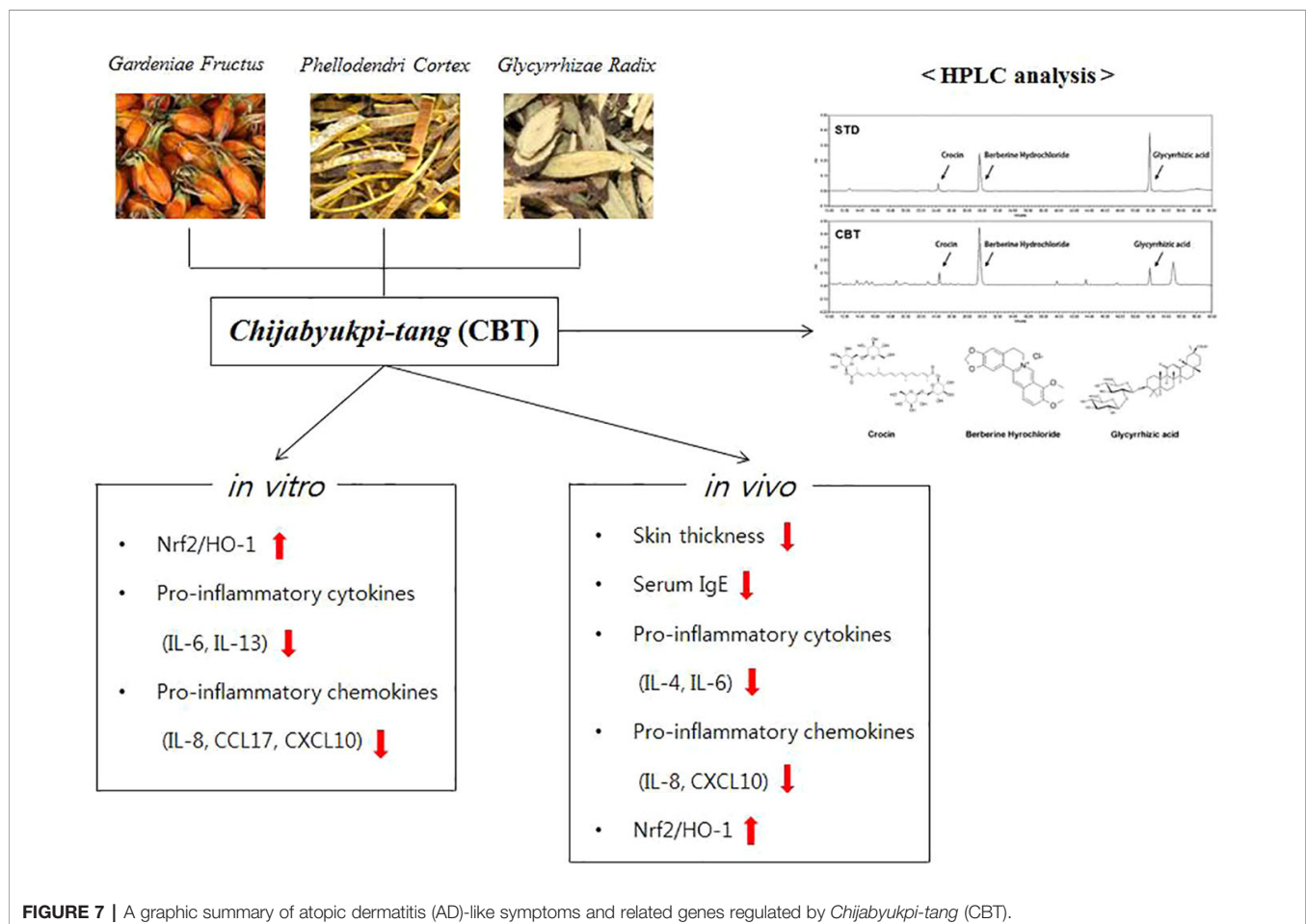
improved the external condition of the dorsal skin and reduced its thickness. In addition, it has also been observed that the reduction in the moisture content of dorsal skin induced by DNCB-treatment is reversed by oral administration of CBT. DNCB-induced dorsal skin damage leads to AD-like inflammatory skin disease characterized by secretion of a variety of pro-inflammatory cytokines and chemokines by damaged keratinocytes resulting in Th cell activation. In this experiment, serum IgE levels, and expression levels of various cytokines and chemokines in skin tissues were increased by DNCB stimulation. These increased serum IgE and gene expression levels in skin tissues were significantly inhibited by the oral administration of CBT. These data provide experimental evidence for the anti-atopic effect of CBT in AD animal models. In these animal models, we also observed expression levels of Nrf2 and HO-1 in tissues to investigate whether the anti-inflammatory response was mediated through the Nrf2/HO-1 signaling pathway. As a result, we found that the expression levels of the Nrf2 and HO-1 gene were increased in a dose-dependent manner by CBT, similar to the result seen in the HaCaT cells.

In conclusion, CBT induces anti-inflammatory effects by up-regulating Nrf2/HO-1 signaling in TNF-α/IFN-γ-stimulated HaCaT cells. In addition, CBT improves AD-like skin lesions and inhibits inflammatory cytokines and chemokines in DNCB-treated mice models (**Figure 7**). These results suggest that CBT is a potential therapeutic candidate for the treatment of AD. However, the effects of dexamethasone or the individual herbal components (crocin, berberine hydrochloride and glycyrrhizic acid) vs CBT are not yet known, and further studies are required.

DATA AVAILABILITY STATEMENT

All datasets generated for this study are included in the article/ supplementary material.

ETHICS STATEMENT

The animal study was reviewed and approved by the Animal Experiment Ethics Committee of Chonbuk National University (CBNU-IACUC) (Confirmation No. CBNU 2016-0011).

AUTHOR CONTRIBUTIONS

D-KK, MP, J-HL, and J-YL designed the study. J-HL and J-YL performed the experiments, analyzed the date. J-YL wrote the draft manuscript. J-HL rewrote and revised the manuscript. EJ, HN, and SP read the manuscript. All authors contributed to the article and approved the submitted version.

ACKNOWLEDGMENTS

REFERENCES

Ahmed, S. M., Luo, L., Namani, A., Wang, X. J., and Tanga, X. (2017). Nrf2 signaling pathway: Pivotal roles in inflammation. *Biochim. Biophys. Acta Mol. Basis Dis.* 1863 (2), 585–597. doi: 10.1016/j.bbadis.2016.11.005

Akram, M., Shin, I., Kim, K. A., Noh, D., Baek, S. H., Chang, S. Y., et al. (2016). A newly synthesized macakurzin C-derivative attenuates acute and chronic skin inflammation: The Nrf2/heme oxygenase signaling as a potential target. *Toxicol. Appl. Pharmacol.* 307, 62–71. doi: 10.1016/j.taap.2016.07.013

Asahina, R., and Maeda, S. (2017). A review of the roles of keratinocyte-derived cytokines and chemokines in the pathogenesis of atopic dermatitis in humans and dogs. *Vet. Dermatol.* 28 , (1) 16–(1) e5. doi: 10.1111/vde.12351

Chen, X. L., Dodd, G., Thomas, S., Zhang, X., Wasserman, M. A., Rovin, B. H., et al. (2006). Activation of Nrf2/ARE pathway protects endothelial cells from oxidant injury and inhibits inflammatory gene expression. *Am. J. Physiol. Heart. Circ. Physiol.* 290 (5), 1862–1870. doi: 10.1152/ajpheart.00651.2005

Chen, F. P., Chen, F. J., Jong, M. S., Tsai, H. L., Wang, J. R., and Hwang, S. J. (2009). Modern use of Chinese herbal formulae from Shang-Han Lun. *Chin. Med. J.* 122 (16), 1889–1894. doi: 10.3760/cma.j.issn.0366-6999.2009.16.010

Choi, W. Y., and Lee, S. J. (2017). Two Case Reports treated with Chijabackpi-tang based on Shanghanlun provisions. *J. Kor. Med. Assoc. Clin. Sanghan-Geumgwe.* 9 (1), 101–113. doi: 10.22891/kmedia.2017.9.1.101

Choi, J. H., Jin, S. W., Han, E. H., Park, B. H., Kim, H. G., Khanal, T., et al. (2014). Platycodon grandiflorum root-derived saponins attenuate atopic dermatitis-like skin lesions via suppression of NF-kappaB and STAT1 and activation of Nrf2/ARE-mediated heme oxygenase-1. *Phytomedicine* 21 (8-9), 1053–1061. doi: 10.1016/j.phymed.2014.04.011

Cury Martins, J., Martins, C., Aoki, V., Gois, A. F., Ishii, H. A., and da Silva, E. M. (2015). Topical tacrolimus for atopic dermatitis. *Cochrane Database Syst. Rev.* 1 (7), CD009864. doi: 10.1002/14651858.CD009864.pub2

Darlenski, R., Kazandjieva, J., Hristakieva, E., and Fluhr, J. W. (2014). Atopic dermatitis as a systemic disease. *Clin. Dermatol.* 32 (3), 409–413. doi: 10.1016/j.clindermatol.2013.11.007

Debnath, T., Lee, Y. M., Lim, J. H., and Lim, B. O. (2018). Anti-allergic and anti-atopic dermatitis effects of Gardenia Fructus extract. *Food. Agr. Immunol.* 29 (1), 665–674. doi: 10.1080/09540105.2018.1436523

Dupuy, P. (1994). Does atopic dermatitis result from cytokine dysregulation? *J. Invest. Dermatol.* 102 (5), 741. doi: 10.1111/1523-1747.ep12398629

Fagot, D., Pham, D. M., Laboureau, J., Planel, E., Guerin, L., Nègre, C., et al. (2018). Crocin, a natural molecule with potentially beneficial effects against skin ageing. *Int. J. Cosmet. Sci.* 40 (4), 388–400. doi: 10.1111/ics.12472

Fan, H. J., Xie, Z. P., Lu, Z. W., Tan, Z. B., Bi, Y. M., Xie, L. P., et al. (2018). Anti-inflammatory and immune response regulation of Si-Ni-San in 2,4-dinitrochlorobenzene-induced atopic dermatitis-like skin dysfunction. *J. Ethnopharmacol.* 222, 1–10. doi: 10.1016/j.jep.2018.04.032

Giustizieri, M. L., Mascia, F., Frezzolini, A., Pità, O. D., Chinni, L. M., Giannetti, A., et al. (2001). Keratinocytes from patients with atopic dermatitis and psoriasis show a distinct chemokine production profile in response to T cell–derived cytokines. *J. Allergy Clin. Immunol.* 107 (5), 871–877. doi: 10.1067/mai.2001.114707

Guttman-Yassky, E., Nograles, K. E., and Krueger, J. G. (2011). Contrasting pathogenesis of atopic dermatitis and psoriasis-part I: clinical and pathologic concepts. *J. Allergy Clin. Immunol.* 127 (5), 1110–1118. doi: 10.1016/j.jaci.2011.01.053

Higashi, Y., and Kanzaki, T. (2006). Effects of Kampo Medicine, Shishi-hakuhi-to, on Elderly Patients with Pruritic Skin Diseases Measured Using a Patient Diary with an Itching Visual Analog Scale. *Nishi. Nihon. Hifuka.* 68 (4), 408–412. doi: 10.2336/nishinihonhifu.68.408

Homey, B., Steinhoff, M., Ruzicka, T., and Leung, D. Y. (2006). Cytokines and chemokines orchestrate atopic skin inflammation. *J. Allergy Clin. Immunol.* 118 (1), 178–189. doi: 10.1016/j.jaci.2006.03.047

Hon, K. L., Chan, B. C., and Leung, P. C. (2011). Chinese herbal medicine research in eczema treatment. *Chin. Med.* 6, 17. doi: 10.1186/1749-8546-6-17

Kapoor, R., Menon, C., Hoffstad, O., Bilker, W., Leclerc, P., and Margolis, D. J. (2008). The prevalence of atopic triad in children with physician-confirmed atopic dermatitis. *J. Am. Acad. Dermatol.* 58 (1), 68–73. doi: 10.1016/j.jaad.2007.06.041

Kiebert, G., Sorensen, S. V., Revicki, D., Fagan, S. C., Doyle, J. J., Cohen, J., et al. (2002). Atopic dermatitis is associated with a decrement in health-related quality of life. *Int. J. Dermatol.* 41 (3), 151–158. doi: 10.1046/j.1365-4362.2002.01436.x

Kirino, M., Kirino, Y., Takeno, M., Nagashima, Y., Takahashi, K., Kobayashi, M., et al. (2008). Heme oxygenase 1 attenuates the development of atopic dermatitis-like lesions in mice: implications for human disease. *J. Allergy Clin. Immunol.* 122 , (2) 290–297. doi: 10.1016/j.jaci.2008.05.031

Lee, J. H., Ki, H. H., Kim, D. K., and Lee, Y. M. (2018). Triticum aestivum sprout extract attenuates 2,4–dinitrochlorobenzene–induced atopic dermatitis–like skin lesions in mice and the expression of chemokines in human keratinocytes. *Mol. Med. Rep.* 18 , (3) 3461–3468. doi: 10.3892/mmr.2018.9339

Leung, D. Y., and Bieber, T. (2003). Atopic dermatitis. *Lancet* 361 (9352), 151–160. doi: 10.1016/S0140-6736(03)12193-9

Leung, D. Y., and Sorter, N. A. (2001). Cellular and immunologic mechanisms in atopic dermatitis. *J. Am. Acad. Dermatol.* 44 (1 Suppl), S1–S12. doi: 10.1067/mjd.2001.109815

Liu, F. T., Goodarzi, H., and Chen, H. Y. (2011). IgE, mast cells, and eosinophils in atopic dermatitis. *Clin. Rev. Allergy Immunol.* 41 (3), 298–310. doi: 10.1007/s12016-011-8252-4

Loboda, A., Damulewicz, M., Pyza, E., Jozkowicz, A., and Dulak, J. (2016). Role of Nrf2/HO-1 system in development, oxidative stress response and diseases: an evolutionarily conserved mechanism. *Cell Mol. Life Sci.* 73 (1), 3221–3247. doi: 10.1007/s00018-016-2223-0

Matsumoto, K., Mizukoshi, K., Oyobikawa, M., Ohshima, H., and Tagami, H. (2004). Establishment of an atopic dermatitis-like skin model in a hairless mouse by repeated elicitation of contact hypersensitivity that enables to conduct functional analyses of the stratum corneum with various non-invasive biophysical instruments. *Skin Res. Technol.* 10 (2), 122–129. doi: 10.1111/j.1600-0846.2004.00062.x

Mie, W., Eiko, S., Kazuhiko, Y., Kazuhiko, U., Masaaki, Y., Yasushi, O., et al. (2009). Shishihakuhito, a traditional Chinese medicine for atopic dermatitis, inhibits IgE-mediated histamine release from rat RBL-2H3 basophilic leukocyte cells. *J. Trad. Med.* 26 (1), 44–49. doi: 10.11339/jtm.26.44

Peng, W., and Novak, N. (2015). Pathogenesis of atopic dermatitis. *Clin. Exp. Allergy* 45 , (3) 566–574. doi: 10.1111/cea.12495

Ryter, S. W., Alam, J., and Choi, A. M. (2006). Heme oxygenase-1/carbon monoxide: from basic science to therapeutic applications. *Physiol. Rev.* 86 (2), 583–650. doi: 10.1152/physrev.00011.2005

Shaw, T. E., Currie, G. P., Koudelka, C. W., and Simpson, E. L. (2011). Eczema prevalence in the United States: data from the 2003 National Survey of Children's Health. *J. Invest. Dermatol.* 131 (1), 67–73. doi: 10.1038/jid.2010.251

Wang, X., Feng, S., Ding, N., He, Y., Li, C., Li, M., et al. (2018). Anti-Inflammatory Effects of Berberine Hydrochloride in an LPS-Induced Murine Model of Mastitis. *Evid. Based Compl. Alternat. Med.* 2018, 5164314. doi: 10.1155/2018/5164314

Yamanaka, K., and Mizutani, H. (2011). The role of cytokines/chemokines in the pathogenesis of atopic dermatitis. *Curr. Probl. Dermatol.* 41, 80–92. doi: 10.1159/000323299

Yang, X. L., Liu, D., Bian, K., and Zhang, D. D. (2013). Study on in vitro anti-inflammatory activity of total flavonoids from Glycyrrhizae Radix et Rhizoma and its ingredients. *Zhongguo Zhong Yao Za Zhi.* 38 (1), 99–104. doi: 10.4268/cjcmm20130120

Ameliorative and Synergic Effects of Derma-H, a New Herbal Formula, on Allergic Contact Dermatitis

Si Yeon Jo[1], Mi Hye Kim[1], Haesu Lee[1], Sun Haeng Lee[2] and Woong Mo Yang[1*]

[1] Department of Convergence Korean Medical Science, College of Korean Medicine, Kyung Hee University, Seoul, South Korea, [2] Department of Clinical Korean Medicine, Graduate School, Kyung Hee University, Seoul, South Korea

Allergic contact dermatitis (ACD) is characterized by itching, skin inflammation, and allergic responses caused by release of immunoglobulin E and T helper 2-specific cytokines. The aim of this study is to investigate the ameliorative and synergic effects of herbal formula, Derma-H, containing *Astragalus membranaceus* Fisch. ex Bunge (AM) and *Nepeta tenuifolia* Benth (NT) which have been used as traditional medicinal herbs for the cure of dryness, edema, and pruritus. 2,4-Dinitrochlorobenzene (DNCB) was applied for ACD induction. AM, NT, and a mixture of AM and NT was topically applied to skin lesions for 11 days. Dermatitis score and number of scratches were significantly diminished in AM, NT, and AM + NT (Derma-H)-treated groups. Especially, Derma-H was more effective than single treatment of AM and NT on skin hyperplasia and mast cell infiltration. Also, NGF expression decreased by NT and a mixture of AM and NT. Additionally, series of TrkA, Raf-1, MEK, and ERK were significantly inhibited by topical AM and NT application. Those findings suggested AM and NT treatment has a synergic effect on DNCB-induced ACD in mice.

Keywords: allergic contact dermatitis, *Astragalus membranaceus* Fisch. ex Bunge, *Nepeta tenuifolia* Benth, pruritus, inflammation

INTRODUCTION

Allergic contact dermatitis (ACD), a delayed-type of hypersensitivity, is caused by a variety of contact allergens. Approximately, 7% of worldwide population suffers from ACD and the prevalence rate of ACD is consistently increasing (Kim et al., 2013). ACD patients suffer from several symptoms including relapsing eczema, swelling, redness, dryness, and itching (Lipozencic and Wolf, 2007). There are several factors to trigger ACD such as stress, irritants, allergens, microorganisms, and environmental factors (Park et al., 2016). Although the pathogenesis of ACD is not fully known, multiple studies reported that inflammatory and pruritic mediators are involved in the progress of ACD (Nedoszytko et al., 2014). T helper (Th) 2 cytokines are typical inflammatory mediators in ACD (Kim et al., 2018). In addition, recruitment of nerve growth factor (NGF) and interleukin (IL)-31 induces severe itching in ACD (Feld et al., 2016). Natural killer cells, T regulatory cells, B cells, epidermal Langerhans cells, and keratinocytes are also involved in ACD (Gober and Gaspari, 2008).

Because the incidence of ACD is still increasing, the therapeutic request for improving ACD is gradually rising (Lee et al., 2016). To alleviate ACD symptoms, there are various drugs such as anti-inflammatory, anti-histamine, and glucocorticosteroid drugs as well as moisturizers (Yuan et al., 2010; Lee et al., 2017). However, long period-use of steroids including dexamethasone causes skin weakening, facial edema, psoriasis, furuncles, dryness, and bleeding (Walling and Swick, 2010). For those reasons, ACD patients hesitate to take such drugs because of their severe side effects (Arkwright et al., 2013). Thus, the development of novel ACD treatment using plant-derived natural compounds remains as a global challenge (Kim et al., 2013).

In East Asia, the dried root of *Astragalus membranaceus* Fisch. ex Bunge (AM) has been used as a conventional medicinal herb for more than 2,000 years (Zhou et al., 2018). Additionally, AM has a therapeutic effect on inflammation, skin-reinforcing, wound healing, and immune-regulation (Cho and Leung, 2007). The dried leaves of *Nepeta tenuifolia* Benth (NT) have been widely used in Japan, China, and Korea as an anti-inflammatory treatment for influenza symptoms such as headache, cough, nasal plug, fever, and severe fatigue (Grewe et al., 1998). Clinically, many prescriptions contain AM and NT such as Danggwieumja (Dangguiyinzi), Haedoknaetaksan (Jieduneituosan), Danggwieum (Dangguiyin), Daegosamhwan (Dakushenwan), and Haedokbangpungtang (Jiedufangfengtang) are used to cure skin diseases. Especially, it is reported that AM preserves cutaneous lesions by alleviating the severity of psoriasis, furuncle, and eczema and regenerating of skin tissues, while NT usually improves allergic, inflammatory, and infectious skin disease. Based on the previous studies (Choi et al., 2013; Choi et al., 2016; Choi et al., 2018), the hypothesis was suggested that a mixture of AM and NT has synergic effects on ACD.

In this study, the effects and its possible mechanism of AM and NT on ACD were investigated in DNCB-induced mice model. Histopathological features of skin lesions and scratching behaviors were analyzed. Especially, to demonstrate the clinical efficacy of AM and NT on pruritus, NGF, Tropomyosin receptor kinase A (TrkA), Raf-1 (Serine/Threonine kinase), MEK (MAPK/ERK kinase), and Extracellular signal-regulated kinases (ERK) pathway and interleukin (IL)-31 were examined. Moreover, expression levels of interleukin (IL)-4, -6, -10, -13, tumor necrosis factor (TNF)-α, and transforming growth factor (TGF)-β in ACD-like skin lesions were confirmed the inhibitory effects of AM and NT on immune responses in ACD.

MATERIALS AND METHODS

Chemicals and Reagents

2,4-dinitrochlorobenzene (DNCB) and Dexamethasone was purchased from Sigma Aldrich (St.Louis, USA). Sodium dodecyl sulfate (SDS) was applied by Biosesang (Sungnam, Korea). Antibodies used in Western blot such as β-actin, Raf-1, p-Raf-1, anti-rabbit, and anti-mouse horseradish peroxidase-

conjugated secondary antibody were obtained from Santa Cruz (CA, USA). ERK, p-ERK, MEK, p-MEK were purchased from Cell Signaling Technology (Danvers, MA, USA). In addition, antibody of TrkA was applied by Abcam (Cambridge, UK). For reverse transcription polymerase chain reaction (RT-PCR) experiment, Maxime RT Premix and Maxime PCR premix were purchased from iNtRON Biotechnology Inc. (Sungnam, Korea). Specific primers such as IL-4, -6, -10, -13, -31, TNF-α, interferon (IFN)-γ, TGF-β, and GAPDH used for amplifying were designed by Bioneer Corp. (Daejeon, Korea).

Preparation of Sample A. membranaceus Fisch. ex Bunge and N. *tenuifolia* Benth, which are originated from Korean medicine, were obtained from Dong-Yang Herb (Seoul, Korea). The batch numbers of *A. membranaceus* Fisch. ex Bunge and N. *tenuifolia* Benth were DY074K02H and DY052S02H. Ten grams of AM and NT, respectively, were extracted with 100 ml of distilled water by refluxing at 100°C for 2 h. The extracts were filtered by vacuum filter and condensed in a rotary evaporator under reducing pressure. Then condensed samples were pre-dried in −80°C about 48 h. Samples were powdered under freeze-dryer for 72 h. The yields of AM and NT were 29.57 and 17.10%.

Standardization of AM and NT

Each of AM and NT extracts were identified by formononetin and pulegone using high-performance liquid chromatography diode array detector (HPLC-DAD). Formononetin and pulegone were chosen to identify AM and NT extracts, respectively, as standard compounds according to the National Standard of Traditional Medicinal (Herbal and Botanical) Materials in the Korean Pharmacopoeia. The HPLC apparatus was a Gilson System equipped with a 234 Autosampler, a UV/VIS-155 detector and a 321 HPLC Pump (Gilson, Seoul, Korea). In case of AM, chromatography was performed at room temperature at a flow rate of 0.5 ml/min and 10 µl was analyzed for 50 min. The retention time of formononetin was 31.7 min. Standardization of NT was based on the content of pulegone. Chromatographical analysis was performed at room temperature at a flow rate of 1.0 ml/min, and 10 µl was analyzed for 30 min. The retention time of pulegone was 18.4 min. Consequently, the concentrations of formononetin and pulegone were 2 mg/g in AM extract and 7.03 mg/g in NT extract, respectively (**Figures S1** and **S2**).

Animals

All of 30 male BALB/c mice aged 5-week-old were purchased from Raonbio Inc. (Yongin, Korea). Animals were housed in a well-controlled animal room with a 12 h light/dark cycle and humid condition of 50 ± 5% at 22–24°C. All mice were fed with standard chow diet and tap water. Animal care and experimental procedures were performed in accordance with the "Guide for the Care and Use of Laboratory Animals" (Department of Health, Education and Welfare, NIH publication #78-23, 1996). This animal experiment was approved by the Guide for the Care and Use of Laboratory Animals of Kyung Hee University, Seoul, Korea (KHUASP(SE)-16-159).

After 1 week of adaptation, mice were divided into six groups (n = 5): (i) NOR: normal control, with no sensitization and

vehicle application; (ii) DNCB: negative control, with DNCB sensitization and vehicle application; (iii) DEX: positive control, with DNCB sensitization and 10 μM (3.9246×10^{-3} mg/ml) of dexamethasone application; (iv) AM: with DNCB sensitization and 30 mg/ml of AM application; (v) NT: with DNCB sensitization and 20 mg/ml of NT application; and (vi) AM + NT: with DNCB sensitization and 50 mg/ml AM and NT, 30 mg AM, and 20 mg NT in 1 ml distilled water, application. The concentrations of AM (30 mg/ml) and NT (20 mg/ml) were determined by each yield to correspond to the same amount of raw materials. A mixture consists of 30 mg of AM and 20 mg of NT dissolved in 1 ml distilled water. Animal experiment was performed as described previously (Choi et al., 2017). Before the experiment, the skin on the upper back was shaved by an electronic shaver. 2,4-dinitrochlorobenzene (DNCB) was used as a sensitization substance for ACD, which initiates skin innate immunity activation. For first challenge of ACD, 200 μl of 1% DNCB in acetone/olive oil (4:1, v/v) was topically applied to the dorsal skin of mice once daily. After 3 days of sensitization, mice did not receive any further treatment during the next 4 days. Then, sodium dodecyl sulfate (SDS), samples, and DNCB were treated every 3 h in order, respectively, at second challenge of ACD. In detail, 200 μl of 4% SDS was applied to the dorsal skin of mice to disrupt the skin barrier and remove cuticle layers. After 3 h, 200 μl of samples including AM, NT, and mixture were topically administrated to the dorsal skin, while DNCB group was received vehicle. Then after 3 h of sample treatment, 200 μl of 0.5% DNCB was treated to the skin lesions of mice. All treatments including 4% SDS, samples, and 0.5% DNCB were repeated for consecutive 11 days. There was no side effects or abnormalities following AM and NT treatment during the experiment. At the end of experiment, all mice were sacrificed.

Measurement of Dermatitis Score

The extent of (1) erythema/hemorrhage, (2) dryness/scarring, (3) edema, and (4) erosion/excoriation was scored as 0 (none), 1 (mild), 2 (moderate), or 3 (severe). All mice were photographed by digital camera (Sony, Tokyo, Japan) under anesthesia. The severity of the dorsal skin was measured by three researchers without group information. The sum of the separate scores was described as the dermatitis score. Before sacrifice, mice were anesthetized with 100 μl of zoletil and rompun mixture. Then the severity of the dorsal skin in all mice was measured by triplicate.

Measurement of Scratching Behavior

The previous day of sacrifice, all mice were set in a separated plastic cage for stabilizing for 1 h after sensitization with 200 μl of 0.5% DNCB. Scratching behavior of each group was recorded for 20 min. The number of scratching was counted by acknowledging the scratches only the back side of the body. The scratching episode of each group was counted by a blind test. The number of scratching of each mouse was averaged from the counts of three researchers.

Histological Analysis for H&E Staining

Skin tissues from the upper back of mice were fixed in 4% formalin for 24 h, dehydrated. After embedding of each specimen, the specimens were sliced to 4 μm of thickness. Sections of skin specimens were stained with hematoxylin and eosin (H&E). Stained specimens were cover-slipped with VECTA Mount permanent mounting medium (VECTOR laboratories, Inc., Burlingame, CA). Digital images were obtained from Leica Application Suite (LAS) Microscope Software (Leica Microsystems Inc., IL, USA). The magnification of H&E staining was ×100.

Histological Analysis for Toluidine Blue Staining

For the evaluation of mast cell infiltration, sliced specimens of 4 μm thickness were stained with toluidine blue solution. Digital images were obtained from Leica Application Suite (LAS) Microscope Software. Then five sites of every stained specimen were chosen for counting mast cells numbers at random with the scale of ×200.

Western Blot Analysis

Each sample of dorsal skins were homogenized in tissue protein extraction buffer (Thermo scientific, Rockford, USA) with protease inhibitor cocktail tablets (Roche, Mannheim, Germany). Twenty micrograms of protein from dorsal skin was denatured with 5% SDS loading buffer. The prepared samples were loaded on 10% SDS-polyacrylamide gel electrophoresis. Then electro-transferred to activated polyvinylidene fluoride membranes. Membranes were blocked by 3% bovine serum albumin in tris-buffered saline (TBS) containing 1% tween 20 (TBS-T) and incubated with the specific antibodies at 4°C overnight (β-actin, Raf-1, p-Raf-1; Santa Cruz, CA, USA, 1:1,000 dilutions in TBS-T, ERK, p-ERK, MEK, p-MEK; Cell Signaling Technology, Danvers, MA, USA, 1:1,000 dilution in TBS-T, TrkA; Abcam, Cambridge, UK, 1:1,000 dilution in TBS-T). After washing of those membranes for 10 min three times, membranes were incubated with anti-rabbit and anti-mouse horseradish peroxidase-conjugated secondary antibody (Santa Cruz, 1:2,000 dilutions in TBS-T) for 1 h at room temperature. Then proteins were developed with an enhanced chemiluminescence detection reagent (AbClon, Seoul, Korea) by a Davinch-Western imaging system (Davinch-K, Seoul, Korea).

Measurement of Inflammatory Cytokine Levels

Total RNA from dorsal skin lesions was extracted with RNA extraction solution (Nanohelix, Daejeon, Korea) following the manufacturer's instruction. Isolated total 2 μg RNA was synthesized into cDNA using Maxime RT Premix (iNtRON Biotechnology Inc., Sungnam, Korea). Synthesis of cDNA was arranged as follows: stage 1: 45°C for 60 min; stage 2: 95°C for 5 min. The cDNA was amplified with using Maxime PCR premix (iNtRON Biotechnology Inc., Sungnam, Korea) and specific primers such as IL-4, -6, -10, -13, -31, TNF-α, interferon (IFN)-γ, TGF-β, and GAPDH. The primers used for amplifying were designed by Bioneer Corp. (Daejeon, Korea) and listed in **Table 1**. Optimal conditions of each factors for RT-PCR were confirmed by triplicate. Gene expressions were relatively estimated with the

Target gene	5′ → 3′ Forward primer	5′ → 3′ Reverse primer
IL-6	CGGAGAGGAGACTTCACAGAGGA	GGAGAGCATTGGAAATTGGGG
TNF-α	CCTGTAGCCCACGTCGTAGC	TTGACCTCAGCGCTGAGTTG
IL-10	GACCAGCTGGACAACATACTGCTAA	GTTGAGATGATGCTTTGACAGAAG
TGF-β	CGGGGCGACCTGGGCACCATCCATGAC	CTGCTCCACCTTGGGCTTGCGACCCAC
IL-4	ATGGGTCTCAACCCCCAGC	GCTCTTTACGCTTTCCAGGAAGTC
IL-13	ACCACGGTCATTGCTCTCA	GTGTCTCGGACATGCAAGCT
IL-31	TCGGTCATCATAGCACATCTGGAG	GCACAGTCCCTTTGGAGTTAAGTC
IFN-γ	AGCGGCTGACTGAACTCAGATTGTAG	GTCACAGTTTTCAGCTGTATAGGG
GAPDH	GGCATGGACTGTGGTCATGA	TTCACCACCATGGAGAAGGC

housekeeping genes (GAPDH) mRNA levels. The relative changes of target gene expression were analyzed by Gel doc (DAIHAN Scientific Co, Ltd., Wonju-si, Gangwon-do, Korea).

Statistical Analysis

Data are presented as the mean ± standard error of the mean (S.E.M). Differences between control groups and application groups were examined using a one-way analysis of variance (ANOVA) and Tukey's tests. $p < 0.05$ were considered statistically significant.

RESULTS

Effect of AM and NT on Skin Dermatitis Score and Scratching Behavior

Dermatitis symptoms including erythema, dryness, edema, erosion were developed following the DNCB sensitization. As a negative control; dermatitis score of DNCB group was calculated about 6.1, unlike 0 of the normal control group; NOR group. Compared with DNCB group, skin severity in DEX group as a positive control was clearly ameliorated as shown in 56.0% reduction of dermatitis score. The skin severity of each group were improved as following the application of AM and NT. Compared with DNCB group, Dermatitis scores of AM and NT group were decreased by 18.7% and 25.3%, respectively. Moreover, AM + NT group also showed noticeable improvement of skin severity. The score of AM + NT group was decreased by 27.5% compared with DNCB group (**Figure 1A**).

Additionally, DNCB-treated mice showed a noticeable increase of scratching actions than NOR group about 24.8 folds. As a positive control, DEX treatment depressed the number of scratching behavior up to 32.1% compared with DNCB group. Each of AM and NT treatment ameliorated the scratching behavior up to 30.0 and 25.6%. In addition, topical application of AM and NT reduced the scratching behavior up to 31.2% compared with DNCB group (**Figure 1B**).

Effect of AM and NT on Histological Changes

As follow H&E staining, the DNCB group indicated skin hyperplasia of the epidermis and lichenification. Thickness of epidermis and dermis were increased 6.1- and 2.1 folds in DNCB group compared with NOR group. There were significant reductions of epidermal and dermal thickness in all treatment groups compared with DNCB group. Each AM and NT treatment influenced skin hyperplasia compared with DNCB group (Epidermis: AM 50.1%, NT 54.7%; dermis: AM 18.9%, NT 31.6%). Similarly, the treatment of mixture, Derma-H, markedly inhibited hyperplasia of the epidermis and dermis similar to DEX (Epidermis: AM + NT 55.2%, DEX 64.4%; dermis: AM + NT 35.2%, DEX 25.8%) (**Figures 2A, B**).

Effect of AM and NT on Mast Cell Degranulation

As follow toluidine blue staining, the infiltration of mast cells in DNCB group was 8.7 folds higher than that in NOR group. Each treatment of AM and NT also reduced mast cell infiltration about 38.5 and 43.0%, respectively. In addition, the number of mast cells was significantly reduced by 49.0% in AM and NT treated mice (**Figure 3**).

Effect of AM and NT on NGF-TrkA Signaling Pathway-Related Factors

To identify the pruritic effects of AM and NT mixture, the expressions of NGF-TrkA signaling pathway-related factors were estimated (**Figure 4A**). Expression of NGF in DNCB group was 2.1 folds higher than NOR group. Topical treatment of DEX reduced NGF expression about 42.0% compared with DNCB group. Compared with DNCB group, the expressions of NGF in AM and NT treated groups were reduced about 11.8 and 16.3% respectively. Similar to the result of DEX group, a mixture of AM and NT down-regulated the expression of NGF up to 32.5% (**Figure 4B**).

Series of TrkA, Raf-1, MEK, and ERK levels were analyzed by Western blot analysis. Phosphorylation of TrkA, Raf-1, MEK, and ERK were considerably increased by 2.9, 2.8, 4.1, and 2.7 folds in DNCB-induced ACD skin, compared with NOR group. With the treatment of AM and NT, series of TrkA, Raf-1, MEK, and ERK expressions were remarkably inhibited by 56.2, 77.6, 73.6, and 33.5% compared with DEX group about 58.7, 22.6, 74.8, and 39.3% (**Figures 4C–F**). Also, Raf-1, MEK, and ERK phosphorylation were decreased in AM and NT groups, respectively (Raf-1: AM 42.5%, NT 50.0%; MEK: AM 61.0%, NT 72.8%; ERK: AM 6.5%, NT 15.7%).
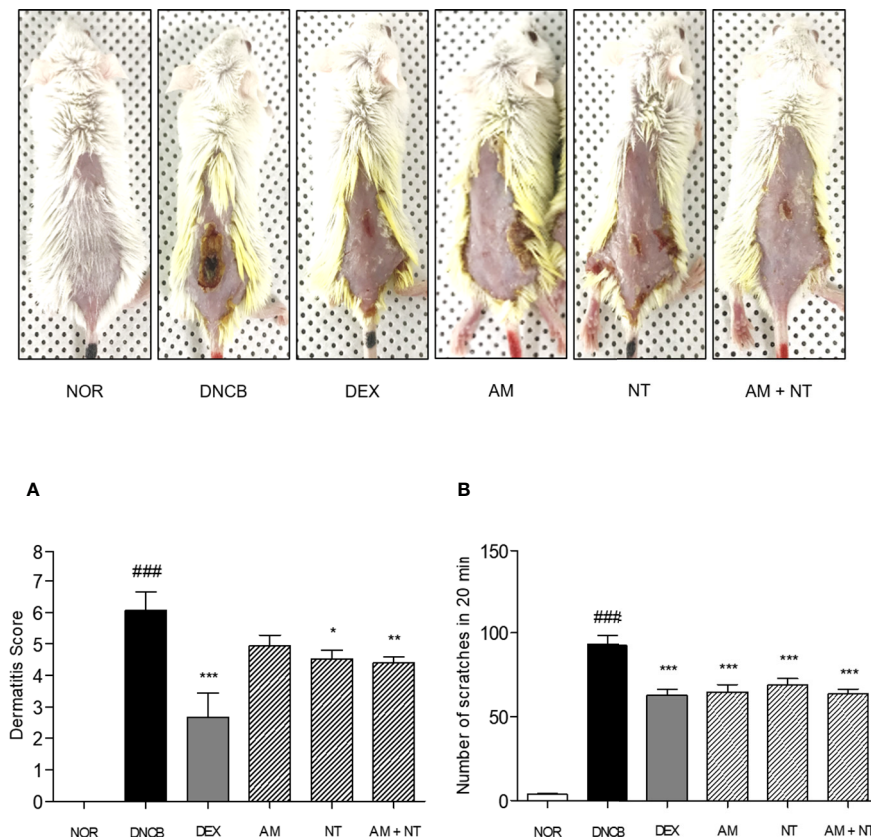
FIGURE 1 | Effects of AM, NT, and a mixture of AM and NT on skin dermatitis scores **(A)** and scratching behaviors **(B)** with allergic contact dermatitis skin lesions. The scratching behavior was evaluated 1 h after the last DNCB application on the day before sacrifice. Data were presented as means ± S.E.M (n = 5). $^{###}p < 0.001$ *vs.* NOR; $^{*}p < 0.05$, $^{**}p < 0.01$, and $^{***}p < 0.001$ *vs.* DNCB.

Effect of AM and NT on Inflammatory Cytokines

To investigate the anti-inflammatory effects of AM and NT, mRNA expression levels of inflammatory-mediators including pro-inflammatory cytokines (IL-6 and TNF-α), counter-regulatory cytokines (IL-10 and TGF-β), Th2 cytokines (IL-4, -13, and -31), and Th1 cytokine (IFN-γ) in the dorsal skin was analyzed by RT-PCR. DNCB group up-regulated the expressions of pro-inflammatory cytokines and Th2-specific cytokines while down-regulated the counter-regulatory cytokines. The recruitment of pro-inflammatory cytokines including IL-6 and TNF-α were increased about 2.5 and 3.0 folds compared with NOR group. Anti-inflammatory cytokines including IL-10 and TGF-β down-regulated about 0.2 and 0.1 folds in DNCB group. Each of AM and NT treatment have regulatory effects on pro-inflammatory cytokines and anti-inflammatory cytokines with the decreases of IL-6 and TNF-α (IL-6: AM 33.9%, NT 48.6%; TNF-α: AM 47.0%, NT 49.0%) (**Figure 5A**) and the increases of IL-10 and TGF-β (IL-10: AM 56.6%, NT 53.8%; TGF-β: AM 82.7%, NT 84.9%) (**Figure 5B**). Compared with DNCB group, topical treatment of AM and NT diminished the levels of IL-6 and TNF-α about 59.3 and 65.3% and up-regulated IL-10 and TGF-β about 53.1 and 85.0%.

Additionally, the expression levels of IL-4, -13, and -31 in DNCB group were 2.6, 4.2, and 4.1 folds higher than NOR group. The expressions of IL-4, -13, and -31 were significantly decreased in AM, NT, and AM + NT groups (IL-4: AM 38.4%, NT 44.1%, AM + NT 48.0%; IL-13: AM 68.2%, NT 69.9%, AM + NT 73.1%; IL-31: AM 64.0%, NT 44.7%, AM + NT 75.5%) (**Figure 5C**). However, Th1-specific cytokine IFN-γ did not appear any increase in AM, NT, and AM + NT groups (**Figure 5D**).

DISCUSSION

ACD is an inflammatory skin disease associated with skin barrier disruption, leading to intense itching and typically characterized by hyperkeratosis, skin thickening, dryness, excoriation, redness, scars, and edema (Grewe et al., 1998; Napolitano et al., 2016). Dermatitis scores, indicated by erythema/hemorrhage, dryness/scarring, edema, and erosion/excoriation, were improved by AM, NT, and a mixture of AM and NT. Through the histological analysis, skin hyperplasia and swelling were appeared in DNCB group and those symptoms were alleviated by treatment of AM and NT. Single administration of AM and NT, respectively, recovered the characteristics of ACD, such as erythema,
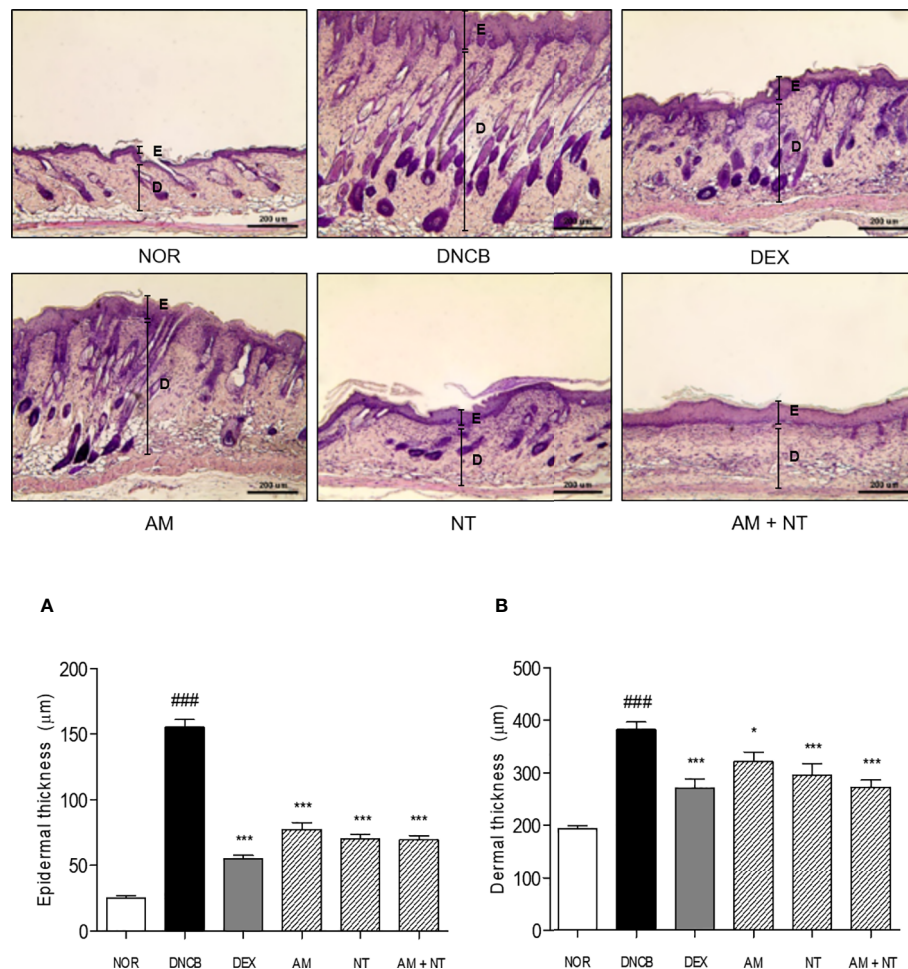
FIGURE 2 | Effects of AM, NT, and a mixture of AM and NT on histopathological features with allergic contact dermatitis skin lesions. Epidermis **(A)** and dermis **(B)** thickness were stained with hematoxylin and eosin and measured microscopically. The magnification was ×100. Data were presented as means ± S.E.M (n = 5). $^{###}p < 0.001$ vs. NOR; $^{*}p < 0.05$ and $^{***}p < 0.001$ vs. DNCB. Black lines indicate the layer of epidermis (E) and dermis (D).

hemorrhage, dryness, scarring, erosion, and skin hyperplasia. AM and NT had similar or better inhibitory effects on the development of ACD.

About 60% of ACD patients, especially children, have experienced sleep disturbance regardless of clinical treatment (Fishbein et al., 2018). Because scratching aggravates dermatitis, the susceptibility to itching is increased, resulting in the degeneration of skin lesions (Koblenzer, 1999; Feld et al., 2016). Therefore, the regulation of pruritus and scratching behaviors can be a new therapeutic method for treating ACD (Choi et al., 2018). As described in the previous studies (Choi et al., 2016), topical AM treatment significantly inhibited the scratching behavior by 30.0%. In addition, the number of scratches were decreased at the ratio of 31.2% by treatment of AM and NT, while topical NT application reduced the itching by 25.6%.

There are several pathways to cause scratching and itching in ACD patients such as histamine 1 and 4 receptor, neuropeptides, cytokines, and various inflammatory factors like NGF and mast cell degranulation (Stander and Luger, 2010). Mast cell is the first defender to protect cellular barriers in the cutaneous lesions, the mucous membrane, and digestive and respiratory tracts. Mast cells have been not only associated with acute and chronic responses but also featured by inflammation (Metz et al., 2007). It is well established that the number of mast cells was markedly increased in ACD-like skin lesions (Kawakami et al., 2009). The number of mast cells was remarkably ameliorated in AM, NT, and AM + NT groups as compared with DNCB group.

In association with the mast cells activation, NGF and its receptor (TrkA) have been considered to act as a leading part in the pruritus by inducing "itch-scratch cycle" (Roblin et al., 2015). NGF is a significant neuropeptide that activates nervous system in central and peripheral parts. In addition, NGF correlated inflammatory responses by mast cells, B cells, T cells, neutrophils, and eosinophils (Kritas et al., 2014). TrkA is one of NGF receptors and have a binding with NGF, as a strong affinity nerve growth factor receptor (Mahadeo et al., 1994). This membrane-bounded receptor auto-phosphorylated upon
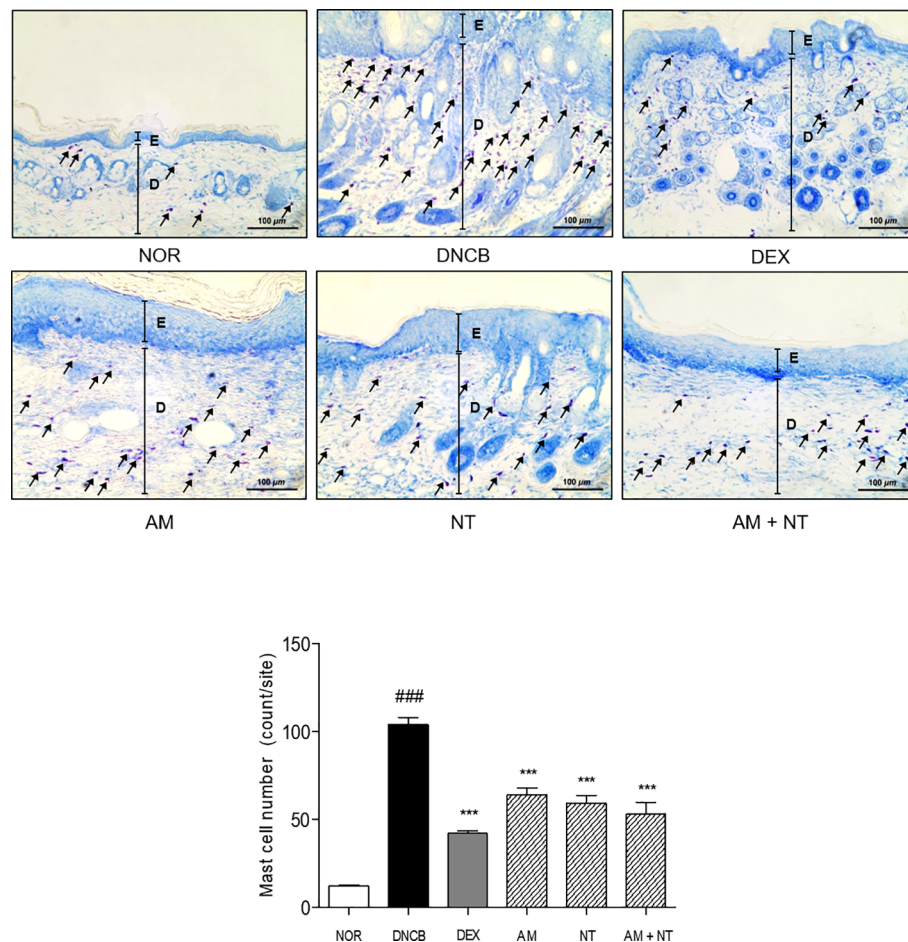
FIGURE 3 | Effects of AM, NT, and a mixture of AM and NT on mast cell degranulation with allergic contact dermatitis skin lesions. Mast cell infiltration in dorsal skin lesions were indicated by Toluidine blue staining. The magnification is ×200. Data were presented as means ± S.E.M (n = 5). [###]$p < 0.001$ *vs.* NOR; [***]$p < 0.001$ *vs.* DNCB. Black lines indicate the layer of epidermis (E) and dermis (D). Arrows indicate the toluidine blue-stained mast cells.

neurotrophin binding (Joca et al., 2015). Activated TrkA triggers Raf-1 to be phosphorylated. Activation of MEK, as a result from phosphorylation by Raf-1, phosphorylates ERK (Roblin et al., 2015). In this study, topical NT and a mixture of AM and NT treatment significantly decreased the expressions of NGF in ACD-like skin lesions, while AM did not affect the NGF expression. The expression of TrkA was markedly diminished in AM and NT treated skin tissues. In consistent with the NGF-TrkA expression, the phosphorylation of series of Raf-1, MEK, and ERK was markedly inhibited in AM, NT, and a mixture of AM and NT treated ACD-like lesions compared with DNCB group. Treatment of AM and NT appeared to be more effective in NGF-TrkA pathway than that of NT.

In addition to itchy lesions, Th cell immune responses are clinical features in ACD (Biedermann et al., 2015). The production of IL-6 and TNF-α initiates the pro-inflammatory reaction in acute stage of ACD. Additionally, counter-regulatory cytokines such as IL-10 and TGF-β are down-regulated by DNCB sensitization, indicating that IL-10 and TGF-β are regarded as anti-inflammatory cytokines. Furthermore, Th2

cells mainly mediate the onset of ACD, while Th1 cells are predominant in the chronic phase of ACD (Leung et al., 2004). Imbalanced Th2/Th1 cell-mediated cytokine is one of critical causes of developing ACD (Racke et al., 1994). IL-4, IL-13, and IL-31 are typical Th2-mediated cytokines in the progress of ACD development (Neis et al., 2006). In contrast, Th1 cells activation increases the release of IFN-γ (Bradley et al., 1996). Especially, Th2-specific cytokines promotes the degranulation of mast cells, that leads to itching sensation. Therefore, inhibition of Th2-mediated cytokines is expected to ameliorate the scratching behavior in ACD. In this study, treatment of AM, NT, and a mixture of AM and NT inhibited the production of pro-inflammatory cytokines, IL-6 and TNF-α, along with increases of anti-inflammatory cytokines, IL-10 and TGF-β. Th2-specific cytokines including IL-4, -13, and -31 were down-regulated, while Th1-specific cytokine IFN-γ was not affected by AM, NT, and a mixture of AM and NT. These results demonstrate that AM and NT had beneficial effects on the down-regulation of Th2-mediated cytokines rather than the up-regulation of Th1-mediated cytokine. Interestingly, the degree of itch score
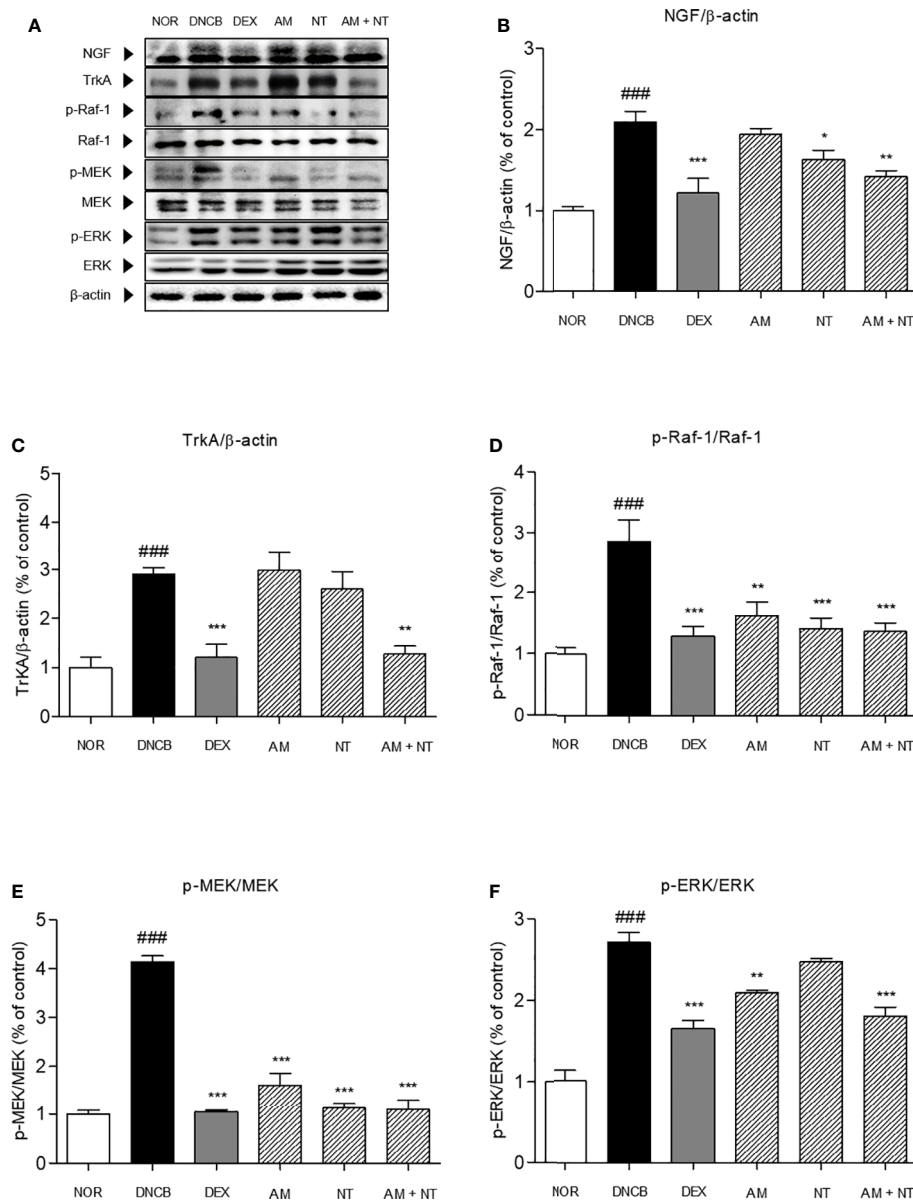
FIGURE 4 | Effects of AM, NT, and a mixture of AM and NT on NGF-TrkA signaling related factors with allergic contact dermatitis skin lesions. **(A)** The expressions of NGF-TrkA signaling related factors, such as **(B)** NGF, **(C)** TrkA, **(D)** Raf-1, **(E)** MEK, and **(F)** ERK were determined on the dorsal skin by Western blot analysis. Data were presented as means ± S.E.M (n = 5). $^{###}p < 0.001$ vs. NOR; $^*p < 0.05$, $^{**}p < 0.01$, and $^{***}p < 0.001$ vs. DNCB.

correlates with the IL-31 cytokine production in ACD lesions (Neis et al., 2006). AM treatment showed lower IL-31 expression (64.2%) than NT treatment (44.7%). Although AM did not affect the NGF-TrkA signaling, itching-related cytokine IL-31 was inhibited by AM treatment, resulting in a decrease of scratching behavior.

In this experiment, AM and NT had anti-inflammatory effect on Th and mast cells in clinical phase of ACD. Moreover, they had regulatory effect on keratinocyte which has a role in

initiation and termination phase of ACD (Gober and Gaspari, 2008). Astragaloside IV from AM stimulated proliferation and migration of keratinocytes via regulation of the Wnt signaling pathway (Li et al., 2012). And NT promoted keratinocyte migration and wound healing (Isohama, 2014).

Epidermal Langerhans cells and dermal dendritic cells may regulate an immune response by presenting allergens to T cells in the paracortical areas of regional lymph nodes in elicitation phase of ACD (Gober and Gaspari, 2008). Further studies
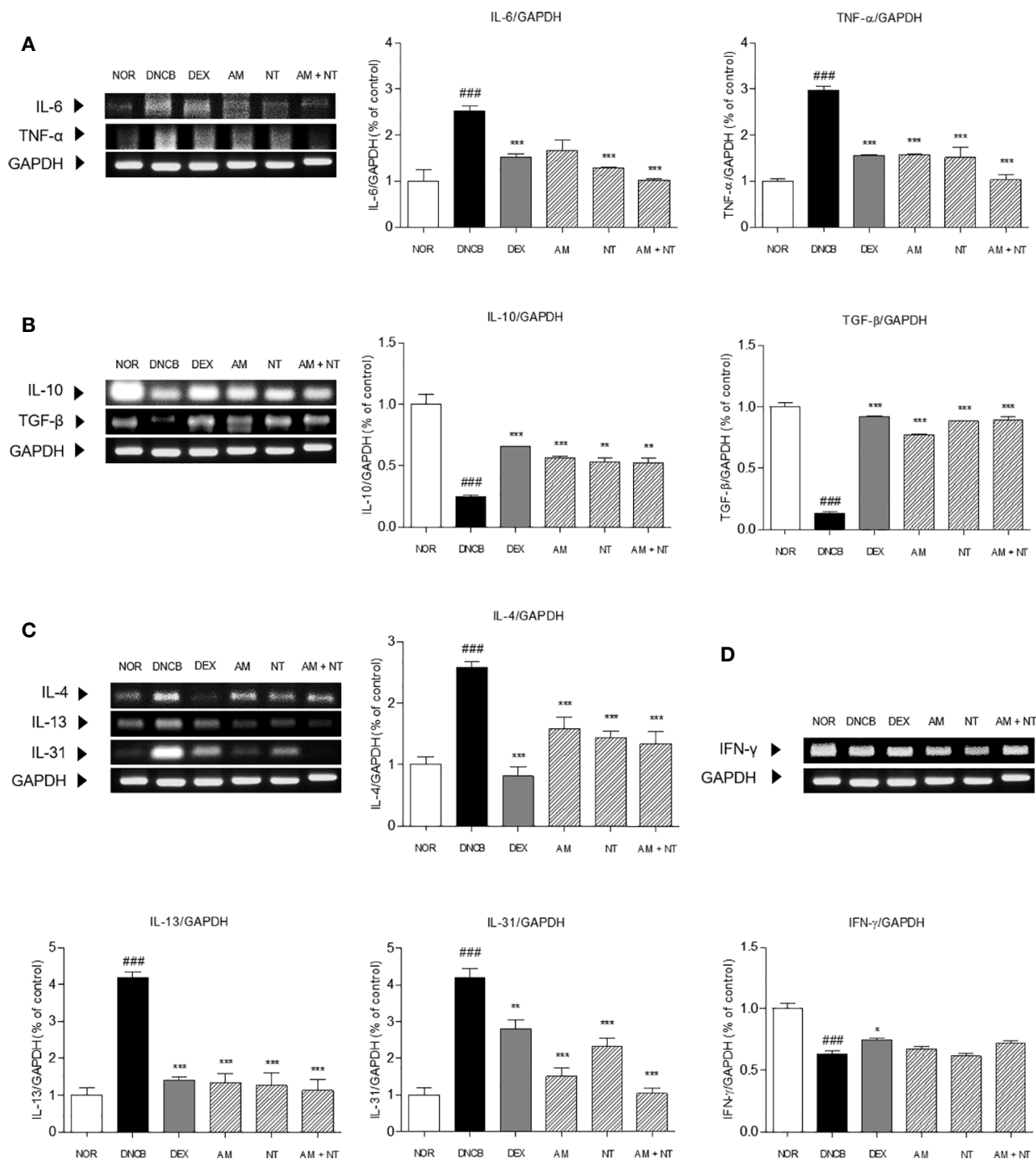
FIGURE 5 | Effects of AM, NT, and a mixture of AM and NT on inflammatory cytokine levels: **(A)** pro-inflammatory cytokines; interleukin (IL)-6 and TNF-α, **(B)** anti-inflammatory cytokines; IL-10 and TGF-β, **(C)** Th2 specific cytokines; IL-4, -13, and -31; and **(D)** Th1 specific cytokines; IFN-γ in mice with allergic contact dermatitis skin lesions. Data were presented as means ± S.E.M (n = 5). $^{###}p < 0.001$ *vs.* NOR; $^{*}p < 0.05$, $^{**}p < 0.01$, and $^{***}p < 0.001$ *vs.* DNCB.
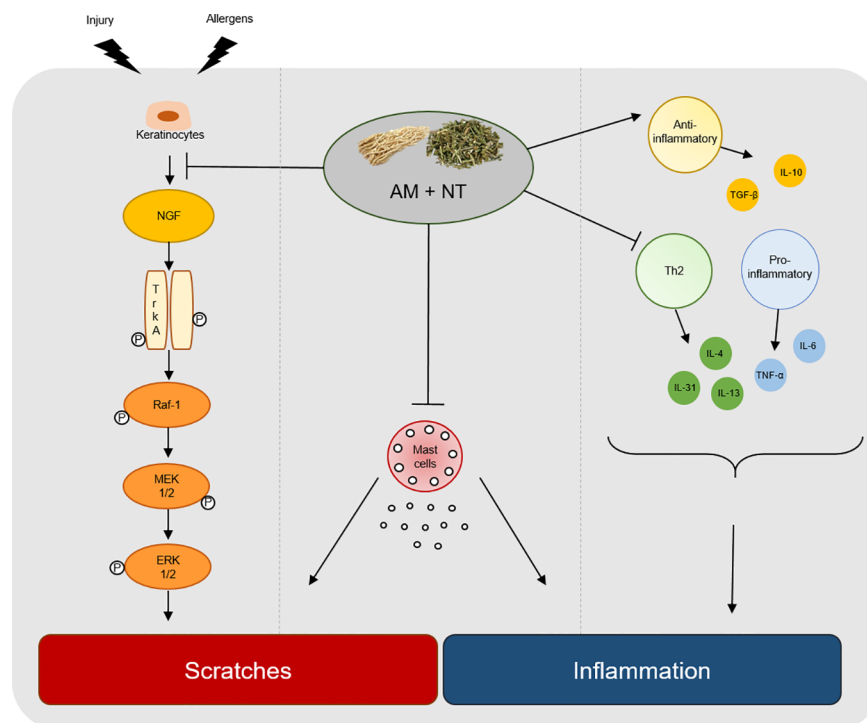
FIGURE 6 | Graphical summary of key process by a mixture of AM and NT, Derma-H, in ACD. Derma-H, a mixture of AM and NT, improved scratches by inhibiting the release of NGF-TrkA signaling and decreasing the number of mast cells. In addition, pro-inflammatory, Th2-specific cytokines and anti-inflammatory cytokines were effectively regulated by Derma-H. Consequently, Derma-H has ameliorative effects on ACD.

confirming the effect of AM or NT on epidermal Langerhans cells or dermal dendritic cells will clearly reveal the mechanism for improving allergic contact dermatitis.

Taken together, AM showed the anti-inflammatory effect by decreasing the expression of Th2-mediated cytokines. In addition, NT inhibited NGF-TrkA signaling as an anti-pruritic effect on DNCB-induced skin lesions. In conclusion, a mixture of AM and NT has a synergic effect on pruritus and inflammation in DNCB-induced ACD (**Figure 6**). It may be hypothesized that AM and NT may be further developed as a new alternative therapy for ACD once further experimental work has clarified the concentration of treatment and various clinical effect.

DATA AVAILABILITY STATEMENT

All datasets generated for this study are included in the article/**Supplementary Material**.

ETHICS STATEMENT

The animal study was reviewed and approved by the Guide for the Care and Use of Laboratory Animals of Kyung Hee University, Seoul, Korea (KHUASP(SE)-14-030).

AUTHOR CONTRIBUTIONS

All authors contributed to the article and approved the submitted version. SJ and WY contributed to analysis design. SJ, MK, HL, and SL analyzed data. SJ and WY drafted the manuscript. WY provided supervision of study.

FUNDING

SUPPLEMENTARY MATERIAL

The Supplementary Material for this article can be found online at: https://www.frontiersin.org/articles/10.3389/fphar.2020.01019/full#supplementary-material

FIGURE S1 | Standardization of *Astragalus membranaceus* Fisch. ex Bunge using high-performance liquid chromatography (HPLC) systems. HPLC chromatograms of external standard formononetin **(A)** and AM **(B)**.

FIGURE S2 | Standardization of *Nepeta tenuifolia* Benth using high-performance liquid chromatography (HPLC) systems. HPLC chromatograms of external standard pulegone **(A)** and NT **(B)**.

REFERENCES

Arkwright, P. D., Motala, C., Subramanian, H., Spergel, J., Schneider, L. C., and Wollenberg, A. (2013). Management of difficult-to-treat atopic dermatitis. *J. Allergy Clin. Immunol. Pract.* 1 (2), 142–151. doi: 10.1016/j.jaip.2012.09.002

Biedermann, T., Skabytska, Y., Kaesler, S., and Volz, T. (2015). Regulation of T Cell Immunity in Atopic Dermatitis by Microbes: The Yin and Yang of Cutaneous Inflammation. *Front. Immunol.* 6, 353. doi: 10.3389/fimmu.2015.00353

Bradley, L. M., Dalton, D. K., and Croft, M. (1996). A direct role for IFN-gamma in regulation of Th1 cell development. *J. Immunol.* 157 (4), 1350–1358.

Cho, W. C., and Leung, K. N. (2007). In vitro and in vivo immunomodulating and immunorestorative effects of Astragalus membranaceus. *J. Ethnopharmacol.* 113 (1), 132–141. doi: 10.1016/j.jep.2007.05.020

Choi, Y. Y., Kim, M. H., Kim, J. H., Jung, H. S., Sohn, Y., Choi, Y. J., et al. (2013). Schizonepeta tenuifolia inhibits the development of atopic dermatitis in mice. *Phytother. Res.* 27 (8), 1131–1135. doi: 10.1002/ptr.4833

Choi, Y. Y., Kim, M. H., Hong, J., Kim, K., and Yang, W. M. (2016). Effect of Dangguibohyul-Tang, a Mixed Extract of Astragalus membranaceus and Angelica sinensis, on Allergic and Inflammatory Skin Reaction Compared with Single Extracts of Astragalus membranaceus or Angelica sinensis. *Evid. Based. Complement Alternat. Med.* 2016, 5936354. doi: 10.1155/2016/5936354

Choi, Y. Y., Kim, M. H., Lee, H., Ahn, K. S., Um, J., Lee, S., et al. (2017). Cynanchum atratum inhibits the development of atopic dermatitis in 2,4-dinitrochlorobenzene-induced mice. *BioMed. Pharmacother.* 90, 321–327. doi: 10.1016/j.biopha.2017.03.065

Choi, Y. Y., Kim, M. H., Lee, H., Jo, S. Y., and Yang, W. M. (2018). (R)-(+)-pulegone suppresses allergic and inflammation responses on 2,4-dinitrochlorobenzene-induced atopic dermatitis in mice model. *J. Dermatol. Sci.* 91 (3), 292–300. doi: 10.1016/j.jdermsci.2018.06.002

Feld, M., Garcia, R., Buddenkotte, J., Katayama, s., Lewis, K., Muirhead, G., et al. (2016). The pruritus- and TH2-associated cytokine IL-31 promotes growth of sensory nerves. *J. Allergy Clin. Immunol.* 138 (2), 500–508.e524. doi: 10.1016/j.jaci.2016.02.020

Fishbein, A. B., Mueller, K., Kruse, L., Boor, P., Sheldon, S., Zee, P., et al. (2018). Sleep disturbance in children with moderate/severe atopic dermatitis: A case-control study. *J. Am. Acad. Dermatol.* 78 (2), 336–341. doi: 10.1016/j.jaad.2017.08.043

Gober, M. D., and Gaspari, A. A. (2008). Allergic contact dermatitis. *Curr. Dir. Autoimmun.* 10, 1–26. doi: 10.1159/000131410

Grewe, M., Bruijnzeel-Koomen, C. A., Schopf, E., Thepen, T., Langeveld-Wildschut, A. G., Ruzicka, T., et al. (1998). A role for Th1 and Th2 cells in the immunopathogenesis of atopic dermatitis. *Immunol. Today* 19 (8), 359–361. doi: 10.1016/S0167-5699(98)01285-7

Isohama, Y. (2014). [Increase in aquaporin 3 expression in keratinocytes by Schizonepeta tenuifolia]. *Nihon Yakurigaku Zasshi* 143 (3), 115–119. doi: 10.1254/fpj.143.115

Joca, S. R., Moreira, F. A., and Wegener, G. (2015). Atypical Neurotransmitters and the Neurobiology of Depression. *CNS Neurol. Disord. Drug Targets* 14 (8), 1001–1011. doi: 10.2174/1871527314666150909114804

Kawakami, T., Ando, T., Kimura, M., Wilson, B. S., and Kawakami, Y. (2009). Mast cells in atopic dermatitis. *Curr. Opin. Immunol.* 21 (6), 666–678. doi: 10.1016/j.coi.2009.09.006

Kim, M. H., Choi, Y. Y., Yang, G., Cho, I. H., Nam, D., and Yang, W. M. (2013). Indirubin, a purple 3,2- bisindole, inhibited allergic contact dermatitis via regulating T helper (Th)-mediated immune system in DNCB-induced model. *J. Ethnopharmacol.* 145 (1), 214–219. doi: 10.1016/j.jep.2012.10.055

Kim, Y. A., Kim, D. H., Park, C. B., Park, T. S., and Park, B. J. (2018). Anti-Inflammatory and Skin-Moisturizing Effects of a Flavonoid Glycoside Extracted from the Aquatic Plant Nymphoides indica in Human Keratinocytes. *Molecules* 23 (9), 2342. doi: 10.3390/molecules23092342

Koblenzer, C. S. (1999). Itching and the atopic skin. *J. Allergy Clin. Immunol.* 104 (3 Pt 2), S109–S113. doi: 10.1016/S0091-6749(99)70052-7

Kritas, S. K., Caraffa, A., Antinolfi, P., Saggini, A., Pantalone, A., Rosati, M., et al. (2014). Nerve growth factor interactions with mast cells. *Int. J. Immunopathol. Pharmacol.* 27 (1), 15–19. doi: 10.1177/039463201402700103

Lee, H. J., Kim, M. H., Choi, Y. Y., Kim, E. H., Hong, J., Kim, K., et al. (2016). Improvement of atopic dermatitis with topical application of Spirodela polyrhiza. *J. Ethnopharmacol.* 180, 12–17. doi: 10.1016/j.jep.2016.01.010

Lee, J. H., Lee, Y. J., Lee, J. Y., and Park, Y. M. (2017). Topical Application of Eupatilin Ameliorates Atopic Dermatitis-Like Skin Lesions in NC/Nga Mice. *Ann. Dermatol.* 29 (1), 61–68. doi: 10.5021/ad.2017.29.1.61

Leung, D. Y., Boguniewicz, M., Howell, M. D., Nomura, I., and Hamid, Q. A. (2004). New insights into atopic dermatitis. *J. Clin. Invest.* 113 (5), 651–657. doi: 10.1172/jci21060

Li, F. L., Li, X., Wang, Y. F., Xiao, X. L., Xu, R., Chen, J., et al. (2012). Astragaloside IV Downregulates beta-Catenin in Rat Keratinocytes to Counter LiCl-Induced Inhibition of Proliferation and Migration. *Evid. Based. Complement Alternat. Med.* 2012, 956107. doi: 10.1155/2012/956107

Lipozencic, J., and Wolf, R. (2007). Atopic dermatitis: an update and review of the literature. *Dermatol. Clin.* 25 (4), 605–612. doi: 10.1016/j.det.2007.06.009

Mahadeo, D., Kaplan, L., Chao, M. V., and Hempstead, B. L. (1994). High affinity nerve growth factor binding displays a faster rate of association than p140trk binding. Implications for multi-subunit polypeptide receptors. *J. Biol. Chem.* 269 (9), 6884–6891.

Metz, M., Grimbaldeston, M. A., Nakae, S., Piliponsky, A. M., Tsai, M., and Galli, S. J. (2007). Mast cells in the promotion and limitation of chronic inflammation. *Immunol. Rev.* 217, 304–328. doi: 10.1111/j.1600-065X.2007.00520.x

Napolitano, M., Megna, M., Patruno, C., Gisondi, P., Ayala, F., and Balato, N. (2016). Adult atopic dermatitis: a review. *G. Ital. Dermatol. Venereol.* 151 (4), 403–411.

Nedoszytko, B., Sokolowska-Wojdylo, M., Ruckemann-Dziurdzinska, K., Roszkiewicz, J., and Nowicki, R. J. (2014). Chemokines and cytokines network in the pathogenesis of the inflammatory skin diseases: atopic dermatitis, psoriasis and skin mastocytosis. *Postepy Dermatol. Alergol.* 31 (2), 84–91. doi: 10.5114/pdia.2014.40920

Neis, M. M., Peters, B., Dreuw, A., Wenzel, J., Bieber, T., Mauch, C., et al. (2006). Enhanced expression levels of IL-31 correlate with IL-4 and IL-13 in atopic and allergic contact dermatitis. *J. Allergy Clin. Immunol.* 118 (4), 930–937. doi: 10.1016/j.jaci.2006.07.015

Park, K. D., Pak, S. C., and Park, K. K. (2016). The Pathogenetic Effect of Natural and Bacterial Toxins on Atopic Dermatitis. *Toxins (Basel)* 9 (1), 3. doi: 10.3390/toxins9010003

Racke, M. K., Bonomo, A., Scott, D. E., Cannella, B., Levine, A., Raine, C. S., et al. (1994). Cytokine-induced immune deviation as a therapy for inflammatory autoimmune disease. *J. Exp. Med.* 180 (5), 1961–1966. doi: 10.1084/jem.180.5.1961

Roblin, D., Yosipovitch, G., Boyce, B., Robinson, J., Sandy, J., Mainero, V., et al. (2015). Topical TrkA Kinase Inhibitor CT327 is an Effective, Novel Therapy for the Treatment of Pruritus due to Psoriasis: Results from Experimental Studies, and Efficacy and Safety of CT327 in a Phase 2b Clinical Trial in Patients with Psoriasis. *Acta Derm Venereol.* 95 (5), 542–548. doi: 10.2340/00015555-2047

Stander, S., and Luger, T. A. (2010). Itch in atopic dermatitis - pathophysiology and treatment. *Acta Dermatovenerol. Croat.* 18 (4), 289–296.

Walling, H. W., and Swick, B. L. (2010). Update on the management of chronic eczema: new approaches and emerging treatment options. *Clin. Cosmet. Invest. Dermatol.* 3, 99–117. doi: 10.2147/CCID.S6496

Yuan, X. Y., Liu, W., Zhang, P., Wang, R. Y., and Guo, J. Y. (2010). Effects and mechanisms of aloperine on 2, 4-dinitrofluorobenzene-induced allergic contact dermatitis in BALB/c mice. *Eur. J. Pharmacol.* 629 (1-3), 147–152. doi: 10.1016/j.ejphar.2009.12.007

Zhou, R., Chen, H., Chen, J., Chen, X., Wen, Y., and Xu, L. (2018). Extract from Astragalus membranaceus inhibit breast cancer cells proliferation via PI3K/AKT/mTOR signaling pathway. *BMC Complement Altern. Med.* 18 (1), 83. doi: 10.1186/s12906-018-2148-2

Hyaluronic Acid-Mediated Drug Delivery System Targeting for Inflammatory Skin Diseases: A Mini Review

Kang Nien How[1], Wei Hsum Yap[2], Calvin Lai Hock Lim[2], Bey Hing Goh[3,4] and Zee Wei Lai[2]*

[1] Dermatology Unit, Faculty of Medicine and Health Sciences, Universiti Putra Malaysia, Serdang, Malaysia, [2] Faculty of Medical and Health Sciences, School of Biosciences, Taylor's University, Subang Jaya, Malaysia, [3] College of Pharmaceutical Sciences, Zhejiang University, Hangzhou, China, [4] Biofunctional Molecule Exploratory Research Group (BMEX), School of Pharmacy, Monash University Malaysia, Bandar Sunway, Malaysia

OPEN ACCESS

Hyaluronic acid (HA), a major component of extracellular matrix has been widely applied in pharmaceutical and cosmetic industries due to its reported pharmacological properties. Various types of HA drug delivery system including nanoparticles, cryogel-based formulations, microneedle patches, and nano-emulsions were developed. There are studies reporting that several HA-based transdermal delivery systems exhibit excellent biocompatibility, enhanced permeability and efficient localized release of anti-psoriasis drugs and have shown to inhibit psoriasis-associated skin inflammation. Similarly HA is found in abundant at epidermis of atopic dermatitis (AD) suggesting its role in atopic AD pathology. Anti-allergenic effect of atopic eczema can be achieved through the inhibition of CD44 and protein kinase C alpha (PKCα) interaction by HA. Herein, we aim to evaluate the current innovation on HA drug delivery system and the other potential applications of HA in inflammatory skin diseases, focusing on atopic dermatitis and psoriasis. HA is typically integrated into different delivery systems including nanoparticles, liposomes, ethosomes and microneedle patches in supporting drug penetration through the stratum corneum layer of the skin. For instance, ethosomes and microneedle delivery system such as curcumin-loaded HA-modified ethosomes were developed to enhance skin retention and delivery of curcumin to CD44-expressing psoriatic cells whereas methotrexate-loaded HA-based microneedle was shown to enhance skin penetration of methotrexate to alleviate psoriasis-like skin inflammation. HA-based nanoparticles and pluronic F-127 based dual responsive (pH/temperature) hydrogels had been described to enhance drug permeation through and into the intact skin for AD treatment.

Keywords: hyaluronic acid, inflammatory skin diseases, psoriasis, atopic dermatitis, drug delivery, CD44 receptor
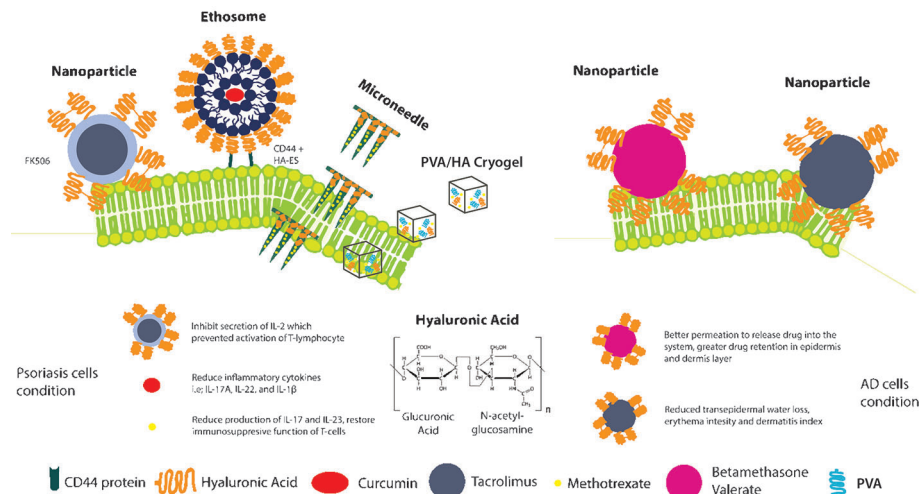
GRAPHICAL ABSTRACT | HA-mediated Drug Delivery System Targeting Inflammatory Skin Diseases (Psoriasis and Atopic Dermatitis).

INTRODUCTION

Skin as the first line of defense against infection is made up of three main layers which vary in functions and anatomy: epidermis (outer layer), dermis (middle layer) and hypodermis (bottom layer) (Prost-Squarcioni, 2006). As it interacts with environment, skin acts as a protector against diseases, excessive water loss, UV damage, mechanical injury, and also helps in regulate body temperature (Logger et al., 2019). Skin and subcutaneous diseases are the 4th leading cause of disability globally in 2013 excluding mortality, with dermatitis being the greatest burden among all costing approximately 9.3 million disability-adjusted life years (Karimkhani et al., 2017). Psoriasis is reported to affect 2% of worldwide population due to genetic and environmental factors (Mohd Affandi et al., 2018). Psoriasis is an inflammatory skin diseases which is chronic with strong genetic predisposition and autoimmune pathogenic traits (Du et al., 2019) that is causing burden to patient either physically or physiologically (Boehncke and Schön, 2015). For mild to moderate psoriasis, topical corticosteroids are the first-line treatment. However, long term application of topical corticosteroids can produce adverse effects such as epidermal thinning, atrophy, ulceration and facial erythema (Coondoo et al., 2014).

Atopic dermatitis (AD), a common chronic inflammatory skin disease poses a significant threat to both patient and the economy. It also affects the quality of individual life as well as their families (Kapur et al., 2018). The disease is believed to arise due to the complex interplay between skin barrier malfunction, immune dysregulation and infectious agents from environment factor (Kapur et al., 2018). In Canada, it was reported that an estimated cost of $1.4 billion annually is incurred to assist AD patient in getting treatment, like emollients application, as well as frequent physician visits which impacted the economy (Barbeau and Lalonde, 2006). AD has significant impact on the patients quality of life as there will be constant itchiness which can lead to skin trauma and sleep deprivation (Kapur et al., 2018).

CD44, a receptor for HA is found to be highly expressed in psoriatic skin. The concentration is negatively correlated with HA distribution (Zhang et al., 2019). It was found that anti-allergenic effect can be achieved through the inhibition of CD44 and PKCα interaction by HA (Kim et al., 2008). Based on the understanding of the characteristic of HA and HA-CD44 pathway, HA is widely used as a nano-drug delivery system to enhance the therapeutic effect of drug at the lesion site (Taetz et al., 2009). HA assisted drug delivery systems that has been described include nanoparticle, ethosomes and microneedle. It is an important vehicle to enhance drug-skin penetration and an important vehicle to retain moisture in AD in view of barrier dysfunction. The objective of this review is to review the role of HA as a drug delivery system in inflammatory skin diseases namely psoriasis and atopic dermatitis.

STRUCTURAL AND FUNCTIONAL CHARACTERISTICS OF HYALURONIC ACID

Hyaluronic acid (HA), a major component of extracellular matrix has been widely applied in pharmaceutical and cosmetic industries

---

Abbreviations: HA, hyaluronic acid; AD, atopic dermatitis; LMWHA, low molecular weight hyaluronic acid; HMWHA, high molecular weight hyaluronic acid; IL, interleukin; SC, stratum corneum; PKCα; protein kinase C alpha; HaCat, human keratinocyte cell line.

due to its reported pharmacological properties which includes anti-aging (Bukhari et al., 2018), anti-inflammatory (Chen, 2018), skin repairing (Narurkar et al., 2016), tissue regeneration (Bukhari et al., 2018) and wound recovery properties (Chen, 2018). HA possess good biocompatibility, high moisture retention, and tuneable viscoelastic properties (Sze et al., 2016). It is a natural unbranched polymer composed of repeating disaccharide units of D-glucuronic acid and N-acetylglucosamine linked by a glucuronidic β (1–3) bond. HA with different molecular weights exhibit distinct properties. For instance, low molecular weight HA (LMW-HA) is reported to be associated with promoting angiogenesis whereas high molecular weight HA (HMW-HA) inhibits angiogenesis. The appropriate balance between synthesis and degradation of HA is vital in the regulation of various biological functions including cell proliferation, migration, differentiation (Bychkov and Kuzmina, 2015), vasculogenesis and angiogenesis (Pardue et al., 2008), as well as regulating cell adhesion and motility (Kouvidi et al., 2011), as determined by their molecular weight. LMW-HA on the other hand exerts opposite effect as compared to HMW-HA where it demonstrates biological activities such as antioxidant properties and pronounced free radical scavenging has been developed in recent years (Ke et al., 2011). In addition, LMW-HA has also shown to induce inflammatory genes in T-24 carcinoma cells, in eosinophils (Ohkawara et al., 2000) as well as dendritic cells (Termeer et al., 2000). Both sizes of HA are safe and efficacious, and the market is expecting a continuing emergence of HA-based products in the coming years (Tabassum and Hamdani, 2014).

PSORIASIS

Psoriasis is a chronic inflammatory autoimmune skin disease characterized by marked epidermal proliferation and abnormal differentiation with activation of both innate and acquired immunity (Rendon and Schäkel, 2019). This autoimmune disorder is multifactorial, and inflammation is known to play a major role in its development. Research have showed that activated Th1 and Th17 T cells (CD4+ T cells), CD8+ T cells, as well as increased levels of cytokines such as IL-17, IL-23, TNF-α and IL-27, have been directly implicated in psoriasis immunopathogenesis (Luger and Loser, 2018). The immunology and genetics studies of psoriasis have provided insights into the heterogeneity and regulatory pathways that govern psoriasis, and assist in the development of therapy based on patients biogenetic markers and identify new avenues for treatment based on a more complete understanding of the immunological mechanisms. Topical administration is one of the important approaches to treat psoriasis. Drugs are applied directly to the affected skin lesions to inhibit inflammatory symptoms of psoriasis. Topical administration of drugs with narrow therapeutic window can reduce systemic absorption compared to drugs delivered through oral and intravenous routes which help to reduce adverse systemic effects. Though topically applied drugs provide prolonged duration of action, the stratum corneum limits the amount of drugs being percutaneously absorbed, resulting in poor clinical efficacy. Hence, novel and improved percutaneous delivery system to overcome the stratum corneum barrier of psoriatic skin is vital to antipsoriatic drug for topical therapy.

HA AS A DRUG DELIVERY SYSTEM IN PSORIASIS

Currently, HA is widely incorporated as part of the transdermal delivery system to enhance drug penetration in psoriasis treatment. Various forms of drug delivery systems including HA-based nanoparticles, ethosomes, cryogels, and microneedle patches have been developed to enhance drug permeation through and into the intact skin for psoriasis treatment. The excellent solubility properties of HA resulted in its development as one of the most important topical carriers for the localized delivery of drugs to the skin and also as a drug delivery agent for ophthalmic, nasal, pulmonary, parenteral and topical routes of administration (Brown and Jones, 2005). HA acts as mucoadhesive, retaining the drug at specific site of action/absorption. It also can modify the *in vivo* release and absorption rate of the therapeutic agent and it is able to localize delivery of drug to the epidermis. The types of psoriasis drugs that have been incorporated into these HA-based delivery systems include methotrexate, tacrolimus, and corticosteroids, all which are first-line treatments for moderate to severe psoriasis.

One of the novel nano-topical drug delivery system developed using HA-modified ethosomes target CD44 in the inflamed epidermis (Zhang et al., 2019). Ethosomes are novel deformable liposomes derived from dispersing liposomes in small-chain biocompatible alcohols and they are demonstrated to be more superior than classic liposomes which significantly increase skin retention of drugs (Touitou et al., 2000). The incorporation of curcumin in HA-modified ethosomes target CD44 in the inflamed epidermis (Zhang et al., 2019). Recent studies have found that CD44 protein is highly expressed in the epidermis of psoriatic inflamed skin, suggesting that CD44 can serve as a potential target of novel active-targeting nanocarriers for topical administration to increase skin drug retention and enhance drug efficacy (Lindqvist et al., 2012). The HA-modified ethosomes showed specific adhesion CD44 in imiquimod-induced psoriasis-like inflamed skin, and that the increased topical drug delivery of curcumin reduced TNF-α, IL-17A, IL-17F, IL-22, and IL-1β mRNA levels; and lower CCR6 protein expression.

Another formulated hybrid nanoparticle system based on the combination of amphiphilic conjugations of HA–Cholesterol-self-assembled nanoparticles and hydrotropic nicotinamide was developed to enhance the permeation of tacrolimus (FK506) in the treatment of psoriasis (Wan et al., 2017). Commercial FK506 is an ointment formulation use to treat atopic dermatitis, but it is applied to other skin diseases like psoriasis (Malecic and Young, 2016). FK506 is a type of macrolide immunosuppressive drug

which prevents activation of T-lymphocyte through inhibition of IL-2, a cytokine that is responsible for the development and persistence of psoriasis lesions (Goebel et al., 2011). However, topical treatment of tacrolimus ointment on hyperkeratotic psoriatic plaques did not promote FK506 deposition due to its high hydrophobicity and high molecular weight (Zonnevdd et al., 1998). The combination of HA–Cholesterol nanoparticles exhibited a significant synergistic effect on the permeation of FK506 ointment and that it presented a synergistic effect on antipsoriasis which might increase the therapeutic effect and minimize systemic side effects (Wan et al., 2017).

Synthetic biodegradable polymers have significant versatility and diverse biomedical applications owing to their tailorable designs or modifications. Poly(vinyl alcohol) (PVA) is a water soluble biodegradable synthetic polymer with good biocompatibility, and it can be physically cross-linked by the freeze-thaw method (Stauffer and Peppast, 1992) to form hydrogels useful in pharmaceutical formulations. The development of PVA/HA cryogels loaded with methotrexate showed good *in vivo* biocompatibility after systemic and topical administration in laboratory animals. The pH-responsive swelling and releasing abilities of these PVA/HA cryogels allow these systems to be developed as topical formulations for psoriasis therapy.

Meanwhile, development of pH-responsive biodegradable poly-L-glutamic acid (PGA)-fluocinolone acetonide (FLUO) conjugate allows the controlled release of the FLUO to reduce skin inflammation (Dolz-Pérez et al., 2020). However, PGA-FLUO showed limitations in the release of drug in the epidermis which bring about the application of PGA-FLUO within hyaluronic acid (HA)-poly-L-glutamate cross polymer (HA-CP) resulted in slower and sustained drug transfer in the epidermis allowing sufficient residence time for drug activity (Dolz-Pérez et al., 2020).

Microneedle patch is a highly efficient and versatile device which attracted extensive scientific and industrial interests in the past decades due to prominent properties including painless penetration, low cost, excellent therapeutic efficacy, and relative safety. The robust microneedle enabling transdermal delivery has a paramount potential to create advanced functional devices with superior nature for biomedical applications. Methotrexate, an analogue of folic acid has been used as a drug to treat psoriasis skin condition (Czarnecka-Operacz and Sadowska-Przytocka, 2014). Methotrexate has been shown to down-regulate interleukin-17 and interferon-c, inhibit proliferation of effector T cells and restore the immunosuppressive function of regulatory T cells (Chen, 2018). Nevertheless, its high molecular weight, hydrophilicity and inability to maintain a stable form at physiological pH restricted the permeability of methotrexate by passive diffusion through the stratum corneum (Alvarez-Figueroa et al., 2001). The development of methotrexate-loaded HA-based microneedle patch successfully penetrated imiquimod (IMQ)-induced thickened epidermis in mice and alleviated the psoriasis-like skin inflammation (Du et al., 2019). In addition, the methotrexate-loaded HA-based microneedle patches were significantly more efficacious than taking the same dose of drug orally. This significantly reduced the amount of methotrexate required for the microneedle patch delivery system required for a comparable amelioration, which in turn lowered its systemic toxicity (Du et al., 2019).

HA AS A BIOMARKER IN PSORIASIS

Serum HA had been utilized as a biomarker for psoriasis as studies reported that concentration of serum HA increases significantly in patients with serious cutaneous psoriasis (Yamamoto et al., 1997). This is due to the ability of low molecular weight HA (LMWHA) in inducing inflammatory cytokine gene expression and serving as a ligand for toll-like receptors (TLRs). In addition, presence of IL-1β, tumor necrosis factor-α (TNF-α) and degradative enzymes such as metalloproteinases will lead to an increase in hyaluronan synthetases (HAS) 1–3 and hyaluronidases that synthesize LMWHA by degrading HMWHA (Mehta et al., 2011; Hellman et al., 2019). In psoriasis, TLRs play a vital role as innate immune responses through activation of TLR7 and TLR9 and also the secretion of interleukin-23 (IL-23) *via* autoimmune plasmacytoid dendritic cell activation which releases interferon-a, that further signals Tip-DC (tumor necrosis factor-a and inducible nitric oxide synthase-producing dendritic cell) activation (Yamamoto, 2015). Other TLRs including TLR2 and TLR4 contribute to the pathogenesis of psoriasis plaque, guttate (Garcia-Rodriguez et al., 2013) and also psoriatic arthritis (Carrasco et al., 2011). HA is highly abundant in psoriatic skin, and it signals through TLR4 and TLR2. Meanwhile the binding of HA on CD44 also induces secretion of IL-6 and inflammation in T cells and neutrophils (Jiang et al., 2011).

ATOPIC DERMATITIS

Atopic dermatitis (AD) is the most common chronic inflammatory skin disease affecting infants and children (Siegfried and Hebert, 2015). Factors causing AD includes defect in terminal epithelial differentiation, immune dysregulation, altered skin microbiome and altered composition of stratum corneum (SC) intracellular lipids leading to barrier dysfunction (Bieber et al., 2017; Nakatsuji et al., 2017). Impairment of the SC permeability barrier functions cause dehydration due to an increase of transepidermal water loss, followed by inflammation due to the increasing release of cytokines, chemokines and interleukines (Damiani et al., 2019). Skin hydration, anti-bacterial measures and topical immunosuppressant therapy using topical corticosteroids calcineurin inhibitors are the common approaches in the management of AD (Sathishkumar and Moss, 2016).

HA'S ROLE IN ATOPIC DERMATITIS

HA is found to be related to inflammatory skin dermatoses (Ohtani et al., 2009; Barnes et al., 2012) The synthesis of HA is regulated by hyaluronan synthases (HAS). In normal circumstances, HAS1 is found to be regulating epidermal differentiation. However, role of HAS3 becomes apparent during pathological condition (Malaisse et al., 2014). The earlier studies provide conflicting evidences on HA role in epidermal differentiation (Maytin et al., 2004; Passi et al., 2004; Bourguignon et al., 2006; Farwick et al., 2011). Latest evidence by Malaisse et al. (2014) acknowledge the fact that though HA present at high level, it is not necessary for homeostatic epidermal differentiation (Malaisse et al., 2014). However, HA become important in pathological condition. During inflammation, HAS3 is upregulated while HAS1 is downregulated. Heparin binding-epidermal growth factor. (HB-EGF) is found to be possibly linked to HAS expression in AD lesions. However, how HAS involved in the pathomechanism of keratinocyte inflammation is still unclear and thus requiring further studies (Malaisse et al., 2014).

HA IN MEDICAL DEVICE MOISTURIZERS

The basic principle AD treatment is optimal skin care that address the skin barrier defect. Moisturizers restore the ability of lipid bilayer to restore, retain and redistribute water. They penetrate and contribute to the reorganization of the structure of the skin layers. Thus, moisturizers play an important role in AD management (Giam et al., 2016). Moisturizers can be categorized into three main groups, namely humectant, occlusive and emollients. These products are formulated in various delivery system including gel, foam, cream, ointment and lotion. They also contain various composition to enhance its efficacy. Humectants work by attracting fluids from the deeper epidermis to SC and has a biological similarities to the natural moisturizing factors of the corneocytes (Giam et al., 2016). HA being a natural component of the skin, has been one of the most favorite humectant used in almost all nutricosmetic products with moisturizing properties (Bukhari et al., 2018). It helps in attracting and retaining fluid, and skin barrier repair (Maytin et al., 2004; Goh et al., 2019). However it is rarely used primarily as a sole ingredient, but rather working synergistically with other category of moisturizer to achieve its role in skin repair (Draelos, 2011; Frankel et al., 2011; Pacha and Hebert, 2012; Micali et al., 2018). The molecular weight of HA shall be considered, as HA with a molecular weight higher than 50 kDa may reduce skin penetration. Thus, HMWHA is used to form a film to impede epidermal water loss, while LMWHA is utilized to improve skin penetration to restore a sustained physiological and hydrated microenvironment for optimize skin rejuvenation and tissue repair (Symonette et al., 2014).

HA AS A DRUG DELIVERY SYSTEM IN ATOPIC DERMATITIS

Similar to psoriasis, various forms of drug delivery systems including HA-based nanoparticles and pluronic F-127 based dual responsive (pH/temperature) hydrogels have been described to enhance drug permeation through and into the intact skin for AD treatment. The types of drugs that have been incorporated into these HA-based delivery systems include tacrolimus, bethamethasone valerate and gallic acid, a principal component of traditional Chinese medicine Cortex Moutan.

Topical calcineurin inhibitor, namely tacrolimus ointment (Protropic®) and pimecrolimus cream (Elidel®) are steroid sparing agents for the treatment of atopic dermatitis. However the potency of tacrolimus 0.1% was only found to be equivalent to medium potency topical steroid(Eichenfield et al., 2014), possibly due to the limited skin penetration due to its large molecular size. A novel HA-coated tacrolimus-loaded nanoparticles (HA-TCS-CS-NPs) was described (Zhuo et al., 2018). It was noted that the physiochemical properties had been optimized, *in vivo* drug release was more sustained, drug permeation and retention had been improvised, and anti-AD efficacy in AD mice model was found to be superior in comparison with tacrolimus solution (Zhuo et al., 2018). However, this study did not compare their nanoparticles with the marketed Protropic®. Similar technology had been used to encapsulate betamethasone valerate (BMV), a medium potency topical corticosteroid. It was found that (HA-BMV-CS-NP) demonstrated optimum physicochemical characteristics, including fine particle size, high zeta potential, high entrapment efficacy and loading capacity. It also demonstrated higher drug permeation and drug retention(Pandey et al., 2019).

Pluronic F-127 (PF127) is a non-ionic triblock copolymer of poly(ethylene oxide)-b-poly(propylene oxide)-b-poly(ethylene oxide), thermo-responsive polymer capable to form gel from its aqueous solution. Chitosan is a cationic pH-responsive biopolymer that swells in acidic pH and shrinks in basic pH, while HA is an anionic pH-responsive biopolymer that can swell in basic pH and shrink in acidic pH (Chatterjee et al., 2019). The conjugation of these polymers formed a dual-responsive hydrogels [PF127/HA-Ala-Chito(oligo)]. It had been used to incorporate gallic acid, the principal component of traditional Chinese medicine Cortex Moutan, recommended in the treatment of atopic dermatitis. This anti-inflammatory and anti-allergic herbal medicine is claimed to have similar effect like corticosteroids without their side effects. PF127/HA-Ala-chito(oligo) drug delivery system was found to have improve rheological properties, mechanical stability and pH responsiveness. This drug delivery system was found to exhibit better gallic acid release under neutral pH condition. The mechanical stability and sustain drug release property despite increasing acidity in the external environment. However, further modification of this drug delivery system is required to involve non-toxic biomaterials (Chatterjee et al., 2019).

CONCLUSION

HA is widely utilized in dermatology as it is a natural, non-immunogenic polysaccharide with good biocompatibility and degradability (Huang and Huang, 2018). The moisturizing properties of HA made it exist in almost all moisturizing and antiaging cosmetics. The identification of CD44 receptors and HA on both psoriasis and AD epidermis had led to many researchers exploring this component as a possible new way for drug delivery Research on this field flourishes further even more with the improve understanding of nanomedicine. However, the current research are mainly in the pre-clinical phase. There are still large gaps in terms of best material to be utilized to improve the safety and efficacy of drug delivery. The mechanism of HA based drug delivery system is still unclear. The role of HA and its receptor on both AD and psoriasis is also yet to be well defined. Thus, more work needs to be done on all aspect of HA and its receptors on patho-mechanism of inflammatory skin diseases and its potential role in improvising future drug delivery.

AUTHOR CONTRIBUTIONS

KNH, ZWL, and WHY conceived the idea and wrote the manuscript. All authors contributed to the article and approved the submitted version.

FUNDING

REFERENCES

Alvarez-Figueroa, M. J., Delgado-Charro, M. B., and Blanco-Méndez, J. (2001). Passive and iontophoretic transdermal penetration of methotrexate. *Int. J. Pharm.* 212, 101–107. doi: 10.1016/s0378-5173(00)00599-8

Barbeau, M., and Lalonde, H. (2006). Burden of atopic dermatitis in Canada. *Int. J. Dermatol.* 45, 31–36. doi: 10.1111/j.1365-4632.2004.02345.x

Barnes, L., Carraux, P., Saurat, J. H., and Kaya, G. (2012). Increased expression of CD44 and hyaluronate synthase 3 is associated with accumulation of hyaluronate in spongiotic epidermis. *J. Invest. Dermatol.* 132 (3), 736. doi: 10.1038/jid.2011.384

Bieber, T., D'Erme, A. M., Akdis, C. A., Traidl-Hoffmann, C., Lauener, R., Schäppi, G., et al. (2017). Clinical phenotypes and endophenotypes of atopic dermatitis: Where are we, and where should we go? *J. Allergy Clin. Immunol.* 139, S58–S64. doi: 10.1016/j.jaci.2017.01.008

Boehncke, W. H., and Schön, M. P. (2015). Psoriasis. *Lancet* 386, 983–994. doi: 10.1016/S0140-6736(14)61909-7

Bourguignon, L. Y., Ramez, M., Gilad, E., Singleton, P. A., Man, M. Q., Crumrine, D. A., et al. (2006). Hyaluronan-CD44 interaction stimulates keratinocyte differentiation, lamellar body formation/secretion, and permeability barrier homeostasis. *J. Invest. Dermatol.* 126 (6), 1356–1365. doi: 10.1038/sj.jid.5700260

Brown, M. B., and Jones, S. A. (2005). Hyaluronic acid: a unique topical vehicle for the localized delivery of drugs to the skin. *J. Eur. Acad. Dermatol. Venereology JEADV* 19 (3), 308–318. doi: 10.1111/j.1468-3083.2004.01180.x

Bukhari, S. N. A., Roswandi, N. L., Waqas, M., Habib, H., Hussain, F., Khan, S., et al. (2018). Hyaluronic acid, a promising skin rejuvenating biomedicine: A review of recent updates and pre-clinical and clinical investigations on cosmetic and nutricosmetic effects. *Int. J. Biol. Macromol.* 120, 1682–1695. doi: 10.1016/j.ijbiomac.2018.09.188

Bychkov, S. M., and Kuzmina, S. A. (2015). "The Biological Role of Hyaluronic Acid," in *Hyaluronic Acid* (Chichester, UK: John Wiley & Sons, Ltd), 9–75. doi:10.1002/9781118695920.ch2.

Carrasco, S., Neves, F., Fonseca, M., Gonçalves, C., Saad, C., Sampaio-Barros, P., et al. (2011). Toll-like receptor (TLR) 2 is upregulated on peripheral blood monocytes of patients with psoriatic arthritis: a role for a gram-positive inflammatory Trigger. *Clin. Exp. Rheumatol.* 29, 958–962.

Chatterjee, S., Hui, P. C., Kan, C., and Wang, W. (2019). Dual-responsive (pH/temperature) Pluronic F-127 hydrogel drug delivery system for textile-based transdermal therapy. *Sci. Rep.* 9 (1), 1–13. doi: 10.1038/s41598-019-48254-6

Chen, Z. (2018). What's new about the mechanism of methotrexate action in psoriasis? *Br. J. Dermatol.* 179, 818–819. doi: 10.1111/bjd.16908

Coondoo, A., Phiske, M., Verma, S., and Lahiri, K. (2014). Side-effects of topical steroids: A long overdue revisit. *Indian Dermatol. Online J.* 5, 425. doi: 10.4103/2229-5178.142483

Czarnecka-Operacz, M., and Sadowska-Przytocka, A. (2014). The possibilities and principles of methotrexate treatment of psoriasis - The updated knowledge. *Postep. Dermatologii i Alergol.* 31, 392–400. doi: 10.5114/pdia.2014.47121

Damiani, G., Eggenhöffner, R., Pigatto, P. D. M., and Bragazzi, N. L. (2019). Nanotechnology meets atopic dermatitis: Current solutions, challenges and future prospects. Insights and implications from a systematic review of the literature. *Bioact. Mater.* 4, 380–386. doi: 10.1016/j.bioactmat.2019.11.003

Dolz-Pérez, I., Sallam, M. A., Masiá, E., Morelló-Bolumar, D., Pérez del Caz, M. D., Graff, P., et al. (2020). Polypeptide-corticosteroid conjugates as a topical treatment approach to psoriasis. *J. Control. Release.* 318, 210–222. doi: 10.1016/j.jconrel.2019.12.016

Draelos, Z. D. (2011). A clinical evaluation of the comparable efficacy of hyaluronic acid-based foam and ceramide-containing emulsion cream in the treatment of mild-to-moderate atopic dermatitis. *J. Cosmet. Dermatol.* 10 (3), 185–188. doi: 10.1111/j.1473-2165.2011.00568.x

Du, H., Liu, P., Zhu, J., Lan, J., Li, Y., Zhang, L., et al. (2019). Hyaluronic Acid-Based Dissolving Microneedle Patch Loaded with Methotrexate for Improved Treatment of Psoriasis. *ACS Appl. Mater. Interfaces.* 11 (46), 43588–43598. doi: 10.1021/acsami.9b15668

Eichenfield, L. F., Tom, W. L., Berger, T. G., Krol, A., Paller, A. S., Schwarzenberger, K., et al. (2014). Guidelines of care for the management of atopic dermatitis: Section 2. Management and treatment of atopic dermatitis with topical therapies. *J. Am. Acad. Dermatol.* 71 (1), 116–132. doi: 10.1016/j.jaad.2014.03.023

Farwick, M., Gauglitz, G., Pavicic, T., Köhler, T., Wegmann, M., Schwach-Abdellaoui, K., et al. (2011). Fifty-kDa hyaluronic acid upregulates some epidermal genes without changing TNF-α expression in reconstituted epidermis. *Skin Pharmacol. Physiol.* 24 (4), 210–217. doi: 10.1159/000324296

Frankel, A., Sohn, A., Patel, R. V., and Lebwohl, M. (2011). Bilateral comparison study of pimecrolimus cream 1% and a ceramide-hyaluronic acid emollient foam in the treatment of patients with atopic dermatitis. *J. Drugs Dermatol.* 10 (6), 666. doi: 10.1016/j.jaad.2010.09.266

Garcia-Rodriguez, S., Arias-Santiago, S., Perandrés-López, R., Castellote, L., Zumaquero, E., Navarro, P., et al. (2013). Increased gene expression of Toll-like receptor 4 on peripheral blood mononuclear cells in patients with psoriasis. *J. Eur. Acad. Dermatol. Venereol.* 27, 242–250. doi: 10.1111/j.1468-3083.2011.04372.x

Giam, Y. C., Hebert, A. A., Dizon, M. V., Van Bever, H., Tiongco-Recto, M., Kim, K.-H., et al. (2016). A review on the role of moisturizers for atopic dermatitis. *Asia Pac. Allergy* 6 (2), 120–128. doi: 10.5415/apallergy.2016.6.2.120

Goebel, A. S. B., Neubert, R. H. H., and Wohlrab, J. (2011). Dermal targeting of tacrolimus using colloidal carrier systems. *Int. J. Pharm.* 404, 159–168. doi: 10.1016/j.ijpharm.2010.11.029

Goh, J. X. H., Tan, L. T.-H., Yew, H. C., Pusparajah, P., Lingham, P., Long, C. M., et al. (2019). Hydration effects of moisturizing gel on normal skin: A pilot study. *Prog. Drug Discovery Biomed. Sci.* 2 (1), a0000023. doi: 10.36877/pddbs.a0000023

Hellman, U., Engström-Laurent, A., Larsson, A., and Lindqvist, U. (2019). Hyaluronan concentration and molecular mass in psoriatic arthritis: biomarkers of disease severity, resistance to treatment, and outcome. *Scand. J. Rheumatol.* 48, 284–293. doi: 10.1080/03009742.2019.1577490

Huang, G., and Huang, H. (2018). Hyaluronic acid-based biopharmaceutical delivery and tumor-targeted drug delivery system. *J. Control. Release.* 278, 122–126. doi: 10.1016/j.jconrel.2018.04.015

Jiang, D., Liang, J., and Noble, P. W. (2011). Hyaluronan as an immune regulator in human diseases. *Physiol. Rev.* 91, 221–264. doi: 10.1152/physrev.00052.2009

Kapur, S., Watson, W., and Carr, S. (2018). Atopic dermatitis. *Allergy Asthma Clin. Immunol.* 14 (suppl 2), 44–52. doi: 10.1186/s13223-018-0281-6

Karimkhani, C., Dellavalle, R. P., Coffeng, L. E., Flohr, C., Hay, R. J., Langan, S. M., et al. (2017). Global skin disease morbidity and mortality an update from the global burden of disease study 2013. *JAMA Dermatol.* 153, 406–412. doi: 10.1001/jamadermatol.2016.5538

Ke, C., Sun, L., Qiao, D., Wang, D., and Zeng, X. (2011). Antioxidant acitivity of low molecular weight hyaluronic acid. *Food Chem. Toxicol.* 49 (10), 2670–2675. doi: 10.1016/j.fct.2011.07.020

Kim, Y., Lee, Y. S., Hahn, J. H., Choe, J., Kwon, H. J., Ro, J. Y., et al. (2008). Hyaluronic acid targets CD44 and inhibits FcεRI signaling involving PKCδ, Rac1, ROS, and MAPK to exert anti-allergic effect. *Mol. Immunol.* 45, 2537–2547. doi: 10.1016/j.molimm.2008.01.008

Kouvidi, K., Berdiaki, A., Nikitovic, D., Katonis, P., Afratis, N., Hascall, V. C., et al. (2011). Role of receptor for hyaluronic acid-mediated motility (RHAMM) in low molecular weight hyaluronan (LMWHA)-mediated fibrosarcoma cell adhesion. *J. Biol. Chem.* 286 (44), 38509–38520. doi: 10.1074/jbc.M111.275875

Lindqvist, U., Pihl-Lundin, I., and Engström-Laurent, A. (2012). Dermal distribution of hyaluronan in psoriatic arthritis: Coexistence of CD44, MMP3 and MMP9. *Acta Derm. Venereol.* 92 (4), 372–377. doi: 10.2340/00015555-1286

Logger, J., Olydam, J., Woliner-van der Weg, W., and van Erp, P. (2019). Noninvasive Skin Barrier Assessment: Multiparametric Approach and Pilot Study. *Cosmetics* 6:20. doi: 10.3390/cosmetics6010020

Luger, T. A., and Loser, K. (2018). Novel insights into the pathogenesis of psoriasis. *Clin. Immunol. (Orlando Fla.)* 186, 43–45. doi: 10.1016/j.clim.2017.07.014

Malaisse, J., Bourguignon, V., De Vuyst, E., Lambert De Rouvroit, C., Nikkels, A. F., Flamion, B., et al. (2014). Hyaluronan metabolism in human keratinocytes and atopic dermatitis skin is driven by a balance of hyaluronan synthases 1 and 3. *J. Invest. Dermatol.* 134, 2174–2182. doi: 10.1038/jid.2014.147

Malecic, N., and Young, H. (2016). Tacrolimus for the management of psoriasis: Clinical utility and place in therapy. *Psoriasis Targets Ther.* 6, 153–163. doi: 10.2147/PTT.S101233

Maytin, E. V., Chung, H. H., and Seetharaman, V. M. (2004). Hyaluronan participates in the epidermal response to disruption of the permeability barrier in vivo. *Am. J. Pathol.* 165, 1331–1341. doi: 10.1016/S0002-9440(10)63391-3

Mehta, N. N., Yu, Y. D., Saboury, B., Foroughi, N., Krishnamoorthy, P., Raper, A., et al. (2011). Systemic and vascular inflammation in patients with moderate to severe psoriasis as measured by [18F]-fluorodeoxyglucose positron emission tomography-computed tomography (FDG-PET/CT): A pilot study. *Arch. Dermatol.* 147, 1031–1039. doi: 10.1001/archdermatol.2011.119

Micali, G., Paternò, V., Cannarella, R., Dinotta, F., and Lacarrubba, F. (2018). Evidence-based treatment of atopic dermatitis with topical moisturizers. *G. Ital. di Dermatologia e Venereol.* 153, 396–402. doi: 10.23736/S0392-0488.18.05898-4

Mohd Affandi, A., Khan, I., and Ngah Saaya, N. (2018). Epidemiology and Clinical Features of Adult Patients with Psoriasis in Malaysia: 10-Year Review from the Malaysian Psoriasis Registry, (2007-2016). *Dermatol. Res. Pract.* 2018, 1–8. doi: 10.1155/2018/4371471

Nakatsuji, T., Chen, T. H., Narala, S., Chun, K. A., Two, A. M., Yun, T., et al. (2017). Antimicrobials from human skin commensal bacteria protect against Staphylococcus aureus and are deficient in atopic dermatitis. *Sci. Transl. Med.* 9 eaah4680. doi: 10.1126/scitranslmed.aah4680

Narurkar, V. A., Cohen, J. L., Dayan, S., Kaminer, M. S., Rivkin, A., Shamban, A., et al. (2016). A Comprehensive Approach to Multimodal Facial Aesthetic Treatment: Injection Techniques and Treatment Characteristics From the HARMONY Study. *Dermatologic Surg.* 42 (Suppl 2), S177–S191. doi: 10.1097/DSS.0000000000000743

Ohkawara, Y., Tamura, G., Iwasaki, T., Tanaka, A., Kikuchi, T., and Shirato, K. (2000). Activation and transforming growth factor-β production in eosinophils by hyaluronan. *Am. J. Respir. Cell Mol. Biol.* 23, 444–451. doi: 10.1165/ajrcmb.23.4.3875

Ohtani, T., Memezawa, A., Okuyama, R., Sayo, T., Sugiyama, Y., Inoue, S., et al. (2009). Increased hyaluronan production and decreased E-cadherin expression by cytokine-stimulated keratinocytes lead to spongiosis formation. *J. Invest. Dermatol.* 129 (6), 1412–1420. doi: 10.1038/jid.2008.394

Pacha, O., and Hebert, A. A. (2012). Treating atopic dermatitis: Safety, efficacy, and patient acceptability of a ceramide hyaluronic acid emollient foam. *Clin. Cosmet. Investig. Dermatol.* 5, 39. doi: 10.2147/CCID.S23269

Pandey, M., Choudhury, H., Gunasegaran, T. A. P., Nathan, S. S., Md, S., Gorain, B., et al. (2019). Hyaluronic acid-modified betamethasone encapsulated polymeric nanoparticles: fabrication, characterisation, in vitro release kinetics, and dermal targeting. *Drug Deliv. Transl. Res.* 9, 520–533. doi: 10.1007/s13346-018-0480-1

Pardue, E. L., Ibrahim, S., and Ramamurthi, A. (2008). Role of hyaluronan in angiogenesis and its utility to angiogenic tissue engineering. *Organogenesis* 4 (4), 203–214. doi: 10.4161/org.4.4.6926

Passi, A., Sadeghi, P., Kawamura, H., Anand, S., Sato, N., White, L. E., et al. (2004). Hyaluronan suppresses epidermal differentiation in organotypic cultures of rat keratinocytes. *Exp. Cell Res.* 296 (2), 123–134. doi: 10.1016/j.yexcr.2004.01.031

Prost-Squarcioni, C. (2006). Histologie de la peau et des follicules pileux. *Medecine/Sciences* 22, 131–137. doi: 10.1051/medsci/2006222131

Rendon, A., and Schäkel, K. (2019). Psoriasis pathogenesis and treatment. *Int. J. Mol. Sci.* 20 (6), 1475. doi: 10.3390/ijms20061475

Sathishkumar, D., and Moss, C. (2016). Topical therapy in atopic dermatitis in children. *Indian J. Dermatol.* 61, 656–661. doi: 10.4103/0019-5154.193677

Siegfried, E., and Hebert, A. (2015). Diagnosis of Atopic Dermatitis: Mimics, Overlaps, and Complications. *J. Clin. Med.* 4, 884–917. doi: 10.3390/jcm4050884

Stauffer, S. R., and Peppast, N. A. (1992). Poly(vinyl alcohol) hydrogels prepared by freezing-thawing cyclic processing. *Polymer* 33 (18), 3932–3936. doi: 10.1016/0032-3861(92)90385-A

Symonette, C. J., Kaur Mann, A., Tan, X. C., Tolg, C., Ma, J., Perera, F., et al. (2014). Hyaluronan-Phosphatidylethanolamine Polymers Form Pericellular Coats on Keratinocytes and Promote Basal Keratinocyte Proliferation. *BioMed. Res. Int.* 2014. doi: 10.1155/2014/727459

Sze, J. H., Brownlie, J. C., and Love, C. A. (2016). Biotechnological production of hyaluronic acid: a mini review. *3 Biotech.* 6, 1–9. doi: 10.1007/s13205-016-0379-9

Tabassum, N., and Hamdani, M. (2014). Plants used to treat skin diseases. *Pharmacogn. Rev.* 8, 52–60. doi: 10.4103/0973-7847.125531

Taetz, S., Bochot, A., Surace, C., Arpicco, S., Renoir, J. M., Schaefer, U. F., et al. (2009). Hyaluronic acid-modified DOTAP/DOPE liposomes for the targeted delivery of anti-telomerase siRNA to CD44-expressing lung cancer cells. *Oligonucleotides* 19, 103–115. doi: 10.1089/oli.2008.0168

Termeer, C. C., Hennies, J., Voith, U., Ahrens, T., M. Weiss, J., Prehm, P., et al. (2000). Oligosaccharides of Hyaluronan Are Potent Activators of Dendritic Cells. *J. Immunol.* 165, 1863–1870. doi: 10.4049/jimmunol.165.4.1863

Touitou, E., Dayan, N., Bergelson, L., Godin, B., and Eliaz, M. (2000). Ethosomes - novel vesicular carriers for enhanced delivery: characterization and skin penetration properties. *J. Controlled release* 65 (3), 403–418. doi: 10.1016/s0168-3659(99)00222-9

Wan, T., Pan, W., Long, Y., Yu, K., Liu, S., Ruan, W., et al. (2017). Effects of nanoparticles with hydrotropic nicotinamide on tacrolimus: Permeability through psoriatic skin and antipsoriatic and antiproliferative activities. *Int. J. Nanomedicine.* 12, 1485. doi: 10.2147/IJN.S126210

Yamamoto, T., Matsuuchi, M., Irimajiri, J., Katayama, I., and Nishioka, K. (1997). John Libbey Eurotext - European Journal of Dermatology - Elevated circulating

hyaluronan in patients with generalized pustular psoriasis. *Eur. J. Dermatol.* 7 (6), 409–411.

Yamamoto, T. (2015). Hyaluronic acid in psoriasis. *J. Eur. Acad. Dermatol. Venereol.* 29, 2487–2487. doi: 10.1111/jdv.12581

Zhang, Y., Xia, Q., Li, Y., He, Z., Li, Z., Guo, T., et al. (2019). CD44 assists the topical anti-psoriatic efficacy of curcumin-loaded hyaluronan-modified ethosomes: A new strategy for clustering drug in inflammatory skin. *Theranostics* 9 (1), 48. doi: 10.7150/thno.29715

Zhuo, F., Abourehab, M. A. S., and Hussain, Z. (2018). Hyaluronic acid decorated tacrolimus-loaded nanoparticles: Efficient approach to maximize dermal targeting and anti-dermatitis efficacy. *Carbohydr. Polym.* 197, 478–489. doi: 10.1016/j.carbpol.2018.06.023

Zonnevdd, I. M., Rubins, A., Jablonska, S., Dobozy, A., Ruzicka, T., Kind, P., et al. (1998). Topical tacrolimus is not effective in chronic plaque psoriasis: A pilot study. *Arch. Dermatol.* 134, 1101–1102. doi: 10.1001/archderm.134.9.1101

frontiers
in Pharmacology

Microalgae as Potential Anti-Inflammatory Natural Product Against Human Inflammatory Skin Diseases

Wu-Thong Choo[1], Ming-Li Teoh[1,2,3]*, Siew-Moi Phang[2,4]*, Peter Convey[5], Wei-Hsum Yap[1], Bey-Hing Goh[6,7] and John Beardall[8]

[1] School of Biosciences, Taylor's University, Lakeside Campus, Subang Jaya, Malaysia, [2] Institute of Ocean and Earth Sciences, University of Malaya, Kuala Lumpur, Malaysia, [3] National Antarctic Research Centre, Institute of Graduate Studies, University of Malaya, Kuala Lumpur, Malaysia, [4] Faculty of Applied Sciences, UCSI University, Kuala Lumpur, Malaysia, [5] British Antarctic Survey, NERC, Cambridge, United Kingdom, [6] Biofunctional Molecule Exploratory Research Group (BMEX), School of Pharmacy, Monash University Malaysia, Bandar Sunway, Malaysia, [7] College of Pharmaceutical Sciences, Zhejiang University, Hangzhou, China, [8] School of Biological Sciences, Monash University, Clayton, VIC, Australia

The skin is the first line of defense against pathogen and other environmental pollutant. The body is constantly exposed to reactive oxygen species (ROS) that stimulates inflammatory process in the skin. Many studies have linked ROS to various inflammatory skin diseases. Patients with skin diseases face various challenges with inefficient and inappropriate treatment in managing skin diseases. Overproduction of ROS in the body will result in oxidative stress which will lead to various cellular damage and alter normal cell function. Multiple signaling pathways are seen to have significant effects during ROS-mediated oxidative stress. In this review, microalgae have been selected as a source of natural-derived antioxidant to combat inflammatory skin diseases that are prominent in today's society. Several studies have demonstrated that bioactive compounds isolated from microalgae have anti-inflammation and anti-oxidative properties that can help remedy various skin diseases. These compounds are able to inhibit production of pro-inflammatory cytokines and reduce the expression of inflammatory genes. Bioactive compounds from microalgae work in action by altering enzyme activities, regulating cellular activities, targeting major signaling pathways related to inflammation.

Keywords: microalgae, bioactive compounds, anti-inflammation, anti-oxidant, skin disease

INTRODUCTION

The skin is the outermost layer and considered the largest organ in the human body. It plays an important protective role by providing a major boundary between the host and the external environment (Benson and Watkinson, 2012). The skin is also well equipped with effective defenses against pathogens and other environmental pollution (Wang H. et al., 2013). Exogenous threats such as UV radiation and oral introduction of potentially toxic dietary and drug metabolites, all of these factors may influence the health and appearance of the skin (Sander et al., 2004). The body

is constantly exposed to these environmental agents and endogenous metabolites that may have either short-term or long-term side effects to the host. Because of that, they may directly or indirectly promote the production of reactive oxygen species (ROS) that stimulate the inflammatory process in the skin (Kohen, 1999; Trouba et al., 2002). The surface of the skin is constantly exposed to ROS as its first line of defense against pathogens and external pollutants. Many studies have linked ROS to various inflammatory skin diseases (atopic dermatitis [AD], psoriasis, and vitiligo), skin aging, and carcinogenesis (Briganti and Picardo, 2003; Sander et al., 2004; Okayama, 2005).

Skin diseases are the fourth most common cause of non-fatal disease burden and 18th leading cause of global disability-adjusted life years (DALYs) worldwide within the year of 2010–2013 (Karimkhani et al., 2017). Dermatitis (consisting of atopic, seborrheic, and contact categories) is the highest burden among of the skin conditions, make up a total of 9.3 million DALYs (Karimkhani et al., 2017). Skin diseases may present similarly across racial and ethnic groups; however, some features may be either more prominent in patients with darker skin (Mei-Yen Yong and Tay, 2017; Kaufman et al., 2018). Besides that, patients with skin diseases face challenges with ineffective and inappropriate treatment, such as oral antihistamines, oral corticosteroids, or traditional medicines, which may have low potency or have significant side effects for certain individual (Lopez Carrera et al., 2019). Therefore, natural derived ingredients may be potential in combating against skin diseases (Jahan et al., 2017).

ROS consist of reactive molecules and free radicals that are oxygen based and are often associated with the principle of oxidative stress, which suggests that ROS induce cell damage by interfering with lipids, proteins, and DNA within the body (Cross, 1987). ROS are produced during the reduction of molecular oxygen as follow:

$$O_2 + 1e^- + H^+ \rightarrow H_2O \rightarrow H^+ + O_2^-$$

$$H_2O + 1e^- + H^+ \rightarrow H_2O_2$$

$$H_2O_2 + 1e^- + H^+ \rightarrow H_3O_2 \rightarrow H_2O + OH$$

$$OH + 1e^- + H^+ \rightarrow H_2O$$
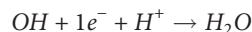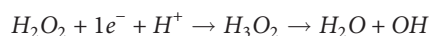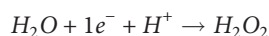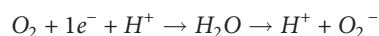
Superoxide anion (O_2^-), hydroxyl radicals (OH.), hydrogen peroxide (H_2O_2), and molecular oxygen (O_2) at low levels in the body are involved in various cellular process such as, cell proliferation, apoptosis, immune responses, and cell differentiation (Kumar and Pandey, 2015). In contrast, overproduction of ROS will result in oxidative stress, which will further lead to altered metabolism, dysregulated signal transduction, and biomolecular cell damage, which cause pathological changes in normal cell function (Trouba et al., 2002). Biomolecular damage that occurs as a result of increasing ROS levels has considered as lipid peroxidation, DNA mutation, enzyme inactivation/activation, and protein oxidation/degradation. Such damages will usually cause further damaging effects as the result of ROS. Thus, the amount of ROS level is displayed to be hormesis, whereby low dose stimulation showing beneficial effects and high dose stimulation showing toxic effect (Di Meo et al., 2016).

RELATIONSHIP BETWEEN OXIDATIVE STRESS AND SKIN INFLAMMATION DISEASE

Inflammation triggers when the body detects the presence of pathogens or irritants that are present in the body. Many studies have linked that there is correlation between oxidative stress and various inflammatory skin disease. Evidence shows that ROS-mediated oxidative stress stimulates the production of oxidative products which can cause damage to proteins, triggers cell apoptosis, cause DNA modification, lipid peroxidation, and promotes the release of proinflammatory mediators, such as cytokines and chemokines, which may be the main cause of several inflammatory skin disease to occur (Meffert et al., 1976). In addition, ROS acts as a secondary messenger in influencing cellular signal transduction pathways proinflammatory signaling pathways and modulate the expression of several gene involved in inflammation (Finkel and Holbrook, 2000). The most significant effects were seen in MAPK/AP-1, NF-κβ, and JAK-STAT signaling pathways during early stage of every inflammatory disorders (**Figure 1**) (Dhar et al., 2002; Wolk

FIGURE 1 | Reactive oxygen species (ROS)-mediated activation of various cell signaling pathways in the skin. Chemical irritants, allergens, or inflammatory agents that cause the production of ROS during the pathogenesis of various skin disease and activation of a various number of signaling pathways. Signaling pathways with the most significant effects are MAPK/AP-1, NF-κβ, and JAK-STAT pathways. Activation of these pathways will result in protein damge, cell apoptosis, DNA modification, lipid peroxidation, and production of proinflammatory mediators.

et al., 2004; Kim et al., 2005; Wang et al., 2006). Activation of these signal transduction cascades results in the production of growth factors, cytokines, neurotransmitters, and other signaling molecules, thus leading to cell proliferation, differentiation, and apoptosis.

MECHANISM OF ANTI-OXIDANTS IN SKIN

Anti-oxidants functions to delay or prevent ROS-induced cellular damage. They can help to reduce oxygen radicals, inhibiting chain initiation reactions, binding catalysts that generate ROS, and attenuating hydrogen radicals (Trouba et al., 2002). Anti-oxidants can be categorized as enzymatic and non-enzymatic in the intracellular and extracellular environment (Frei et al., 1988).

Rice-Evans and Diplock (1993) proposed that anti-oxidants had two principle mechanism of action against ROS. The first is a chain breaking mechanism whereby anti-oxidant donates an electron to the free radical that is present in the systems. The second mechanism involves removal of ROS/RNS initiators by quenching chain-initiating catalyst. Anti-oxidants may cultivate different mechanism to combat radicals in the biological systems such as, electron donation, metal ion chelation, co-antioxidants, or by gene expression regulation (Krinsky, 1992).

SKIN DISORDERS

Atopic Dermatitis

Atopic dermatitis (AD) is a chronic, itching, inflammatory disease and is predominantly between 10 and 20% of pediatric population (Kowalska-Olędzka et al., 2019). Symptoms of AD appear in 60% of patients before reaching 1 year of age (Kowalska-Olędzka et al., 2019). AD is believed to be caused by combination of genetic and environmental factors (Eigenmann and Calza, 2000; Hill and Hosking, 2004). It is characterized by having papules and plaques. The earliest lesion is a small erythematous papule or papulovesicle. These papules may then later become erythematous plaques with clinical features of weeping, crusting, or scaling, depending on the severity of the lesions form (Simpson, 2010). The most problematic symptom of AD is itch. The "itch-scratch" cycle involves scratching on affected areas on the skin to relieve AD associated itch and would further worsen the disease (**Figure 2**). These symptoms would usually accompany with sleep disturbance and social stigma of visible skin disorder, therefore having negative impact to the quality of life to the patient and family (Bender et al., 2008).

Symptoms of AD often reduces the barrier function of the skin as demonstrated by elevated trans-epidermal water loss and increase permeation of environmental irritants and allergens. Antigen-presenting cells (APC), such as Langerhan's cells, process antigens and present it to lymphocytes, where the process will stimulate helper T-cells into the skin. These cells then stimulate the production of proinflammatory cytokines into
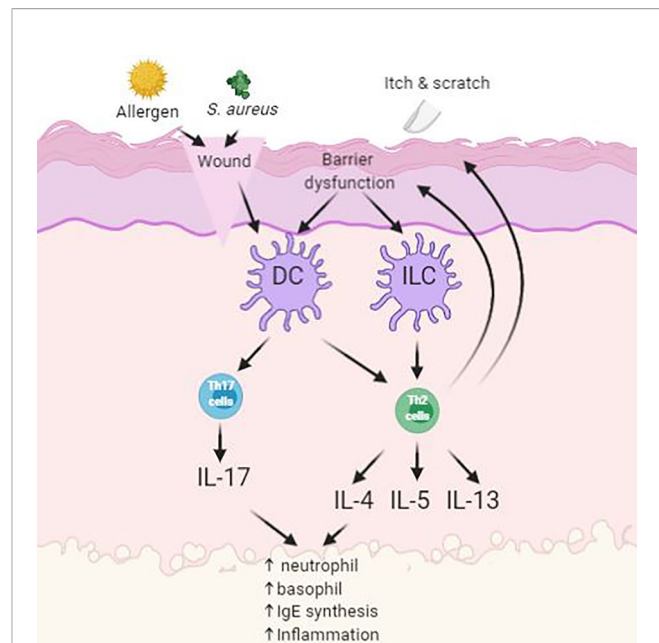
FIGURE 2 | Simplified schematic of pathogenesis of atopic dermatitis (AD) with skin barrier defect. Impact of infections, allergens and itch leads to upregulation of inflammatory pathways.

the inflamed area. This will then enable the activation of imbalanced growth factors, cytokines (IL-1, IL-6, GM-CSF, TNF-α), and chemokines that interfere with the normal mechanism of the innate immune system of the skin (Nesterova et al., 2019). Overproduction levels of cytokines will oppose the mechanism of innate immunity in the skin and consequently cause secondary bacterial infection at site of inflammation (Albanesi and Pastore, 2010). Patients with AD are prone to acquiring secondary cutaneous infections such as *Staphylococcus aureus* infections. These infections are usually present in the form of impetigo or folliculitis due to further worsening from scratching (Leyden et al., 1974).

Other than avoiding irritants and moisturizing the skin with emollients, the most common method to treat AD is by applying topical corticosteroids (Spergel, 2008). Topical corticosteroids produce instant results in short-term treatment on skin itching and inflammation of skin. However, long-term usage of such treatment may lead to adverse effects, such as skin atrophy and telangiectasia (Van der Aa et al., 2010). Besides that, long term use of topical corticosteroids will cause thinning of the stratum corneum, therefore allowing irritants and allergens entry into the skin.

Psoriasis

Psoriasis is a chronic autoimmune disease characterized by raised, red scaly plaques (Lowes et al., 2014). This disease affects 2–3% of the world population, resulting in psychological stress and poor quality of life (Perera et al., 2012). The most common type of psoriasis is psoriasis vulgaris which accounted about 85–90% of all cases of psoriasis. Psoriasis is caused by hyperproliferation of keratinocytes and infiltration of activated

immune cells triggered by several factors such as physical and psychological stress, bacterial infections, or injury (Dika et al., 2007; Lowes et al., 2007).

Several studies have identified that overexpression of various cytokines occurred in psoriasis, such as interleukins (ILs), tumor necrosis factor (TNF), and interferon-γ (IFN-γ) (**Figure 3**) (Nickoloff et al., 2007). Furthermore, development of psoriasis was closely linked to complex cellular interactions among epidermal keratinocytes, leukocytes, neutrophils, dendritic cells, and activated T cells, growth factors, cytokines, and chemokines (Nickoloff et al., 2007).

The mitogen-activated protein kinase signaling pathways composed of extracellular-regulated kinase (ERK1/2 and ERK3/4) (Seternes et al., 2004), Jun N-terminal kinase (JNK) (Davis, 1994; Cano and Mahadevan, 1995), p38 kinase (Cano and Mahadevan, 1995; Cobb and Goldsmith, 1995), and big mitogen activated protein kinase 1 (BMK1) (Kato et al., 2000). Several studies have demonstrated that ROS may trigger pathogenesis of psoriasis through ERK1/2, JNK, and p38 MAPK pathways (Takahashi et al., 2002; Johansen et al., 2005; Yu et al., 2007). However, no reports have found that ERK3/4 and BMK1 pathway being involved in the pathogenesis of psoriasis due to oxidative stress as of now.

During cell stimulation, Iκβ (inhibitor of κβ) proteins are rapidly phosphorylated and degraded by the proteasome, the unbound NF-κβ translocate into the nucleus to regulate multiple gene expressions (Hayden, 2004). These genes may encode for TNF super family, IL-1, IL-6, IL-8, iNOS, major histocompatibility complex class 1 (MHC class 1) antigens,

E-selectin, and vascular cell adhesion molecule 1 (VCAM-1), which are mostly involved in psoriasis (Wajant et al., 2003; Schottelius et al., 2004).

Although MAPK/AP-1 and NF-κβ signaling pathways is triggered by ROS in the pathogenesis of psoriasis, there is solid evidence showing that there's a correlation between these two signal transduction pathways. This is because the response to AP-1 is highly stimulated due to the presence of NF-κβ and thus NF-κβ positively modulates the expression of c-Fos and AP-1 activity (Stein et al., 1993; Fujioka et al., 2004).

The JAK-STAT signal pathway also plays an important role in immune and inflammatory responses (Kishimoto et al., 1994). Studies shown that STAT1 is upregulated by IFN-γ and IL-20 and thus induce inflammatory mediators in a type 1 cytokine pathway model of psoriasis pathogenesis (Wang et al., 2006). Another study had demonstrated that STAT3 pathway is believed to play a role in the pathogenesis of psoriasis where STAT3 is activated by IL-22 and result in the increased expression of β-defensin 2/3 (Wolk et al., 2004).

The most common conventional treatment of psoriasis consists of corticosteroids, Vitamin D analogues, phototherapy, and systemic treatments (Novelli et al., 2014). However, long-term usage of conventional treatments may cause severe health issues to patients, such as poor tolerability and cumulative toxicity (Rahman et al., 2012). Topical glucocorticosteroids and Vitamin D analogues are commonly used to treat psoriasis by regulating keratinocyte function and inflammatory response. Nonetheless, long term treatment of corticosteroid can cause several health issues, such as cutaneous atrophy, short remission duration, and cause psoriasis to be rebound (Chong and Fonacier, 2015). Regardless of their reduce side effects in comparison to corticosteroid, vitamin D analogues still fail to have a rapid activation in the body (Smith and Barker, 2006). Another widely used treatment for psoriasis, methotrexate, due to its reasonable price and its high efficacy (Boehncke, 2003; Heydendael et al., 2003). However, prolonged usage of the drug may cause patients to suffer liver fibrosis and cirrhosis (Deng et al., 2016).

Vitiligo

Vitiligo is a skin disorder characterized by depigmented macules from melanocyte dysfunction in the epidermis (Boniface et al., 2017). Vitiligo affects approximately 0.5–1% of the world population and both genders are equally affected (Taïeb and Picardo, 2009). Studies have suggest that destruction of melanocytes is the main cause of the pathogenesis of vitiligo (Poole et al., 1993). Oxidative stress may be the main pathogenic reason in melanocyte loss (Maresca et al., 1997; Schallreuter, 1999).

Patients in active phase of vitiligo has high levels of ROS in the epidermal layer, primarily consists of hydrogen peroxide (H_2O_2) and peroxynitrite (Schallreuter et al., 1991; Schallreuter et al., 1999). This damage is due to local and systemic imbalance in enzymatic and non-enzymatic anti-oxidant systems in the skin (Shajil and Begum, 2006). Studies have demonstrated that vitiligo patients have high levels of tetrahydrobiopterin (6BG4) and the isomer 7BH4 in the epidermis and inhibits the enzymes
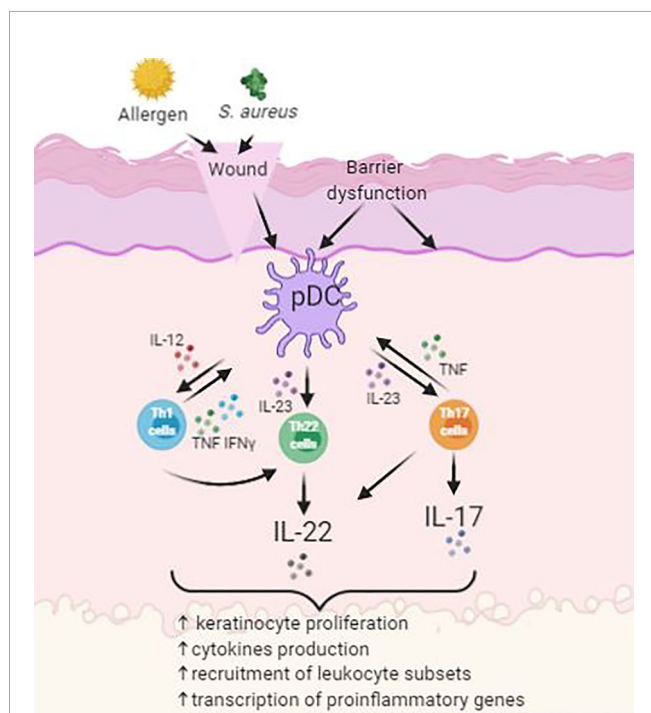
FIGURE 3 | Simplified schematic of pathogenesis of psoriasis with activation of Th22 and Th17 cells.

involved in melanogenesis and increases the production of H_2O_2 (Schallereuter et al., 1994; Hasse et al., 2004).

In melanocytes, the alteration of calcium homeostasis due to the increase in level of H_2O_2 systemically and locally would indirectly interfere with the intake of L-phemylalanine, an amino acid precursor of tyrosine (Schallreuter et al., 2007). Proopiomelanocortin-derived bioactive peptides ACTH and a-MSH plays crucial role in melanogenesis by activating a cascade of intracellular signals that promotes relevant enzymes in melanin production, such as tyrosinase and tyrosinase-related proteins 1 and tyrosinase-related proteins 2. Presence of ROS may oxidize or inhibit these signaling pathways for melanin synthesis (Tachibana, 2000).

Accumulation of ROS may induce DNA damage, lipid peroxidation, increased production of proinflammatory, and antimelanogenic cytokines (Mahendra et al., 2019a; Mahendra et al., 2019b). Altered enzymes that play a key role in melanogenesis may show partial or complete dysfunction due to damage done from oxidative stress (Denat et al., 2014).

Recent studies have linked Nrf2-anti-oxidant response element (ARE) pathway being affected by oxidative stress in regulating vitiligo skin homeostasis (Jian et al., 2011; Jian et al., 2014; Qiu et al., 2014). Nrf2-ARE is an anti-oxidant pathway that regulates the transcription of stress-related cytoprotective genes and thus protecting cells from radical molecules (Jian et al., 2011). One example of such gene is the heme oxygenase-1 (HO-1). Another study had shown that vitiligo melanocytes have decrease HO-1 expression and abnormal redox balance due to reduced Nrf2 nuclear translocation and transcriptional activity. For this reason, the same studies were conducted in a clinical setting and showed that vitiligo patients have low expression levels of HO-1 gene when compared to healthy controls (Jian et al., 2014).

Corticosteroids are still the first line therapy for vitiligo and can use either as topical or systemic treatment. Topical corticosteroids help to decrease the destruction of melanocyte and repopulate melanocyte and melanin production (Bleehen, 1976; Hann et al., 1993). However, corticosteroids still pose to have various side effects which includes skin atrophy, telangiectasia, and striae distensae, steroid folliculitis, and acne formation on the skin (Speeckaert and van Geel, 2017). In contrast, oral corticosteroid therapy in moderate doses helps in arresting the progression of vitiligo (Speeckaert and van Geel, 2017). Side effects include acne formation, disturbance in sleep patterns, weight gain, agitation, hypertrichosis, and menstrual abnormalities, when consume on a long-term basis (Radakovic-Fijan et al., 2001).

Phototherapy is also a common treatment to induce repigmentation in vitiligo patients. Phototherapy involves usage of both UVA and UVB to promote melanocyte migration and proliferation (Wu et al., 2007). Common side effects patients may receive from psoralen and ultraviolet a (PUVA) treatment includes erythema, pruritus, headache, and nausea (Valkova et al., 2004). Patients may also suffer from second-degree burns when incorrect radiation doses from phototherapy (Herr et al., 2007). PUVA also carries a higher risk in gaining non-melanoma skin cancer and melanoma (Park et al., 2003; Patel et al., 2009).

MICROALGAE AS NATURAL SOURCE OF BIOACTIVE COMPOUNDS

Microalgae are unicellular microorganism that can be found in freshwater or marine environments. They are autotrophic as they are capable to undergo photosynthesis with the aid of sunlight, they can convert water and carbon dioxide into organic compounds like terrestrial plants (Metting, 1996). Microalgae have many advantages over terrestrial plants as they are fast growing, easily cultivate, and do not compete directly with agricultural crops. Microalgae are capable to live in extreme conditions and environment by adopting surviving strategies by producing various bioactive compounds with diverse structure and unique activity to counter environmental stress (Christaki et al., 2012). Therefore, microalgae has drawn great attention as candidate for natural products to be use in the medical, pharmaceutical, cosmetic, and biofuel industries (Sathasivam et al., 2019).

Microalgae produce various bioactive compounds that exhibit potential pharmacological effects, including anticancer, antidiabetic, anti-inflammatory, and anti-oxidative activities (Fu et al., 2017). These bioactive compounds include fatty acids, phycobiliproteins, chlorophylls, carotenoids, and vitamins. Microalgae-derived bioactive compounds have been proven to be able to overcome inflammatory skin disorders, given by their tremendous structural diversity and biological availability. Furthermore, the culture condition of microalgae can be easily manipulate to favor production of specific bioactive compounds by addition or removal of certain nutrients (Fu et al., 2017).

Bioactive compounds of microalgae from primary metabolism are directly involved in cell growth and reproduction. Primary metabolites from microalgae are usually consists of carbohydrates, lipid, and proteins (Wen et al., 2015). Secondary metabolites have gained several attentions over the past decades due to their wide health benefiting properties. These metabolites are mainly involved in adaption of microalgae to the environment (Bourgaud et al., 2001). In most microalgae species, the bioactive compounds are accumulated in the form of their biomass; while in some cases, they are excreted into the medium.

Protective Effects of Microalgae Against Inflammatory Skin Diseases

Microalgae extracts possess anti-inflammatory properties as they are able to inhibit production of pro-inflammatory cytokines and reduce the expression of inflammatory genes (Robertson et al., 2015). Bioactive compounds from microalgae works in various ways in inhibiting skin inflammation which includes altering enzyme activities, regulating cellular activities, nitric oxide synthase (NOS), and targeting major signaling pathways, such as NF-κβ and MAPKs pathway (Hussain et al., 2016). Both of these pathways are major mediators of various inflammatory producer. Besides having anti-inflammatory, microalgae extracts

may also possess anti-oxidative properties too (Arulselvan et al., 2016).

KEY METABOLITES IN MICROALGAE

Carotenoids

Carotenoids are mostly found in plants, marine algae, fungi, and bacteria. Carotenoids are divided into two classes, carotenes and xanthophylls (Sathasivam and Ki, 2018). Xanthophylls contain oxygen group in their structure while it is absent in carotenes. Carotenoids have a common chemical backbone which composed mainly of polyene chain with a long conjugated double bond system. The ending of the chain may be terminated with cyclic groups containing oxygen-bearing substitutes. The electron-rich conjugated system of the polyene and its cyclic end groups determine the functional anti-oxidant properties of carotenoids (Martin et al., 1999).

In microalgae, carotenoids play a role in protecting the chlorophyll from long-term exposure of light by scavenging ROS, phototropism, and photoaxis (Esteban et al., 2009). Carotenoids can scavenge harmful radicals through three different ways, which are, electron transfer, radical adduct formation, and hydrogen atom transfer (Burton and Ingold, 1984; Rice-Evans et al., 1997; Paiva and Russell, 1999; Skibsted, 2012).

$$Car + R^\bullet \rightarrow Car^{\bullet +} + R^- \ (electron\ transfer)$$

$$Car + R^\bullet \rightarrow [Car \cdots R]^\bullet \ (radical\ adduct\ formation)$$

$$Car + R^\bullet \rightarrow Car(-H)^\bullet + RH \ (hydrogen\ atom\ transfer)$$
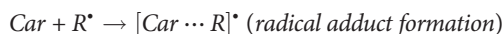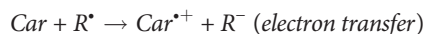
Carotenoids are potential to be used to treat and control chronic inflammation as research shown that they are capable to inhibit pro-inflammatory cytokines (Zhang et al., 2014). Carotenoids are able to regulate chronic inflammatory disorder by inhibiting the effects from nitric oxide production, pro-inflammatory cytokines, expression of pro-inflammatory genes, and pro-inflammatory enzyme activities (Hussain et al., 2016).

Astaxanthin

Astaxanthin is a lipid soluble pigment and is classified as a xanthophyll. It is a secondary metabolite and is mainly found in the marine environment as a red-orange pigment. Astaxanthin is primarily synthesized naturally by microalgae, zooplankton, crustaceans, and certain species of fish, such as salmonids. Although astaxanthin can be synthesized from plants, bacteria, and microalgae, one particular species of microalgae, namely *Haematococcus pluvialis*, is known to produce the highest content of astaxanthin (Boussiba, 2000).

Astaxanthin has reported to have higher bioactive properties than zeaxanthin, lutein, and β-carotene. This is due to the presence of a keto- and hydroxyl group on each end of its structure. Because of its unique structure, astaxanthin has the potential to be used in promoting human health. The polar end groups of astaxanthin are able to quench free radicals, the double bond chains of the structure help remove high-energy electrons. Because of its unique structure, astaxanthin has a higher anti-oxidant activity than other carotenoids (Higuera-Ciapara et al., 2006). When it come to the characteristics of its existence, astaxanthin is polar in nature and hence its rate in absorption is rather easy with a moderate consumption. Besides the integrity of membrane is preserved by conveniently instilling themselves in between bilayers. With this feature, astaxanthin can also preserve the functionality of the mitochondria that lead to the protection of the redox state of the body (Wolf et al., 2010; Kidd, 2011).

Studies on rat models on the effects of astaxanthin on lipopolysaccharide-induced inflammatory reactions shows that astaxanthin (100 mg/kg) has a higher anti-inflammatory activity than that of 10 mg/kg of prednisolone, a common anti-inflammatory drug. Further results showed that astaxanthin inhibits production of NO, prostaglandin E_2 (PGE_2), TNF-α, and interleukin-1β, and also blocks the NOS enzyme in RAW 264.7 cells (Ohgami et al., 2003).

Other reports stating that human neutrophil treated with 5 mM astaxanthin has improved phagocytic and microbicidal activity. Besides that, oxidative damage to proteins and lipids in human neutrophil were significantly lower after astaxanthin treatment due to the fact that astaxanthin is effective in quenching ROS (Macedo et al., 2010).

Another study has demonstrated that U937 cells (human lymphoma cell line) pre-incubated in 10 mM astaxanthin before inducing H_2O_2 showed lower cytokines levels than cells that were not treated with astaxanthin. In addition, cells that were pre-incubated in astaxanthin had shown higher levels of SHP-1 (protein tyrosine phosphate), an enzyme that removes phosphate groups from phosphorylated tyrosine residue from proteins, and lower levels of NF-ƙβ expression (Speranza et al., 2012).

Studies also shown that HaCaT keratinocytes treated with astaxanthin were able to decrease UV-induced release of migration inhibitory factor (MIF), 1L-1β, and TNF-α at both the protein and mRNA levels. Astaxanthin treatment were able to reduce the UVB-induced production of pro-inflammatory cytokines, thus inhibited the cells from undergoing apoptosis and also protected the skin from inflammation. Furthermore, astaxanthin treatment significantly reduced the UVB-induced caspase-3 and caspase-9 activity while no reduction was observed in UVC-induced caspase-3 activity. Therefore, astaxanthin treatment may have a stronger protective effect against UVB-induced apoptosis than UVC-induced apoptosis. Besides that, astaxanthin also decreases the expression levels of inducible nitric oxide synthase (iNOS) and cycloosygenase-2 (COX-2) and decreases production of PGE_2 in UV-induced HaCaT keratinocyte (Yoshihisa et al., 2014).

Lutein

Lutein is a yellow pigment and is classified as a xanthophyll. Lutein helps protect green microalgae from ROS damage. Microalgae have been considered the main natural source for lutein production as they produce higher lutein content compare to plants source (Lin et al., 2015). *Dunaliella salina* has been

shown to be potential in producing lutein by manipulating its growth conditions (Fu et al., 2012). Other microalgae strain, such as *Chlorella sorokiniana* and *Chlorella prothecoides* have also been suggested as source of lutein production by manipulating growth conditions (Shi et al., 2002; Cordero et al., 2011). Lutein has been widely studied in the treatment of macular degeneration. However, studies suggest that lutein is capable of quenching oxygen radicals and scavenging free radicals (Jahns and Holzwarth, 2012).

Microsporine-Like Amino Acid

Studies have proven that mycosporine-Gly possess anti-oxidative activity and may protect against skin inflammation caused by UV radiation. Anti-oxidative activity of mycosporine-Gly (0.3mM) extracted from *Chlamydomonas hedleyi* was high and UV-elevated COX-2 gene were suppressed. This shown that the regulation of COX-2 may be link to the oxidative process from mycrosporine-Gly (Suh et al., 2014).

Sterols

Sterols are found in almost all living organism. Microalgae produce a wide variety of sterols and plant derivative sterols are termed as phytosterols. Phytosterols extracted from microalgae found to possess anti-inflammatory properties (Yasukawa et al., 1996). A study demonstrated that extract from the microalgae, *Nannochloropsis oculata*, was able to induce anti-inflammatory effect on RAW 264.7 cells. Anti-inflammatory of the extract were accomplished by the decrease expression of iNOS and COX-2 proteins (Sanjeewa et al., 2016).

Polysaccharides

The cell walls of microalgae are rich in sulphated polysaccharide (SPs) and it exhibit various health benefiting properties such as anticoagulant, anti-oxidant, antiviral, anticancer, and anti-inflammatory activities (Wang J. et al., 2013; De Jesus Raposo et al., 2015). Therefore, SPs from microalgae have potential to be incorporate in nutraceutical, pharmaceutical, and cosmeceutical products. The biological and pharmacological activities of SPs are due to the complex interaction of the structure feature, such as the sulphation level, distribution of sulphate groups along the backbone of the molecule, molecular weight, sugar residue composition, and stereochemistry (Damonte et al., 2004; Ghosh et al., 2009). Several studies have demonstrated SPs for its potent anti-inflammatory properties. For instance, a study on *Chlorella stigmatophora* and *Phaeodactylum tricornutum* had demonstrated anti-inflammatory activity on paw edema. Carrageenan extracted from both microalgae strain had better anti-inflammatory activity on *in vivo* and *in vitro* models compared to the anti-inflammatory drug, indomethacin (Guzmán et al., 2003). Besides that, inhibition of leukocyte migration has a correlation with the anti-inflammatory activity of polysaccharides. Leukocyte movement to site of injury promotes cytokine release and production of nitric oxide. SPs from *Porphyridium* had demonstrated to inhibit the movement and adhesion of polymorphonuclear leukocytes and development of erythema *in vivo* (Matsui et al., 2003).

Besides inhibiting inflammatory cytokines and chemokines, studies also shown that *P. cruentum* is capable of inhibiting biomembrane peroxidation and for its immunomodulatory activities (Sun et al., 2009; Sun et al., 2012). Studies had demonstrated that low molecular fractions of exopolysachharide (EPS) from *P. creuntum* can stimulate the production of macrophages and nitric oxide (NO). NO is a free radical produced by phagocytes and plays a role in the immune system. In addition, other study also justified that SPs from cyanobacteria can promote immune system by triggering the cell and humor stimulation (Namikoshi and Rinehart, 1996).

Conclusion

ROS are prevalent in nature and are constantly produced at minute amount in aerobic systems. Living organism are capable to produce a wide range of anti-oxidant to eliminate or inhibit ROS to maintain homeostasis. Our body is constantly exposed to various pro-oxidants from the environment, such as consumption of drugs, solar radiation, pollutant, food additives, synthetic cosmetic products, which are capable to induce ROS in skin. ROS mostly target DNA, proteins, and lipid-rich membranes to induce toxicity effects to the body. Such damages to the skin may result in numerous skin diseases ranging from AD to vitiligo. Therefore, discovery of novel anti-inflammatory drugs from natural products that could potentially eliminate or inhibit ROS could bring new insight for biomedical research and industry (Fernando et al., 2016). Microalgae has become the main interest among consumers and industry due to their ability to produce a wide variety of bioactive compounds with health promoting properties and anti-inflammatory can be isolated from them. However, further pre-clinical investigation is still needed to understand the mechanism of these novel compounds in tackling skin inflammation diseases.

REFERENCES

Albanesi, C., and Pastore, S. (2010). Pathobiology of Chronic Inflammatory Skin Diseases: Interplay Between Keratinocytes and Immune Cells as a Target for Anti-Inflammatory Drugs. *Curr. Drug Metab.* 11 (3), 210–227. doi: 10.2174/138920010791196328

Arulselvan, P., Fard, M., Tan, W., Gothai, S., Fakurazi, S., Norhaizan, M., et al. (2016). Role of Antioxidants and Natural Products in Inflammation. *Oxid. Med. Cell. Longevity* 2016, 1–15. doi: 10.1155/2016/5276130

Bender, B., Ballard, R., Canono, B., Murphy, J., and Leung, D. (2008). Disease severity, scratching, and sleep quality in patients with atopic dermatitis. *J. Am. Acad. Dermatol.* 58 (3), 415–420. doi: 10.1016/j.jaad.2007.10.010

Benson, H., and Watkinson, A. (2012). *Transdermal and topical drug delivery.* Hoboken, N.J.: Wiley, pp. 3–5.

Bleehen, S. (1976). The treatment of vitiligo with topical corticosteroids. *Br. J. Dermatol.* 94 (s12), 43–50. doi: 10.1111/j.1365-2133.1976.tb02268.x

Boehncke, W. (2003). Immunomodulatory drugs for psoriasis. *BMJ* 327 (7416), 634–635. doi: 10.1136/bmj.327.7416.634

Boniface, K., Seneschal, J., Picardo, M., and Taïeb, A. (2017). Vitiligo: Focus on Clinical Aspects, Immunopathogenesis, and Therapy. *Clin. Rev. Allergy Immunol.* 54 (1), 52–67. doi: 10.1007/s12016-017-8622-7

Bourgaud, F., Gravot, A., Milesi, S., and Gontier, E. (2001). Production of plant secondary metabolites: a historical perspective. *Plant Sci.* 161 (5), 839–851. doi: 10.1016/S0168-9452(01)00490-3

Boussiba, S. (2000). Carotenogenesis in the green alga *Haematococcus pluvialis*: Cellular physiology and stress response. *Physiol. Plant.* 108 (2), 111–117. doi: 10.1034/j.1399-3054.2000.108002111.x

Briganti, S., and Picardo, M. (2003). Antioxidant activity, lipid peroxidation and skin diseases. What's new. *J. Eur. Acad. Dermatol. Venereol.* 17 (6), 663–669. doi: 10.1046/j.1468-3083.2003.00751.x

Burton, G., and Ingold, K. (1984). beta-Carotene: an unusual type of lipid antioxidant. *Science* 224 (4649), 569–573. doi: 10.1126/science.6710156

Cano, E., and Mahadevan, L. (1995). Parallel signal processing among mammalian MAPKs. *Trends Biochem. Sci.* 20 (3), 117–122. doi: 10.1016/S0968-0004(00)88978-1

Chong, M., and Fonacier, L. (2015). Treatment of Eczema: Corticosteroids and Beyond. *Clin. Rev. Allergy Immunol.* 51 (3), 249–262. doi: 10.1007/s12016-015-8486-7

Christaki, E., Bonos, E., Giannenas, I., and Florou-Paneri, P. (2012). Functional properties of carotenoids originating from algae. *J. Sci. Food Agric.* 93 (1), 5–11. doi: 10.1002/jsfa.5902

Cobb, M., and Goldsmith, E. (1995). How MAP Kinases Are Regulated. *J. Biol. Chem.* 270 (25), 14843–14846. doi: 10.1074/jbc.270.25.14843

Cordero, B., Obraztsova, I., Couso, I., Leon, R., Vargas, M., and Rodriguez, H. (2011). Enhancement of Lutein Production in *Chlorella sorokiniana* (Chorophyta) by Improvement of Culture Conditions and Random Mutagenesis. *Mar. Drugs* 9 (9), 1607–1624. doi: 10.3390/md9091607

Cross, C. (1987). Oxygen Radicals and Human Disease. *Ann. Internal Med.* 107 (4):526. doi: 10.7326/0003-4819-107-4-526

Damonte, E., Matulewicz, M., and Cerezo, A. (2004). Sulfated Seaweed Polysaccharides as Antiviral Agents. *Curr. Med. Chem.* 11 (18), 2399–2419. doi: 10.2174/0929867043364504

Davis, R. (1994). MAPKs: new JNK expands the group. *Trends Biochem. Sci.* 19 (11), 470–473.

De Jesus Raposo, M., de Morais, A., and de Morais, R. (2015). Marine Polysaccharides from Algae with Potential Biomedical Applications. *Mar. Drugs* 13 (5), 2967–3028. doi: 10.3390/md13052967

Denat, L., Kadekaro, A., Marrot, L., Leachman, S., and Abdel-Malek, Z. (2014). Melanocytes as Instigators and Victims of Oxidative Stress. *J. Invest. Dermatol.* 134 (6), 1512–1518. doi: 10.1038/jid.2014.65

Deng, Y., Chang, C., and Lu, Q. (2016). The Inflammatory Response in Psoriasis: a Comprehensive Review. *Clin. Rev. Allergy Immunol.* 50 (3), 377–389. doi: 10.1007/s12016-016-8535-x

Dhar, A., Young, M., and Colburn, N. (2002). The role of AP-1, NF-kappaB and ROS/NOS in skin carcinogenesis: the JB6 model is predictive. *Mol. Cell. Biochem.* 234/235 (1), 85–193. doi: 10.1023/A:1015948505117

Di Meo, S., Reed, T., Venditti, P., and Victor, V. (2016). Harmful and Beneficial Role of ROS. *Oxid. Med. Cell. Longevity* 2016, 1–3. doi: 10.1155/2016/7909186

Dika, E., Bardazzi, F., Balestri, R., and Maibach, H. (2007). Environmental Factors and Psoriasis1. *Environ. Factors Skin Dis.* 35, 118–135. doi: 10.1159/000106419

Eigenmann, P., and Calza, A. (2000). Diagnosis of IgE-mediated food allergy among Swiss children with atopic dermatitis. *Pediatr. Allergy Immunol.* 11 (2), 95–100. doi: 10.1034/j.1399-3038.2000.00071.x

Esteban, R., Martínez, B., Fernández-Marín, B., María Becerril, J., and García-Plazaola, J. (2009). Carotenoid composition in Rhodophyta: insights into xanthophyll regulation in *Corallina elongate*. *Eur. J. Phycol.* 44 (2), 221–230. doi: 10.1080/09670260802439109

Fernando, I., Nah, J., and Jeon, Y. (2016). Potential anti-inflammatory natural products from marine algae. *Environ. Toxicol. Pharmacol.* 48, 22–30. doi: 10.1016/j.etap.2016.09.023

Finkel, T., and Holbrook, N. (2016). Oxidants, oxidative stress and the biology of ageing. *Nature* 408, 239–247. doi: 10.1038/35041687

Frei, B., Stocker, R., and Ames, B. (1988). Antioxidant defenses and lipid peroxidation in human blood plasma. *Proc. Natl. Acad. Sci.* 85 (24), 9748–9752. doi: 10.1073/pnas.85.24.9748

Fu, W., Guðmundsson, Ó., Paglia, G., Herjólfsson, G., Andrésson, Ó., Palsson, B., et al. (2012). Enhancement of carotenoid biosynthesis in the green microalga *Dunaliella salina* with light-emitting diodes and adaptive laboratory evolution. *Appl. Microbiol. Biotechnol.* 97 (6), 2395–2403. doi: 10.1007/s00253-012-4502-5

Fu, W., Nelson, D., Yi, Z., Xu, M., Khraiwesh, B., Jijakli, K., et al. (2017). Bioactive Compounds From Microalgae: Current Development and Prospects. *Stud. Natural Prod. Chem.* 54, 199–225. doi: 10.1016/B978-0-444-63929-5.00006-1

Fujioka, S., Niu, J., Schmidt, C., Sclabas, G., Peng, B., Uwagawa, T., et al. (2004). NF-$_k$B and AP-1 Connection: Mechanism of NF- B-Dependent Regulation of AP-1 Activity. *Mol. Cell. Biol.* 24 (17), 7806–7819. doi: 10.1128/MCB.24.17.7806-7819.2004

Ghosh, T., Chattopadhyay, K., Marschall, M., Karmakar, P., Mandal, P., and Ray, B. (2009). Focus on antivirally active sulfated polysaccharides: From structure–activity analysis to clinical evaluation. *Glycobiology* 19 (1), 2–15. doi: 10.1093/glycob/cwn092

Guzmán, S., Gato, A., Lamela, M., Freire-Garabal, M., and Calleja, J. (2003). Anti-inflammatory and immunomodulatory activities of polysaccharide from *Chlorella stigmatophora* and *Phaeodactylum tricornutum*. *Phytother. Res.* 17 (6), 665–670. doi: 10.1002/ptr.1227

Hann, S., Kim, H., Im, S., Park, Y., Cui, J., and Bystryn, J. (1993). The change of melanocyte cytotoxicity after systemic steroid treatment in vitiligo patients. *J. Dermatol. Sci.* 6 (3), 201–205. doi: 10.1016/0923-1811(93)90039-R

Hasse, S., Gibbons, N., Rokos, H., Marles, L., and Schallreuter, K. (2004). Perturbed 6-Tetrahydrobiopterin Recycling via Decreased Dihydropteridine Reductase in Vitiligo: More Evidence for H$_2$O$_2$ Stress. *J. Invest. Dermatol.* 122 (2), 307–313. doi: 10.1046/j.0022-202X.2004.22230.x

Hayden, M. (2004). Signaling to NF- B. *Genes Dev.* 18 (18), 2195–2224. doi: 10.1101/gad.1228704

Herr, H., Cho, H., and Yu, S. (2007). Burns caused by accidental overdose of photochemotherapy (PUVA). *Burns* 33 (3), 372–375. doi: 10.1016/j.burns.2006.07.005

Heydendael, V., Spuls, P., Opmeer, B., de Borgie, C., Reitsma, J., Goldschmidt, W., et al. (2003). Methotrexate versus Cyclosporine in Moderate-to-Severe Chronic Plaque Psoriasis. *New Engl. J. Med.* 349 (7), 658–665. doi: 10.1056/NEJMoa021359

Higuera-Ciapara, I., Félix-Valenzuela, L., and Goycoolea, F. (2006). Astaxanthin: A Review of its Chemistry and Applications. *Crit. Rev. Food Sci. Nutr.* 46 (2), 185–196. doi: 10.1080/10408690590957188

Hill, D., and Hosking, C. (2004). Food allergy and atopic dermatitis in infancy: an epidemiologic study. *Pediatr. Allergy Immunol.* 15 (5), 421–427. doi: 10.1111/j.1399-3038.2004.00178.x

Hussain, T., Tan, B., Yin, Y., Blachier, F., Tossou, M., and Rahu, N. (2016). Oxidative Stress and Inflammation: What Polyphenols Can Do for Us? *Oxid. Med. Cell. Longevity* 2016 1–9. doi: 10.1155/2016/7432797

Jahan, A., Ahmad, I., Fatima, N., Ansari, V., and Akhtar, J. (2017). Algal bioactive compounds in the cosmeceutical industry: a review. *Phycologia* 56 (4), 410–422. doi: 10.2216/15.58.1

Jahns, P., and Holzwarth, A. (2012). The role of the xanthophyll cycle and of lutein in photoprotection of photosystem II. *Biochim. Biophys. Acta (BBA) - Bioenerg.* 1817 (1), 182–193. doi: 10.1016/j.bbabio.2011.04.012

Jian, Z., Li, K., Liu, L., Zhang, Y., Zhou, Z., Li, C., et al. (2011). Heme Oxygenase-1 Protects Human Melanocytes from H2O2-Induced Oxidative Stress via the Nrf2-ARE Pathway. *J. Invest. Dermatol.* 131 (7), 1420–1427. doi: 10.1038/jid.2011.56

Jian, Z., Li, K., Song, P., Zhu, G., Zhu, L., Cui, T., et al. (2014). Impaired Activation of the Nrf2-ARE Signaling Pathway Undermines H 2 O 2 -Induced Oxidative Stress Response: A Possible Mechanism for Melanocyte Degeneration in Vitiligo. *J. Invest. Dermatol.* 134 (8), 2221–2230. doi: 10.1038/jid.2011.56

Johansen, C., Kragballe, K., Westergaard, M., Henningsen, J., Kristiansen, K., and Iversen, L. (2005). The mitogen-activated protein kinases p38 and ERK1/2 are increased in lesional psoriatic skin. *Br. J. Dermatol.* 152 (1), 37–42. doi: 10.1111/j.1365-2133.2004.06304.x

Karimkhani, C., Dellavalle, R., Coffeng, L., Flohr, C., Hay, R., Langan, S., et al. (2017). Global Skin Disease Morbidity and Mortality. *JAMA Dermatol.* 153 (5), 406. doi: 10.1001/jamadermatol.2016.5538

Kato, Y., Chao, T., Hayashi, M., Tapping, R., and Lee, J. (2000). Role of BMK1 in Regulation of Growth Factor-Induced Cellular Responses. *Immunol. Res.* 21 (2-3), 233–238. doi: 10.1385/IR:21:2-3:233

Kaufman, B., Guttman-Yassky, E., and Alexis, A. (2018). Atopic dermatitis in diverse racial and ethnic groups-Variations in epidemiology, genetics, clinical presentation and treatment. *Exp. Dermatol.* 27 (4), 340–357. doi: 10.1111/exd.13514

Kidd, P. (2011). Astaxanthin, cell membrane nutrient with diverse clinical benefits and anti-aging potential. *Altern. Med. Rev.* 16 (4), 355–364.

Kim, A., Labasi, J., Zhu, Y., Tang, X., McClure, K., Gabel, C., et al. (2005). Role of p38 MAPK in UVB-Induced Inflammatory Responses in the Skin of SKH-1 Hairless Mice. *J. Invest. Dermatol.* 124 (6), 1318–1325. doi: 10.1111/j.0022-202X.2005.23747.x

Kishimoto, T., Taga, T., and Akira, S. (1994). Cytokine signal transduction. *Cell* 76 (2), 253–262. doi: 10.1016/0092-8674(94)90333-6

Kohen, R. (1999). Skin antioxidants: Their role in aging and in oxidative stress — New approaches for their evaluation. *Biomed. Pharmacother.* 53 (4), 181–192. doi: 10.1016/S0753-3322(99)80087-0

Kowalska-Oledzka, E., Czarnecka, M., and Baran, A. (2019). Epidemiology of atopic dermatitis in Europe. *J. Drug Assess.* 8 (1), 126–128. doi: 10.1080/21556660.2019.1619570

Krinsky, N. (1992). Mechanism of Action of Biological Antioxidants. *Exp. Biol. Med.* 200 (2), 248–254. doi: 10.3181/00379727-200-43429

Kumar, S., and Pandey, A. (2015). Free Radicals: Health Implications and their Mitigation by Herbals. *Br. J. Med. Med. Res.* 7 (6), 438–457. doi: 10.9734/BJMMR/2015/16284

Leyden, J., Marples, R., and Kligman, A. (1974). *Staphylococcus aureus* in the lesions of atopic dermatitis. *Br. J. Dermatol.* 90 (5), 525–525. doi: 10.1111/j.1365-2133.1974.tb06447.x

Lin, J., Lee, D., and Chang, J. (2015). Lutein production from biomass: Marigold flowers versus microalgae. *Biores.s Technol.* 184, 421–428. doi: 10.1016/j.biortech.2014.09.099

Lopez Carrera, Y., Al Hammadi, A., Huang, Y., Llamado, L., Mahgoub, E., and Tallman, A. (2019). Epidemiology, Diagnosis, and Treatment of Atopic Dermatitis in the Developing Countries of Asia, Africa, Latin America, and the Middle East: A Review. *Dermatol. Ther.* 9, 685–705. doi: 10.1007/s13555-019-00332-3

Lowes, M., Bowcock, A., and Krueger, J. (2007). Pathogenesis and therapy of psoriasis. *Nature* 445 (7130), 866–873. doi: 10.1038/nature05663

Lowes, M., Suárez-Fariñas, M., and Krueger, J. (2014). Immunology of Psoriasis. *Annu. Rev. Immunol.* 32 (1), 227–255. doi: 10.1146/annurev-immunol-032713-120225

Macedo, R., Bolin, A., Marin, D., and Otton, R. (2010). Astaxanthin addition improves human neutrophils function: in vitro study. *Eur. J. Nutr.* 49 (8), 447–457. doi: 10.1007/s00394-010-0103-1

Mahendra, C., Tan, L., Yap, W., Chan, C., Lingham, P., Pusparajah, P., et al. (2019a). Model of Experimentation for Photoprotective Properties of Natural Products Against Ultraviolet C (UVC) Damage: A Case Study On Rosmarinic Acid. *Prog. Drug Discovery Biomed. Sci.* 2, 1. doi: 10.36877/pddbs.a0000027

Mahendra, C., Tan, L., Yap, W., Chan, C., Pusparajah, P., and Goh, B. (2019b). An Optimized Cosmetic Screening Assay for Ultraviolet B (UVB) Protective Property of Natural Products. *Prog. Drug Discovery Biomed. Sci.* 2, 1. doi: 10.36877/pddbs.a0000021

Maresca, V., Roccella, M., Roccella, F., Camera, E., Del Porto, G., Passi, S., et al. (1997). Increased Sensitivity to Peroxidative Agents as a Possible Pathogenic Factor of Melanocyte Damage in Vitiligo. *J. Invest. Dermatol.* 109 (3), 310–313. doi: 10.1111/1523-1747.ep12335801

Martin, H., Jäger, C., Ruck, C., Schmidt, M., Walsh, R., and Paust, J. (1999). Anti- and Prooxidant Properties of Carotenoids. *J. Für Praktische Chem.* 341 (3), 302–308. doi: 10.1002/(SICI)1521-3897(199904)341:3<302::AID-PRAC302>3.0.CO;2-6

Matsui, M., Muizzuddin, N., Arad, S., and Marenus, K. (2003). Sulfated Polysaccharides from Red Microalgae Have Antiinflammatory Properties *In Vitro* and *In Vivo. Appl. Biochem. Biotechnol.* 104 (1), 13–22. doi: 10.1385/ABAB:104:1:13

Meffert, H., Diezel, W., and Sönnichsen, N. (1976). Stable lipid peroxidation products in human skin: detection, ultraviolet light-induced increase, pathogenic importance. *Experientia* 32 (11), 1397–1398. doi: 10.1007/BF01937397

Mei-Yen Yong, A., and Tay, Y. (2017). Atopic Dermatitis: Racial and Ethnic Differences. *Dermatol. Clinics* 35 (3), 395–402. doi: 10.1016/j.det.2017.02.012

Metting, F. (1996). Biodiversity and application of microalgae. *J. Ind. Microbiol. Biotechnol.* 17 (5-6), 477–489. doi: 10.1007/BF01574779

Namikoshi, M., and Rinehart, K. (1996). Bioactive compounds produced by cyanobacteria. *J. Ind. Microbiol. Biotechnol.* 17 (5-6), 373–384. doi: 10.1007/BF01574768

Nesterova, A., Klimov, E., Zharkova, M., Sozin, S., Sobolev, V., Shkrob, M., et al. (2019). *Disease pathways. 1st ed.* Elsevier, pp. 493–532.

Nickoloff, B., Xin, H., Nestle, F., and Qin, J. (2007). The cytokine and chemokine network in psoriasis". *Clinics Dermatol.* 25 (6), 568–573. doi: 10.1016/j.clindermatol.2007.08.011

Novelli, L., Chimenti, M., Chiricozzi, A., and Perricone, R. (2014). The new era for the treatment of psoriasis and psoriatic arthritis: Perspectives and validated strategies. *Autoimmun. Rev.* 13 (1), 64–69. doi: 10.1016/j.autrev.2013.08.006

Ohgami, K., Shiratori, K., Kotake, S., Nishida, T., Mizuki, N., Yazawa, K., et al. (2003). Effects of Astaxanthin on Lipopolysaccharide-Induced Inflammation *In Vitro* and *In Vivo. Invest. Opthalmol. Visual Sci.* 44 (6), 2694. doi: 10.1167/iovs.02-0822

Okayama, Y. (2005). Oxidative Stress in Allergic and Inflammatory Skin Diseases. *Curr. Drug Target -Inflamm. Allergy* 4 (4), 517–519. doi: 10.2174/1568010054526386

Paiva, S., and Russell, R. (1999). ß-Carotene and Other Carotenoids as Antioxidants. *J. Am. Coll. Nutr.* 18 (5), 426–433. doi: 10.1080/07315724.1999.10718880

Park, H., Lee, Y., and Chun, D. (2003). Squamous cell carcinoma in vitiligo lesion after long-term PUVA therapy. *J. Eur. Acad. Dermatol. Venereol.* 17 (5), 578–580. doi: 10.1046/j.1468-3083.2003.00815.x

Patel, R., Clark, L., Lebwohl, M., and Weinberg, J. (2009). Treatments for psoriasis and the risk of malignancy. *J. Am. Acad. Dermatol.* 60 (6), 1001–1017. doi: 10.1016/j.jaad.2008.12.031

Perera, G., Di Meglio, P., and Nestle, F. (2012). Psoriasis. *Annu. Rev. Pathol.: Mech. Dis.* 7 (1), 385–422. doi: 10.1016/j.jaad.2008.12.031

Poole, I., Das, P., Wijngaard, R., Bos, J., and Westerhof, W. (1993). Review of the etiopathomechanism of vitiligo: A convergence theory. *Exp. Dermatol.* 2 (4), 145–153. doi: 10.1111/j.1600-0625.1993.tb00023.x

Qiu, L., Song, Z., and Setaluri, V. (2014). Oxidative Stress and Vitiligo: The Nrf2–ARE Signaling Connection. *J. Invest. Dermatol.* 134 (8), 2074–2076. doi: 10.1038/jid.2014.241

Radakovic-Fijan, S., Fürnsinn-Friedl, A., Hönigsmann, H., and Tanew, A. (2001). Oral dexamethasone pulse treatment for vitiligo. *J. Am. Acad. Dermatol.* 44 (5), 814–817. doi: 10.1067/mjd.2001.113475

Rahman, M., Alam, K., Ahmad, M., Gupta, G., Afzal, M., Akhter, S., et al. (2012). Classical to Current Approach for Treatment of Psoriasis: A Review. *Endocr. Metab. Immune Disord. - Drug Targets* 12 (3), 287–302. doi: 10.2174/187153012802002901

Rice-Evans, C., Sampson, J., Bramley, P., and Holloway, D. (1997). Why Do We Expect Carotenoids to be Antioxidantsin vivo? *Free Radical Res.* 26 (4), 381–398. doi: 10.3109/10715769709097818

Rice-Evans, C., and Diplock, A. (1993). Current status of antioxidant therapy. *Free Radical Biol. Med.* 15 (1), 77–96. doi: 10.1016/0891-5849(93)90127-g

Robertson, R., Guihéneuf, F., Bahar, B., Schmid, M., Stengel, D., Fitzgerald, G., et al. (2015). The Anti-Inflammatory Effect of Algae-Derived Lipid Extracts on Lipopolysaccharide (LPS)-Stimulated Human THP-1 Macrophages. *Mar. Drugs* 13 (8), 5402–5424. doi: 10.3390/md13085402

Sander, C., Chang, H., Hamm, F., Elsner, P., and Thiele, J. (2004). Role of oxidative stress and the antioxidant network in cutaneous carcinogenesis. *Int. J. Dermatol.* 43 (5), 326–335. doi: 10.1111/j.1365-4632.2004.02222.x

Sanjeewa, K., Fernando, I., Samarakoon, K., Lakmal, H., Kim, E., Kwon, O., et al. (2016). Anti-inflammatory and anti-cancer activities of sterol rich fraction of cultured marine microalga *Nannochloropsis oculata*. ALGAE 31 (3), 277–287. doi: 10.4490/algae.2016.31.6.29

Sathasivam, R., and Ki, J. (2018). A Review of the Biological Activities of Microalgal Carotenoids and Their Potential Use in Healthcare and Cosmetic Industries. *Mar. Drugs* 16 (1):26. doi: 10.3390/md16010026

Sathasivam, R., Radhakrishnan, R., Hashem, A., and Abd_Allah, E. (2019). Microalgae metabolites: A rich source for food and medicine. *Saudi J. Biol. Sci.* 26 (4), 709–722. doi: 10.1016/j.sjbs.2017.11.003

Schallereuter, K., Wood, J., Ziegler, I., Lemke, K., Pittelkow, M., Lindsey, N., et al. (1994). Defective tetrahydrobiopterin and catecholamine biosynthesis in the depigmentation disorder vitiligo. *Biochim. Biophys. Acta (BBA) - Mol. Basis Dis.* 1226 (2), 181–192. doi: 10.1016/0925-4439(94)90027-2

Schallreuter, K., Wood, J., and Berger, J. (1991). Low Catalase Levels in the Epidermis of Patients with Vitiligo. *J. Invest. Dermatol.* 97 (6), 1081–1085. doi: 10.1111/1523-1747.ep12492612

Schallreuter, K., Moore, J., Wood, J., Beazley, W., Gaze, D., Tobin, D., et al. (1999). *In Vivo* and *In Vitro* Evidence for Hydrogen Peroxide (H$_2$O$_2$) Accumulation in the Epidermis of Patients with Vitiligo and its Successful Removal by a UVB-Activated Pseudocatalase. *J. Invest. Dermatol. Symp. Proc.* 4 (1), 91–96. doi: 10.1038/sj.jidsp.5640189

Schallreuter, K., Gibbons, N., Zothner, C., Abou Elloof, M., and Wood, J. (2007). Hydrogen peroxide-mediated oxidative stress disrupts calcium binding on calmodulin: More evidence for oxidative stress in vitiligo. *Biochem. Biophys. Res. Commun.* 360 (1), 70–75. doi: 10.1016/j.bbrc.2007.05.218

Schallreuter, K. (1999). Successful Treatment of Oxidative Stress in Vitiligo. *Skin Pharmacol. Physiol.* 12 (3), 132–138. doi: 10.1159/000029867

Schottelius, A., Moldawer, L., Dinarello, C., Asadullah, K., Sterry, W., and Edwards, C. (2004). Biology of tumor necrosis factor-alpha- implications for psoriasis. *Exp. Dermatol.* 13 (4), 193–222. doi: 10.1111/j.0906-6705.2004.00205.x

Seternes, O., Mikalsen, T., Johansen, B., Michaelsen, E., Armstrong, C., Morrice, N., et al. (2004). Activation of MK5/PRAK by the atypical MAP kinase ERK3 defines a novel signal transduction pathway. *EMBO J.* 23 (24), 4780–4791. doi: 10.1038/sj.emboj.7600489

Shajil, E., and Begum, R. (2006). Antioxidant status of segmental and non-segmental vitiligo. *Pigment Cell Res.* 19 (2), 179–180. doi: 10.1111/j.1600-0749.2006.00299.x

Shi, X., Jiang, Y., and Chen, F. (2002). High-Yield Production of Lutein by the Green Microalga *Chlorella protothecoides* in Heterotrophic Fed-Batch Culture. *Biotechnol. Prog.* 18 (4), 723–727. doi: 10.1021/bp0101987

Simpson, E. (2010). Atopic dermatitis: a review of topical treatment options. *Curr. Med. Res. Opin.* 26 (3), 633–640. doi: 10.1185/03007990903512156

Skibsted, L. (2012). Carotenoids in Antioxidant Networks. Colorants or Radical Scavengers. *J. Agric. Food Chem.* 60 (10), 2409–2417. doi: 10.1021/jf2051416

Smith, C., and Barker, J. (2006). Psoriasis and its management. *BMJ* 333 (7564), 380–384. doi: 10.1136/bmj.333.7564.380

Speeckaert, R., and van Geel, N. (2017). Vitiligo: An Update on Pathophysiology and Treatment Options. *Am. J. Clin. Dermatol.* 18 (6), 733–744. doi: 10.1007/s40257-017-0298-5

Speranza, L., Pesce, M., Patruno, A., Franceschelli, S., Lutiis, M., Grilli, A., et al. (2012). Astaxanthin Treatment Reduced Oxidative Induced Pro-Inflammatory Cytokines Secretion in U937: SHP-1 as a Novel Biological Target. *Mar. Drugs* 10 (12), 890–899. doi: 10.3390/md10040890

Spergel, J. (2008). Immunology and Treatment of Atopic Dermatitis. *Am. J. Clin. Dermatol.* 9 (4), 233–244. doi: 10.2165/00128071-200809040-00003

Stein, B., Baldwin, A., Ballard, D., Greene, W., Angel, P., and Herrlich, P. (1993). Cross-coupling of the NF-kappa B p65 and Fos/Jun transcription factors produces potentiated biological function. *EMBO J.* 12 (10), 3879–3891. doi: 10.1002/j.1460-2075.1993.tb06066.x

Suh, S., Hwang, J., Park, M., Seo, H., Kim, H., Lee, J., et al. (2014). Anti-Inflammation Activities of Mycosporine-Like Amino Acids (MAAs) in Response to UV Radiation Suggest Potential Anti-Skin Aging Activity. *Mar. Drugs* 12 (10), 5174–5187. doi: 10.3390/md12105174

Sun, L., Wang, C., Shi, Q., and Ma, C. (2009). Preparation of different molecular weight polysaccharides from *Porphyridium cruentum* and their antioxidant activities. *Int. J. Biol. Macromol.* 45 (1), 42–47. doi: 10.1016/j.ijbiomac.2009.03.013

Sun, L., Wang, L., and Zhou, Y. (2012). Immunomodulation and antitumor activities of different-molecular-weight polysaccharides from *Porphyridium cruentum*. *Carbohydr. Polymers* 87 (2), 1206–1210. doi: 10.1016/j.carbpol.2011.08.097

Tachibana, M. (2000). MITF: A Stream Flowing for Pigment Cells. *Pigment Cell Res.* 13 (4), 230–240. doi: 10.1034/j.1600-0749.2000.130404.x

Taïeb, A., and Picardo, M. (2009). Vitiligo. *New Engl. J. Med.* 360 (2), 160–169. doi: 10.1056/NEJMcp0804388

Takahashi, H., Ibe, M., Nakamura, S., Ishida-Yamamoto, A., Hashimoto, Y., and Iizuka, H. (2002). "Extracellular regulated kinase and c-Jun N-terminal kinase are activated in psoriatic involved epidermis". *J. Dermatol. Sci.* 30 (2), 94–99. doi: 10.1016/S0923-1811(02)00064-6

Trouba, K., Hamadeh, H., Amin, R., and Germolec, D. (2002). Oxidative Stress and Its Role in Skin Disease. *Antioxid. Redox Signaling* 4 (4), 665–673. doi: 10.1089/15230860260220175

Valkova, S., Trashlieva, M., and Christova, P. (2004). Treatment of vitiligo with local khellin and UVA: comparison with systemic PUVA. *Clin. Exp. Dermatol.* 29 (2), 180–184. doi: 10.1111/j.1365-2230.2004.01462.x

Van der Aa, L., Heymans, H., van Aalderen, W., and Sprikkelman, A. (2010). Probiotics and prebiotics in atopic dermatitis: review of the theoretical background and clinical evidence. *Pediatr. Allergy Immunol.* 21 (2p2), e355–e367. doi: 10.1111/j.1399-3038.2009.00915.x

Wajant, H., Pfizenmaier, K., and Scheurich, P. (2003). Tumor necrosis factor signaling. *Cell Death Differ.* 10 (1), 45–65. doi: 10.1038/sj.cdd.4401189

Wang, F., Lee, E., Lowes, M., Haider, A., Fuentes-Duculan, J., Abello, M., et al. (2006). Prominent Production of IL-20 by CD68+/CD11c+ Myeloid-Derived Cells in Psoriasis: Gene Regulation and Cellular Effects. *J. Invest. Dermatol.* 126 (7), 1590–1599. doi: 10.1038/sj.jid.5700310

Wang, H., Chou, Y., Wen, Z., Wang, C., Chen, C., and Ho, M. (2013). Novel Biodegradable Porous Scaffold Applied to Skin Regeneration. *PloS One* 8 (11). doi: 10.1371/journal.pone.0056330

Wang, J., Jin, W., Hou, Y., Niu, X., Zhang, H., and Zhang, Q. (2013). Chemical composition and moisture-absorption/retention ability of polysaccharides extracted from five algae. *Int. J. Biol. Macromol.* 57, 26–29. doi: 10.1016/j.ijbiomac.2013.03.001

Wen, W., Li, K., Alseekh, S., Omranian, N., Zhao, L., Zhou, Y., et al. (2015). Genetic Determinants of the Network of Primary Metabolism and Their Relationships to Plant Performance in a Maize Recombinant Inbred Line Population. *Plant Cell* 27 (7), 1839–1856. doi: 10.1105/tpc.15.00208

Wolf, A., Asoh, S., Hiranuma, H., Ohsawa, I., Iio, K., Satou, A., et al. (2010). Astaxanthin protects mitochondrial redox state and functional integrity against oxidative stress. *J. Nutr. Biochem.* 21 (5), 381–389. doi: 10.1016/j.jnutbio.2009.01.011

Wolk, K., Kunz, S., Witte, E., Friedrich, M., Asadullah, K., and Sabat, R. (2004). IL-22 Increases the Innate Immunity of Tissues. *Immunity* 21 (2), 241–254. doi: 10.1016/j.immuni.2004.07.007

Wu, C., Lan, C., Wang, L., Chen, G., Wu, C., and Yu, H. (2007). Effects of psoralen plus ultraviolet A irradiation on cultured epidermal cells in vitro and patients with vitiligo in vivo. *Br. J. Dermatol.* 156 (1), 122–129. doi: 10.1111/j.1365-2133.2006.07584.x

Yasukawa, K., Akihisa, T., Kanno, H., Kaminaga, T., Izumida, M., Sakoh, T., et al. (1996). Inhibitory Effects of Sterols Isolated from *Chlorella vulgaris* on 12-O-Tetradecanoylphorbol-13-acetate-Induced Inflammation and Tumor Promotion in Mouse Skin. *Biol. Pharm. Bull.* 19 (4), 573–576. doi: 10.1248/bpb.19.573

Yoshihisa, Y., Rehman, M., and Shimizu, T. (2014). Astaxanthin, a xanthophyll carotenoid, inhibits ultraviolet-induced apoptosis in keratinocytes. *Exp. Dermatol.* 23 (3), 178–183. doi: 10.1111/exd.12347

Yu, X., Li, C., Dai, H., Cai, D., Wang, K., Xu, Y., et al. (2007). Expression and localization of the activated mitogen-activated protein kinase in lesional psoriatic skin. *Exp. Mol. Pathol.* 83 (3), 413–418. doi: 10.1016/j.yexmp.2007.05.002

Zhang, J., Sun, Z., Sun, P., Chen, T., and Chen, F. (2014). Microalgal carotenoids: beneficial effects and potential in human health. *Food Funct.* 5 (3), 413. doi: 10.1039/C3FO60607D

Conflict of Interest: The authors declare that the research was conducted in the absence of any commercial or financial relationships that could be construed as a potential conflict of interest.

Efficacy and Safety of Socheongryong-Tang Among Atopic Dermatitis Patients With Respiratory Disorders: A Double-Blinded, Randomized, Placebo-Controlled Clinical Trial

Ju Hyun Lee[1], Eun Heui Jo[2], Jee Youn Jung[3], Young-Eun Kim[4], Mi-Ju Son[3], Su Jin Kang[5], Geum Jin Yang[6], Yu Hwa Shim[6] and Min Cheol Park[7]*

[1]Department of Korean Medicine Ophthalmology and Otolaryngology and Dermatology, Wonkwang University Korean Medicine Hospital, Iksan, South Korea, [2]Department of Acupuncture and Moxibustion, Wonkwang University Korean Medicine Hospital and Research Center of Traditional Korean Medicine, Wonkwang University, Deokjingu, South Korea, [3]Clinical Medicine Division, Korea Institute of Oriental Medicine, Daejeon, South Korea, [4]Future Medicine Division, Korea Institute of Oriental Medicine, Daejeon, South Korea, [5]Department of Korean Medicine Obstetrics and Gynecology, Wonkwang University Korean Medicine Hospital, Iksan, South Korea, [6]Korean Medicine Dermatology Clinical Research Center of Wonkwang University, Iksan, South Korea, [7]Department of Korean Medicine Ophthalmology and Otolaryngology and Dermatology, Wonkwang University Korean Medicine Hospital and Research Center of Traditional Korean Medicine, Wonkwang University, Iksan, South Korea

Atopic dermatitis is a chronic inflammatory skin disease that affects the growth and development of children. The prevalence of atopic dermatitis has been continually increasing, and this has also been accompanied by rising socioeconomic costs. Interest has been growing in alternative medicine as a means of alleviating the burden of atopic dermatitis. This was a single-center, double-blinded, randomized, placebo-controlled investigator-led clinical trial including 60 atopic dermatitis patients. The participants were classified into an experimental group (30 persons) and a control group (30 persons), who were administered, respectively, socheongryong-tang or a placebo for 4 weeks. After 4 weeks of treatment, the participants visited the trial center again and assess their efficacy and safety. The researchers performed statistical comparisons of the changes in the SCORAD Index, amount and frequency of ointment use, and height and weight to assess the efficacy. To assess the safety, diagnostic tests and vital sign checks were performed at each visit, and the presence or absence of adverse events was observed. As a result, the frequency and the amount of steroid ointment application in both groups increased, but the experimental group showed less tendency ($p = 0.081$). Results of analyzing the children in the experimental group in relation to growth showed a significantly greater height growth than the control group ($p < 0.05$). In addition, all study participants did not show any remarkable abnormal signs in the safety evaluation. In conclusion, compared to the control group, the experimental group, who took socheongryong-tang showed a tendency to be less dependent on steroid ointment and statistically significant increase in height.

Keywords: allergy, atopic dermatitis, clinical trials, height growth, socheongryong-tang

INTRODUCTION

Atopic dermatitis (AD, also called atopic eczema) is a chronic relapsing inflammatory skin disorder that is accompanied by itching, is caused by genetic and environmental factors (Nutten, 2015; Otsuka et al., 2017), and is common in infants (Eichenfield et al., 2013). Due to the "allergic march", patients who suffered from AD in infancy are more likely to develop respiratory disorders such as allergic asthma or rhinitis in childhood (Bantz et al., 2014). Several studies on allergic disease have reported that atopic disease affects the growth and development of children. Although the mechanisms by which allergic diseases impair height growth have not yet been elucidated (Kristmundsdottir and David, 1987), children with a history of respiratory allergy or AD are more likely to be shorter than their peers (Ferguson et al., 1982; Kristmundsdottir and David, 1987; Sant'Anna et al., 1996).

The prevalence of AD has been persistently increasing to date (Deckers et al., 2012; Nutten, 2015), and this has been accompanied by rising socioeconomic costs. There has been growing interest in alternative medicine as a means of reducing the socioeconomic burden of AD. However, excluding a study analyzing the growth-promoting ingredients in boyangsungjang-tang (Hong et al., 2012) or studies demonstrating the efficacy of gamisasangja-tang (Park et al., 2015) and taeumjowi-tang (Park et al., 2019) for alleviating AD, there have been hardly any clinical studies demonstrating the efficacy of alternative medicine for AD and growth.

Socheongryong-tang (SCRT, also known as Sho-Seiru-To and Xiao-Qing-Long-Tang) is a type of herbal medicine that has been used for centuries to treat respiratory and allergic diseases in countries across East Asia (Ko et al., 2004; Das et al., 2009). However, in spite of these effects of SCRT, there have been almost no studies demonstrating its effects on AD and childhood growth. This research aims to evaluate the efficacy and safety of SCRT, vs. placebo, for the treatment of AD with respiratory disorders and as a growth promoter for short children.

MATERIALS AND METHODS

Sample Size Calculation

To evaluate SCRT efficacy in AD patients, we used SCORAD scores. In SCRT and placebo groups, It was hypothesized that the mean SCORAD scores change after intervention will be 7.9 (μc) and 13.8 (μt), respectively, with a standard deviation of 8.2. Based on the estimated dropout rate (20%), 60 participants in total were needed to achieve significance level of 0.05 in a 2-tailed test and a statistical power of 80%.

Study Design and Participants

This study was designed as a single-center, double-blinded, randomized, placebo-controlled, investigator-led clinical trial. The participants were divided into an experimental group (30 persons) and a control group (30 persons), who were administered SCRT or placebo, respectively, for 4 weeks. After 4 weeks of medication, the participants visited the trial center again, and the efficacy and safety of the treatments were assessed. The trial design of this study has already been published in the form of a protocol paper (Kang et al., 2020). This clinical trial was conducted from June 13, 2019 (first registration date) to December 13, 2019 (last visit date).

Patient Enrollment

A total of 65 persons were enrolled in the study, of which five persons were excluded during screening. The reasons for exclusion were contravening the exclusion criteria (two persons), contravening the inclusion criteria (two persons), and withdrawal of consent (one person). Investigator-led clinical trials were for trend search rather than statistical and clinical significance, and n number was selected as 30 cases per group considering 20% dropout rate.

Inclusion and Exclusion Criteria

Among patients who had heard and fully understood a thorough explanation of the study, voluntarily decided to participate, and gave written consent to adhere to the study precautions, those who satisfied all the following inclusion criteria and did not fit any of the exclusion criteria were defined as participants.

Inclusion Criteria

(1) Male or female individuals aged 7–65 years, having mild-moderate atopic dermatitis (SCORAD score ≥15 and <50), and with ≥3 major clinical symptoms and ≥3 minor clinical symptoms according to the Hanifin & Rajka diagnostic criteria (Hanifin and Rajka, 1980)
(2) Individuals who checked ≥1 respiratory disease or related symptom corresponding to the allergy march in the questionnaire for symptom classification

Exclusion Criteria

(1) Patients receiving intensive drug treatment for severe AD
(2) Patients who have used oral antihistamines, steroids, antibiotics, systemic photochemotherapy, or other immune-suppressants less than 4 weeks before the start of the trial
(3) Patients with a systemic infection or receiving systemic antibiotic therapy, or taking interferon therapy
(4) Patients with severe skin disease or pigment deposition other than AD, or with extensive scarring in the region of AD
(5) Patients with liver disease, kidney disease, severe acute cardiovascular disease, gastrointestinal disorders, excessive sweating, voiding dysfunction, or chronic disease
(6) Patients with a platelet count ≤100,000/mm³ due to liver dysfunction caused by chronic hepatitis
(7) Patients who have taken potassium-containing agents, licorice-containing agents, glycyrrhizic acid, salt-containing agents, loop diuretics (furosemide, ethacrynic acid), thiazide diuretics (trichlormethiazide), ephedra/ephedrine-containing agents, MAO inhibitors, thyroid-related drugs, catecholamines, or xanthines less than 4 weeks before the start of the trial

TABLE 1 | Ingredients of the SCRT granules and placebo.

	Ingredient name	Amount (g)	Extract (g)		Ingredient name	Amount (g)
Main Ingredient	*Pinellia ternata* (Thunb.) Makino	2.00	1.05	Excipient	Lactose hydrate	1.490
	Ephedra sinica Stapf	1.00			Corn starch	1.490
	Paeonia lactiflora Pall.	1.00		Colorant	Caramel pigment	0.010
	Glycyrrhiza uralensis Fisch.	1.00		Fragrance	Ginseng flavor powder	0.010
	Cinnamomum cassia (L.) J. Presl	1.00		—	—	—
	Asiasarum heterotropoides var. *mandshuricum* (Maxim.) F. Maek.	1.00	—	—	—	—
	Zingiber officinale Roscoe	1.00	—	—	—	—
	Schisandra chinensis (Turcz.) Baill.	1.00	—	—	—	—
			—	—	—	—
Excipient	Lactose hydrate	—	0.82	—	—	—
	Cornstarch	—	1.13	—	—	—
Total	—	—	3.00	Total	—	3.00

(8) Patients who have taken antipsychotic drugs less than 2 months before screening

(9) Patients who have participated in another clinical trial within the last 4 months

(10) Patients with a history of drug/alcohol abuse, hypersensitivity to any drugs used in this clinical trial or ingredients in those drugs

(11) Women who are pregnant, breastfeeding or capable of childbearing (i.e., women who have not undergone surgical sterilization) and do not accept the use of appropriate contraceptive methods

(12) Patients with thyroid dysfunction, indicated by thyroid-stimulating hormone (TSH) ≤0.1 or ≥10.0 µU/ml in screening

Investigated Drug and Placebo

The experimental group took SCRT granules (Batch number: 18423; Hanpoong Pharm and Foods, Jeonju, Jeollabuk-do, South Korea) and the control group took a placebo (Batch number: 18001; Hanpoong Pharm and Foods), which are all water extracted brown granules (**Table 1**). The participants took SCRT or the placebo three times per day for 4 weeks, taking one sachet before each meal. The one-time dose of SCRT or placebo was determined with reference to the regulations on reporting product licenses for herbal medicines published by the Korean Food and Drug Administration, differentiating according to age. The participants aged 7–14 years took a dose of 6.0 g per day, and the participants aged 15–65 years took a dose of 9.0 g per day.

To provide the minimal treatment for AD, all participants were supplied with Lacticare (Hydrocortisone acetate 1%) ointment, which is a Class 7 steroid, corresponding to the classification of "the least potent agent" (Ference and Last, 2009). Lacticare is a white lotion manufactured by Korea Pharma Co., Ltd. (Hwaseong, Gyeonggi-do, South Korea). All the participants were instructed to rub a thin layer of the ointment broadly into the affected area, in accordance with their physician's guidance. Each drug was stored at room temperature (20–30°C) in a sealed container, and storage, management, and distribution of the drugs was conducted under the guidance of the principal investigator and a traditional Korean medicine physician acting as a trial administrator.

Randomization and Blinding
Randomization

The participants who gave written consent to participate in the trial were allocated a screening number by researchers according to the order in which they gave consent. Of these, participants who satisfied the inclusion/exclusion criteria were assigned a randomization number in the order in which they visited. Treatment prescribed to the participants was based on these numbers assigned to the participants.

The randomization table contains information about the administration group assigned to the participants according to the randomization number. A block randomization method was used to randomize based on a 1:1 allocation ratio within a block of a certain size (e.g., 4, 6, 8). After generating the randomization table, for each participant, the corresponding drug was packaged, a label with the randomization number was attached, and the drug was sent to the pharmacist or traditional Korean medicine physician administrator at the trial center before the start of the trial.

Blinding

To ensure scientific results for the trial, double-blinding was performed, so that the investigators and participants were both unaware of the group allocation of each participant. In the event of unblinding due to adverse events, this was to be reported to the IRB and the petitioner was to be informed in accordance with the unblinding protocol.

Efficacy Assessment
SCORAD Index

The SCORAD Index is a scale for assessing AD that was developed in 1996 and has been used to date (European Task Force on Atopic Dermatitis, 1993). The investigators used the SCORAD Index to ascertain objective symptoms, such as the extent and severity of lesions, used the VAS to quantify and calculate subjective symptoms, such as pruritus

and sleep disorders. Based on this data, the changes in the SCORAD Index were compared statistically between the two groups.

Ointment Application

Drugs that were prescribed for treatment purposes and could affect the results, such as antihistamines, steroids, and NSAIDs, were thoroughly banned. However, in order to provide the minimal treatment for AD, all participants were provided with the steroid ointment Lacticare. The study participants were instructed to apply an appropriate amount of steroid ointment to the skin lesion with a cotton swab whenever atopic dermatitis symptoms occurred. To prevent adverse reactions, the maximum number of applications per day of steroid ointment was limited to 1 to 3 times. The participants recorded their own frequency of ointment use every day in a notebook, and based on this record, they visited the research institute again on Week 4 to calculate the total number of times they used the ointment. The total amount of ointment used was measured using scales when the patients visited the trial center again 4 weeks after the start of the trial. Based on these measurements, the change in ointment use was compared statistically between the two groups.

Body Measurement

The investigators measured and recorded the participants' height and body weight when they visited the trial center at baseline and in Week 4. Based on these measurements, changes in height and weight were compared between the two groups.

Safety Assessment
Adverse Reaction

In this study, all harmful, unintended signs, symptoms, and diseases that the participants developed after receiving a drug in the trial were defined as adverse reactions. In the event of an adverse reaction, the investigators compiled a case record form including the name of the adverse reaction, the date of onset and recovery, by severity, relatedness to the drug taken, related procedures and treatments, and treatment outcomes. Abnormal laboratory results or vital signs that were considered to be clinically significant were also recorded as adverse reactions.

Diagnostic Test

For safety assessment, all participants were subjected to laboratory tests for a total of 20 items, including complete blood cell (CBC), renal function test (RFT), liver function test (LFT), blood lipid, and urine PH. The tests were performed twice, at baseline and in Week 4.

Vital Sign Monitoring

The investigators measured all participants' body temperature, pulse rate, and blood pressure when they visited the trial center at baseline and in Week 4. Changes in vital signs were monitored before and after taking the prescribed drug, and judged to be normal or abnormal based on the results.

Statistical Analyses

SAS for Windows was used for statistical analysis; the statistical significance level was set at 5% and the power at 80%, and 95% confidence intervals were provided for the differences between the groups. For test results, means, standard deviations, and frequencies were shown. Paired t-tests were used to compare the efficacy outcome variables between baseline and Week 4, and independent t-tests were used to analyze differences between the two groups. However, when normality was not satisfied through the normality test, nonparametric analysis was performed using Wilcoxon signed-rank test and Mann-Whitney test. The participants' gender and ratio of participants who developed adverse reactions was calculated and compared between the two groups using a chi-square test. The chi-square test, Fisher's exact test, and independent t-test were used for comparative analysis of factors that influence height growth. Means and standard deviations were shown for laboratory test results and vital signs, and independent t-tests and paired t-tests were used to compare the results, respectively, within groups between baseline and Week 4, and between groups. Missing values (e.g., due to dropout) were imputed using last observation carried forward (LOCF).

RESULTS

Demographic Information

There were no statistically significant differences in sex or age between the two groups. Statistical analysis in this study included a total of 49 participants, excluding the four participants who dropped out and seven participants who, in a MAST test for around 60 allergens to test for respiratory allergies, diverged from the normal distribution for an item on the statistically significant boundary between the two groups. The seven participants showing differences in the MAST test were all in the experimental group, and showed allergic reactions to garlic (one person), Cladosporium (three persons), *Alternaria alternata* (one person), and dog (two persons).

In order to precisely ascertain the extent of growth, participants who were aged <18 years were classified as children. A total of 30 children were recruited (15 in the experimental group and 15 in the control group). Among the children, there were no statistically significant differences in sex or age between the two groups (**Table 2**). One person in the experimental group and three persons in the control group dropped out during the trial. The reason for dropout in the experimental group was concomitant medication with a banned drug, and TSH outside the normal range in the placebo group. Among the children, one participant of the experimental group dropped out due to violation of exclusion criteria. Excluding the patients who dropped out, 56 patients completed the whole clinical trial in accordance with the prepared protocol (**Figure 1**).

TABLE 2 | Demographic information.

		Experimental group (n = 30)	Control Group (n = 30)	Total (n = 60)	p-value[a]
Total participants	Sex (M/F)	16/14	9/21	25/35	0.067[b]
	Age (years)	22.53 ± 14.67	25.47 ± 16.89	24.00 ± 15.75	0.476
		Experimental group (n = 15)	Control group (n = 15)	Total (n = 30)	p-value[a]
Children participants	Sex (M/F)	9/6	6/9	15/15	0.273[b]
	Age (years)	10.00 ± 1.96	10.13 ± 2.10	10.07 ± 2.00	0.859

[a]Values are presented as mean ± SD: analyzed by independent t-test.
[b]Values are presented as mean ± SD: analyzed by chi-square test.

FIGURE 1 | Study flow chart describing the randomized controlled trial.
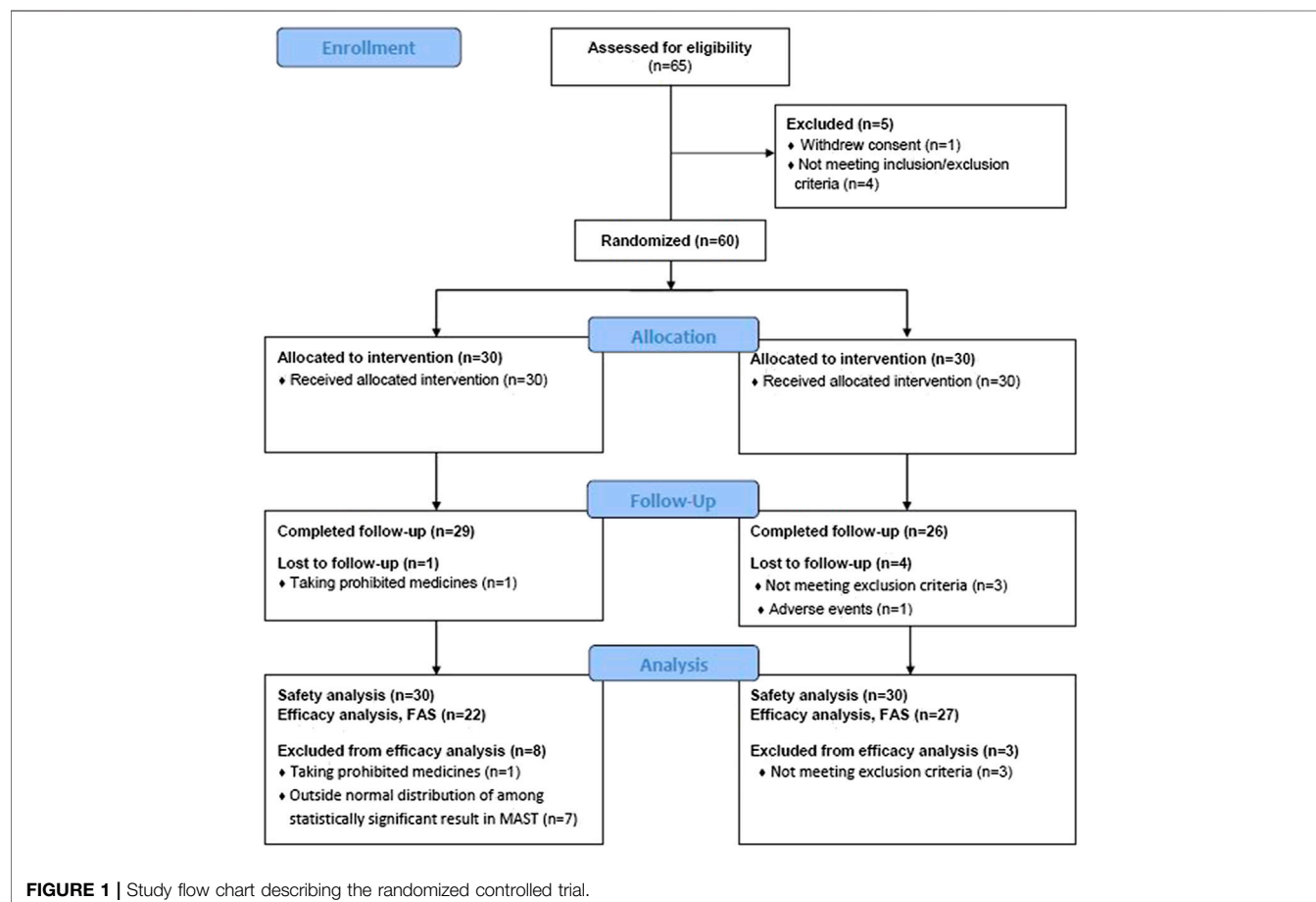
Compliance

The experimental group took a mean of 76.97 ± 12.01 doses of the prescribed drug, showing 94.55 ± 5.18% compliance. The control group took a mean of 76.33 ± 18.16 doses of the prescribed drug, showing 93.67 ± 6.21% compliance. Compliance was over 90% in both groups, and there was no statistically significant different between the two groups.

Efficacy Evaluation
SCORAD Index

In the efficacy evaluation in Week 4, the objective, subjective, and total SCORAD scores all showed statistically significant decreases compared to baseline in both the experimental group and the control group ($p < 0.05$). However, there were no significant differences when SCORAD scores were compared between the two groups (**Table 3**).

Ointment Application

The mean amount of ointment used in the experimental group increased by 2.50 ± 7.63 g at Week 4 compared to baseline, and the frequency of use increased by 3.00 ± 12.17. Meanwhile, the amount of ointment used in the control group increased by 11.85 ± 21.93 g, and the frequency of use increased by 7.33 ± 11.63. There were no statistically significant differences

TABLE 3 | Changes in the SCORAD index.

	Experimental group (n = 22)				Control group (n = 27)				p-value[b]
	Baseline	Week 4	Change value	p-value[a]	Baseline	Week 4	Change value	p-value[a]	
Extent of lesion	33.14 ± 12.13	23.77 ± 11.41	−9.36 ± 10.30	0.0003***	32.41 ± 15.86	23.37 ± 12.75	−9.04 ± 8.39	<0.0001***	0.903
Severity of lesion	4.27 ± 1.39	3.18 ± 1.40	−1.09 ± 0.92	<0.0001***	4.19 ± 1.44	3.11 ± 1.45	−1.07 ± 0.83	<0.0001***	0.947
Subjective symptoms	9.36 ± 3.37	6.59 ± 3.32	−2.77 ± 2.49	<0.0001***	8.52 ± 3.62	6.26 ± 3.72	−2.26 ± 2.46	<0.0001***	0.473
Total score	30.95 ± 7.72	22.48 ± 9.07	−8.46 ± 5.93	<0.0001***	29.65 ± 9.44	21.82 ± 9.06	−7.83 ± 5.53	<0.0001***	0.699

[a]Values are presented as mean ± SD: analyzed by paired t-test.
[b]Values are presented as mean ± SD: analyzed by independent t-test.
***p < 0.001.

TABLE 4 | Changes in the amount and frequency of ointment use.

	Experimental group (n = 22)				Control group (n = 27)				p-value[b]
	Baseline	Week 4	Change value	p-value[a]	Baseline	Week 4	Change value	p-value[a]	
Frequency of use (times)	3.68 ± 3.98	6.18 ± 8.70	2.50 ± 7.63	0.139	5.93 ± 8.81	13.26 ± 14.55	7.33 ± 11.63	0.003**	0.100
Amount of use (g)	7.59 ± 10.83	10.59 ± 13.00	3.00 ± 12.17	0.260	6.59 ± 14.35	18.44 ± 21.68	11.85 ± 21.93	0.009**	0.081

[a]Values are presented as mean ± SD: analyzed by paired t-test.
[b]Values are presented as mean ± SD: analyzed by independent t-test.
**p < 0.01.

TABLE 5 | Changes in children's height and weight.

	Experimental group (n = 14)				Control group (n = 15)				p-value[b]
	Baseline	Week 4	Change value	p-value[a]	Baseline	Week 4	Change value	p-value[a]	
Height (cm)	146.43 ± 16.20	147.00 ± 16.10	0.57 ± 0.65	0.006**	146.80 ± 11.93	146.87 ± 11.78	0.07 ± 0.26	0.334	0.015*
Weight (kg)	40.21 ± 10.52	40.53 ± 10.73	0.31 ± 0.95	0.239	45.91 ± 14.30	46.47 ± 14.38	0.56 ± 1.66	0.212	0.632
BMI (kg/m^2)	18.56 ± 2.82	18.55 ± 2.89	−0.01 ± 0.39	0.946	20.84 ± 4.86	21.09 ± 4.83	0.25 ± 0.74	0.205	0.243

[a]Values are presented as mean ± SD: analyzed by paired t-test.
[b]Values are presented as mean ± SD: analyzed by independent t-test.
*p < 0.05.
**p < 0.01.

between the two groups in the amount or frequency of ointment use. However, there was a trend for a less amount of ointment use in the experimental group compared to the control group (p = 0.08; **Table 4**).

Body Measurement

The mean height of the children in the experimental group was 146.43 ± 16.20 cm at baseline, and the mean growth after medication was 0.57 ± 0.65 cm. The mean height of the children in the control group was 146.80 ± 11.93 cm at baseline, and the mean growth after medication was 0.07 ± 0.26 cm. In statistical analysis, the height of the experimental group and the control group at baseline did not show a statistically significant difference. However, at Week 4, the experimental group showed a significant level of height growth, while the control group did not show any significant change. As a result, the experimental group showed significantly more growth than the control group (p < 0.05). On the other hand, there were no significant differences between the two groups in changes in body weight or BMI (**Table 5**).

In the analysis of the children and their parents, such as the parents' age, parents' education level, parents' occupation, family income, weight and height at birth, breastfeeding experience, which can affect height growth, no statistically significant difference was observed between the experimental group and the control group (**Table 6**). In addition, residential life (type of resident, residential environment, construction period, new/repaired house or new furniture, etc.), eating habits and other matters (cooking method, whether to take dietary supplements, number and type of eating out, type of snack, the number of exercise, participants' ethnicity etc.) did not show any significant difference between both groups (**Table 6**).

Safety Evaluation
Adverse Reaction

The adverse reactions reported by the participants were mild abdominal pain (two persons), acute palmoplantar vesicular eczema (one person), and fever and coughing (one person). Of these, the eczema and fever and coughing were considered to be unrelated to the prescribed drug, and disappeared promptly after monitoring. The two cases of abdominal pain were both in the

TABLE 6 | Analysis of influencing factors related to children's height growth.

			Experimental group (n = 15)	Control group (n = 15)	*p*-value
General characteristics of parents	Parent's age	Under 30	1 (6.67%)	0 (0.00%)	1.000[a]
		30–34	1 (6.67%)	1 (6.67%)	
		35–39	4 (26.67%)	4 (26.67%)	
		Over 40	9 (60.00%)	10 (66.67%)	
	Education level	High school graduate	5 (33.33%)	7 (46.67%)	0.456[b]
		College graduate	10 (66.67%)	8 (53.33%)	
	Occupation	Employed	11 (73.33%)	12 (80.00%)	1.000[a]
		Unemployed	4 (26.67%)	3 (20.00%)	—
	Family income (US dollor)	Under 200	2 (13.33%)	1 (6.67%)	0.582[a]
		200–300	1 (6.67%)	2 (13.33%)	
		300–400	6 (40.00%)	3 (20.00%)	
		Over 400	6 (40.00%)	9 (60.00%)	
General characteristics of children	Weight at birth (kg)	—	3.34 ± 0.38	3.26 ± 0.49	0.592[c]
	Height at birth (cm)	—	50.37 ± 1.60	49.93 ± 1.98	0.519[c]
	Breastfeeding experience	No lactation	3 (20.00%)	2 (13.33%)	0.775[a]
		Colostrum lactation	2 (13.33%)	2 (13.33%)	
		Under 6 months	6 (40.00%)	4 (26.67%)	
		Over 1 year	4 (26.67%)	7 (46.67%)	

[a]*Values are presented as mean ± SD or number (%): analyzed by Fisher's exact test.*
[b]*Values are presented as mean ± SD or number (%): analyzed by chi-square test.*
[c]*Values are presented as mean ± SD or number (%): analyzed by independent* t-test.

TABLE 7 | Changes in children's TSH and Vital sign.

	Experimental group (n = 14)				Control group (n = 15)				*p*-value[b]
	Baseline	Week 4	Change value	*p*-value[a]	Baseline	Week 4	Change value	*p*-value[a]	
TSH (uIU/ml)	1.46 ± 0.48	1.21 ± 0.36	−0.25 ± 0.32	0.012*	1.40 ± 0.68	1.89 ± 1.23	0.49 ± 1.08	0.103	0.022*
SBP (mmHg)	100.86 ± 10.73	100.79 ± 10.36	−0.07 ± 10.20	0.980	103.93 ± 14.56	106.27 ± 15.10	2.33 ± 11.33	0.438	0.554
DBP (mmHg)	59.93 ± 7.15	59.57 ± 9.47	−0.36 ± 12.07	0.911	63.00 ± 11.96	63.27 ± 12.04	0.27 ± 8.42	0.904	0.872
Body temperature (°C)	36.79 ± 0.21	36.78 ± 0.32	−0.01 ± 0.38	0.890	36.67 ± 0.22	36.77 ± 0.22	0.09 ± 0.28	0.224	0.396
Pulse (times/min)	85.57 ± 5.46	82.36 ± 5.88	−3.21 ± 8.34	0.146	81.33 ± 6.79	83.67 ± 5.05	2.33 ± 5.14	0.100	0.039*

[a]*Values are presented as mean ± SD: analyzed by paired* t-test.
[b]*Values are presented as mean ± SD: analyzed by independent* t-test.
*$*p < 0.05$.

placebo group, and one of these patients showed recovery without separate treatment. The other patient withdrew their consent and dropped out of the clinical trial due to the abdominal pain.

Diagnostic Test and Vital Sign Monitoring

In blood tests and vital sign monitoring after 4 weeks of medication, pulse and TSH levels of the children in the experimental group showed a significantly greater decrease from baseline compared to the control group ($p < 0.05$). The body temperature, SBP, DBP of the children in the experimental group also showed a decrease compared to the baseline. However, this change in TSH and vital sign was within the normal range, and all study participants did not show any abnormal signs in laboratory tests or vital sign monitoring throughout the study (**Table 7**).

DISCUSSION

AD is a relapsing, pruritic, inflammatory skin disease, reported to be caused by interactions between the immune system,

microbial exposure, genetic and environmental factors, and skin barrier dysfunction (Flohr and Mann, 2014; Otsuka et al., 2017). For treatment of AD, depending on the etiology and the severity of symptoms, methods such as avoidance strategies, topical anti-inflammatory therapy, and phototherapy are used (Wollenberg et al., 2018a; Wollenberg et al., 2018b). Of these, application of steroidal ointment is the most commonly recommended treatment method to alleviate symptoms (Arellano et al., 2007). However, long-term steroid use can cause adverse reactions such as acne, steroid rosacea, telangiectasia, perioral dermatitis, and atrophy. For patients who do not respond to steroid treatment, AD can recur (Fukaya, 2000; Atherton, 2003).

The incidence of AD has been gradually increasing over several centuries, and currently affects around 20% of the world population (Bantz et al., 2014). The need to develop new therapeutic agents has become prominent due to the increasing socioeconomic costs of AD (Carroll et al., 2005; Suh et al., 2007), and this has been accompanied by growing interest in the potential of alternative medicine.

SCRT is a herbal medicine that has been used in East Asia to treat diseases related to the allergic march, such as allergic rhinitis and asthma, for hundreds of years (Shin et al., 2018). SCRT is reported to have an "anti-allergic effect" (Ikeda et al., 2002) and an "anti-inflammatory effect" (Shin et al., 2018). However, to date, there have been almost no clinical studies investigating the effects of SCRT for AD.

With the aim of verifying the efficacy of SCRT for AD, this study evaluated efficacy and safety in patients taking SCRT or a placebo. In the efficacy assessment, there were no statistically significances between the two groups in objective, subjective, and total SCORAD scores. This is thought to be due to the effects of the steroidal ointment supplied to all participants to provide the minimal treatment.

There were also no statistically significant differences between the two groups in the change in amount and frequency of ointment use. However, the experimental group showed a trend for less ointment use than the control group ($p = 0.081$). The reason for this phenomenon seems to be that the previously reported anti-allergic effect such as inhibiting IL-4 and $CD4^+$ of SCRT and its ingredients (Ikeda et al., 2002) affected the progression and remission of atopic dermatitis. This indicates that medication with SCRT could reduce AD patients' dependency on steroidal ointment.

In anthropometric analysis only including children (participants aged <18 years), the experimental group showed a significantly greater increase in height from baseline to Week 4 than the control group ($p < 0.05$). Most of the children in this study belonged to the school-age (7–12 years old), and in the statistical analysis conducted on these participants (13 from the experimental group and 12 from the control group), the experimental group showed a statistically significant height growth compared to the control group ($p = 0.016$). The remaining five participants (two from the experimental group and three from the control group) belonged to adolescence (over 13 years old), and in the height growth, no statistically significant difference was shown between the experimental group and control group. However, because the number of adolescence participants was too small, it was judged to have no statistical significance. In addition, as a result of investigating and comparing factors that can affect height growth such as parents' socioeconomic environment, physical information of the children, residential life, eating habits, participants' ethnicity and exercise, the experimental group and the control group didn't show any statistically significant differences in these items. This suggests that SCRT has a significant effect as a growth promoter for children with AD.

In blood tests and vital sign monitoring after 4 weeks of medication, TSH levels of the children in the experimental group showed a significantly greater decrease from baseline compared to the control group ($p < 0.05$). Thyroid hormones are known to have a major effect on children's growth and development (Tarım, 2011). The fact that the experimental group of this study showed height growth and TSH reduction after 4 weeks of SCRT administration suggests that there may be some association between SCRT, TSH, and children's height growth. However, considering the fact that the relationship between SCRT and TSH has not been clearly identified, further studies are needed to clarify this association.

In adverse reaction monitoring, vital sign monitoring, and laboratory tests to evaluate the safety of SCRT, there were no abnormal findings. Considering that previous studies have reported allergic diseases, such as allergic asthma and AD, leading to short stature in children (Ferguson et al., 1982; Kristumundsdottir and David, 1987; Snat'Anna et al., 1996), the growth-promoting effects of SCRT are thought to be mediated not only by hormones, but also by amelioration of allergic disease. The results of this study provide evidence to support claims that SCRT is a safe treatment method without adverse effects that can be used in children with AD as an alternative to growth hormone, which is controversial.

The mechanisms behind the growth-promoting effects of SCRT are unclear, and other factors affecting growth such as parental height could not be actively controlled. In addition, it is difficult to generalize the results as the number of research participants analyzed for height growth is relatively small. However, if independent studies of SCRT or a long-term, large-scale study of the effects on AD relief and growth factors such as T3, T4, and IGF-1 were performed, the mechanisms could be revealed more precisely.

CONCLUSION

The experimental group that took SCRT showed a trend for reduced dependence on steroidal ointment compared to the control group. In addition, SCRT treatment resulted in a significant promotion of height growth in children with AD. Also in safety evaluation, all study participants did not show any abnormal signs including laboratory tests or vital sign monitoring throughout the study.

DATA AVAILABILITY STATEMENT

The original contributions presented in the study are included in the article/supplementary material, further inquiries can be directed to the corresponding author.

ETHICS STATEMENT

The studies involving human participants were reviewed and approved by The institutional review board of the Wonkwang University Korean Medicine Hospital. Written informed consent to participate in this study was provided by the participants' legal guardian/next of kin.

AUTHOR CONTRIBUTIONS

JL: Conceptualization, Visualization, Writing of the original draft. EJ: Methodology, Revision and editing of the draft. JJ: Methodology, Revision and editing of the draft. Y-EK: Methodology. M-JS: Methodology. SK: Resources. GY: Resources. YS: Data curation, Resources. MP: Conceptualization, Project administration, Supervision, Revision and editing of the draft.

REFERENCES

Arellano, F. M., Wentworth, C. E., Arana, A., Fernández, C., and Paul, C. F. (2007). Risk of lymphoma following exposure to calcineurin inhibitors and topical steroids in patients with atopic dermatitis. *J. Invest. Dermatol.* 127, 808–816. doi:10.1038/sj.jid.5700622.

Atherton, D. J. (2003). Topical corticosteroids in atopic dermatitis. *BMJ* 327, 942–943. doi:10.1136/bmj.327.7421.942.

Bantz, S. K., Zhu, Z., and Zheng, T. (2014). The atopic march: progression from atopic dermatitis to allergic rhinitis and asthma. *J. Clin. Cell. Immunol.* 5 (2), 202. doi:10.4172/2155-9899.1000202.

Carroll, C. L., Balkrishnan, R., Feldman, S. R., Fleischer, A. B., Jr, and Manuel, J. C. (2005). The burden of atopic dermatitis: impact on the patient, family, and society. *Pediatr. Dermatol.* 22, 192–199. doi:10.1111/j.1525-1470.2005.22303.x.

Das, A. K., Mizuguchi, H., Kodama, M., Dev, S., Umehara, H., Kitamura, Y., et al. (2009). Sho-seiryu-to suppresses histamine signaling at the transcriptional level in TDI-sensitized nasal allergy model rats. *Allergol. Int.* 58, 81–88. doi:10.2332/allergolint.o-07-526.

Deckers, I. A. G., McLean, S., Linssen, S., Mommers, M., van Schayck, C. P., and Sheikh, A. (2012). Investigating international time trends in the incidence and prevalence of atopic Eczema 1990-2010: a systematic review of epidemiological studies. *PLoS One* 7, e39803. doi:10.1371/journal.pone.0039803.

Eichenfield, L. F., Tom, W. L., Chamlin, S. L., Feldman, S. R., Hanifin, J. M., Simpson, E. L., et al. (2014). Guidelines of care for the management of atopic dermatitis: section 1. Diagnosis and assessment of atopic dermatitis. *J. Am. Acad. Dermatol.* 70, 338–351. doi:10.1016/j.jaad.2013.10.010.

European Task Force on Atopic Dermatitis (1993). Severity scoring of atopic dermatitis: the SCORAD index. *Dermatology* 186, 23–31.

Ference, J. D., and Last, A. R. (2009). Choosing topical corticosteroids. *Am. Fam. Physician.* 79, 135–140.

Ferguson, A., Murray, A., and Tze, W. (1982). Short stature and delayed skeletal maturation in children with allergic disease. *J. Allergy Clin. Immunol.* 69, 461–466. doi:10.1016/0091-6749(82)90122-1.

Flohr, C., and Mann, J. (2014). New insights into the epidemiology of childhood atopic dermatitis. *Allergy* 69, 3–16. doi:10.1111/all.12270.

Fukaya, M. (2000). Why do patients with atopic dermatitis refuse to apply topical corticosteroids? *Dermatology* 201, 242–245. doi:10.1159/000018495.

Hanifin, J. M., and Rajka, G. (1980). Diagnostic features of atopic dermatitis. *Acta Derm. Venereol. Suppl.* 59, 44–47. doi:10.2340/00015555924447

Hong, H.-S., Lee, J.-Y., and Kim, D.-G. (2012). Analysis of factors enhancing growth effect of Boyangsungjang-Tang. *J. Korean Oriental Pediatr.* 26, 62–71. doi:10.7778/jpkm.2012.26.2.062.

Ikeda, Y., Kaneko, A., Yamamoto, M., Ishige, A., and Sasaki, H. (2002). Possible involvement of suppression of Th2 differentiation in the anti-allergic effect of Sho-seiryu-to in mice. *Jpn. J. Pharmacol.* 90, 328–336. doi:10.1254/jjp.90.328.

Kang, S.-J., Cho, H.-B., Jo, E.-H., Yang, G.-J., Hong, J.-E., Lee, J.-H., et al. (2020). Efficacy and safety of So-Cheong-Ryong-Tang in patients with atopic dermatitis and respiratory disorders. *Medicine*, 99. e18565. doi:10.1097/MD.0000000000018565.

Ko, E., Rho, S., Cho, C., Choi, H., Ko, S., Lee, Y., et al. (2004). So-cheong-ryong-tang, tradititional Korean medicine, suppresses Th2 lineage development. *Biol. Pharm. Bull.* 27, 739–743. doi:10.1248/bpb.27.739.

Kristmundsdottir, F., and David, T. J. (1987). Growth impairment in children with atopic eczema. *J. R. Soc. Med.* 80, 9–12. doi:10.1177/014107688708000106.

Nutten, S. (2015). Atopic dermatitis: global epidemiology and risk factors. *Ann. Nutr. Metab.* 66, 8–16. doi:10.1159/000370220.

Otsuka, A., Nomura, T., Rerknimitr, P., Seidel, J. A., Honda, T., and Kabashima, K. (2017). The interplay between genetic and environmental factors in the pathogenesis of atopic dermatitis. *Immunol. Rev.* 278, 246–262. doi:10.1111/imr.12545.

Park, B.-K., Park, Y.-C., Jung, I. C., Kim, S.-H., Choi, J. J., Do, M., et al. (2015). Gamisasangja-tang suppresses pruritus and atopic skin inflammation in the NC/Nga murine model of atopic dermatitis. *J. Ethnopharmacol.* 165, 54–60. doi:10.1016/j.jep.2015.02.040.

Park, J., Youn, D.-H., Kang, J., Ahn, K. S., Kwak, H. J., and Um, J.-Y. (2019). Taeumjowi-tang, a traditional Korean Sasang remedy, improves obesity-atopic dermatitis comorbidity by regulating hypoxia-inducible factor 1 alpha. *Front. Pharmacol.* 10, 1458. doi:10.3389/fphar.2019.01458.

Sant'Anna, C. A., Solé, D., and Naspitz, C. K. (1996). Short stature in children with respiratory allergy. *Pediatr. Allergy Immunol.* 7, 187–192. doi:10.1111/j.1399-3038.1996.tb00131.x.

Shin, N.-R., Kim, C., Seo, C.-S., Ko, J.-W., Cho, Y.-K., Kim, J.-C., et al. (2018). So-Cheong-Ryoung-Tang attenuates pulmonary inflammation induced by cigarette smoke in bronchial epithelial cells and experimental mice. *Front. Pharmacol.* 9, 1064. doi:10.3389/fphar.2018.01064.

Suh, D.-C., Sung, J., Gause, D., Raut, M., Huang, J., and Choi, I.-S. (2007). Economic burden of atopic manifestations in patients with atopic dermatitis–analysis of administrative claims. *J. Manag. Care Pharm.* 13, 778–789. doi:10.18553/jmcp.2007.13.9.778.

Tarım, Ö. (2011). Thyroid hormones and growth in health and disease. *J. Clin. Res. Pediatr. Endocrinol.* 3 (2), 51–55. doi:10.4274/jcrpe.v3i2.11.

Wollenberg, A., Barbarot, S., Bieber, T., Christen-Zaech, S., Deleuran, M., Fink-Wagner, A., et al. (2018a). Consensus-based European guidelines for treatment of atopic eczema (atopic dermatitis) in adults and children: part I. *J. Eur. Acad. Dermatol. Venereol.* 32, 657–682. doi:10.1111/jdv.14891.

Wollenberg, A., Barbarot, S., Bieber, T., Christen-Zaech, S., Deleuran, M., Fink-Wagner, A., et al. (2018b). Consensus-based European guidelines for treatment of atopic eczema (atopic dermatitis) in adults and children: part II. *J. Eur. Acad. Dermatol. Venereol.* 32, 850–878. doi:10.1111/jdv.14888.

Natural Xanthones and Skin Inflammatory Diseases: Multitargeting Mechanisms of Action and Potential Application

Natalie Vivien Gunter[1], Soek Sin Teh[2], Yang Mooi Lim[3,4] and Siau Hui Mah[1,5]*

[1]School of Biosciences, Taylor's University, Subang Jaya, Malaysia, [2]Engineering and Processing Division, Energy and Environment Unit, Malaysian Palm Oil Board, Kajang, Malaysia, [3]Centre for Cancer Research, Faculty of Medicine and Health Sciences, Universiti Tunku Abdul Rahman, Kajang, Malaysia, [4]Department of Pre-Clinical Sciences, Faculty of Medicine and Health Sciences, Universiti Tunku Abdul Rahman, Kajang, Malaysia, [5]Centre for Drug Discovery and Molecular Pharmacology, Faculty of Health and Medical Sciences, Taylor's University, Subang Jaya, Malaysia

The pathogenesis of skin inflammatory diseases such as atopic dermatitis, acne, psoriasis, and skin cancers generally involve the generation of oxidative stress and chronic inflammation. Exposure of the skin to external aggressors such as ultraviolet (UV) radiation and xenobiotics induces the generation of reactive oxygen species (ROS) which subsequently activates immune responses and causes immunological aberrations. Hence, antioxidant and anti-inflammatory agents were considered to be potential compounds to treat skin inflammatory diseases. A prime example of such compounds is xanthone (xanthene-9-one), a class of natural compounds that possess a wide range of biological activities including antioxidant, anti-inflammatory, antimicrobial, cytotoxic, and chemotherapeutic effects. Many studies reported various mechanisms of action by xanthones for the treatment of skin inflammatory diseases. These mechanisms of action commonly involve the modulation of various pro-inflammatory cytokines such as interleukin (IL)-1β, IL-6, IL-8, and tumor necrosis factor α (TNF-α), as well as anti-inflammatory cytokines such as IL-10. Other mechanisms of action include the regulation of NF-κB and MAPK signaling pathways, besides immune cell recruitment via modulation of chemokines, activation, and infiltration. Moreover, disease-specific activity contributed by xanthones, such as antibacterial action against *Propionibacterium acnes* and *Staphylococcus epidermidis* for acne treatment, and numerous cytotoxic mechanisms involving pro-apoptotic and anti-metastatic effects for skin cancer treatment have been extensively elucidated. Furthermore, xanthones have been reported to modulate pathways responsible for mediating oxidative stress and inflammation such as PPAR, nuclear factor erythroid 2-related factor and prostaglandin cascades. These pathways were also implicated in skin inflammatory diseases. Xanthones including the prenylated α-mangostin (**2**) and γ-mangostin (**3**), glucosylated mangiferin (**4**) and the caged xanthone gambogic acid (**8**) are potential lead compounds to be further developed into pharmaceutical agents for the treatment of skin inflammatory diseases. Future studies on the structure-activity relationships, molecular mechanisms, and applications of xanthones for the treatment of skin inflammatory diseases are thus highly recommended.

Keywords: acne, anti-inflammatory, antioxidant, atopic dermatitis, skin cancer, psoriasis

INTRODUCTION

Skin inflammatory diseases are mediated by multiple mechanisms that induce chronic inflammation (Pleguezuelos-Villa et al., 2019). For instance, the pathogenesis of skin inflammatory diseases such as atopic dermatitis (AD), acne, psoriasis and skin malignancies have been extensively associated with immunological alterations in cytokine expression and immune cell activity. Inflammatory responses were additionally linked to the generation of oxidative stress by external aggressors such as ultraviolet (UV) radiation and xenobiotics that also disrupts the normal intracellular redox state and cellular protein structures (Li et al., 2012; Cidade et al., 2017). These inflammatory responses in skin inflammatory diseases are commonly modulated through NF-κB, MAPK and PI3K/Akt signaling pathways which contribute to the activation of immune cells and production of pro-inflammatory cytokines such as interleukin (IL)-1β, IL-6, IL-8 and tumor necrosis factor α (TNF-α) (Wang et al., 2017; Guo et al., 2019). Thus, the potential lead compounds that possess both anti-inflammatory and antioxidant activities such as xanthones have received great attention for the treatment for skin inflammatory diseases (Pleguezuelos-Villa et al., 2019).

Xanthones are versatile scaffolds consisting of a tricyclic xanthene-9-one structure (1) and are commonly found in higher plants, fungi, and lichens (Aye et al., 2020). Various plants have been reported to be rich in naturally occurring xanthones, including *Garcinia mangostana* L. (Im et al., 2017), *G. cowa* Roxb. ex Choisy (Auranwiwat et al., 2014), *G. hanburyi* Hook.f. (Xu et al., 2015), *Mangifera indica* L. (Garrido et al., 2004), *Hypericum oblongifolium* Wall. (Ali et al., 2011), *Tripterospermum lanceolatum* (Hayata) H. Hara ex Satake (Hsu et al., 1997), *Mesua beccariana* (Baill.) Kosterm., *M. ferrea* L. (Teh et al., 2017), *Iris sibirica* L. (Tikhomirova and Ilyicheva, 2020), *I. adriatica* Trinajstic ex Mitic (Alperth et al., 2018), *Calophyllum inophyllum* L. (Mah et al., 2019) and *C. soulattri* Burm.f. (Mah et al., 2019). Furthermore, plants of the genera *Calophyllum*, *Cratoxylum*, *Garcinia*, *Gentiana*, *Hypericum* and *Swertia* were proposed to possess great developmental prospect due to their rich content of xanthones (Ruan et al., 2017). This class of compounds possess a wide range of biological activities including anti-inflammatory (Teh et al., 2017; Mah et al., 2019; Aye et al., 2020; Ng et al., 2020), antioxidant (Wang et al., 2018a), antimicrobial (Koh et al., 2013; Auranwiwat et al., 2014), chemotherapeutic (Beninati et al., 2014) and chemopreventive (Purnaningsih et al., 2018) activities. Thus, xanthones are promising lead compounds for treating skin inflammatory diseases.

Many reviews to date discuss on various biological activities of xanthones (Ibrahim et al., 2016; Aizat et al., 2019; Feng et al., 2020; Ong et al., 2020) with a recent review discussing the modulatory ability of xanthones on macrophage function and associated inflammatory diseases (Ng and Chua, 2019). The reviews on the potential of xanthones as anti-inflammatory agents for skin diseases are limited and no review has been focused extensively on their mechanisms of action in the context of skin inflammatory diseases. Thus, in this review, we focused on the studies of naturally occurring xanthones within the past two decades for the treatment of skin inflammatory diseases, particularly atopic dermatitis, acne, psoriasis, and skin cancers, while simultaneously highlighting the mechanisms of action and signaling pathways involved. A summary of the mechanisms of action for xanthone derivatives with anti-inflammatory, anti-bacterial, chemotherapeutic and cytoprotective effects are summarized in **Table 1**; **Figure 1**. The basic structure of xanthone is presented in **Figure 2**, together with its naturally available derivatives that exhibit these biological activities. The potential applications of xanthones with regards to cellular pathways implicated in skin inflammatory diseases are also included in this review.

XANTHONES INVOLVED IN THE TREATMENT OF SKIN INFLAMMATORY DISEASES

Atopic Dermatitis

AD, also known as atopic eczema, is the most common chronic skin disorder affecting 3-20% of the global population (Lopez Carrera et al., 2019; Schwingen et al., 2020). AD is commonly characterized by pruritic skin lesions with concurrent allergic inflammation and augmented immunoglobulin E (IgE) and histamine levels (Higuchi et al., 2013; Zhao et al., 2017). Allergic inflammation and augmented serum IgE levels underlie the immunological dysregulation and subsequent dysfunction of the skin barrier (Higuchi et al., 2013). Reactive oxygen species (ROS) have also been associated with the pathogenesis of skin allergic reactions (Bickers and Athar 2006; Sivaranjani et al., 2013). ROS causes lipid peroxidation and damages cellular components, initiating cell death (Okayama 2005; Sivaranjani et al., 2013). The generation of ROS also activates immune responses by inducing leukocyte infiltration and altering cytokine expression profiles of Th1 and Th2 cells (Bickers and Athar 2006). Thus, antioxidants and anti-inflammatory agents such as xanthones are highly beneficial to treat AD (Okayama 2005; Sivaranjani et al., 2013).

Anti-itching Activity & Histamine Modulation by Xanthones

Xanthones were found to attenuate various clinical symptoms of AD such as skin lesions and possess anti-itching effect. The xanthone-rich mangosteen rind of *G. mangostana* L. extracted with 70% ethanol was studied by Higuchi et al. (2013) as a potential preventative agent for AD. The extract was administered orally at a dose of 250 mg/kg/day to 6-week-old NC/Tnd mice which decreased the frequency and duration of scratching per 20 minutes in treated-NC-Tnd mice. This finding was linked to the decreased keratinocyte and fibroblast

TABLE 1 | Xanthones and their mechanism of action for treatment of skin inflammatory diseases.

Disease	Xanthone	Mechanism of Action	References
Atopic dermatitis	Xanthene-9-one (**1**)	Reduced serum levels of histaminein DNFB-induced mice	Aye et al. (2020)
		Suppressed histamine and TSLP release by PMA-CI-stimulated HMC-1 mast cells	
		Reduced mRNA expression of IL-1β, IL-6, IL-8, TARC and MDC in mice	
		Reduced serum levels of IgE	
		Reduced population of mast cells in skin lesions	
		Inhibited phosphorylation of IκBα and NF-κB in HaCaT cells	
	α-mangostin (**2**)	Reduced skin lesions and hyperplasia in DNFB-induced mice	Aye et al. (2020)
		Anti-itching effects by decreasing production of NGF and nerve extensions	Nakatani et al. (2002)
		Antagonist of H1 receptors by competitive inhibition	Chairungsrilerd et al. (1996a), Chairungsrilerd et al. (1996b)
		Inhibited mRNA expression of TSLP and IFN-γ	Higuchi et al. (2013)
		Suppressed IgE production by stimulated splenic B cells	Jang et al. (2012), Higuchi et al. (2013)
		Inhibited allergen-IgE-induced mast cell activation	Jang et al. (2012)
		Reduced eosinophil population in skin of NC/Tnd mice by suppressing PI3K recruiting and activating activity	Higuchi et al. (2013)
		Inhibited NF-κB and MAPK pathways	Jang et al. (2012), Xu et al. (2018)
	γ-mangostin (**3**)	Antagonist of H1 receptor	Sukma et al. (2011)
		Suppressed IgE production by stimulated splenic B cells	Jang et al. (2012), Higuchi et al. (2013)
		Inhibited allergen-IgE-induced mast cell activation	Jang et al. (2012)
		Reduced eosinophil population in skin of NC/Tnd mice by suppressing PI3K recruiting and activating activity	Higuchi et al. (2013)
	Mangiferin (**4**)	Reduced serum levels of IL-4, IL-5, IL-13, IL-17A and TNF-α	Guo et al. (2014), Zhao et al. (2017), Yun et al. (2019)
		Increased serum levels of IL-10 and TGF-β	Guo et al. (2014), Zhao et al. (2017), Yun et al. (2019)
		Reduced secretion of IL-1β, IL-6 and iNOS by RAW264.7 macrophages	Zhao et al. (2017)
		Decreased Th9 and Th17, and increased Treg subsets in the spleen	Yun et al. (2019)
		Restored imbalanced Th1/Th2 cell ratio	Guo et al. (2014)
		Reduced inflammatory cell infiltration and eosinophil population in the skin	Guo et al. (2014), Zhao et al. (2017), Yun et al. (2019)
		Inhibited phosphorylation of IκB and reduced levels of NF-κB2	Zhao et al. (2017)
Acne	α-mangostin (**2**)	Bacteriostatic and bacteriocidal activity on Gram-positive bacteria	Koh et al. (2013), Tatiya-Aphiradee et al. (2016), Sivaranjani et al. (2019)
		Antibacterial activity against *P. acnes* and *S. epidermidis*	Auranwiwat et al. (2014), Sivaranjani et al. (2017), Xu et al. (2018)
		Targeted and disrupted cellular membrane integrity, causing rapid loss of intracellular components	Koh et al. (2013)
		Inhibited mRNA expression of IL-1β, IL-6 and TNF-α in *P. acnes*-induced HaCaT cells	Xu et al. (2018)
		Inhibited activation of NF-κB and MAPK pathways by suppressing phosphorylation of IκB, p65, p38, ERK and JNK	Xu et al. (2018)
		Inhibited lipase activity of *P. acnes*	Xu et al. (2018)
	γ-mangostin (**3**)	Antibacterial activity against *P. acnes*	Xu et al. (2018)
		Inhibited mRNA expression of IL-1β, IL-6 and TNF-α in P. acnes-induced HaCaT cells	
		Inhibited activation of NF-κB and MAPK pathways by suppressing phosphorylation of IκB, p65, p38, ERK and JNK	
		Inhibited lipase activity of *P. acnes*	
	β-mangostin (**5**)	Antibacterial activity against *S. epidermidis*	Auranwiwat et al. (2014)
	Garcicowanone A (**6**)	Antibacterial activity against *S. epidermidis*	Auranwiwat et al. (2014)

78

TABLE 1 | (*Continued*) Xanthones and their mechanism of action for treatment of skin inflammatory diseases.

Disease	Xanthone	Mechanism of Action	References
Skin cancer and melanoma	α-mangostin (**2**)	Inhibited *in vitro* cell proliferation, adhesion and invasion of SK-MEL-28, B16-F10 and A375 cells	Wang et al. (2011), Beninati et al. (2014)
		Inhibited tumor incidence and hyperplasia in DMBA-TPA-induced mice	Wang et al. (2017)
		Increased caspase-3 activity and caused loss of mitochondrial membrane potential	Wang et al. (2011)
		Increased expression of Bax, Bad and caspase-3	Wang et al. (2017)
		Downregulation of Bcl-2 and Bal-xL	Wang et al. (2017)
		Induced cell differentiation and aggregation in B16-F10 cells	Beninati et al. (2014)
		Anti-metastatic effect by reducing MMP-1 and MMP-9 activity	Beninati et al. (2014), Im et al. (2017)
		Decreased phosphorylation of PI3K, Akt and TOR proteins	Wang et al. (2017), Xia and Sun (2018)
		Induced ROS generation	Xia and Sun (2018)
		Downregulated IL-1β, IL-4 and IL-18 in DMBA-TPA-induced skin tumorigenesis in mice	Im et al. (2017), Wang et al. (2017)
		Upregulated IL-10 in DMBA-TPA-induced skin tumorigenesis in mice	Wang et al. (2017)
		Chemoprevention by photoprotective and antioxidative activity	Im et al. (2017), Purnaningsih et al. (2018)
	γ-mangostin (**3**)	Inhibited *in vitro* cell proliferation of SK-MEL-28 cells	Wang et al. (2011)
		Induced apoptosis by causing the loss of mitochondrial membrane potential	
		Chemoprevention by photoprotective and antioxidative activity	Im et al. (2017), Purnaningsih et al. (2018)
	Mangiferin (**4**)	Anti-metastatic and anti-angiogenic effect by selectively inhibiting the expression of *VEGFR2*, *MMP-19* and *PGF* genes	Delgado-Hernández et al. (2019)
		Selectively inhibited NF-κB genes including *IL-6*, *TNF*, *IFN-γ* and *CCL2*	Delgado-Hernández et al. (2019)
		Increased activity of SOD in skin of UVB-irradiated SKH-1 mice	Petrova et al. (2011)
		Chemoprevention by photoprotective and antioxidative activity	Magcwebeba et al. (2016a), Magcwebeba et al. (2016b)
	β-mangostin (**5**)	Chemoprevention by photoprotective and antioxidative activity	Im et al. (2017), Purnaningsih et al. (2018)
	8-deoxygartanin (**7**)	Inhibited *in vitro* cell proliferation of SK-MEL-28 cells	Wang et al. (2011)
		Induced apoptosis by causing the loss of mitochondrial membrane potential	
	Gambogic acid (**8**)	Inhibited cell proliferation and viability in B16-F10 and A375 cells	Zhao et al. (2008), Xu et al. (2009)
		Decreased *in vivo* expression of Akt1 and Akt2	Liang et al. (2018)
		Induced apoptosis by increasing Bax/Bcl-2 ratio and activation of caspase-3	Xu et al. (2009)
		Modulated mitochondrial p66shc/ROS-p53/Bax signaling	Liang and Zhang (2016)
		Modulated miR-199a-3p/ZEB1 signaling	Liang et al. (2018)
		Anti-metastatic effect by downregulating α4 integrin and fibronectin adhesion	Zhao et al. (2008)
	Gambogenic acid (**9**)	Induced apoptosis via PI3K/Akt/mTOR signaling pathway	Cheng et al. (2014)
	33-hydroxyepigambogic acid (**10**)	Cytotoxic activity against SK-MEL-28 cells	Xu et al. (2015)
		Induced cell cycle arrest at S or G2/M phase	
		Induced apoptosis by increasing the activity of caspase-3/7	
	35-hydroxyepigambogic acid (**11**)	Cytotoxic activity against SK-MEL-28 cells	Xu et al. (2015)
		Induced cell cycle arrest at S or G2/M phase	
		Induced apoptosis by increasing the activity of caspase-3/7	
	Xanthone V$_1$ (**12**)	Induced cell cycle arrest at S phase	Kuete et al. (2011)
		Induced apoptosis by increasing activation of caspase-3/7	
	Norathyriol (**13**)	Inhibited skin carcinogenesis in SKH-1 hairless mice exposed to solar UV	Li et al. (2012)
		Induced cell cycle arrest at G2/M phase by increasing cyclin B1 and phosphorylated Cdk 1	
		Inhibited activation of MAPK and NF-κB cascades by competitively inhibiting ERK2 kinases	
	Gentiacaulein (**15**)	Chemoprevention by photoprotection and quenching of excited riboflavin	Hirakawa et al. (2005)
	Norswertianin (**16**)	Chemoprevention by photoprotection and quenching of excited riboflavin	Hirakawa et al. (2005)

(Continued on following page)

production of nerve growth factors (NGF) and nerve extension that relieved the itching.

Histamines, also known as imidazolethylamine, play an important role in cutaneous inflammation and contribute to the characteristic redness, wheal, flare and pruritis of AD (Buddenkotte et al., 2010). It affects the integrity of the skin barrier and modulates inflammatory immune responses via the activation of eosinophils, mast cells and basophils (Buddenkotte et al., 2010; Ohsawa and Hirasawa 2014). Furthermore, this allergic mediator is capable of activating Th2 cells, subsequently increasing the production of Th2 cytokines such as IL-4, IL-5, and IL-13 (Ohsawa and Hirasawa, 2014). While the pruritic role of histamines in AD is still being debated, administration of antihistamines did help to mitigate itching (Ohsawa and Hirasawa, 2014). A study on the anti-inflammatory activity of the 40% ethanol extract of mangosteen hull (*G. mangostana* L.) revealed more than 80% inhibition of histamine release from IgE-sensitized RBL-2H3 basophil cells, besides inhibiting the synthesis of prostaglandin E_2 (PGE2) at 300 μg/mL (Nakatani et al., 2002). The key compound contributing to the anti-inflammatory effect of the extract was suggested to be a xanthone named as α-mangostin (**2**). Meanwhile, **1** was revealed to be capable of reducing serum levels of histamine in 2,4-dinitrofluorobenzene (DNFB)-induced AD mice model with 0.001-1.000 mM in a dose-dependent manner (Aye et al., 2020). DNFB is a hapten which is topically applied to animal models to mimic the pathophysiology and skin inflammation of AD (Aye et al., 2020). Furthermore, **1** demonstrated significant reduction in skin lesions and hyperplasia in DNFB-induced mice at doses of 0.2, 2.0 and 20.0 mg/kg (Aye et al., 2020). *In vitro* experiments further highlighted the ability of **1** at 0.001-1.000 mM to suppress histamine and thymic stromal lymphopoietin (TSLP) released by HMC-1 mast cells that was stimulated by phorbol myristate acetate (PMA) and calcium ionophore A23187 (CI). The synergistic combination of PMA-CI was established as powerful tools to study accessory-independent activation of T cells (Heinze and Mohr, 1990).

α-Mangostin (**2**) was previously reported to be a selective and competitive inhibitor of histamine H1 receptors (Chairungsrilerd et al., 1996a; Chairungsrilerd et al., 1996b). The antihistamine effect of **2** via the inhibition of histamine release and antagonism of histamine H1 receptors disclosed the xanthone as a potential candidate to alleviate histamine-mediated effects in allergic reactions such as AD. Besides **2**, γ-mangostin (**3**) is another major xanthone found in mangosteen rind and hull extracts (Nakatani et al., 2002; Higuchi et al., 2013). As shown in **Figure 2**, both **2** and **3** are similar in structures and only differ by demethylation of 7-OH in **2**. An early histamine-induced contraction study on **3** showed that it lacked of histamine H1 receptor antagonism on the isolated rabbit aorta at 5 μM (Chairungsrilerd et al., 1996b). However, a later study on neuroblastoma cells by Sukma et al. (2011) contradicted the findings by Chairungsrilerd et al. (1996b). The authors suggested that the increase in mRNA expression of H1 receptors is compensatory against the antagonistic effect of **3** (Sukma et al., 2011). Further

TABLE 1 | (*Continued*) Xanthones and their mechanism of action for treatment of skin inflammatory diseases.

Disease	Xanthone	Mechanism of Action	References
Psoriasis	Mangiferin (**4**)	Cytoprotective effects on $H_2O_2^-$ stressed 3T3 fibroblast cells Reduced inflammatory infiltrates and MPO activity Inhibited *in vitro* keratinocyte proliferation of HaCaT cells	Pleguezuelos-Villa et al. (2019)
	Gambogic acid (**8**)	Inhibited activation of NF-κB by suppressing the TNF-α-induced translocation of p65 into nucleus Downregulation of CD3$^+$, IL-17 and IL-22 Decreased leukocyte recruitment and accumulation by downregulating ICAM-1, E-selectin, VEGFR-2 and p-VEGFR2	Wen et al. (2014)

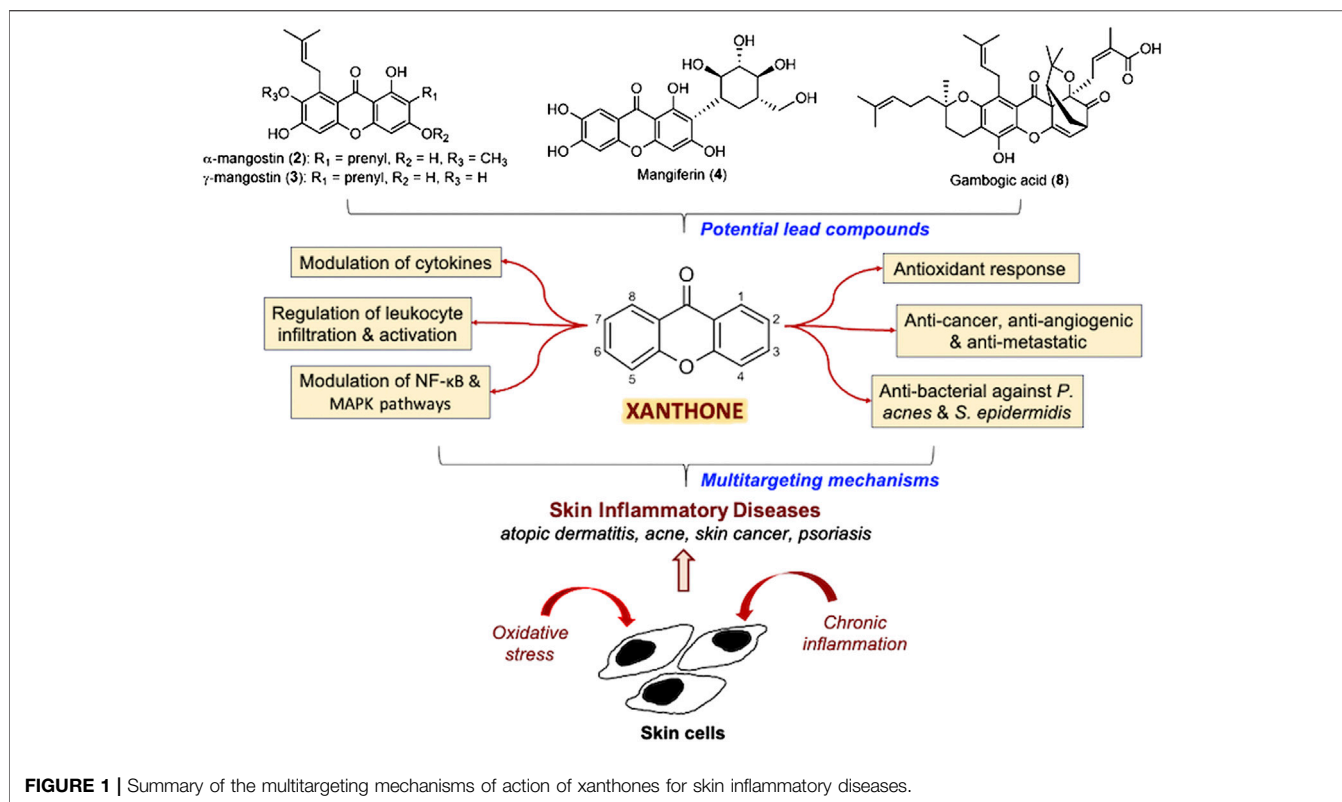*IL, interleukin; TNF-α, tumor necrosis factor α*

FIGURE 1 | Summary of the multitargeting mechanisms of action of xanthones for skin inflammatory diseases.
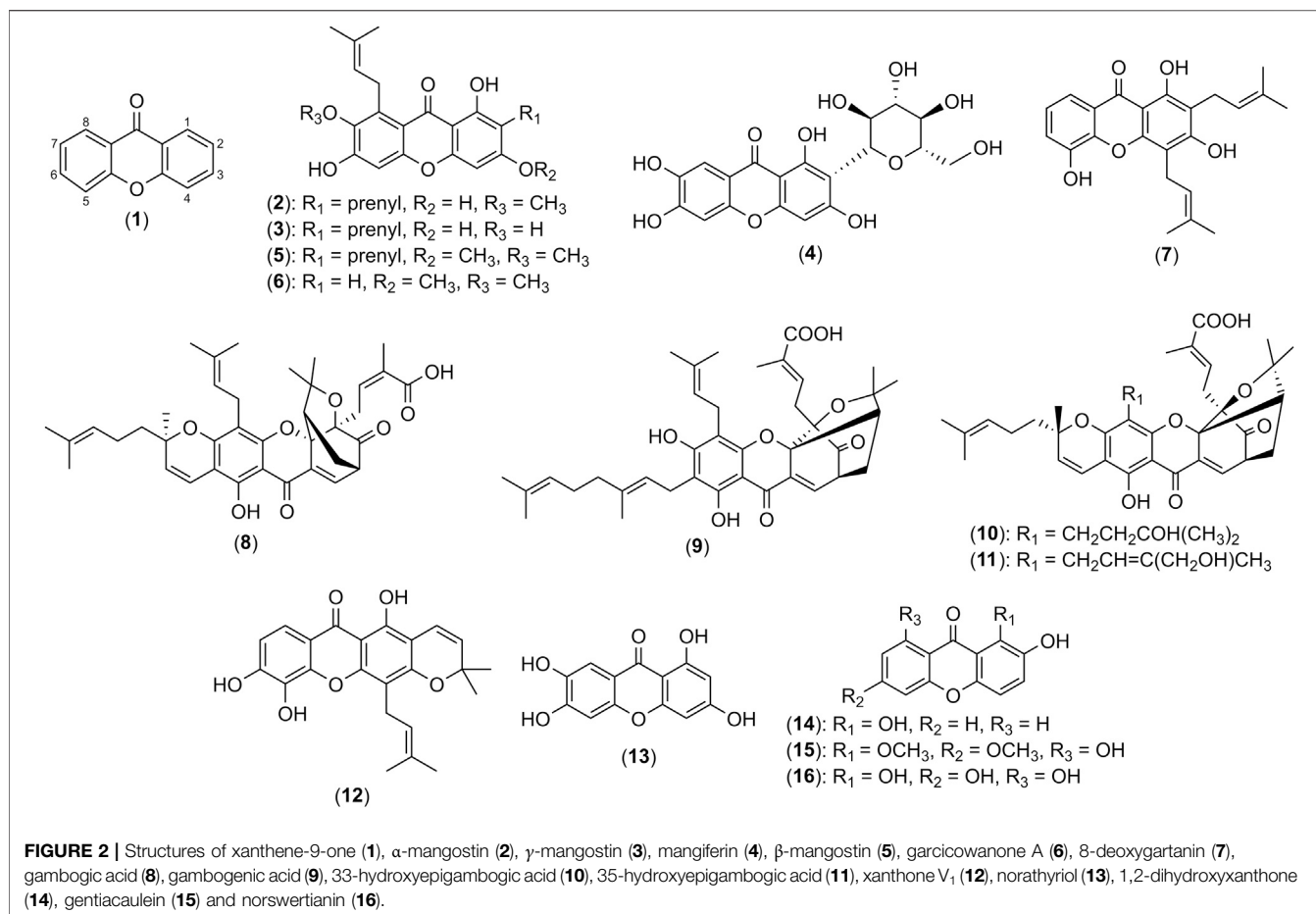
investigation on the structure-activity relationship of xanthone on histamine antagonism may be worthwhile.

Modulation of Cytokine Expression and IgE by Xanthones

Xanthones are involved in the modulation of immune inflammatory responses and the expression of cytokines and IgE. The pristine xanthone **1** was found to reduce the mRNA expression of immunomodulatory mediators and ILs responsible for recruiting immune cells to the site of skin inflammation in mice at doses of 0.2, 2.0 and 20.0 mg/kg (Aye et al., 2020). The mediators involved are IL-1β, IL-6, IL-8, thymus and activation-regulated chemokine (TARC) and macrophage derived chemokine (MDC) (Aye et al., 2020). Xanthone **1** also reduced the serum levels of IgE, as well as the population of mast cells in skin lesions at the same doses. Furthermore, **1** increased the survival rate of anaphylactic shock by 83.3%, further highlighting its immunomodulatory capabilities. It is worthwhile to note that **1** did not induce any cytotoxicity to HaCaT normal keratinocyte cells at 0.001-10.000 mM (Aye et al., 2020). Another study on the xanthone-rich mangosteen rind ethanol extract using AD mice models revealed the suppression of mRNA expression of various pro-inflammatory cytokines such as IL-4, interferon-γ (IFN-γ) and TSLP when treated with 250 mg/kg/day of the extract (Higuchi et al., 2013). TSLP was suggested to be the most crucial target of the extract against AD development. Besides that, the extract at the same dose suppressed the mRNA expression of Th2 chemokines MDC and eotaxin-2 involved in T cell-mediated inflammation and recruitment of

eosinophils, respectively (Watanabe et al., 2002; Higuchi et al., 2013). However, the expression of pro-inflammatory cytokines commonly associated with AD such as IL-4, IL-5 and IL-13 were not affected by treatment with the extract (Higuchi et al., 2013). Xanthone **2** was identified as the most abundant xanthone and main active compound of the mangosteen rind ethanol extract (Higuchi et al., 2013). The isolated **2** was further reported to inhibit the mRNA expression of TSLP and IFN-γ with IC_{50} values of 0.4 and 3.6 μM, respectively.

In contrast, mangiferin (**4**), a natural xanthone glucoside, was able to alleviate the imbalanced expression of cytokines in the serum of oxazolone-induced AD in C57BL/6 mice model with oral administration of 50 mg/kg/day (Zhao et al., 2017). Treatment with **4** restored the Th1/Th2 cytokine imbalance by reducing serum levels of pro-inflammatory cytokines including IL-4, IL-5, IL-13, IL-17A and TNF-α, while increasing the levels of anti-inflammatory cytokines IL-10 and transforming growth factor β (TGF-β) (Guo et al., 2014; Zhao et al., 2017; Yun et al., 2019). Besides that, 20 and 100 μM of **4** were shown to modulate cytokine expression of macrophages which play a crucial role in skin inflammation and reduce the levels of IL-1β, IL-6 and inducible nitric oxide synthase (iNOS) secreted by RAW264.7 cells (Zhao et al., 2017). Interestingly, **4** also directly affected the T cell population, particularly Th1, Th2, Th9, Th17 and Treg cells whereby imbalance of these subsets characterizes the impaired immune response in AD (Auriemma et al., 2013). Compound **4** can restore the aberrant Th1/Th2 cell ratio found in allergic inflammatory disorders while decreasing Th9 and Th17 proportions and increasing proportions of Treg cells in the spleen

FIGURE 2 | Structures of xanthene-9-one (**1**), α-mangostin (**2**), γ-mangostin (**3**), mangiferin (**4**), β-mangostin (**5**), garcicowanone A (**6**), 8-deoxygartanin (**7**), gambogic acid (**8**), gambogenic acid (**9**), 33-hydroxyepigambogic acid (**10**), 35-hydroxyepigambogic acid (**11**), xanthone V$_1$ (**12**), norathyriol (**13**), 1,2-dihydroxyxanthone (**14**), gentiacaulein (**15**) and norswertianin (**16**).

with oral administration of 50-200 mg/kg/day (Guo et al., 2014; Yun et al., 2019). The modulation of the Th1/Th2 cytokine and cell differentiation imbalance by **4** may involve the inhibition of STAT6 signaling pathway (Guo et al., 2014). Collectively, these anti-inflammatory mechanisms exhibited by **4** may contribute to the alleviation of skin inflammation in AD mice model (Zhao et al., 2017).

Besides that, **2** suppressed the IgE production induced by IL-4 and lipopolysaccharide (LPS)-stimulated splenic B cells with an IC$_{50}$ value of 2.5 μM whereas a xanthone of similar structure, **3** showed an IC$_{50}$ value of 1.6 μM (Higuchi et al., 2013). This finding was also previously described by Jang et al. (2012) where both **2** and **3** at the doses of 10 and 30 mg/kg/day were able to decrease the secretion of IgE in an airway inflammation model induced by ovalbumin, an allergen commonly used in immunological studies to imitate allergic reactions. Furthermore, the authors suggested the ability of **2** and **3** to inhibit allergen-IgE-induced mast cell activation while attenuating the production of IgE, therefore exhibiting anti-inflammatory effects through multiple mechanisms.

Other Anti-inflammatory Mechanisms of Xanthones

Besides mediating cytokine expression, xanthones were found to modulate the recruitment of eosinophils. Since eosinophils play a key role in allergic diseases, minimal recruitment of the cell

consequently reduces the associated inflammation (Guo et al., 2014). Mangosteen rind ethanol extracts that primarily contain **2** and **3** reduced the population of eosinophils in the skin of NC/Tnd mice at a dose of 250 mg/kg/day (Higuchi et al., 2013). The finding may be associated with the ability of **2** and **3** to suppress PI3K activity, a signal transduction pathway commonly involved in the recruitment and activation of eosinophils, at a dose of 30 mg/kg/day (Jang et al., 2012). Similarly, **4** was able to dose-dependently suppress eosinophilia with comparable effects with dexamethasone (1-dehydro-9α-fluoro-16α-methylhydrocortisone), a topical corticosteroid used in the treatment of AD (Kalz 1960; Guo et al., 2014; Yun et al., 2019). This finding was consolidated by histological examination of the skin of oxazolone-induced AD in C57BL/6 mice that revealed a decrease in inflammatory cell infiltration after oral administration of **4** at 50 mg/kg/day (Zhao et al., 2017).

The inflammatory NF-κB pathway has been associated with AD. This pathway mainly involves the MAPK/NF-κB cascade and NF-κB/caspase-1 axis which induce the expression of numerous pro-inflammatory cytokines such as TNF-α, IL-8 and IL-1β (Lee et al., 2015; Guo et al., 2019). Modulation of the NF-κB pathway appears to be a common anti-inflammatory mechanism exhibited by xanthones. Xanthone **1** significantly attenuated the phosphorylation of IκBα and NF-κB in HaCaT cells at 0.001 to 10.000 mM, demonstrating the inhibition of an allergic

inflammatory response (Aye et al., 2020). Besides that, **1** was also shown to regulate the MAPK and caspase-1 pathways in keratinocytes and mast cells (Aye et al., 2020). Its derivatives such as **2** was reported to inhibit the NF-κB pathway at 10 and 30 mg/kg/day in ovalbumin-induced airway inflammation in mice models, resulting in anti-inflammatory action (Jang et al., 2012). Compound **4** also suppressed the activation of the NF-κB pathway *in vivo* when oxazolone-induced dermatitis mice were treated with 50 mg/kg/day of the xanthone by reducing the level of NF-κB2 and inhibiting the phosphorylation of IκB. Thus, **4** was proposed to be a good lead compound for treating AD (Zhao et al., 2017). Similarly, xanthones **1** and **2** are potential lead compounds for treating AD as they exhibit anti-inflammatory effects.

Acne

Acne vulgaris, a cutaneous inflammatory disease of the pilosebaceous follicle is listed as the eighth most prevalent disease worldwide and is estimated to affect 9.38% of the global population (Heng and Chew, 2020). Commensal skin bacteria *Propionibacterium acnes* and *Staphylococcus epidermidis* are associated with the onset and development of inflammatory acne via production of neutrophil chemotactic factors as well as pro-inflammatory cytokines such as IL-1, IL-6, IL-8 and TNF-α (Chomnawang et al., 2005; Asasutjarit et al., 2013; Xu et al., 2018). Recruitment of immune cells subsequently induced the generation of ROS which contributes to the irritation of the follicular epithelium that often leads to skin damage and scarring (Chomnawang et al., 2007). These acne-causing bacteria are quickly gaining resistance to classic antibiotics, hence the search for natural antibacterial and anti-acne compounds is ongoing (Asasutjarit et al., 2013). Xanthones are compounds that can be potentially used in treating acne.

Anti-acne Activity of Xanthone-rich Extracts

Garcinia mangostana L. ethanol extracts and its primary xanthone **2** were proven to exhibit anti-acne effects (Chomnawang et al., 2007; Pan-In et al., 2015). Early studies reported that the xanthone-rich ethanol extract showed the strongest inhibitory effects with minimum inhibitory concentration (MIC) of 0.039 mg/mL on both *P. acnes* and *S. epidermidis* when compared to eighteen Thai medicinal plant extracts with MICs ranging from 0.625 to more than 5 mg/mL using disc diffusion and broth dilution methods (Chomnawang et al., 2005). The extracts were analyzed using bioautographic detection in thin layer chromatography, and silica gel column chromatography which identified the main components of the extract to be **2** and **3** (Chomnawang et al., 2005; Tatiya-Aphiradee et al., 2016). Another study demonstrated the anti-microbial effects of aqueous extracts of *G. mangostana* L. on both acne-causing bacteria using a similar disc diffusion assay, further supporting Chomnawang and colleagues' discoveries (Bhaskar et al., 2009). Later studies reported that the dichloromethane extract of mangosteen fruit rind (*G. mangostana* L.) obtained using Soxhlet extraction showed the strongest bacteriostatic and bactericidal activity against *P. acnes* and *S. epidermidis* with minimal bactericidal concentration (MBC) of 3.91 and

15.63 μg/mL, respectively (Pothitirat et al., 2010). Similarly, **2** was isolated and identified to be the key active compound in the rind extract. The concentration of **2** in the extract was significantly correlated to antibacterial activity against *P. acnes* and *S. epidermidis* (Pothitirat et al., 2010). Meanwhile, in a 3-week randomized, double-blinded and placebo-controlled study, mangosteen rind extract capsules were orally prescribed thrice daily to 94 patients with mild and moderate acne (Sutono 2013). The study reported a decrease of 63% and 35% in non-inflamed and inflamed acne lesions respectively, with no adverse effects (Sutono 2013). It was concluded that oral administration of the rind extract significantly decreased the severity of mild and moderate acne compared to a placebo.

Antibacterial Activity of Xanthones for Acne Treatment

Further investigations on isolated xanthone **2** from *G. mangostana* L. pericarp ethanol extract reveal its bacteriostatic (Tatiya-Aphiradee et al., 2016) and bactericidal effects (Koh et al., 2013) on Gram-positive bacteria using broth dilution and time-kill kinetics assays. Koh et al. (2013) identified the isoprenyl group attached at C-8 of **2** to be crucial in its antibacterial effect as it allowed the xanthone to associate with bacterial lipid alkyl chains and penetrate into the bacteria. Furthermore, a separate study highlighted that **2** mimics the chemical structure of *meta*-phenylene ethynylene, a membrane-targeting cationic antimicrobial peptide (Sivaranjani et al., 2017). Consequently, rapid penetration of the xanthone into the bacterium deranged the cytoplasmic membrane integrity, causing swift loss of intracellular components within 5-10 minutes at concentrations as low as 7.61 μM as proven in an ethidium bromide uptake assay, together with SYTOX green and calcein leakage assays (Koh et al., 2013). Thus, it was postulated that the primary target of **2** in antibacterial mechanisms of Gram-positive bacteria, such as *P. acnes* and *S. epidermidis* is the bacterial inner membrane. This discovery was also corroborated by Auranwiwat and colleagues (2014) that found the prenyl substituent at C-8 in α-mangostin (**2**), β-mangostin (**5**) and garcicowanone A (**6**), a novel xanthone identified in the unripe fruits of *Garcinia cowa* Roxb. ex Choisy, to confer to their remarkable antimicrobial activity against Gram-positive bacteria. Xanthones **2**, **5** and **6** are similar in structure, differing by prenyl substituents at C-2, and hydroxyl or methoxy groups at C-3 positions as shown in **Figure 2**. Moreover, **2**, **5** and **6** demonstrated significant activity against *S. epidermidis* with MIC values between 2-4 μg/mL, where **2** is the most potent among the xanthones (Auranwiwat et al., 2014). Hence, it was postulated that prenyl and hydroxyl groups attached at C-2 and C-3 positions, respectively of **2** were the important functional groups for antibacterial activity. Additionally, **2** significantly inhibited biofilm formation of *S. epidermidis*, a crucial virulence factor of the bacterium at concentrations as low as 12.18 μM (Sivaranjani et al., 2017). Another study reported the anti-*P. acnes* activity of **2** and **3** (Xu et al., 2018). Interestingly, while **2** and **3** displayed similar MIC values of 4.0 μM on *P. acnes* growth, **3** achieved a larger maximum inhibition zone of 20 mm diameter compared to 12 mm diameter by **2** in the disc diffusion method. This finding suggests **3** to be a more potent anti-bacterial agent

against *P. acnes* compared to **2** though there is still a lack of research study on the anti-acne activity of **3** (Xu et al., 2018). Thus far, no comparative studies have been done on the anti-acne activity of **2**, **3** and **5** which have closely related structures with prenyl substituent at C-2 and C-8.

Previous studies reported that **2** is effective against methicillin-resistant *Staphylococcus aureus* (MRSA) strains in an *in vivo* model by using superficial skin infection mouse model (Tatiya-Aphiradee et al., 2016). Topical treatment with 100 μL of 1.32% of **2** significantly reduced the number of MRSA colonies after 3 days to levels comparable to the control (Tatiya-Aphiradee et al., 2016). Interestingly, studies to date reported no resistance development towards **2** in MRSA with insignificant changes in the MIC of 3.80 μM when tested in a 20-passage multistep resistance selection study (Koh et al., 2013). Similarly, *S. epidermidis* did not develop resistance towards **2** despite continuous exposure at 0.38-3.05 μM across 19 passages in both planktonic and biofilm cells (Sivaranjani et al., 2017). A later study conducted by Sivaranjani et al. (2019) revealed molecular antibacterial mechanisms of **2** on *S. epidermidis* by downregulating the expression of genes responsible for bacterial cytoplasmic membrane integrity, cell division, teichoic acid and fatty acid biosynthesis, as well as DNA replication and repair systems. The target on multiple metabolic pathways by **2** minimized the risk of resistance development which greatly increased the potential of the xanthone as anti-bacterial agents for acne treatment.

Anti-inflammatory Mechanisms of Xanthones

Investigations on the potential of *G. mangostana* L. pericarps ethanol extracts for acne treatment revealed its anti-inflammatory effects by suppressing the production of pro-inflammatory cytokine, TNF-α. The pericarp extract suppressed the production of TNF-α by 94.59% at 50 μg/mL in an *in vitro* cytokine production assay in peripheral blood mononuclear cells stimulated with heat-killed *P. acnes*. (Chomnawang et al., 2007). The extract also possessed antioxidative activity by free radical scavenging mechanisms as shown in DPPH scavenging assay (IC_{50} = 6.13 μg/mL). The authors suggested the potential anti-inflammatory mechanisms was due to the attenuation of oxidative stress. A recent study revealed **2** and **3** to exhibit anti-acne activities via multiple anti-inflammatory mechanisms (Xu et al., 2018). The mRNA expression of pro-inflammatory cytokines IL-1β, IL-6 and TNF-α in *P. acnes*-stimulated HaCaT cells was significantly inhibited by **2** and **3** at concentration of 2-8 μM, as shown in a qRT-PCR analysis (Xu et al., 2018). Furthermore, **2** and **3** also suppressed the activation of NF-κB and MAPK pathways by decreasing the phosphorylation of pathway-related proteins IκB, p65, p38, ERK and JNK in a dose-dependent manner (Xu et al., 2018). Moreover, these xanthones completely inhibited the activity of lipases, a pro-inflammatory and virulence factor of *P. acnes*, at concentrations as low as 4 μM. Consequently, **2** and **3** halted the inflammatory response induced by *P. acnes* (Xu et al., 2018). Various anti-inflammatory mechanisms exhibited by these xanthones contribute to their biological potential as anti-acne agents.

Development of Xanthone Formulations for Acne Treatment

As a hydrophobic prenylated xanthone, flux of **2** through the stratum corneum is undesirable for acne treatment as it limits drug retention and absorption in hair follicles and sebaceous glands (Bhaskar et al., 2009; Pan-In et al., 2015). Numerous topical formulations were hence designed to maximize the retention of active compounds within the epidermis, ideally attaching to the bacterial surface and directly releasing the xanthone to the bacteria (Bhaskar et al., 2009; Pan-In et al., 2015). For example, an anti-acne gel formulation in aqueous based Carbopol-934 (1% w/w) containing aqueous extracts of *G. mangostana* L. and *Aloe vera* (L.) Burm.f. was developed for the topical therapy of mild acne (Bhaskar et al., 2009). The formulation had an ideal hydrophilic-lipophilic balance for epidermal permeation and showed larger maximum zone of inhibition of 1.7 cm against *P. acnes* compared to the marketed clindamycin phosphate gel of 1.1 cm when 1.5 g of the gels were tested using a zone of inhibition assay (Bhaskar et al., 2009). Interestingly, the formulated gel was claimed to be advantageous as there was no development of tolerance or resistance by the bacteria. Identification of **2** as the crucial phytochemical in these mangosteen extracts led to the anti-acne studies involving the film-forming solutions of a purified α-mangostin (**2**)-rich mangosteen fruit rind extract (*G. mangostana* L.) (Asasutjarit et al., 2013). The optimized formulations utilized 8% w/w of Klucel LF and Eudragit RL PO in a 5:1 ratio as film-forming polymers and 1% w/w triethyl citrate as a plasticizer. With 1 mg/g of **2** loaded, the films showed significant anti-bacterial activity against *P. acnes* in the disc diffusion method, producing a inhibition zone diameter of 23.5±1.5 mm. Similarly, nanoemulsions of **2** showed anti-bacterial activity against *P. acnes* while also being non-toxic to HaCaT cells at concentration of 0.2% w/w of **2** in nanoemulsions (Asasutjarit et al., 2019). In addition, other studies employed cellulose-based nanoparticles for delivery of **2** and showed insignificant skin irritation *in vivo* on human volunteers in a 4-week-randomized, double-blind, placebo-controlled, split-face study with topical application of 0.3, 0.6 and 1.2% w/w **2**-loaded nanoparticles (Pan-In et al., 2015). The non-irritancy may be associated with the non-cytotoxicity of **2** towards normal keratinocytes and fibroblasts. For example, an *in vitro* examination showed the formulation of the xanthone-rich extract to be non-toxic to normal skin fibroblast cells and was regarded to be non-irritant and safe for skin use (Asasutjarit et al., 2013). This finding was also supported by Xu et al. (2018) that showed **2** and **3**, the major xanthones of mangosteen pericarps (*G. mangostana* L.), to be non-toxic to HaCaT keratinocyte cells despite showing effective antibacterial activity against *P. acnes*. Moreover, these xanthones inhibited *P. acnes*-induced hyperproliferation of HaCaT cells at 2-8 μM in a dose-dependent manner. There was no significant effect on the proliferation of non-induced HaCaT cells at the same concentrations which excluded the non-specific cytotoxicity of the xanthones as a mechanism of action.

Skin Cancer & Melanoma

Skin cancer is classified as either melanoma or non-melanoma where melanoma is regarded as the most aggressive form of skin cancer (Delgado-Hernández et al., 2019). Non-melanoma skin cancer is also ranked as the fifth most common cancer worldwide by the World Health Organization (WHO) (Khazaei et al., 2019). Meanwhile, the incidence of melanoma is increasing at a faster rate than any other cancer with worrying mortality rates (Purnaningsih et al., 2018; Khazaei et al., 2019). UV radiation in particular has been strongly associated with skin carcinogenesis, causing oxidative damage, pro-inflammatory responses and DNA mutations (Hiraku et al., 2007; Kapadia et al., 2013; Im et al., 2017). Inflammation was described to be crucial in this skin disease as the inflammatory environment supports tumorigenesis and promotes invasion and metastasis (Pittayapruek et al., 2016; Wang et al., 2017). The extent of inflammation is commonly assessed by the detection of pro-inflammatory cytokines such as TNF-α, IL-1β, IL-4, IL-6 and IL-18 (Wang et al., 2017). ROS was also implicated in the initiation, promotion and progression stages of skin carcinogenesis by causing structural alterations in DNA and proteins (Bickers and Athar, 2006). Accumulation of ROS triggers inflammation and the production of matrix metalloproteinases (MMPs) that promote tumor invasion, metastasis and angiogenesis by mediating TGF-β and vascular endothelial growth factor (VEGF) (Pittayapruek et al., 2016; Im et al., 2017). The mechanism of action of xanthones commonly involve the apoptotic Bax and anti-apoptotic Bcl-2 proteins which are two of the most important markers of apoptosis (Wang et al., 2017). Activation of Bax and inhibition of Bcl-2 induce mitochondrial outer membrane permeabilization, apoptosome formation and activation of the executioner caspases-3 and -7 (Campbell and Tait, 2018). Consequently, the cell begins to dismantle, and apoptosis occurs. Other mechanisms of action include cell cycle arrest, and the disruption of MAPK and PI3K/Akt signaling pathways which modulate the growth and proliferation of skin cancer cells (Hambright et al., 2015).

There is a lack of a reliable therapy for this skin malignancy (Delgado-Hernández et al., 2019). Nowadays, multitargeted treatment is urgently required as singularly targeting a kinase or pathway is ineffective to cease malignant proliferation, angiogenesis, and metastasis. Therefore, xanthones with its multitargeting mechanisms are promising pharmacophore candidates for cancer treatment (Delgado-Hernández et al., 2019).

Cytotoxic Mechanisms of Xanthones

The cytotoxic mechanisms of various natural xanthones have been thoroughly investigated. The natural prenylated xanthone, **2** inhibited the *in vitro* proliferation, adhesion, and invasion of several melanoma cell lines, namely SK-MEL-28, B16-F10 and A375 in a dose-dependent manner (Wang et al., 2011; Beninati et al., 2014). This xanthone also induced apoptosis in melanoma SK-MEL-28 cells whereby it increased the proportion of early apoptotic cells from 1.7% (control) to 59.6% at concentration of 24.36 μM (Wang et al., 2011). The observed apoptotic effect was linked to the 25-fold increase in caspase-3 activity and loss of mitochondrial membrane potential ($\Delta\Psi_m$) (Wang et al., 2011). This finding was supported by Wang et al. (2017) who reported an increased expression of pro-apoptotic proteins, Bax, BAD and caspase-3 with concurrent downregulation of anti-apoptotic proteins, Bcl-2 and Bal-xL after *in vivo* treatment of mice with 5 and 20 mg/kg/day of **2**. Furthermore, the study by Wang and colleagues (2017) showed that **2** was active *in vivo* as it inhibited tumor incidence and hyperplasia induced by carcinogen 9,10-dimethylbenz[a]anthracene (DMBA) and skin tumor promoter 12-O-tetra-decanoylphorbol-13-acetate (TPA) in ICR mice following daily intraperitoneal administration of 5 mg/kg or 20 mg/kg of the xanthone (Wang et al., 2017). The inhibition of cancer cell proliferation was hypothesized to be linked to the suppression of the PI3K/Akt signaling pathway by decreasing the phosphorylation of PI3K, Akt and TOR proteins (Wang et al., 2017; Xia and Sun 2018). The use of 5 μM of **2** as an adjunct to kinase inhibitors of the PI3K pathway such as rapamycin was also shown to be effective in inhibiting the proliferation of SK-MEL-28 cells (Xia and Sun 2018). Interestingly, despite antioxidative and ROS scavenging activity of **2** (Pedraza-Chaverri et al., 2009; Pérez-Rojas et al., 2009), the induction of ROS generation in melanoma cells may be a cytotoxic mechanism exhibited by the synergistic combination of **2** and kinase inhibitors (Xia and Sun 2018). The structurally similar xanthone, **3** and another prenylated xanthone, 8-deoxygartanin (**7**) also exhibited similar inhibitory effects on SK-MEL-28 cell proliferation while increasing apoptotic rate and loss of $\Delta\Psi_m$ when tested at 2.5, 5.0 and 10.0 μg/mL (Wang et al., 2011). Among these three xanthones, **2** was the most potent as it exhibited the highest apoptotic and anti-proliferative activity against SK-MEL-28 cells.

The anti-metastatic effect of **2** was also reported where it induced cancer cell differentiation after treatment with 10 and 15 μM of the xanthone as evidenced by the intracellular increase of the differentiation marker PpIX in B16-F10 cells (Beninati et al., 2014). Furthermore, **2** reduced the plasticity of melanoma cells by up to 80% as seen in 3D-invasion assays (Beninati et al., 2014). The activity of MMP-9 which promotes angiogenesis and tumor invasion was reduced by 63% whereas cell aggregation increased by 3-fold when treated with 15 μM of **2**. Similarly, later studies conducted by Im et al. (2017) reported a reduction in MMP-1 and MMP-9 enzyme levels in the skin of UVB-irradiated mice after treatment with 100 mg/kg/day of **2**. These MMPs mediate the degradation of extracellular matrix which allow cancer cells to detach from the original tumor site and spread to other locations (Pittayapruek et al., 2016). Numerous mechanisms exhibited by **2** result in the anti-metastatic effect of xanthones.

Another xanthone with significant anti-cancer activity found in the resins of *Garcinia hanburyi* Hook.f. is gambogic acid (**8**) (Zhao et al., 2008). This caged xanthone exerted *in vitro* cytotoxicity on B16-F10 (IC_{50} = 1.71 μM) and A375 melanoma cells (IC_{50} = 2.50 μM), inhibiting the viability and cell proliferation in a dose-dependent manner (Zhao et al., 2008; Xu et al., 2009). Various mechanisms such as cell cycle arrest, release of cytochrome c from mitochondria as well as the induction of apoptosis and necrosis have been attributed to the cytotoxic effects of **8** (Zhao et al., 2008; Xu et al., 2009).

For instance, treatment with 3.96-11.89 μM of **8** increased the number of early apoptotic A375 cells by at least 7-fold after 36 hours where the observed finding was associated with an increase in Bax, a decrease in Bcl-2, and subsequent increased activation of caspase-3 (Xu et al., 2009). Interestingly, co-treatment of **8** with cisplatin, a standard chemotherapy drug significantly increased cisplatin-induced cytotoxicity on cisplatin-resistant A375 melanoma cells, suggesting the potential of xanthone in combination therapy (Liang et al., 2018). Later studies reported the involvement of other apoptotic pathways in melanoma cells such as mitochondrial p66^{shc}/ROS-p53/Bax (Liang and Zhang 2016) and a novel miR-199a-3p/ZEB1 signaling (Liang et al., 2018) in the anti-tumour mechanism of **8**. Besides that, **8** inhibited the migration and adhesion of B16-F10 melanoma cells to fibronectin via the downregulation of the cell adhesion molecule α_4 integrin with 0.01-0.60 μM of **8** in a dose-dependent manner (Zhao et al., 2008). Moreover, lung metastases were significantly suppressed with an inhibitory rate of 94.14% by 1.5 mg/kg of **8** in an artificial *in vivo* metastasis assay in mice (Zhao et al., 2008). The anti-proliferative effect on the *in vivo* tumors was also associated with the decreased expressions of Akt1 and Akt2, proteins of the PI3K/Akt pathway which regulate cell proliferation (Hambright et al., 2015; Liang et al., 2018).

Similarly, another caged xanthone, gambogenic acid (**9**) induced apoptosis in B16 cells via the PI3K/Akt/mTOR signaling pathway (Cheng et al., 2014). This xanthone decreased phosphorylated levels of PI3K, Akt and mTOR in a time-dependent manner, limiting the activation of this proliferation-inducing pathway (Cheng et al., 2014). Cytotoxicity evaluation of the compounds isolated from *G. hanburyi* Hook.f. revealed two derivatives of **8**, 33-hydroxyepigambogic acid (**10**) and 35-hydroxyepigambogic acid (**11**) to have potent activity against SK-MEL-28 cells with IC$_{50}$ values of 0.82 and 0.73 μM, respectively (Xu et al., 2015). Similar to **8**, these two caged xanthones instigated cell cycle arrest in S or G2/M phases and induced apoptosis through amplification of caspase-3/7 activity (Xu et al., 2015). Likewise, xanthone V$_1$ (**12**), a compound isolated from a Cameroonian medicinal plant, *Vismia laurentii* De Wild. caused cell cycle arrest at the S phase and apoptosis via caspase-3/7 activation (Kuete et al., 2011). Interestingly, previous studies highlighted the apparent selectivity of **2**, **3** and **7** for cancer cells with higher IC$_{50}$ values for CCD-1064Sk, a normal skin fibroblast cell line of 17.71, 28.58 and 27.21 μM, respectively when compared to SK-MEL-28 cells with IC$_{50}$ of 14.42, 8.95 and 10.07 μM, respectively (Wang et al., 2011). Other compounds such as **12** was also found to be less toxic to AML12 normal hepatic cells (IC$_{50}$ > 0.051 μM) compared to Colo-38 melanoma cells (IC$_{50}$ = 0.003 μM) (Kuete et al., 2011).

Meanwhile, the glycosylated xanthone **4** did not exhibit significant cytotoxic effects on B16-F10 melanoma and EA.hy926 endothelial cells (Delgado-Hernández et al., 2019). Instead, this xanthone dose-dependently suppressed basic fibroblast growth factor (bFGF)-induced cell motility, metastasis, and angiogenesis at 30-120 μM as shown in an *in vitro* wound healing model, as well as chorioallantoic membrane and endothelial fibrin gel sandwich assays. Furthermore, genes such as VEGFR2, MMP-19 and PGF that contribute to cancer angiogenesis and metastasis processes were selectively inhibited by **4**, consequently ceasing cell invasion and migration (Delgado-Hernández et al., 2019). Meanwhile, its metabolite norathyriol (**13**) was found to inhibit cell proliferation of JB6 P+ mouse skin epidermal cells at 10 and 25 μM by causing cell arrest at the G2/M phase (Li et al., 2012). Furthermore, *in vivo* experiments showed the inhibition of skin carcinogenesis in SKH-1 hairless mice upon topical application of 0.5 or 1.0 mg of **13** in 200 μL of acetone before solar UV irradiation. These findings suggested **13** that possesses chemopreventive effects (Li et al., 2012).

Anti-inflammatory Mechanisms of Xanthones

Anti-inflammatory activity is a potential mechanism to treat skin cancers (Rayburn et al., 2009). The anti-inflammatory activity of **2** on immune cells RAW264.7 and THP-1, as well as various cancer cell lines such as HepG2, Caco-2 and HT-29 have been previously investigated (Gutierrez-Orozco et al., 2013; Mohan et al., 2018). A recent study reported the ability of 5 and 20 mg/kg/day of **2** to suppress the inflammation caused by DMBA-TPA-induced skin tumorigenesis in mice by downregulating skin and systemic levels of pro-inflammatory cytokines IL-1β, IL-4 and IL-18, and upregulating anti-inflammatory cytokine IL-10 (Wang et al., 2017). This xanthone also downregulated the inflammatory IL-1β, IL-6 and TNF-α at a transcriptional level in UVB-exposed hairless mice with oral administration of 100 mg/kg/day of **2** (Im et al., 2017). Meanwhile, 240 μM of **4** was found to suppress lipid and calcium signaling as well as cancer-inflammation via selective inhibition of multiple pro-inflammatory NF-κB genes, including IL-6, TNF, IFN-γ and CCL2 genes (Delgado-Hernández et al., 2019). Furthermore, **4** was found to significantly increase the antioxidant superoxide dismutase (SOD) activity in the skin of UVB-irradiated SKH-1 mice upon topical application of 100 μL of 4 mg/mL of **4** in ethanol:acetone (1:1, v/v). However, the activity and expression of antioxidant enzymes catalase (CAT) and cyclooxygenase (COX)-2 were not affected (Petrova et al., 2011). Nevertheless, **4** was capable of inhibiting UVB-induced edema in SKH-1 mice by 73.33% with topical application of 4 mg/mL of the xanthone (Petrova et al., 2011).

Norathyriol (**13**) showed anti-inflammatory activity *in vitro* via competitive inhibition of MAPK1 at its ATP-binding site at 10 and 100 μM (Li et al., 2012). The xanthone moiety acts as an adenine mimic, forming hydrogen bonds and hydrophobic interactions in the hinge region of MAPK1. Consequently, MAPK cascades as well as the UVB-induced activation and activity of pro-inflammatory transcription factors AP-1 and NF-κB were halted (Li et al., 2012). A recent fascinating study by Silva and colleagues (2019) investigated the modulatory activity of synthetic 1,2-dihydroxyxanthone (**14**) on THP-1 macrophage activity and A375-C5 melanoma cells (Silva et al., 2019). Treatment with 50 and 100 μM of **14** suppressed the expression of IL-1β and IL-10 by THP-1 macrophages. However, the production of TNF-α was found to increase, suggesting favorability for melanoma treatment based on a previous meta-analysis that linked the development of skin cancers to the use of TNF inhibitors (Mariette et al., 2011; Silva et al., 2019). However, this finding highlighted the

contradictions in current literature on the role of TNF-α in skin cancer and melanoma whereby other studies did not support the benefits of upregulating the cytokine (Smith et al., 2014; Mercer et al., 2017). Further studies on the immune modulation and underlying mechanisms in skin cancers should hence be considered.

Photoprotective Activity of Xanthones for Chemoprevention

While anti-inflammatory action potentially attenuates cancer development and progression, the anti-inflammatory effect of xanthones may also protect normal tissues from cellular damage (Rayburn et al., 2009). Hence, xanthones were highlighted to be photoprotective and chemopreventive agents. A recent study by Purnaningsih et al. (2018) demonstrated the chemopreventive activity of topical applications of 100, 200 and 400 ppm of mangosteen skin (*G. mangostana* L.) ethanol extracts which predominantly consists of **2**, **3** and **5** using a DMBA-induced mice skin cancer model. The authors hypothesized that the observed chemopreventive effect of the extract came from the antioxidant activity and attenuation of ROS production by **2**, **3** and **5** (Purnaningsih et al., 2018). This hypothesis was also consolidated by previous studies that showed **2** isolated from *G. mangostana* L. pericarps to exhibit antioxidative activity by increasing the antioxidant activity of SOD and CAT, halting the generation of oxidative stress (Im et al., 2017).

Besides that, the ethanol and aqueous extracts of two species of honeybush, *Cyclopia intermedia* E.Mey. and *C. subternata* Vogel, which predominantly contain **4** were found to exert *in vitro* cytoprotective effects with negligible effects on the cell viability of normal HaCaT keratinocytes and CRL-7761 fibroblasts (Magcwebeba et al., 2016a). The lack of activity may be associated with poor solubility of the xanthone or influenced by the xanthone-flavanone ratio in the extract. Nonetheless, the study highlighted the high redox potential of **4** and its ability to counter oxidative stress via nuclear factor erythroid 2-related factor 2 (Nrf2) modulation which may additively or synergistically act with other polyphenolic constituents in the honeybush extract to protect against UVB irradiation (Magcwebeba et al., 2016a; Magcwebeba et al., 2016b). Another study highlighted the cytoprotective ability of **4** to inhibit UVB-induced edema and lipid peroxidation in an *in vivo* study (Petrova et al., 2011). Moreover, this xanthone reduced metal-induced oxidative stress and mitochondrial dysfunction via iron-chelating mechanisms in lipid membranes (Magcwebeba et al., 2016a). It was proposed that antioxidative compounds are able to relieve cancer-inflammatory damages as a result of oxidative stress and prolonged UV exposure (Kapadia et al., 2013). Therefore, **4** was suggested to be effective photoprotective agents with potential applications as sunscreens, cosmetics or skin care products to protect against UVB-induced oxidative stress and the resulting skin inflammation (Petrova et al., 2011; Magcwebeba et al., 2016b). Interestingly, two other xanthone derivatives gentiacaulein (**15**) and norswertianin (**16**) were identified to be chemopreventive agents that utilized a novel quenching mechanism instead of antioxidation or physical sunscreen effects (Hirakawa et al.,

2005). Using fluorescence spectroscopic techniques and *ab initio* molecular orbital calculations, the DNA photoprotective effects of these xanthones were found to involve the quenching of the triplet photoexcited state of riboflavin (Hirakawa et al., 2005).

Psoriasis

Psoriasis is a chronic T-cell mediated skin inflammatory disease characterized by thickened and scaly plaques and skin lesions (Wen et al., 2014; Owczarek and Jaworski, 2016). Pathogenesis of this disease involves interaction between genetic and environmental factors. Histological symptoms commonly involve keratinocyte hyperproliferation, abnormal keratinocyte differentiation and infiltration of inflammatory cells (Wen et al., 2014; Pleguezuelos-Villa et al., 2019). The production of inflammatory cytokines such as the Th17 signature IL-17A, IL-22, IL-23 and IFN-γ is a key characteristic of psoriasis (Schön, 2019). Dysregulated effector T-cell function and differentiation as well as the NF-κB pathway were also associated to the inflammatory response in psoriasis. Besides that, the influx of neutrophils in psoriatic lesions is a histological characteristic of psoriasis (Guérard et al., 2013). Neutrophils were reported to play a crucial role in psoriasis besides being a key source of the pro-inflammatory cytokines IL-8 and IL-17A (Biasi et al., 1998; Wang and Jin, 2020). Recently, the role of ROS and oxidative stress in psoriasis was demonstrated (Khmaladze et al., 2015; Pleguezuelos-Villa et al., 2019). The ROS generated by keratinocytes, fibroblasts and skin endothelial cells produces chemotactic effects towards neutrophils thereby increasing their infiltration into psoriasis lesions. The activated neutrophils generate a large amount of superoxide anion ($O_2^{\bullet-}$) in a process known as respiratory or oxidative burst (Khmaladze et al., 2015). The interaction between psoriatic keratinocytes and neutrophils was reported to increase the lifespan of this immune cell and augment its production of $O_2^{\bullet-}$, resulting in the oxidative stress (Guérard et al., 2013). Thus, it was suggested that the use of antioxidants are ideal to treat this inflammatory disorder (Pleguezuelos-Villa et al., 2019). As a rich source of natural antioxidants and anti-inflammatory compounds, all parts of the xanthone-rich *G. mangostana* L. plant were traditionally consumed and utilized for the treatment of psoriasis (Ibrahim et al., 2018a; Ibrahim et al., 2018b; Vemu et al., 2019).

Anti-inflammatory Mechanisms of Xanthones

Gambogic acid (**8**) was investigated for its potential use in psoriasis treatment. This compound can counter keratinocyte hyperproliferation, a hallmark of psoriasis as it was shown to be able to inhibit *in vitro* proliferation of normal HaCaT keratinocytes with an IC$_{50}$ of 0.09 μM (Wen et al., 2014). Treatment with **8** also suppressed the translocation of p65 into the nucleus upon TNF-α induction and therefore prevented the subsequent activation of NF-κB and its inflammatory response. In addition, *in vivo* studies on the K14-VEGF transgenic mice model which develops a psoriasis-like cutaneous inflammation showed a dose- and time-dependent inhibition of epidermal hyperplasia, inflammatory infiltrates and hyperkeratosis with topical application of a cream containing 0.10, 0.25 or 0.50% of **8**

(Wen et al., 2014). The anti-psoriatic effect of **8** was also observed in psoriasis-like guinea pig and mouse tail models with great improvement in morphological and histological examinations (Wen et al., 2014). In the same study, immunostaining of CD3^{+}, IL-17 and IL-22 revealed downregulation of these inflammatory factors upon treatment with creams containing 0.10, 0.25 or 0.50% of **8**. Downregulation of cell adhesion molecules such as ICAM-1 and E-selectin which play a crucial role in leukocyte recruitment and accumulation in the psoriatic skin was also observed after the treatment. Furthermore, the expression and phosphorylation of VEGF signaling transducer, VEGFR-2 was downregulated by **8**, consequently suppressing VEGF-mediated angiogenesis and production of adhesion molecules during inflammation (Wen et al., 2014).

Studies on naturally derived xanthones for psoriasis treatment are still limited. As an inflammatory disease, treatment of psoriasis commonly involves anti-TNF agents (Zhao et al., 2017). Inhibitory effects towards TNF-α are commonly observed as exhibiting anti-inflammatory effects of xanthones including **2** (Gutierrez-Orozco et al., 2013; Lee et al., 2013; Im et al., 2017; Herrera-Aco et al., 2019), **3** (Xu et al., 2018; Chiu et al., 2020), **5** (Lee et al., 2013) and **8** (Wang et al., 2018b) are considered potential compounds for psoriasis treatment. A complication commonly associated with psoriasis is inflammatory arthritis where pathogenesis involves similar immunological aberrations of inflammatory cytokines such as IL-17, IL-22, IL-23 and IFN-γ (Sankowski et al., 2013; Schön, 2019). The inflammatory effects of xanthones against arthritis have been previously studied, hence further investigations for the application of these natural xanthones for psoriasis may be considered. One of these xanthones, **2** exhibited anti-inflammatory effects in collagen-induced arthritis in the classic arthritis DBA/1J mice with oral administration of 10 and 40 mg/kg/day via the reduction of pro-inflammatory cytokines IL-6 and IL-33, as well as chemokines CXCL5, CXCL10, CXCL9 and CCL5 which are responsible for the recruitment of inflammatory cells (Herrera-Aco et al., 2019). Similarly, inhibitory effects on the secretion of TNF-α and IL-6 were observed in LPS-stimulated mice with ED_{50} of less than 100 mg/kg (Lee et al., 2013). Besides that, **3** was able to relieve inflammatory symptoms of osteoarthritis by inhibiting the expression of pro-inflammatory transcription factors STAT3 and NF-κB, as well as the expression of cytokines IL-6 and TNF-α (Chiu et al., 2020).

Recent studies proposed that xanthones such as **4** have great potential in treating psoriasis due to its ability to inhibit the pro-inflammatory effects of TNF-α (Zhao et al., 2017). For instance, the anti-inflammatory effects of **4** was highlighted to suppress TNF-α, IL-1β and IL-6 expressions in collagen-induced inflammatory arthritis DBA/1J mice by attenuating the activation of the inflammatory NF-κB and MAPK pathways after oral administration of 100 and 400 mg/kg/day of the xanthone (Tsubaki et al., 2015; Delgado-Hernández et al., 2019). However, the applications of xanthones are usually limited by their low bioavailability (Pleguezuelos-Villa et al., 2019). Thus, a recent study developed biocompatible glycethosome vesicles to stably incorporate **4** and deliver it to the epidermis besides permitting drug accumulation in the skin. Since oxidative stress is involved in psoriasis pathogenesis, the antioxidant effects of glycethosome vesicles containing 2, 4, 6, and 8 mg/mL of **4** was investigated *in vitro* using H_2O_2-stressed 3T3 fibroblast cells and the results showed virtually 100% cytoprotective effects on the cells (Pleguezuelos-Villa et al., 2019). Furthermore, in TPA-induced mice models, topical application of the **4**-loaded vesicles reduced inflammatory infiltrates, myeloperoxidase (MPO) activity, edema as well as abnormal epidermal alterations (Pleguezuelos-Villa et al., 2019).

MPO levels are considered as a marker of neutrophil activation and oxidative tissue injury (Ibrahim et al., 2018b). Tovophyllin A (**17**), a xanthone isolated from *G. mangostana* L. significantly reduced the hepatic levels of MPO in mice induced with acetaminophen after pre-treated with 50 and 100 mg/kg/day of the xanthone. The effect was linked to the suppression of neutrophil infiltration into the liver (Ibrahim et al., 2018b). Similarly, **2** was reported to inhibit carrageenan-induced inflammation in ICR mice with a reduction of neutrophil infiltration of 82% upon an administration of 25 mg/kg (Mohan et al., 2018). The decrease in the levels of TNF-α and IL-1β in the peritoneal fluids of the mice was simultaneously observed following treatment with **2** (Mohan et al., 2018). Meanwhile, **13** was reported to inhibit the generation of $O_2^{\bullet-}$ and oxygen consumption induced by formylmethionyl-leucyl-phenylalanine (fMLP) and dihydrocytochalasin B (CB) in rat neutrophils via the concentration-dependent inhibition of phospholipase C (PLC) pathway and NADPH oxidase activity (Hsu et al., 1997). Moreover, other xanthones isolated from the twigs of *Hypericum oblongifolium* Wall. include hypericorin A (**18**), hypericorin B (**19**), kielcorin (**20**), 3,4,5-trihydroxyxanthone (**21**) and 1,3,7-trihydroxyxanthone (**22**) possessed significant inhibition on the production of $O_2^{\bullet-}$ respiratory burst of neutrophils with IC_{50} values of 816.23, 985.20, 965.21, 907.20 and 975.20 μM, respectively. The chemical structures of **17-22** are shown in **Figure 3**. It was postulated that the potent activity of these xanthones is due to the presence of 1,4-dioxane ring and hydroxyl groups that promote their absorptions into the immune cells (Ali et al., 2011). The capability of these xanthones to decrease neutrophil influx and activity in the areas of inflammation suggested them as suitable drug candidates for psoriasis treatment (Ali et al., 2011).

PROSPECTS FOR FUTURE STUDIES AND APPLICATIONS OF XANTHONES

The immune response is a complex system with crosstalk between many pathways where the anti-inflammatory activity of xanthones have been revealed to involve a variety of mechanisms. Several targets of xanthones and their signaling pathways such as peroxisome proliferator-activated receptors (PPARs), Nrf2 and prostaglandins have been extensively linked to skin inflammatory diseases. This section focuses on the xanthones that were previously reported to modulate the activity or expression of these molecular targets and their relation to skin inflammatory diseases.
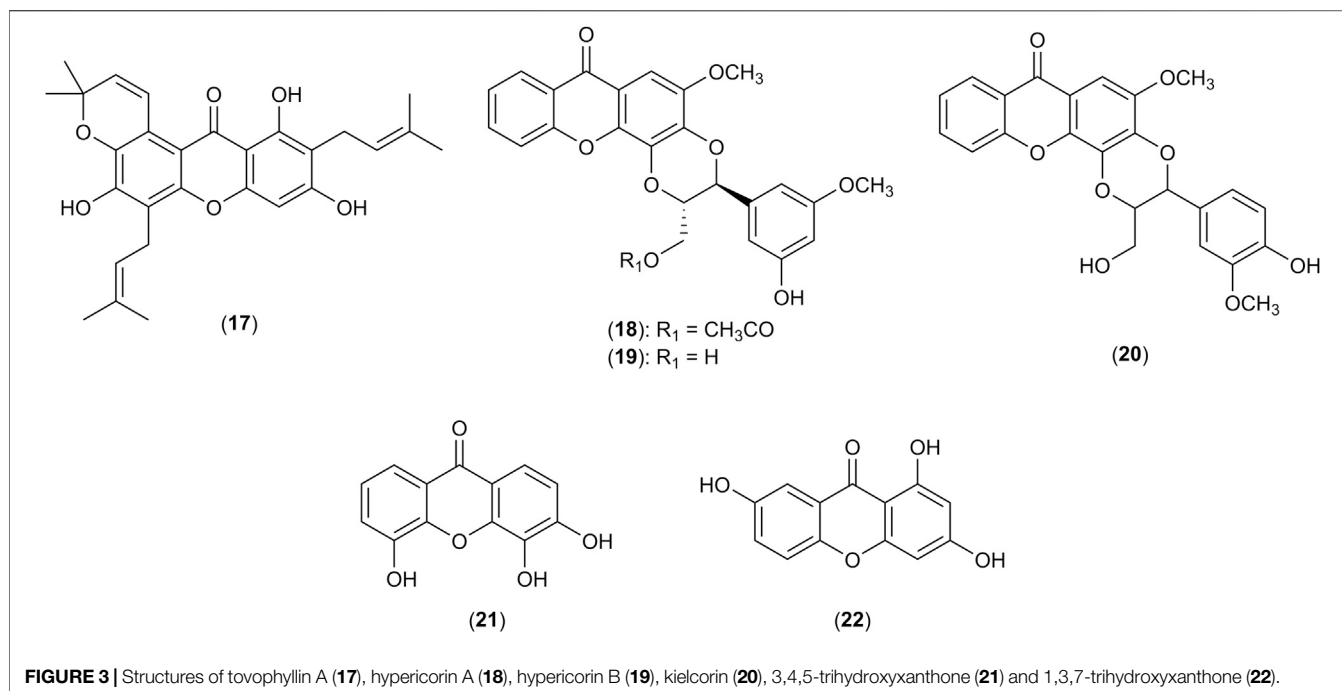
FIGURE 3 | Structures of tovophyllin A (**17**), hypericorin A (**18**), hypericorin B (**19**), kielcorin (**20**), 3,4,5-trihydroxyxanthone (**21**) and 1,3,7-trihydroxyxanthone (**22**).

Peroxisome Proliferator-Activated Receptors as a Target of Xanthones

PPARs and its α, β and γ isoforms have been previously associated with keratinocyte proliferation, differentiation and inflammation (Kim et al., 2006; Sertznig et al., 2008). Downregulation or inactivation of PPAR isoforms disrupts epithelial homeostasis and causes inflammation (Dubrac and Schmuth, 2011). The role of PPARs for skin inflammatory diseases such as psoriasis, skin cancer and acne have been previously reviewed (Sertznig et al., 2008; Sertznig and Reichrath, 2011). Activation of the PPARβ isoform which is also known as PPARδ was reported to selectively initiate terminal differentiation of keratinocytes while simultaneously inhibiting their uncontrolled proliferation (Kim et al., 2006). Additionally, PPARα plays a role in regulating skin inflammation in diseases such as AD and psoriasis by modulating cytokine expression, T cell proliferation, as well as the maturation and migration of Langerhans cells (Dubrac and Schmuth, 2011). Crosstalk with MAPK and NF-κB inflammatory pathways also occurs whereby the activation of these inflammatory pathways results in the inhibition of PPARγ activity (Bumrungpert et al., 2009). Conversely, PPARγ activation antagonizes and inhibits the resulting inflammatory response of NF-κB and AP-1 (Bumrungpert et al., 2010; Mao et al., 2019). Thus, PPAR isoforms were suggested to be a suitable molecular target to treat skin diseases with aberrated cell proliferation such as psoriasis and skin cancers (Kim et al., 2006; Sertznig et al., 2008; Ramot et al., 2015).

Xanthone derivatives such as **2** were found to upregulate PPARγ expression in the preadipocytes in rat retroperitoneal tissue of insulin-resistant mice models following treatment with 5, 10 and 20 mg/kg of the xanthone (Ratwita et al., 2018).

Similarly, **3** was shown to act as an agonist of PPARα and PPARδ using a luciferase reporter assay, approximately doubling the luciferase activity in Cos-1 kidney fibroblasts at 2.5 μM (Matsuura et al., 2013). Furthermore, both **2** and **3** when evaluated at 3, 10 and 30 μM restored the mRNA expression of PPARγ that was suppressed by LPS in macrophages (Bumrungpert et al., 2009; Bumrungpert et al., 2010). The restoration of PPARγ expression consequently alleviated inflammation by downregulating the expression of inflammatory cytokines TNF-α, IL-1β and IL-6 (Bumrungpert et al., 2010). Meanwhile, **4** at doses of 10 and 20 mg/kg exhibited cytoprotective effects against oxidative injury in gastric mucosal ischemia/reperfusion mice model via the upregulation of PPARγ expression and concurrent downregulation of NF-κB signaling (Mahmoud-Awny et al., 2015). This anti-inflammatory mechanism exhibited by **4** was further linked to the inhibition of IL-1β, E-selectin and neutrophil infiltration (Mahmoud-Awny et al., 2015). Interestingly, **4** showed no effect on PPAR transactivation whereas its metabolite, **13** successfully inhibited the transactivation of PPARγ, PPARα and PPARβ isoforms in Cos-7 kidney fibroblasts with IC$_{50}$ values of 153.3, 92.8 and 102.4 μM, respectively (Wilkinson et al., 2008). The difference in terms of the ability to transactivate the PPAR isoforms shown by **4** and **13** highlighted the importance of metabolism for the bioactivities of xanthones.

Nuclear Factor Erythroid 2-Related Factor 2 as a Target of Xanthones

Nrf2 is a transcription factor commonly recognized as the master regulator of cytoprotection and antioxidant defense signaling pathways. This transcription factor is generally activated in

response to ROS production and oxidative stress, inducing the downstream expression of antioxidative and phase II detoxification enzymes within the antioxidant response elements (ARE) such as heme oxygenase-1 (HO-1), NAD(P)H quinone oxidoreductase 1 (NQO1), glutathione *S*-transferase, CAT and SOD (Wang et al., 2018a; Helou et al., 2019). The role of oxidative stress and Nrf2 has been extensively implicated with the pathogenesis of skin inflammation and carcinogenesis (Bickers and Athar 2006; Helou et al., 2019; Hennig et al., 2020). Early studies by Braun et al. (2002) identified Nrf2 to be crucial in modulating inflammation in wound healing where persistent and prolonged inflammation associated with IL-1β, IL-6 and TNF-α was observed in Nrf2-knockout mice. Other studies highlighted the anti-inflammatory role of Nrf2 signaling in reducing the levels of IL-1β and IL-6 to alleviate skin inflammation (Saw et al., 2010) besides suppressing the activation of inflammatory NF-κB and NLRP3 pathways (Bulugonda et al., 2017; Helou et al., 2019; Hennig et al., 2020). The Nrf2 signaling pathway was also associated with chemopreventive effects by exerting photoprotection against UVB-induced skin carcinogenesis besides protecting against inflammatory damage on the extracellular matrix (Saw et al., 2010; Saw et al., 2014). Hence, Nrf2 pathway and its central roles in antioxidant defense and anti-inflammation are potential targets in the treatment of various skin inflammatory diseases.

In recent years, the modulatory roles of Nrf2 signaling by xanthones were reported. For example, **4** was reported to activate Nrf2/ARE pathway in response to oxidative stress, inflammation and DNA damage in neurons (Liu et al., 2016), liver (Pan et al., 2016), gastric ulcer models (Mahmoud-Awny et al., 2015) as well as hematopoietic cells (Zhang et al., 2015). Moreover, anti-inflammatory mechanisms of **4** in macrophages also involved the inactivation of NLRP3 inflammasome complex (Bulugonda et al., 2017; Helou et al., 2019). Similarly, **17**, a xanthone isolated from *G. mangostana* L. activated Nrf2 and protected against acetaminophen-induced oxidative stress injury in liver mice models when given 50 and 100 mg/kg/day (Ibrahim et al., 2018b). Other xanthones such as **2** and **3** were also shown to exert antioxidant effects via Nrf2 activation in retinal (Fang et al., 2016) and liver cells (Wang et al., 2018a), respectively.

However, it is also important to understand the possible double-edged effects of Nrf2 activation. In cancer cells, the Nrf2 pathway is upregulated in response to the high ROS production from the increased metabolism of cells (Hambright et al., 2015). Activation of Nrf2 results in cytoprotective effects and prolongs cancer cell survival that in turn antagonizes chemotherapeutic action (Yanaka 2018). Moreover, the constitutive and increased expression of Nrf2 was linked to poor clinical prognosis as it enhances cancer proliferation, angiogenesis, chemoresistance, and radioresistance (Wu et al., 2019). For example, the mRNA and protein expression of Nrf2 in B16-F10 melanoma cells was increased after an exposure to ionizing radiation (Gao et al., 2018). Subsequent knockdown of Nrf2 using small interfering RNAs (siRNAs) coupled with ionizing radiation reduced the migration and invasion of B16-F10 melanoma cells while increasing cellular apoptosis via caspase-3 activity (Gao et al., 2018). Hence, the incorporation of Nrf2 inhibitors in cancer therapy has recently received increasing

attention, as reported by Panieri and Saso (2019). In other words, even though Nrf2 pathway is a potential target for skin inflammatory diseases, researchers should be wary on the negative implications in malignancies because an activation of Nrf2 may be beneficial in cytoprotection and chemoprevention whereas the inhibition of Nrf2 may be a valuable strategy in targeting skin malignancies.

Prostaglandin as a Target of Xanthones

Prostaglandins, also known as eicosanoids, are powerful lipids that modulate immune responses and inflammation (Bull and Dowd, 1993). Several forms of prostaglandins such as prostaglandin E_2 (PGE$_2$) (Bull and Dowd, 1993; Kabashima et al., 2007) and prostaglandin D_2 (PGD$_2$) (Satoh et al., 2006) have been associated with skin inflammation. The enzyme prostaglandin H synthase, which is involved in the synthesis of eicosanoids, generates hydroxyl-endoperoxides that contributes to the co-oxidation of various substrates and the resulting cutaneous inflammation (Bickers and Athar, 2006). Early studies showed the mediatory role of prostaglandins in generating cutaneous inflammation upon UV exposure (Bull and Dowd, 1993). Release of PGE$_2$ after UV irradiation subsequently induced histamine secretion from mast cells. Later studies showed the crucial involvement of PGE$_2$-EP2/EP4 signaling that resulted in UV-induced acute skin inflammation (Kabashima et al., 2007). This was later supported by Lee et al. (2019) that elucidated the role of PGE$_2$-EP2/EP4 signaling in driving inflammation by Th17 cells in IL-23-induced psoriasis mouse models. The underlying involvement of prostaglandins in skin inflammation thus makes them attractive targets for the treatment of inflammatory diseases.

Xanthones were reported to exhibit anti-inflammatory effects by inhibiting the synthesis and release of prostaglandins, as well as downregulating the activity of COX enzymes. For instance, **3** is capable of competitively inhibiting the activities of COX-1 and COX-2 in microsomes of C6 rat glioma cells which consequently prevented the conversion of arachidonic acid to PGE$_2$ with an IC$_{50}$ of 17 μM (Nakatani et al., 2002). Subsequent studies reported that **3** suppressed LPS-induced expression of COX-2 at protein and mRNA levels in C6 cells with an IC$_{50}$ of 10 μM while COX-1 expression was not affected (Nakatani et al., 2004). Furthermore, **3** halted the release of PGE$_2$ induced by Ca^{2+} ionophores in C6 rat glioma cells in a concentration-dependent manner (IC$_{50}$ = 5 μM) (Nakatani et al., 2002). The antioxidant formulation VIMANG® used in Cuba is an aqueous extract of *Mangifera indica* L. which predominantly consists of **4**. The formulation was shown to be capable of inhibiting PGE$_2$ release in stimulated RAW264.7 macrophages with IC$_{50}$ of 64.1 μg/mL (Garrido et al., 2004). Xanthone **4** was isolated and reported to potently inhibit PGE$_2$ biosynthesis in RAW264.7 macrophages by 84.3% when treated with 0.024 μM of the compound. In addition, **4** was able to suppress COX-2 expression and production of PGE$_2$ in the rat brain when given oral gavages of 30 and 60 mg/kg/day, thereby attenuating inflammation and subsequent oxidative damage (Márquez et al., 2012). Similarly, **13** exerted inhibitory effects on the activities of COX-1, COX-2 as well as lipoxygenases-5 and -12, besides inhibiting the formation of PGD$_2$ in neutrophils with

IC_{50} values of 16.2, 19.6, 1.8 and 1.2 μM, respectively (Hsu et al., 2004). Thus, **13** was proposed to be a potential therapeutic agent to treat inflammatory diseases due to its multitargeting anti-inflammatory mechanisms.

Potential Applications of Xanthones for Wound Healing

The application of mangiferin (**4**) in skin wound healing showcased the anti-inflammatory and cytoprotective effects of the xanthone. Recently, 10, 20 and 40 μM of **4** was loaded in hydrogels (Mao et al., 2018) and liposomes (Mao et al., 2019) to enhance random skin flap regeneration which is commonly disrupted by oxidative stress and inflammation-induced apoptosis. Development of delivery systems for **4** solved the issue of hydrophobicity of xanthone which caused aggregation and poor dispersibility of the compound (Mao et al., 2018). This xanthone was found to modulate apoptosis via the Bax/Bcl-2/caspase-3 pathway, exhibiting protective effects by upregulating the Bcl-2/Bax ratio and reducing cleaved caspase-3 expression (Mao et al., 2018). Studies also showed that liposomes loaded with 10, 20 and 40 μM of **4** suppressed the expression and activation of NF-κB while concurrently increasing PPARγ mRNA and protein levels, consequently protecting against inflammation (Mao et al., 2019). Similarly, **4**-hydrogel dose-dependently decreased levels of CD68 and average macrophage density, hence relieving mild local inflammation in a random skin flap animal model (Mao et al., 2018). The observation was supplemented by *in vivo* studies which revealed a decreased necrosis rate and inflammation in a random patterned skin flap rat model, further highlighting the potential wound healing capabilities of **4** (Mao et al., 2019). Besides that, **4** was reported to dose-dependently affect cell proliferation and angiogenesis with an increase of protein expressions of VEGF and bFGF when tested with HUVEC cells (Mao et al., 2018; Mao et al., 2019). However, the observation contradicted the anti-angiogenic effect of **4** on B16-F10 melanoma cells as discussed earlier. The discrepancy may be linked to cell-specific effects which suggests **4** to be a highly versatile compound for numerous potential applications in skin disorders.

Perspectives for Xanthone in Skin Inflammatory Diseases Research

The ideal therapeutic approach, whether single-targeting or multitargeting, is still being debated within the scientific community. Numerous publications to date discuss the shifting paradigm in drug development (Talevi, 2015; Ramsay et al., 2018). The "one drug, one target" strategy is traditionally associated with high selectivity and hence lower risks of off-target effects (Ramsay et al., 2018). This concept has been the basis of drug development for decades and resulted in immeasurable success for the pharmaceutical industry. Nonetheless, the efficacy of single-targeting drugs may be limited against complex and multifactorial diseases due to compensatory mechanisms or overlapping biological functions in immune pathophysiology (Makhoba et al., 2020). Thus, the concept of polypharmacology which aims to develop single drugs that

recognize multiple molecular targets emerged rapidly as a popular strategy in drug design and development (Bolognesi, 2013; Makhoba et al., 2020). Moreover, 21% of new drugs approved by the Food and Drug Administration (FDA) between 2015 to 2017 were multitarget drugs (Ramsay et al., 2018).

In relation to skin inflammatory diseases, multitargeting mechanisms of action may be advantageous for diseases such as acne and skin malignancies due to the development of drug resistance. For instance, single-targeting mechanisms are ineffective in cancer therapeutics to counter cancer proliferation and metastasis (Delgado-Hernández et al., 2019). However, it must be acknowledged that with an increase in the number of targets, the risk of off-target effects simultaneously increases. The advantages and disadvantages of single targeting versus multitargeting drugs in the context of skin inflammatory diseases have yet to fully addressed. However, the complexity and overlapping immune responses relating to skin inflammatory diseases implied that multitargeting compounds such as xanthones may have good potential in the treatment of these diseases.

Nevertheless, despite the advancing research of xanthones for skin inflammatory diseases, the molecular mechanisms of action are still not completely elucidated. Furthermore, numerous studies do not move past experiments using *in vivo* mice models. Minimal data on the pharmacokinetic and pharmacodynamic properties of xanthones including their bioavailability and safety profile thus limit the progression of xanthones through the drug development process (Ng and Chua, 2019). In addition, the issue of bioavailability has also driven the researchers to develop drug carriers or formulations to improve xanthone delivery to the target site (Asasutjarit et al., 2013; Pan-In et al., 2015; Mao et al., 2018; Pleguezuelos-Villa et al., 2019). These studies are nonetheless still limited and have great rooms to be researched on, thus further studies are recommended to fill these gaps.

CONCLUSION

Xanthones possess a wide range of biological properties such as antioxidant, anti-inflammatory and chemotherapeutic effects that are effective in treating various skin diseases such as acne, atopic dermatitis, psoriasis, and skin cancer. However, the modulatory effects of xanthones on other mediators of inflammation such as PPARs, Nrf2 and prostaglandins have yet to be thoroughly explored in skin inflammatory diseases despite publications highlighting these mediators to be potential molecular targets. As privileged structures and versatile scaffolds, xanthones such as α-mangostin (**2**), γ-mangostin (**3**), mangiferin (**4**) and gambogic acid (**8**) are potential lead compounds to be further developed into pharmaceutical agents for skin inflammatory diseases. Prospective applications of xanthones are vast with synthetic opportunities remaining uncharted. Further studies on the structure-activity relationships, molecular mechanisms, and applications of xanthones for the treatment of skin inflammatory diseases are recommended.

AUTHOR CONTRIBUTIONS

NG, ST, YL, and SM contributed to the idea and drafted the manuscript. All authors contributed to the article and approved the submitted version.

REFERENCES

Aizat, W. M., Jamil, I. N., Ahmad-Hashim, F. H., and Noor, N. M. (2019). Recent updates on metabolite composition and medicinal benefits of mangosteen plant. *PeerJ* 7, e6324. doi:10.7717/peerj.6324

Ali, M., Arfan, M., Ahmad, M., Singh, K., Anis, I., Ahmad, H., et al. (2011). Anti-inflammatory xanthones from the twigs of *Hypericum oblongifolium* wall. *Planta Med.* 77 (18), 2013–2018. doi:10.1055/s-0031-1280114

Alperth, F., Mitić, B., Mayer, S., Maleš, Ž., Kunert, O., Hruševar, D., et al. (2018). Metabolic profiling of rhizomes of native populations of the strictly endemic *Croatian* species *Iris adriatica*. *Plant Biosys.* 153 (2), 317–324. doi:10.1080/11263504.2018.1478906

Asasutjarit, R., Larpmahawong, P., Fuongfuchat, A., Sareedenchai, V., and Veeranondha, S. (2013). Physicochemical properties and anti-*Propionibacterium acnes* activity of film-forming solutions containing alpha-mangostin-rich extract. *AAPS PharmSciTech* 15 (2), 306–316. doi:10.1208/s12249-013-0057-8

Asasutjarit, R., Meesomboon, T., Adulheem, P., Kittiwisut, S., Sookdee, P., Samosornsuk, W., et al. (2019). Physicochemical properties of alpha-mangostin loaded nanomeulsions prepared by ultrasonication technique. *Heliyon* 5 (9), e02465. doi:10.1016/j.heliyon.2019.e02465

Auranwiwat, C., Trisuwan, K., Saiai, A., Pyne, S. G., and Ritthiwigrom, T. (2014). Antibacterial tetraoxygenated xanthones from the immature fruits of *Garcinia cowa*. *Fitoterapia* 98, 179–183. doi:10.1016/j.fitote.2014.08.003

Auriemma, M., Vianale, G., Amerio, P., and Reale, M. (2013). Cytokines and T cells in atopic dermatitis. *Eur. Cytokine Netw.* 24 (1), 37–44. doi:10.1684/ecn.2013.0333

Aye, A., Song, Y. J., Jeon, Y. D., and Jin, J. S. (2020). Xanthone suppresses allergic contact dermatitis *in vitro* and *in vivo*. *Int. Immunopharm.* 78 (106061). doi:10.1016/j.intimp.2019.106061

Beninati, S., Oliverio, S., Cordella, M., Rossi, S., Senatore, C., Liguori, I., et al. (2014). Inhibition of cell proliferation, migration and invasion of B16-F10 melanoma cells by α-mangostin. *Biochem. Biophys. Res. Commun.* 450 (4), 1512–1517. doi:10.1016/j.bbrc.2014.07.031

Bhaskar, G., Arshia, S., and Priyadarshini, S. (2009). Formulation and evaluation of topical polyherbal antiacne gels containing *Garcinia mangostana* and *Aloe vera*. *Phcog. Mag.* 5 (19), 93–99.

Biasi, D., Carletto, A., Caramaschi, P., Bellavite, P., Maleknia, T., Scambi, C., et al. (1998). Neutrophil functions and IL-8 in psoriatic arthritis and in cutaneous psoriasis. *Inflammation* 22 (5), 533–543. doi:10.1023/a:1022354212121

Bickers, D. R., and Athar, M. (2006). Oxidative stress in the pathogenesis of skin disease. *J. Invest. Dermatol.* 126 (12), 2565–2575. doi:10.1038/sj.jid.5700340

Bolognesi, M. L. (2013). Polypharmacology in a single drug: multitarget drugs. *Curr. Med. Chem.* 20 (13), 1639–1645. doi:10.2174/0929867311320130004

Braun, S., Hanselmann, C., Gassmann, M. G., auf dem Keller, U., Born-Berclaz, C., Chan, K., et al. (2002). Nrf2 transcription factor, a novel target of keratinocyte growth factor action which regulates gene expression and inflammation in the healing skin wound. *Mol. Cell. Biol.* 22 (15), 5492–5505. doi:10.1128/mcb.22.15.5492-5505.2002

Buddenkotte, J., Maurer, M., and Steinhoff, M. (2010). Histamine and antihistamines in atopic dermatitis. *Adv. Exp. Med. Biol.* 709, 73–80. doi:10.1007/978-1-4419-8056-4_8

Bull, H. A., and Dowd, P. M. (1993). Prostaglandins, interleukins, and cutaneous inflammation. *Immunomethods* 2 (3), 219–226. doi:10.1006/immu.1993.1025

Bulugonda, R. K., Kumar, K. A., Gangappa, D., Beeda, H., Philip, G. H., Rao, D. D., et al. (2017). Mangiferin from *Pueraria tuberosa* reduces inflammation *via* inactivation of NLRP3 inflammasome. *Sci. Rep.* 7, 42683. doi:10.1038/srep42683

Bumrungpert, A., Kalpravidh, R. W., Chitchumroonchokchai, C., Chuang, C.-C., West, T., Kennedy, A., et al. (2009). Xanthones from mangosteen prevent lipopolysaccharide-mediated inflammation and insulin resistance in primary cultures of human adipocytes. *J. Nutr.* 139 (6), 1185–1191. doi:10.3945/jn.109.106617

Bumrungpert, A., Kalpravidh, R. W., Chuang, C.-C., Overman, A., Martinez, K., Kennedy, A., et al. (2010). Xanthones from mangosteen inhibit inflammation in human macrophages and in human adipocytes exposed to macrophage-conditioned media. *J. Nutr.* 140 (4), 842–847. doi:10.3945/jn.109.120022

Campbell, K. J., and Tait, S. W. G. (2018). Targeting BCL-2 regulated apoptosis in cancer. *Open Biol.* 8 (5), 180002. doi:10.1098/rsob.180002

Chairungsrilerd, N., Furukawa, K.-I., Ohta, T., Nozoe, S., and Ohizumi, Y. (1996b). Histaminergic and serotonergic receptor blocking substances from the medicinal PlantGarcinia mangostana. *Planta Med.* 62 (5), 471–472. doi:10.1055/s-2006-957943

Chairungsrilerd, N., Furukawa, K.-I., Ohta, T., Nozoe, S., and Ohizumi, Y. (1996a). Pharmacological properties of α-mangostin, a novel histamine H1 receptor antagonist. *Eur. J. Pharmacol.* 314 (3), 351–356. doi:10.1016/s0014-2999(96)00562-6

Cheng, H., Zhang, X., Su, J. J., and Li, Q. L. (2014). Study of gambogenic acid-induced apoptosis of melanoma B16 cells through PI3K/Akt/mTOR signaling pathways. *Zhongguo Zhongyao Zazhi* 39 (9), 1666–1669 [in Chinese].

Chiu, Y.-S., Wu, J.-L., Yeh, C.-T., Yadav, V. K., Huang, H.-S., and Wang, L.-S. (2020). γ-Mangostin isolated from *Garcinia mangostana* L. suppresses inflammation and alleviates symptoms of osteoarthritis via modulating miR-124-3p/IL-6/NF-κB signaling. *Aging* 12 (8), 6630–6643. doi:10.18632/aging.103003

Chomnawang, M. T., Surassmo, S., Nukoolkarn, V. S., and Gritsanapan, W. (2005). Antimicrobial effects of Thai medicinal plants against acne-inducing bacteria. *J. Ethnopharmacol.* 101 (1–3), 330–333. doi:10.1016/j.jep.2005.04.038

Chomnawang, M. T., Surassmo, S., Nukoolkarn, V. S., and Gritsanapan, W. (2007). Effect of *Garcinia mangostana* on inflammation caused by *Propionibacterium acnes*. *Fitoterapia* 78 (6), 401–408. doi:10.1016/j.fitote.2007.02.019

Cidade, H., Rocha, V., Palmeira, A., Marques, C., Tiritan, M. E., Ferreira, H., et al. (2017). *In silico* and *in vitro* antioxidant and cytotoxicity evaluation of oxygenated xanthone derivatives. *Arab. J. Chem.* 13 (1), 17–26. doi:10.1016/j.arabjc.2017.01.006

Delgado-Hernández, R., Hernández-Balmaseda, I., Rodeiro-Guerra, I., Gonzalez, J. C. R., De Wever, O., Logie, E., et al. (2019). Anti-angiogenic effects of mangiferin and mechanism of action in metastatic melanoma. *Melanoma Res.* 30 (1), 39–51. doi:10.1097/CMR.0000000000000647

Dubrac, S., and Schmuth, M. (2011). PPAR-alpha in cutaneous inflammation. *Derm. Endocrinol.* 3 (1), 23–26. doi:10.4161/derm.3.1.14615

Fang, Y., Su, T., Qiu, X., Mao, P., Xu, Y., Hu, Z., et al. (2016). Protective effect of alpha-mangostin against oxidative induced-retinal cell death. *Sci. Rep.* 6, 21018. doi:10.1038/srep21018

Feng, Z., Lu, X., Gan, L., Zhang, Q., and Lin, L. (2020). Xanthones, a promising anti-inflammatory scaffold: structure, activity, and drug likeness analysis. *Molecules* 25 (3), 598. doi:10.3390/molecules25030598

Gao, Y., Zhao, Z., Meng, X., Chen, H., and Fu, G. (2018). Migration and invasion in B16-F10 mouse melanoma cells are regulated by Nrf2 inhibition during treatment with ionizing radiation. *Oncol. Lett.* 16 (2), 1959–1966. doi:10.3892/ol.2018.8799

Garrido, G., González, D., Lemus, Y., García, D., Lodeiro, L., Quintero, G., et al. (2004). *In vivo* and *in vitro* anti-inflammatory activity of *Mangifera indica* L. extract (VIMANGS). *Pharmacol. Res.* 50 (2), 143–149. doi:10.1016/j.phrs.2003.12.003

Guérard, S., Allaeys, I., Martin, G., Pouliot, R., and Poubelle, P. E. (2013). Psoriatic keratinocytes prime neutrophils for an overproduction of superoxide anions. *Arch. Dermatol. Res.* 305 (10), 879–889. doi:10.1007/s00403-013-1404-z

FUNDING

Guo, H.-W., Yun, C.-X., Hou, G.-H., Du, J., Huang, X., Lu, Y., et al. (2014). Mangiferin attenuates Th1/Th2 cytokine imbalance in an ovalbumin-induced asthmatic mouse model. *PLoS One* 9 (6), e100394. doi:10.1371/journal.pone.0086881

Guo, H., Liu, H., Jian, Z., Cui, H., Fang, J., Zuo, Z., et al. (2019). Nickel induces inflammatory activation via NF-κB, MAPKs, IRF3 and NLRP3 inflammasome signaling pathways in macrophages. *Aging* 11 (23), 11659–11672. doi:10.18632/aging.102570

Gutierrez-Orozco, F., Chitchumroonchokchai, C., Lesinski, G. B., Suksamrarn, S., and Failla, M. L. (2013). α-Mangostin: anti-inflammatory activity and metabolism by human cells. *J. Agric. Food Chem.* 61 (16), 3891–3900. doi:10.1021/jf4004434

Hambright, H. G., Meng, P., Kumar, A. P., and Ghosh, R. (2015). Inhibition of PI3K/AKT/mTOR axis disrupts oxidative stress-mediated survival of melanoma cells. *Oncotarget* 6 (9), 7195–7208. doi:10.18632/oncotarget.3131

Heinze, H., and Mohr, H. (1990). "Phorbol myristate acetate and calcium ionophore A23187 induce two waves of lymphokine mRNA transcription in stimulted human peripheral blood lymphocytes,"in *Cytokines in hemopoiesis, oncology, and AIDS.* Editors M. Freund, H. Link, and K. Welte (Berlin, Heidelberg: Springer), 359–363.

Helou, D. G., Martin, S. F., Pallardy, M., Chollet-Martin, S., and Kerdine-Römer, S. (2019). Nrf2 involvement in chemical-induced skin innate immunity. *Front. Immunol.* 10, 1004. doi:10.3389/fimmu.2019.01004

Heng, A. H. S., and Chew, F. T. (2020). Systematic review of the epidemiology of acne vulgaris. *Sci. Rep.* 10 (1), 5754. doi:10.1038/s41598-020-62715-3

Hennig, P., Fenini, G., Di Filippo, M., and Beer, H. D. (2020). Electrophiles against (skin) diseases: more than Nrf2. *Biomolecules* 10 (2), 271. doi:10.3390/biom10020271

Herrera-Aco, D. R., Medina-Campos, O. N., Pedraza-Chaverri, J., Sciutto-Conde, E., Rosas-Salgado, G., and Fragoso-González, G. (2019). Alpha-mangostin: anti-inflammatory and antioxidant effects on established collagen-induced arthritis in DBA/1J mice. *Food Chem. Toxicol.* 124, 300–315. doi:10.1016/j.fct.2018.12.018

Higuchi, H., Tanaka, A., Nishikawa, S., Oida, K., Matsuda, A., Jung, K., et al. (2013). Suppressive effect of mangosteen rind extract on the spontaneous development of atopic dermatitis in NC/Tnd mice. *J. Dermatol.* 40 (10), 786–796. doi:10.1111/1346-8138.12250

Hirakawa, K., Yoshida, M., Nagatsu, A., Mizukami, H., Rana, V., Rawat, M. S. M., et al. (2005). Chemopreventive action of xanthone derivatives on photosensitized DNA damage¶. *Photochem. Photobiol.* 81 (2), 314–319. doi:10.1562/2004-07-29-ra-252.1

Hiraku, Y., Ito, K., Hirakawa, K., and Kawanishi, S. (2007). Photosensitized DNA damage and its protection via a novel mechanism. *Photochem. Photobiol.* 83 (1), 205–212. doi:10.1562/2006-03-09-ir-840

Hsu, H., Lin, C.-N., Lu, M.-C., and Wang, J.-P. (2004). Inhibition of the arachidonic acid cascade by norathyriol via blockade of cyclooxygenase and lipoxygenase activity in neutrophils. *N. Schmied. Arch. Pharmacol.* 369 (5), 507–515. doi:10.1007/s00210-004-0922-9

Hsu, M.-F., Raung, S.-L., Tsao, L.-T., Lin, C.-N., and Wang, J.-P. (1997). Examination of the inhibitory effect of norathyriol in formylmethionyl-leucyl-phenylalanine-induced respiratory burst in rat neutrophils. *Free Radic. Biol. Med.* 23 (7), 1035–1045. doi:10.1016/s0891-5849(97)00132-9

Ibrahim, M. Y., Hashim, N. M., Mariod, A. A., Mohan, S., Abdulla, M. A., Abdelwahab, S. I., et al. (2016). α-Mangostin from *Garcinia mangostana* Linn: an updated review of its pharmacological properties. *Arab. J. Chem.* 9 (3), 317–329. doi:10.1016/j.arabjc.2014.02.011

Ibrahim, S. R. M., Abdallah, H. M., El-Halawany, A. M., Nafady, A. M., and Mohamed, G. A. (2018a). Mangostanaxanthone VIII, a new xanthone from *Garcinia mangostana* and its cytotoxic activity. *Nat. Prod. Res.* 33 (2), 258–265. doi:10.1080/14786419.2018.1446012

Ibrahim, S. R. M., El-Agamy, D. S., Abdallah, H. M., Ahmed, N., Elkablawy, M. A., and Mohamed, G. A. (2018b). Protective activity of tovophyllin A, a xanthone isolated from *Garcinia mangostana* pericarps, against acetaminophen-induced liver damage: role of Nrf2 activation. *Food Funct.* 9 (6), 3291–3300. doi:10.1039/c8fo00378e

Im, A. R., Kim, Y. M., Chin, Y. W., and Chae, S. (2017). Protective effects of compounds from *Garcinia mangostana* L. (Mangosteen) against UVB damage in HaCaT cells and hairless mice. *Int. J. Mol. Med.* 40 (6), 1941–1949. doi:10.3892/ijmm.2017.3188

Jang, H.-Y., Kwon, O.-K., Oh, S.-R., Lee, H.-K., Ahn, K.-S., and Chin, Y.-W. (2012). Mangosteen xanthones mitigate ovalbumin-induced airway inflammation in a mouse model of asthma. *Food Chem. Toxicol.* 50 (11), 4042–4050. doi:10.1016/j.fct.2012.08.037

Kabashima, K., Nagamachi, M., Honda, T., Nishigori, C., Miyachi, Y., Tokura, Y., et al. (2007). Prostaglandin E2 is required for ultraviolet B-induced skin inflammation via EP2 and EP4 receptors. *Lab. Invest.* 87 (1), 49–55. doi:10.1038/labinvest.3700491

Kalz, F. (1960). The effect of prolonged therapy of atopic dermatitis with triamcinolone, dexamethasone and 6-methyl prednisolone. *Dermatology* 120, 65–74. doi:10.1159/000255301

Kapadia, G. J., S. Rao, G., Takayasu, J., Takasaki, M., Iida, A., Suzuki, N., et al. (2013). Evaluation of skin cancer chemoprevention potential of sunscreen agents using the Epstein-Barr virus early antigen activationin vitroassay. *Int. J. Cosmet. Sci.* 35 (2), 143–148. doi:10.1111/ics.12015

Khazaei, Z., Ghorat, F., Jarrahi, A. M., Adineh, H. A., Sohrabivafa, M., and Goodarzi, E. (2019). Global incidence and mortality of skin cancer by histological subtype and its relationship with the human development index (HDI); an ecology study in 2018. *World Cancer Res. J.* 6, e1265. doi:10.32113/wcrj_20194_1265

Khmaladze, I., Nandakumar, K. S., and Holmdahl, R. (2015). Reactive oxygen species in psoriasis and psoriasis arthritis: relevance to human disease. *Int. Arch. Allergy Immunol.* 166 (2), 135–149. doi:10.1159/000375401

Kim, D. J., Bility, M. T., Billin, A. N., Willson, T. M., Gonzalez, F. J., and Peters, J. M. (2006). PPARβ/δ selectively induces differentiation and inhibits cell proliferation. *Cell Death Differ.* 13 (1), 53–60. doi:10.1038/sj.cdd.4401713

Koh, J.-J., Qiu, S., Zou, H., Lakshminarayanan, R., Li, J., Zhou, X., et al. (2013). Rapid bactericidal action of alpha-mangostin against MRSA as an outcome of membrane targeting. *Biochim. Biophys. Acta Biomembr.* 1828 (2), 834–844. doi:10.1016/j.bbamem.2012.09.004

Kuete, V., Wabo, H. K., Eyong, K. O., Feussi, M. T., Wiench, B., Krusche, B., et al. (2011). Anticancer activities of six selected natural compounds of some Cameroonian medicinal plants. *PLoS One* 6 (8), e21762. doi:10.1371/journal.pone.0021762

Lee, D.-J., Du, F., Chen, S.-W., Nakasaki, M., Rana, I., Shih, V. F. S., et al. (2015). Regulation and function of the caspase-1 in an inflammatory microenvironment. *J. Invest. Dermatol.* 135 (8), 2012–2020. doi:10.1038/jid.2015.119

Lee, J., Aoki, T., Thumkeo, D., Siriwach, R., Yao, C., and Narumiya, S. (2019). T cell-intrinsic prostaglandin E2-EP2/EP4 signaling is critical in pathogenic Th17 cell-driven inflammation. *J. Allergy Clin. Immunol.* 143 (2), 631–643. doi:10.1016/j.jaci.2018.05.036

Lee, L.-T., Tsai, Y.-F., Hu, N.-Y., Wang, C.-W., Huang, K.-K., Hsiao, J.-K., et al. (2013). Anti-arthritis effect of mangostins from *G. Mangostana*. *Biomed. Prevent. Nutr.* 3 (3), 227–232. doi:10.1016/j.bionut.2012.10.002

Li, J., Malakhova, M., Mottamal, M., Reddy, K., Kurinov, I., Carper, A., et al. (2012). Norathyriol suppresses skin cancers induced by solar ultraviolet radiation by targeting ERK kinases. *Cancer Res.* 72 (1), 260–270. doi:10.1158/0008-5472.can-11-2596

Liang, L. and Zhang, Z. (2016). Gambogic acid inhibits malignant melanoma cell proliferation through mitochondrial p66shc/ROS-p53/Bax-mediated apoptosis. *Cell. Physiol. Biochem.* 38 (4), 1618–1630. doi:10.1159/000443102

Liang, L., Zhang, Z., Qin, X., Gao, Y., Zhao, P., Liu, J., et al. (2018). Gambogic acid inhibits melanoma through regulation of miR-199a-3p/ZEB1 signalling. *Basic Clin. Pharmacol. Toxicol.* 123 (6), 692–703. doi:10.1111/bcpt.13090

Liu, Y.-W., Cheng, Y.-Q., Liu, X.-L., Hao, Y.-C., Li, Y., Zhu, X., et al. (2016). Mangiferin upregulates glyoxalase 1 through activation of Nrf2/ARE signaling in central neurons cultured with high glucose. *Mol. Neurobiol.* 54 (6), 4060–4070. doi:10.1007/s12035-016-9978-z

Lopez Carrera, I., Al Hammadi, A., Huang, Y. H., Llamado, L. J., Mahgoub, E., Tallman, A. M., et al. (2019). Epidemiology, diagnosis, and treatment of atopic dermatitis in the developing countries of Asia, Africa, Latin America, and the Middle East: a review. *Dermatol. Ther.* 9 (4), 685–705. doi:10.1007/s13555-019-00332-3

Magcwebeba, T. U., Riedel, S., Swanevelder, S., Swart, P., De Beer, D., Joubert, E., et al. (2016a). The potential role of polyphenols in the modulation of skin cell viability by *Aspalathus linearis* and *Cyclopia* spp. herbal tea extracts *in vitro*. *J. Pharm. Pharmacol.* 68 (11), 1440–1453. doi:10.1111/jphp.12629

Magcwebeba, T. U., Swart, P., Swanevelder, S., Joubert, E., and Gelderblom, W. C. A. (2016b). Anti-inflammatory effects of *Aspalathus linearis* and *Cyclopia* spp. extracts in a UVB/keratinocyte (HaCaT) model utilising interleukin-1α accumulation as biomarker. *Molecules* 21 (10), 1323. doi:10.3390/molecules21101323

Mah, S., Teh, S., and Lian Ee, G. (2019). Comparative studies of selected *Calophyllum* plants for their anti-inflammatory properties. *Phcog. Mag.* 15 (60), 135–139. doi:10.4103/pm.pm_212_18

Mahmoud-Awny, M., Attia, A. S., Abd-Ellah, M. F., and El-Abhar, H. S. (2015). Mangiferin mitigates gastric ulcer in ischemia/reperfused rats: involvement of PPAR-γ, NF-κB and Nrf2/HO-1 signaling pathways. *PLoS One* 10 (7), e0132497. doi:10.1371/journal.pone.0132497

Makhoba, X. H., Viegas, C., Jr., Mosa, R. A., Viegas, F. P., and Pooe, O. J. (2020). Potential impact of the multi-target dug approach in the treatment of some complex diseases. *Drug Des. Dev. Ther.* 14, 3235–3249. doi:10.2147/dddt. s257494

Mao, X., Cheng, R., Zhang, H., Bae, J., Cheng, L., Zhang, L., et al. (2018). Self-healing and injectable hydrogel for matching skin flap regeneration. *Adv. Sci.* 6 (13), 1801555. doi:10.1002/advs.201801555

Mao, X., Liu, L., Cheng, L., Cheng, R., Zhang, L., Deng, L., et al. (2019). Adhesive nanoparticles with inflammation regulation for promoting skin flap regeneration. *J. Contr. Release* 297, 91–101. doi:10.1016/j.jconrel.2019.01.031

Mariette, X., Matucci-Cerinic, M., Pavelka, K., Taylor, P., van Vollenhoven, R., Heatley, R., et al. (2011). Malignancies associated with tumour necrosis factor inhibitors in registries and prospective observational studies: a systematic review and meta-analysis. *Ann. Rheum. Dis.* 70 (11), 1895–1904. doi:10. 1136/ard.2010.149419

Márquez, L., García-Bueno, B., Madrigal, J. L. M., and Leza, J. C. (2012). Mangiferin decreases inflammation and oxidative damage in rat brain after stress. *Eur. J. Nutr.* 51 (6), 729–739. doi:10.1007/s00394-011-0252-x

Matsuura, N., Gamo, K., Miyachi, H., Iinuma, M., Kawada, T., Takahashi, N., et al. (2013). γ-mangostin from *Garcinia mangostana* pericarps as a dual agonist that activates both PPARα and PPARδ *Bioscience. Biotechnol. Biochem.* 77 (12), 2430–2435. doi:10.1271/bbb.130541

Mercer, L. K., Askling, J., Raaschou, P., Dixon, W. G., Dreyer, L., Hetland, M. L., et al. (2017). Risk of invasive melanoma in patients with rheumatoid arthritis treated with biologics: results from a collaborative project of 11 European biologic registers. *Ann. Rheum. Dis.* 76 (2), 386–391. doi:10.1136/annrheumdis-2016-209285

Mohan, S., Syam, S., Abdelwahab, S. I., and Thangavel, N. (2018). An anti-inflammatory molecular mechanism of action of α-mangostin, the major xanthone from the pericarp of *Garcinia mangostana*: an *in silico, in vitro* and *in vivo* approach. *Food Funct.* 9 (7), 3860–3871. doi:10.1039/c8fo00439k

Nakatani, K., Nakahata, N., Arakawa, T., Yasuda, H., and Ohizumi, Y. (2002). Inhibition of cyclooxygenase and prostaglandin E2 synthesis by γ-mangostin, a xanthone derivative in mangosteen, in C6 rat glioma cells. *Biochem. Pharmacol.* 63 (1), 73–79. doi:10.1016/s0006-2952(01)00810-3

Nakatani, K., Yamakuni, T., Kondo, N., Arakawa, T., Oosawa, K., Shimura, S., et al. (2004). γ-mangostin inhibits inhibitor-κB kinase activity and decreases lipopolysaccharide-induced cyclooxygenase-2 gene expression in C6 rat glioma cells. *Mol. Pharmacol.* 66 (3), 667–674. doi:10.1124/mol.104.002626

Ng, I. M. J. and Chua, C. L. L. (2019). The potential of xanthones as a therapeutic option in macrophage-associated inflammatory diseases. *Phcog. Rev.* 13 (25), 28–33. doi:10.4103/phrev.phrev_25_18

Ng, I. M. J., Mah, S. H., and Chua, C. L. L. (2020). Immuno-modulatory effects of macluraxanthone on macrophage phenotype and function. *Nat. Prod. Res.* 1–6. doi:10.1080/14786419.2020.1775223

Ohsawa, Y. and Hirasawa, N. (2014). The role of histamine H1 and H4 receptors in atopic dermatitis: from basic research to clinical study. *Allergol. Int.* 63 (4), 533–542. doi:10.2332/allergolint.13-ra-0675

Okayama, Y. (2005). Oxidative stress in allergic and inflammatory skin diseases. *Curr. Drug Targets - Inflamm. Allergy* 4 (4), 517–519. doi:10.2174/ 1568010054526386

Ong, Y. S., Murugaiyah, V., Goh, B. H., and Khaw, K. Y. (2020). "Bioactive xanthones from Garcinia mangostana," in *Plant-derived Bioactives*. Editors M. Swamy (Singapore, Singapore: Springer), 281–300.

Owczarek, K. and Jaworski, M. (2016). Quality of life and severity of skin changes in the dynamics of psoriasis. *Adv. Dermatol. Allergol.* 33 (2), 102–108. doi:10. 5114/pdia.2015.54873

Pan, C. W., Pan, Z. Z., Hu, J. J., Chen, W. L., Zhou, G. Y., Lin, W., et al. (2016). Mangiferin alleviates lipopolysaccharide and D-galactosamine-induced acute liver injury by activating the Nrf2 pathway and inhibiting NLRP3 inflammasome activation. *Eur. J. Pharmacol.* 770, 85–91. doi:10.1016/j. ejphar.2015.12.006

Pan-In, P., Wongsomboon, A., Kokpol, C., Chaichanawongsaroj, N., and Wanichwecharungruang, S. (2015). Depositing alpha-mangostin

nanoparticles to sebaceous gland area for acne treatment. *J. Pharmacol. Sci.* 129 (4), 226–232. doi:10.1016/j.jphs.2015.11.005

Panieri, E. and Saso, L. (2019). Potential applications of Nrf2 inhibitors in cancer therapy. *Oxidat. Med. Cell. Longev.* 2019, 8592348. doi:10.1155/2019/8592348

Pedraza-Chaverri, J., Reyes-Fermín, L. M., Nolasco-Amaya, E. G., Orozco-Ibarra, M., Medina-Campos, O. N., Gonzalez-Cuahutencos, O., et al. (2009). ROS scavenging capacity and neuroprotective effect of α-mangostin against 3-nitropropionic acid in cerebellar granule neurons. *Exp. Toxicol. Pathol.* 61 (5), 491–501. doi:10.1016/j.etp.2008.11.002

Pérez-Rojas, J. M., Cruz, C., García-López, P., Sánchez-González, D. J., Martínez-Martínez, C. M., Ceballos, G., et al. (2009). Renoprotection by α-mangostin is related to the attenuation to the renal oxidative/nitrosative stress induced by cisplatin nephrotoxicity. *Free Radic. Res.* 43 (11), 1122–1132. doi:10.1080/ 10715760903214447

Petrova, A., Davids, L. M., Rautenbach, F., and Marnewick, J. L. (2011). Photoprotection by honeybush extracts, hesperidin and mangiferin against UVB-induced skin damage in SKH-1 mice. *J. Photochem. Photobiol. B Biol.* 103 (2), 126–139. doi:10.1016/j.jphotobiol.2011.02.020

Pittayapruek, P., Meephansan, J., Prapapan, O., Komine, M., and Ohtsuki, M. (2016). Role of matrix metalloproteinases in photoaging and photocarcinogenesis. *Int. J. Mol. Sci.* 17 (6), 868. doi:10.3390/ijms17060868

Pleguezuelos-Villa, M., Diez-Sales, O., Manca, M. L., Manconi, M., Sauri, A. R., Escribano-Ferrer, E., et al. (2019). Mangiferin glycethosomes as a new potential adjuvant for the treatment of psoriasis. *Int. J. Pharm.* 573, 118844. doi:10.1016/j. ijpharm.2019.118844

Pothitirat, W., Chomnawang, M. T., Supabphol, R., and Gritsanapan, W. (2010). Free radical scavenging and anti-acne activities of mangosteen fruit rind extracts prepared by different extraction methods. *Pharmaceut. Biol.* 48 (2), 182–186. doi:10.3109/13880200903062671

Purnaningsih, D., Djawad, K., Wahab, S., Massi, N., Alam, G., and Bahar, B. (2018). Protective effect of mangosteen skin extract on albino mice skin with dimethyl-benz(α)anthracene (DMBA) induction: analysis on p53 protein level. *Int. J. Med. Rev. Case Rep.* 3, 213–215.

Ramot, Y., Mastrofrancesco, A., Camera, E., Desreumaux, P., Paus, R., and Picardo, M. (2015). The role of PPARγ-mediated signalling in skin biology and pathology: new targets and opportunities for clinical dermatology. *Exp. Dermatol.* 24 (4), 245–251. doi:10.1111/exd.12647

Ramsay, R. R., Popovic-Nikolic, M. R., Nikolic, K., Uliassi, E., and Bolognesi, M. L. (2018). A perspective on multi-target drug discovery and design for complex diseases. *Clin. Transl. Med.* 7 (1), 3. doi:10.1186/s40169-017-0181-2

Ratwita, W., Sukandar, E. Y., Kurniati, N. F., and Adnyana, I. K. (2018). Alpha mangostin and xanthone from mangosteen (*Garcinia mangostana* L.) role on insulin tolerance and PPAR-γ in preclinical model diabetes mellitus. *J. Pharm. Nutr. Sci.* 8, 83–90. doi:10.6000/1927-5951.2018.08.03.1

Rayburn, E. R., Ezell, S. J., and Zhang, R. (2009). Anti-inflammatory agents for cancer therapy. *Mol. Cell. Pharmacol.* 1 (1), 29–43. doi:10.4255/mcpharmacol. 09.05

Ruan, J., Zheng, C., Liu, Y., Qu, L., Yu, H., Han, L., et al. (2017). Chemical and biological research on herbal medicines rich in xanthones. *Molecules* 22 (10), 1698. doi:10.3390/molecules22101698

Sankowski, A. J., Łebkowska, U. M., Ćwikła, J., Walecka, I., and Walecki, J. (2013). Psoriatic arthritis. *Pol. J. Radiol.* 78 (1), 7–17. doi:10.12659/PJR.883763

Satoh, T., Moroi, R., Aritake, K., Urade, Y., Kanai, Y., Sumi, K., et al. (2006). Prostaglandin D2 plays an essential role in chronic allergic inflammation of the skin via CRTH2 receptor. *J. Immunol.* 177 (4), 2621–2629. doi:10.4049/ jimmunol.177.4.2621

Saw, C. L., Huang, M. T., Liu, Y., Khor, T. O., Conney, A. H., and Kong, A. N. (2010). Impact of Nrf2 on UVB-induced skin inflammation/photoprotection and photoprotective effect of sulforaphane. *Mol. Carcinog.* 50 (6), 479–486. doi:10.1002/mc.20725

Saw, C. L., Yang, A. Y., Huang, M. T., Liu, Y., Lee, J. H., Khor, T. O., et al. (2014). Nrf2 null enhances UVB-induced skin inflammation and extracellular matrix damages. *Cell Biosci.* 4, 39. doi:10.1186/2045-3701-4-39

Schön, M. P. (2019). Adaptive and innate immunity in psoriasis and other inflammatory disorders. *Front. Immunol.* 10, 1764. doi:10.3389/fimmu.2019. 01764

Schwingen, J., Kaplan, M., and Kurschus, F. C. (2020). Review-current concepts in inflammatory skin diseases evolved by transcriptome analysis: in-depth analysis

of atopic dermatitis and psoriasis. *Int. J. Mol. Sci.* 21, 3. doi:10.3390/ijms21030699

Sertznig, P. and Reichrath, J. (2011). Peroxisome proliferator-activated receptors (PPARs) in dermatology. *Derm. Endocrinol.* 3 (3), 130–135. doi:10.4161/derm.15025

Sertznig, P., Seifert, M., Tilgen, W., and Reichrath, J. (2008). Peroxisome proliferator-activated receptors (PPARs) and the human skin. *Am. J. Clin. Dermatol.* 9 (1), 15–31. doi:10.2165/00128071-200809010-00002

Silva, V., Cerqueira, F., Nazareth, N., Medeiros, R., Sarmento, A., Sousa, E., et al. (2019). 1,2-Dihydroxyxanthone: effect on A375-C5 melanoma cell growth associated with interference of THP-1 human macrophage activity. *Pharmaceuticals* 12 (2), 85. doi:10.3390/ph12020085

Sivaranjani, M., Leskinen, K., Aravindraja, C., Saavalainen, P., Pandian, S. K., Skurnik, M., et al. (2019). Deciphering the antibacterial mode of alpha-mangostin on *Staphylococcus epidermidis* RP62A through an integrated transcriptomic and proteomic approach. *Front. Microbiol.* 10, 150. doi:10.3389/fmicb.2019.00150

Sivaranjani, M., Prakash, M., Gowrishankar, S., Rathna, J., Pandian, S. K., and Ravi, A. V. (2017). *In vitro* activity of alpha-mangostin in killing and eradicating *Staphylococcus epidermidis* RP62A biofilms. *Appl. Microbiol. Biotechnol.* 101 (8), 3349–3359. doi:10.1007/s00253-017-8231-7

Sivaranjani, N., Rao, S. V., and Rajeev, G. (2013). Role of reactive oxygen species and antioxidants in atopic dermatitis. *J. Clin. Diagn. Res.* 7 (12), 2683–2685. doi:10.7860/JCDR/2013/6635.3732

Smith, M. P., Sanchez-Laorden, B., O'Brien, K., Brunton, H., Ferguson, J., Young, H., et al. (2014). The immune microenvironment confers resistance to MAPK pathway inhibitors through macrophage-derived TNFα. *Cancer Discov.* 4 (10), 1214–1229. doi:10.1158/2159-8290.cd-13-1007

Sukma, M., Tohda, M., Suksamran, S., and Tantisira, B. (2011). γ-mangostin increases serotonin 2A/2C, muscarinic, histamine and bradykinin receptor mRNA expression. *J. Ethnopharmacol.* 135 (2), 450–454. doi:10.1016/j.jep.2011.03.039

Sutono, T. (2013). Efficacy of *Garcinia mangostana* L. (mangosteen rind extract) to reduce acne severity. *Med. J. Indonesia* 22 (3), 167–172. doi:10.13181/mji.v22i3.586

Talevi, A. (2015). Multi-target pharmacology: possibilities and limitations of the "skeleton key approach" from a medicinal chemist perspective. *Front. Pharmacol.* 6, 205. doi:10.3389/fphar.2015.00205

Tatiya-Aphiradee, N., Chatuphonprasert, W., and Jarukamjorn, K. (2016). *In vivo* antibacterial activity of *Garcinia mangostana* pericarp extract against methicillin-resistant *Staphylococcus aureus* in a mouse superficial skin infection model. *Pharmaceut. Biol.* 54 (11), 2606–2615. doi:10.3109/13880209.2016.1172321

Teh, S. S., Ee, G. C. L., and Mah, S. H. (2017). Evaluation of nitric oxide inhibition effect in LPS-stimulated RAW 264.7 macrophages by phytochemical constituents from *Mesua beccariana, Mesua congestiflora*, and *Mesua ferrea*. *Med. Chem. Res.* 26 (12), 3240–3246. doi:10.1007/s00044-017-2017-4

Tikhomirova, L. I. and Ilyicheva, T. N. (2020). Preparation of biotechnological raw materials of *Iris sibirica* L. with a given content of mangiferin and antiviral activity. *IOP Conf. Ser. Earth Environ. Sci.* 421, 022049. doi:10.1088/1755-1315/421/2/022049

Tsubaki, M., Takeda, T., Kino, T., Itoh, T., Imano, M., Tanabe, G., et al. (2015). Mangiferin suppresses CIA by suppressing the expression of TNF-α, IL-6, IL-1β, and RANKL through inhibiting the activation of NF-κB and ERK1/2. *Am. J. Tourism Res.* 7 (8), 1371–1381.

Vemu, B., Nauman, M. C., Veenstra, J. P., and Johnson, J. J. (2019). Structure activity relationship of xanthones for inhibition of cyclin dependent kinase 4 from mangosteen (*Garcinia mangostana* L.). *Int. J. Nutr.* 4 (2), 38–45. doi:10.14302/issn.2379-7835.ijn-19-2845

Wang, A., Li, D., Wang, S., Zhou, F., Li, P., Wang, Y., et al. (2018a). γ-Mangostin, a xanthone from mangosteen, attenuates oxidative injury in liver via NRF2 and SIRT1 induction. *J. Funct. Foods* 40, 544–553. doi:10.1016/j.jff.2017.11.047

Wang, F., Ma, H., Liu, Z., Huang, W., Xu, X., and Zhang, X. (2017). α-mangostin inhibits DMBA/TPA-induced skin cancer through inhibiting inflammation and promoting autophagy and apoptosis by regulating PI3K/Akt/mTOR signaling pathway in mice. *Biomed. Pharmacother.* 92, 672–680. doi:10.1016/j.biopha.2017.05.129

Wang, J. J., Sanderson, B. J. S., and Zhang, W. (2011). Cytotoxic effect of xanthones from pericarp of the tropical fruit mangosteen (*Garcinia mangostana* Linn.) on

human melanoma cells. *Food Chem. Toxicol.* 49 (9), 2385–2391. doi:10.1016/j.fct.2011.06.051

Wang, Q. L., Yang, D. Z., and Lv, C. (2018b). Antiinflammatory effects of gambogic acid in murine collageninduced arthritis through PI3K/Akt signaling pathway. *Mol. Med. Rep.* 17 (3), 4791–4796. doi:10.3892/mmr.2018.8389

Wang, W. M. and Jin, H. Z. (2020). Role of neutrophils in psoriasis. *J. Immunol. Res.* 2020, 3709749. doi:10.1155/2020/3709749

Watanabe, K., Jose, P. J., and Rankin, S. M. (2002). Eotaxin-2 generation is differentially regulated by lipopolysaccharide and IL-4 in monocytes and macrophages. *J. Immunol.* 168 (4), 1911–1918. doi:10.4049/jimmunol.168.4.1911

Wen, J., Pei, H., Wang, X., Xie, C., Li, S., Huang, L., et al. (2014). Gambogic acid exhibits anti-psoriatic efficacy through inhibition of angiogenesis and inflammation. *J. Dermatol. Sci.* 74 (3), 242–250. doi:10.1016/j.jdermsci.2014.03.001

Wilkinson, A. S., Monteith, G. R., Shaw, P. N., Lin, C. N., Gidley, M. J., and Roberts-Thomson, S. J. (2008). Effects of the mango components mangiferin and quercetin and the putative mangiferin metabolite norathyriol on the transactivation of peroxisome proliferator-activated receptor isoforms. *J. Agric. Food Chem.* 56 (9), 3037–3042. doi:10.1021/jf800046n

Wu, S., Lu, H., and Bai, Y. (2019). Nrf2 in cancers: a double-edged sword. *Cancer Med.* 8 (5), 2252–2267. doi:10.1002/cam4.2101

Xia, Y. and Sun, J. (2018). Synergistic inhibition of cell proliferation by combined targeting with kinase inhibitors and dietary xanthone is a promising strategy for melanoma treatment. *Clin. Exp. Dermatol.* 43 (2), 149–157. doi:10.1111/ced.13283

Xu, L., Lao, Y., Zhao, Y., Qin, J., Fu, W., Zhang, Y., et al. (2015). Screening active compounds from *Garcinia* species native to China reveals novel compounds targeting the STAT/JAK signaling pathway. *BioMed Res. Int.* 2015, 910453. doi:10.1155/2015/910453

Xu, N., Deng, W., He, G., Gan, X., Gao, S., Chen, Y., et al. (2018). Alpha- and gamma-mangostins exhibit anti-acne activities via multiple mechanisms. *Immunopharmacol. Immunotoxicol.* 40 (5), 415–422. doi:10.1080/08923973.2018.1519831

Xu, X., Liu, Y., Wang, L., He, J., Zhang, H., Chen, X., et al. (2009). Gambogic acid induces apoptosis by regulating the expression of Bax and Bcl-2 and enhancing caspase-3 activity in human malignant melanoma A375 cells. *Int. J. Dermatol.* 48 (2), 186–192. doi:10.1111/j.1365-4632.2009.03946.x

Yanaka, A. (2018). Role of Nrf2 in protection of gastrointestinal tract against oxidative stress. *J. Clin. Biochem. Nutr.* 63 (1), 18–25. doi:10.3164/jcbn.17-139

Yun, C., Chang, M., Hou, G., Lan, T., Yuan, H., Su, Z., et al. (2019). Mangiferin suppresses allergic asthma symptoms by decreased Th9 and Th17 responses and increased Treg response. *Mol. Immunol.* 114, 233–242. doi:10.1016/j.molimm.2019.07.025

Zhang, B., Zhao, J., Li, S., Zeng, L., Chen, Y., and Fang, J. (2015). Mangiferin activates the Nrf2-ARE pathway and reduces etoposide-induced DNA damage in human umbilical cord mononuclear blood cells. *Pharmaceut. Biol.* 53 (4), 503–511. doi:10.3109/13880209.2014.927890

Zhao, J., Qi, Q., Yang, Y., Gu, H. Y., Lu, N., Liu, W., et al. (2008). Inhibition of α4 integrin mediated adhesion was involved in the reduction of B16-F10 melanoma cells lung colonization in C57BL/6 mice treated with gambogic acid. *Eur. J. Pharmacol.* 589 (1–3), 127–131. doi:10.1016/j.ejphar.2008.04.063

Zhao, Y., Wang, W., Wu, X., Ma, X., Qu, R., Chen, X., et al. (2017). Mangiferin antagonizes TNF-α-mediated inflammatory reaction and protects against dermatitis in a mice model. *Int. Immunopharm.* 45, 174–179. doi:10.1016/j.intimp.2017.02.014 5

Burn Ointment Promotes Cutaneous Wound Healing by Modulating the PI3K/AKT/mTOR Signaling Pathway

Dali Gan[1†], Qiyuan Su[2†], Hanwen Su[3†], Li Wu[1], Jun Chen[4], Bing Han[5*] and Meixian Xiang[1*]

[1]School of Pharmaceutical Sciences, South-Central University for Nationalities, Wuhan, China, [2]Department of Statistics, University of Illinois at Urbana-Champaign, Urbana, IL, United States, [3]Department of Clinical Laboratory, Renmin Hospital of Wuhan University, Wuhan, China, [4]Department of Pharmacy, Wuhan No.1 Hospital (Wuhan Hospital of Traditional Chinese and Western Medicine), Wuhan, China, [5]Department of Pathology, Penn State College of Medicine, Milton S. Hershey Medical Center, Hershey, PA, United States

Burn ointment (BO) is a clinically useful medicine for the treatment of burns and scalds. However, there is no enough scientific evidence to report the effect of BO on wound healing and its analgesic and anti-inflammatory efficacy. The aim of this work was to evaluate the anti-inflammatory and analgesic efficacy of BO and to reveal the potential wound healing properties and related mechanisms of BO. In this work, the content of active ingredients of BO was determined by high-performance liquid chromatography (HPLC). Two animal models of inflammation were used to study its anti-inflammatory activity, and a hot plate method was used to evaluate its analgesic effect. In addition, mouse incision and rat burn models were used to investigate the effect of BO on the anti-inflammatory and wound healing mechanisms. The results showed that BO was safe for topical application, and BO could significantly inhibit auricular swelling in mice and paw swelling in rats and significantly prolong the latency period of paw licking in the hot plate experiment in mice. It can also accelerate wound healing and repair scars by promoting the formation of new epithelial tissues in rat burn models. In addition, BO significantly downregulated the serum level of TNF-α and significantly increased the serum levels of VEGF and TGF-β1. Also, BO promoted the expression of collagen I and increased the ratio in p-PI3K/PI3K, p-AKT/AKT, and p-mTOR/mTOR pathways. Our results demonstrate the safety and efficacy of BO and suggest that activation of the PI3K/AKT/mTOR signaling pathway may play an important role in the promotion of wound healing by BO.

Keywords: burn ointment, safety evaluation, burn wounds healing, analgesia, anti-inflammatory, PI3K/AKT/mTOR pathway

Abbreviations: AKT, protein kinase B; AST, aspartate transaminase; BMS, burn moisturizing scald ointment; BO, burn ointment; Cr, creatinine; DAB, diaminobenzidine; ELISA, enzyme-linked immunosorbent assay; H&E, hematoxylin-eosin; GAPDH, glyceraldehyde phosphate dehydrogenase; mTOR, mammalian target of rapamycin; PAGE, SDS-polyacrylamide gel electrophoresis; PBS, phosphate buffered saline; PDK-1, 3-phosphoinositide-dependent kinases; PI3K, phosphatidylinositol 3-kinase; PIP3: phosphatidylinositol (3,4,5) P3; PVDF, polyvinylidene difluoride; SDS, sodium dodecyl sulfate; TCM, traditional Chinese medicine; TGF-β1, transforming growth factor-beta1; TNF-α, tumor necrosis factor-alpha; VEGF, vascular endothelial growth factor; PIP2, phosphorylates phosphatidylinositol (4, 5) P2.

Graphical Abstract |
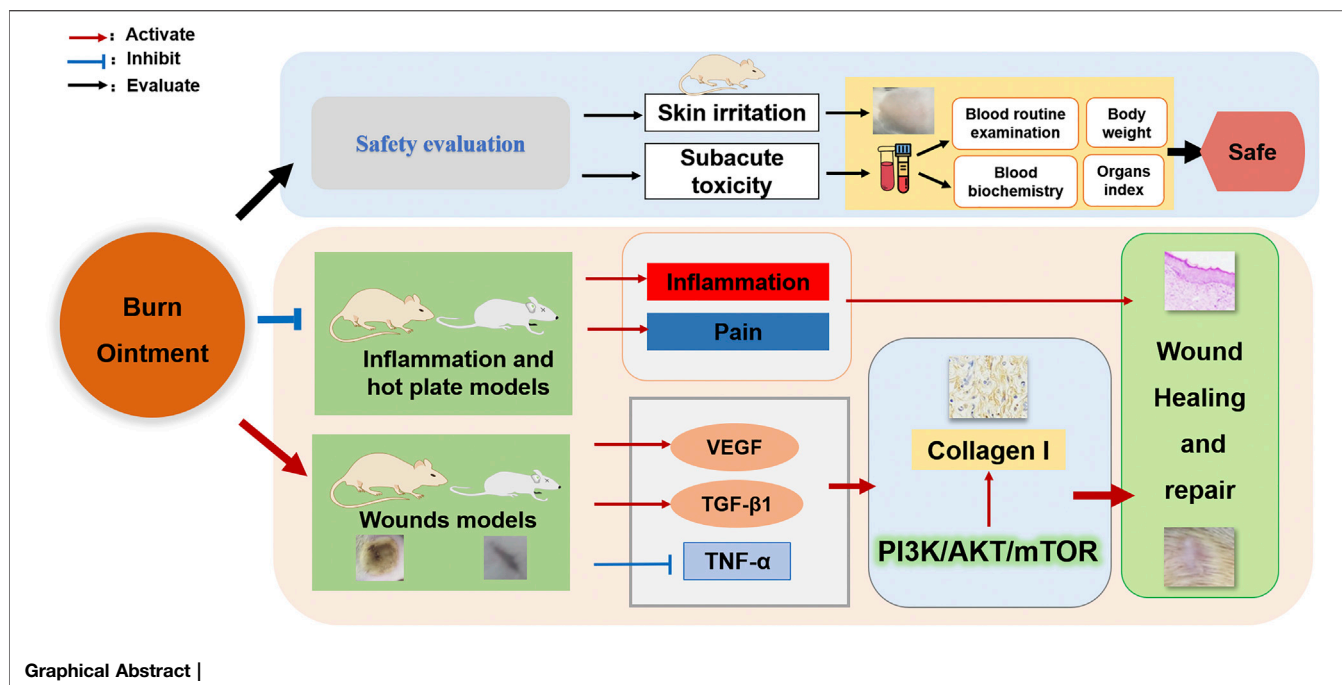
1 INTRODUCTION

Burns are one of the most serious skin-related injuries, and their incidence is on the rise globally (Shan et al., 2015). In the United States, the number of burn victims is estimated as 1.2 million per year. Of these injuries, an average of 50,000 burn victims are severely burned and require hospital treatment (Kaddoura et al., 2017).

The largest organ of the human body is the skin, and it is able to resist external infections and maintain the stability of the internal environment of our body (Riepl, 2020). Mild scalding will damage the skin tissue, but severe burns will be life-threatening. Additionally, the burns can cause inflammation, pain, and other complications (Wang et al., 2018). There are three phases that can be concluded in the dynamic healing process of wounds, including the inflammatory phase, the proliferation phase, and the maturation phase.

Many researches have indicated that several key cellular factors are involved in the process of burn repair, such as tumor necrosis factor-alpha (TNF-α), vascular endothelial growth factor (VEGF), and transforming growth factor-beta1 (TGF-β1) (Kim et al., 2020; Yaseen et al., 2020). If the body acquires an infection when the skin is damaged, it is stimulated to secrete the proinflammatory cytokines, such as TNF-α. After a while, the cytokine initiates an inflammatory cascade reaction to remove necrotic tissues and cells (Zelova and Hosek, 2013). However, overactive inflammation can cause systemic inflammatory response syndrome and immune dysfunction in patients, which will endanger their lives (Boldeanu et al., 2020). Therefore, anti-inflammatory treatments are essential for burn wound healing processes. Once the inflammation subsides, macrophages and other cells begin to secrete growth factors,

such as VEGF. VEGF is an essential cell factor for forming new blood vessels, and it can promote vascular endothelial cell proliferation to produce new blood vessels (Roskoski, 2017). The new blood vessels can provide nutrition to the injured area and accelerate wound healing (Eming et al., 2014). Besides, TGF-β1 is also a necessary cell factor for the healing process, because it promotes fibroblasts to proliferate and differentiate, forms granulation tissues, and synthesizes type I collagen (Kim et al., 2018a). Collagens help with wound contraction and restore skin elasticity to heal the burn wound by filling the space between cells (Gonzalez et al., 2016).

Currently, most of the known medications for burns have the obvious limitation of leaving scars easily. Traditional Chinese medicine compound burn ointment offers a more advanced alternative that avoids such limitations. BO is a traditional Chinese medical formulation, which contains *Rheum palmatum* L., *Angelica sinensis* (Oliv.) Diels, *Codonopsis pilosula* (Franch.) Nannf., *Asarum sieboldii* Miq., *Borneolum syntheticum*, and *Calomelas*. Traditionally, *Rheum palmatum* L. can be used to cure burn wounds *in vitro* (Committee of the Pharmacopoeia of PR China, 2015) due to its antimicrobial and anti-inflammatory qualities (Cao et al., 2017), and it can promote recovery of muscle; *Angelica sinensis* (Oliv.) Diels and *Codonopsis pilosula* (Franch.) Nannf. can remove stasis and analgesia (Wei et al., 2016; Gao et al., 2018), promoting the skin recovery of the wounded area. Modern research has revealed that the extract of *Rheum palmatum* L. could accelerate the progress of wound healing in rats, and its efficacy was better when it combined with the extract of *Angelica dahurica* (Fisch. Ex Hoffm.) Benth. et Hook. f (Yang et al., 2017). Moreover, many studies have shown the enormous potential of BO in treating burns as well, such that many chemicals of *Rheum palmatum* L.

and *Angelica sinensis* (Oliv.) Diels could reduce the liberation of proinflammatory cytokines, including IL-1β, IL-6, TNF-alpha, and IL-33 (Kim et al., 2018b; Shen et al., 2019). They have an anti-inflammatory and analgesic effect (Wei et al., 2016), induce cell proliferation (Gundogdu et al., 2019), and protect cells from injuries (Zhang et al., 2019b). But, the activity of BO in anti-inflammation, analgesia, and promoting skin wound healing, and its specific mechanism are still unclear. Therefore, this study attempted to elucidate the efficacy, the involved molecular mechanisms of BO in the healing process of burn wounds, and their complications. This research would contribute to the development and application of new drugs to treat burns and scalds.

2 MATERIAL AND METHODS

2.1 Materials and Reagents

BO (pharmaceutical batch number: 201671HZ) was supplied by the Department of Pharmacy at the Wuhan Integrated Traditional and Western Medicine Hospital (Wuhan, China). The BO used in this study is a hospital preparation which contains *Rheum palmatum* L., *Angelica sinensis* (Oliv.) Diels, *Codonopsis pilosula* (Franch.) Nannf., *Asarum sieboldii* Miq., *Borneolum syntheticum,* and Calomelas. Burn moisturizing scald ointment (BMS) was purchased from Meibao Pharmaceutical Co., Ltd. (Shantou, China); ELISA kits were obtained from Neobioscience Technology Co., Ltd. (Shenzhen, China); Collagen I primary antibody; phosphorylated PI3K, AKT, and mTOR; unphosphorylated PI3K, AKT, and mTOR polyclonal antibody; and HRP-labeled secondary antibody were purchased from Servicebio (Wuhan, China); Microscope (XSP-C204) was from Motic China group and microscope camera was purchased from Cognex (Massachusetts, United States); Toe volume measuring instrument (PV-200) was from TECHMEN Co., Ltd. (Chengdu, China); full-wavelength microplate reader 1,510 was obtained from Thermo Fisher Scientific (Massachusetts, United States); Ultimate 3000 series HPLC system consisting of the computer-controlled system with the CHROMELEONTM software and a SQL database, equipped with a WPS-3000 autosampler, was from Dionex (California, United States).

2.2 Animals

Kunming (KM) mice (20 ± 2 g), Sprague Dawley (SD) rats (200 ± 20 g), and Sprague Dawley (SD) rats (90 ± 10 g) were purchased from the Experimental Animal Center (certificate of experimental animals: SCXK 2015–0089 for rats and SCXK 2015–0018 for mice), Institute of Health and Epidemic Prevention (Wuhan, China), and housed in the standard specific pathogen-free (SPF) environment for three days. License number of the experimental unit was SYXK (Hubei province) 2016–0089, Experimental Animal Center of Central South University for Nationalities. All animals were allowed free access to food and water. The animal experiments were approved by the Institutional Animal Ethical Committee of Central South University for Nationalities and were performed under the guidelines of the committee; the permit number for the use of animals was no. 2020-scuec-029.

2.3 HPLC Analysis of BO's Chemical Components and Stability

20 mg BO was extracted with 10 ml methanol for 20 min using the ultrasonic method. The obtained extract was separated and transferred to a 10 mL volumetric flask and the volume was adjusted to 10 ml with methanol to obtain a 1 mg/mL sample solution. HPLC was then used to analyze the sample solution to quantify the content of aloe-emodin, emodin, rhein, chrysophanol, ferulic acid, lobetyolin, asarinin, and borneol and evaluate their stability on the 30th day or beyond. The samples were subjected to HPLC analysis on a C_{18} column (Agilent 250 mm × 4.6 mm, 5 μm) by a single injection of 10 μl detected at 254 nm; mobile phase: gradient elution by methyl alcohol (A) and water (B). The gradient program was set as follows: 0–4 min, 5–21% A; 4–8 min, 21–26% A; 8–10 min, 26–32% A; 10–14 min, 32–36% A; 14–18 min, 36–48% A; 18–22 min, 48–55% A; 22–25 min, 55–65% A; 25–30 min, 65% A; column temperature: 25°C; flow rate: 0.8 ml/min.

2.4 Doses and Methods of BO in Animal Models

Mice were randomly divided into several groups: canola oil (Con) group, burn moisturizing scald ointment (BMS) group, and BO group, with 10 mice in each group. The BO dosages of 0.1 g, 0.2 g, and 0.4 g/cm^2 were used to assess the subacute toxicity.

2.5 Skin Irritation Experiment in Rats

One day before the experiment, twenty SD rats were shaved for an area of approximately 4 × 2 cm^2 on the dorsal side. These shaved rats were randomly divided into two groups of ten: the canola oil group (Con) and the BO-treated group (BO). Then 0.2 g/cm^2 BO or Con was applied evenly on the shaved area of animals three times per day for one day. One hour after the last treatment, the treated skin was cleaned with cotton and water. After the application of BO, any signs, symptoms, and other skin changes were observed for 4 h (Ghosh et al., 2019).

2.6 Subacute Toxicity Assessment

Forty SD rats were shaved, weighed, and categorized into four groups of ten: 0.1 g, 0.2 g, and 0.4 g/cm^2 with BO and 0.2 g/cm^2 with Con. All animals received BO or Con 3 times per day for a total of 28 days. The body weight was recorded once per week. At the end of the experiment, all animals were fasted for 12 h and then anesthetized for blood and organ collection (Upadhyay et al., 2009). Hematological and biochemical analyses were run in a clinical laboratory, Wuhan University Renmin Hospital.

2.7 The Hot-Plate Test

The hot-plate test was used to examine the potential analgesic effect of BO. First, 40 KM mice were screened for their pain threshold within 5–30 s. In brief, the temperature of the plate surface was kept at 54 ± 1°C. The interval time that the mice licked

its toe or jumped from the plate was detected three times. Twenty-seven mice were selected and randomly divided into the following groups: the Con group, the BO group, and the BMS group. All mice were applied 0.2 g/cm^2 drug each time on the hind paws, 3 times per day for 7 days. The response latency of mice at the first hind paw lick or jump was recorded and analyzed 30 min after the last dose on day 1 and day 7, respectively (Ariyo et al., 2020). The following formula was used to calculate the pain threshold change:

Pain threshold change (s) = Pain threshold after treatment (s) − Pain threshold before treatment (s).

2.8 The Xylene-Induced Mouse Ear Swelling

Thirty KM mice were randomly divided into three groups of ten: the Con, the BO, and the BMS groups. The animals' ears were treated with 0.2 g/cm^2 drug each time, 3 times per day for 5 days. On the sixth day, 100 μl of xylene was dripped on the right ear with a pipette. After the model was established successfully, the animals were immediately sacrificed, and both ears were removed. The samples were immediately weighed after being punched (Xavier-Santos et al., 2018). The following formula was used to calculate the degree of the ear swelling:

The degree of ear swelling: Δm (mg) = The right ear mass (mg) − The left ear mass (mg).

2.9 Carrageenan-Induced Toe Swelling

Thirty SD rats were randomly divided into three groups of ten, the Con group, the BO group, and the BMS group, with 0.2 g/cm^2 drug topically applied evenly on the right hind paw 3 times/day for a total of 5 days. On the sixth day, each rat's right hind paw was injected with 0.1 ml carrageenan (1%). Rats' right hind paw was marked by black marker at its ankle, then, the paw volume before and after injection at 1–5 h was measured by Toes Volume Measuring Instrument, with three measurements each time point (Zahra et al., 2020). The following formula was used to calculate the toe swelling:

The swelling volume (ΔV) (ml) = V_t (ml) − V_0 (ml), where Vt is the right hind paw volume (ml) at test time and V_0 is the right bind paw volume (ml) before carrageenan injection.

2.10 Incision Wound Model

Twenty mice were randomly divided into two groups of ten, the Con group and the BO group. After dorsal fur shaving and anesthesia, a 1.5-cm long, lateral incision near the tail's root was made on the back. Then, 0.2 g/cm^2 of Con or BO was topically applied over the incision three times per day for 16 days (Getachew et al., 2019). The changes in the wound were observed and recorded.

2.11 Thermal Burn Wounds Model

The dorsal hairs of 36 SD rats were shaved 24 h before the induction of burn. After disinfection and anesthesia, the thermal burn injuries were induced on the dorsal of rats by a metal block (1.5 cm^2) heated over the flame for 10 s. After half an hour, all animals were awakened and randomly evenly divided into the Con group, the BO group, and the BMS group, with 0.2 g/cm^2 drug topically applied each time, 3 times per day for 28 days.

The wounded skin tissue was collected for H&E staining and Western blot test at the 1st, 7th, 14th, and 28th day after the model was established. Blood samples were collected from the abdominal aorta for TNF-α, VEGF, and TGF-β1 measurements, following the commercial kit instructions (Neobioscience, Shenzhen, China).

The wound contraction was evaluated by tracing the wound, using transparent paper and permanent marker, on the 1st, 7th, 14th, and 28th postwounding day. The wound area was retraced on the paper, and the changes in area were calculated, which indicated the wound contraction (Ghosh et al., 2019). The percentage of wound closure was calculated using this formula:

Wound contraction = [(wound area day1− wound area day n)/ wound area day1] ×100%, n = 7th, 14th, and 28th after wound.
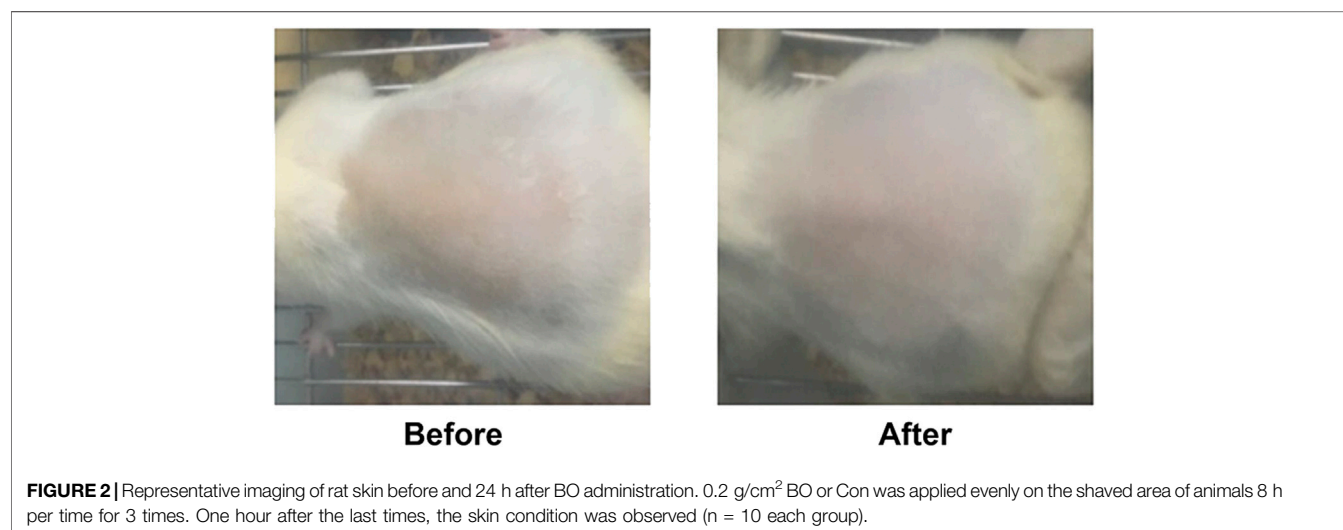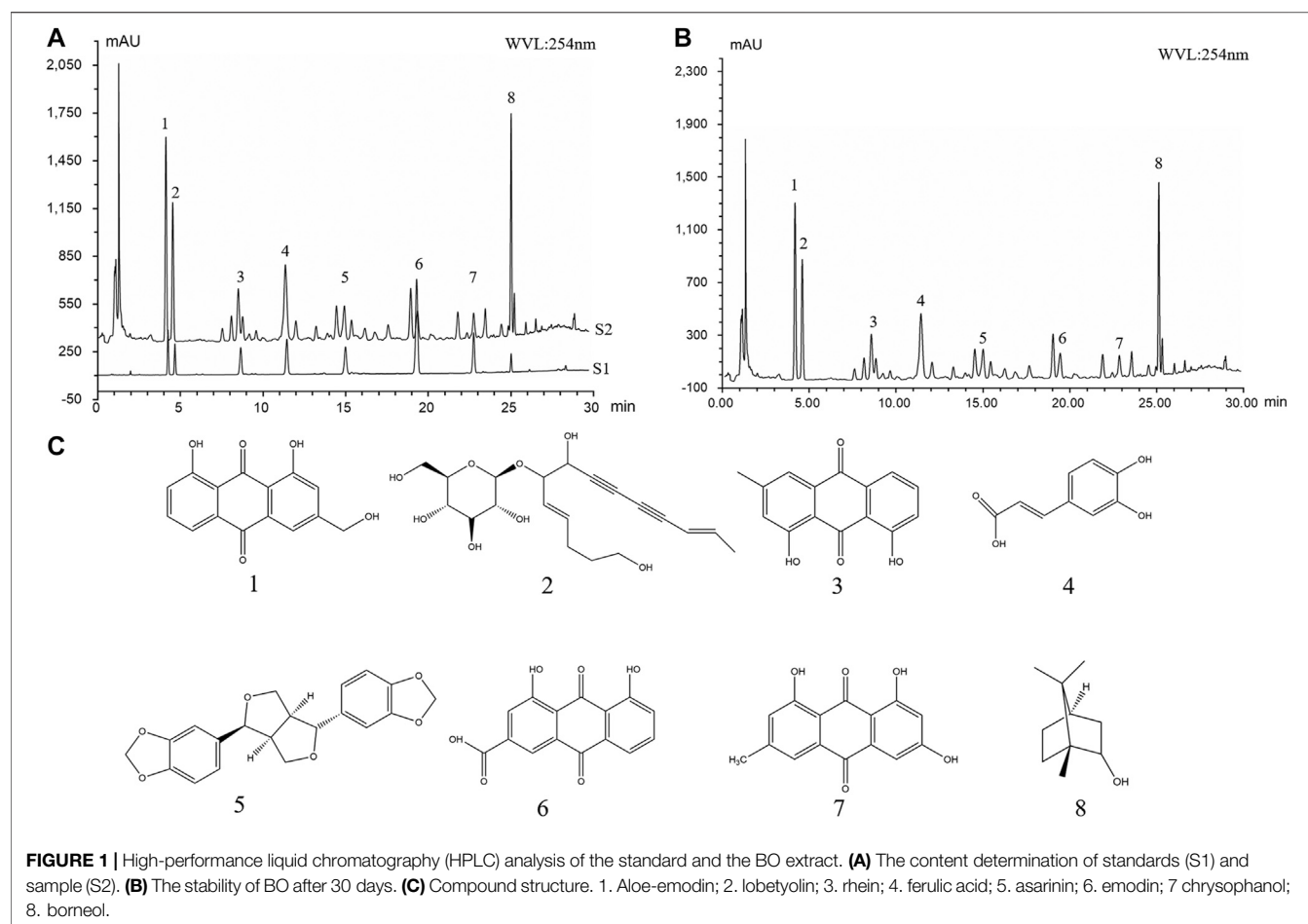
2.12 Histopathological Evaluation and Type I Collagen Staining on Burn Wound Tissue

The burn wound tissue was collected and H&E stained for histopathological evaluation. The pretreated sample tissues from rats were embedded in paraffin wax. The embedded wax blocks were then cut into 4-μm sections. The sections were routinely deparaffinized with xylene and different concentration alcohol. After the conventional staining, alcohol gradient dehydration, then, the samples were sealed with neutral resin. The observations included the epidermis, dermis, blood vessels, cells, and organelles. Two pathologists blindly read and evaluated histopathological changes with a scoring system. The detail score criteria included the regeneration of epithelial tissues, inflammatory cell infiltration, angiogenesis, and the thickness of the granulation; scores from 0 to 3 indicated from lack of recovery to full recovery. The four variables were summed to represent the histopathological score (total score: 0–12, respectively) (Kazemi et al., 2020).

The immunohistochemistry was applied to determine the type I collagen expression. In brief, after head-based antigen retrieval, each section was incubated with collagen I rabbit poly-Ab (Servicebio, 1:100), 4°C overnight. Then these sections were incubated with HRP-labeled goat anti-rabbit Ab (Servicebio, 1:200) for 2 h at room temperature. Finally, the section was stained with DAB and counterstained with hematoxylin. The sections were observed and photographed. The type I collagen expression was analyzed using ImageJ software (National Institutes of Health, Bethesda, MD, United States). The immunohistochemistry (IHC) Image Analysis Toolbox Plug-tool was first used to identify areas of positive staining. Thirty-six images were then converted to the RGB scale and the threshold tool was used to calculate the percentage area positively stained (SenthilKumar et al., 2020).

2.13 Western Blot Analysis

The protein samples (30 μg) from wound skin tissue lysates of burn rats were concentrated and separated respectively by 5 and 10% SDS-polyacrylamide gel electrophoresis (PAGE). Then, they

FIGURE 1 | High-performance liquid chromatography (HPLC) analysis of the standard and the BO extract. **(A)** The content determination of standards (S1) and sample (S2). **(B)** The stability of BO after 30 days. **(C)** Compound structure. 1. Aloe-emodin; 2. lobetyolin; 3. rhein; 4. ferulic acid; 5. asarinin; 6. emodin; 7 chrysophanol; 8. borneol.

FIGURE 2 | Representative imaging of rat skin before and 24 h after BO administration. 0.2 g/cm^2 BO or Con was applied evenly on the shaved area of animals 8 h per time for 3 times. One hour after the last times, the skin condition was observed (n = 10 each group).

were electrotransferred to PVDF membranes. Then, the membranes were blocked with a Western blocking solution (Tris-buffered saline with 0.05% Tween-20 and 5% nonfat dry milk) for 90 min and incubated at 4°C overnight with primary antibodies, phosphorylated and unphosphorylated PI3K, AKT, and mTOR polyclonal antibody (1:1000, Servicebio, Wuhan,

TABLE 1 | Changes of weight in rats (n = 10, mean ± SEM).

Days	Con	BO		
		0.1 g/cm²	0.2 g/cm²	0.4 g/cm²
1	100.75 ± 0.99	100.63 ± 1.65	102.63 ± 1.09	103.63 ± 1.83
7	127.25 ± 1.56	132.25 ± 2.44	131.13 ± 1.88	135.25 ± 3.50
14	196.50 ± 1.58	200.88 ± 4.10	207.88 ± 3.73	199.88 ± 5.35
21	239.38 ± 2.32	251.13 ± 6.24	261.13 ± 4.78	252.00 ± 4.52
28	288.25 ± 3.10	300.50 ± 8.42	310.38 ± 5.16	302.38 ± 6.00

*Con: canola oil and BO: burn ointment. The data are expressed as the mean ± SEM (n = 10), compared with the Con group; *p < 0.05, **p < 0.01.*

TABLE 2 | Effect of BO on rat organ coefficient (mg/g) (n = 10, mean ± SEM).

Organs	Con	BO		
		0.1 g/cm²	0.2 g/cm²	0.4 g/cm²
Heart	3.38 ± 0.02	3.60 ± 0.09	3.65 ± 0.07	3.66 ± 0.08
Liver	27.22 ± 0.67	28.58 ± 2.29	28.12 ± 0.4	27.89 ± 0.42
Spleen	2.07 ± 0.02	1.94 ± 0.05	2.34 ± 0.09	2.15 ± 0.17
Lungs	4.19 ± 0.20	4.27 ± 0.15	3.93 ± 0.13	4.03 ± 0.01
Kidney L	3.45 ± 0.08	3.60 ± 0.04	3.49 ± 0.01	3.69 ± 0.09
Kidney R	3.51 ± 0.03	3.72 ± 0.08	3.59 ± 0.08	3.79 ± 0.09
Testes L	6.65 ± 0.17	6.54 ± 0.05	6.26 ± 0.18	6.49 ± 0.02
Testes R	6.67 ± 0.19	6.58 ± 0.03	6.86 ± 0.01	6.53 ± 0.08
Thymus	1.64 ± 0.01	1.85 ± 0.09	1.71 ± 0.13	1.73 ± 0.06

*Con: canola oil and BO: burn ointment. The data are expressed as the mean ± SEM (n = 10), compared with the Con group; *p < 0.05, **p < 0.01.*

China), followed by washing 3 times in TBST, 5 min/time and incubation with the HPR-labeled goat anti-rabbit secondary antibodies (1:1000, Servicebio, Wuhan, China) at room temperature for 1 h. The membranes were washed 3 times in TBST, 5 min/time. Finally, the protein levels were detected by gel imaging analyzing system (Bio-Rad, California, United States) and normalized to GAPDH.

TABLE 4 | The effect of BO on blood biochemistry in rats (n = 10, mean ± SEM).

	Con	BO		
		0.1 g/cm²	0.2 g/cm²	0.4 g/cm²
ALT (U/L)	44.33 ± 1.11	45.00 ± 1.38	48.00 ± 1.92	40.67 ± 2.46
AST (U/L)	167.67 ± 4.79	191.33 ± 9.87	156.67 ± 4.13	142.33 ± 9.34
Urea (mmol/L)	7.67 ± 0.15	7.57 ± 0.21	9.23 ± 0.17	8.33 ± 0.05
Cr (μmol/L)	25.33 ± 1.46	24.33 ± 0.36	24.00 ± 0.84	22.33 ± 0.48

*ALT: alanine transaminase; AST: aspartate transaminase; Cr, creatinine; Con: canola oil, BO: burn ointment. The data are expressed as the mean ± SEM (n = 10), compared with the Con group; *p < 0.05, **p < 0.01.*

2.14 Statistical Analysis

The data were expressed as the means ± standard error of mean (SEM). Statistical analysis was performed via Student's *T* test and one-way ANOVA (SPSS Program, version 11.5; SPSS, Inc., Chicago, IL, United States). Significant differences were considered when *p* < 0.05.

3 RESULTS

3.1 Result of HPLC Analysis

HPLC was used to detect the active ingredients in the BO and its stability within 30 days. Eight main peaks were obtained, indicating aloe emodin, emodin, rhein, chrysophanol, ferulic acid, lobetyolin, asarinin, and borneol, respectively. (**Figure 1**). The result was identical with the peaks of a single compound of aloe emodin, emodin, rhein, chrysophanol, ferulic acid, lobetyolin, asarinin, and borneol. And the result suggested that BO was stable within 30 days (**Figure 1B**).

3.2 Safety Assessment of BO

The skin irritation experiment in rats was used to evaluate the safety of BO. We did not observe significant differences in the exposed skin in terms of irritation, swelling, inflammation, redness, or other abnormal changes before and after treatment
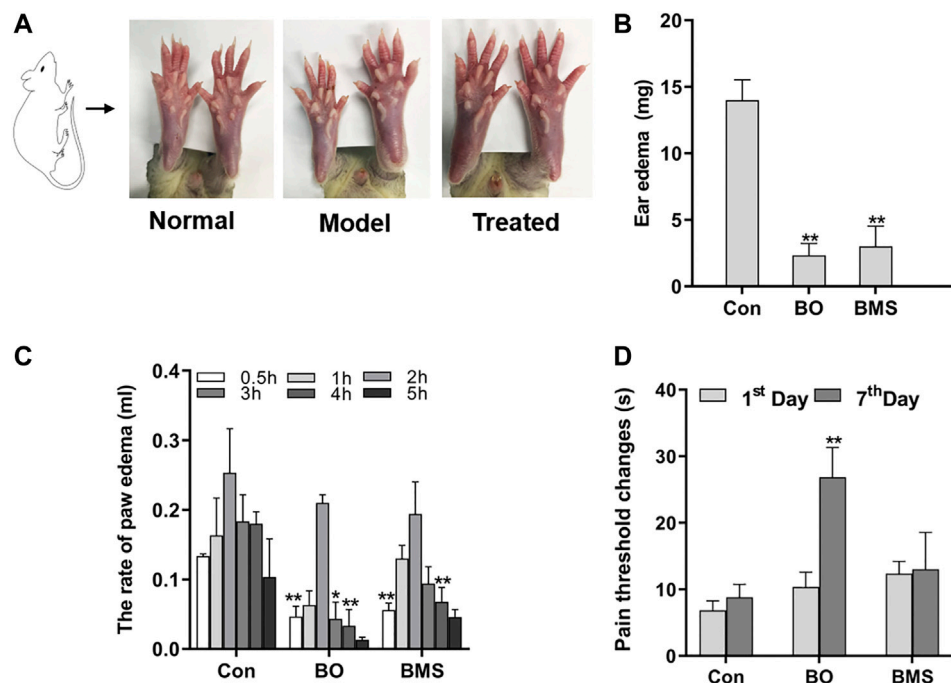
TABLE 3 | Effect of BO on blood routine (n = 10, mean ± SEM).

	Con	BO		
		0.1 g/cm²	0.2 g/cm²	0.4 g/cm²
WBC (×10⁹/L)	9.61 ± 1.18	10.45 ± 1.44	9.33 ± 1.37	8.34 ± 0.21
RBC (×1,012/L)	8.37 ± 0.13	7.67 ± 0.27	8.02 ± 0.23	8.35 ± 0.07
HB (g/L)	149.00 ± 2.39	147.67 ± 1.74	155.33 ± 1.59	160.67 ± 1.20
HCT (L/L)	0.46 ± 0.01	0.46 ± 0.00	0.48 ± 0.00	0.50 ± 0.00
MCV (fL)	54.60 ± 0.30	59.93 ± 1.55	60.03 ± 1.24	59.50 ± 0.65
MCH (pg)	17.80 ± 0.14	19.40 ± 0.44	19.43 ± 0.36	19.23 ± 0.15
MCHC (g/L)	326.00 ± 0.84	323.33 ± 1.32	324.00 ± 0.55	323.33 ± 1.80
PLT (×10⁹/L)	1098.67 ± 46.97	896.33 ± 51.98	1184.33 ± 18.58	1140.00 ± 24.26
PCT (%)	1098.67 ± 46.97	896.33 ± 51.98	1184.33 ± 18.58	1140.00 ± 24.26
MPV (fL)	7.73 ± 0.08	7.90 ± 0.09	7.87 ± 0.10	7.80 ± 0.06
PDW (fL)	8.30 ± 0.11	8.47 ± 0.15	8.53 ± 0.08	8.40 ± 0.08
P-LCR (%)	9.53 ± 0.43	10.13 ± 0.69	10.10 ± 0.57	9.70 ± 0.46

*WBC: leukocyte; RBC: erythrocyte; HB: hemoglobin; HCT: hematocrit value; MCV: mean corpuscular volume; MCH: mean corpuscular hemoglobin; MCHC: mean corpuscular hemoglobin concentration; PLT: platelet; PCT: procalcitonin; MPV: mean platelet volume; PDW: platelet distribution width; P-LCR: platelet-larger cell ratio; Con: canola oil, BO: burn ointment. The data are expressed as the mean ± SEM (n = 10), compared with the Con group; *p < 0.05, **p < 0.01.*

FIGURE 3 | The anti-inflammatory and analgesic effects among Con, BO and BMS. **(A)** Representative imaging of rat toe before and after model induction, before and after treatment. **(B)** On the 6th day, BO pretreatment reduced mouse ear edema; the data were shown as the mean ± SEM (n = 10 each group), compared with the control group; *$p < 0.05$, **$p < 0.01$. **(C)** On the 6th day, BO pretreatment decreased rats' toe swelling; the data are expressed as the mean ± SEM (n = 10 each group), compared with the control group; *$p < 0.05$, **$p < 0.01$. **(D)** BO pretreatment enhanced pain threshold; the data were expressed as the mean ± SEM (n = 9 each group), compared with the control group; *$p < 0.05$, **$p < 0.01$.

(**Figure 2**). Similarly, the preclinical trial for subacute toxicity showed no striking difference among rats treated with BO groups (0.1 g, 0.2 g, and 0.4 g/cm^2) and Con group in rat body weight (**Table 1**), the relative organ weight (**Table 2**), blood routine (**Table 3**), and biochemical analysis (**Table 4**). Thus, our results indicated that BO was safe for rats.

3.3 Effect of BO on Analgesic

As revealed in **Figure 3D**, on the 7th day, the pain threshold of the BO group was significantly increased compared to that of the Con group ($p < 0.01$), while there was no difference in the Con and the BMS group. The results indicated that BO had an analgesic effect.

3.4 Effect of BO on Inhibiting Inflammation

In the model of carrageenan-induced toe swelling, we observed that the rats treated with BO demonstrated a significant reduction in swelling at 3 h after injection (*$p < 0.05$ or **$p < 0.01$, respectively) (**Figure 3C**). In the second model, auricle swelling was significantly reduced in the BO-treated group (**$p < 0.01$) (**Figure 3B**). These results indicated that BO could inhibit inflammation.

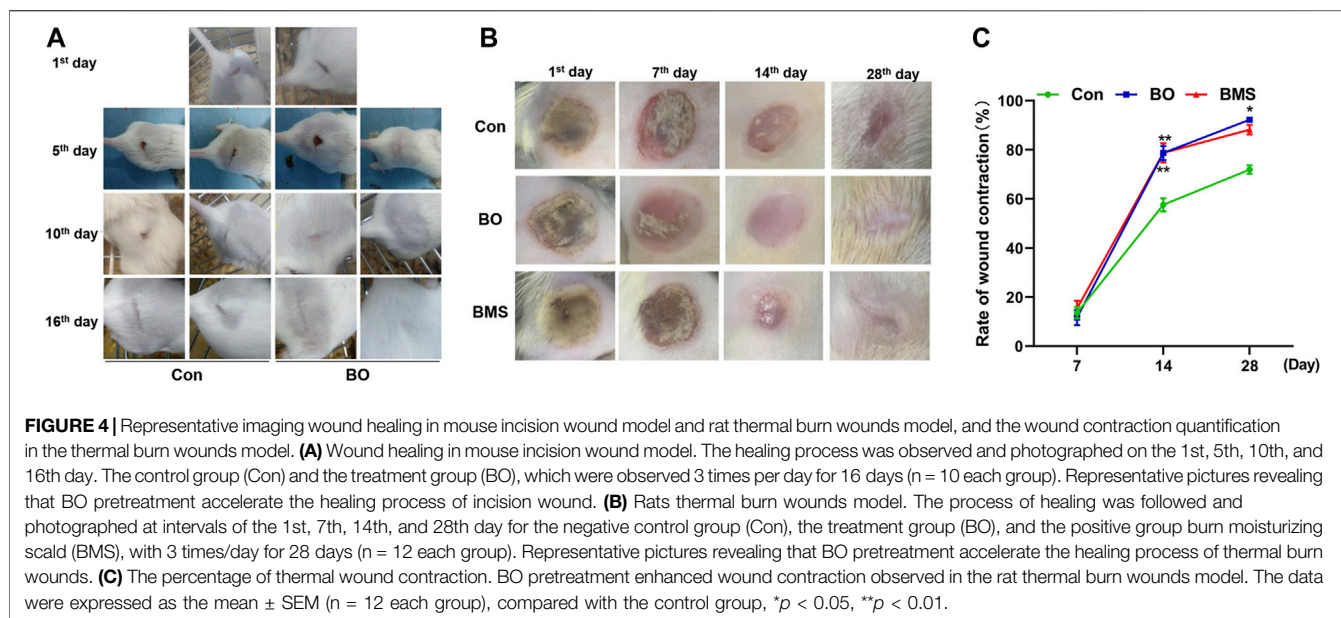## 3.5 Effects of BO on Promoting Wounds Healing

The healing process of the incision wound was observed on the 1st, 5th, 10th, and 16th day after wounding, which is demonstrated in **Figure 4A**. The observation revealed that

incision wounds treated with BO healed considerably faster in comparison with that of the Con on the 16th day. The wounds treated with BO initiated to form scar and shed the eschar gradually in contrast with the Con group. On the 16th day after the incision wound, the wounds of the BO group almost completely disappeared, whereas the scar in the Con group was still predominant. Consistent with the scar change, hair grew vigorously in the wound area in the BO-treated mice, which were entirely covered by the new epidermis.

The impact of BO on the healing process was also observed using the rat burn wound model, in which the percentage contraction ability on the 1st, 7th, 14th, and 28th day after wounding was recorded, as shown in **Figure 4B,C**. The result showed a significant ($p < 0.01$) increase in wound closure in the BO-treated group compared with the Con group on the 14th dayafter wound. On the last day, compared with the Con group, the scar of the BO group had entirely cured, and new fur had been growing on the scar, with the percentage of wound healing at 90.27 ± 2.06, which was significantly higher than that of the Con group (71.92 ± 5.92, $p < 0.01$). These results suggested that BO could promote wound healing.

3.6 Effects of BO on Skin Tissue Development

The representative H&E images of the burn wound skin (100 × magnificent) are shown in **Figure 5A**, and the histopathological assessment is given in **Figure 5B**. The epidermis was fragmented,

FIGURE 4 | Representative imaging wound healing in mouse incision wound model and rat thermal burn wounds model, and the wound contraction quantification in the thermal burn wounds model. **(A)** Wound healing in mouse incision wound model. The healing process was observed and photographed on the 1st, 5th, 10th, and 16th day. The control group (Con) and the treatment group (BO), which were observed 3 times per day for 16 days (n = 10 each group). Representative pictures revealing that BO pretreatment accelerate the healing process of incision wound. **(B)** Rats thermal burn wounds model. The process of healing was followed and photographed at intervals of the 1st, 7th, 14th, and 28th day for the negative control group (Con), the treatment group (BO), and the positive group burn moisturizing scald (BMS), with 3 times/day for 28 days (n = 12 each group). Representative pictures revealing that BO pretreatment accelerate the healing process of thermal burn wounds. **(C)** The percentage of thermal wound contraction. BO pretreatment enhanced wound contraction observed in the rat thermal burn wounds model. The data were expressed as the mean ± SEM (n = 12 each group), compared with the control group, $*p < 0.05$, $**p < 0.01$.

blood vessels and subcutaneous tissues under the dermis were severely damaged upon the burn wound creation. The BO-treated group healed faster than that of the Con group, with reduced inflammatory cell infiltration, increased fibroblast and blood vessels, and accelerated dermal and epidermal formation, at different time points. On the 28th day, the group treated with BO demonstrated an almost completely healed skin structure with normal epithelization, few inflammatory cell infiltrations, and the junction between the epidermis and dermis layers was tight and seamless when compared with the Con group. Moreover, the epidermis of rats treated with BO was much more uniform in thickness than that of the BMS group. The histopathological evaluation is shown in **Figure 5B**, which supported that the BO group was significantly improved than the Con group on the 7th, 14th, and 28th day ($p < 0.05$, respectively).

3.7 Effects of BO on Increasing Type I Collagen

The microscopic images of IHC stained burn wound skin (100× magnificent) and the percentage of collagen I changes are presented in **Figure 5C,D**, respectively. The results showed a significant increase ($p < 0.05$) in the percentage of collagen I in the BO group when compared with the Con group. In the total study period of 28 days, the irregular collagen I areas of the BO group were increased and arranged tightly and evenly. In contrast, the group treated with canola oil was slowly increased. Similarly, the maximum positive area of collagen I observed was on the 28th day in the BO group ($p < 0.01$). The results indicated that BO played an important role in promoting an increase in cellular type I collagen.

3.8 Effects of BO on Regulating the Cytokine Production

The TNF-α, VEGF, and TGF-β1 levels were detected by using the ELISA method, as shown in **Figure 6**. The levels of TNF-α were

significantly lower after BO treatment than in the Con group ($p < 0.001$), indicating a potential anti-inflammatory effect of BO (**Figure 6A**).

The VEGF levels of the BO group were significantly increased on the 14th day compared with the Con group ($p < 0.05$). And the maximum significant differences ($p < 0.01$) of the content of VEGF between the BO-treated group and the Con group were obtained on the 28th day (**Figure 6B**). These results showed that BO could increase the content of VEGF in serum after scalding.

As presented in **Figure 6C**, in the first two weeks after wounding, the content of TGF-β1 of the BO group was significantly increased, compared with the content of the Con group. However, compared with the Con group on the 28th day, the content of the BO-treated group was significantly decreased. These results showed that BO could regulate the content of TGF-β1 in blood with time after burning.

3.9 Effects of BO on Activating the PI3K-AKT-mTOR Pathway

As is evidenced in **Figure 7A**, the application of BO resulted in increased phosphorylation of PI3K, AKT, and mTOR. Densitometry of bands showed that BO did not alter the expression of the unphosphorylated protein of PI3K, AKT, and mTOR. However, it significantly upregulated its phosphorylation compared with the Con group in the last two weeks after wounding ($p < 0.01$) (**Figure 7B–D**). These results suggested that BO could upregulate the expression of the PI3K/AKT/mTOR pathway.

4 DISCUSSION

Burn and scald cause local damage to the body and systemic inflammatory response mediated by neuroendocrine (Gokakin et al., 2013), cytokine, and inflammatory mediators. These biomediators resulted in the delay of the healing of local burn
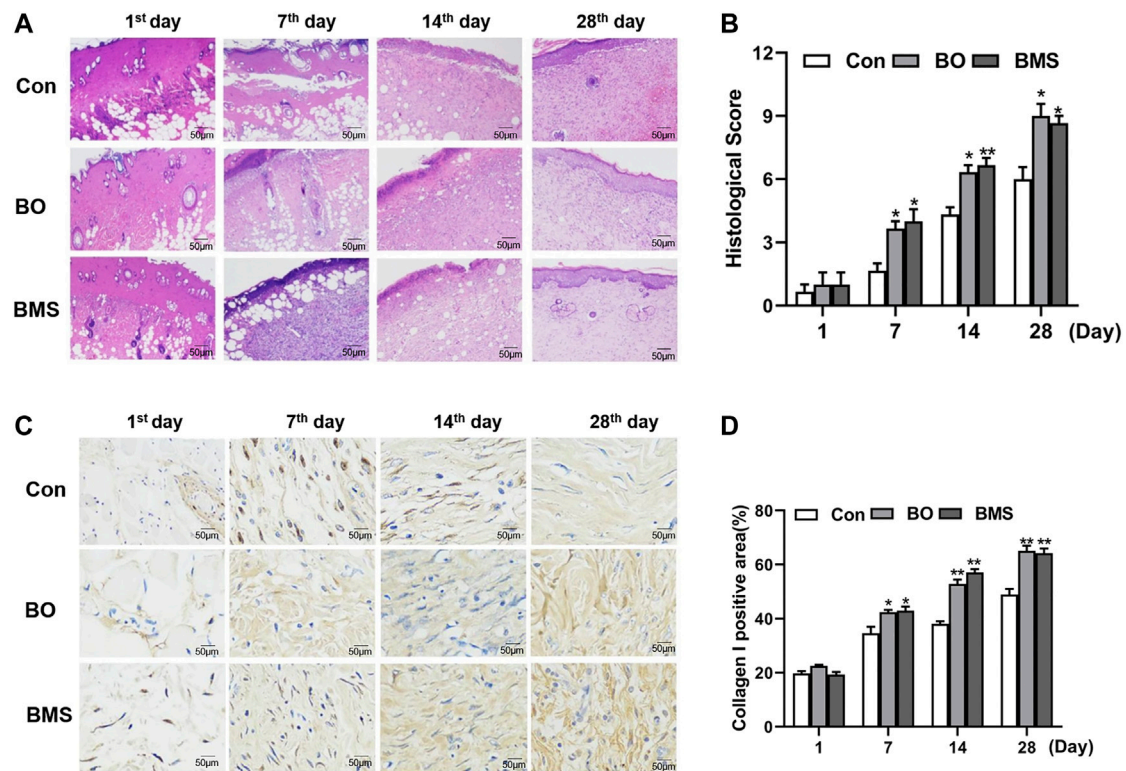
FIGURE 5 | Histopathological evaluation and the type I collagen expression before and after Con, BO, and BMS treatment in the rat thermal burn wounds model. **(A)** Representative H&E imaging of scald wound in rats. Specimens were taken from the 1st, 7th, 14th, and 28th day after modeling. The negative control group (Con), the treatment group (BO), and the positive group burn moisturizing scald (BMS) (n = 12 each group). **(B)** The results of the histological score. Comparing with the Con group, the BO group's wound was significantly healing on the 28th day (*$p < 0.05$), BMS group's wound was prominently healing on the 14th day, and the data were expressed as the mean ± SEM, (*$p < 0.05$, **$p < 0.01$, respectively, n = 12 each group). **(C)** Increased type I collagen expression in the rat scald wound after BO treatment. Specimens were taken from the 1st, 7th, 14th, and 28th day after modeling. The negative control group (Con), the treatment group (BO), and the positive group burn moisturizing scald (BMS) (n = 12 each group). **(D)** The results of collagen Ⅰ expression semiquantitation, compared with the control group. BO could upregulate the collagen Ⅰ of wound area markedly from the 7th day; the data were expressed as the mean ± SEM (n = 12 each group); *$p < 0.05$, **$p < 0.01$, respectively.

and scald wounds and trigger of various, severe complications, such as pain, making treatment difficult (Naseri et al., 2018). The healing of burn and scald wounds involves three complex processes: inflammation, tissue hyperplasia, and regeneration. These three

processes are not independent but overlap and develop in a particular order (Govindaraju et al., 2019). Exogenous damage will stimulate the body to secrete various growth factors, such as VEGF and TGF-β1, which can promote cell migration, proliferation,
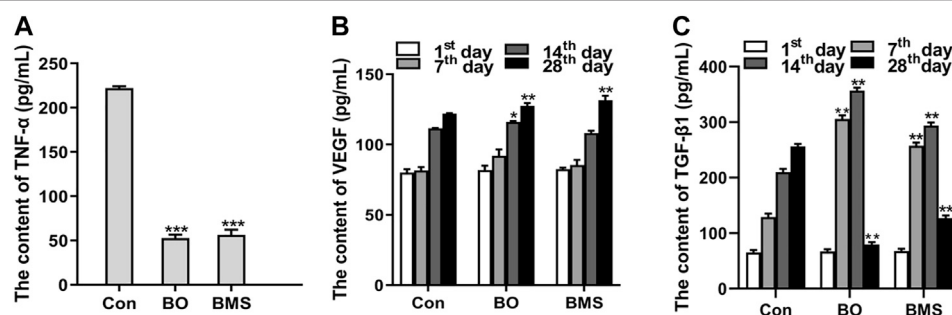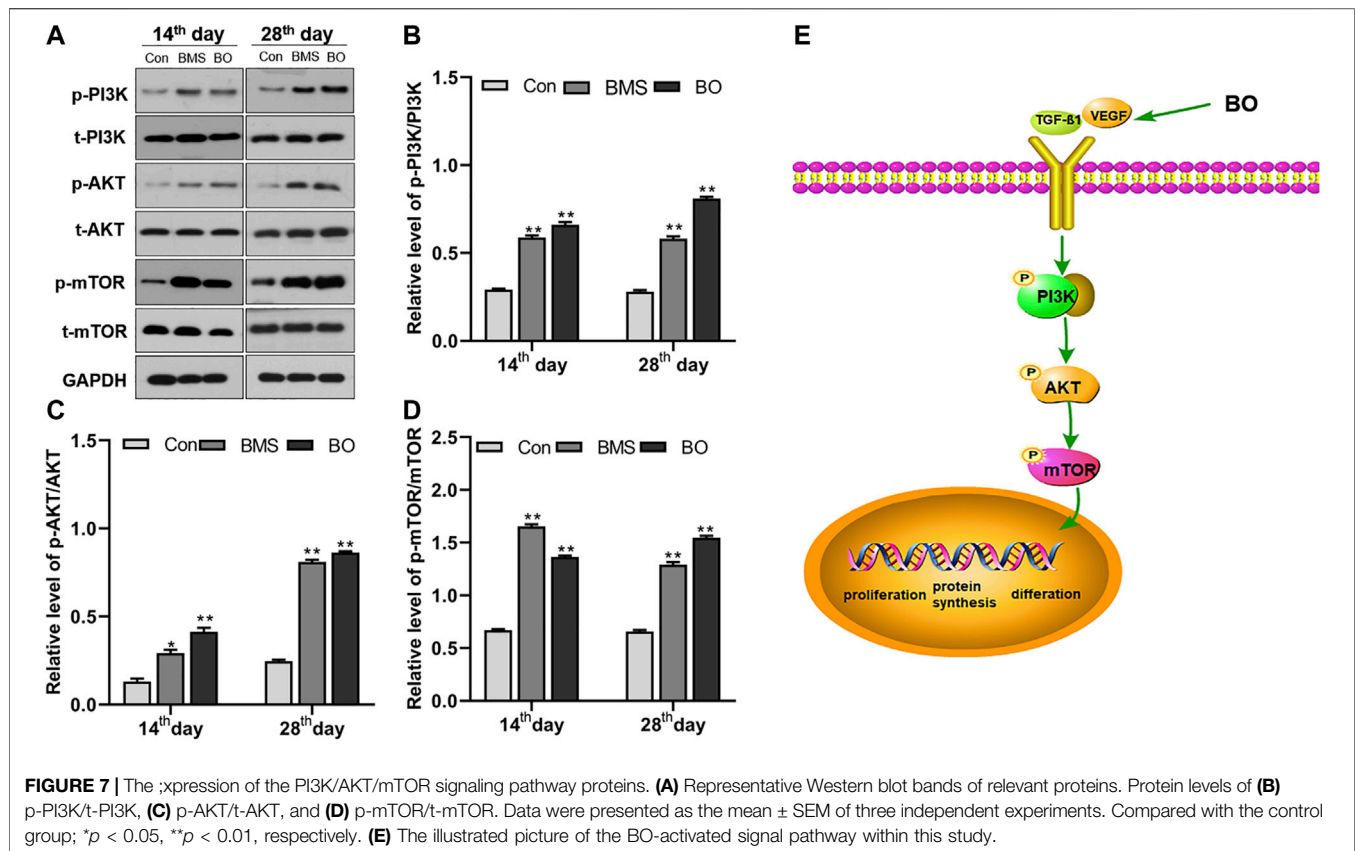

FIGURE 6 | The serum cytokine level before and after Con, BO, and BMS treatment. **(A)** Downregulated TNF-α level after BO treatment. The data are expressed as the mean ± SEM (n = 12 each group), compared with the Con group, ***$p < 0.001$. **(B)** The content of VEGF, which was tested on the 1st, 7th, 14th, and 28th day. The data were expressed as the mean ± SEM (n = 12 each group), compared with the control group; *$p < 0.05$, **$p < 0.01$, respectively. **(C)** The content of TGF-β1, which was tested at the 1st, 7th, 14th, and 28th day. The data were expressed as the mean ± SEM (n = 12 each group), compared with the control group, **$p < 0.01$.

FIGURE 7 | The ;xpression of the PI3K/AKT/mTOR signaling pathway proteins. **(A)** Representative Western blot bands of relevant proteins. Protein levels of **(B)** p-PI3K/t-PI3K, **(C)** p-AKT/t-AKT, and **(D)** p-mTOR/t-mTOR. Data were presented as the mean ± SEM of three independent experiments. Compared with the control group; *$p < 0.05$, **$p < 0.01$, respectively. **(E)** The illustrated picture of the BO-activated signal pathway within this study.

and differentiation, to help wound constriction and recovery. The damaged wound and these biomediators can also activate signaling pathways associated with wound repair, such as the PI3K/AKT/mTOR pathway (Cho et al., 2019; Zhang et al., 2020).

The inflammatory response is the first step after tissue damage and is essential for skin repair (Glim et al., 2015). A prolonged inflammatory response will be harmful to the body and lead to unexpected complications. Therefore, it is crucial to suppress inflammation and pain during tissue recovery. The clinical signs of inflammation are redness, swelling, heat, and pain (Yu et al., 2014). Swelling is a pathological manifestation of inflammation, and it is generally believed that eliminating swelling can achieve anti-inflammatory effects (Srivastava et al., 2018; Chen et al., 2019). To investigate the anti-inflammatory and analgesic effects of BO, we used a variety of classical animal models of inflammation, including mouse auricular swelling, rat toe swelling, and mouse hot plate test. These results showed that BO could inhibit auricular swelling in mice and toe swelling in rats ($p < 0.05$, $p < 0.01$, respectively), indicating its strong anti-inflammatory activity. In addition, the analgesic results showed that BO could relieve pain, and the pain threshold of BO-treated mice was significantly higher than that of control mice ($p < 0.01$), supporting the analgesic effect of BO.

When the wound presents with early inflammation, the body's defense system is activated, with the formation of a protective barrier and several growth factors production (Silvestre et al., 2018). TNF-α and VEGF are two of those cytokines and are critical in the wound

healing process. TNF-α, one of the most vital proinflammatory cytokines, can induce vasodilatation, edema, and leukocyte adhesion to the epithelium. It can also regulate blood coagulation and contribute to oxidative stress in inflammation (Zelova and Hosek., 2013). Studies have shown that medications could decrease the release of inflammatory cytokines, such as TNF-α, reduce the inflammatory response, and promote wound healing (Weimann et al., 2018). In the present study, we found that BO could inhibit TNF-α release, which might be one potential anti-inflammatory mechanism of BO.

The secretion of VEGF in the healing process also exerts a significant effect, as VEGF can promote vascular endothelial cell proliferation and survival, accelerating the formation of new blood vessels (Peng et al., 2016; Wagner et al., 2016; Yan et al., 2017; Yen et al., 2018). The blood vessels are the channels of nutrient delivery in the body (Johnson and Wilgus, 2014), and it will ensure that the tissues and organs are provided with sufficient requirements for new skin formation (Sorg et al., 2018). Our results indicated that when the skin was scalded by high temperature, BO could upregulate the release of VEGF to facilitate wound healing. Also, collagen is necessary for repairing wounds. Studies had illustrated that TGF-β1 could regulate type I collagen gene expression and translation (Guo et al., 2018). However, the continuous increase of collagen I in the tissue will cause pathological scars to develop. Our results showed that the TGF-β1 content in the BO-treated group tended to increase early but decreased later. Based on these results, we speculated that with BO treatment, TGF-β1 stimulated the release of type I collagen

at the early course to promote skin repair. At the later stage, to avoid collagen over-proliferation and scar formation, TGF-β1 expression is downregulated to inhibit the increase of collagen I.

The PI3K/AKT/mTOR signaling pathway is found in various cells and participates in cell growth, proliferation, apoptosis, and differentiation (Polivka and Janku., 2014; Peng et al., 2016; Dong et al., 2020). PI3K can be activated by growth factors, such as VEGF and TGF-β1 (Cui et al., 2017; Kim et al., 2018a; Zhang et al., 2019c). The activated state of growth factor receptors quickly phosphorylates phosphatidylinositol (4,5) P2 (PIP2) to obtain phosphatidylinositol (3,4,5) P3 (PI3P) (Zhang et al., 2019a). Protein kinase B (AKT) is one of the proteins downstream of PI3K; it is recruited by PI3P and phosphorylated by 3-phosphoinositide-dependent kinases (PDK-1) (Yudushkin, 2019). Then, p-AKT can regulate the protein level of phosphorylated mTOR to promote cellular growth and reproduction (Xu et al., 2018). Fibroblasts are a significant factor involved in wound healing. When tissue injury occurs, this signaling pathway is activated by increased VEGF and TGF-β1 levels, initiating fibroblasts migration to the wound site, proliferation, and differentiation into myofiibroblasts (Eming et al., 2014). These cells can help contract the wound border and contribute to producing collagen-like proteins, which are necessary for healing wounds and forming new skin tissue, accelerating the repair of burn wounds (Ohlund et al., 2014; Brenner et al., 2016; Xiao et al., 2017). Our Western blotting analysis showed that compared with the Con group, the BO-treated group had significantly increased activation of the PI3K/AKT/mTOR signaling pathway, with gradually upregulated phosphorylated proteins of this pathway. This finding suggested that the preliminary mechanism by which BO promoted burn repair might be related to the activation of the PI3K/AKT/mTOR signaling pathway.

In order to evaluate the quality and standard of preparations of BO, we detected and analyzed eight quality marker components in BO by HPLC, which contained aloe emodin, emodin, rhein, chrysophanol, ferulic acid, lobetyolin, asarinin, and borneol. The active compounds aloe emodin, emodin, rhein, and chrysophanol were reported to be quality markers of *Rheum palmatum* L. with anti-inflammatory activity and to promote wound healing, and their pathways of action may be involved in the proliferation and differentiation of skin epithelial cells through the regulation of PI3K/AKT pathway (Dong et al., 2016; Wu et al., 2017; Dong et al., 2019; Su et al., 2020). Ferulic acid is a quality marker of *Angelica sinensis* (Oliv.) Diels, which can promote wound healing (Wei et al., 2016). Lobetyolin is a quality marker of *Codonopsis pilosula* (Franch.) Nannf. Ferulic acid and lobetyolin can increase the content of VEGF in blood vessels and promote angiogenesis (Lin et al., 2010; Wang et al., 2020). Asarinin, a quality marker of *Asarum sieboldii* Miq., increases TGF-β content, reduces toe swelling, and regulates inflammation in arthritis model mice through the NF-κB pathway (Dai et al., 2019). And *Borneolum syntheticum*, whose chemical component is borneol, is a natural transdermal absorption enhancer that promotes BO absorption (Dai et al., 2018).

All of the above compounds have been reported to exhibit anti-inflammatory, analgesic, and skin healing promoting effects individually, but the combined effects of these compounds have not been investigated. In the present report, we investigated the role and mechanism of BO containing a mixture of active ingredients in anti-inflammatory and skin healing promotion. Our study showed that BO had a promising effect, which was most likely achieved by modulating the P13K/AKT transduction pathway.

5 CONCLUSION

In conclusion, this study demonstrated that BO is a pharmacologically active traditional Chinese medical formulation for promoting wound healing. It can accelerate wound healing through PI3K/AKT/mTOR signaling pathway and increase the key cytokines VEGF and TGF-β1 to further help tissue recovery. This study provides an insight into the in vivo effects of this preparation and its mechanism of action of BO in the treatment of burns and scalds, which will provide some guidance for the clinical application and development of BO.

DATA AVAILABILITY STATEMENT

The original contributions presented in the study are included in the article/ further inquiries can be directed to the corresponding authors.

ETHICS STATEMENT

The animal study was reviewed and approved by the Institutional Animal Ethical Committee of Central South University for Nationalities and was performed under the guidelines of the committee; the permit number for the use of animals was no. 2020-scuec-029.

AUTHOR CONTRIBUTIONS

MX and BH designed the research and wrote the paper. DG and LW performed animal experiments. QS carried out data sorting and statistics. HS performed biochemistry and immunology tests. JC supplied BO. All authors reviewed the manuscript.

FUNDING

REFERENCES

Ariyo, O. O., Ajayi, A. M., Ben-Azu, B., and Aderibigbe, A. O. (2020). Anti-nociceptive and anti-inflammatory activities of ethanol extract and fractions of Morus mesozygia Stapf (Moraceae) leaves and its underlying mechanisms in rodents. *J. Ethnopharmacol.* 259, 112934. doi:10.1016/j.jep.2020.11293410.1016/j.jep.2020.112934

Boldeanu, L., Boldeanu, M. V., Bogdan, M., Meca, A. D., Coman, C. G., Buca, B. R., et al. (2020). Immunological approaches and therapy in burns (review). *Exp. Ther. Med.* 20 (3), 2361–2367. doi:10.3892/etm.2020.8932

Brenner, A. K., Andersson, T. T., and Bruserud, O. (2016). The complexity of targeting PI3K-Akt-mTOR signalling in human acute myeloid leukaemia: the importance of leukemic cell heterogeneity, neighbouring mesenchymal stem cells and immunocompetent cells. *Molecules* 21 (11), 1512. doi:10.3390/molecules21111512

Cao, Y. J., Pu, Z. J., Tang, Y. P., Shen, J., Chen, Y. Y., Kang, A., et al. (2017). Advances in bio-active constituents, pharmacology and clinical applications of rhubarb. *Chin. Med.* 12, 36. doi:10.1186/s13020-017-0158-5

Chen, J., Si, M., Wang, Y., Liu, L., Zhang, Y., Zhou, A., et al. (2019). Ginsenoside metabolite compound K exerts anti-inflammatory and analgesic effects via downregulating COX_2. *Inflammopharmacology* 27 (1), 157–166. doi:10.1007/s10787-018-0504-y

Cho, H., Kim, J., Park, J., Hong, S., Kim, D., and Seo, K. (2019). Kochia scoparia seed extract suppresses VEGF-induced angiogenesis via modulating VEGF receptor 2 and PI3K/AKT/mTOR pathways. *Pharm. Biol.* 57 (1), 684–693. doi:10.1080/13880209.2019.1672753

Cui, J., Li, Z., Jin, C., and Jin, Z. (2020). Knockdown of fibronectin extra domain B suppresses TGF-β1-mediated cell proliferation and collagen deposition in keloid fibroblasts via AKT/ERK signaling pathway. *Biochem. Bioph. Res. Co.* 526 (4), 1131–1137. doi:10.1016/j.bbrc.2020.04.021

Cui, M., Pan, Z., and Pan, L. (2017). Danggui Buxue extract-loaded liposomes in thermosensitive gel enhance *in vivo* dermal wound healing via activation of the VEGF/PI3K/Akt and TGF-β/Smads signaling pathway. *Evid. Based Complement. Alternat. Med.* 2017, 8407249. doi:10.1155/2017/8407249

Dai, Q., Wang, M., Li, Y., and Li, J. (2019). Amelioration of CIA by asarinin is associated to a downregulation of TLR9/NF-κB and regulation of Th1/Th2/Treg expression. *Biol. Pharm. Bull.* 42 (7), 1172–1178. doi:10.1248/bpb.b19-00083

Dai, X., Wang, R., Wu, Z., Guo, S., Yang, C., Ma, L., et al. (2018). Permeation-enhancing effects and mechanisms of borneol and menthol on ligustrazine: a multiscale study using *in vitro* and coarse-grained molecular dynamics simulation methods. *Chem. Biol. Drug Des.* 92 (5), 1830–1837. doi:10.1111/cbdd.13350

Dong, X., Fu, J., Yin, X., Cao, S., Li, X., Lin, L., et al. (2016). Emodin: a review of its pharmacology, toxicity and pharmacokinetics. *Phytother Res.* 30 (8), 1207–1218. doi:10.1002/ptr.5631

Dong, X., He, Z., Xiang, G., Cai, L., Xu, Z., Mao, C., et al. (2020). Paeoniflorin promotes angiogenesis and tissue regeneration in a full-thickness cutaneous wound model through the PI3K/AKT pathway. *J. Cel Physiol.* 235 (12), 9933–9945. doi:10.1002/jcp.29808

Dong, X., Zeng, Y., Liu, Y., You, L., Yin, X., Fu, J., et al. (2019). Aloe-emodin: a review of its pharmacology, toxicity, and pharmacokinetics. *Phytother Res.* 34 (2), 270–281. doi:10.1002/ptr.6532

Eming, S. A., Martin, P., and Tomic-Canic, M. (2014). Wound repair and regeneration: mechanisms, signaling, and translation. *Sci. Transl. Med.* 6 (265), 265sr6. doi:10.1126/scitranslmed.3009337

Gao, S. M., Liu, J. S., Wang, M., Cao, T. T., Qi, Y. D., Zhang, B. G., et al. (2018). Traditional uses, phytochemistry, pharmacology and toxicology of Codonopsis: a review. *J. Ethnopharmacol.* 219, 50–70. doi:10.1016/j.jep.2018.02.039

Getachew, A., Assefa, B., and Wubayehu, K. (2019). Evaluation of wound healing and anti-inflammatory activity of the leaves of Calpurnia aurea (Ait.) Benth (fabaceae) in mice. *Wound Med.* 25 (1), 100151. doi:10.1016/j.wndm.2019.100151

Ghosh, D., Mondal, S., and Ramakrishna, K. (2019). A topical ointment formulation containing leaves extract of Aegialitis rotundifolia Roxb., accelerates excision, incision and burn wound healing in rats. *Wound Med.* 26 (1), 100168. doi:10.1016/j.wndm.2019.100168

Glim, J. E., Beelen, R. H., Niessen, F. B., Everts, V., and Ulrich, M. M. (2015). The number of immune cells is lower in healthy oral mucosa compared to skin and does not increase after scarring. *Arch. Oral Biol.* 60 (2), 272–281. doi:10.1016/j.archoralbio.2014.10.008

Gokakin, A. K., Deveci, K., Kurt, A., Karakus, B. C., Duger, C., Tuzcu, M., et al. (2013). The protective effects of sildenafil in acute lung injury in a rat model of severe scald burn: A biochemical and histopathological study. *Burns* 39 (6), 1193–1199. doi:10.1016/j.burns.2012.12.017

Gonzalez, A. C., Costa, T. F., Andrade, Z. A., and Medrado, A. R. (2016). Wound healing - a literature review. *Bras Dermatol.* 91 (5), 614–620. doi:10.1590/abd1806-4841.20164741

Govindaraju, P., Todd, L., Shetye, S., Monslow, J., and Puré, E. (2019). CD44-dependent inflammation, fibrogenesis, and collagenolysis regulates extracellular matrix remodeling and tensile strength during cutaneous wound healing. *Matrix Biol.* 75–76, 314–330. doi:10.1016/j.matbio.2018.06.004

Gundogdu, G., Gundogdu, K., Nalci, K. A., Demirkaya, A. K., Yilmaz, T. S., Demirkaya, M. F., et al. (2019). The effect of parietin isolated from *Rheum ribes* L. on *in vitro* wound model using human dermal fibroblast cells. *Int. J. Low Extrem. Wounds* 18 (1), 56–64. doi:10.1177/1534734618819660

Guo, S., Meng, X. W., Yang, X. S., Liu, X. F., Ou-Yang, C. H., and Liu, C. (2018). Curcumin administration suppresses collagen synthesis in the hearts of rats with experimental diabetes. *Acta Pharmacol. Sin.* 39 (2), 195–204. doi:10.1038/aps.2017.92

Johnson, K. E., and Wilgus, T. A. (2014). Vascular endothelial growth factor and angiogenesis in the regulation of cutaneous wound repair. *Adv. Wound Care* 3 (10), 647–661. doi:10.1089/wound.2013.0517

Kaddoura, I., Abu-Sittah, G., Ibrahim, A., Karamanoukian, R., and Papazian, N. (2017). Burn injury: review of pathophysiology and therapeutic modalities in major burns. *Ann. Burns Fire Disasters* 30 (2), 95–102.

Kazemi, M., Mohammadifar, M., Aghadavoud, E., Vakili, Z., Aarabi, M. H., and Talaei, S. A. (2020). Deep skin wound healing potential of lavender essential oil and licorice extract in a nanoemulsion form: biochemical, histopathological and gene expression evidences. *J. Tissue Viability* 29 (2), 116–124. doi:10.1016/j.jtv.2020.03.004

Kim, D., Jo, Y., Garagiola, U., Choi, J., Kang, Y., Oh, J., et al. (2020). Increased level of vascular endothelial growth factors by 4-hexylresorcinol is mediated by transforming growth factor-β1 and accelerates capillary regeneration in the burns in diabetic animals. *Int. J. Mol. Sci.* 21 (10), 3473. doi:10.3390/ijms21103473

Kim, K. K., Sheppard, D., and Chapman, H. A. (2018a). TGF-β1 signaling and tissue fibrosis. *Cold Spring Harb Perspect. Biol.* 10 (4), a022293. doi:10.1101/cshperspect.a022293

Kim, Y. J., Lee, J. Y., Kim, H. J., Kim, D. H., Lee, T. H., Kang, M. S., et al. (2018b). Anti-inflammatory effects of Angelica sinensis (Oliv.) Diels water extract on RAW 264.7 induced with lipopolysaccharide. *Nutrients* 10 (5), 647. doi:10.3390/nu10050647

Lin, C. M., Chiu, J. H., Wu, I. H., Wang, B. W., Pan, C. M., and Chen, Y. H. (2010). Ferulic acid augments angiogenesis via VEGF, PDGF and HIF-1 alpha. *J. Nutr. Biochem.* 21 (7), 627–633. doi:10.1016/j.jnutbio.2009.04.001

lund, D., Elyada, E., and Tuveson, D. (2014). Fibroblast heterogeneity in the cancer wound. *J. Exp. Med.* 211 (8), 1503–1523. doi:10.1084/jem.20140692

Naseri, N., Kalantar, K., and Amirghofran, Z. (2018). Anti-inflammatory activity of *Echium amoenum* extract on macrophages mediated by inhibition of inflammatory mediators and cytokines expression. *Res. Pharm. Sci.* 13 (1), 73–81. doi:10.4103/1735-5362.220970

Peng, N., Gao, S., Guo, X., Wang, G., Cheng, C., Li, M., et al. (2016). Silencing of VEGF inhibits human osteosarcoma angiogenesis and promotes cell apoptosis via VEGF/PI3K/AKT signaling pathway. *Am. J. Transl. Res.* 8 (2), 1005–1015.

Polivka, J. J., and Janku, F. (2014). Molecular targets for cancer therapy in the PI3K/AKT/mTOR pathway. *Pharmacol. Ther.* 142 (2), 164–175. doi:10.1016/j.pharmthera.2013.12.004

Riepl, M. (2020). Compounding pearls: wound care: burn healing, part 1. *Int. J. Pharm. Compd.* 24 (3), 188–193.

Roskoski, R. J. (2017). Vascular endothelial growth factor (VEGF) and VEGF receptor inhibitors in the treatment of renal cell carcinomas. *Pharmacol. Res.* 120, 116–132. doi:10.1016/j.phrs.2017.03.010

SenthilKumar, G., Fisher, M. M., Skiba, J. H., Miller, M. C., Brennan, S. R., Kaushik, S., et al. (2020). FGFR inhibition enhances sensitivity to radiation in non-small

cell lung cancer. *Mol. Cancer Ther.* 19 (6), 1255–1265. doi:10.1158/1535-7163.
MCT-19-0931

Shan, Y., Peng, L., Liu, X., Chen, X., Xiong, J., and Gao, J. (2015). Silk fibroin/gelatin
electrospun nanofibrous dressing functionalized with astragaloside IV induces
healing and anti-scar effects on burn wound. *Int. J. Pharm.* 479 (2), 291–301.
doi:10.1016/j.ijpharm.2014.12.067

Shen, C., Zhang, Z., Xie, T., Ji, J., Xu, J., Lin, L., et al. (2019). Rhein suppresses lung
inflammatory injury induced by human respiratory syncytial virus through
inhibiting NLRP3 inflammasome activation via NF-κB pathway in mice. *Front.
Pharmacol.* 10, 1600. doi:10.3389/fphar.2019.01600

Silvestre, M. C., Sato, M. N., and Reis, V. M. S. D. (2018). Innate immunity and
effector and regulatory mechanisms involved in allergic contact dermatitis. *Bras
Dermatol.* 93 (2), 242–250. doi:10.1590/abd1806-4841.20186340

Sorg, H., Tilkorn, D. J., Mirastschijski, U., Hauser, J., and Kraemer, R. (2018). Panta
Rhei: neovascularization, angiogenesis and nutritive perfusion in wound
healing. *Eur. Surg. Res.* 59 (3–4), 232–241. doi:10.1159/000492410

Srivastava, R. A. K., Cornicelli, J. A., Markham, B., and Bisgaier, C. L. (2018).
Gemcabene, a first-in-class hypolipidemic small molecule in clinical
development, attenuates osteoarthritis and pain in animal models of
arthritis and pain. *Front. Pharmacol.* 9, 471. doi:10.3389/fphar.2018.00471

Su, S., Wu, J., Gao, Y., Luo, Y., Yang, D., and Wang, P. (2020). The pharmacological
properties of chrysophanol, the recent advances. *Biomed. Pharmacother.* 125,
110002. doi:10.1016/j.biopha.2020.110002

Upadhyay, N. K., Kumar, R., Mandotra, S. K., Meena, R. N., Siddiqui, M. S.,
Sawhney, R. C., et al. (2009). Safety and healing efficacy of Sea buckthorn
(*Hippophae rhamnoides* L.) seed oil on burn wounds in rats. *Food Chem.
Toxicol.* 47 (6), 1146–1153. doi:10.1016/j.fct.2009.02.002

Wagner, V. P., Curra, M., Webber, L. P., Nor, C., Matte, U., Meurer, L., et al. (2016).
Photobiomodulation regulates cytokine release and new blood vessel formation
during oral wound healing in rats. *Lasers Med. Sci.* 31 (4), 665–671. doi:10.1007/
s10103-016-1904-0

Wang, C., Hui, J., Zhu, X., Cui, S., Cui, Z., and Xu, D. (2020). Lobetyolin efficiently
promotes angiogenesis and neuronal development in transgenic zebrafish. *Nat.
Product. Commun.* 15 (8), 1–7. doi:10.1177/1934578X20937174

Wang, Y., Beekman, J., Hew, J., Jackson, S., Issler-Fisher, A. C., Parungao, R., et al.
(2018). Burn injury: challenges and advances in burn wound healing, infection,
pain and scarring. *Adv. Drug Deliv. Rev.* 123, 3–17. doi:10.1016/j.addr.2017.
09.018

Wei, W. L., Zeng, R., Gu, C. M., Qu, Y., and Huang, L. F. (2016). Angelica sinensis
in China-A review of botanical profile, ethnopharmacology, phytochemistry
and chemical analysis. *J. Ethnopharmacol.* 190, 116–141. doi:10.1016/j.jep.2016.
05.023

Weimann, E., Silva, M., Murata, G. M., Bortolon, J. R., Dermargos, A., Curi, R.,
et al. (2018). Topical anti-inflammatory activity of palmitoleic acid improves
wound healing. *Plos One* 13 (10), e0205338. doi:10.1371/journal.pone.
0205338

Wu, C., Cao, H., Zhou, H., Sun, L., Xue, J., Li, J., et al. (2017). Research progress on
the antitumor effects of Rhein: literature review. *Anticancer Agents Med. Chem.*
17 (12), 1624–1632. doi:10.2174/1871520615666150930112631

Xavier-Santos, J. B., Félix-Silva, J., Passos, J. G. R., Gomes, J. A. S., Fernandes, J. M.,
Garcia, V. B., et al. (2018). Development of an effective and safe topical anti-
inflammatory gel containing *Jatropha gossypiifolia* leaf extract: results from a
pre-clinical trial in mice. *J. Ethnopharmacol.* 227, 268–278. doi:10.1016/j.jep.
2018.09.007

Xiao, W., Tang, H., Wu, M., Liao, Y., Li, K., Li, L., et al. (2017). Ozone oil promotes
wound healing by increasing the migration of fibroblasts via PI3K/Akt/mTOR
signaling pathway. *Biosci. Rep.* 37 (6), BSR20170658. doi:10.1042/BSR20170658

Xu, J., Wang, S., Feng, T., Chen, Y., and Yang, G. (2018). Hypoglycemic and
hypolipidemic effects of total saponins from Stauntonia chinensis in diabetic
db/db mice. *J. Cell. Mol. Med.* 22 (12), 6026–6038. doi:10.1111/jcmm.13876

Yan, D., He, Y., Dai, J., Yang, L., Wang, X., and Ruan, Q. (2017). Vascular
endothelial growth factor modified macrophages transdifferentiate into
endothelial-like cells and decrease foam cell formation. *Biosci. Rep.* 37 (3),
BSR20170002. doi:10.1042/BSR20170002

Yang, W. T., Ke, C. Y., Wu, W. T., Harn, H. J., Tseng, Y. H., and Lee, R. P. (2017).
Effects of Angelica dahurica and Rheum officinale extracts on excisional wound
healing in rats. *Evid. Based Complement. Alternat. Med.* 2017, 1583031. doi:10.
1155/2017/1583031

Yaseen, H. S., Asif, M., Saadullah, M., MahrukhAsghar, S., Shams, M. U., et al.
(2020). Methanolic extract of Ephedra ciliata promotes wound healing and
arrests inflammatory cascade *in vivo* through downregulation of TNF-α.
Inflammopharmacology 28 (6), 1691–1704. doi:10.1007/s10787-020-00713-7

Yen, Y. H., Pu, C. M., Liu, C. W., Chen, Y. C., Chen, Y. C., Liang, C. J., et al. (2018).
Curcumin accelerates cutaneous wound healing via multiple biological actions:
the involvement of TNF-α, MMP-9, α-SMA, and collagen. *Int. Wound J.* 15 (4),
605–617. doi:10.1111/iwj.12904

Yu, T., Li, Y. J., Bian, A. H., Zuo, H. B., Zhu, T. W., Ji, S. X., et al. (2014). The
regulatory role of activating transcription factor 2 in inflammation. *Mediators
Inflamm.* 2014, 950472. doi:10.1155/2014/950472

Yudushkin, I. (2019). Getting the AKT together: guiding intracellular AKT activity
by PI3K. *Biomolecules* 9 (2), 67. doi:10.3390/biom9020067

Zahra, Z., Khan, M. R., Shah, S. A., Maryam, S., Majid, M., Younis, T., et al. (2020).
Vincetoxicum arnottianum ameliorate inflammation by suppressing oxidative
stress and pro-inflammatory mediators in rat. *J. Ethnopharmacol.* 252, 112565.
doi:10.1016/j.jep.2020.112565

Zelova, H., and Hosek, J. (2013). TNF-α signaling and inflammation: interactions
between old acquaintances. *Inflamm. Res.* 62 (7), 641–651. doi:10.1007/s00011-
013-0633-0

Zhang, M., Jang, H., and Nussinov, R. (2019a). The mechanism of PI3Kα activation
at the atomic level. *Chem. Sci.* 10 (12), 3671–3680. doi:10.1039/c8sc04498h

Zhang, Q., Hu, F., Guo, F., Zhou, Q., Xiang, H., and Shang, D. (2019b). Emodin
attenuates adenosine triphosphate-induced pancreatic ductal cell injury *in vitro*
via the inhibition of the P2X7/NLRP3 signaling pathway. *Oncol. Rep.* 42,
1589–1597. doi:10.3892/or.2019.7270

Zhang, Z., Zhang, X., Zhao, D., Liu, B., Wang, B., Yu, W., et al. (2019c). TGF-β1
promotes the osteoinduction of human osteoblasts via the PI3K/AKT/mTOR/
S6K1 signaling pathway. *Mol. Med. Rep.* 19 (5), 3505–3518. doi:10.3892/mmr.
2019.10051

Zhang, Y., Cai, W., Han, G., Zhou, S., Li, J., Chen, M., et al. (2020). Panax
notoginseng saponins prevent senescence and inhibit apoptosis by regulating
the PI3K-AKT-mTOR pathway in osteoarthritic chondrocytes. *Int. J. Mol. Med.*
45 (4), 1225–1236. doi:10.3892/ijmm.2020.4491

Transcriptomic Analysis of the Mechanisms for Alleviating Psoriatic Dermatitis Using Taodan Granules in an Imiquimod-Induced Psoriasis-like Mouse Model

Le Kuai[1,2†], Ying Luo[2†], Keshen Qu[3†], Yi Ru[2], Yue Luo[1], Xiaojie Ding[1], Meng Xing[2,4], Liu Liu[2], Xiaoying Sun[2], Xin Li[1,2]* and Bin Li[1,4,5]*

[1]Department of Dermatology, Yueyang Hospital of Integrated Traditional Chinese and Western Medicine, Shanghai University of Traditional Chinese Medicine, Shanghai, China, [2]Institute of Dermatology, Shanghai Academy of Traditional Chinese Medicine, Shanghai, China, [3]Department of Traditional Chinese Surgery, Longhua Hospital Shanghai University of Traditional Chinese Medicine, Shanghai, China, [4]Department of Dermatology, Shaanxi Hospital of Traditional Chinese Medicine, Xi'an, China, [5]Shanghai Dermatology Hospital, Tongji University, Shanghai, China

Taodan granules (TDGs) are clinically efficacious for treating psoriasis, buttheir specific mechanisms of action are unclear. In this study, we determined the concentrations of tanshinone IIA and curcumol using high-performance liquid chromatography (HPLC) to establish quality control parameters for assessing the mechanism of TDGs in treating psoriasis. Thereafter, a mouse model of psoriasis was treated with TDGs. TDGs attenuated imiquimod-induced typical erythema, scales, and thickening of the back and ear lesions in the psoriatic mouse model. Furthermore, PCNA and Ki67-positive cells were reduced in the *epidermis* of psoriatic lesions following TDG treatment. Finally, the sequencing results were verified using a multitude of methods, and the mechanism of action of TDGs against psoriasis was found to be via the upregulation of metabolic signaling pathways such as the Gly-Ser-Thr axis, the downregulation of immune and inflammatory pathways, and the decrease in Rac2 and Arhgdib concentrations. Overall, this study clarified the mechanism of TDG treatment for psoriasis and provided evidence for its clinical application.

Keywords: psoriasis, taodan granules, RNA sequencing analysis, Chinese medicine, transcriptomic analysis

BACKGROUND

Psoriasis is a common chronic refractory skin disease, characterized by epidermal hyperkeratosis, angiogenesis, and inflammatory reactions (Armstrong et al., 2020). The prevalence of psoriasis is increasing, ranging from 0.51 to 11.43% in adults, and a cross-sectional study revealed that psoriasis affects approximately 3% of the population and 7.4 million adults in the United States (Rachakonda et al., 2014; Michalek et al., 2017). Furthermore, the disease is associated with a significant economic burden, while the all-cause healthcare cost of each patient with psoriasis per year is generally $12,523 (Al Sawah et al., 2017). Psoriasis also has a serious negative impact on work productivity and health-related quality of life (Lopes et al., 2019). Psoriasis is a systemic disease that not only involves the skin, but is also associated with comorbidities, including cardiovascular disease, chronic obstructive

pulmonary disease, diabetes, obesity, and hyperuricemia (Miele et al., 2009; Li et al., 2015; Yuan et al., 2019; Kovitwanichkanont et al., 2020). Systemic inflammation and oxidative stress in psoriasis are closely related to a variety of complications associated with a conspicuously high risk of death in patients with conditions such as kidney disease and liver disease (Dhana et al., 2019). Inflammation in psoriasis can lead to renal dysfunction by upregulating NADPH oxidases as well as inducible nitric oxide synthase (Al-Harbi et al., 2017a), and it has also been confirmed to induce hepatic inflammation, resulting in protein and lipid metabolism disorders through interleukin (IL)-17 RC/NF-κB signaling (Al-Harbi et al., 2017b). Additionally, the role of psoriatic inflammation enhances allergic airway inflammation via IL-23/signal transducer and activator of transcription 3 (STAT3) signaling in a murine model (Nadeem et al., 2017). Western medicine has made great progress in systematic therapies for psoriasis, such as methotrexate, cyclosporin, retinoic acid, and biological agents (Armstrong et al., 2020). Nonetheless, adverse reactions and contraindications have limited the wide application of these drugs (Sparks et al., 2020; Williams et al., 2020). Currently, Chinese medicine (CM) has become a global alternative medicine that has been gradually adopted for the treatment of psoriasis (Parker et al., 2017).

Taodan granules (TDGs) are composed of *Salvia miltiorrhiza Bunge*, *Curcuma aeruginosa Roxb.*, *Astragalus mongholicus Bunge*, *Glycyrrhiza inflata Batalin* and *Angelica sinensis (Oliv.) Diels*, *Conioselinum anthriscoides "Chuanxiong"*, *Prunus persica (L.) Batsch*, *Cyathula officinalis K. C. Kuan*, and *Smilax china L.*. Our previous clinical studies demonstrated that TDGs were satisfactory for the treatment of mild-to-moderate psoriasis vulgaris, and the reduction of IL-2, IL-4, and IL-6, together with the secretion of neuropeptides in the peripheral blood of patients with psoriasis was observed after TDG treatment for one month; the psoriasis area and severity index (PASI) score improved by 76.65% (Fan et al., 2006a; Fan et al., 2006b). Recently, Ru et al. conducted a high-quality randomized controlled trial to evaluate the clinical efficacy, safety, and recurrence rate of TDGs for psoriasis blood stasis syndrome (Ru et al., 2019). Although TDGs have a positive curative effect on psoriasis without significant AEs, the relative mechanism of action remains elusive.

RNA sequencing (RNA-seq), a progressive technique, is practical for identifying numerous genes regulated by specific medications (Liu et al., 2020). In this study, we used an imiquimod (IMQ)-induced psoriasis-like mouse model to examine the mechanism of action of TDGs against psoriasis. We used RNA-seq to analyze skin lesion samples with and without TDGs treatment, screened for the upregulated and downregulated genes 12 days after the therapy, conducted a bioinformatics study, and verified the aforementioned observations.

MATERIALS AND METHODS

Pharmaceutical Composition of Taodan granule

The TDGs comprised nine Chinese herbs. These herbs (**Supplementary Table S1**) were authenticated by a

pharmacognosist of the Yueyang Hospital of Integrated Traditional Chinese and Western Medicine, Shanghai University of Traditional Chinese Medicine, in accordance with standard protocols.

High-Performance Liquid Chromatography

The extraction and HPLC analysis of the TDGs were performed using the following methods: 1) In line with standard methods of the Chinese Pharmacopeia, all crude drugs listed in **Supplementary Table S1** were boiled and kept at near-boiling temperature for 1 h and then filtered. 2) Another 1,650 ml of water was added to the filtrate, brought to a boil again, kept for 1 h, and then filtered. 3) Two extracts were combined to obtain 1 g/ml of crude drug. Tanshinone IIA (abs47000393, purity ≥98%) and curcumol (abs47005976, purity ≥98%) were examined in the crude drug by using an Agilent 1,200 series HPLC and a ZORBAX SB-C18 chromatographic column (4.6 mm × 250 mm, 5 μm) therewith. The detection chromatographic conditions were as follows: acetonitrile, 0.5% phosphoric aqueous acid solution (70: 30, v/v); column temperature, 30°C; detection wavelength, 210 nm; and injection volume, 20 μl. Tanshinone IIA and curcumol are the main active ingredients of *Salvia miltiorrhiza Bunge* and *Curcuma eruginosa Roxb,* respectively. Hence, TDGs without *Salvia miltiorrhiza Bunge* and *Curcuma eruginosa Roxb.* were used as the negative controls.

Animals

Male specific pathogen-free (SPF)–grade BALB/c mice, with a weight of 25 ± 3 g, were provided by the Shanghai Medical Experimental Animal Center (SCXK Shanghai 2013–0016, Shanghai, China). The mice were maintained in an environment with a temperature of 23 ± 2°C and a 16–8 h light-dark cycle, along with sterile water. The fodder was supplied by Shanghai Pu Lu Tong Biological Technology Co., Ltd. All procedures were reviewed and approved by the Ethics Committee of Yueyang Hospital affiliated to Shanghai University of Traditional Chinese Medicine (no. YYLAC-2020–078–1).

Plant Material and Drugs

The TDGs were acquired from the Pharmacy Department of the Yueyang Hospital of Integrated Traditional Chinese and Western Medicine, Shanghai University of Traditional Chinese Medicine, and stored at 4°C. Petroleum jelly was obtained from Nanchang Baiyun Pharmaceutical Co., Ltd (Jiangxi, China, Drug approval No. F20050006). IMQ cream was obtained from Sichuan Mingxin Pharmaceutical Co., Ltd (Sichuan, China, Drug approval No. H20030128).

Experimental Grouping and Mice Model

Mice were randomly divided into three groups after the back hair was clipped (2×2 cm^2).

a. Control group: ears and back were treated with 62.5 mg petroleum jelly.
b. IMQ group: ears and back were treated with 62.5 mg of 5% IMQ cream for 6 h, followed by intragastric administration of 1.8 g/kg 0.9% NaCl solution.

c. IMQ + TDG group: ears and back were treated with 62.5 mg of 5% IMQ cream for 6 h, followed by intragastric administration of 1.8 g/kg TDGs.

All treatments were executed from the date of applying IMQ cream (day 0), once a day for 12 days. The PASI score was used to determine the severity of skin inflammation on the backs and ears of the mice. Each parameter of the score ranged from 0 to 4, representing the order of severity. The mice were fasted before collecting specimens, but they could drink water for 12 h. Mice were euthanized by inhalation of CO_2 on day 12. Lesions of the back and ear were collected for reserves.

mRNA Sequencing Analysis
Sequencing Method
On day 12, the mice were euthanized. The back lesions were homogenized using TRIzol reagent (Ambion). Total RNA was extracted from the samples, and the DNA was digested with DNase. Magnetic beads with oligo (dT) enriched the mRNA. After adding the interrupting reagent, the mRNA was broken into short fragments, used as a template, and synthesized as one-strand cDNA with six base random primers. Next, a double-strand reaction system was prepared to synthesize double-stranded cDNA, which was purified using the kit. The purified double-stranded cDNA was subjected to terminal repair, with an A-tail connecting the sequencing connector. The fragment size was selected, and PCR amplification was performed. The library qualified with an Agilent 2,100 Bioanalyzer was established, and Illumina HiSeq™ 2,500 was used for sequencing to produce 125–150 bp double-ended data. RNA-seq analysis was performed by Shanghai OE Biotechnology Co., Ltd.

Gene Expression Analysis
Trimmomatic software (version 0.36) preprocessed the quality of the original data, and the number of reads during the entire quality control process was statistically summarized. Hisat2 software (version 2.2.1.0) was used to align CleanReads with the specified reference genome. We applied the known reference gene sequences and annotation files as the database, and the sequence similarity alignment method was adopted to identify the expression abundance of each protein-coding gene in each sample. The htseq-count software (version 0.9.1) was used to obtain the number of reads, compared with the protein-coding genes in each sample. The fragments per kilobase million (FPKM) values, representing the relative gene expression abundance, were calculated using the Cufflinks software (version 2.2.1).

Analysis of Differentially Expressed Genes
Standardization disposal was performed using DESeq software (version 1.18.0) for the gene count of each sample (BaseMean value was used to estimate expression). The multiples were calculated, and the negative binomial distribution test method (NB) was used to verify the significance of the difference in the number of reads. Finally, the different protein-coding genes were screened according to the results of fold changes and the significance of differences.

Gene Ontology and Kyoto Encyclopedia of Genes and Genomes Analysis
After the DEGs were obtained, the significance of the GO and KEGG analyses was analyzed using DAVID (https://david.ncifcrf.gov/). A p-value of <0.05 was considered as the standard for statistically significant differences. The list of target genes was set for "*Homo sapiens*".

Reverse Transcription Polymerase Chain Reactio
On day 12, the mice in each group were euthanized by CO_2 inhalation. The middle portion of the skin lesions was measured. Total RNA was extracted using the TRIzol reagent kit. Afterward, the Reverse Transcription System First Strand cDNA Synthesis Kit was used with 20.0 a reaction volume. Real-time fluorescent PCR was used for the RT-PCR. This specific method was consistent with previous experiments (Kuai et al., 2018). The primer sequences are shown in **Supplementary Table S2**.

Enzyme-Linked Immunosorbent Assay
On day 12, the lesions were collected from the mice for ELISA. The levels of chemokine (C-X-C motif) ligand 13 (CXCL13), IL-17a, tumor necrosis factor-alpha (TNF-α), sarcosine dehydrogenase (Sardh), and phosphoglycerate mutase 2 (Pgam2) protein expression were detected by applying a CXCL13 Mouse ELISA kit (ab212167, Abcam), an IL-17 Mouse ELISA kit (ab100702, Abcam), TNF-α Mouse ELISA kit (ab208348, Abcam), a Sardh Mouse ELISA kit (ABIN5521597), and a Pgam2 Mouse ELISA kit (ABIN5525256), respectively. Antibodies against the Vav 1 oncogene (Vav1) (ABIN6256653), LYN proto-oncogene, Src family tyrosine kinase (Lyn) (ABIN6256754), hematopoietic cell kinase (Hck) (ABIN3184982), protein kinase C, beta (Prkcb) (ABIN3032235), cystathionine beta-synthase (CBS) (ABIN6260518), serine dehydratase-like (Sdsl) (ABIN1092123), glycine N-methyltransferase (GNMT) (ABIN5700022), and Rho, GDP dissociation inhibitor (GDI) beta (Arhgdib) (ABIN5699138) from 4A Biotech Co. Ltd. were used for ELISA.

Hematoxylin-Eosin Solution and Immunohistochemistry
The mice were euthanized by inhalation of CO_2 on day 12. The center of the lesions were fixed with 4% formalin solution and stained with H&E solution, followed by immunohistochemistry (IHC). The quantitative methods for epidermal thickness together with the positive cell rate have been described in previous studies (Luo et al., 2019; Kuai et al., 2020).

The following antibodies were used for immunohistochemistry: anti-Ki-67 antibody (1:50, ab16667, Abcam), anti-PCNA antibody (1:6,400, ab29, Abcam), anti-NF-κB p105/p50 antibody (1:60,000, ab32360, Abcam), and anti-RAS-related C3 botulinum substrate 2 (Rac2) antibody (1:50, ab2244, Abcam).
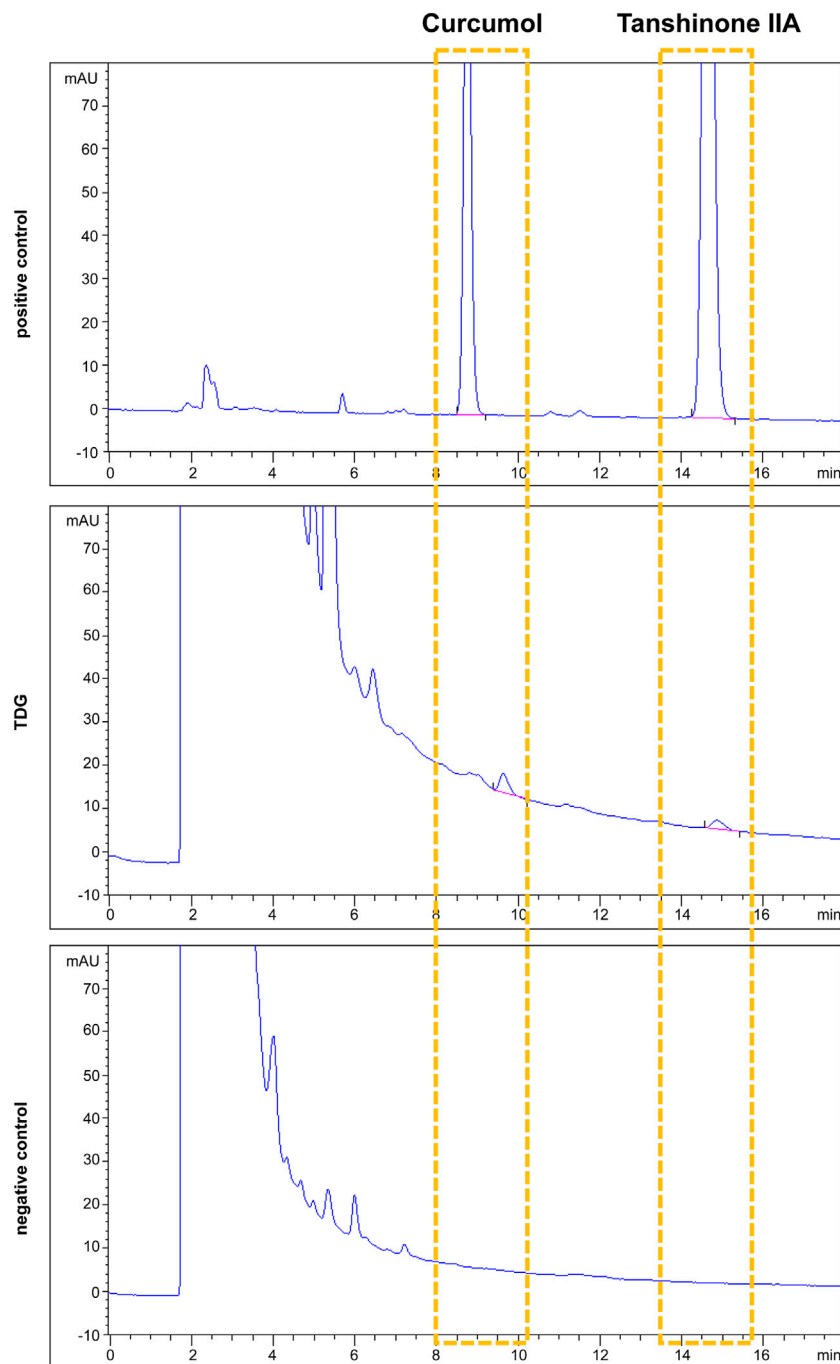
FIGURE 1 | Tanshinone IIA and curcumol were adopted as quality controls for Taodan granule (TDG). Tanshinone IIA and curcumol are detected in both positive control and TDG samples but neither found in the negative control.

Western Blotting

Rac2 and Arhgdib protein expression in the back lesions was measured by western blotting. Briefly, the mice were euthanized by inhalation of CO_2 on day 12. The middle portion of the back lesions was immediately placed in liquid nitrogen and stored at −80°C. The cells were collected. RIPA lysis buffer (Beyotime, Shanghai, China) was used to extract the total protein. The BCA protein analysis kit (TB258438; Bio-Rad, United States) was used to determine protein concentration. The total protein (20 μg per sample) was separated and transferred to a polyvinylidene fluoride membrane. The antibodies for western blotting included anti-Rac2 antibodies (ab2244; Abcam), anti-Arhgdib antibodies (ab181252; Abcam), and β-actin (ab8226; Abcam), and incubated overnight at 4°C. Next, the samples were incubated
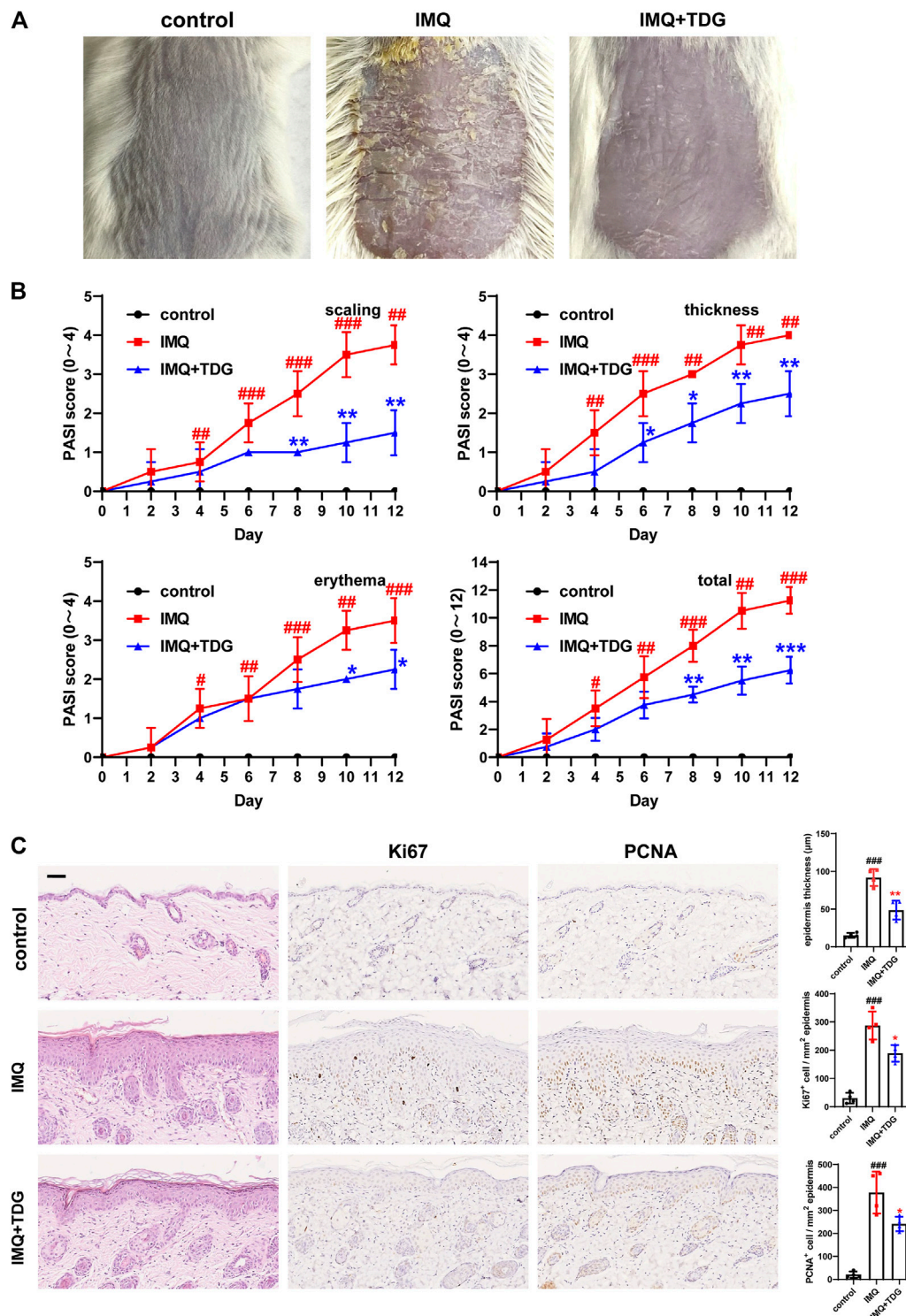
FIGURE 2 | Taodan granules (TDGs) alleviated back lesions in imiquimod (IMQ)-induced psoriasis-like mice and decreased keratinocyte proliferation. (A) The appearance of back lesions in each group on day 12. (B) The psoriasis area severity index (PASI) score (0–4) with scales, thickness, erythema, and a total score. (C) Representative H&E sections of back lesions on day 12 (× 200) (Left). Representative immunohistochemistry sections of Ki67 and PCNA nuclear staining (brown) of the back skin lesions (200×) (Middle and Right). Quantification of *epidermis* thickness as well as Ki67$^+$ and PCNA$^+$ cells in back lesions. Scale bar: 100 μm. The data are expressed as mean ± SD. Four skin lesions from in group were included for analysis. $^{\#}p < 0.05$, $^{\#\#}p < 0.01$, $^{\#\#\#}p < 0.001$, compared with the control group. $^*p < 0.05$, $^{**}p < 0.01$, $^{***}p < 0.001$, compared with the IMQ group.

with the secondary antibody (ab205719; Abcam) for 1 h at room temperature.

Statistical Methods

The data were analyzed using SPSS 24.0 (IBM Corp., Armonk International Business Machines, New York, United States), and they are described as mean ± standard deviation (SD). A t-test was used to compare the two groups. Statistical significance was set at $p < 0.05$.

RESULTS

High-Performance Liquid Chromatography Profiles of Tanshinone IIA and Curcumol in Taodan Granule

Salvia miltiorrhiza Bunge and *Curcuma aeruginosa Roxb.* are the two major components of the TDGs. Our previous study (Li et al., 2012) confirmed that tanshinone IIA, an active lipopolysaccharide of *Salvia miltiorrhiza Bunge*, could lead to cell cycle arrest and apoptosis in keratinocytes (KC) of the target cells in psoriasis. Tanshinone IIA has been shown to inhibit the increase in interferon sensitivity and upregulation of aberrant KC differentiation markers (Pedersen et al., 2012). On the other hand, curcumol is one of the main bioactive components of *Curcuma aeruginosa Roxb.*, and is generally used for the quality control of Chinese herbal compounds, which contains *Curcuma aeruginosa Roxb.* (Lei et al., 2019). Multiple studies have shown that curcumin can inhibit cell proliferation and migration in numerous proliferative diseases (Hashem et al., 2020; Huang et al., 2020; Li et al., 2020). In summary, we chose tanshinone IIA and curcumol to preliminarily establish quality control (**Figure 1**).

Taodan Granules Relieved Back and ear Lesions, as Well as Suppressed Keratinocytes Proliferation in Imiquimod-Induced Psoriasis-like Mice

First, we established an animal model of psoriasis via IMQ induction. Compared with the control group, the IMQ group displayed typical psoriatic skin lesions with scales, erythema, and thickening accompanied by a conspicuous increase in the PASI scores ($p < 0.05$) (**Figures 2A,B**; **Supplementary Figures S1A, B**). Histologically, spinous layer hypertrophy, significantly thickened *epidermis* (back: $p < 0.001$; ear: $p < 0.001$), and obvious inflammation were observed in the IMQ-induced mice on day 12 (**Figure 2C**; **Supplementary Figure S1C**). These results revealed that the IMQ-induced mouse model was consistent with the characteristics of psoriasis.

Next, we determined whether TDGs could inhibit back and ear lesions *in vivo*. With TDG treatment, the skin lesions of IMQ-induced psoriasis-like mice were alleviated, and the PASI scores declined ($p < 0.05$) (**Figures 2A,B**; **Supplementary Figures S1A, B**). The most effective TDG dose was determined to be 1.8 g/kg (**Supplementary Figure S2**). On day 12, the TDG-treated mice

demonstrated reductions in inflammatory cell infiltration and epidermal hyperplasia (back: $p = 0.002$; ear: $p = 0.001$) (**Figure 2C**; **Supplementary Figure S1C**).

We further predicted whether TDGs could prevent excessive KC proliferation in IMQ-induced mice. With TDG treatment, the lesions of the mice were validated by the significantly decreased number of Ki67-positive cells (back: $p = 0.014$; ear: $p = 0.014$) as well as PCNA-positive cells (back: $p = 0.03$; ear: $p = 0.019$) (**Figure 2C**; **Supplementary Figure S1C**).

mRNA Sequencing Analysis of Taodan Granule-Regulated Gene Expression in Imiquimod-Induced Psoriasis-Like Skin Lesions

Expression Analysis

We investigated the difference in gene expression with TDG treatment, RNA was extracted from the back tissues of the IMQ and IMQ + TDG groups for mRNA sequencing on day 12. Sequencing reports suggested that the total reads ranged from 47,337,442 to 50,470,212, and the rate of total mapped reads was between 94.97 and 95.79%. The boxplot for the FPKM values and the two-dimensional diagram of the principal component analysis are shown in **Supplementary Figure S3**.

Differentially Expressed Genes Following Taodan Granule Treatment

DESeq software was used for differential expression analysis to identify candidate genes regulated by TDG treatment (1.18.0). |$\log_2$FoldChange| > 1 and p-value < 0.05 of the genes were judged for differential expression. A total of 1,233 DEGs were identified, of which 539 were upregulated and 694 were downregulated (**Figure 3A**). The 20 most significantly upregulated and downregulated DEGs after TDG treatment are demonstrated in **Table 1**. The mRNA levels for the 10 most significantly upregulated and downregulated DEGs were verified by RT-PCR, which were consistent with the sequencing results (**Supplementary Figure S4**).

The biological characteristics of the potential targets of TDGs were evaluated by KEGG and GO analyses. KEGG analysis results (**Figure 3B**) demonstrated that the most upregulated gene categories were for the neuroactive ligand-receptor interaction, estrogen signaling pathway, biosynthesis of unsaturated fatty acids, and glycine, serine, and threonine (Gly-Ser-Thr) metabolism. The most downregulated gene categories were cytokine-cytokine receptor interaction, *Staphylococcus aureus* infection, osteoclast differentiation, and chemokine signaling pathway. GO analysis results (**Figure 3C**) revealed that the most upregulated gene categories were intermediate filaments, keratin filaments, cellular components, and structural molecule activity. The most downregulated gene categories were inflammatory response, immune system process, extracellular space, and innate immune response. Thus, the above results might reflect abnormalities in biological processes, metabolism, and inflammatory immune-related signaling pathways in psoriasis, and manifest the conceivable mechanism of TDGs.
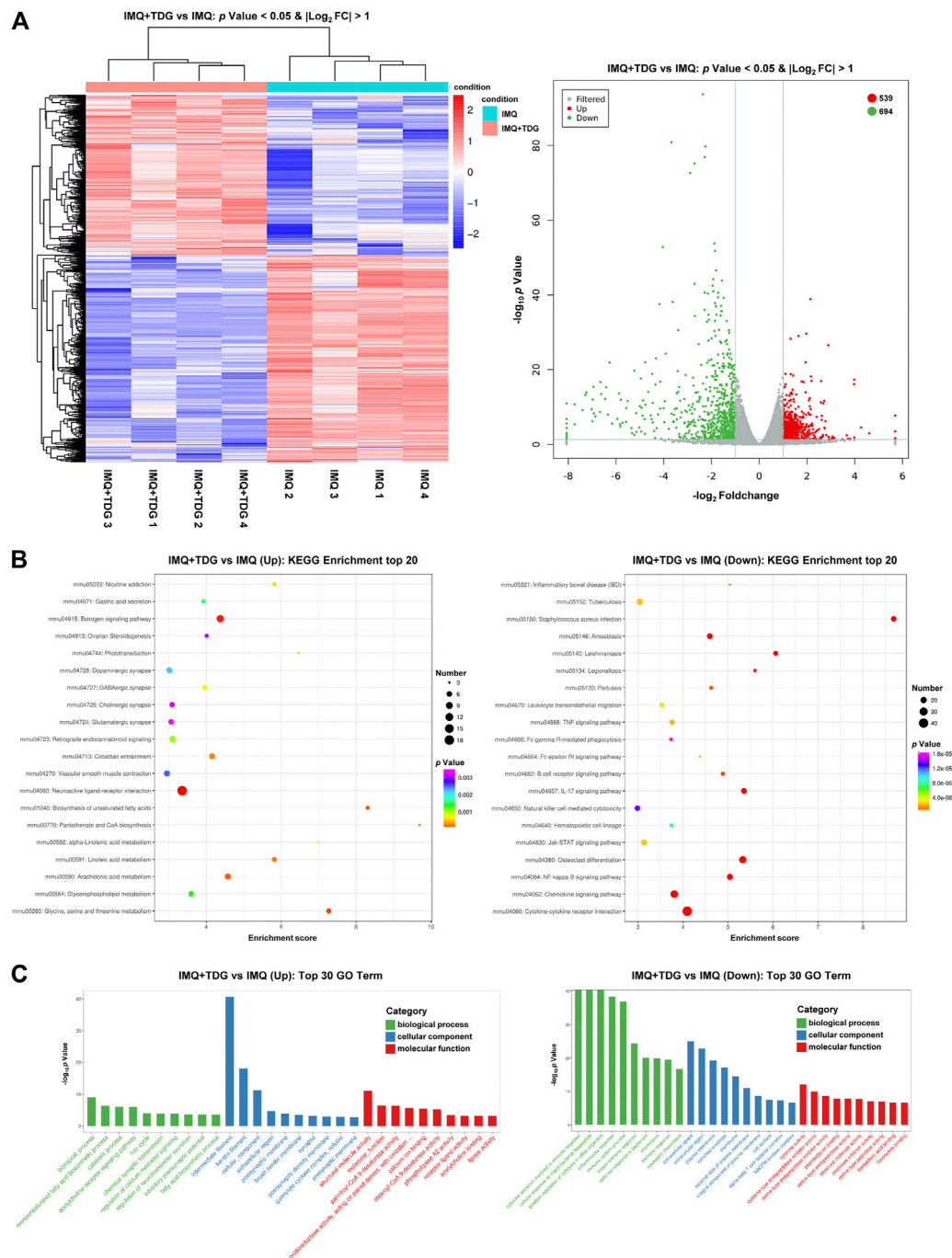
FIGURE 3 | Differentially expressed genes (DEGs) induced after Taodan granule (TDG) treatment. **(A)** Cluster analysis of DEGs among samples and groups. The color of the heat map indicates the relative gene expression. The deeper red color indicates the higher gene expression, whereas the deeper blue color indicates the lower gene expression **(Left)**. The volcano map suggests the overall DEGs in the imiquimod (IMQ)+TDG group, compared with the IMQ group **(Right)**. **(B)** Enriched KEGG analysis of **up-(Left)** and **down-(Right)** regulated DEGs. **(C)** Enriched gene ontology analysis of **up-(Left)** and **down-(Right)** regulated DEGs.

Experimental Verification
Taodan Granules Increased the Gly-Ser-Thr Metabolism Axis and Decreased Chemokine Signaling Pathway and Inflammatory Marker Protein Expression

Several studies (Gelfand et al., 2018; Tollefson et al., 2018; Evans et al., 2020) have shown that the pathogenesis of psoriasis is closely related to metabolic disorders that are frequently aggravated. The Gly-Ser-Thr axis is a major metabolic crossroad connecting several crucial biological pathways (Aon et al., 2020). Based on the sequencing results, the genes of CBS, Sardh, GNMT, Pgam2, and Sdsl in the Gly-Ser-Thr axis were selected for the determination of protein concentrations on day

TABLE 1 | Top 20 upregulated and downregulated genes in the psoriatic skin of the mice models with or without Taodan granules (TDGs) (Genes with |log2FoldChange| > 1 and p-value < 0.05).

Gene ID	Gene name	Gene definition	LOG$_2$|FC|	p-value	Q-value
Top 20 upregulated genes					
66,107	Wfdc21	WAP four-disulfide core domain 21	2.141,861,603	1.34E-39	1.15E-36
432,839	Gprin2	G protein regulated inducer of neurite outgrowth 2	1.969,102,658	2.22E-30	9.29E-28
108,151	Sema3d	Sema domain, immunoglobulin domain (ig), short basic domain, secreted, (semaphorin) 3D	1.643,954,426	8.96E-30	3.66E-27
16,008	Igfbp2	Insulin-like growth factor binding protein 2	1.311,271,087	4.79E-29	1.83E-26
406,220	Krt77	Keratin 77	2.889,566,113	2.87E-27	9.37E-25
230,613	Skint10	Selection and upkeep of intraepithelial T-cells 10	1.940,699,804	1.00E-22	2.61E-20
14,622	Gjb5	Gap junction protein, beta 5	1.0953,902	1.35E-19	2.34E-17
79,362	Bhlhe41	Basic helix-loop-helix family, member e41	1.320,164,851	1.48E-19	2.54E-17
73,442	Hspa12a	Heat shock protein 12 A	1.420,015,579	3.70E-19	6.16E-17
66,203	Lce1m	Late cornified envelope 1 M	2.169,646,121	6.75E-19	1.07E-16
435,350	Serpinb6e	Serine (or cysteine) peptidase inhibitor, clade B, member 6e	3.976,679,949	4.75E-18	6.83E-16
69,117	Adh6a	Alcohol dehydrogenase 6 A (class V)	2.187,395,639	1.07E-17	1.48E-15
238,395	Serpina3j	Serine (or cysteine) peptidase inhibitor, clade a (alpha-1 antiproteinase, antitrypsin), member 3 J	2.590,357,248	1.13E-17	1.56E-15
107,585	Dio3	Deiodinase, iodothyronine type III	1.781,280,765	1.45E-17	1.95E-15
11,519	Add2	Adducin 2 (beta)	1.861,512,402	2.43E-17	3.14E-15
271,047	Serpina3b	Serine (or cysteine) peptidase inhibitor, clade A, member 3 B	3.973,024,928	7.68E-17	9.65E-15
12,411	Cbs	Cystathionine beta-synthase	1.100,796,697	8.20E-17	1.02E-14
68,659	Fam198 b	Family with sequence similarity 198, member B	1.064,341,173	3.47E-16	3.95E-14
192,166	Sardh	Sarcosine dehydrogenase	1.064,351,251	5.48E-16	6.04E-14
18,162	Npr3	Natriuretic peptide receptor 3	1.39,877,771	2.50E-15	2.59E-13
Top 20 downregulated genes					
16,409	Itgam	Integrin alpha M	−2.359,917,295	1.99E-94	3.57E-90
170,677	Cdhr1	Cadherin-related family member 1	−3.677,378,859	1.32E-81	1.19E-77
16,414	Itgb2	Integrin beta 2	−2.253,358,932	1.70E-80	1.02E-76
19,354	Rac2	RAS-related C3 botulinum substrate 2	−2.283,072,327	1.24E-77	5.58E-74
83,382	Siglece	Sialic acid binding ig-like lectin E	−2.712,092,471	6.31E-76	2.27E-72
217,306	Cd300e	CD300 E molecule	−2.896,226,408	2.08E-73	6.24E-70
73,656	Ms4a6c	Membrane-spanning 4-domains, subfamily A, member 6C	−1.87,982,465	1.47E-54	3.76E-51
	Sprr2a3	Small proline-rich protein 2A3	−4.039,888,592	1.45E-53	3.25E-50
100,042,514					
83,490	Pik3ap1	Phosphoinositide-3-kinase adaptor protein 1	−1.852,487,496	1.62E-52	3.23E-49
15,163	Hcls1	Hematopoietic cell specific lyn substrate 1	−1.807,265,374	2.60E-47	4.68E-44
23,880	Fyb	FYN binding protein	−1.927,183,842	5.81E-45	9.50E-42
72,042	Cotl1	Coactosin-like 1 (dictyostelium)	−1.563,171,219	1.30E-44	1.94E-41
246,256	Fcgr4	Fc receptor, IgG, low affinity IV	−2.70,846,219	1.04E-43	1.44E-40
18,173	Slc11a1	Solute carrier family 11 (proton-coupled divalent metal ion transporters), member 1	−1.951,701,945	3.15E-43	4.05E-40
26,888	Clec4a2	C-type lectin domain family 4, member a2	−1.930,263,987	1.02E-41	1.22E-38
65,221	Slc15a3	Solute carrier family 15, member 3	−2.280,078,606	2.26E-41	2.54E-38
14,127	Fcer1g	Fc receptor, IgE, high affinity I, gamma polypeptide	−1.713,529,716	2.48E-41	2.62E-38
244,233	Cd163l1	CD163 molecule-like 1	−2.148,022,202	4.31E-41	4.31E-38
20,525	Slc2a1	Solute carrier family 2 (facilitated glucose transporter), member 1	−1.727,582,584	4.31E-40	4.08E-37
11,433	Acp5	Acid phosphatase 5, tartrate resistant	−1.490,765,474	6.27E-40	5.63E-37

Q-VALUE, A Benjamini value (an adjusted p-value).

12 to explore the involvement of this metabolic pathway in the TDG treatment of psoriasis (**Figure 4A**). Compared with the IMQ group, the skin protein expression of these five genes in the IMQ + TDG group was significantly increased (CBS: $p = 0.030$; Sardh: $p = 0.030$; GNMT: $p = 0.005$; Pgam2: $p = 0.022$; Sdsl: $p = 0.007$), which was consistent with our KEGG enrichment results (**Figure 3B**).

Furthermore, the chemokine signaling pathway, which controls inflammatory response and directional cell migration, is involved in KC hyperplasia, regulating inflammation, the formation of new blood vessels, and other processes linked to psoriasis-related damage. KEGG analysis revealed that the chemokine signaling pathway was downregulated by TDG treatment (**Figure 3B**). Next, we validated the skin protein expression levels of the genes (Vav1, Lyn, Hck, Prkcb, and CXCL13) in this pathway on day 12, and a decrease in the same expression as KEGG was observed (Vav1: $p = 0.016$; Lyn: $p = 0.004$; Hck: $p = 0.032$; Prkcb: $p = 0.005$; CXCL13: $p = 0.020$) (**Figure 4A**).

In addition, compared with the IMQ group, the protein expression of IL-17a ($p = 0.008$) and TNF-α ($p = 0.016$) in the back lesions decreased in the IMQ + TDG group on day 12 (**Figure 4A**), which are inflammatory factors involved in the pathogenesis of psoriasis (Hawkes et al., 2017). We also examined NF-κB in a protein complex that controls the transcriptional regulation of inflammatory cytokines. Previous studies have

shown that NF-κB is activated during psoriasis (Capon et al., 2012). Here, the downregulation of NF-κB by TDGs was observed (back: $p = 0.013$; ear: $p = 0.027$) (**Figure 4B**; **Supplementary Figure S5**). Consistent with the above results, KEGG analysis showed TNF-α together with IL-17a and NF-κB-related pathways were downregulated by TDG treatment (**Figure 3B**).

Taodan Granules Reduced Protein Expressed Levels of Rac2 in Psoriatic Lesions and Serum Arhgdib

Abnormal proliferation and migration of KCs in psoriasis are vital pathogenic factors (Zhang et al., 2019). Rac2, a member of the small Rho GTPase family, centrally regulating cell migration via cytoskeletal rearrangement (Hordijk, 2006). Our mRNA sequencing results demonstrated that Rac2 was significantly downregulated following TDG treatment (**Table 1**). To verify whether TDGs could decrease the expression of Rac2, which influenced the regulation of migration in IMQ-induced psoriasis-like mice, IHC was used to detect Rac2 protein expression on day 12. The TDG-treated lesions demonstrated a significant decrease in the number of Rac2-positive cells (**Figure 5A**; **Supplementary Figure S5**) in the basal layers of the *epidermis* compared to the IMQ group. The same results were found on western blotting to verify back lesions (**Figure 5C**).

To further explore the feasible mechanism by which TDGs regulate Rac2 in psoriasis, we conducted a protein-protein interaction analysis using the Search Tool for the Retrieval of Interaction Gene/Proteins (String) database based on our sequencing results (**Table 2**). The results showed that the Arhgdib, Ncf2, and Cybb genes in DEGs had the highest combined scores for Rac2. We chose to assess the serum expression of the Arhgdib gene, a Rho GDI protein, to test the possible mode action of Rac2 during TDG treatment of psoriasis on day 12. Following TDG treatment, the protein expression of Arhgdib in IMQ-induced psoriasis-like mice was significantly downregulated ($p = 0.040$) (**Figure 5B**), which matched our sequencing results. Simultaneously, we also affirmed the protein expression of Arhgdib in the back lesions through western blotting, consistent with the trend of expression by ELISA (**Figure 5C**). These results suggest that TDGs may alleviate the symptoms of psoriasis by regulating Rac2 and Arhgdib, which are related to the mechanism of cell migration.

DISCUSSION

TDGs have therapeutic effects in relieving psoriasis. Our previous studies have shown that TDGs are effective for the treatment of mild-to-moderate psoriasis vulgaris (Fan et al., 2006a; Fan et al., 2006b), although the mechanism remains unclear. CM mainly exerts therapeutic effects via the interaction of multiple natural products containing an army of targets through numerous pathways, which is a challenge for investigating their mechanisms of action (Zhou et al., 2014). Nonetheless, RNA-seq may provide a new direction for this conundrum. In this study, we performed RNA-seq to determine the mechanism by which TDGs ameliorate psoriasis and verify the observations via *in vivo* experiments.

To clarify the pharmacological mechanism of TDGs, we used HPLC to establish quality control. Based on the excellent curative effect and unclear mechanism of TDGs in this study, we first induced a mouse psoriatic model with IMQ, which is a classic accepted model of psoriasis that we have often used in our previous studies (Kuai et al., 2020; Ru et al., 2020). Our results demonstrated that TDGs attenuated IMQ-induced psoriatic classical symptoms (**Figure 2**; **Supplementary Figure. S1**). To assess whether the remission of psoriatic lesions after TDG treatment may be due to the prevention of the over-proliferation of KCs, we verified the Ki67 and PCNA-positive cells in each group. Ki67 and PCNA are classical markers of cell proliferation in a variety of diseases (Alhosaini et al., 2021; Cai et al., 2021). As expected, following TDG treatment, the number of Ki67 and PCNA-positive cells in IMQ-induced psoriasis-like mice decreased significantly (**Figure 2**; **Supplementary Figure S1**), which is consistent with the results of previous studies (Ru et al., 2020; Thatikonda et al., 2020; Tomalin et al., 2020). Accordingly, we speculated that TDGs could mitigate the excessive proliferation of KCs to effectively alleviate psoriasis.

To further explore the potential mechanism of TDG in psoriasis, we applied RNA-seq to investigate skin lesion samples from IMQ-induced psoriasis-like mice with and without TDG. A total of 1,233 DEGs were identified, of which 539 were upregulated and 694 were downregulated (**Figure 3A**). The mRNA levels of the 10 most significantly upregulated and downregulated DEGs were verified by RT-PCR, consistent with the sequencing results (**Supplementary Figure S4**).

A bioinformatic analysis concluded that the most upregulated gene categories by TDGs were associated with metabolism-related signaling pathways (**Figures 3B,C**); these pathways have been found to mediate psoriasis in several existing reports (Chen et al., 2018; Lin et al., 2019). The Gly-Ser-Thr axis is a metabolic pathway closely related to proliferative disease and lifetime (Aon et al., 2020). Nevertheless, no related studies on this axis in psoriasis have been reported. RNA-seq results confirmed that CBS, Sardh, GNMT, Pgam2, and Sdsl were the top five upregulated genes by TDGs in the Gly-Ser-Thr axis. CBS is primarily a cytosolic enzyme that regulates homocysteine metabolism and is involved in the biosynthesis of hydrogen sulfide. Clinical evidence has strongly supported the negative regulatory role of CBS in proliferative diseases (Kim et al., 2009), which induces autophagy and apoptosis via the PI3K/Akt/mTOR pathway in hepatocellular carcinoma (HCC) cells (Zhu et al., 2018). Sardh and GNMT are pivotal enzymes associated with sarcosine metabolism, and transcription and protein levels are regulated in cancer tissues. Meanwhile, Sardh has been reported to reduce sarcosine levels and attenuate the invasion of DU145 prostate cancer cells (Khan et al., 2013). Pgam2 is a crucial enzyme involved in glycolysis related to oxidative stress, and decreased expression of Pgam2 was observed in proliferative disease induced by local infections (Cladel et al., 2019). In addition, clinical evidence has suggested that Sdsl has specific protein expression in peripheral cholangiocarcinoma (Darby et al., 2010). We verified the upregulation of CBS, Sardh, GNMT, Pgam2, and Sdsl following TDG treatment (**Figure 4A**).
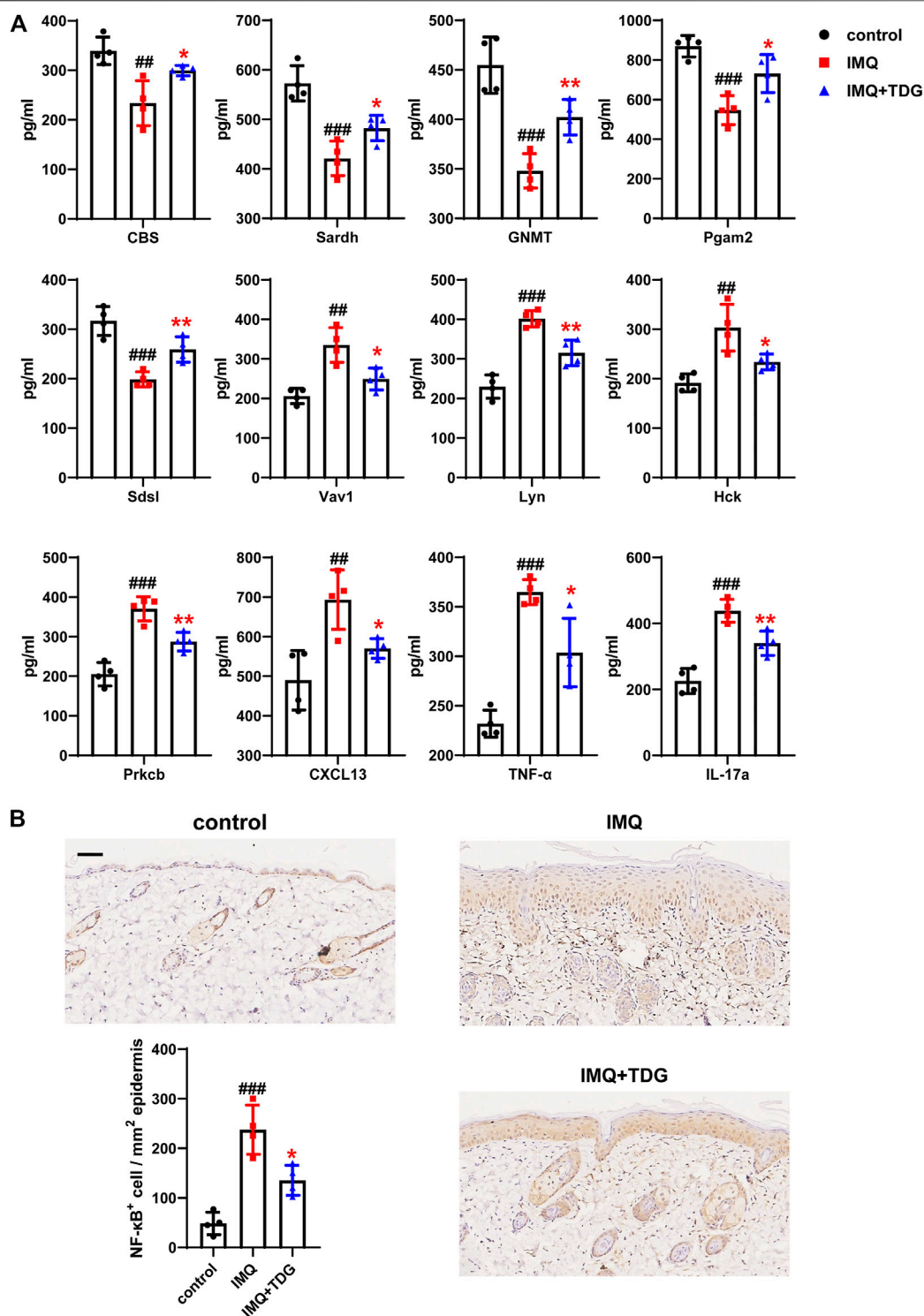
FIGURE 4 | Increased gene expression in Gly-Ser-Thr metabolism axis and decreased gene expression in chemokine signaling pathway as well as inflammatory markers after Taodan granule (TDG) treatment. **(A)** Expression determined by ELISA: CBS, Sardh, GNMT, Pgam2, and Sdsl in Gly-Ser-Thr axis; Vav1, Lyn, Hck, Prkcb, and CXCL13 in chemokine signaling pathway; IL-17a as well as TNF-α protein in lesions. **(B)** Representative immunohistochemistry sections of NF-κB nuclear staining (brown) of the back skin lesions (200×). Quantification of NF-κB^{+} cells in back lesions. Scale bar = 100 μm. The data are expressed as the mean ± SD. Four skin lesions in each group were included for analysis. [#]$p < 0.05$, [##]$p < 0.01$, [###]$p < 0.001$, compared with the control group. [*]$p < 0.05$, [**]$p < 0.01$, [***]$p < 0.001$, compared with the imiquimod (IMQ) group.
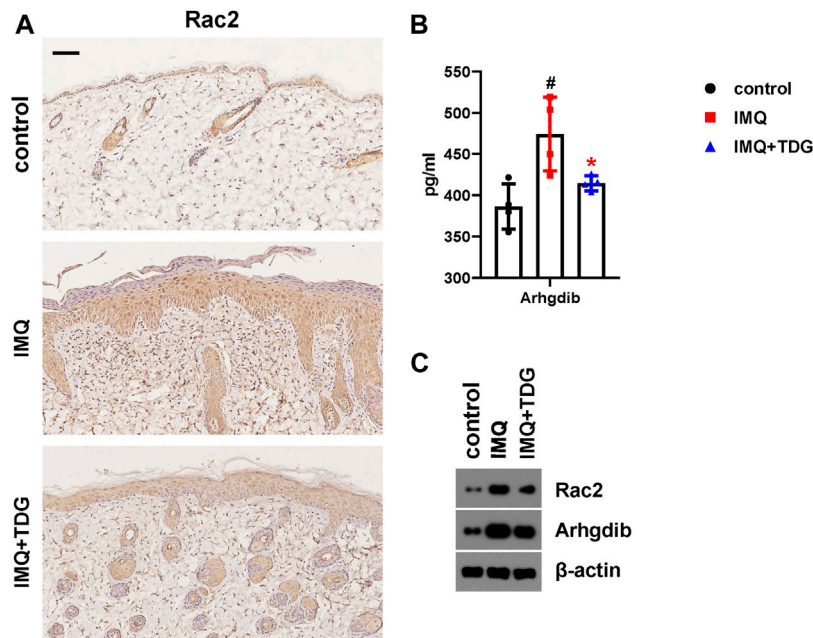
FIGURE 5 | Reduced Rac2 and Arhgdib in lesions following Taodan granule (TDG) treatment. **(A)** Representative images of Rac2 cytoplasm staining (brown) of back lesions from each group (200×). Scale bar = 100 μm. **(B)** The expression of Arhgdib protein in lesions determined by ELISA. **(C)** Western blotting of Rac2 and Arhgdib protein in back lesions on day 12. The data are expressed as mean ± SD. Four skin lesions in each group were included for analysis. $^{\#}p < 0.05$, $^{\#\#}p < 0.01$, $^{\#\#\#}p < 0.001$, compared with the control group. $^{*}p < 0.05$, $^{**}p < 0.01$, $^{***}p < 0.001$, compared with the imiquimod (IMQ) group.

TABLE 2 | Top 20 genes of combined-score with Rac2 (Genes with |log2FoldChange| > 1 and p-value < 0.05).

Gene ID	Gene name	Gene definition	LOG$_2$|FC|	p-value	Q-value	Regulation	Combined-score
11,857	Arhgdib	Rho, GDP dissociation inhibitor (GDI) beta	−1.363,083,474	9.26E-34	4.62E-31	DOWN	994
17,970	Ncf2	Neutrophil cytosolic factor 2	−1.116,136,949	2.99E-14	2.68E-12	DOWN	991
13,058	Cybb	Cytochrome b-245, beta polypeptide	−1.010,635,235	4.13E-08	1.15E-06	DOWN	989
17,972	Ncf4	Neutrophil cytosolic factor 4	−1.477,689,282	5.77E-24	1.62E-21	DOWN	988
22,324	Vav1	Vav 1 oncogene	−1.810,926,467	1.18E-37	8.16E-35	DOWN	987
105,855	Nckap1l	NCK associated protein 1 like	−1.131,010,001	1.11E-21	2.37E-19	DOWN	981
17,969	Ncf1	Neutrophil cytosolic factor 1	−1.299,760,797	1.81E-21	3.70E-19	DOWN	977
277,360	Prex1	Phosphatidylinositol-3,4,5-trisphosphate-dependent rac exchange factor 1	−1.038,248,484	2.29E-19	3.88E-17	DOWN	967
94,176	Dock2	Dedicator of cyto-kinesis 2	−1.092,696,865	1.23E-17	1.67E-15	DOWN	963
171,207	Arhgap4	Rho gtpase activating protein 4	−1.592,067,061	8.27E-28	2.86E-25	DOWN	941
18,707	Pik3cd	Phosphatidylinositol 3-kinase catalytic delta polypeptide	−1.016,119,488	1.31E-14	1.24E-12	DOWN	909
223,881	Rnd1	Rho family gtpase 1	−1.900,093,986	0.000995	0.007526	DOWN	906
23,912	Rhof	ras homolog family member F (in filopodia)	−1.620,812,138	0.000323	0.002942	DOWN	906
320,207	Pik3r5	Phosphoinositide-3-kinase, regulatory subunit 5, p101	−1.91,468,164	9.01E-19	1.42E-16	DOWN	821
18,751	Prkcb	Protein kinase C, beta	−1.350,798,593	1.38E-27	4.66E-25	DOWN	806
15,163	Hcls1	Hematopoietic cell specific lyn substrate 1	−1.807,265,374	2.60E-47	4.68E-44	DOWN	787
22,376	Was	Wiskott-aldrich syndrome	−1.152,788,414	2.68E-09	1.01E-07	DOWN	772
19,264	Ptprc	Protein tyrosine phosphatase, receptor type, C	−1.165,374,311	4.22E-14	3.70E-12	DOWN	772
16,414	Itgb2	Integrin beta 2	−2.253,358,932	1.70E-80	1.02E-76	DOWN	756
107,321	Lpxn	Leupaxin	−1.469,153,083	6.09E-09	2.08E-07	DOWN	751

Q-VALUE, A Benjamini value (an adjusted p-value).

Moreover, the most downregulated gene categories by TDGs were for the canonical immune and inflammatory pathways associated with psoriasis (**Figures 3B,C**). RNA-seq reported that Vav1, Lyn, Hck, Prkcb, and CXCL13 were the top five downregulated genes in the chemokine signaling pathway. Vav1, a key downstream signaling molecule of the T-cell

receptor, can trigger cytoskeleton rearrangement and immune synapse formation, as well as lead to the activation of transcription factors along with cytokine release (NFAT, NF-κB, AP1, etc.) (Bustelo, 2000). During the development of a host of tumor diseases, Vav1 promotes cell proliferation and invasion (Fernandez-Zapico et al., 2005). Lyn is the substrate for caspases in the cysteine protease family and is involved in the regulation of apoptosis and inflammation. Lyn has been validated for specific increases in protein levels in human psoriatic lesions and is involved in regulating the expression of STAT3 and the NF-κB pathway to mediate a chronic inflammatory syndrome resembling human psoriasis in a mouse model by pan-genomic profiling (Marchetti et al., 2009). Hck, a member of the Src family of kinases, is highly expressed in macrophages and is related to various inflammatory responses (Kong et al., 2020). Clinical evidence has shown that the mRNA level of Prkcb in the bone marrow is significantly higher in patients with psoriasis than in healthy individuals. Prkcb is a critical gene for regulating hematopoietic cell development and differentiation, and the abnormal expression of Prkcb may induce dysfunction in the hematopoietic cells of patients with psoriasis (Yin et al., 2011). The inflammatory chemokine CXCL13 is crucial in the homing of B lymphocytes into lymphoid follicles, while CXCL13 mRNA was upregulated in the brain tissues of the IMQ-induced mouse model (McColl et al., 2016). By verifying the sequencing results via ELISA, we found that TDGs could downregulate the expression of these five genes (**Figure 4A**), and the specific mechanism is worthy of further exploration.

Psoriasis has been identified as a T-cell-mediated autoimmune skin disease. Different T-cell subsets such as Th1, Th17, and regulatory T cells are pivotal for psoriatic pathogenesis and inflammation (Armstrong et al., 2020). The psoriatic inflammatory cascade is triggered by plasmacytoid dendritic cells and activated and polarized Th cells, while producing various inflammatory cytokines (IL-23, IL-6, IFN-γ, IL-17a, TNF-α, etc.) (Zhu et al., 2006; Lowes et al., 2013; Wu et al., 2018). These pro-inflammatory factors induce epidermal over-proliferation and activate KCs to produce chemokines and antimicrobial peptides to maintain the inflammatory microenvironment and promote the development of the psoriatic phenotype (Conrad et al., 2018). Our previous studies have demonstrated that the expression levels of IL-23, IL-17, IFN-γ, and TNF-α in the serum of patients with psoriasis were significantly increased (Li et al., 2016). Furthermore, NF-κB is a crucial regulator of inflammation, cell proliferation, differentiation, and apoptosis in the pathogenesis of psoriasis. The NF-κB pathway regulates the expression of pro-inflammatory factors (TNF-α and IL-6) to aggravate the inflammatory process. IL-6 induces IL-17 to produce an inflammatory response, promotes KC hyperproliferation, and increases T-cell aggregation in the *epidermis*. IL-17 and TNF-α promote the expression of CCL20 in KCs and further attract dendritic cells as well as Th17 cells, thereby promoting the formation of chemotaxis rings and exacerbating the inflammatory response in psoriasis (Wang et al., 2015; Yang et al., 2020). Several *in vivo* experiments have also indicated

that the inhibition of NF-κB activity could significantly improve the inflammatory response in psoriasis (Kulkarni et al., 2015; Irrera et al., 2017). To further verify whether TDGs could regulate skin inflammation, we measured the concentrations of IL-17a, TNF-α, and NF-κB proteins in each group. Consistent with previous results (Rerknimitr et al., 2016; Yu et al., 2019), the expression of IL-17a, TNF-α, and NF-κB was significantly reduced after TDG treatment (**Figure 4**; **Supplementary Figure S5**). Based on the above, we inferred that TDGs upregulated metabolic pathways, such as the Gly-Ser-Thr axis, and downregulated immune- and inflammation-related signaling pathways to treat psoriasis.

Rac2, a major isoform of the Rac GTPases, has been shown to play a crucial role in cell migration and is involved in the homing of T-lymphoid progenitor cells (Lu et al., 2020). High expression of Rac2 may be a diagnostic index for clear-cell renal cell carcinoma, as the knockdown of Rac2 *in vitro* attenuates the proliferation, migration, and invasion of renal carcinoma cells (Liu et al., 2019). The hyperproliferation and abnormal migration of KCs, which are responsible for psoriasis-lesioned microenvironments, are critical features of psoriasis (Liu et al., 2020). Our sequencing results demonstrated the downregulation of Rac2 in skin lesions of IMQ-induced psoriasis-like mice by TDGs (**Table 1**). Therefore, IHC and western blotting were used to confirm that Rac2 expression significantly decreased in skin lesions after TDG treatment, to verify the feasible role of TDGs in regulating Rac2 (**Figure 5A**; **Supplementary Figure S5**). Next, based on the protein-protein interaction analysis, we found that the skin protein expression of Arhgdib (had the highest combined scores of Rac2) in IMQ-induced psoriasis-like mice was significantly downregulated (**Figure 5B**). Arhgdib is mainly located in hematopoietic, endothelial, and epithelial cells. Clinical evidence has demonstrated that Arhgdib is often highly expressed in proliferative diseases, and knockout-Arhgdib can reduce proliferation, migration, and invasion of cells *in vitro* (Wang et al., 2020). Hence, we speculate that TDGs may reduce Rac2 and Arhgdib and, consequently, decrease KC proliferation and migration to relieve psoriasis.

CONCLUSION

We explored the feasible mechanism of action of TDG treatment for psoriasis through RNA-seq analysis and experimental verification. We found that TDGs affected KC proliferation and inflammatory responses to alleviate IMQ-induced psoriatic symptoms. The mechanisms of TDG treatment for psoriasis include the upregulation of metabolic signaling pathways, downregulation of immune and inflammatory pathways, and a decrease in Rac2 and Arhgdib genes. Further studies are needed to clarify the mechanisms of TDGs and provide a reference for clinical indications, along with optimal doses. The fuzziness of Chinese herbal compounds is significant; hence, evidence of their effectiveness *in vitro* and *in vivo* is the foundation for all subsequent studies. In future studies, we plan to continue further exploring other signaling pathways involved.

DATA AVAILABILITY STATEMENT

The data generated from this article can be found in the Sequence Read Archive database (https://www.ncbi.nlm.nih.gov/sra/), using accession number SRP292449.

ETHICS STATEMENT

The animal study was reviewed and approved by the Ethics Committee of Yueyang Hospital affiliated to Shanghai University of Traditional Chinese Medicine.

AUTHOR CONTRIBUTIONS

BL, XL, LK, YiL, and KQ conceptualized and planned the experiments. LK, YiL, and KQ performed most of the experiments and completed the original draft. YR and YuL completed the RNA-seq analysis. XD completed HPLC. MX and LL completed the verification experiments. XS and LK analyzed the data. YiL and KQ raised the animals and completed the protein-protein interaction analysis. BL and XL guided the experiments. All authors were involved in the writing and critical review of the manuscript and approved its final version.

FUNDING

SUPPLEMENTARY MATERIAL

The Supplementary Material for this article can be found online at: https://www.frontiersin.org/articles/10.3389/fphar.2021.632414/full#supplementary-material.

REFERENCES

Al Sawah, S., Foster, S. A., Goldblum, O. M., Malatestinic, W. N., Zhu, B., Shi, N., et al. (2017). Healthcare costs in psoriasis and psoriasis sub-groups over time following psoriasis diagnosis. *J. Med. Econ.* 20 (9), 982–990. doi:10.1080/13696998.2017.1345749

Al-Harbi, N. O., Nadeem, A., Al-Harbi, M. M., Zoheir, K. M. A., Ansari, M. A., El-Sherbeeny, A. M., et al. (2017a). Psoriatic inflammation causes hepatic inflammation with concomitant dysregulation in hepatic metabolism via IL-17A/IL-17 receptor signaling in a murine model. *Immunobiology* 222 (2), 128–136. doi:10.1016/j.imbio.2016.10.013

Al-Harbi, N. O., Nadeem, A., Ansari, M. A., Al-Harbi, M. M., Alotaibi, M. R., AlSaad, A. M. S., et al. (2017b). Psoriasis-like inflammation leads to renal dysfunction via upregulation of NADPH oxidases and inducible nitric oxide synthase. *Int. Immunopharmacology* 46, 1–8. doi:10.1016/j.intimp.2017.02.018

Alhosaini, K., Ansari, M. A., Nadeem, A., Attia, S. M., Bakheet, S. A., Al-Ayadhi, L. Y., et al. (2021). Dysregulation of ki-67 expression in T cells of children with autism spectrum disorder. *Children* 8 (2), 116. doi:10.3390/children8020116

Aon, M. A., Bernier, M., Mitchell, S. J., Di Germanio, C., Mattison, J. A., Ehrlich, M. R., et al. (2020). Untangling determinants of enhanced health and lifespan through a multi-omics approach in mice. *Cel Metab.* 32 (1), 100–116 e104. doi:10.1016/j.cmet.2020.04.018

Armstrong, A. W., and Read, C. (2020). Pathophysiology, clinical presentation, and treatment of psoriasis. *JAMA* 323 (19), 1945–1960. doi:10.1001/jama.2020.4006

Bustelo, X. R. (2000). Regulatory and signaling properties of the Vav family. *Mol. Cel. Biol.* 20 (5), 1461–1477. doi:10.1128/mcb.20.5.1461-1477.2000

Cai, H.-Q., Zhang, M.-J., Cheng, Z.-J., Yu, J., Yuan, Q., Zhang, J., et al. (2021). FKBP10 promotes proliferation of glioma cells via activating AKT-CREB-PCNA axis. *J. Biomed. Sci.* 28 (1), 13. doi:10.1186/s12929-020-00705-3

Capon, F., Burden, A. D., Trembath, R. C., and Barker, J. N. (2012). Psoriasis and other complex trait dermatoses: from Loci to functional pathways. *J. Invest. Dermatol.* 132 (3 Pt 2), 915–922. doi:10.1038/jid.2011.395

Chen, H.-X., Liu, Y.-S., and Zhang, X.-J. (2018). TargetScore used to reveal potential targets of miRNA203 and miRNA-146a in psoriasis by integrating microRNA overexpression and microarray data. *Medicine (Baltimore)* 97 (41), e12671. doi:10.1097/MD.0000000000012671

Cladel, N. M., Jiang, P., Li, J. J., Peng, X., Cooper, T. K., Majerciak, V., et al. (2019). Papillomavirus can be transmitted through the blood and produce infections in blood recipients: evidence from two animal models. *Emerging Microbes & Infections* 8 (1), 1108–1121. doi:10.1080/22221751.2019.1637072

Conrad, C., and Gilliet, M. (2018). Psoriasis: from pathogenesis to targeted therapies. *Clinic Rev. Allerg Immunol.* 54 (1), 102–113. doi:10.1007/s12016-018-8668-1

Darby, I. A., Vuillier-Devillers, K., Pinault, É., Sarrazy, V., Lepreux, S., Balabaud, C., et al. (2010). Proteomic analysis of differentially expressed proteins in peripheral cholangiocarcinoma. *Cancer Microenvironment* 4 (1), 73–91. doi:10.1007/s12307-010-0047-2

Dhana, A., Yen, H., Yen, H., and Cho, E. (2019). All-cause and cause-specific mortality in psoriasis: a systematic review and meta-analysis. *J. Am. Acad. Dermatol.* 80 (5), 1332–1343. doi:10.1016/j.jaad.2018.12.037

Evans, E. A., Sayers, S. R., Kodji, X., Xia, Y., Shaikh, M., Rizvi, A., et al. (2020). Psoriatic skin inflammation induces a pre-diabetic phenotype via the endocrine actions of skin secretome. *Mol. Metab.* 41, 101047. doi:10.1016/j.molmet.2020.101047

Fan, B., Li, B., Shen, J. X., Zhang, Y., Tang, H., and Wang, J. (2006a). Effects of herbal medicine on cytokines in patients with psoriasis at different stages. *Chin. J. Dermatol. Venereol.* (02), 70–71.

Fan, B., Li, B., Zhang, Y., Shen, J. X., and Zhao, X. L. (2006b). Effects of Chinese herbal medicine on the secretion of Substance P and -endorphins in plasma of patients with psoriasis during progressive and inactive stages. *Shanghai J. Traditional Chin. Med.* (10), 34–35. doi:10.16305/j.1007-1334.2006.10.017

Fernandez-Zapico, M. E., Gonzalez-Paz, N. C., Weiss, E., Savoy, D. N., Molina, J. R., Fonseca, R., et al. (2005). Ectopic expression of VAV1 reveals an unexpected role in pancreatic cancer tumorigenesis. *Cancer Cell* 7 (1), 39–49. doi:10.1016/j.ccr.2004.11.024

Gelfand, J. M., and Wan, M. T. (2018). Psoriasis: a novel risk factor for type 2 diabetes. *Lancet Diabetes Endocrinol.* 6 (12), 919–921. doi:10.1016/S2213-8587(18)30127-X

Hashem, S., Nisar, S., Sageena, G., Macha, M. A., Yadav, S. K., Krishnankutty, R., et al. (2020). Therapeutic effects of curcumol in several diseases; an overview. *Nutr. Cancer* 73, 181–195. doi:10.1080/01635581.2020.1749676

Hawkes, J. E., Chan, T. C., and Krueger, J. G. (2017). Psoriasis pathogenesis and the development of novel targeted immune therapies. *J. Allergy Clin. Immunol.* 140 (3), 645–653. doi:10.1016/j.jaci.2017.07.004

Hordijk, P. L. (2006). Regulation of NADPH oxidases. *Circ. Res.* 98 (4), 453–462. doi:10.1161/01.RES.0000204727.46710.5e

Huang, X., Qian, J., Li, L., Zhang, X., Wei, G., Lv, J., et al. (2020). Curcumol improves cisplatin sensitivity of human gastric cancer cells through inhibiting PI3K/AKT pathway. *Drug Dev. Res.* 81, 1019. doi:10.1002/ddr.21719

Irrera, N., Vaccaro, M., Bitto, A., Pallio, G., Pizzino, G., Lentini, M., et al. (2017). BAY 11-7082 inhibits the NF-κB and NLRP3 inflammasome pathways and protects against IMQ-induced psoriasis. *Clin. Sci. (Lond).* 131 (6), 487–498. doi:10.1042/CS20160645

Khan, A. P., Rajendiran, T. M., Bushra, A., Asangani, I. A., Athanikar, J. N., Yocum, A. K., et al. (2013). The role of sarcosine metabolism in prostate cancer progression. *Neoplasia* 15 (5), 491–IN13. doi:10.1593/neo.13314

Kim, J., Hong, S. J., Park, J. H., Park, S. Y., Kim, S. W., Cho, E. Y., et al. (2009). Expression of cystathionine β-synthase is downregulated in hepatocellular carcinoma and associated with poor prognosis. *Oncol. Rep.* 21 (6), 1449–1454. doi:10.3892/or_00000373

Kong, X., Liao, Y., Zhou, L., Zhang, Y., Cheng, J., Yuan, Z., et al. (2020). Hematopoietic cell kinase (HCK) is essential for NLRP3 inflammasome activation and lipopolysaccharide-induced inflammatory response in vivo. *Front. Pharmacol.* 11, 581011. doi:10.3389/fphar.2020.581011

Kovitwanichkanont, T., Chong, A. H., and Foley, P. (2020). Beyond skin deep: addressing comorbidities in psoriasis. *Med. J. Aust.* 212 (11), 528–534. doi:10.5694/mja2.50591

Kuai, L., Song, J.-k., Zhang, R.-x., Xing, M., Luo, Y., Ru, Y., et al. (2020). Uncovering the mechanism of Jueyin granules in the treatment of psoriasis using network pharmacology. *J. Ethnopharmacology* 262, 113214. doi:10.1016/j.jep.2020.113214

Kuai, L., Zhang, J.-t., Deng, Y., Xu, S., Xu, X.-z., Wu, M.-f., et al. (2018). Sheng-ji Hua-yu formula promotes diabetic wound healing of re-epithelization via Activin/Follistatin regulation. *BMC Complement. Altern. Med.* 18 (1), 32. doi:10.1186/s12906-017-2074-8

Kulkarni, N. M., Muley, M. M., Jaji, M. S., Vijaykanth, G., Raghul, J., Reddy, N. K. D., et al. (2015). Topical atorvastatin ameliorates 12-O-tetradecanoylphorbol-13-acetate induced skin inflammation by reducing cutaneous cytokine levels and NF-κB activation. *Arch. Pharm. Res.* 38 (6), 1238–1247. doi:10.1007/s12272-014-0496-0

Lei, L., Wu, K., and Wang, G. L. (2019). HPLC method was used to simultaneously determine the content of 6 components in xiaoji Huazhong powder. *Chin. Med.* 22 (02), 340–343.

Li, F.-L., Xu, R., Zeng, Q.-c., Li, X., Chen, J., Wang, Y.-F., et al. (20122012). Tanshinone IIA inhibits growth of keratinocytes through cell cycle arrest and apoptosis: underlying treatment mechanism of psoriasis. *Evidence-Based Complement. Altern. Med.* 2012, 1. doi:10.1155/2012/927658

Li, S., Zhou, G., Liu, W., Ye, J., Yuan, F., and Zhang, Z. (2020). Curcumol inhibits lung adenocarcinoma growth and metastasis via inactivation of PI3K/AKT and Wnt/ss-catenin pathway. *Oncol. Res.* doi:10.3727/096504020X15917007265498

Li, X., Kong, L., Li, F., Chen, C., Xu, R., Wang, H., et al. (2015). Association between psoriasis and chronic obstructive pulmonary disease: a systematic review and meta-analysis. *PLoS One* 10 (12), e0145221. doi:10.1371/journal.pone.0145221

Li, X., Xiao, Q.-q., Li, F.-l., Xu, R., Fan, B., Wu, M.-f., et al. (2016). Immune signatures in patients with psoriasis vulgaris of blood-heat syndrome: a systematic review and meta-analysis. *Evidence-Based Complement. Altern. Med.* 2016, 1. doi:10.1155/2016/9503652

Lin, C.-Y., Hsu, C.-Y., Elzoghby, A. O., Alalaiwe, A., Hwang, T.-L., and Fang, J.-Y. (2019). Oleic acid as the active agent and lipid matrix in cilomilast-loaded nanocarriers to assist PDE4 inhibition of activated neutrophils for mitigating psoriasis-like lesions. *Acta Biomater.* 90, 350–361. doi:10.1016/j.actbio.2019.04.002

Liu, L., Song, B., Ma, J., Song, Y., Zhang, S.-Y., Tang, Y., et al. (2020). Bioinformatics approaches for deciphering the epitranscriptome: recent progress and emerging topics. *Comput. Struct. Biotechnol. J.* 18, 1587–1604. doi:10.1016/j.csbj.2020.06.010

Liu, T., Zhang, X., and Wang, Y. (2020). miR-183-3p suppresses proliferation and migration of keratinocyte in psoriasis by inhibiting GAB1. *Hereditas* 157 (1), 28. doi:10.1186/s41065-020-00138-w

Liu, Y., Cheng, G., Song, Z., Xu, T., Ruan, H., Cao, Q., et al. (2019). RAC2 acts as a prognostic biomarker and promotes the progression of clear cell renal cell carcinoma. *Int. J. Oncol.* 55 (3), 645–656. doi:10.3892/ijo.2019.4849

Lopes, N., Dias, L. L. S., Azulay-Abulafia, L., Oyafuso, L. K. M., Suarez, M. V., Fabricio, L., et al. (2019). Humanistic and economic impact of moderate to severe plaque psoriasis in Brazil. *Adv. Ther.* 36 (10), 2849–2865. doi:10.1007/s12325-019-01049-7

Lowes, M. A., Russell, C. B., Martin, D. A., Towne, J. E., and Krueger, J. G. (2013). The IL-23/T17 pathogenic axis in psoriasis is amplified by keratinocyte responses. *Trends Immunol.* 34 (4), 174–181. doi:10.1016/j.it.2012.11.005

Lu, X., Zhang, Y., Liu, F., and Wang, L. (2020). Rac2 regulates the migration of T lymphoid progenitors to the thymus during zebrafish embryogenesis. *J.I.* 204 (9), 2447–2454. doi:10.4049/jimmunol.1901494

Luo, Y., Ru, Y., Zhao, H., Liu, L., Hong, S., Sun, X., et al. (20192019). Establishment of mouse models of psoriasis with blood stasis syndrome complicated with glucose and lipid metabolism disorders. *Evidence-Based Complement. Altern. Med.* 2019, 1. doi:10.1155/2019/6419509

Marchetti, S., Gamas, P., Belhacène, N., Grosso, S., Pradelli, L. A., Colosetti, P., et al. (2009). The caspase-cleaved form of LYN mediates a psoriasis-like inflammatory syndrome in mice. *EMBO. J.* 28 (16), 2449–2460. doi:10.1038/emboj.2009.183

McColl, A., Thomson, C. A., Nerurkar, L., Graham, G. J., and Cavanagh, J. (2016). TLR7-mediated skin inflammation remotely triggers chemokine expression and leukocyte accumulation in the brain. *J. Neuroinflammation.* 13 (1), 102. doi:10.1186/s12974-016-0562-2

Michalek, I. M., Loring, B., and John, S. M. (2017). A systematic review of worldwide epidemiology of psoriasis. *J. Eur. Acad. Dermatol. Venereol.* 31 (2), 205–212. doi:10.1111/jdv.13854

Miele, L., Vallone, S., Cefalo, C., La Torre, G., Di Stasi, C., Vecchio, F. M., et al. (2009). Prevalence, characteristics and severity of non-alcoholic fatty liver disease in patients with chronic plaque psoriasis. *J. Hepatol.* 51 (4), 778–786. doi:10.1016/j.jhep.2009.06.008

Nadeem, A., Al-Harbi, N. O., Ansari, M. A., Al-Harbi, M. M., El-Sherbeeny, A. M., Zoheir, K. M. A., et al. (2017). Psoriatic inflammation enhances allergic airway inflammation through IL-23/STAT3 signaling in a murine model. *Biochem. Pharmacol.* 124, 69–82. doi:10.1016/j.bcp.2016.10.012

Parker, S., Zhang, C. S., Yu, J. J., Lu, C., Zhang, A. L., and Xue, C. C. (2017). Oral Chinese herbal medicine versus placebo for psoriasis vulgaris: a systematic review. *J. Dermatol. Treat.* 28 (1), 21–31. doi:10.1080/09546634.2016.1178377

Pedersen, E., Wang, Z., Stanley, A., Peyrollier, K., Rösner, L. M., Werfel, T., et al. (2012). RAC1 in keratinocytes regulates crosstalk to immune cells by Arp2/3-dependent control of STAT1. *J. Cel Sci* 125 (Pt 22), 5379–5390. doi:10.1242/jcs.107011

Rachakonda, T. D., Schupp, C. W., and Armstrong, A. W. (2014). Psoriasis prevalence among adults in the United States. *J. Am. Acad. Dermatol.* 70 (3), 512–516. doi:10.1016/j.jaad.2013.11.013

Rerknimitr, P., Nitinawarat, J., Weschawalit, S., Wititsuwannakul, J., Wongtrakul, P., Jutiviboonsuk, A., et al. (2016). The efficacy ofGynura pseudochina DC.var.hispida thv. Ointment in treating chronic plaque psoriasis: a randomized controlled trial. *J. Altern. Complement. Med.* 22 (8), 669–675. doi:10.1089/acm.2016.0100

Ru, Y., Li, H., Zhang, R., Luo, Y., Song, J., Kuai, L., et al. (2020). Role of keratinocytes and immune cells in the anti-inflammatory effects of Tripterygium wilfordii Hook. f. in a murine model of psoriasis. *Phytomedicine* 77, 153299. doi:10.1016/j.phymed.2020.153299

Ru, Y., Yan, X.-N., Yang, S.-Q., Gong, L.-P., Li, L.-E., Chen, J., et al. (2019). Oral Taodan granules for mild-to-moderate psoriasis vulgaris: protocol for a randomized, double-blind, multicenter clinical trial. *Ann. Transl. Med.* 7 (18), 488. doi:10.21037/atm.2019.09.05

Sparks, J. A., Dellaripa, P. F., Glynn, R. J., Paynter, N. P., Xu, C., Ridker, P. M., et al. (2020). Pulmonary adverse events in patients receiving low-dose methotrexate in the randomized, double-blind, placebo-controlled cardiovascular inflammation reduction trial. *Arthritis Rheumatol.* 72, 2065. doi:10.1002/art.41452

Thatikonda, S., Pooladanda, V., Sigalapalli, D. K., and Godugu, C. (2020). Piperlongumine regulates epigenetic modulation and alleviates psoriasis-like skin inflammation via inhibition of hyperproliferation and inflammation. *Cell Death Dis* 11 (1), 21. doi:10.1038/s41419-019-2212-y

Tollefson, M. M., Van Houten, H. K., Asante, D., Yao, X., and Maradit Kremers, H. (2018). Association of psoriasis with comorbidity development in children with psoriasis. *JAMA Dermatol.* 154 (3), 286–292. doi:10.1001/jamadermatol.2017.5417

Tomalin, L. E., Russell, C. B., Garcet, S., Ewald, D. A., Klekotka, P., Nirula, A., et al. (2020). Short-term transcriptional response to IL-17 receptor-A antagonism in the treatment of psoriasis. *J. Allergy Clin. Immunol.* 145 (3), 922–932. doi:10.1016/j.jaci.2019.10.041

Wang, X., Bi, X., Huang, X., Wang, B., Guo, Q., and Wu, Z. (2020). Systematic investigation of biomarker-like role of ARHGDIB in breast cancer. *Cbm* 28 (1), 101–110. doi:10.3233/CBM-190562

Wang, Y., Zhao, J., Zhang, L., Di, T., Liu, X., Lin, Y., et al. (2015). Suppressive effect of β, β-dimethylacryloyl alkannin on activated dendritic cells in an imiquimod-induced psoriasis mouse model. *Int. J. Clin. Exp. Pathol.* 8 (6), 6665–6673.

Williams, A. L., Pace, N. D., and DeSesso, J. M. (2020). Teratogen update: topical use and third-generation retinoids. *Birth Defects Res.* 112, 1105. doi:10.1002/bdr2.1745

Wu, R., Zeng, J., Yuan, J., Deng, X., Huang, Y., Chen, L., et al. (2018). MicroRNA-210 overexpression promotes psoriasis-like inflammation by inducing Th1 and Th17 cell differentiation. *J. Clin. Invest.* 128 (6), 2551–2568. doi:10.1172/JCI97426

Yang, L., Zhang, T., Zhang, C., Xiao, C., Bai, X., and Wang, G. (2020). Upregulated E3 ligase tripartite motif-containing protein 21 in psoriatic *epidermis* ubiquitylates nuclear factor-κB p65 subunit and promotes inflammation in keratinocytes*. *Br. J. Dermatol.* 184, 111. doi:10.1111/bjd.19057

Yin, G., Li, J., Wan, Y., Hou, R., Li, X., Zhang, J., et al. (2011). Abnormality of RUNX1 signal transduction in psoriatic CD34+ bone marrow cells. *Br. J. Dermatol.* 164 (5), 1043–1051. doi:10.1111/j.1365-2133.2010.10192.x

Yu, Q., Tong, Y., Cui, L., Zhang, L., Gong, Y., Diao, H., et al. (2019). Efficacy and safety of etanercept combined plus methotrexate and comparison of expression of pro-inflammatory factors expression for the treatment of moderate-to-severe plaque psoriasis. *Int. Immunopharmacology* 73, 442–450. doi:10.1016/j.intimp.2019.05.042

Yuan, Y., Liu, M., Liu, W., and Du, H. (2019). The association of serum uric acid levels in psoriasis patients. *Medicine (Baltimore)* 98 (44), e17643. doi:10.1097/MD.0000000000017643

Zhang, X., Yin, M., and Zhang, L.-j. (2019). Keratin 6, 16 and 17-critical barrier alarmin molecules in skin wounds and psoriasis. *Cells* 8 (8), 807. doi:10.3390/cells8080807

Zhou, X., Menche, J., Barabási, A.-L., and Sharma, A. (2014). Human symptoms-disease network. *Nat. Commun.* 5, 4212. doi:10.1038/ncomms5212

Zhu, H., Blake, S., Chan, K. T., Pearson, R. B., and Kang, J. (2018). Cystathionineβ-synthase in physiology and cancer. *Biomed. Res. Int.* 2018, 1. doi:10.1155/2018/3205125

Zhu, K. J., Cheng, H., Mao, X. H., Lao, L. M., Cen, J. P., and Ye, J. (2006). Increased endocytic activity in monocyte-derived dendritic cells in patients with psoriasis vulgaris. *Indian J. Med. Res.* 123 (1), 43–50.

Systems Pharmacology Approach and Experiment Evaluation Reveal Multidimensional Treatment Strategy of LiangXueJieDu Formula for Psoriasis

Jingxia Zhao[1,2†], Yan Wang[1,2†], Weiwen Chen[1], Jing Fu[1,2], Yu Liu[1,2,3], Tingting Di[1,2], Cong Qi[1,2], Zhaoxia Chen[1,2] and Ping Li[1,2]*

[1]Beijing Hospital of Traditional Chinese Medicine, Capital Medical University, Beijing, China, [2]Beijing Key Laboratory of Clinic and Basic Research with Traditional Chinese Medicine on Psoriasis, Beijing Institute of Traditional Chinese Medicine, Beijing, China, [3]Beijing University of Chinese Medicine, Beijing, China

Clinical studies have demonstrated the anti-psoriatic effect of the LiangXueJieDu (LXJD) herbal formula. However, the systemic mechanism and the targets of the LXJD formula have not yet been elucidated. In the present study, a systems pharmacology approach, metabolomics, and experimental evaluation were employed. First, by systematic absorption-distribution-metabolism-excretion (ADME) analysis, 144 active compounds with satisfactory pharmacokinetic properties were identified from 12 herbs of LXJD formula using the TCMSP database. These active compounds could be linked to 125 target proteins involved in the pathological processes underlying psoriasis. Then, the networks constituting the active compounds, targets, and diseases were constructed to decipher the pharmacological actions of this formula, indicating its curative effects in psoriasis treatment and related complications. The psoriasis-related pathway comprising several regulatory modules demonstrated the synergistic mechanisms of LXJD formula. Furthermore, the therapeutic effect of LXJD formula was validated in a psoriasis-like mouse model. Consistent with the systems pharmacology analysis, LXJD formula ameliorated IMQ-induced psoriasis-like lesions in mice, inhibited keratinocyte proliferation, improved keratinocyte differentiation, and suppressed the infiltration of CD3+ T cells. Compared to the model group, LXJD formula treatment remarkably reduced the expression of inflammatory cytokines and factors, such as IL-1β, IL-6, TNF-α, Cox2, and inhibited the phosphorylation of p-P65, p-IκB, p-ERK, p-P38, p-PI3K, p-AKT, indicating that LXJD formula exerts its therapeutic effect by inhibiting the MAPK, PI3K/AKT, and NF-κB signaling pathways. The metabolic changes in the serum of psoriasis patients were evaluated by liquid chromatography coupled with orbitrap mass spectrometry (LC-MS). The LXJD formula improved two perturbed metabolic pathways of glycerophospholipid metabolism and steroid hormone biosynthesis. Overall, this study revealed the complicated anti-psoriatic mechanism of LXJD formula and also offered a reliable strategy to elucidate the complex therapeutic mechanism of this Chinese herbal formula in psoriasis from a holistic perspective.

INTRODUCTION

Psoriasis is an immune-mediated, chronic skin condition that follows a relapsing and remitting course. It poses a significant public health challenge with a high prevalence rate of 0.09–11.43% worldwide and multiple co-morbidities, including arthritis, cardiovascular disease, obesity, diabetes mellitus, reduced quality of life, and depression/anxiety (World health organization, 2016). Psoriasis vulgaris is the most common form of psoriasis, encompassing about 80% of psoriasis patients. Clinical manifestations comprise well-demarcation, scaling, and erythematous plaques that appear anywhere on the body. Histologically, psoriasis is characterized by parakeratosis, acanthosis with downward elongation of rete ridges, thin/no granular cell layer, Munro's microabscesses (neutrophils in parakeratotic scale), increased mitotic figures above basal layer, and mixed dermal infiltrate of lymphocytes and neutrophils.

Current treatments for psoriasis are categorized as follows: topical therapies (topical corticosteroids, tar-based preparations, dithranol, vitamin D analogs, salicylic acid, and topical retinoids), oral medication (methotrexate, acitretin, and cyclosporine), biological agents (infliximab, adalimumab, etanercept, and ustekinumab), and Ultraviolet phototherapy (UV-B and psoralen-UV-A) (Heng et al., 2000; Gamret et al., 2018). However, 52.3% of patients with psoriasis reported dissatisfaction with their medical treatment because of the inefficacy of the methods and adverse effects (Kurd et al., 2008). Thus, the utilization of complementary and alternative medicine among psoriasis patients is common, with prevalence varying between 42 and 69% (Ben-Arye et al., 2003; Damevska et al., 2014; Talbott and Duffy, 2015). These methods constitute herbal therapies and traditional Chinese medicine (TCM) that have gained popularity in recent years. The application of TCM in the treatment of psoriasis has a long history. According to the theory of TCM, psoriasis vulgaris is classified as three main blood-related syndromes: blood heat, blood stasis, and blood dryness. The blood-heat syndrome is frequently observed at the active stage, accounting for 53.8% of the condition in psoriasis vulgaris (Zhang et al., 2009). LiangXueJieDu (LXJD) formula is commonly used to treat psoriasis vulgaris with blood-heat syndrome and has proven to be a safe remedy with better efficacy compared to conventional therapy in a multicenter randomized controlled study (Sun et al., 2020). However, the mechanisms underlying LXJD formula-alleviated psoriasis remain unclear.

TCM is based on its own theory of medicine with multiple ingredients' interactions. Relative to Western medicine, TCM treats the function and dysfunction of the body using a holistic approach. However, the complexity of the ingredients and their *in vivo* activity could interfere with identifying the targets and understanding the mechanisms of TCM. Systems pharmacology is an emerging systematic methodology that combines oral bioavailability screening, multiple drug targets prediction and validation, and network pharmacology, providing a holistic approach to explore the targets and mechanisms of TCM. In recent years, systems pharmacology has been widely used to reveal the potential mechanism of TCM formulas (Liu et al., 2016; Yuan et al., 2020).

Based on the proved clinical efficacy, we applied the systems pharmacology method to explore the pharmacological targets and mechanisms of LXJD formula in the treatment of psoriasis in this study. Next, we verified the mechanism of LXJD formula on the main targets and those integrated by systemic pharmacology in the samples from psoriasis patients and psoriasis-like mice.

MATERIALS AND METHODS

Reagents

High performance liquid chromatography (HPLC)-grade acetonitrile and methanol were purchased from Merck (Darmstadt, Germany). Purified water (18.2 MΩ) was obtained from a Milli-Q water purification system (Millipore, United States). Formic acid was obtained from Sigma-Aldrich (St. Louis, United States). Chlorogenic acid, caffeic acid, paeoniflorin, taxifolin, astilbin, albiflorin, resveratrol, rosmarinic acid, 5-O-methylvisammioside, quercetin, naringenin, luteolin, kaempferol, and isorhamnetin (all 98%, pure) were purchased from the National Institutes for Food and Drug Control (Beijing, China) (**Table 1**). All other chemicals were of analytical grade. CD3, Ki67, and loricrin antibodies were purchased from Abcam (Cambridge, MA, United States).
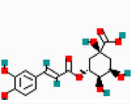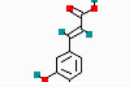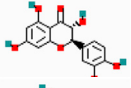
Database Construction
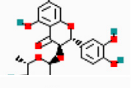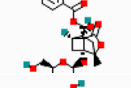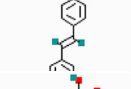
A total of 864 chemical ingredients of 12 herbs in LXJD formula were collected manually from PubMed, the China National Knowledge Infrastructure (CNKI), and the Traditional Chinese Medicines Systems Pharmacology (TCMSP) databases (http://lsp.nwsuaf.edu.cn/) (Ru et al., 2014).
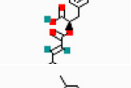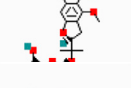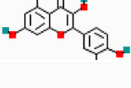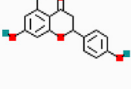
Screening of Active Compounds

We employed an *in silico* integrative model-ADME (absorption, distribution, metabolism, and excretion of drugs) to screen out the compounds with favorable pharmacokinetics properties. Oral bioavailability (OB) is one of the most desirable attributes of new drugs representing the ratio of the orally administered dose that reaches the circulation system with unaltered activity.
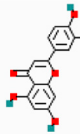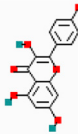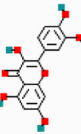
In the present study, the OBioavail1.1 model was utilized to estimate the OB values. The compounds from LXJD formula which satisfy the criteria of OB ≥ 30% were selected as candidate active molecules for further screening (Ru et al., 2014; Yuan et al., 2020). Drug-likeness (DL) is a major factor in the absorption, distribution, metabolism, and elimination of the molecules in the human body. It is estimated from the molecular structure before the substance is synthesized and tested. Herein, a compound with

TABLE 1 | Identification of the chemical constituents of LXJD formula by UHPLC-ESI-MS analysis.

No	Retention time (min)	Selected ion	Measured mass (m/z)	Error (ppm)	Identification	Formula	Chemical structure
1	20.41	(M–H)	353.0878	–0.02	Chlorogenic acid	$C_{16}H_{18}O_9$	
2	20.68	(M–H)	179.0351	0.63	Caffeic acid	$C_9H_8O_4$	
3	21.24	(M + H)	481.1712	–0.63	Paeoniflorin	$C_{23}H_{28}O_{11}$	
4	23.90	(M–H)	303.0510	–0.001	Taxifolin	$C_{15}H_{12}O_7$	
5	25.23	(M–H)	449.1090	0.03	Astilbin	$C_{21}H_{22}O_{11}$	
6	25.95	(M + H)	481.1713	–0.56	Albiflorin	$C_{23}H_{28}O_{11}$	
7	26.43	(M–H)	227.0714	–0.08	Resveratrol	$C_{14}H_{12}O_3$	
8	26.72	(M-H)	359.077	0.76	Rosmarinic acid	$C_{18}H_{16}O_8$	
9	27.74	(M + H)	453.1760	1.04	5-O-methylvisammioside	$C_{22}H_{28}O_{10}$	
10	29.45	(M–H)	301.0352	–0.63	Quercetin	$C_{15}H_{10}O_7$	
11	29.58	(M–H)	271.0612	–0.03	Naringenin	$C_{15}H_{12}O_5$	

TABLE 1 | (Continued) Identification of the chemical constituents of LXJD formula by UHPLC-ESI-MS analysis.

No	Retention time (min)	Selected ion	Measured mass (m/z)	Error (ppm)	Identification	Formula	Chemical structure
12	30.23	(M−H)	285.0403	−0.73	Luteolin	$C_{15}H_{10}O_6$	
13	31.24	(M−H)	285.0404	−0.20	Kaempferol	$C_{15}H_{10}O_6$	
14	31.66	(M−H)	315.0510	−0.10	Isorhamnetin	$C_{16}H_{12}O_7$	

DL $\geq$ 0.18 was selected as the active compound of herbs for subsequent studies (Ru et al., 2014; Yuan et al., 2020). The oral absorption of drugs was realized *via* intestinal epithelial cells (IECs). In this study, a computer Caco-2 permeability prediction model was applied to predict the intestinal permeability of the components in TCMSP (Lv et al., 2019). The chemical ingredients with Caco-2 cell permeability ≥ -0.4 were filtered out as candidate active compounds. The oil-water partition coefficient AlogP is the logarithm of the ratio of the partition coefficient of the substance in n-octanol and water. Lipophilicity is a leading physical and chemical parameter reflecting the permeability in biofilms. ALOGPS2.1 software was used to calculate AlogP, and the threshold was set to <5 according to Lipinski's rule of five (Lipinski et al., 2001; Tetko and Bruneau, 2004).

Target Fishing

A weighted ensemble similarity (WES) model was implemented to predict the potential target molecules of the candidate active compounds in LXJD formula. Then, a similarity search based on chemical fingerprinting was applied to obtain potential targets (http://sea.bkslab.org/search/). Finally, the targets from different sources were analyzed against the Pharmacogenomics knowledgebase (PharmGKB, https://www.pharmgkb.org/), Therapeutic Targets Database (TTD, http://database.idrb.cqu.edu.cn/TTD/), and Comparative Toxicogenomics Database (CTD, http://ctdbase.org/) to eliminate redundant and erroneous molecules, thereby guaranteeing the accuracy of the database.

Gene Ontology Enrichment and Clustering Analysis for Targets

To identify the targets associated with the physiological features of psoriasis, a Gene Ontology (GO) enrichment analysis was performed using DAVID (http://david.abcc.ncifcrf.gov) for classification. In this section, the GOBP (biological process) analysis result was highlighted. Then, functional annotation clustering analysis was carried out based on the GOBP enrichment data. *p*-value <0.05 indicated statistical significance.

Network Construction

TCM is a complex system consisting of multiple effective compounds, multiple targets of action, and related diseases. To illustrate the pharmacological mechanisms of LXJD formula in psoriasis treatment and clarify the complicated associations among the active compounds, targets, and diseases at a systems level, the network visualization analysis Cytoscape software was used to establish the compound-target network, target-disease network, and target-pathway network, respectively. In order to further interpret the molecular mechanism of LXJD formula against psoriasis, an integrated map of "psoriasis-related pathways" was constructed by integrating the key pathway obtained from the Kyoto Encyclopedia of Genes and Genomes (KEGG) database (http://www.kegg.jp/) using target-pathway network analysis.

Preparation of LiangXueJieDu Formula

LXJD formula, consisting of Tu Fu Ling (*Smilax glabra* Roxb.) (ratio 1:5), Huai Hua (Styphnolobium japonicum (L.) Schott

syn. Sophora japonica L.) (ratio 1:10), Di Huang (Rehmannia glutinosa (Gaertn.) DC.) (ratio 1:10), Zi Cao (Arnebia euchroma (Royle ex Benth.) I.M.Johnst.) (ratio 1:15), Quan Shen (Bistorta officinalis Delarbre syn. Polygonum (Isatis tinctoria L.) (ratio 1: 15), Bai Mao Gen (Imperata cylindrica (L.) P.Beauv.) (ratio 1:15), Bai Xian Pi (Dictamnus dasycarpus Turcz.) (ratio 1:15), Bai Hua She She Cao (Scleromitrion diffusum (Willd.) R.J.Wang syn. Hedyotis diffusa Willd.) (ratio 1:15), Fang Feng (Saposhnikovia varzcata (Turcz.) Schischk.) (ratio 1:15), and Mu Dan Pi (Paeonia x suffruticosa Andr), were decocted and provided by the TCM Pharmacy of Beijing Hospital of Traditional Chinese Medicine. Briefly, 150 g of the crude drugs of LXJD formula were soaked and decocted in 400 ml of pure water for 30 min. Then, the water decoction was concentrated to 200 ml, and the final dosage of crude drugs was 0.75 g/ml.

All raw herbs were purchased from Beijing Xinglin Pharmaceutical (Beijing, China, Voucher number 20150301). The voucher specimen, identified by Professor Wei He, was deposited in our laboratory at Beijing Traditional Chinese Medical Hospital.

Preparation of Standard Solutions and Liquid Chromatography

A standard working solution of the 14 reference substances (**Table 1**, purities>98%) were prepared in concentrations ranging from 0.032 to 0.058 mg/ml in methanol and stored at 4°C. The 14 reference substances were used as standard control to identify the major components of LXJD formula by the UPLC-MS method.

The UPLC separation was performed on an ACQUITY UPLC™ BEH C18 column (100 × 2.1, 1.7 mm). Both negative and positive modes were examined. A gradient elution was used with 0.1% formic acid in methanol as solvent A and 0.1% formic acid in water as solvent B, at a flow rate of 0.2 ml min^{-1}. The following gradient elution scheme was used: 0–2 min, 100–100% B; 2–10 min, 100–93% B; 10–40 min, 93–0% B; 40–45 min, 0–0% B; 45–45.1 min, 0–100% B; and 45.1–60 min, 100–100% B. The injection volume was 10 μl.

Mass Spectrometric Conditions

A Thermo Q Exactive™ Plus Orbitrap™ mass spectrometer was used for the qualitative analysis of the constituents in LXJD formula. Mass spectrometric parameters were: sheath gas flow rate of 35; aux gas flow rate of 10; sweep gas flow rate of 0; S-lens RF level of 50. The spray voltage was 3.5 kV for the positive and −4.5 kV for the negative ion mode. The capillary temperature and aux gas heater temperature were set to 320 and 350 °C, respectively. The m/z ranged from 100–1200 and 150–2000 for the positive and negative ion modes, respectively.

Study Design

A total of 40 psoriasis patients were recruited from the Beijing Traditional Chinese Medical Hospital according to the specified inclusion and exclusion criteria.

The inclusion criteria were as follows: 1) Psoriasis vulgaris was diagnosed according to the "Clinical Guidelines of Psoriasis 2008" reported by the Chinese Medical Association; 2) age 18–65 years; 3) willing to sign a written informed consent; 4) psoriasis patients were diagnosed with blood-heat syndrome based on the theory of TCM; 4) PASI score >5.

Exclusion criteria (patients who met one of the following conditions were excluded): 1) Those who were allergic to LXJD formula or the composition; 2) women who were pregnant or in the lactation stage; 3) those who had been treated with steroids orally in the past 2 weeks or with retinoid orally or steroid topically in the past week; 4) arthropathic, pustular, or erythrodermic psoriasis; 5) those with severe heart, cerebrovascular, liver, kidney, hematopoietic system, cancer, or psychosis diseases.

The treatment group received the Chinese herbal medicine LXJD formula for 8 weeks. Each dose of LXJD formula (150 g of crude drugs) was decocted in 400 ml of water. Then, the water decoction was concentrated to 200 ml, and the final dosage of crude drugs was 0.75 g/ml. In total, 100 ml of the decoction was taken orally 30 min before breakfast and the other 100 ml 30 min before dinner. Serum samples were collected from each patient before and 8 weeks after LXJD formula treatment.

The study duration was 8 weeks. Patients were evaluated before the start of treatment and were followed up every 2 weeks during the trial period. Clinical symptoms, examination of psoriatic skin lesions, and psoriasis area and severity index (PASI) scores were documented. The PASI is a composite index of the severity of the three main characteristics of psoriatic plaques (erythema, scaling, and thickness) weighted by the amount of coverage of these plaques in the four main body areas (i.e., head, trunk, upper extremities, and lower extremities). PASI scores can range from 0 to 72, wherein higher scores indicate greater severity.

Out of a total of 40 potentially eligible patients, 15 patients were subsequently excluded from this study, of which 7 patients were excluded from the Chinese medicine treatment group for failing to adhere to the clinical trial protocol and eight patients were excluded because of the progression and evolution of patients' symptoms.
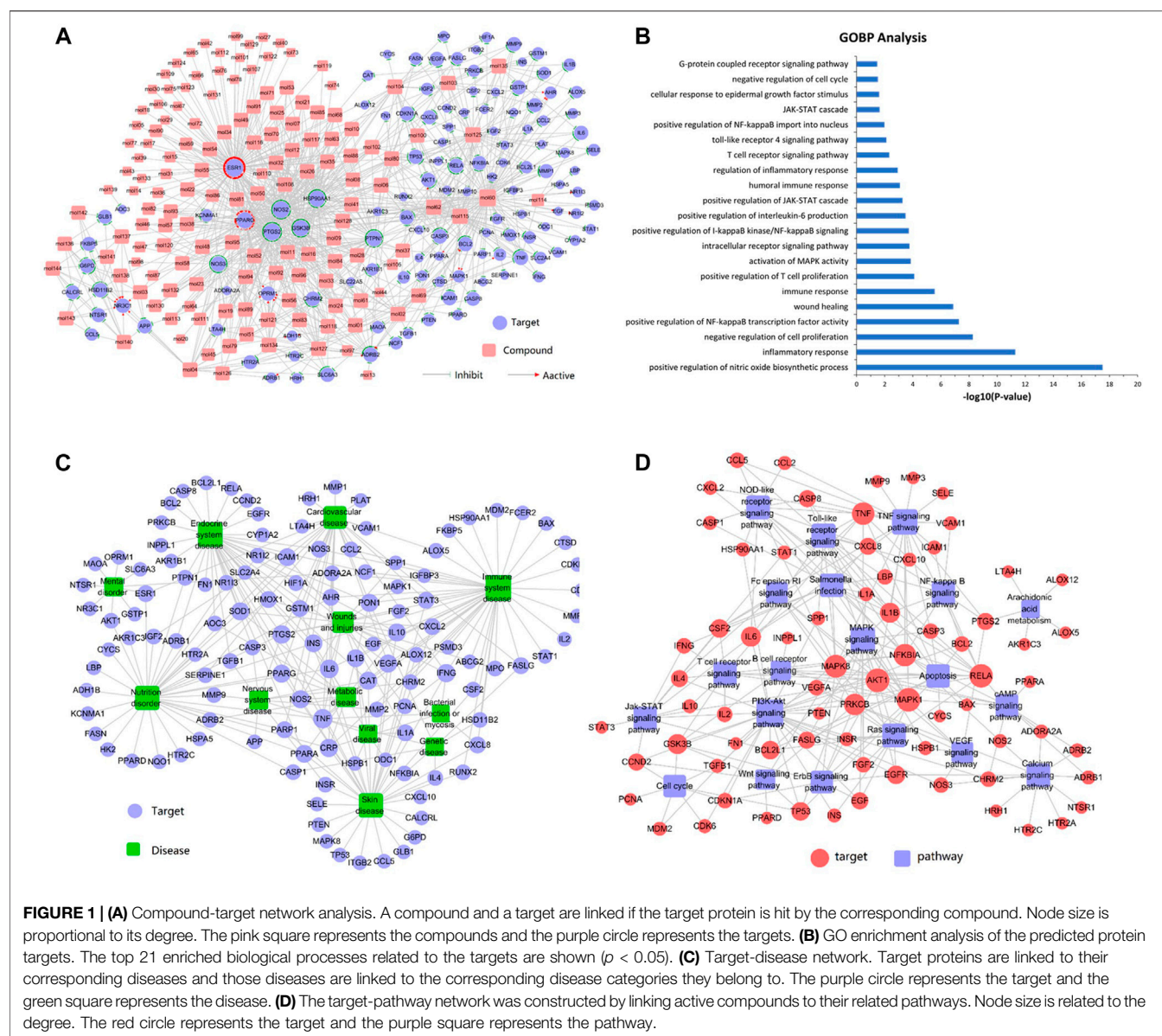
Of the remaining 25 patients, 52% of patients (13 in 25) after LXJD treatment achieved PASI60 and were considered as responders to LXJD treatment. Serum metabolomics were analyzed in these 13 responders' samples only.

Ethics Statement

Informed consent was given by the patients and this study was approved by the Ethics Committee of Beijing Traditional Chinese Medical Hospital (NO. 2017BL-073–01).

Sample Preparation

Serum (100 μl) was added into methanol (400 μl), vortex-mixed for 30 s, and the proteins were precipitated by centrifugation at 12,000 rpm for 15 min. Subsequently, the dried residue was reconstituted in 100 μl of acetonitrile-water (10:90, v/v) and then injected for LC-MS analysis.

FIGURE 1 | (A) Compound-target network analysis. A compound and a target are linked if the target protein is hit by the corresponding compound. Node size is proportional to its degree. The pink square represents the compounds and the purple circle represents the targets. **(B)** GO enrichment analysis of the predicted protein targets. The top 21 enriched biological processes related to the targets are shown ($p < 0.05$). **(C)** Target-disease network. Target proteins are linked to their corresponding diseases and those diseases are linked to the corresponding disease categories they belong to. The purple circle represents the target and the green square represents the disease. **(D)** The target-pathway network was constructed by linking active compounds to their related pathways. Node size is related to the degree. The red circle represents the target and the purple square represents the pathway.

Metabolic Profiling

The chromatographic analysis of the serum sample was performed in a Thermo LC system (Thermo, Ultimate 3000 LC, Orbitrap Elite) equipped with a Hypergod C18 column (4.6 mm × 100 mm, 3.0 μm). The column was maintained at 40°C, and the flow rate was set at 0.30 ml/min. The mobile phase was composed of water (A) and acetonitrile (B), each containing 0.1% formic acid. The linear gradient program was optimized as follows: 0–2.0 min, 5% B; 2.0–12 min, 5–95% B; 12–15 min, washing with 95% B for 15–17 min, and equilibration with 5% B. A volume of 4 μl was injected in all the cases and analyzed on a Thermo mass spectrometer equipped with an electrospray ionization source (ESI) operating in positive and negative ion modes. The optimized parameters of TOF were set as follows: the spray voltage was 3.0 kV (ES+) and 3.2 kV (ES−) with the

capillary temperature at 350°C, and sheath gas flow and auxiliary gas flow were set at 45 and 15, respectively. The mass range was set at 100–1000 m/z with 70,000 mass resolution at 400 m/z. The accepted scientific names must be updated using Medicinal Plant Name Service - KEW (https://mpns.science.kew.org/mpns-portal/).

The MS raw data of serum samples were processed using SIEVE software (Thermo Corp., Manchester, United Kingdom). This process included deconvolution, normalization, and alignment, and a dataset including retention time and mass pairs with the corresponding intensities of each metabolite was obtained. Then, the processed dataset was introduced into the SIMCA-P software package (v13.0, Umetric, Umeå, Sweden) to perform principal component analysis (PCA) and orthogonal to partial least squares-discriminate analysis (OPLS-DA). In the

OPLS-DA model, the variable importance of project (VIP) value and *S*-plot were employed as standards to select potential biomarkers.

Animals

Eight-week-old male C57BL/6 mice were purchased from Beijing Huafakang Biological Technology Co., Ltd. (Beijing, China) and maintained under specific pathogen-free conditions. All experiments adhered to the principles of the Declaration of Helsinki and were conducted using the protocols approved by the Beijing Institute of Traditional Chinese Medicine.

Establishment of Imiquimod (IMQ)-Induced Psoriasis-like Mouse Models

Mice were divided into four groups (10 mice/group): Control group, model group, MTX group, and LXJD group. All mice except those in the control group received a daily topical application of 42 mg of IMQ cream (5%) (MedShine, Chengdu, China) on their shaved back for seven consecutive days to establish a model of psoriasiform lesions. LXJD and MTX treatment started with the application of IMQ. From days 1–7, mice in the LXJD and MTX (positive control) groups were treated with LXJD (29.4 g herb/kg/day) and MTX (1 mg/kg/day) by gavage, respectively. Mice in the control group (control) and model group (model) were given saline by intragastric administration. On day seven, the animals were sacrificed, and skin samples were collected from their backs.

Histology, Immunohistochemistry, and Immunofluorescence Staining

The mouse back skin was fixed in formalin and embedded in paraffin. Partial sections were stained with hematoxylin-eosin (H&E) for pathological observation by microscopy. Partial sections were stained with anti-Rabbit CD3 (1:100, Abcam, United States) and anti-Loricrin (1:200, Abcam, United States), and Diaminobezidin (DAB) (Zhongshan Golden Bridge Biotechnology, China) was used for color development. For immunofluorescence, Ki-67 (proliferation) level was evaluated in skin sections using anti-Ki67 antibody (1:200, Abcam), following the manufacturer's instructions. For CD3^{+}, Ki-67+, and Loricrin+ cells, three areas in three sections of each sample were selected randomly, and the number of positive cells was calculated.

Quantitative RT-PCR Analysis (qRT-PCR)

Total RNA was extracted from the skin lesion and cultured cells using an ultrapure RNA extraction kit (Kang Biotechnology, China). Reverse transcription was carried out using the HiFi-MMLV cDNA first-strand synthesis kit (Kang Biotechnology). Quantitative real-time PCR amplification was performed on ABI 7500 Real-Time PCR Systems (Applied Biosystems, United States). A housekeeping gene was utilized as an internal reference standard. The relative gene expression was calculated using the $2^{-\Delta\Delta Ct}$ method.

Western Blot

The tissue extracts were prepared using RIPA buffer (50 mM of Tris-HCl pH 7.4, 150 mM of NaCl, 1 mM of EDTA, 1% Triton X-100, 0.1% SDS, 0.5% deoxycholate) supplemented with a complete protease inhibitor cocktail (Roche) and a PhosSTOP phosphatase inhibit or cocktail (Roche). Samples were subjected to SDS-PAGE and the resolved proteins were then transferred onto a polyvinylidene difluoride (PVDF) membrane (Millipore). The immunoblots were probed with indicated antibodies and visualized using a SuperSignal West Pico chemiluminescence ECL kit (Pierce). GAPDH was used as an internal control.

Statistical Analysis

All quantitative data are presented as means ± SD and analyzed for statistical significance using GraphPad Prism 5.0 (GraphPad Software Inc., San Diego, CA, United States). One-way analysis of variance (ANOVA) followed by Tukey's post hoc test and unpaired Student's t-test was used to analyze the statistical significance among multiple groups and between two groups, respectively. A two-tailed Student's *t*-test was performed in a clinical study using the Statistical Package for Social Science program (SPSS 20.0, Chicago, IL, United States). $p < 0.05$ indicated statistically significant difference.
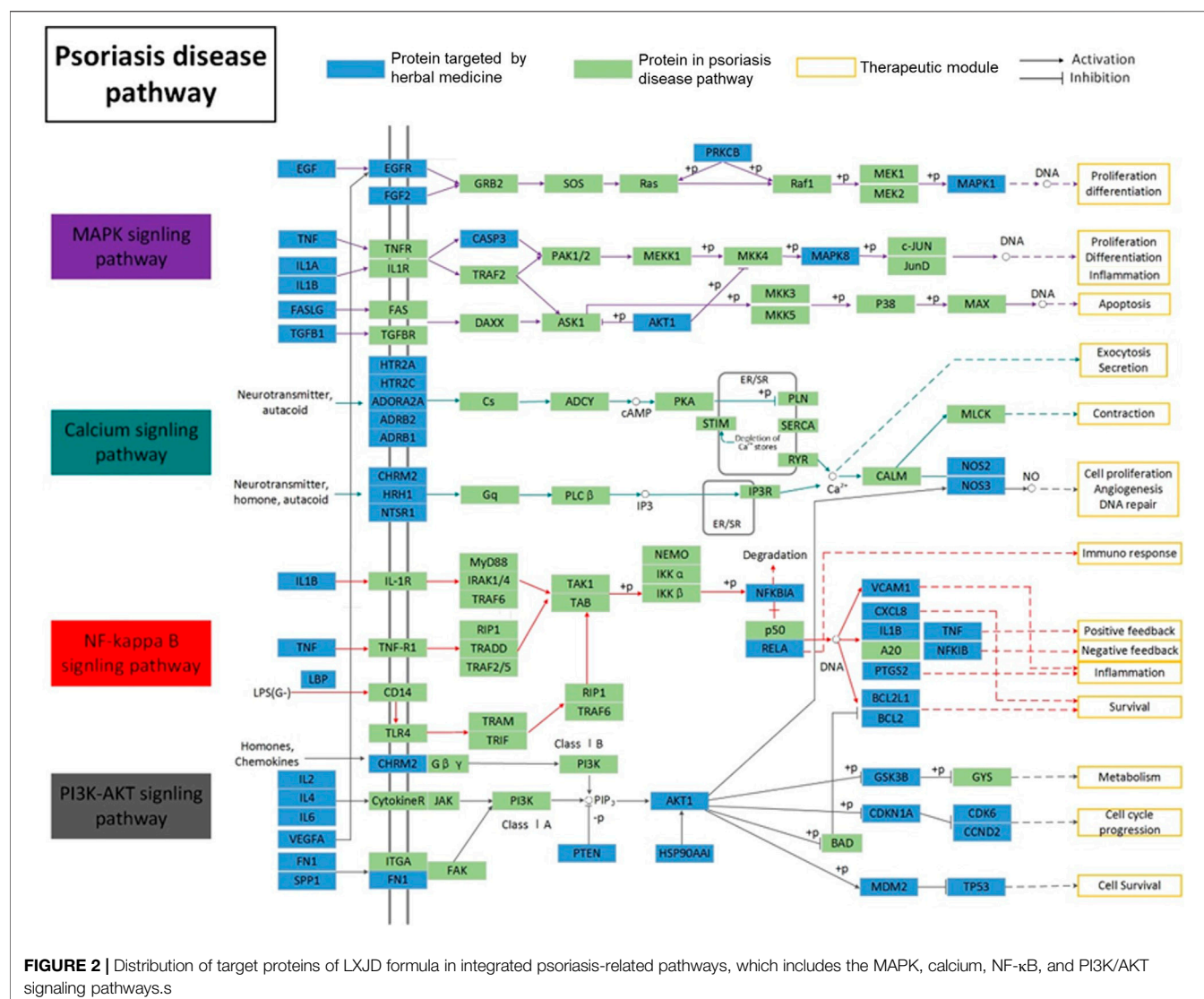
RESULTS

Bioactive Compounds Identification for Each Herb in LiangXueJieDu Formula

In the current study, 864 chemical ingredients and their pharmaceutical properties in the LXJD formula were obtained from the TCMSP database. A combination of OB (≥30%), Caco-2 permeability (Caco-2) (>−0.4), prediction of permeability (AlogP <5), and drug-likeness (DL) ≥0.18 properties was applied to identify the active compounds of LXJD formula. Based on a previous report, some compounds that did not agree with the threshold of compounds screening were also likely to produce therapeutic effects, and hence, retained as active compounds in this study, such as palmitic acid (Dogra et al., 2018), sitosterol (REISS and JAIMOVICH, 1958), stigmasterol (Srivastava, 2014), trametenolic acid (Ma et al., 2013), lignoceric acid (Tsoukalas et al., 2019), tirucallane (Mireku et al., 2015), etc. These compounds have bioactivity and are reported as anti-psoriatic or anti-inflammatory molecules. Finally, 144 active compounds (**Supplementary Table S1**), including 37 in Isatis tinctoria, 8 in Scleromitrion diffusum, 10 in Dictamnus dasycarpus, 9 in Paeonia lactiflora, 11 in Rehmannia glutinosa, 14 in Arnebia euchroma, 3 in Paeonia x suffruticosa, 18 in Saposhnikovia varzcata, 5 in Smilax glabra, 8 in Imperata cylindrica, 7 in Bistorta officinalis, and 14 in Paeonia lactiflora, were obtained.

Target Identification and Analysis

TCM formulas exert their pharmacological activities through synergistic interactions between multiple compounds and targets. To identify the relevant targets of the potential compounds in LXJD formula, the TCMSP database and WES algorithms were used. A final list of 125 potential targets for 144 bioactive compounds was obtained. These targets were further subject to PharmGkb, CTD, and TTD for sanity checks. As shown

FIGURE 2 | Distribution of target proteins of LXJD formula in integrated psoriasis-related pathways, which includes the MAPK, calcium, NF-κB, and PI3K/AKT signaling pathways.s

in **Supplementary Table S2**, most active compounds could act on multiple targets simultaneously, and one target could also be linked to multiple active compounds. PTGS2, also known as cyclooxygenase-2 (COX-2), is one of the potential targets that play a critical role in inflammation (Yalçin et al., 2007). It was predicted that PTGS2 is linked to 86 active compounds in the LXJD formula to exert therapeutic effect synergistically. The active compound quercetin (MOL60) was found to be connected to 79 targets, reflecting the multiple targets of herbal medicine.
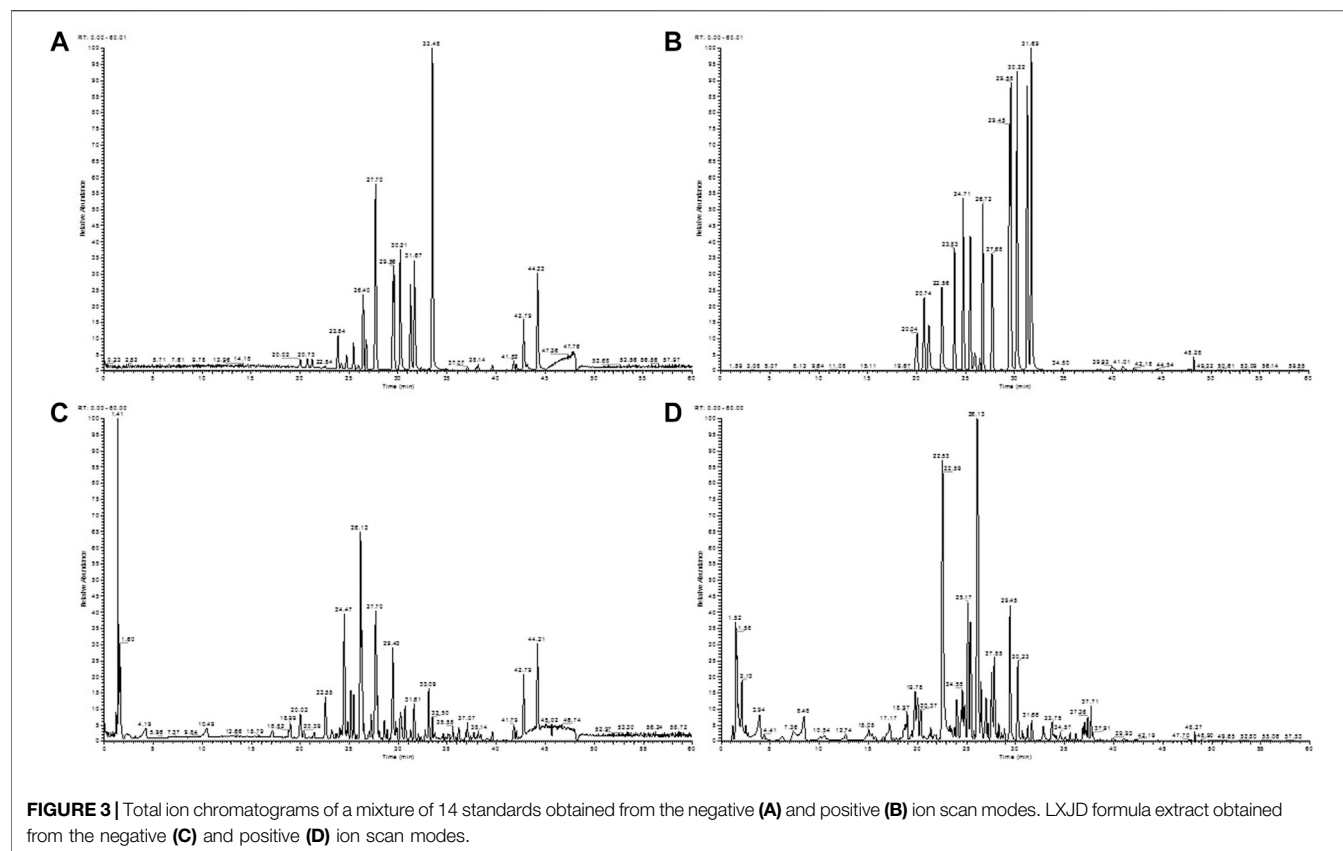
Gene Ontology Enrichment Analysis for Potential Targets

To validate whether the 125 potential targets in the network are associated with psoriasis, we performed GO term (BP) enrichment analysis. The top 21 significant GO terms responsible for psoriasis were enriched. As shown in

Figure 1B, inflammatory response, positive regulation of NF-κB transcription factor activity, positive regulation of T cell proliferation, regulation of inflammatory response, and IL-6 production was intricately linked to the pathogenesis of psoriasis. These results suggested that the potential targets were significantly involved in the pathogenesis of psoriasis.

Compound-Target Network Analysis

Figure 1A shows that the compound-target network consisted of 144 active compounds, 125 targets, and 901 compound-target interactions (269 nodes and 901 edges). The results displayed an average of 7.2° per compound and 6.3° per target protein, respectively. In the correlations between compounds and targets (**Supplementary Table S3**), MOL60 exhibited the highest number of target interactions (79°), followed by MOL125 (35°), MOL115 (34°), and MOL62 (33°), which was consistent with the multi-component and multi-target traits of herbal medicines. Regarding the candidate targets, estrogen

FIGURE 3 | Total ion chromatograms of a mixture of 14 standards obtained from the negative **(A)** and positive **(B)** ion scan modes. LXJD formula extract obtained from the negative **(C)** and positive **(D)** ion scan modes.

receptor (ESR1) showed the highest degree (113°), followed by PTGS2 (86°), NOS2 (81°), PPARG (60°), and GSK3B (56°), which demonstrated the potential therapeutic effect of each drug in LXJD formula for ameliorating psoriasis.

Target-Disease Network

In order to elucidate the correlation between LXJD formula and diseases, a target-disease network, including 122 target proteins and 12 corresponding diseases, was constructed based on the DrugBank, TTD, and PharmGKB databases. As shown in **Figure 1C**, LXJD formula was related to 12 types of diseases, including immune system disease (41°), endocrine system disease (37°), skin disease (35°), nutrition disorder (35°), cardiovascular disease (27°) wounds and injuries (29°), metabolic disease (14°), nervous system disease (10°), mental disorder (9°), genetic disease (7°), viral disease (7°), and bacterial infection or mycosis (4°). The target-disease network might explain the theory of "homotherapy for heteropathy" in TCM.

Target-Pathway Network Analysis

To further elucidate the therapeutic mechanisms underlying the LXJD formula in the treatment of psoriasis, all the predicted target proteins were mapped to enrich the relevant pathways. The target-pathway network containing 73 targets and 20 corresponding pathways is shown in **Figure 1D**. The majority of the target proteins were involved in multiple pathways,

indicating that the target proteins of the LXJD formula interplayed with each other in different pathways and exerted synergistic effects in the treatment of psoriasis. As shown in **Supplementary Table S4**, the crucial target protein-associated pathways included the PI3K/AKT signaling pathway (27°), TNF signaling pathway (21°), MAPK signaling pathway (16°), toll-like receptor signaling pathway (15°), NOD-like receptor signaling pathway (13°), *salmonella* infection pathway (13°), Ras signaling pathway (13°), apoptosis pathway (12°), calcium signaling pathway (12°), NF-κB signaling pathway (11°), T cell receptor signaling pathway (11°), and JAK-STAT signaling pathway (11°). These results suggested that multiple targets affect various pathways regulating the pathological processes underlying psoriasis, thereby promoting a potent therapeutic approach for these diseases.

Psoriasis-Related Pathway Analysis

Based on the complex mechanism of the LXJD formula in the treatment of psoriasis, an integrated map of "psoriasis-related pathways" was constructed by integrating the key pathways obtained from the KEGG database using target-pathway network analysis. As shown in **Figure 2**, psoriasis-related pathways consist of four important pathways: the MAPK signaling pathway, calcium signaling pathway, PI3K/AKT signaling pathway, and NF-κB signaling pathway. These pathways were associated with several biological functions,
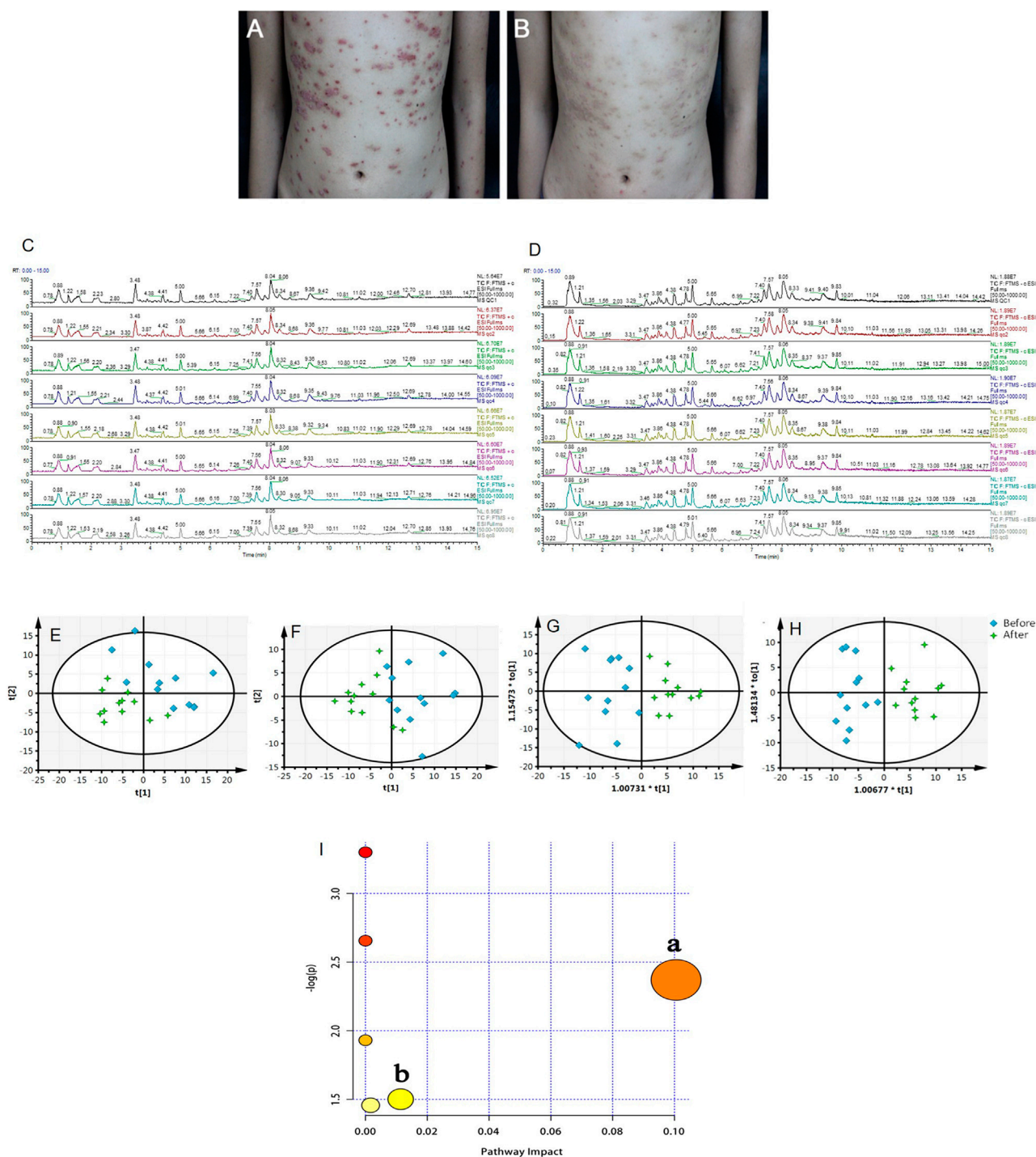
FIGURE 4 | (A, B) Representative photographs of the patient with psoriasis taken at baseline (week 0, A) and after 8 weeks (B) of treatment with LiangxueJiedu formula. Total ions chromatogram of QC samples from the positive (C) and negative (D) ion scan modes. (E, F) PCA score plots of serum samples collected from psoriasis patients before and after 8 weeks of LiangxueJiedu formula treatment measured in (E, R^2X = 0.724, Q^2 = 0.495) positive and (F, R^2X = 0.574, Q^2 = 0.371) negative mode. (G, H) OPLS-DA score plots of serum samples collected from psoriasis patients before and after 8 weeks of LiangxueJiedu formula treatment based on UPLC-Q-TOF/MS technology in (G, R^2X = 0.557, R^2Y = 0.782, Q^2 = 0.671) positive and (H, R^2X = 0.410, R^2Y = 0.852, Q^2 = 0.453) negative mode. (I) Summary of pathway analysis with MetPA, a: glycerophospholipid metabolism; b: steroid hormone biosynthesis.

TABLE 2 | Characteristics of the study cohorts.

	Before treatment	After treatment
Gender	7/6	7/6
PASI	13.6 ± 5.97	$3.8 \pm 2.1^{**}$

*Values are reported as the mean ± SD. Units for cholesterol and triglycerides are mmol/L, PASI, psoriasis area, and severity index. Gender balance: male/female. p < 0.05 indicated statistical significance for PASI scores before and after treatment (**p < 0.01).*

such as inflammation, proliferation, metabolism, cell survival, cell cycle, and immune response, indicating the therapeutic effect of the LXJD formula in psoriasis.

Identification of Major Components of LiangXueJieDu Formula

The total ion chromatograms of the LXJD formula extracted in both the positive and negative ion modes are shown in **Figure 3**. The MS data exhibited high precision with the mass accuracy within 5 ppm. Based on the MS spectra and fragmentation pattern using public databases (Chemspider and MassBank) or literature, 14 compounds were identified (**Table 1**). Chlorogenic acid, caffeic acid, paeoniflorin, taxifolin, astilbin, albiflorin, resveratrol, rosmarinic acid, 5-O-methylvisammioside, quercetin, naringenin, luteolin, kaempferol, and isorhamnetin were the main components of the LXJD formula extract, which was consistent with the systems pharmacology prediction. These results also demonstrated that the UPLC-MS method was suitable for identifying these compounds.

Effect of LiangXueJieDu Formula in Psoriasis Patients

After 8 weeks of treatment with LXJD formula, the skin symptoms of all patients improved. In addition, psoriasis area and severity index (PASI) scoring, a critical index to evaluate psoriasis in the clinic, decreased significantly ($p < 0.05$) following LXJD formula treatment (**Figures 4A,B** and **Table 2**).

Serum Metabolomics Study of Psoriasis Patients

Serum metabolic profiling of psoriasis patients was acquired to explore the protective effect of the LXJD formula. UPLC/Q-TOF-MS was applied for analysis. The quality-control (QC) sample was used to monitor the precision, repeatability, and reliability of the LC-MS measurements and peak intensity data (**Figures 4C,D**). These results indicated that methods were suitable for subsequent sample analysis. Principal component analysis (PCA) was employed to obtain unsupervized multivariate statistical analysis of serum metabolomics. In **Figures 4E,F**, serum metabolites in positive and negative ion modes were displayed by score plots, the cluster of psoriasis patients before LXJD formula treatment was clearly separated from those after 8 weeks of LXJD formula treatment in both modes. The OPLS-DA models were established to identify the discriminating ions

contributing to the classification before and after LXJD formula treatment patients (**Figures 4G,H** and **Table 3**). The score plots based on the serum metabolomics of these two groups in positive and negative ion modes are shown in **Figures 4G,H**, the values of R^2X, R^2Y, and Q^2 were 0.557, 0.782, and 0.671 in the positive ion mode, 0.410, 0.852, and 0.453 in the negative ion mode, indicating the classification was well suited for the models. A total of 11 metabolites in the positive mode and seven metabolites in the negative mode were altered after LXJD formula treatment. These included cortisone (S1), L-urobilinogen (S2), PA[15:1(9Z)/22:4(7Z,10Z,13Z,16Z)] (S3), PC[18:0/18:4(6Z,9Z,12Z,15Z)] (S4), PC[18:1(9Z)/4:0] (S5), PC[20:0/14:1(9Z)] (S6), PC[20:4(8Z,11Z,14Z,17Z)/18:3(6Z,9Z,12Z)] (S7), PG[12:0/20:5(5Z,8Z,11Z,14Z,17Z)] (S8), PG[P-18:0/20:4(5Z,8Z,11Z,14Z)] (S9), phenyllactic acid (S10), traumatic acid (S11), 16-hydroxy hexadecanoic acid (S12), 4-hydroxybutanoic acid (S13), L-gamma-glutamyl-L-isoleucine (S14), MG[0:0/16:1(9Z)/0:0] (S15), PA[20:4(5Z,8Z,11Z,14Z)/18:4(6Z,9Z,12Z,15Z)] (S16), PG[20:3(8Z,11Z,14Z)/20:0] (S17), and PS[21:0/18:3(6Z,9Z,12Z)] (S18). To probe the associations between the key metabolic pathways and the regulatory effects of LXJD formula, metabolic pathway analysis (MetPA) (software of MetaboAnalyst 3.0; http://www.metaboanalyst.ca/) was performed by the integration of all serum potential metabolites. As a result, two disturbed metabolic pathways, glycerophospholipid metabolism and steroid hormone biosynthesis were considered as the most relevant pathways involved in psoriasis (**Figure 4I**). LXJD formula treatment improved both perturbed metabolic pathways.

LiangXueJieDu Formula Improved the Differentiation of Keratinocytes and Alleviated the Proliferation of Keratinocytes in an Establishment of Imiquimod-Induced Psoriasis-Like Mouse Model

To assess whether LXJD formula exerts therapeutic effects in a psoriasis mouse model, we applied IMQ on the shaved back skin of the animals for seven consecutive days. Subsequently, the skin developed typical erythema, scaling, and thickening. Consistent with the systems pharmacology analysis, mice treated with LXJD formula had smoother skin, less erythema, and sparser scales (**Figure 5A**). H&E staining of the skin lesion in the model group showed increased epidermal thickening, parakeratosis, and residual condensation of nuclei in the stratum corneum, representing typical characteristics of psoriasis-like skin lesions. These pathological features were ameliorated by LXJD formula (**Figures 5B,F**).

Loricrin is a keratinocyte differentiation marker that is mainly expressed in the cytoplasm and distributed throughout the stratum corneum of normal mouse skin. In the model group, low levels of loricrin indicated abnormal keratinocyte differentiation, which was reversed in animals treated with LXJD ($p < 0.01$) (**Figures 5D,H**). The expression of Ki-67, a marker strongly associated with cell proliferation and immune dysregulation (Alhosaini et al., 2021), was dramatically decreased in the LXJD-treated groups ($p < 0.01$) (**Figures 5E,I**), indicating that the IMQ-induced uncontrolled proliferation of basal keratinocytes was ameliorated.

TABLE 3 | Potential metabolites characterized in the serum profile and the altered trends in different groups.

NO.	Metabolites	VIP	m/z	Rt	p-value	Fold-change (B/A)
S1	Cortisone	1.025	360.1936	4.487	0.018	0.268
S2	L-Urobilinogen	1.111	596.3528	7.711	0.009	−0.854
S3	PA[15:1(9Z)/22:4(7Z,10Z,13Z,16Z)]	1.187	708.4561	3.832	0.005	−0.229
S4	PC[18:0/18:4(6Z,9Z,12Z,15Z)]	1.122	781.5589	10.116	0.008	0.899
S5	PC[18:1(9Z)/4:0]	1.075	591.3974	7.707	0.012	−0.672
S6	PC[20:0/14:1(9Z)]	1.070	759.5765	11.030	0.013	0.486
S7	PC(20:4[8Z,11Z,14Z,17Z)/18:3(6Z,9Z,12Z)]	1.103	803.5414	10.122	0.010	1.014
S8	PG[12:0/20:5(5Z,8Z,11Z,14Z,17Z)]	1.031	712.4401	8.479	0.017	−0.701
S9	PG[P-18:0/20:4(5Z,8Z,11Z,14Z)]	1.159	782.5629	10.828	0.006	0.650
S10	Phenyllactic acid	1.037	166.0626	4.306	0.016	0.633
S11	Traumatic acid	1.145	228.1364	6.101	0.007	−0.489
S12	16-hydroxy hexadecanoic acid	1.015	272.2349	7.480	0.019	−0.424
S13	4-hydroxybutanoic acid	1.106	104.0476	1.624	0.010	−0.694
S14	L-gamma-glutamyl-L-isoleucine	1.004	258.1369	5.235	0.021	−0.758
S15	MG[0:0/16:1(9Z)/0:0]	1.133	328.2605	11.324	0.008	−0.576
S16	PA[20:4(5Z,8Z,11Z,14Z)/18:4(6Z,9Z,12Z,15Z)]	1.043	716.4334	8.207	0.016	−0.756
S17	PG[20:3(8Z,11Z,14Z)/20:0]	1.030	828.5686	11.208	0.017	0.481
S18	PS[21:0/18:3(6Z,9Z,12Z)]	1.048	827.5646	11.112	0.015	0.508

Potential metabolites are characterized in the serum profile and their altered trends in different groups. Fold-change (B/A) represents the changing trend before and after LXJD formula treatment based on log 2 (B/A).

LiangXueJieDu Formula Inhibited T Cell Infiltration in an Establishment of Imiquimod-Induced Psoriasis-Like Mouse Model

We further examined the effect of LXJD formula on CD3+ T cell infiltration in the dermis. The control mice showed fewer CD3+ T cells in the dermis. The T cell infiltration in the dermis and epidermis was markedly higher in the model group than in the control group. On the other hand, LXJD and MTX groups showed reduced CD3+ T cell infiltration in the skin ($p < 0.01$) (**Figures 5C,G**).

LiangXueJieDu Formula Regulated the Expression of Inflammatory Cytokines and Factors in an Establishment of Imiquimod-Induced Psoriasis-Like Mouse Model

We determined the mRNA expression of several inflammatory cytokines and factors in the skin lesions and found that the levels of *Il1b, Il6, Tnfa, Cox2, Nos2,* and *Gsk3b* were significantly increased, while those of *Esr1* and *Pparg* mRNAs were suppressed in the lesions of the model group. Moreover, compared to the model group, the expression of *Il1b, Il6, Tnfa, Cox2, Nos2,* and *Gsk3b* mRNA declined in the LXJD group ($p < 0.01$ or $p < 0.05$), and that of *Esr1* and *Pparg* mRNAs reversed after LXJD formula administration ($p < 0.01$ or $p < 0.05$) (**Figure 6**).

LiangXueJieDu Formula Improved the Establishment of Imiquimod-Induced Psoriasis-Like Dysfunction Pathway

To further validate the prediction of systematic pharmacological analysis, we examined the effect of LXJD formula on key proteins in integrated psoriasis-related pathways, including MAPK, calcium, PI3K/AKT, and NF-κB signaling pathways using Western blot. IMQ application significantly increased the level of p-P65, p-IκB, p-ERK, p-P38, p-JNK, p-PI3K, p-AKT, and p-CAMKΙΙ in skin lesions. Compared to the model group, LXJD formula treatment remarkably inhibited the phosphorylation of p-P65, p-IκB, p-ERK, p-P38, p-PI3K, and p-AKT ($p < 0.01$ or $p < 0.05$), but showed a negligible inhibitory effect on p-JNK and p-CAMKΙΙ phosphorylation, indicating that LXJD formula exerts its therapeutic effect by inhibiting the MAPK, PI3K/AKT, and NF-κB signaling pathways to a large extent (**Figure 7**).

DISCUSSION

TCM has been used in clinical treatment in China for more than 2000 years and has accumulated a wealth of experience in the treatment of psoriasis. Our previous study has shown that the administration of LXJD formula in psoriasis vulgaris patients with blood-heat syndrome was associated with significantly better outcomes and a lower recurrence rate compared to standard Western medicine (cetirizine hydrochloride, vitamin C, and vitamin B complex) (Sun et al., 2020). However, bioactive ingredients with potential anti-psoriatic activities and specific targets have not yet been identified. TCM is a complex material system encompassing multiple active compounds, multiple targets of action, and related diseases; while it does not correspond to the theory of "single gene, single target, and single disease" (Lv et al., 2019). Therefore, exploring the targets and mechanism of LXJD formula in the treatment of psoriasis through a systems pharmacology method combined with a screening of active compounds, drug targets, and network analysis is essential.

In this study, we identified 144 compounds in the active fractions of LXJD formula using an *in silico* integrative model-ADME system with the following thresholds: OB ≥ 30%, DL ≥
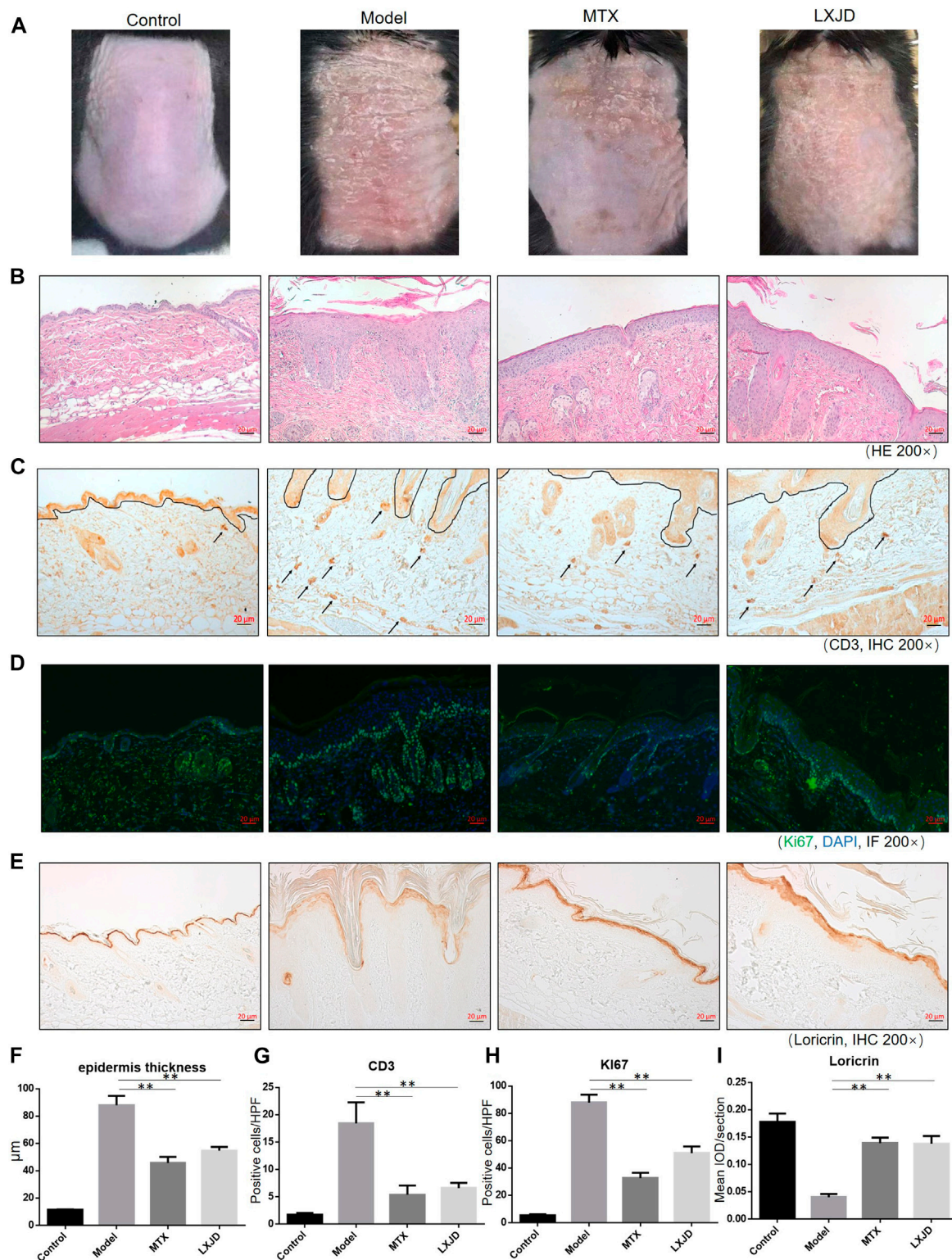
FIGURE 5 | C57 BL/6 mice were treated daily with IMQ cream on the shaved back skin to induced psoriasis-like dermatitis, while the control group (CTRL) was treated with matrix. The IMQ-treated mice were administered saline (model) [methotrexate (MTX) serves as a positive control] or LXJD formula for a total of 7 days. **(A)** Phenotypic presentation of the back skin on day 7 after IMQ treatment. **(B)** Histological analyses of mouse back skin by H&E staining. **(C)** Immunohistochemical staining of CD3+ cells in skin lesions. Mouse back skin was stained for Ki67 **(D)** and loricrin **(E)**. **(F–I)** Quantification analysis for epidermis thickness, CD3+ and Ki-67+, and loricrin was performed. Data are shown as mean ± SD. n = 5 mice. *$p < 0.05$ and **$p < 0.01$ vs. model group.
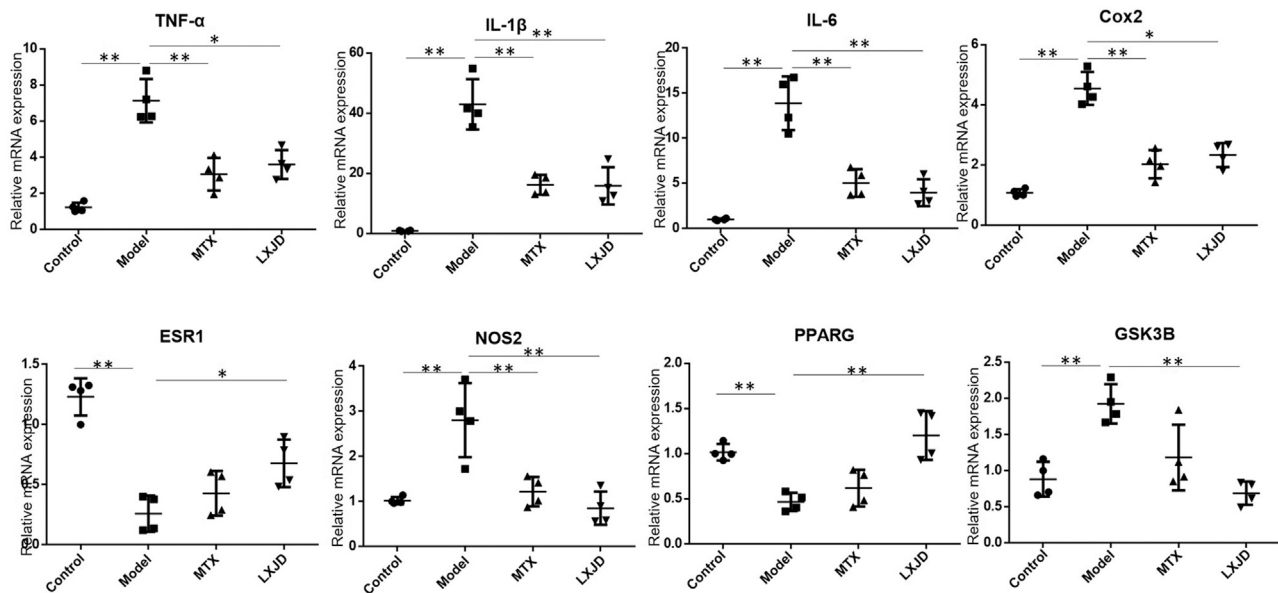
FIGURE 6 | The mRNA expression of key inflammatory cytokines and predicted genes in the skin lesion of the psoriasis-like mouse model. Values were normalized to β-actin and expressed relative to the control group. Data are shown as mean ± SD. n = 4 mice. *$p < 0.05$ and **$p < 0.01$ vs. model group.
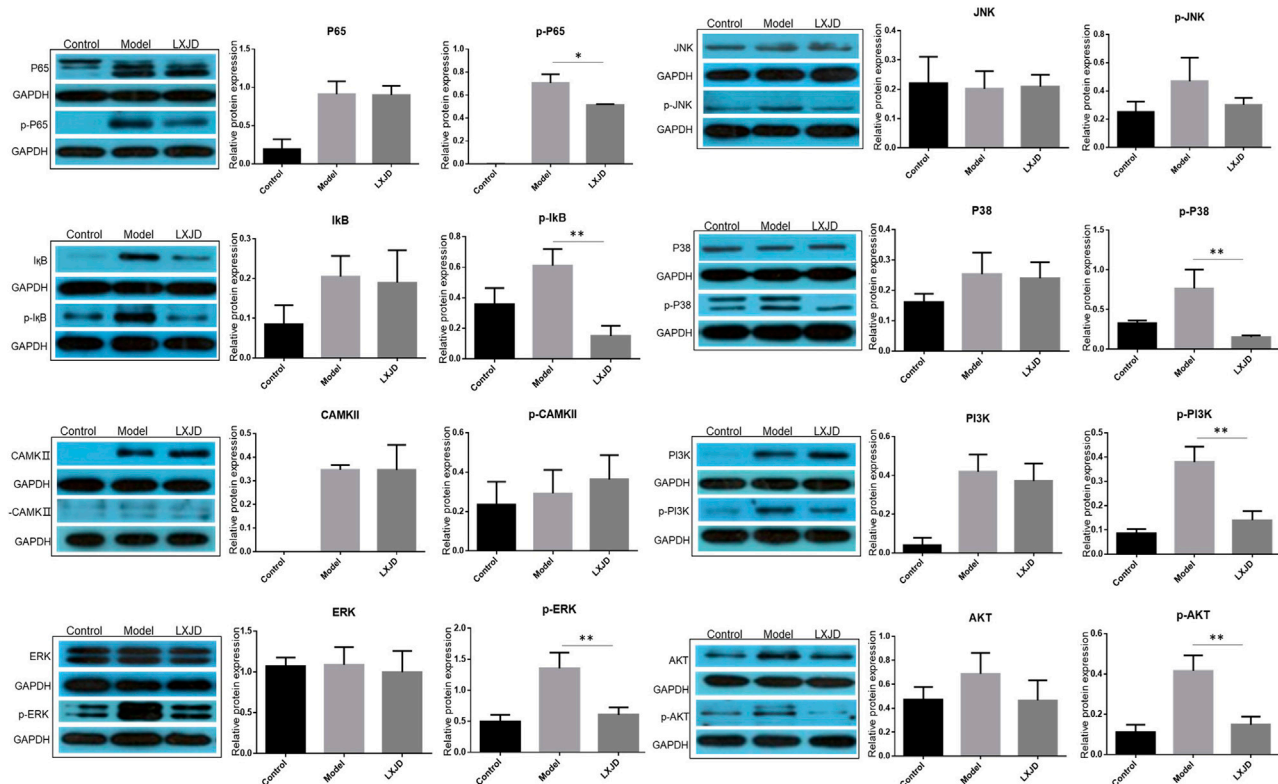

FIGURE 7 | Effects of LXJD formula on IMQ-induced psoriasis-like dysfunction pathway. Levels of P65, p-P65, IκB, p-IκB, CAMKII, p-CAMKII, ERK, p-ERK, P38, p-P38, JNK, p-JNK, PI3K, p-PI3K, AKT, and p-AKT proteins in skin lesions are detected by Western blot. Semiquantitative analysis was performed. *$p < 0.05$, **$p < 0.01$ indicating significant inhibition of LXJD as compared to model group. Data are shown as mean ± SD. n = 3 mice.

0.18, Caco-2 > -0.4, and AlogP <5. Subsequently, a final list of 125 potential targets for the 144 bioactive compounds was obtained by several integrated approaches, including the WES algorithm, TCMSP database, PharmGkb, Comparative Toxicogenomics database, and Therapeutic Targets database. These potential targets could be classified into the following subgroups: cytokines and chemokines, enzymes, signaling molecules, and transcription factors, and nuclear receptors. Most of these targets exhibited abnormal expression and were designated as the therapeutic targets in psoriasis, such as the cytokines and chemokines (IL-1β, IL-6, TNF, IFN-γ, CXCL8, CCL2). As expected, drugs targeting TNF-α have been applied in the clinic and have shown promising therapeutic effects on psoriasis (Chima and Lebwohl, 2018). Moreover, a total of 125 potential targets were significantly enriched as GO terms (BPs), including inflammatory response, cell proliferation, inflammatory response, NF-κB transcription factor activity, and cytokine production, which are strongly associated with the pathogenesis of psoriasis. Then, the compound-target network was constructed, showing complex interactions between 144 active compounds and 125 targets. Among these, ESR1 was the most common target of 113 compounds, constituting up to 77.1% of the total candidates. Reportedly, *ESR1* is the top-ranked hub gene, which is downregulated in psoriasis and related to anti-apoptotic functions (Zeng et al., 2016), deeming it as a potential therapeutic target for psoriasis. Consistently, our compound-target network indicated that the active compounds from LXJD formula could activate ESR1. Moreover, *IL1B* and *STAT3* were also reported as hub genes in psoriasis (Choudhary et al., 2020) and targets of LXJD formula. In this compound-target network, most of the active compounds were connected to multiple targets and exerted pharmacological effects. For example, quercetin exhibited the highest number of target interactions. Quercetin possesses anti-tumor activity (Xu et al., 2015) and anti-proliferative effects (Delgado et al., 2014); also, it is shown to have appreciable anti-psoriasis effects in IMQ-induced mice. The underlying mechanism might involve the improvement of antioxidant, anti-inflammatory activity, and inhibition on NF-κB signaling pathway activation (Chen et al., 2017). In addition, the anti-psoriasis effects of Paeonol (Meng et al., 2017), Baicalin (Hung et al., 2018), Paeoniflorin (Zhao et al., 2016), and Wogonin (Chi et al., 2003) have been demonstrated in an IMQ-induced psoriasis-like mouse model.

To further elucidate the complex mechanism of LXJD formula in the treatment of psoriasis, we established an integrated map of "psoriasis-related pathways" by integrating the key pathways obtained from the KEGG database using target-pathway network analysis. This map showed that the active compounds in LXJD formula interacting with these predicted targets are associated with the MAPK, calcium, PI3K/AKT, and NF-κB signaling pathways. These interactions regulate inflammation, cell proliferation, metabolism, cell survival, cell cycle, and immune response, and ultimately improve psoriasis.

Different complex diseases caused by the same disease gene exhibit overlapping protein-protein interactions and biological processes. Therefore, when a drug acts on the proteins associated with multiple diseases, it might show multiple

therapeutic effects (Li et al., 2012). For example, peroxisome proliferator-activated receptor gamma (PPARG or PPAR-γ), a nuclear receptor, is one of the primary targets of LXJD formula, according to our compound-target network. PPAR-γ can bind to DNA and regulate the transcription of genes involved in lipid and glucose metabolism. Activation of PPAR-γ has favorable effects on adipocyte function, insulin sensitivity, lipoprotein metabolism, and vascular structure and function. PPAR-γ has been recognized as a therapeutic target in cardiovascular disease and diabetes mellitus. In addition, several studies demonstrated that PPAR-γ agonists may have antidepressant properties, open-label administration of the PPAR-γ agonist, pioglitazone, was associated with improvement in depressive symptoms and reduced cardiometabolic risk (Kemp et al., 2014). In the skin, PPAR-γ has a critical role in keratinocyte homeostasis, exhibiting pro-differentiation, antiproliferation, and immunomodulatory functions. The expression of PPAR-γ was reduced in a psoriasis hyperproliferative epidermis (Lima et al., 2013). Reportedly, diabetic patients treated with troglitazone (PPAR-γ agonist) showed substantial improvement in their psoriatic plaques (Pershadsingh et al., 1998). In addition to relieving the symptoms of patients with chronic psoriasis, this drug has modified the abnormal phenotype of transplanted psoriatic skin (Hanley et al., 1999). Furthermore, treatment with thiazolidinediones (PPAR-γ agonist) in patients with plaque psoriasis improved their cutaneous symptoms (Pershadsingh et al., 1998; Ellis et al., 2000). Based on the target-disease network, we could speculate that LXJD formula has potential pharmacological effects on immune system disease, endocrine system disease, skin disease, cardiovascular disease, metabolic disease, and mental disorder. Consistently, a previous study identified that psoriasis is not confined to skin impairment, and an increased morbidity of metabolic syndrome, cardiovascular disease, depression, and anxiety are also associated complications (Lima et al., 2013). Chronic inflammation caused by disorganized immune activation and correlated systemic abnormalities might underpin the common pathogenesis of psoriasis and related diseases. There is evidence that an imbalance between different T cells, e.g., T helper cells 17 (Th17) vs. regulatory T cells (Treg) and abnormal cytokine production are the driving forces in common for the progression and development of mental disorder and immune system disease (Ahmad et al., 2017; Ahmad et al., 2017; Bakheet et al., 2019; Ahmad et al., 2020). Many compounds, which have been shown to have promising effects in multiple immune-mediated inflammatory disorders such as asthma, rheumatoid arthritis, and alcoholic liver disease, have therapeutic potential in psoriatic inflammation as well (Alzahrani et al., 2019; Al-Harbi et al., 2020; Nadeem et al., 2020). Collectively, the herbs in LXJD formula exhibit efficacy in psoriasis treatment and in treating related complications, indicating that multiple diseases may be treated using a common herbal medicine.

Metabolomics data might provide useful information to explore the mechanisms underlying these associated diseases, especially metabolism disorders (Lee et al., 2003). Herein, we employed LC-MS to analyze psoriasis patients' serum metabolomics and investigate the metabolic changes associated with LXJD formula treatment. In concordance with the previous study, the elements of

glycerophospholipid metabolism were significantly altered in the plasma of psoriatic patients (Zeng et al., 2017). The current metabolomics results indicated that glycerophospholipid metabolism involving 11 metabolites was significantly influenced in psoriasis patients according to MetPA, and the most influencing targets were related to the therapeutic intervention of LXJD formula against psoriasis. The compound-target network showed that PPAR-γ could be activated by LXJD formula. There is evidence that the PPAR-γ agonist could regulate glycerophospholipid metabolism (Tan et al., 2017), which is consistent with our metabolomics data showing that LXJD formula improved the perturbed metabolic pathways of glycerophospholipid metabolism. Based on this, we inferred that LXJD formula might regulate the glycerophospholipid metabolism through activating PPAR-γ. In addition, abnormalities in glycerophospholipid metabolism are the characteristics of diabetes mellitus (Xu et al., 2013). Dang et al. also revealed that the alteration of glycerophospholipid metabolism pathways is associated with atherosclerosis (Dang et al., 2016). Therefore, glycerophospholipid metabolism might be a drug target for psoriasis and related complications, including diabetes mellitus and atherosclerosis. LXJD formula could treat these associated diseases by regulating the altered metabolism.

Finally, we utilized an IMQ-induced psoriasis-like mouse model to validate the predicted targets and mechanisms of LXJD formula. In line with the current findings from systems pharmacology, LXJD formula could ameliorate psoriasis lesions, inhibit keratinocytes proliferation, improve keratinocytes differentiation, and suppress the infiltration of CD3+ T cells in an IMQ-induced psoriasis-like mouse model. This therapeutic effect was mediated by inhibiting the MAPK, PI3K/AKT, and NF-κB signaling pathways and reducing the subsequent release of inflammatory cytokines.

CONCLUSION AND LIMITATION

In conclusion, our systems pharmacological network identified active compounds and potential target proteins and elucidated the pharmacological mechanism of LXJD formula for the treatment of psoriasis and related diseases. These targets have been validated by our *in vivo* experiments. The metabolic changes associated with LXJD formula treatment adequately complemented the interaction between the Chinese herbal compounds and body metabolism, thereby revealing the underlying mechanism. These studies provided convincing evidence and a biological basis for LXJD formula in the treatment of psoriasis, contributing to its clinical application and generalization.

Certainly, there are still some limitations in our study. Even though LXJD formula has been proven as a safe treatment for psoriasis (Sun et al., 2020) and been used widely in China for decades, it still cause concerns about its toxicity due to different sources of herbs and different types of concoctions. In this animal study, no significant impact on body weight was found after LXJD formula treatment (data not shown). Nonetheless, further toxicity/safety evaluation studies need to be done in future. Components of Chinese herbal medicine are complicated, it is not clarified whether there are new intermediate metabolites or

side effects caused by the interaction between compounds. We were not able to validate all of the 144 compounds in this formula by UPLC-MS analysis. Besides, a new intermediate metabolite might have an effect on psoriasis in a pre-clinical *in vivo* psoriasis model and/or human trial testing as well. We investigated the whole formula effect on a psoriasis-like animal model and corresponding predicted targets, but the effect of individual compounds on corresponding predicted targets remains unclear. Despite these potentially interesting associations, cautious interpretation and further validation tests are warranted.

Although further validation tests will be required to support deep assessments, the current study combining systems pharmacology, metabolomics, and experiment evaluation illustrated the correlation among active compounds, targets, and metabolism, contributing to the understanding of the mechanism of LXJD formula in the treatment of psoriasis.

DATA AVAILABILITY STATEMENT

The original contributions presented in the study are included in the article/**Supplementary Material**, further inquiries can be directed to the corresponding author.

ETHICS STATEMENT

The studies involving human participants were reviewed and approved by the Ethics Committee of Beijing Traditional Chinese Medical Hospital. The patients/participants provided their written informed consent to participate in this study. The animal study was reviewed and approved by Beijing Institute of Traditional Chinese Medicine.

AUTHOR CONTRIBUTIONS

This work includes significant contributions from all authors. JZ, YW, and PL conceived the study and designed the experiments. JZ and YW carried out the systems pharmacology analysis, JF identified the main components in the LXJD formula extract, YW, WC, and ZC performed the clinical study and metabolomics analysis. JZ, YL, TD, and CQ conducted animal experiments. JZ wrote the manuscript. YW and PL edited the manuscript. All authors read and approved the final manuscript.

FUNDING

SUPPLEMENTARY MATERIAL

The Supplementary Material for this article can be found online at: https://www.frontiersin.org/articles/10.3389/fphar.2021.626267/full#supplementary-material

REFERENCES

Ahmad, S. F., Ansari, M. A., Nadeem, A., Bakheet, S. A., Al-Ayadhi, L. Y., Alsaad, A. M. S., et al. (2020). Upregulation of Interleukin (IL)-31, a Cytokine Producing CXCR1 Peripheral Immune Cells, Contributes to the Immune Abnormalities of Autism Spectrum Disorder. *J. Neuroimmunology* 349, 577430. doi:10.1016/j.jneuroim.2020.577430

Ahmad, S. F., Nadeem, A., Ansari, M. A., Bakheet, S. A., Attia, S. M., Zoheir, K. M. A., et al. (2017). Imbalance between the Anti- and Pro-inflammatory Milieu in Blood Leukocytes of Autistic Children. *Mol. Immunol.* 82, 57–65. doi:10.1016/j.molimm.2016.12.019

Ahmad, S. F., Zoheir, K. M. A., Ansari, M. A., Nadeem, A., Bakheet, S. A., Al-Ayadhi, L. Y., et al. (2017). Dysregulation of Th1, Th2, Th17, and T Regulatory Cell-Related Transcription Factor Signaling in Children with Autism. *Mol. Neurobiol.* 54 (6), 4390–4400. doi:10.1007/s12035-016-9977-0

Al-Harbi, N. O., Nadeem, A., Ahmad, S. F., Bakheet, S. A., El-Sherbeeny, A. M., Ibrahim, K. E., et al. (2020). Therapeutic Treatment with Ibrutinib Attenuates Imiquimod-Induced Psoriasis-like Inflammation in Mice through Downregulation of Oxidative and Inflammatory Mediators in Neutrophils and Dendritic Cells. *Eur. J. Pharmacol.* 877, 173088. doi:10.1016/j.ejphar.2020.173088

Alhosaini, K., Ansari, M. A., Nadeem, A., Attia, S. M., Bakheet, S. A., Al-Ayadhi, L. Y., et al. (2021). Dysregulation of Ki-67 Expression in T Cells of Children with Autism Spectrum Disorder. *Children* 8 (2), 116. doi:10.3390/children8020116

Alzahrani, K. S., Nadeem, A., Ahmad, S. F., Al-Harbi, N. O., Ibrahim, K. E., El-Sherbeeny, A. M., et al. (2019). Inhibition of Spleen Tyrosine Kinase Attenuates Psoriasis-like Inflammation in Mice through Blockade of Dendritic Cell-Th17 Inflammation axis. *Biomed. Pharmacother.* 111, 347–358. doi:10.1016/j.biopha.2018.12.060

Bakheet, S. A., Ansari, M. A., Nadeem, A., Attia, S. M., Alhoshani, A. R., Gul, G., et al. (2019). CXCR3 Antagonist AMG487 Suppresses Rheumatoid Arthritis Pathogenesis and Progression by Shifting the Th17/Treg Cell Balance. *Cell Signal.* 64, 109395. doi:10.1016/j.cellsig.2019.109395

Ben-Arye, E., Ziv, M., Frenkel, M., Lavi, I., and Rosenman, D. (2003). Complementary Medicine and Psoriasis: Linking the Patient's Outlook with Evidence-Based Medicine. *Dermatology* 207 (3), 302–307. doi:10.1159/000073094

Chen, H., Lu, C., Liu, H., Wang, M., Zhao, H., Yan, Y., et al. (2017). Quercetin Ameliorates Imiquimod-Induced Psoriasis-like Skin Inflammation in Mice via the NF-Kb Pathway. *Int. Immunopharmacology* 48, 110–117. doi:10.1016/j.intimp.2017.04.022

Chi, Y. S., Lim, H., Park, H., and Kim, H. P. (2003). Effects of Wogonin, a Plant Flavone from Scutellaria Radix, on Skin Inflammation: *In Vivo* Regulation of Inflammation-Associated Gene Expression. *Biochem. Pharmacol.* 66 (7), 1271–1278. doi:10.1016/s0006-2952(03)00463-5

Chima, M., and Lebwohl, M. (2018). TNF Inhibitors for Psoriasis. *Sem Cutan. Med. Surg.* 37 (3), 134–142. doi:10.12788/j.sder.2018.039

Choudhary, S., Pradhan, D., Khan, N. S., Singh, H., Thomas, G., and Jain, A. K. (2020). Decoding Psoriasis: Integrated Bioinformatics Approach to Understand Hub Genes and Involved Pathways. *Cpd* 26, 3619–3630. doi:10.2174/1381612826666200311130133

Damevska, K., Neloska, L., Nikolovska, S., Gocev, G., and Duma, S. (2014). Complementary and Alternative Medicine Use Among Patients with Psoriasis. *Dermatol. Ther.* 27 (5), 281–283. doi:10.1111/dth.12139

Dang, V. T., Huang, A., Zhong, L. H., Shi, Y., and Werstuck, G. H. (2016). Comprehensive Plasma Metabolomic Analyses of Atherosclerotic Progression Reveal Alterations in Glycerophospholipid and Sphingolipid Metabolism in Apolipoprotein E-Deficient Mice. *Sci. Rep.* 6, 35037. doi:10.1038/srep35037

Delgado, L., Fernandes, I., González-Manzano, S., de Freitas, V., Mateus, N., and Santos-Buelga, C. (2014). Anti-proliferative Effects of Quercetin and Catechin Metabolites. *Food Funct.* 5 (4), 797–803. doi:10.1039/c3fo60441a

Dogra, N. K., Kumar, S., Thakur, K., and Kumar, D. (2018). Antipsoriatic Effect of Fatty Acid Enriched Fraction of Vernonia Anthelmintica Willd. Fruits. *J. Ethnopharmacology* 224, 85–90. doi:10.1016/j.jep.2018.05.038

Ellis, C. N., Varani, J., Fisher, G. J., Zeigler, M. E., Benson, S. C., Chi, Y., et al. (2000). Troglitazone Improves Psoriasis and Normalizes Models of Proliferative Skin Disease: Ligands for Peroxisome Proliferator-Activated Receptor-Gamma Inhibit Keratinocyte Proliferation. *Arch. Dermatol.* 136, 609–616. doi:10.1001/archderm.136.5.609

Gamret, A. C., Price, A., Fertig, R. M., Lev-Tov, H., and Nichols, A. J. (2018). Complementary and Alternative Medicine Therapies for Psoriasis. *JAMA Dermatol.* 154 (11), 1330–1337. doi:10.1001/jamadermatol.2018.2972

Hanley, K., Kömüves, L. G., Bass, N. M., He, S., Jiang, Y., Crumrine, D., et al. (1999). Fetal Epidermal Differentiation and Barrier Development *In Vivo* Is Accelerated by Nuclear Hormone Receptor Activators1. *J. Invest. Dermatol.* 113, 788–795. doi:10.1046/j.1523-1747.1999.00743.x

Heng, M. C. Y., Song, M. K., Harker, J., and Heng, M. K. (2000). Drug-induced Suppression of Phosphorylase Kinase Activity Correlates with Resolution of Psoriasis as Assessed by Clinical, Histological and Immunohistochemical Parameters. *Br. J. Dermatol.* 143 (5), 937–949. doi:10.1046/j.1365-2133.2000.03767.x

Hung, C.-H., Wang, C.-N., Cheng, H.-H., Liao, J.-W., Chen, Y.-T., Chao, Y.-W., et al. (2018). Baicalin Ameliorates Imiquimod-Induced Psoriasis-like Inflammation in Mice. *Planta Med.* 84 (15), 1110–1117. doi:10.1055/a-0622-8242

Kemp, D. E., Schinagle, M., Gao, K., Conroy, C., Ganocy, S. J., Ismail-Beigi, F., et al. (2014). PPAR-γ Agonism as a Modulator of Mood: Proof-Of-Concept for Pioglitazone in Bipolar Depression. *CNS Drugs* 28 (6), 571–581. doi:10.1007/s40263-014-0158-2

Kurd, S. K., Smith, N., VanVoorhees, A., Troxel, A. B., Badmaev, V., Seykora, J. T., et al. (2008). Oral Curcumin in the Treatment of Moderate to Severe Psoriasis Vulgaris: a Prospective Clinical Trial. *J. Am. Acad. Dermatol.* 58 (4), 625–631. doi:10.1016/j.jaad.2007.12.035

Lee, C.-H., Olson, P., and Evans, R. M. (2003). Minireview: Lipid Metabolism, Metabolic Diseases, and Peroxisome Proliferator-Activated Receptors. *Endocrinology* 144, 2201–2207. doi:10.1210/en.2003-0288

Li, X., Xu, X., Wang, J., Yu, H., Wang, X., Yang, H., et al. (2012). A System-Level Investigation into the Mechanisms of Chinese Traditional Medicine: Compound Danshen Formula for Cardiovascular Disease Treatment. *PLoS One* 7 (9), e43918. doi:10.1371/journal.pone.0043918

Lima, E. D. A., Lima, M. M. D. D. A., Marques, C. D. L., Duarte, A. L. B. P., Pita, I. D. R., and Pita, M. G. D. R., (2013). Peroxisome Proliferator-Activated Receptor Agonists (PPARs): a Promising prospect in the Treatment of Psoriasis and Psoriatic Arthritis. *Bras. Dermatol.* 88 (6), 1029–1035. doi:10.1590/abd1806-4841.20132653

Lipinski, C. A., Lombardo, F., Dominy, B. W., and Feeney, P. J, (2001). Experimental and Computational Approaches to Estimate Solubility and Permeability in Drug Discovery and Development Settings. *Adv. Drug Deliv. Rev.* 46 (1-3), 3–26. doi:10.1016/s0169-409x(00)00129-0

Liu, J., Mu, J., Zheng, C., Chen, X., Guo, Z., Huang, C., et al. (2016). Systems-Pharmacology Dissection of Traditional Chinese Medicine Compound Saffron Formula Reveals Multi-Scale Treatment Strategy for Cardiovascular Diseases. *Sci. Rep.* 6, 19809. doi:10.1038/srep19809

Lv, W. J., Liu, C., Li, Y. F., Chen, W-Q., Li, Z-Q., Li, Y., et al. (2019). Systems Pharmacology and Microbiome Dissection of Shen Ling Bai Zhu San Reveal Multiscale Treatment Strategy for IBD. *Oxid Med. Cel Longev* 2019, 8194804. doi:10.1155/2019/8194804

Ma, L., Chen, H., Dong, P., and Lu, X, (2013). Anti-inflammatory and Anticancer Activities of Extracts and Compounds from the Mushroom Inonotus Obliquus. *Food Chem.* 139 (1-4), 503–508. doi:10.1016/j.foodchem.2013.01.030

Meng, Y., Wang, M., Xie, X., Di, T., Zhao, J., Lin, Y., et al. (2017). Paeonol Ameliorates Imiquimod-Induced Psoriasis-like Skin Lesions in BALB/c Mice by Inhibiting the Maturation and Activation of Dendritic Cells. *Int. J. Mol. Med.* 39 (5), 1101–1110. doi:10.3892/ijmm.2017.2930

Mireku, E. A., Kusari, S., Eckelmann, D., Mensah, A. Y., Talontsi, F. M., and Spiteller, M. (2015). Anti-inflammatory Tirucallane Triterpenoids from Anopyxis Klaineana Pierre (Engl.), (Rhizophoraceae). *Fitoterapia* 106, 84–91. doi:10.1016/j.fitote.2015.08.007

Nadeem, A., Ahmad, S. F., Al-Harbi, N. O., El-Sherbeeny, A. M., Alasmari, A. F., Alanazi, W. A., et al. (2020). Bruton's Tyrosine Kinase Inhibitor Suppresses Imiquimod-Induced Psoriasis-like Inflammation in Mice through Regulation of IL-23/IL-17A in Innate Immune Cells. *Int. Immunopharmacology* 80, 106215. doi:10.1016/j.intimp.2020.106215

Pershadsingh, H. A., Sproul, J. A., Benjamin, E., Finnegan, J, and Amin, N. M (1998). Treatment of Psoriasis with Troglitazone Therapy. *Arch. Dermatol.* 134, 1304–1305. doi:10.1001/archderm.134.10.1304

Reiss, F., and Jaimovich, L. (1958). The Influence of Sitosterol upon Psoriasis Vulgaris. *Dermatology* 117 (5), 393–401. doi:10.1159/000255614

Ru, J., Li, P., Wang, J., Zhou, W, Li, B, Huang, C., et al. (2014). TCMSP: a Database of Systems Pharmacology for Drug Discovery from Herbal Medicines. *J. Cheminform* 6, 13. doi:10.1186/1758-2946-6-13

Srivastava, R. (2014). A Review on Phytochemical, Pharmacological, and Pharmacognostical Profile of Wrightia Tinctoria: Adulterant of Kurchi. *Phcog Rev.* 8 (15), 36–44. doi:10.4103/0973-7847.125528

Sun, L., Li, T., Zhou, D., Yang, X., Tian, J., Zhao, J., et al. (2020). "Efficacy and Safety of Liangxue Jiedu Decoction for the Treatment of Progressive Psoriasis Vulgaris: a Multicenter, Randomized, Controlled Study". *J. Tradit Chin. Med.* 40 (2), 296–304.

Talbott, W., and Duffy, N. (2015). Complementary and Alternative Medicine for Psoriasis: what the Dermatologist Needs to Know. *Am. J. Clin. Dermatol.* 16 (3), 147–165. doi:10.1007/s40257-015-0128-6

Tan, J., Wang, Y., Wang, S., Zhang, N., Wu, S., Yuan, Z., et al. (2017). Untargeted Metabolomics Analysis of Adipogenic Transformation in OP9-DL1 Cells Using Liquid Chromatography-Mass Spectrometry: Implications for Thymic Adipogenesis. *Cell Biol Int* 41 (4), 447–456. doi:10.1002/cbin.10740

Tetko, I. V., and Bruneau, P. (2004). Application of ALOGPS to Predict 1-octanol/water Distribution Coefficients, logP, and logD, of AstraZeneca In-house Database. *J. Pharm. Sci.* 93 (12), 3103–3110. doi:10.1002/jps.20217

Tsoukalas, D., Fragoulakis, V., Sarandi, E., Docea, A. O, Tsilimidos, G, Aschner, M, et al. (2019). Targeted Metabolomic Analysis of Serum Fatty Acids for the Prediction of Autoimmune Diseases. *Front. Mol. Biosci.* 6, 120. doi:10.3389/fmolb.2019.00120

World health organization (2016). *Global Report on Psoriasis*, 2016, 7–9.

Xu, F., Tavintharan, S., Sum, C. F., Woon, K., Lim, S. C., and Ong, C. N. (2013). Metabolic Signature Shift in Type 2 Diabetes Mellitus Revealed by Mass Spectrometry-Based Metabolomics. *J. Clin. Endocrinol. Metab.* 98 (6), E1060–E1065. doi:10.1210/jc.2012-4132

Xu, G., Shi, H., Ren, L., Gou, H., Gong, D., Gao, X., et al. (2015). Enhancing the Anti-colon Cancer Activity of Quercetin by Self-Assembled Micelles. *Int. J. Nanomedicine* 10, 2051–2063. doi:10.2147/IJN.S75550

Yalçin, B., Tezel, G. G., Arda, N., Erman, M., and Alli, N. (2007). Vascular Endothelial Growth Factor, Vascular Endothelial Growth Factor Receptor-3 and Cyclooxygenase-2 Expression in Psoriasis. *Anal. Quant Cytol. Histol.* 29 (6), 358–364.

Yuan, N., Gong, L., Tang, K., He, L, Hao, W, Li, X, et al. (2020). An Integrated Pharmacology-Based Analysis for Antidepressant Mechanism of Chinese Herbal Formula Xiao-Yao-San. *Front. Pharmacol.* 11, 284. doi:10.3389/fphar.2020.00284

Zeng, C. W., Wen, B., Hou, G. X., Lei, L, Jia, X, Chen, X., et al. (2017). Lipidomics Profiling Reveals the Role of Glycerophospholipid Metabolism in Psoriasis. *Gigascience* 6 (10), 1–11. doi:10.1093/gigascience/gix087

Zeng, X., Zhao, J., Wu, X., Shi, H., Liu, W., Cui, B., et al. (2016). PageRank Analysis Reveals Topologically Expressed Genes Correspond to Psoriasis and Their Functions Are Associated with Apoptosis Resistance. *Mol. Med. Rep.* 13 (5), 3969–3976. doi:10.3892/mmr.2016.4999

Zhang, G.-z., Wang, J.-S., Wang, P., Jiang, C.-Y., Deng, B.-X., Li, P., et al. (2009). Distribution and Development of the TCM Syndromes in Psoriasis Vulgaris. *J. Traditional Chin. Med.* 29 (3), 195–200. doi:10.1016/s0254-6272(09)60064-9

Zhao, J., Di, T., Wang, Y., Wang, Y., Liu, X., Liang, D., et al. (2016). Paeoniflorin Inhibits Imiquimod-Induced Psoriasis in Mice by Regulating Th17 Cell Response and Cytokine Secretion. *Eur. J. Pharmacol.* 772, 131–143. doi:10.1016/j.ejphar.2015.12.040

Check for updates

Isovitexin Inhibits Ginkgolic Acids-Induced Inflammation Through Downregulating SHP2 Activation

Yiwei Zhang[1], Zhipeng Qi[1], Wenjie Wang[1], Lei Wang[1], Fuliang Cao[2], Linguo Zhao[1,2] and Xianying Fang[1]*

[1]College of Chemical Engineering, Nanjing Forestry University, Nanjing, China, [2]Co-Innovation Center for Sustainable Forestry in Southern China, Nanjing Forestry University, Nanjing, China

It has been reported that *Celtis sinensis* Pers. is employed as a folk medicine for the treatment of inflammatory diseases. But the mechanism supporting its use as anti-inflammatory remains unclear. To investigate the anti-inflammatory of *Celtis sinensis* Pers. ICR mice were provided *Celtis sinensis* Pers. leaf extract (CLE) at 100, 200 mg/kg after ginkgolic acids (GA) sensitization. Our data showed that CLE and the main flavonoid isovitexin in CLE could ameliorate GA-induced contact dermatitis in mice. Ear swelling, inflammatory cell infiltration and splenomegaly were inhibited significantly by isovitexin, while the weight loss of mice in the isovitexin-treated group was much better than that in the dexamethasone-treated group (positive control drug). It has been reported in previous research that GA-induced inflammation is closely related to the T cell response. Therefore, T cells were the focus of the anti-inflammatory effect of isovitexin in this paper. The *in vivo* results showed that isovitexin (10, 20 mg/kg) inhibited the expression of proinflammatory cytokines (TNF-α, IFN-γ, IL-2 and IL-17A) in lymph nodes, inhibited the secretion of cytokines into the serum from mice with contact dermatitis and promoted the expression of apoptosis-related proteins. *In vitro*, isovitexin also induced apoptosis and inhibited proinflammatory cytokine expression in Con A-activated T cells. Further study showed that the MAPK and STAT signaling pathways and the phosphorylation of SHP2 were inhibited by isovitexin. Both molecular docking and biological experiments indicated that SHP2 may be an anti-inflammatory target of isovitexin in T cells. Taken together, isovitexin can serve as a potential natural agent for the treatment or prevention of GA-induced inflammatory problems.

Keywords: isovitexin, ginkgolic acids, dermatitis, inflammation, SHP2, *Celtis sinensis* Pers. leaf

INTRODUCTION

Ginkgo seeds has been used as a nutritious food for thousands of years, and a variety of medicinal effects have been attributed to the ginkgo seeds. The main active pharmaceutical ingredients in *Ginkgo biloba* include oxyglycoside flavonoids, terpene trilactones, proanthocyanidins and so on (Zhou et al., 2018; Omidkhoda et al., 2019). However, food poisoning by Ginkgo seeds has been reported in Japan and China, which presents as frequent vomiting and generalized convulsions (Miwa et al., 2001). Ginkgolic acids (GA), the alkylphenol constituents in ginkgo seeds, have been considered one of the potential toxic components in *Ginkgo biloba*. The functional disorders are probably due to GA (Qian et al., 2017). It has also been reported that contact allergic dermatitis (ACD) can be induced by ginkgolic acids when people contact ginkgo leaf during the picking of Ginkgo seeds (Hotta et al., 2013; Mei et al., 2017). *Ginkgo*

biloba leaf exhibit useful applications in health, food and dietary supplements but are also controversial in the application of some aspects because of the existence of GA. Under some conditions, GA can be separated by organic solvent extraction or column chromatography (Van Beek and Montoro, 2009). However, for raw material products such as Ginkgo seeds and ginkgo tea, the GA removal process cannot be performed (Fransen et al., 2010; Fang et al., 2019). Other methods, such as detoxification by compatibility, need to be taken to solve the GA-caused toxicity problems in the application of Ginkgo seeds and ginkgo tea.

GA, a derivative of alkyl-substituted salicylic acid, is similar to the chemical structure of urushiol and differs by carbon number and unsaturation, classified as C13:0, C15:1, C15:0, and C17:1 (Wang et al., 2014). Allergies were caused by paint occur frequently in our daily lives. As an allergen from paint, urushiol can cause intense, persistent itch, skin rashes and a burning sensation in severe cases (Boelman, 2010). The clinical manifestations of GA-induced ACD are similar to urushiol-induced ACD, followed by the appearance of erythematous edematous plaques and papulovesicles accompanied by intense pruritus on the forearms in severe cases (Han et al., 2016). These inflammatory reactions can lead to a series of problems, such as skin injury, immune liver injury, gastrointestinal inflammatory injury and so on. With an important role in the immune response, T cells appear to proliferate and differentiate. However, overdeveloped T cells are associated with cutaneous allergic and inflammatory responses, which exacerbate skin inflammation, tissue injury and other immunopathies. In a previous study, reports suggested that the mechanism of GA-induced ACD may be consistent with urushiol-induced ACD. Numerous experimental animal models have validated GA as a hapten with the ability to activate T cells against innocuous or autoantigens and induce type IV allergic reactions (Ude et al., 2013). A study has shown that T cells in rats sensitized with GA are differentiated into $CD4^+$ T cells, suggesting that GA may act as an allergen to enhance body sensitivity, induce T cell division and proliferation and enhance the cellular immune response.

Celtis sinensis Pers. has been used as a traditional herbal remedy for thousands of years in China. It uses to treat urushiol-induced dermatitis. There is a folk tale, from the Maolan karst forest, that if someone contacted poison ivy inadvertently, he could be treated by putting the leaf of *Celtis sinensis Pers.* into his mouth. Isovitexin, the most abundant flavonoid in the leaf of *Celtis sinensis* (Zehrmann et al., 2010), is a widely found natural carbon glycoside flavonoid. Isovitexin has various pharmacological activities, such as antineoplastic (Cao et al., 2019), antioxidant (Liu et al., 2020a), and neurological protective effects (Liu et al., 2020b). This compound has also shown anti-inflammatory efficacy against human diseases (Fransen et al., 2010; Fang et al., 2019). It has been reported that isovitexin inhibits the MAPK and NF-κB pathways in macrophages in acute lung injury (Fransen et al., 2010; Fang et al., 2019). In lymphocytes, a number of ACD-associated cytokines are dependent on JAK-STAT signaling, and antigen presentation is dependent on MAPK signaling for the effects on cellular transcription and activation. In this study, a contact-hypersensitivity mouse model induced by GA was established to reveal the mechanisms underlying the anti-inflammatory effect of

isovitexin. In summary, this study provides supporting data for isovitexin ameliorating GA-induced allergic contact dermatitis.
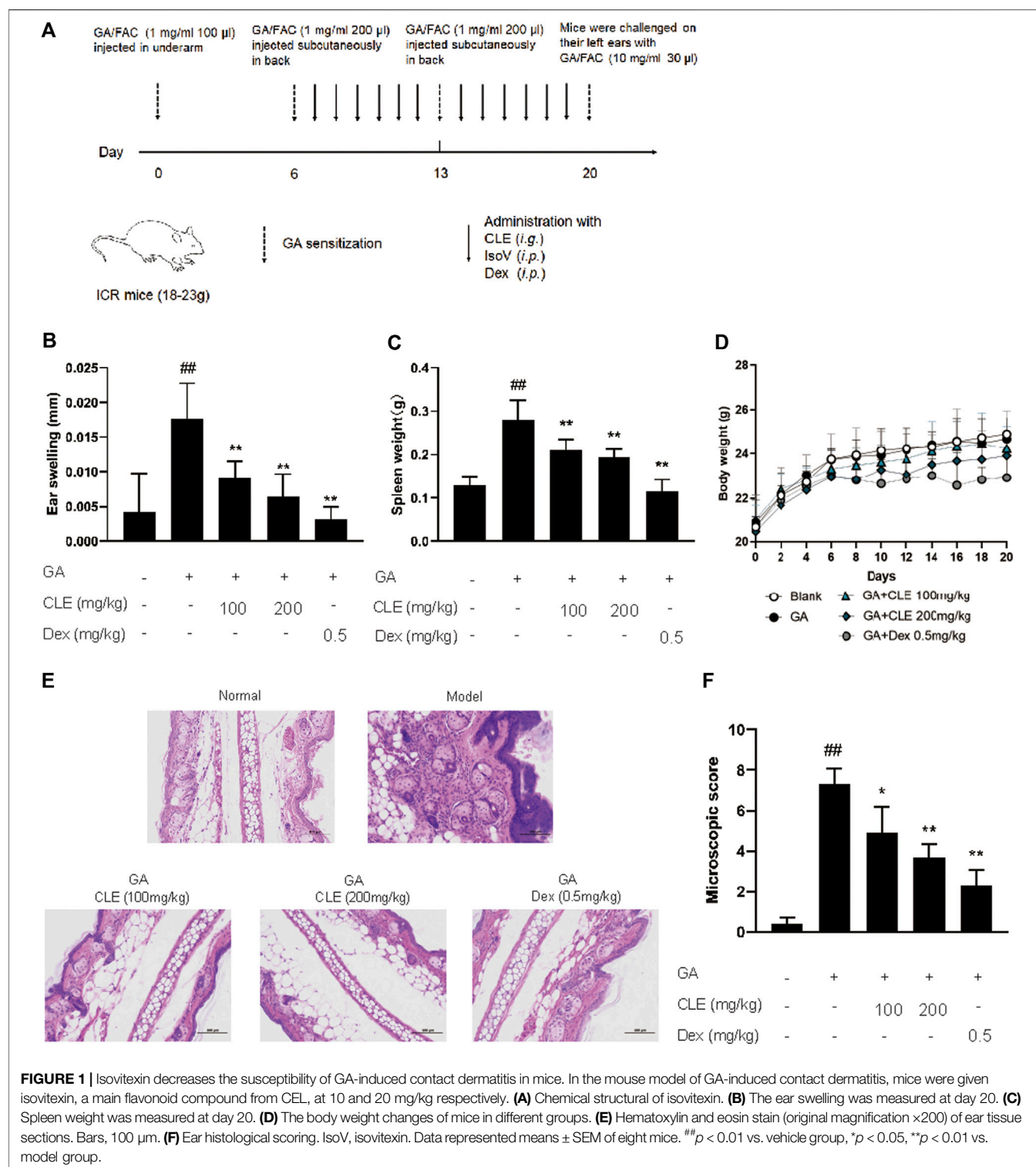
MATERIALS AND METHODS

Reagents

Isovitexin (CAS No. 38953-85-4, purity: 98.01%) was obtained from Mansite Biotechnology, Chengdu, China) was dissolved in 100% DMSO at a concentration of 100 mM as a stock solution and diluted test concentration with culture medium before each experiment. The concentration of final DMSO did not extend 0.1% throughout the trail. Ginkgolic acids were purchased from Jingzhu Medical Technology (Nanjing, China). The Annexin V-FITC/PI apoptosis kit and ELISA kits for murine (TNF-α, IFN-γ, IL-2, IL-17A) were purchased from MultiSciences (Lianke) Biotech Co., Ltd. (Hangzhou, China). SHP099, the SHP2 inhibitor, purchased from Selleckchem. Concanavalin A (Con A), MTT, Freund's Adjuvant Complete (FAC) and Dexamethasone (Dex) were purchased from Sigma-Aldrich (St Louis, MO). Antibodies against phospho-STAT3 (Tyr705), phospho-AKT (Ser473), Anti-ERK, phospho-P38 (Thr180/Tyr182), phospho-JNK (Thr183/Tyr185), phospho-ERK1/2 (Thr 202/Tyr 204), Caspase-3, Caspase-8, Cleaved Caspase-3 (Asp175), Cleaved Caspase-8 (Asp387), Cleaved PARP (Asp214) were purchased from Cell Signal Technology (Beverly, MA). Antibodies against phospho-SHP2 (Tyr 542) was purchased from Abcam (Cambridge, United Kingdom). Anti-β-actin, Anti-AKT, Anti-PARP, Anti-P38, Anti-JNK, Anti-AKT, Anti-STAT6 was purchased from Proteintech Group (Wuhan, China). Anti-STAT3, Anti-SHP2 was purchased from Santa cruz Biotechnology.

Animal

Female ICR mice and BALB/c mice, 18–23 g, 6–8 weeks old, were obtained from the Experimental Animal Center of Yangzhou University (Yangzhou, China). The mice were maintained in plastic cages with free access to eat food and drink water, temperature kept at 21 ± 2°C and kept on a 12 h light/dark cycle. Animal welfare and experimental procedures were subjected to the Guide for the Care and Use of Laboratory Animals (National Institutes of Health, United States), and the study protocol was approved by the Animal Care and Protection Committee of Nanjing University-Gulou Hospital (SYXK 2004-0013). The authors confirmed that all animals received human care and all animal experiments were performed in accordance with the relevant guidelines and regulations. All the authors complied with the ARRIVE guidelines experiments.

Experimental design for GA-induced contact hypersensitivity is shown in **Figure 1A**. On the first day (day 0), female ICR mice were sensitized with FAC emulsified GA (GA/FAC, 1 mg/ml, 100 μl) in the right flank by subcutaneous injection. On Day 6 and day 13, mice were sensitized with FAC emulsified GA (GA/FAC, 1 mg/ml, 200 μl) in the back by subcutaneous injection of multipoints. On the last day (day 20), mice were challenged on their left ears with GA/FAC (10 mg/ml, 30 μl). 24 h after the challenge, the ear thickness was measured with a digimatic

FIGURE 1 | Isovitexin decreases the susceptibility of GA-induced contact dermatitis in mice. In the mouse model of GA-induced contact dermatitis, mice were given isovitexin, a main flavonoid compound from CEL, at 10 and 20 mg/kg respectively. **(A)** Chemical structural of isovitexin. **(B)** The ear swelling was measured at day 20. **(C)** Spleen weight was measured at day 20. **(D)** The body weight changes of mice in different groups. **(E)** Hematoxylin and eosin stain (original magnification ×200) of ear tissue sections. Bars, 100 μm. **(F)** Ear histological scoring. IsoV, isovitexin. Data represented means ± SEM of eight mice. [##]$p < 0.01$ vs. vehicle group, [*]$p < 0.05$, [**]$p < 0.01$ vs. model group.

micrometer. Ears' swelling was evaluated by the thickness difference between the left and right. Mice in normal group were normally sensitized with FAC and challenged with olive oil without GA. CLE (100, 200 mg/kg, intragastrically) or isovitexin (10, 20 mg/kg, intraperitoneally) or dexamethasone (0.5 mg/kg, intraperitoneally) was administered once a day from day 6 to day 20. Mice in the normal group and model group were given saline as control.

Cell Culture and Proliferation Assay

T cells, isolated from female Balb/c mice Lymph nodes, were cultured in 96-well plates in 1,640 medium at the density of 5×10^6 cells/well and stimulated with 5 µg/ml of Con A for 48 h under a humidified 5% (v/v) CO_2 atmosphere at 37°C. MTT with concentration of 4 mg/ml dissolves in PBS, 20 µl of MTT was added in each well 4 h before the end of incubation. Then culture media was removed and 200 µl DMSO was added to dissolve the crystals. Measuring the absorbance value at 540 nm.

Plant Material Extraction of Celtis Leaf

The plant name, *Celtis sinensis Pers.*, were confirmed with the Medicinal Plant Names Services (http://mpns.kew.org). Celtis leaves were collected from Guizhou, China, and were authenticated as *C. sinensis* based on the morphological characteristics by the international Cultivar Registration Center (Nanjing Forestry University). A voucher specimen (voucher number GZCS200503) of this plant was deposited at 2,304 laboratory, college of chemical engineering, Nanjing Forestry University, China.

The method of extraction followed with few modifications as described by Lee et al. (2018). The air-dried leaf of Celtis sinensis (5 kg) were ground in a cutting mill and soaked with ethyl alcohol (25L′3, for 1.5 h each) at 70°C. After the crude extract was dried under reduced pressure, a crude dark green residue was suspended in water with freeze-dried preservation.

Quantitative RT-PCR

Total RNA was extracted from popliteal fossa lymph nodes and reverse transcribed to cDNA. Quantitative PCR was performed with the ABI Prism 7,000 sequence detection system (Applied Biosystems, Foster City, CA)using SYBR Green I dye (Biotium, Inc.) Threshold cycle numbers were obtained using ABI Prism 7000 SDS software version 1.0. PCR cycling conditions were as follows: one cycle of 94 8C for 5 min followed by 40 cycles of 94 8C for 30 s, 58 8C for 30 s, and 72 8C for 45 s. The primer sequences used were as follows:

tnf-α forward 5′-CCCTCACACTCAGATCATCTTCT-3′,
tnf-α reverse 5′-GCTACGACGTGGGCTACAG-3′;
ifn-γ forward 5′-GCCACGGCACAGTCATTGA-3′,
ifn-γ reverse 5′-TGCTGATGGCCTGATTGTCTT-3′;
il-2 forward 5′-GTGCTCCTTGTCAACAGCG-3′,
il-2 reverse 5′-GGGGAGTTTCAGGTTCCTGTA-3′;
il-17a forward 5′-TTTAACTCCCTTGGCGCAAAA-3′,
il-17a reverse 5′-CTTTCCCTCCGCATTGACAC-3′;
β-actin forward 5′-GTGACGTTGACATCCGTAAAGA-3′,
β-actin reverse 5′-GCCGGACTCATCGTACTCC-3′.

Relative message RNA (mRNA) expression was calculated as a ratio to actin.

Cytokine Assay

Cytokine levels were measured using ELISA kits from MultiSciences (Lianke) Biotech Co., Ltd. (Hangzhou, China) according to the manufacturer's instructions.

Western Blot Analysis

Cells isolated from lymph node were cultured in 6-well plates at a density of 1×10^7 cells/well in RPMI1640 medium and stimulated with Con A (5 µg/ml). Proteins lyzed from cultured cells were separated by SDS-PAGE and electrophoretically transferred onto PVDF membranes (Millipore, Bedford, MA). After treatment with blocking buffer in 5% BSA at RT for 1 h, membranes were incubated with primary antibodies at 4°C overnight, and the secondary antibody incubation at RT for 2 h. Antibody reactivity was detected by using ECL luminescence reagent (Tanon, Shanghai).

Histological Analysis

The 5 mm thickness of ear sections were obtained by formalin-fixed, paraffin-embedded and stained with hematoxylin and eosin. Histological parameter was following as described before (Omidkhoda et al., 2019): the level of leukocyte infiltration and vascular congestion (Zhou et al., 2018); the erosion and anabrosis of epidermal cells (Miwa et al., 2001); affection of the other side of the ears (Luo et al., 2011). We scored each of the histological assessment on a scale of 1–4 and the higher score means more serious inflammation.

Molecular Docking Analysis

The molecular docking analysis was conducted in Maestro v11.1 (Schrödinger, LLC) by the default protocols (Wang et al., 2020). We prepared the ligand isovitexin and SHP2 protein (Protein Data Bank ID:3o5x). The docking grid was generated based on the position of the tyrosine phosphatase SHP2 with the default protocol. Subsequently, glide docking was performed and induce-fit docking was conducted based on the results of glide docking.

Statistical Analysis

All Data were represented means ± SEM from triplicate experiments performed in a parallel manner. Data were statistically compared and one-way analysis of variance ANOVA followed by Dunnett's test between the vehicle group and multiple dose groups (Szczepanski et al., 2020). The level of significance was set at $p < 0.05$.

RESULTS

Celtis sinensis Leaf Extract Protects Mice From Allergic Contact Dermatitis

Celtis sinensis is employed as a folk medicine for treating inflammation, skin infections and other diseases (Rojas-Bedolla et al., 2018). To study the possibility of using *Celtis sinensis* to treat inflammation in GA-induced allergic contact dermatitis, a mouse model of GA-induced hypersensitive contact dermatitis was established. We stimulated the popliteal lymph nodes and the left ear of ICR mice by GA (**Figure 1A**). Mice challenged by GA displayed definite inflammation, as indicated by splenomegaly and ear swelling, compared with the vehicle group.
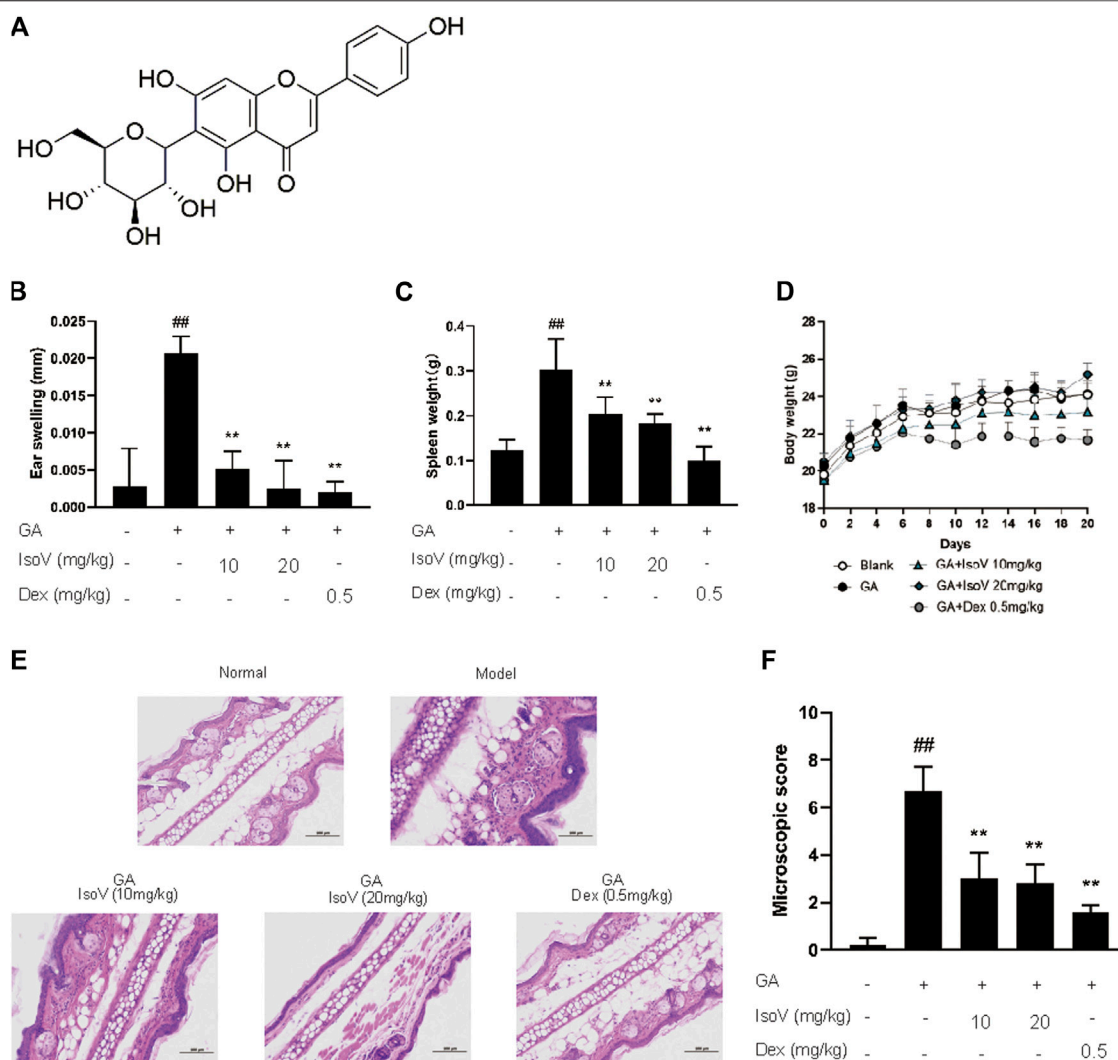
FIGURE 2 | *Celtis sinensis* leaf Extract (CLE) ameliorates ginkgolic acids (GA)-induced contact dermatitis in mice. **(A)** The mouse model of GA-induced contact dermatitis, drugs were administered once a day from day 6 to day 20. **(B)** The mice were given CLE at 100 and 200 mg/kg respectively, and the ear swelling was measured 24 h after challenge at day 20. **(C)** Spleen weight was measured at day 20. **(D)** The body weight changes of mice in different groups. **(E)** Hematoxylin and eosin stain (original magnification ×200) of ear tissue sections. Bars, 100 μm. **(F)** Ear histological scoring. Data represent means ± SEM of eight mice. $^{##}p < 0.01$ vs. vehicle group, $^{*}p < 0.05$, $^{**}p < 0.01$ vs. model group.

Celtis sinensis leaf extract (investigational ingredient, CLE) and dexamethasone (positive control drug, Dex) were used to treat the degree of ear swelling. Notably, mice that received CLE exhibited significantly reduced susceptibility to GA-induced allergic contact dermatitis, as shown by the milder splenomegaly and ear swelling compared with the model group (**Figures 1B,C**). Indeed, CLE did not decrease the body weight of mice, but it appeared in mice that received dexamethasone (**Figure 1D**). Histopathologically, mice that received CLE displayed significantly alleviated leukocyte infiltration, epidermal anabrosis and affection damage compared with the vehicle group (**Figures 1E,F**). Collectively, intragastric instillation of CLE confers protection from GA-induced allergic contact dermatitis in ICR mice.

Isovitexin, the Main Flavonoid in the Leaf of *Celtis sinensis*, Ameliorates GA-Induced Allergic Contact Dermatitis in Mice

Since isovitexin (chemical structure is shown in **Figure 2A**) is the predominant flavone of *Celtis sinensis* (Ota et al., 2017), we further examined the possible role of isovitexin in dermal inflammation. Mice that received isovitexin exhibited ameliorative ear swelling and splenomegaly compared with the model group (**Figures 2B,C**). Meanwhile, consistent with the

CLE experiments, isovitexin did not show body weight loss, suggesting that compared with dexamethasone, isovitexin displayed significant anti-inflammatory function without serious side effects (**Figure 2D**). Histopathologically, mice that received isovitexin displayed directly reduced leukocyte chemotaxis and ameliorated proinflammatory cytokine release (**Figures 2E,F**). Therefore, isovitexin, a natural flavone, exerts immunosuppressive effects in GA-induced allergic contact dermatitis.

Isovitexin Inhibits T Cell-Mediated Inflammation in Mice With GA-Induced Allergic Contact Dermatitis

Stimulation with GA also exacerbated the release of inflammatory cytokines (TNF-α, IFN-γ, IL-2, and IL-17A) in serum. The upregulation of these T cell-specific cytokines indicates that GA-induced allergic contact dermatitis mainly triggers inflammatory activation of T cells rather than macrophage-mediated innate inflammation. Anti-inflammatory effects of isovitexin were presumably attributed to a decrease in T cell-specific cytokines in serum (**Figure 3A**). We then evaluated the mRNA level of T cell-associated cytokines in popliteal lymph nodes. Compared with inflamed dermatitis mice, the contents of *tnf-α, ifn-γ, il-2,* and *il-17a* were significantly lower in mice that received isovitexin (**Figures 3B,C**). Moreover, we observed that proapoptotic proteins (cleaved caspase-3 and cleaved PARP) were activated and that proliferation proteins (phosphor-AKT and phospho-ERK1/2) were inhibited in isovitexin-treated T cells from allergic mice (**Figures 3D,E**). Taken together, these data clearly demonstrate that isovitexin may inhibit T cell-mediated inflammatory responses in dermatitis.

Isovitexin Inhibits the Proliferation and Promotes Apoptosis of Con A-Activated T Cells *in vitro*

The above findings prompted us to suppose that isovitexin diminished T cell proinflammatory activities in response to GA stimulation. Furthermore, we used Con A-activated T cells to explore the mechanisms underlying the antagonizing effects of isovitexin on metabolic disorders. Con A is a plant lectin that induces the mitogenic activity of T lymphocytes and increases the production of inflammatory cytokines such as IL-2, TNF-α and IFN-γ (Shinohara and Tsukimoto, 2017). The MTT assay was used to assess cell viability. As showing in **Figure 4B**, Con A (5 μg/ml) strongly promoted T cell proliferation. In addition, cell culture with the addition of 0–100 μM isovitexin was not toxic to naïve T cells, but it inhibited the proliferation of Con A-activated T cells (**Figures 4A,B**). On the other hand, isovitexin triggered apoptosis of Con A-activated T cells, as analyzed by the Annexin V/PI staining assay (**Figure 4C**). The percentages of early apoptotic T cells significantly increased with different doses of isovitexin after 24 h of incubation. To define the pathway of apoptosis, western blotting was used to analyze the cleavage of poly (ADP-ribose) polymerase (PARP) and caspase. Strong cleavage of PARP together with activation of caspase-3 and -8 were observed in the Con A-activated T cells

treated with isovitexin, which is consistent with the results of animal experiments (**Figures 4D,E**). These observations indicate that isovitexin inhibits the proliferation of Con A-activated T cells by promoting apoptosis.

Isovitexin Inhibits the Production of Proinflammatory Cytokines in Con A-Activated T Cells

Numerous apoptotic cells have been shown to inhibit proinflammatory cytokine production, preventing chronic inflammation (Voll et al., 1997). For this claim, we examined whether isovitexin is linked with the production of proinflammatory cytokines, including TNF-α, IFN-γ, IL-2 and IL-17A. ELISA was performed to measure the release of cytokines in the culture supernatant, and RT-PCR was carried out to measure the expression of these cytokines from Con A–activated T cells (**Figures 5A–C**). Interestingly, at a concentration of 100 μM, isovitexin significantly reduced the levels of proinflammatory cytokines (TNF-α, IFN-γ, IL-2 and IL-17A) at both the mRNA and protein levels.

The MAPK and STAT Signaling Pathways are Regulated by Isovitexin in Con A-Activated T Cells

The MAPK and STAT signaling pathways govern the expression of most proinflammatory genes (Huang et al., 2010; Villarino et al., 2017). To understand how isovitexin modulates inflammatory responses in T cells, we examined the relationship between isovitexin and these pathways. Mechanistically, T cells treated with 100 μM isovitexin exhibited markedly reduced phosphorylation of proteins such as P38, JNK, and ERK1/2 in Con A-induced T cells, which are the central kinases in the MAPK signaling pathway that cause inflammation. On the other hand, isovitexin dose-dependently decreased the level of IκB phosphorylation. The kinase is activated by a highly diverse group of extracellular signals, including inflammatory cytokines, growth factors, and chemokines. Unexpectedly, isovitexin did not affect the expression of p65 in whole cell lysate, and whether p65 is in the core needs to be further proven. Western blotting was also used to explore whether isovitexin decreased the phosphorylation of STAT3, STAT6, and SHP2, which play important roles in the proliferation and differentiation of T cells. Thus, isovitexin serves as a negative regulator of the MAPK and STAT signaling pathways (**Figures 6A,B**).

Molecular Docking Analyses of the Interaction Between Isovitexin and SHP2 Protein

Next, we sought to determine the molecular mechanisms by which isovitexin modulates the MAPK and STAT signaling pathways in Con A-activated T cells. We first tested whether isovitexin might interact with SHP2. The interaction between the SHP2 protein and isovitexin was demonstrated by molecular docking analysis. As shown in the figure, there is a certain
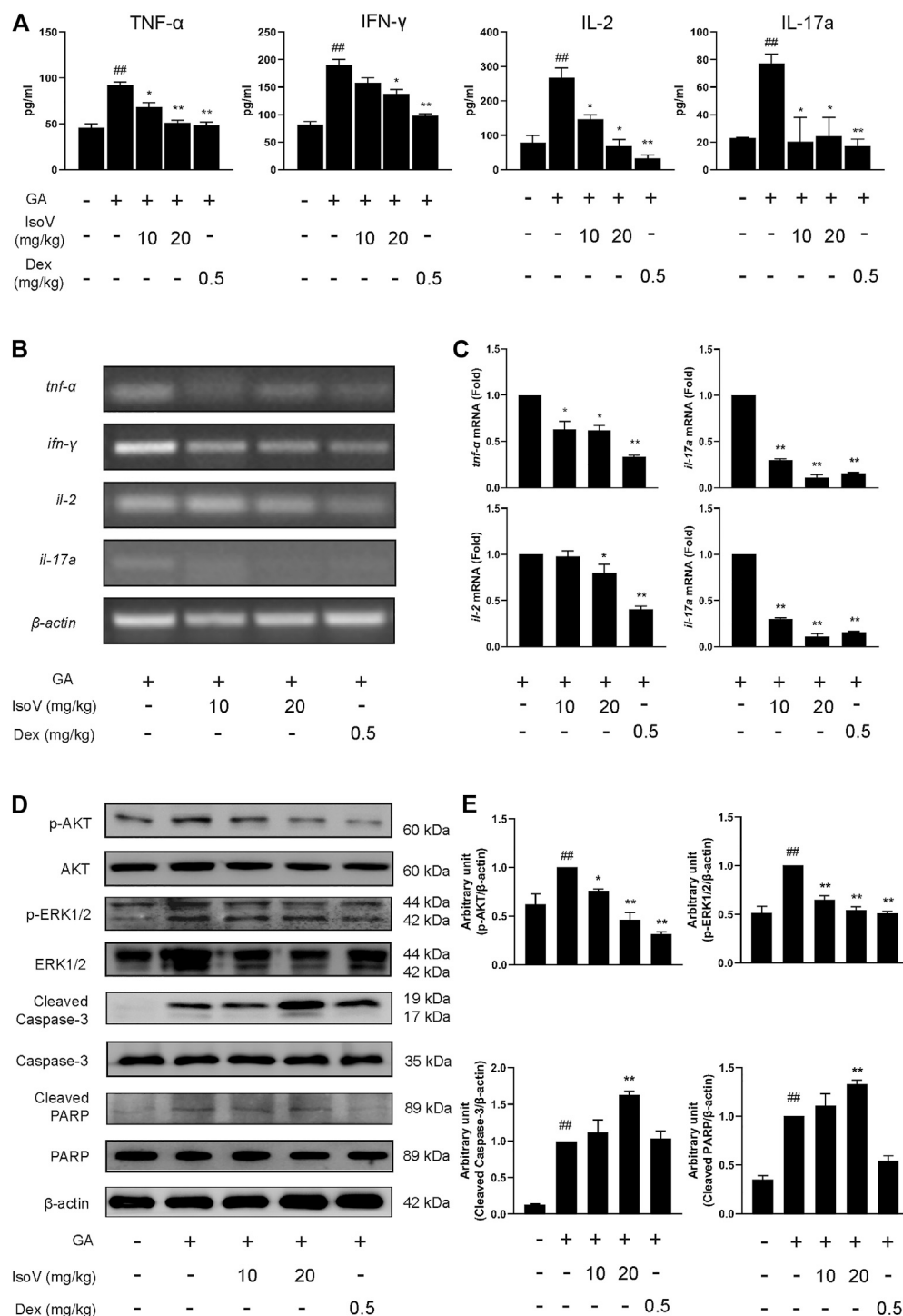
FIGURE 3 | Isovitexin inhibits the expression of pro-inflammatory cytokines in lymph nodes and serum from mice with contact dermatitis and promotes the expression of apoptosis-related proteins. In the mouse model of GA-induced contact dermatitis, **(A)** the effect of isovitexin on the levels of pro-inflammatory cytokines in the serum was determined by ELISA. Data are representative of three independent experiments; **(B,C)** the effect of isovitexin on the inflammatory cytokines mRNA expression in lymph nodes was measured by RT-PCR, and the relative band density was analyzed using ImageJ; **(D,E)** the lymph node cells were harvested and lyzed, and the effect of isovitexin on the protein levels of p-AKT, Cleaved PARP, Cleaved Caspase-3, p-ERK1/2 were analyzed by western blotting, and the relative band density was analyzed using ImageJ. The grouping of gels were cropped from different parts of the different gels. Data represented means ± SEM of three independent time. $^{\#\#}p < 0.01$ vs. vehicle group, $^{*}p < 0.05$, $^{**}p < 0.01$ vs. model group.
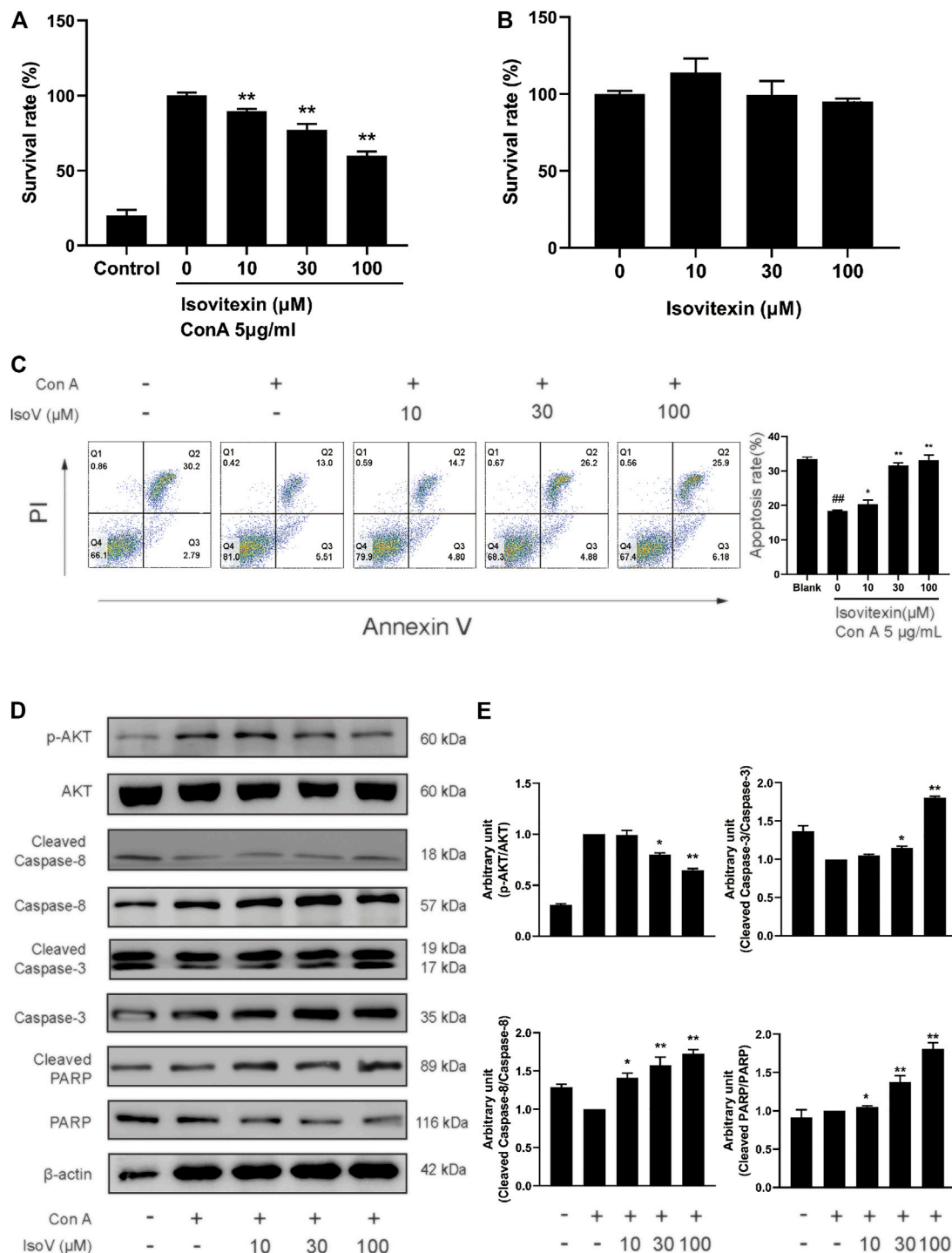
FIGURE 4 | Isovitexin induces the apoptosis of Con A-activated T cells. **(A)** Con A-activated T cells were treated with different concentrations of isovitexin for 48 h, and the cell survival was determined by MTT assay. **(B)** T cells were treated with different concentrations of isovitexin for 24 h, and the cell survival was determined by MTT assay. Cells incubated without Con A and isovitexin were used as control. Con A-activated T cells were seeded in 12-well plates and incubated with 0, 10, 30 and 100 μM isovitexin for 24 h. **(C)** Cells were stained with Annexin V and PI, and the apoptosis of the cells was determined by flow cytometry assay of Annexin V/PI staining. Annexin V positive cells of three independent experiments were shown in column statistics. **(D,E)** Cells treated with different concentrations of isovitexin were harvested and lyzed. The protein levels of p-AKT, Cleaved caspase-3, Cleaved caspase-8, Cleaved PARP in T cells were measured by western blotting, and the relative band density was analyzed using ImageJ. The grouping of gels were cropped from different parts of the different gels. Data represented mean ± SEM of three independent experiments. $^{##}p < 0.01$ vs. Blank group, $^*p < 0.05$, $^{**}p < 0.01$ vs. control (Con A-activated T cells).
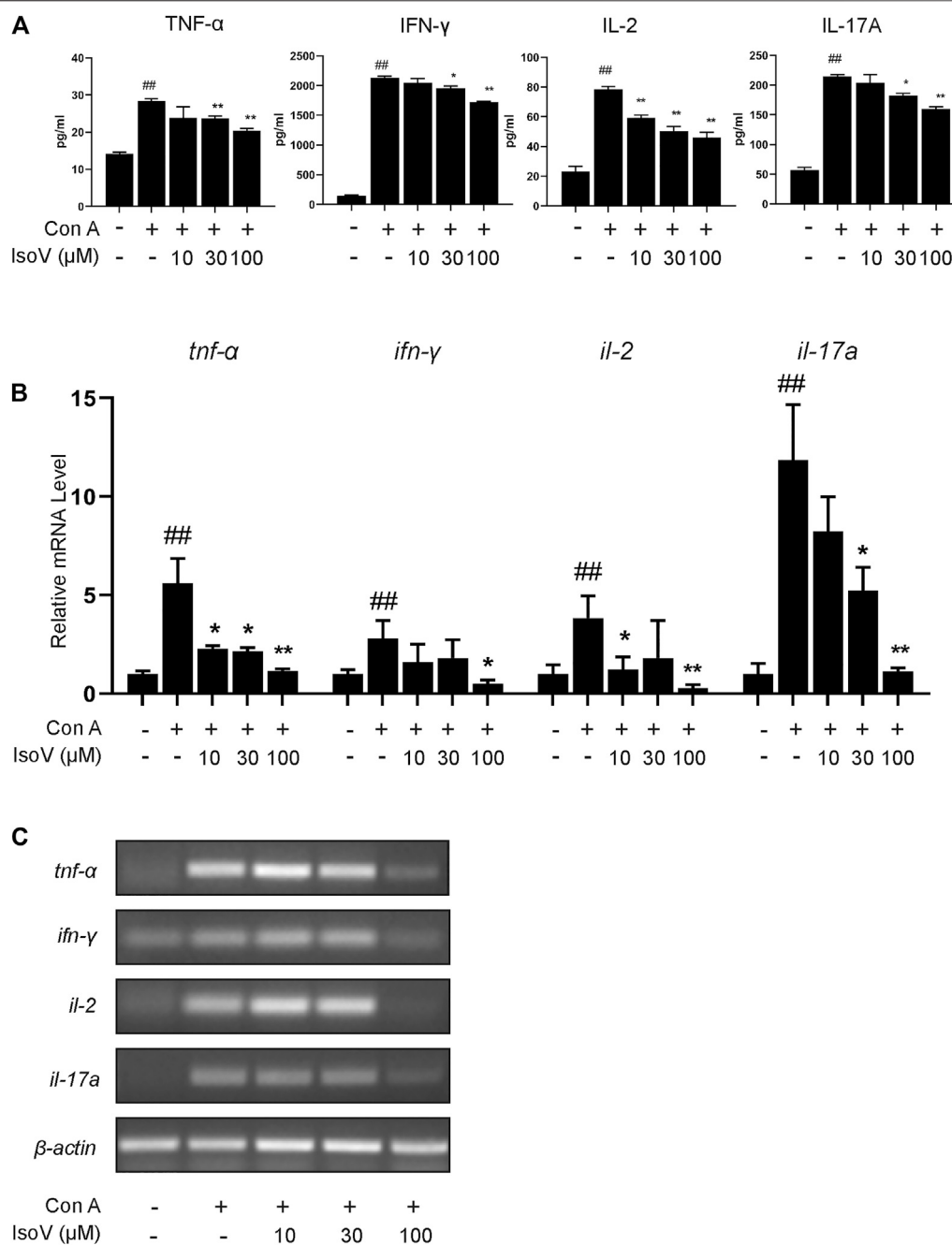
FIGURE 5 | Isovitexin inhibits T cells proinflammatory cytokines production in activated mouse T cells. Con A-activated T cells were treated with different concentrations of isovitexin for 24 h; **(A)** Proinflammatory cytokines, in culture supernatants of the indicated groups, were determined by ELISA; **(B,C)** Relative *tnf-α, ifn-γ, il-2, il-17a* mRNA level was determined by Q-PCR **(B)** and RT-PCR **(C)**. Data are mean ± SEM and are representative of at least three independent experiments. Significant differences are expressed as [##]$p < 0.01$ vs. Blank group, *$p < 0.05$, **$p < 0.01$ vs. control (Con A-activated T cells).

intensity of interaction between SHP2 and isovitexin, and the best induced-fit docking score is −5.414 kcal/mol, where isovitexin can insert into the active domain of SH2 kinase and interact by hydrogen bonding and π–π interactions (**Figure 6C**). The docking results suggest that there is obvious π-π conjugation between TYR279, the B ring and the C ring of isovitexin. There may be two hydrogen bond interactions between SHP2

and isovitexin: one formed between the ASN281 residue and 4′-OH on the C ring of isovitexin, and the other formed between GLN and the carbonyl group on the B ring of isovitexin. Indeed, the A ring of isovitexin forms seven kinds of hydrogen bonds with SHP2 with ASP425, LYS366, AGR465, TRP423 and GLY427, which confer stability to the docking conformation (**Figure 6D**).
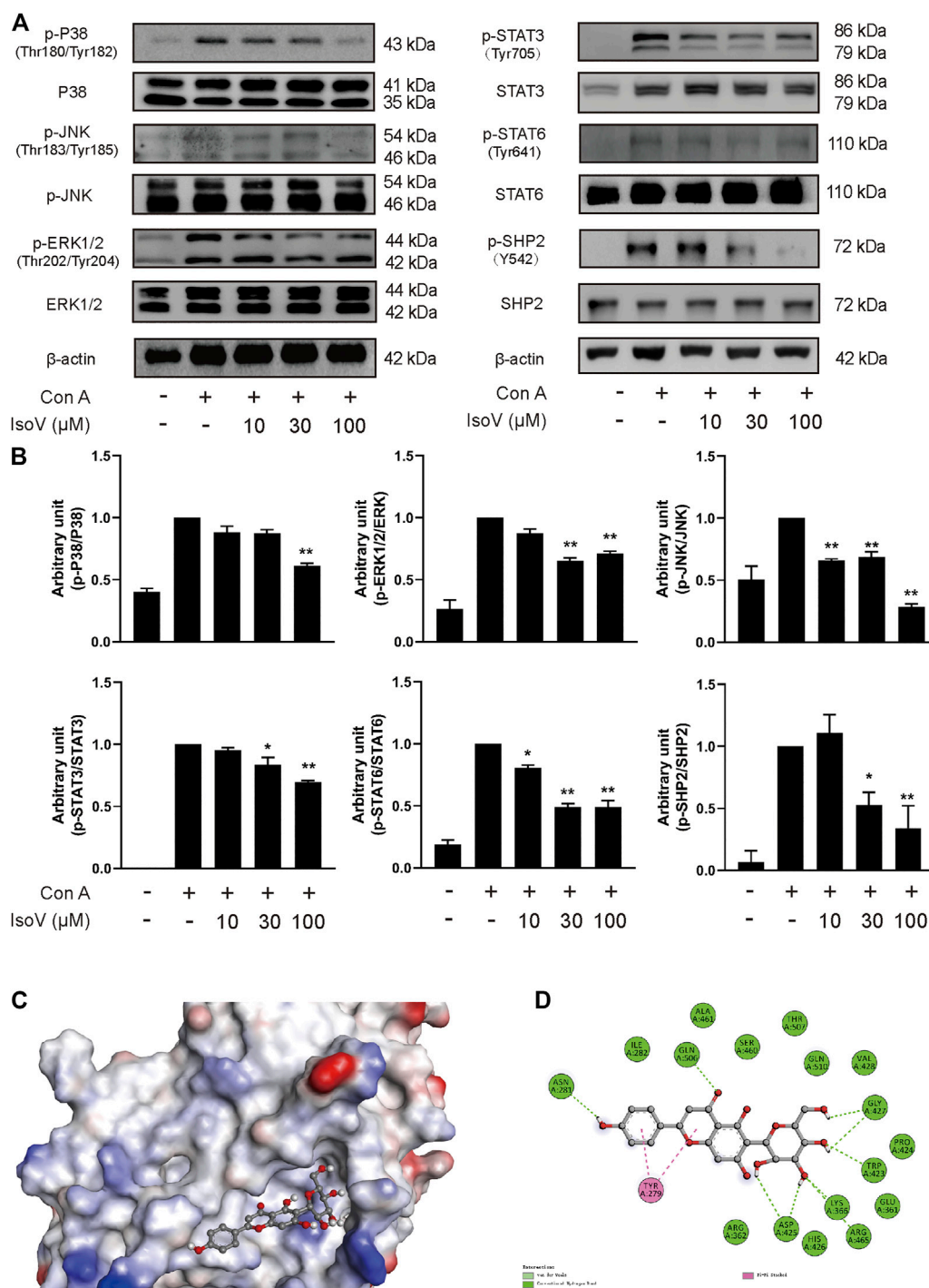
FIGURE 6 | Isovitexin inhibits MAPK, STAT signaling and decreases the phosphorylated SHP2 level in Con A–activated T cells. **(A,B)** T cells isolated from the lymph nodes of Balb/c mice were stimulated with 5 μg/ml Con A and various doses of isovitexin for 24 h. The protein levels of p-P38, p-JNK, p-ERK1/2, p-STAT3, p-STAT6, p-SHP2 in T cells were measured by western blotting, and the relative band density was analyzed using ImageJ Data are mean ± SEM and are representative of at least three independent experiments. The grouping of gels were cropped from different parts of the different gels. Significant differences are expressed as *$p < 0.05$, **$p < 0.01$ vs. the Con A group. **(C,D)** The induced fit docking analysis of isovitexin and SHP2 protein (PDB:3o5x). Hydrogen bonds and π-π stacking were indicated with green and pink dot line, respectively.
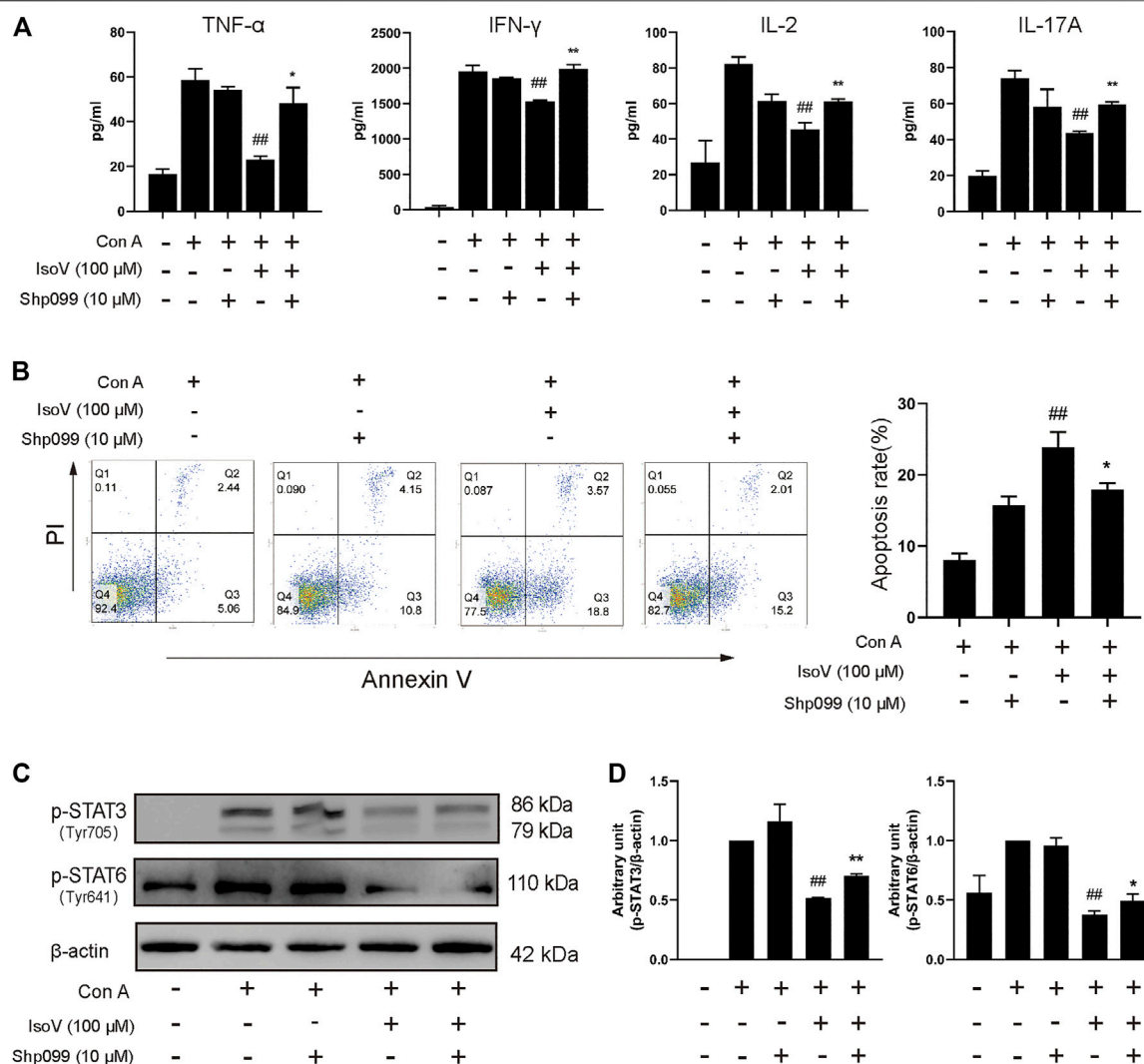
FIGURE 7 | The SHP2-specific inhibitor SHP099 reversed the effects of isovitexin on activated T cells. Con A-activated T cells were treated with 100 μM isovitexin and added with 10 μM SHP2 or not; **(A)** The levels of proinflammatory cytokines in cell culture supernatants were determined using ELISA kits after 24 h cultivation. **(B)** Cells were stained with Annexin V and PI, and the apoptosis of the cells was determined by flow cytometry assay of Annexin V/PI staining. Annexin V positive cells of three independent experiments were shown in column statistics. **(C,D)** Lymph nodes cells were harvested and lyzed and the phosphorylation of STAT3 and STAT6 was evaluated by Western blot. The grouping of blots was cropped from different parts of the same gel. Data are mean ± SEM and are representative of two independent experiments. Significant differences are expressed as [##]$p < 0.01$ vs. Con A group, [*]$p < 0.05$, [**]$p < 0.01$ vs. the isovitexin group.
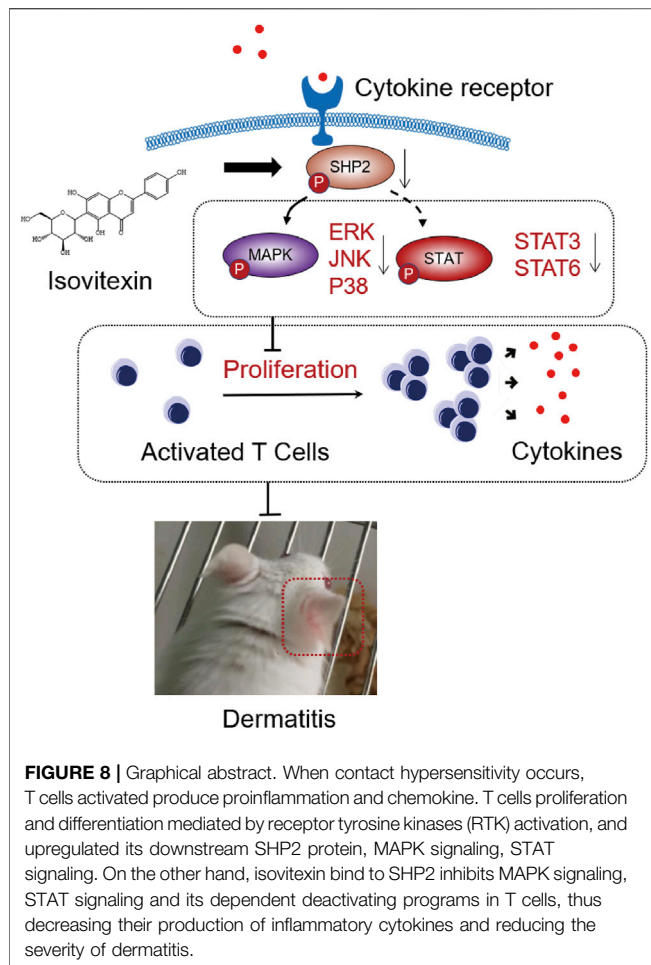
The Effects of Isovitexin on Con A-Activated T Cells can be Reversed by the SHP2-Specific Inhibitor SHP099

SHP099, a selective SHP2 inhibitor, binds to protein tyrosine phosphatase domains, inhibiting SHP2 activity through an allosteric mechanism (Pádua et al., 2018). We investigated whether isovitexin suppressed the release of cytokines by regulating SHP2 in Con A-activated T cells, and the effects were examined in SHP099-treated cells. The results showed that the inhibitory effects of isovitexin on T cell proliferation and proinflammatory cytokine production were partially reversed by SHP099 (**Figures 7A,B**). Moreover, In the SHP099 group, the phosphorylation levels of STAT3 and

STAT6 were higher than isovitexin group (**Figures 7C,D**). The presumed reason is that SHP099 inhibited MAPK signaling pathway, and STAT as a supplementary pathway the phosphorylation level of increased. In summary, our study proved that isovitexin restrains p-SHP2 and controls dermatitis inflammation (**Figure 8**).

DISCUSSION

Allergic contact dermatitis is a skin disease caused by environmental or occupational allergens. As a general concept of the antigen presentation process in the sensitization phase of ACD, allergens activate innate immunity through keratinocyte

FIGURE 8 | Graphical abstract. When contact hypersensitivity occurs, T cells activated produce proinflammation and chemokine. T cells proliferation and differentiation mediated by receptor tyrosine kinases (RTK) activation, and upregulated its downstream SHP2 protein, MAPK signaling, STAT signaling. On the other hand, isovitexin bind to SHP2 inhibits MAPK signaling, STAT signaling and its dependent deactivating programs in T cells, thus decreasing their production of inflammatory cytokines and reducing the severity of dermatitis.

release of proinflammatory cytokines and chemokines to recruit T cells. Hapten-specific T cells are guided to inflammatory sites and produce cytokines, such as TNF-α, IFN-γ and IL-17A. In turn, these cytokines then stimulate skin-resident cells, which lead to further recruitment of T cells and induce an inflammatory cascade (Honda et al., 2013; Leonard and Guttman-Yassky, 2019). Indeed, dysregulation of the skin immune system occurs in nearly all ACD cases, which highlights the importance of appropriate immune regulation in preventing ACD. However, studies of contact-hypersensitivity mouse models have mostly used synthetic experimental allergens, such as DNFB. Different allergens cause widely divergent immune responses, resulting in the eventual failure of the therapeutic strategies for ACD. We therefore optimized a mouse model of GA-induced ACD to identify inflammation and ear swelling. We identified a critical role of proinflammatory cytokines such as TNF-α, IFN-γ, IL-2 and IL-17A in skin inflammation in this model (**Figures 3A,B**) and revealed that these cytokines may be regulated by SHP2 *in vitro* (**Figure 6A**).

As an environmental allergen, GA-induced ACD is usually treated with NSAIDs or immunosuppressive drugs, and long-term use may result in serious side effects, including effects on the gastrointestinal tract and infection susceptibility (Rosa et al., 2016). In this context, new pharmacological strategies are being

sought, such as resolution of inflammation with fewer side effects. In the present study, we have provided proof that CLE, especially isovitexin, may dampen proinflammatory signaling and the clearance of proinflammatory mediators to attenuate inflammation. In conclusion, isovitexin acts as an inflammatory inhibitor to ameliorate GA-induced ACD (**Figures 1**, **2**).

Isovitexin is the most abundant flavone in the leaf of *Celtis sinensis*. It has anti-inflammatory pharmacological properties. In a previous study, isovitexin attenuated the LPS-induced phosphorylation of all three MAPKs, reduced NF-κB activation and promoted M2 polarization in macrophages (Lv et al., 2016; Liu et al., 2019). However, few studies targeting the anti-inflammatory effects of T lymphocytes by isovitexin treatment have been reported. To reveal the regulatory effects of isovitexin on ACD, which is characterized by the Th1 response (Owen et al., 2018), we used T cells from mouse lymph node cells under Con A stimulation. In this study, we found that isovitexin dose-dependently upregulated apoptosis and suppressed the cytokines TNF-α, IFN-γ, IL-2 and IL-17A (**Figure 5**). This result is consistent with animal experiments, indicating that isovitexin exerts an immunomodulatory effect when facing an inflammatory challenge.

To further reveal the underlying mechanisms of isovitexin on T cell apoptosis and signaling pathways. We further examined the effects of isovitexin on cleaved caspase-3, cleaved caspase-8, MAPK signaling and STAT signaling in activated T cells. In this study, we have provided several lines of evidence that suggest that cleaved caspase-3 and cleaved caspase-8 are significantly enhanced by isovitexin treatment in a dose-dependent manner (**Figure 4**). These cleaved proteins lead to increasing apoptosis. MAPK signaling and STAT signaling, along with countless studies linking to inflammatory pathologies, provide the rationale for applying potent inhibitors in the treatment of immune-system-mediated diseases (Villarino et al., 2017; Yahfoufi et al., 2018). Our research result is somewhat consistent with a previous report in which isovitexin normalized the phosphorylation of all three MAPKs and the STAT signaling pathway. In addition, isovitexin dampens proinflammatory signaling and promotes the resolution of inflammation (**Figure 6**).

SHP2, a nonreceptor protein tyrosine phosphatase, was the first reported oncogenic tyrosine phosphatase and has attracted much attention. The function of SHP2 was reported to regulate cell survival and proliferation primarily through activation of the RAS-ERK signaling pathway and to mediate the immune checkpoint pathways (Chen et al., 2016). Moreover, SHP2 is an important mediator in lupus erythematosus, ERK/MAPK signaling normalization and reduced production of IFN-γ and IL-17a cytokines involved in inflammation can occur by directly inhibiting SHP2 (Wang et al., 2016). Meanwhile, SHP2 is required for full activation of the JAK/STAT pathway, a major signaling cascade in inflammation (Frankson et al., 2017). SHP2 has been characterized as a positive regulator of JAK2/STAT3 signaling in rheumatoid arthritis diseases (Ganesan and Rasool, 2017). Here, molecular docking showed that isovitexin may bind to the PTP domain with hydrogen bonding and π–π interactions (**Figure 6B**). Western blotting experiments suggested that isovitexin normalized Src-homology two domain-containing phosphatase tyrosine (Y542) phosphatase, which upregulates phosphatase activity (Jiang et al., 2019). Indeed, downregulated SHP2 reduces the downstream MAPK and STAT signaling pathways, which decreases the level

of proinflammatory cytokine release and ameliorates ACD. It also prevents the T cell-decreased MAPK signaling, which would cause autoreactivity and autoimmunity (Gorelik et al., 2007). In summary, isovitexin blockade of SHP2 may be a novel and effective therapy for the treatment of patients with GA-induced ACD.

SHP099, an inhibitor that binds to the allosteric site of SHP2 and stabilizes the closed form of SHP2 by interacting with the N-SH2 and PTP domains, has been used to provide several lines of evidence, which suggested functional expression and a physiological signaling role of SHP2 in Con A-active T cells. First, the Annexin V/PI staining results showed that T cells treated with isovitexin and SHP099 had an increased proportion of living cells vs. the isovitexin group alone (**Figure 7B**). These results indicated that isovitexin promotes T lymphocyte apoptosis by downregulating SHP2 activation. Moreover, SHP099 also reversed the inhibitory effects of isovitexin on MAPK and STAT signaling (**Figure 7C**). Our results indicate that isovitexin exerts SHP2-dependent inhibitory effects in Con A-activated T cells.

In summary, our study demonstrates that isovitexin from Celtis sinensis is a potential therapeutic agent against GA-induced allergic contact dermatitis. The MAPK and STAT signaling pathways can be regulated by isovitexin, and SHP2 may be a potential anti-inflammatory target of isovitexin in T cells. Isovitexin can be used to solve anti-inflammatory problems induced by GA.

DATA AVAILABILITY STATEMENT

The original contributions presented in the study are included in the article/**Supplementary Material**, further inquiries can be directed to the corresponding author.

ETHICS STATEMENT

The animal study was reviewed and approved by Animal welfare and experimental procedures were subjected to the Guide for the Care and Use of Laboratory Animals (National Institutes of Health, United States) and the related ethical regulations of our university. All efforts were carried out to reduce the number of animals used and minimize animal suffering.

AUTHOR CONTRIBUTIONS

Conceptualization, XF, LZ; Methodology, YZ, ZQ, LW; Writing–Original Draft Preparation, YZ, Writing–Review and Editing, WW; Supervision, FC; Funding Acquisition XF, LZ.

FUNDING

SUPPLEMENTARY MATERIAL

The Supplementary Material for this article can be found online at: https://www.frontiersin.org/articles/10.3389/fphar.2021.630320/full#supplementary-material

REFERENCES

Boelman, D. J. (2010). Emergency: Treating Poison Ivy, Oak, and Sumac. *Am. J. Nurs.* 110, 49–52. doi:10.1097/01.NAJ.0000377690.87350.36

Cao, X., Liu, L., Yuan, Q., Li, X., Cui, Y., Ren, K., et al. (2019). Isovitexin Reduces Carcinogenicity and Stemness in Hepatic Carcinoma Stem-like Cells by Modulating MnSOD and FoxM1. *J. Exp. Clin. Cancer Res.* 38, 264. doi:10.1186/s13046-019-1244-6

Chen, Y.-N. P., Lamarche, M. J., Chan, H. M., Fekkes, P., Garcia-Fortanet, J., Acker, M. G., et al. (2016). Allosteric Inhibition of SHP2 Phosphatase Inhibits Cancers Driven by Receptor Tyrosine Kinases. *Nature* 535, 148–152. doi:10.1038/nature18621

Fang, X., Dong, Y., Xie, Y., Wang, L., Wang, J., Liu, Y., et al. (2019). Effects of β-glucosidase and α-rhamnosidase on the Contents of Flavonoids, Ginkgolides, and Aroma Components in Ginkgo Tea Drink. *Molecules* 24, 2009. doi:10.3390/molecules24102009

Frankson, R., Yu, Z.-H., Bai, Y., Li, Q., Zhang, R.-Y., and Zhang, Z.-Y. (2017). Therapeutic Targeting of Oncogenic Tyrosine Phosphatases. *Cancer Res.* 77, 5701–5705. doi:10.1158/0008-5472.CAN-17-1510

Fransen, H. P., Pelgrom, S. M. G. J., Stewart-Knox, B., De Kaste, D., and Verhagen, H. (2010). Assessment of Health Claims, Content, and Safety of Herbal Supplements Containing Ginkgo Biloba. *Food Nutr. Res.* 54, 5221. doi:10.3402/fnr.v54i0.5221

Ganesan, R., and Rasool, M. (2017). Interleukin 17 Regulates SHP-2 and IL-17RA/STAT-3 Dependent Cyr61, IL-23 and GM-CSF Expression and RANKL Mediated Osteoclastogenesis by Fibroblast-like Synoviocytes in Rheumatoid Arthritis. *Mol. Immunol.* 91, 134–144. doi:10.1016/j.molimm.2017.09.003

Gorelik, G., Fang, J. Y., Wu, A., Sawalha, A. H., and Richardson, B. (2007). Impaired T Cell Protein Kinase Cδ Activation Decreases ERK Pathway Signaling in Idiopathic and Hydralazine-Induced Lupus. *J. Immunol.* 179, 5553–5563. doi:10.4049/jimmunol.179.8.5553

Han, E. J., Park, H. L., and Kim, S. H. (2016). Allergic Reaction to Ginkgo Nut on FDG PET/CT. *Clin. Nucl. Med.* 41, 716–717. doi:10.1097/RLU.0000000000001276

Honda, T., Egawa, G., Grabbe, S., and Kabashima, K. (2013). Update of Immune Events in the Murine Contact Hypersensitivity Model: toward the Understanding of Allergic Contact Dermatitis. *J. Invest. Dermatol.* 133, 303–315. doi:10.1038/jid.2012.284

Hotta, E., Tamagawa-Mineoka, R., and Katoh, N. (2013). Allergic Contact Dermatitis Due to Ginkgo Tree Fruit and Leaf. *Eur. J. Dermatol.* 23, 548–549. doi:10.1684/ejd.2013.2102

Huang, P., Han, J., and Hui, L. (2010). MAPK Signaling in Inflammation-Associated Cancer Development. *Protein Cell* 1, 218–226. doi:10.1007/s13238-010-0019-9

Jiang, L., Xu, W., Chen, Y., and Zhang, Y. (2019). SHP2 Inhibitor Specifically Suppresses the Stemness of KRAS-Mutant Non-small Cell Lung Cancer Cells. *Artif. Cell Nanomedicine, Biotechnol.* 47, 3231–3238. doi:10.1080/21691401.2019.1646748

Lee, S., Lee, D., Lee, J. C., Kang, K. S., Ryoo, R., Park, H.-J., et al. (2018). Bioactivity-Guided Isolation of Anti-inflammatory Constituents of the Rare Mushroom Calvatia Nipponica in LPS-Stimulated RAW264.7 Macrophages. *Chem. Biodiversity* 15, e1800203. doi:10.1002/cbdv.201800203

Leonard, A., and Guttman-Yassky, E. (2019). The Unique Molecular Signatures of Contact Dermatitis and Implications for Treatment. *Clinic Rev. Allerg Immunol.* 56, 1–8. doi:10.1007/s12016-018-8685-0

Liu, B., Huang, B., Hu, G., He, D., Li, Y., Ran, X., et al. (2020). Corrigendum: Isovitexin-Mediated Regulation of Microglial Polarization in

Lipopolysaccharide-Induced Neuroinflammation via Activation of the CaMKKβ/AMPK-PGC-1α Signaling Axis. *Front. Immunol.* 11, 41. doi:10.3389/fimmu.2020.00041

Liu, B., Huang, B., Hu, G., He, D., Li, Y., Ran, X., et al. (2019). Isovitexin-Mediated Regulation of Microglial Polarization in Lipopolysaccharide-Induced Neuroinflammation via Activation of the CaMKKβ/AMPK-PGC-1α Signaling Axis. *Front. Immunol.* 10, 2650. doi:10.3389/fimmu.2019.02650

Liu, S., Zhang, X., and Wang, J. (2020). Isovitexin Protects against Cisplatin-Induced Kidney Injury in Mice through Inhibiting Inflammatory and Oxidative Responses. *Int. Immunopharmacology* 83, 106437. doi:10.1016/j.intimp.2020.106437

Luo, Q., Gu, Y., Zheng, W., Wu, X., Gong, F., Gu, L., et al. (2011). Erlotinib Inhibits T-Cell-Mediated Immune Response via Down-Regulation of the C-Raf/ERK cascade and Akt Signaling Pathway. *Toxicol. Appl. Pharmacol.* 251, 130–136. doi:10.1016/j.taap.2010.12.011

Lv, H., Yu, Z., Zheng, Y., Wang, L., Qin, X., Cheng, G., et al. (2016). Isovitexin Exerts Anti-inflammatory and Anti-oxidant Activities on Lipopolysaccharide-Induced Acute Lung Injury by Inhibiting MAPK and NF-Kb and Activating HO-1/Nrf2 Pathways. *Int. J. Biol. Sci.* 12, 72–86. doi:10.7150/ijbs.13188

Mei, N., Guo, X., Ren, Z., Kobayashi, D., Wada, K., and Guo, L. (2017). Review ofGinkgo Biloba-Induced Toxicity, from Experimental Studies to Human Case Reports. *J. Environ. Sci. Health C* 35, 1–28. doi:10.1080/10590501.2016.1278298

Miwa, H., Iijima, M., Tanaka, S., and Mizuno, Y. (2001). Generalized Convulsions after Consuming a Large Amount of Gingko Nuts. *Epilepsia* 42, 280–281. doi:10.1046/j.1528-1157.2001.33100.x

Omidkhoda, S. F., Razavi, B. M., and Hosseinzadeh, H. (2019). Protective Effects of *Ginkgo Biloba L.* Against Natural Toxins, Chemical Toxicities, and Radiation: A Comprehensive Review. *Phytotherapy Res.* 33, 2821–2840. doi:10.1002/ptr.6469

Ota, A., Višnjevec, A. M., Vidrih, R., Prgomet, Ž., Nečemer, M., Hribar, J., et al. (2017). Nutritional, Antioxidative, and Antimicrobial Analysis of the Mediterranean Hackberry (Celtis australisL.). *Food Sci. Nutr.* 5, 160–170. doi:10.1002/fsn3.375

Owen, J. L., Vakharia, P. P., and Silverberg, J. I. (2018). The Role and Diagnosis of Allergic Contact Dermatitis in Patients with Atopic Dermatitis. *Am. J. Clin. Dermatol.* 19, 293–302. doi:10.1007/s40257-017-0340-7

Pádua, R. A. P., Sun, Y., Marko, I., Pitsawong, W., Stiller, J. B., Otten, R., et al. (2018). Mechanism of Activating Mutations and Allosteric Drug Inhibition of the Phosphatase SHP2. *Nat. Commun.* 9, 4507. doi:10.1038/s41467-018-06814-w

Qian, Y., Peng, Y., Shang, E., Zhao, M., Yan, L., Zhu, Z., et al. (2017). Metabolic Profiling of the Hepatotoxicity and Nephrotoxicity of Ginkgolic Acids in Rats Using Ultra-performance Liquid Chromatography-High-Definition Mass Spectrometry. *Chemico-Biological Interactions* 273, 11–17. doi:10.1016/j.cbi.2017.05.020

Rojas-Bedolla, E. I., Gutiérrez-Pérez, J. L., Arenas-López, M. I., González-Chávez, M. M., Zapata-Morales, J. R., Mendoza-Macías, C. L., et al. (2018). Chemical Characterization, Pharmacological Effects, and Toxicity of an Ethanol Extract of *Celtis Pallida Torr.* (Cannabaceae) Aerial Parts. *J. Ethnopharmacology* 219, 126–132. doi:10.1016/j.jep.2018.03.014

Rosa, S. I. G., Rios-Santos, F., Balogun, S. O., and Martins, D. T. d. O. (2016). Vitexin Reduces Neutrophil Migration to Inflammatory Focus by Down-Regulating Pro-inflammatory Mediators via Inhibition of P38, ERK1/2 and JNK Pathway. *Phytomedicine* 23, 9–17. doi:10.1016/j.phymed.2015.11.003

Shinohara, Y., and Tsukimoto, M. (2017). Adenine Nucleotides Attenuate Murine T Cell Activation Induced by Concanavalin A or T Cell Receptor Stimulation. *Front. Pharmacol.* 8, 986. doi:10.3389/fphar.2017.00986

Szczepanski, A. P., Zhao, Z., Sosnowski, T., Goo, Y. A., Bartom, E. T., and Wang, L. (2020). ASXL3 Bridges BRD4 to BAP1 Complex and Governs Enhancer Activity in Small Cell Lung Cancer. *Genome Med.* 12, 63. doi:10.1186/s13073-020-00760-3

Ude, C., Schubert-Zsilavecz, M., and Wurglics, M. (2013). *Ginkgo Biloba* Extracts: a Review of the Pharmacokinetics of the Active Ingredients. *Clin. Pharmacokinet.* 52, 727–749. doi:10.1007/s40262-013-0074-5

Van Beek, T. A., and Montoro, P. (2009). Chemical Analysis and Quality Control of Ginkgo Biloba Leaves, Extracts, and Phytopharmaceuticals. *J. Chromatogr. A* 1216, 2002–2032. doi:10.1016/j.chroma.2009.01.013

Villarino, A. V., Kanno, Y., and O'shea, J. J. (2017). Mechanisms and Consequences of Jak-STAT Signaling in the Immune System. *Nat. Immunol.* 18, 374–384. doi:10.1038/ni.3691

Voll, R. E., Herrmann, M., Roth, E. A., Stach, C., Kalden, J. R., and Girkontaite, I. (1997). Immunosuppressive Effects of Apoptotic Cells. *Nature* 390, 350–351. doi:10.1038/37022

Wang, J., Mizui, M., Zeng, L.-F., Bronson, R., Finnell, M., Terhorst, C., et al. (2016). Inhibition of SHP2 Ameliorates the Pathogenesis of Systemic Lupus Erythematosus. *J. Clin. Invest.* 126, 2077–2092. doi:10.1172/JCI87037

Wang, J., Wang, J.-Q., Cai, C.-Y., Cui, Q., Yang, Y., Wu, Z.-X., et al. (2020). Reversal Effect of ALK Inhibitor NVP-Tae684 on ABCG2-Overexpressing Cancer Cells. *Front. Oncol.* 10, 228. doi:10.3389/fonc.2020.00228

Wang, M., Zhao, J., Avula, B., Wang, Y.-H., Avonto, C., Chittiboyina, A. G., et al. (2014). High-Resolution Gas Chromatography/Mass Spectrometry Method for Characterization and Quantitative Analysis of Ginkgolic Acids inGinkgo bilobaPlants, Extracts, and Dietary Supplements. *J. Agric. Food Chem.* 62, 12103–12111. doi:10.1021/jf503980f

Yahfoufi, N., Alsadi, N., Jambi, M., and Matar, C. (2018). The Immunomodulatory and Anti-inflammatory Role of Polyphenols. *Nutrients* 10, 1618. doi:10.3390/nu10111618

Zehrmann, N., Zidorn, C., and Ganzera, M. (2010). Analysis of Rare Flavonoid C-Glycosides in *Celtis Australis L.* By Micellar Electrokinetic Chromatography. *J. Pharm. Biomed. Anal.* 51, 1165–1168. doi:10.1016/j.jpba.2009.11.028

Zhou, G., Ma, J., Tang, Y., Wang, X., Zhang, J., Yao, X., et al. (2018). Optimization of Ultrasound-Assisted Extraction Followed by Macroporous Resin Purification for Maximal Recovery of Functional Components and Removal of Toxic Components from *Ginkgo Biloba* Leaves. *Biomed. Res. Int.* 2018, 1–15. doi:10.1155/2018/4598067

Advantages of publishing in Frontiers

OPEN ACCESS
Articles are free to read for greatest visibility and readership

FAST PUBLICATION
Around 90 days from submission to decision

HIGH QUALITY PEER-REVIEW
Rigorous, collaborative, and constructive peer-review

TRANSPARENT PEER-REVIEW
Editors and reviewers acknowledged by name on published articles

REPRODUCIBILITY OF RESEARCH
Support open data and methods to enhance research reproducibility

DIGITAL PUBLISHING
Articles designed for optimal readership across devices

FOLLOW US
@frontiersin

IMPACT METRICS
Advanced article metrics track visibility across digital media

EXTENSIVE PROMOTION
Marketing and promotion of impactful research

LOOP RESEARCH NETWORK
Our network increases your article's readership